Targeted and untargeted lipid analysis of platelets by liquid chromatography coupled to mass spectrometry

Dissertation

der Mathematisch-Naturwissenschaftlichen Fakultät

der Eberhard Karls Universität Tübingen

zur Erlangung des Grades eines

Doktors der Naturwissenschaften

(Dr. rer. nat.)

vorgelegt von

Małgorzata Cebo,

aus Geburtsort

Częstochowa, Polen

Tübingen

2020

Gedruckt mit Genehmigung der Mathematisch-Naturwissenschaftlichen Fakultät der Eberhard Karls Universität Tübingen.

Tag der mündlichen Qualifikation: 07.12.2020

Stellvertretender Dekan: *Prof. Dr. József Fortágh*

1. Berichterstatter: *Prof. Dr. Michael Lämmerhofer*

2. Berichterstatter: *Prof. Dr. Pierre Koch*

The research described in this thesis was conducted between September 1st 2016 and 31st January 2020 at the Institute of Pharmaceutical Sciences, Division Pharmaceutical (Bio)Analysis, Eberhard Karls Universität Tübingen under the supervision of Prof. Dr. Michael Lämmerhofer.

To my parents, Czesława and Sławomir Cebo

TABLE OF CONTENTS

SUMMARY

Lipids play various roles in cells, e.g. membrane building, energy storage and signalling. A distinctive class of lipids, important for bioactive signalling, consists of oxylipins. Oxylipins are formed by oxidation of polyunsaturated fatty acids which in turn might have been released from more complex lipids by the enzymatic activity of phospholipases. Lipids including oxylipins play a major role in platelet activation. Analysis of a changing platelet lipidome during their activation allows researchers to learn about biochemical pathways associated with this process and to select new therapeutic targets for novel drugs against diseases, in which platelets are involved.

The last decades have brought unprecedented technological innovations in analytical chemistry including separation science (e.g. highly efficient sub-2 µm particles for stationary phases, capillary columns for liquid chromatography (LC) and novel chiral materials) and mass spectrometry (MS) (e.g. high resolution instrument, increased sensitivity, novel analytical strategies like untargeted profiling with sequential window acquisition of all theoretical fragment ion mass spectra (SWATH)). The inventions have enabled the exponential growth in various 'omics' branches, also lipidomics.

In my first project, a combined targeted-untargeted LC-MS/MS method was developed for the analysis of oxylipins and fatty acids in platelet releasates. The MS data was acquired with the SWATH approach and the acquisition windows were optimized to ensure wide coverage of analytes and to provide high sensitivity and low limits of detection for the 3 targeted compounds: thromboxane B2 (TXB2), 12-hydroxy-5*Z*,8*E*,10*E*-heptadecatrienoic acid (HHT) and 12-keto-5*Z*,8*E*,10*E*-heptadecatrienoic acid (KHT). In this context, a general synthesis method for keto-analogues of hydroxy fatty acids in presence of double bonds was proposed for the preparation of standards. The sample analysis revealed that activated platelets release high amounts of TXB2, HHT and KHT: in average 13, 15 and 0.6 attomoles per platelet, respectively. Furthermore, untargeted analysis showed a significantly increased release in other oxylipins upon the activation, but also in polyunsaturated fatty acids (PUFA). There is less awareness of the release of a broad range of biologically active oxylipins and PUFA during platelet activation and the biological implications are not fully understood at the moment.

My second study involved the development of a new LC method for oxylipin separation with a capillary column (inner diameter equal to 0.5 mm). Scheduled selected reaction monitoring (SRM) for MS/MS detection provided high sensitivity, accuracy and precision

for quantification of 42 oxylipins. Thirteen internal standards were spread across the LC separation and used for normalization of analyte signals. Moreover, various extraction protocols and calibration methods were compared. The Bond Elut Certify II cartridges (mixed-mode reversed-phase/anion-exchange material) for solid phase extraction and external matrix-matched calibrants were used in the final method. The method was validated with concentrated plasma, which was an easily available, but challenging biological matrix. The final analysis detected 19 oxylipins in resting platelets.

The third analytical method, which was developed in this work, utilized a modern chiral LC column for enantiomeric separation of oxylipins. The method showed an outstanding peak resolution and great sensitivity provided by SRM MS/MS detection. Nineteen enantiomeric pairs and one diastereomeric pair of hydroxy fatty acids were quantified in on air autoxidized PUFA and in platelet releasates. The autoxidized samples contained, as expected, racemic mixtures, but the single enantiomers were mostly detected in platelet samples with 12(*S*)-hydroxyeicosatetraenoic (12(*S*)-HETE) being the highest abundant oxylipin in the thrombin activated samples. An interesting observation was made about 12-hydroxyeicosatrienoic acid (12-HETrE), which seems to be synthetized in platelets via 2 different enzymatic reactions.

Parallel to the more specific methods, described above, sets of platelets were analysed with a reversed-phase LC-MS/MS method for the general lipid analysis. The sets included platelets treated in-vitro with a selective CXCR7 receptor agonist, untreated control, thrombin-activated platelets as well as CXCR7 agonist/thrombin activated platelets, and the untargeted SWATH data acquisition was utilized for lipid profiling. What is more, a novel approach for post-acquisition data processing by targeted feature extraction on MS1 and MS2 level including improved peak picking, lipid identification and quantification was developed and it provided higher assay specificity then conventional methods. The lipid identification was supported by the characteristic elution pattern in reversed-phase LC and quantification was done mostly using extracted ion chromatograms (EIC) of fragments from SWATH. The final results of platelet lipidomes showed that changes typical for platelet activation (e.g. increase in the concentration of oxylipins and lysophosphatidylinositols) were highly supressed in the samples, where the CXCR7 agonist was added. That means that the agonist is capable of reducing platelet activation. On the other hand, the agonist itself also influenced the platelet lipidome, as it showed increased level of acylcarnitines and decrease in diglycerides, when compared to resting platelets.

ZUSAMMENFASSUNG

Lipide haben unterschiedliche Funktionen in biologischen Zellen, z.B. Membranaufbau, Energiespeicherung und Signalübertragung. Eine charakteristische Klasse von Lipiden, die für die bioaktive Signalübertragung wichtig ist, besteht aus Oxylipinen. Oxylipine werden durch Oxidation von Fettsäuren gebildet, die ihrerseits durch die enzymatische Aktivität von Phospholipasen aus komplexen Lipiden freigesetzt werden können. Lipide, einschließlich der Oxylipine, spielen eine wichtige Rolle bei der Aktivierung von Thrombozyten. Forscher interessieren sich nun für das Lipidom in Thrombozyten und für dessen Änderung während ihrer Aktivierung und wollen so die an diesem Prozess beteiligten biochemischen Wege kennenlernen, um schließlich neue therapeutische Ansätze gegen Krankheiten zu finden, an denen Thrombozyten beteiligt sind.

Die letzten Jahrzehnte haben beispiellose technologische Innovationen in der analytischen Chemie gebracht, wie in der Chromatographie (z.B. hocheffiziente sub-2-µm-Partikel für stationäre Phasen, Kapillarsäulen für die Flüssigkeitschromatographie (LC), neuartige chirale Materialien) oder in der Massenspektrometrie (MS) (z.B. Massenspektrometer mit erhöhter Auflösung oder erhöhter Empfindlichkeit, neuartige Analysestrategien wie nicht-zielgerichtetes Profiling mittels so genannter “sequential window acquisition of all theoretical fragment ion mass spectra” (SWATH)-Datenerfassung). Diese Neuerungen haben das exponentielle Wachstum in den verschiedenen „Omics“ -Wissenschaften, wie auch in der Lipidomik vorangetrieben.

In meinem ersten Projekt wurde eine kombinierte zielgerichtete LC-MS/MS-Methode zur Analyse von Oxylipinen und Fettsäuren entwickelt, und in Zellüberständen von Thrombozyten angewendet. Die MS-Daten wurden mit der SWATH- Datenerfassung erfasst und die Methode dahingehend optimiert, eine breite Abdeckung der Analyten sicherzustellen und die erforderliche Empfindlichkeit und niedrige Nachweisgrenzen für die 3 Zielverbindungen, Thromboxan B2 (TXB2), 12-Hydroxy-5*Z*,8*E*,10*E*-Heptadecatriensäure (HHT) und 12-Keto-5*Z*,8*E*,10*E*-Heptadecatriensäure (KHT), zu gewährleisten. Darüber hinaus wurde eine neue allgemeine Synthesemethode für Ketoanaloga von Hydroxyfettsäuren beschrieben. Die Studie ergab schließlich, dass aktivierte Blutplättchen hohe Mengen an TXB2, HHT und KHT freisetzen: durchschnittlich 13, 15 bzw. 0,6 attomol pro Blutplättchen. Darüber hinaus zeigte eine nicht-zielgerichtete Analyse einen signifikanten Anstieg anderer Oxylipine und mehrfach ungesättigter Fettsäuren (PUFA), die bei der Aktivierung freigesetzt werden. Über dieses Phänomen ist bisher wenig bekannt und seine biologische Bedeutung ist noch nicht vollständig geklärt.

Meine zweite Studie befasste sich mit der Entwicklung einer neuen LC-Methode zur Oxylipin-Trennung mit einer Kapillarsäule (Innendurchmesser gleich 0,5 mm). Ein so genanntes „scheduled selected reaction monitoring“ (SRM-MS/MS) lieferte hohe Empfindlichkeit, Genauigkeit und Präzision für die Quantifizierung von 42 Oxylipinen. 13

interne Standards wurden über die LC-Trennung verteilt und zur Normalisierung der Analyten verwendet. Darüber hinaus wurden verschiedene Extraktionsprotokolle und Kalibrierungsmethoden verglichen. Die optimierte Methode verwendet Bond Elut Certify II-Kartuschen (mit Mixed-Mode reversed-phase/Anionenaustauscher Material) zur Festphasenextraktion und externe matrix-matched Kalibranten. Die Methode wurde mit konzentriertem Plasma validiert, das eine leicht verfügbare, wenngleich herausfordernde biologische Matrix war. Es konnten somit 19 Oxylipine in nicht-aktivierten Blutplättchen nachgewiesen werden.

Die dritte, von mir entwickelte Analysemethode verwendete eine moderne chirale LC-Säule zur Enantiomerentrennung von Oxylipinen. Das Verfahren zeigte eine hervorragende Peakauflösung und eine hohe Empfindlichkeit, die durch die SRM-MS/MS-Detektion bereitgestellt wurden. Neunzehn Enantiomerenpaare und ein Diastereomerenpaar von Hydroxyfettsäuren wurden in an der Luft autoxidierten PUFA und in Zellüberständen von Thrombozyten quantifiziert. Die autoxidierten Proben enthielten erwartungsgemäß racemische Gemische, wohingegen die einzelnen Enantiomere meist in den Thrombozytenproben nachgewiesen wurden. Dabei war die 12(*S*)-Hydroxyeicosatetraensäure (12(*S*)-HETE) das höchst abundante Oxylipin in den Thrombin-aktivierten Proben. Weitere interessante Beobachtungen wurden über die 12-Hydroxyeicosatriensäure (12-HETrE) gemacht, die offenbar über 2 verschiedene enzymatische Reaktionen in Blutplättchen synthetisiert werden kann.

Parallel zu den oben beschriebenen, gezielten Methoden wurden Thrombozytengruppen mit einer Umkehrphasen-LC-MS/MS-Methode für die allgemeine nicht-zielgerichtete Lipidanalyse analysiert. Die Sets enthielten Thrombozyten, die in vitro mit einem selektiven CXCR7-Rezeptoragonisten behandelt wurden, neben Kontrollen ohne diesem Agonist, Gruppen mit Plättchen die durch Thrombin aktiviert wurden sowie mit Thrombin und CXCR7 Agonist, und die nicht-zielgerichtete SWATH-Datenerfassung wurde für das Lipid Profiling verwendet. Darüber hinaus wurde ein neuartiger Ansatz für die Datenverarbeitung nach der SWATH Datenerfassung entwickelt, der ein verbessertes Peak-Picking, eine Lipididentifikation und Lipidquantifizierung umfasst und eine höhere Spezifität als herkömmliche Methoden bietet. Die Lipididentifikation wurde durch ein charakteristisches Elutionsmuster in Umkehrphasen-LC unterstützt, und die Quantifizierung erfolgte hauptsächlich unter Verwendung extrahierter Ionenchromatogramme (EIC) von Fragmenten aus SWATH. Die Endergebnisse der Thrombozytenlipidomen zeigten, dass Änderungen, die für die Thrombozytenaktivierung typisch sind (z.B. Erhöhung der Konzentration von Oxylipin und Lysophosphatidylinositol), nach Zugabe des CXCR7-Agonisten, stark unterdrückt waren. Dies bedeutet, dass der Agonist die Thrombozytenaktivierung reduzieren kann. Andererseits beeinflusste der Agonist selbst auch das Thrombozytenlipidom, da er im Vergleich zu ruhenden Thrombozyten einen erhöhten Acylcarnitinspiegel und eine Abnahme der Diglyceride aufwies.

LIST OF PUBLICATIONS INCLUDED IN THIS THESIS

Publication I

M. Cebo, J. Schlotterbeck, M. Gawaz, M. Chatterjee, and M. Lämmerhofer, "Simultaneous targeted and untargeted UHPLC-ESI-MS/MS method with data-independent acquisition for quantification and profiling of (oxidized) fatty acids released upon platelet activation by thrombin" *Analytica Chimica Acta*, vol. 1094, pp. 57-69, 2020/01 2020, doi: 10.1016/j.aca.2019.10.005.

Publication II

M. Cebo, X. Fu, M. Gawaz, M. Chatterjee, and M. Lämmerhofer, "Micro-UHPLC-MS/MS method for analysis of oxylipins in plasma and platelets" *J Pharm Biomed Anal*, vol. 189, p. 113426, Jun 20 2020, doi: 10.1016/j.jpba.2020.113426.

Publication III

M. Cebo, X. Fu, M. Gawaz, M. Chatterjee, and M. Lämmerhofer, "Enantioselective ultra-high performance liquid chromatography-tandem mass spectrometry method based on sub-2μm particle polysaccharide column for chiral separation of oxylipins and its application for the analysis of autoxidized fatty acids and platelet releasates" *J Chromatogr A*, vol. 1624, p. 461206, Aug 2 2020, doi: 10.1016/j.chroma.2020.461206.

Publication IV (manuscript ready for submission)

M. Cebo, J. Schlotterbeck, C. Calderón Castro, M. Gawaz, M. Chatterjee, and M. Lämmerhofer, "Untargeted UHPLC-ESI-QTOF-MS/MS analysis with improved lipid identification and quantification for describing total platelet lipidome and its changes upon thrombin-activation and treatment with a platelet inhibitor"

AUTHOR CONTRIBUTIONS

Publication I

Simultaneous targeted and untargeted UHPLC-ESI-MS/MS method with data-independent acquisition for quantification and profiling of (oxidized) fatty acids released upon platelet activation by thrombin.

Małgorzata Cebo
General concept
Method development
Sample preparation and analysis
Data processing and interpretation
Main writing of the manuscript

Dr. Jörg Schlotterbeck
Discussion of results and interpretation
LC-MS instruments maintenance
Proofreading of the manuscript

Prof. Dr. Meinrad Gawaz
Coordination and financing of the biological part of the project
Proofreading of the manuscript

Dr. Madhumita Chatterjee
Platelets collection, isolation and in-vitro treatment
Biological interpretation
Correction and editing of the manuscript
Corresponding author

Prof. Dr. Michael Lämmerhofer
Generation, initiation, coordination and financing of the project
Discussion of results and interpretation
Partial writing and editing of the manuscript
Proofreading and final approval of the manuscript
Corresponding author

Publication II

Micro-UHPLC-MS/MS method for analysis of oxylipins in plasma and platelets.

Małgorzata Cebo
General concept
Method development
Sample preparation and analysis
Data processing and interpretation
Main writing of the manuscript

Xiaoqing Fu
Sample preparation and analysis
LC-MS instruments maintenance
Proofreading of the manuscript

Prof. Dr. Meinrad Gawaz
Coordination and financing of the biological part of the project
Proofreading of the manuscript

Dr. Madhumita Chatterjee
Platelets collection, isolation and in-vitro treatment
Biological interpretation
Correction and editing of the manuscript

Prof. Dr. Michael Lämmerhofer
Generation, initiation, coordination and financing of the project
Discussion of results and interpretation
Partial writing and editing of the manuscript
Proofreading and final approval of the manuscript
Corresponding author

Publication III

Enantioselective ultra-high performance liquid chromatography-tandem mass spectrometry method based on sub-2µm particle polysaccharide column for chiral separation of oxylipins and its application for the analysis of autoxidized fatty acids and platelet releasates.

Małgorzata Cebo
General concept
Method development
Sample preparation and analysis
Data processing and interpretation
Main writing of the manuscript

Xiaoqing Fu
Sample preparation and analysis
LC-MS instruments maintenance
Proofreading of the manuscript

Prof. Dr. Meinrad Gawaz
Coordination and financing of the biological part of the project
Proofreading of the manuscript

Dr. Madhumita Chatterjee
Platelets collection, isolation and in-vitro treatment
Biological interpretation
Correction and editing of the manuscript

Prof. Dr. Michael Lämmerhofer
Generation, initiation, coordination and financing of the project
Discussion of results and interpretation
Partial writing and editing of the manuscript
Proofreading and final approval of the manuscript
Corresponding author

Publication IV

Untargeted UHPLC-ESI-QTOF-MS/MS analysis with improved lipid identification and quantification for describing total platelet lipidome and its changes upon thrombin-activation and treatment with a platelet inhibitor.

Małgorzata Cebo
General concept (lipidomics analysis)
Sample preparation and analysis
Data processing and interpretation
Main writing of the manuscript

Dr. Jörg Schlotterbeck
Discussion of results and interpretation
LC-MS instruments maintenance

Dr. Carlos Calderón Castro
Sample preparation
Discussion of results
LC-MS instruments maintenance

Prof. Dr. Meinrad Gawaz
Coordination and financing of the biological part of the project
Proofreading of the manuscript

Dr. Madhumita Chatterjee
General concept (platelet treatment)
Platelets collection., isolation and in-vitro treatment
Biological interpretation
Correction and editing of the manuscript

Prof. Dr. Michael Lämmerhofer
Generation, initiation, coordination and financing of the project
Discussion of results and interpretation
Partial writing and editing of the manuscript
Proofreading and final approval of the manuscript
Corresponding author

LIST OF OTHER PUBLICATIONS PREPARED DURING THE RESEARCH PERIOD

Publication V (in preparation)

M. Cebo, K. Dittrich, M. Manke, J. Rheinlaender, H. Eysmondt, N. Ferreirós, J. Sudman, M. Büttcher, A. Witte, O. Borst, D. Rath, T. Bakchoul, M. Gawaz, T. Schäffer, M. Lämmerhofer, Madhumita Chatterjee, "Targeting chemokine receptor CXCR7 favours anti-platelet lipids over a pro-thrombotic lipidome and regulates thrombo-inflammation: implications for anti-thrombotic strategy in coronary artery disease"

Publication VI

J. Schlotterbeck, M. Cebo, A. Kolb, and M. Lämmerhofer, "Quantitative analysis of chemoresistance-inducing fatty acid in food supplements using UHPLC-ESI-MS/MS," *Anal Bioanal Chem*, vol. 411, no. 2, pp. 479-491, Jan 2019,
doi: 10.1007/s00216-018-1468-x.

Publication VII

C. Calderon, L. Rubarth, M. Cebo, I. Merfort, and M. Lämmerhofer, "Lipid Atlas of Keratinocytes and Betulin Effects on its Lipidome Profiled by Comprehensive UHPLC-MS/MS with Data Independent Acquisition Using Targeted Data Processing," *Proteomics*, vol. 20, no. 11, p. e1900113, Jun 2020,
doi: 10.1002/pmic.201900113.

Publication VIII

X. Fu, M. Cebo, T. Ikegami, and M. Lämmerhofer, "Retention characteristics of poly(N-(1H-tetrazole-5-yl)-methacrylamide)-bonded stationary phase in hydrophilic interaction chromatography," *J Chromatogr A*, vol. 1609, p. 460500, Jan 4 2020,
doi: 10.1016/j.chroma.2019.460500.

Publication IX

X. Fu, M. Cebo, T. Ikegami, and M. Lämmerhofer, "Separation of carbohydrate isomers and anomers on poly-N-(1H-tetrazole-5-yl)-methacrylamide-bonded stationary phase by hydrophilic interaction chromatography as well as determination of anomer interconversion energy barriers," *J Chromatogr A*, vol. 1620, p. 460981, Jun 7 2020,
doi: 10.1016/j.chroma.2020.460981.

LIST OF POSTER PRESENTATIONS

The 32nd International Symposium on Chromatography (ISC) 2018, Cannes-Mandelieu, France, September 23rd – 27th.

Analysis of platelet fatty acids and oxylipins by combined targeted and untargeted LC-MS method.

Małgorzata Cebo, Jörg Schlotterbeck, Meinrad Gawaz, Madhumita Chatterjee, Michael Lämmerhofer

The 4th Lipidomics Forum 2018, Dortmund, Germany, November 11th – 13th.

Analysis of fatty acids and oxylipins in platelets by combined targeted and untargeted LC-MS/MS method.

Małgorzata Cebo, Jörg Schlotterbeck, Meinrad Gawaz, Madhumita Chatterjee, Michael Lämmerhofer

The 23rd International Symposium on Separation Sciences (ISSS) 2017, Vienna, Austria, September 19th – 22nd.

Combined targeted and untargeted UHPLC-ESI-MS/MS method with data-independent acquisition for quantification of platinum-induced fatty acids and profiling of oxylipins in platelets.

Małgorzata Cebo, Jörg Schlotterbeck, Meinrad Gawaz, Madhumita Chatterjee, Michael Lämmerhofer

LIST OF ORAL PRESENTATIONS

48th International Symposium on High-Performance Liquid Phase Separations and Related Techniques (HPLC) 2019, Milan, Italy, June 16th – 20th.

Lipidomics of platelets: LC-MS analysis and improved data processing by lipid identification and quantification with SWATH

Małgorzata Cebo, Michael Lämmerhofer

4th Cardiology Winterschool 2019, Haigerloch, Germany, January 11th – 12th.

Receptor CXCR7: thrombotic response through changes in the platelet lipidome

Małgorzata Cebo, Madhumita Chatterjee, Michael Lämmerhofer

ABBREVIATIONS

AA	arachidonic acid
ACar	acylcarnitine
ACD	acid-citrate-dextrose buffer
ACN	acetonitrile
ADC	analogue-to-digital converter
ADP	adenosine diphosphate
AIF	all ion fragmentation
ALA	α-linolenic acid
APCI	atmospheric pressure chemical ionisation
ATP	adenosine triphosphate
BHT	butylated hydroxytoluene
BPR	back pressure regulator
cAMP	cyclic adenosine monophosphate
CE	cholesteryl ester
CE	collision energy
CEM	continuous electron multiplier
Cer	ceramide
CES	collision energy spread
cGMP	cyclic guanosine monophosphate
CID	collision-induced dissociation
COX	cyclooxygenase
CSP	chiral stationary phase
CV	coefficient of variation
CXCL	chemokine
CXCR	chemokine receptor
CYP450	cytochrome P450
DB	double bond
DC	direct current
DDA	data dependent acquisition
DG	diglyceride
DGLA	dihomo-γ-linolenic acid
DHA	4*Z*,7*Z*,10*Z*,13*Z*,16*Z*,19*Z*-docosahexaenoic acid
DIA	data independent acquisition
DiHETE	dihydroxyeicosatetraenoic acid
DTS	dense tubular system
EET	epoxyeicosatetraenoic acid
EIC	extracted ion chromatogram
EPA	5*Z*,8*Z*,11*Z*,14*Z*,17*Z*-eicosapentaenoic acid
ePC	etherphosphatidylcholine
ePE	etherphosphatidylethonolamine

ESI	electrospray ionisation
FA	fatty acid
FA	formic acid
FAME	fatty acid methyl ester
FC	fold change
FT-ICR	Fourier-transform ion cyclotron resonance
FWHM	full width at half maximum
GC	gas chromatography
GP	glycoprotein
GTP	guanosine triphosphate
HAc	acetic acid
HDoHE	hydroxydocosahexaenoic acid
HEPE	hydroxyeicosapentaenoic acid
HETE	hydroxyeicosatetraenoic acid
HETrE	hydroxyeicosatrienoic acid
HexCer	hexosylceramide
HHT	12*S*-hydroxy-5*Z*,8*E*,10*E*-heptadecatrienoic acid
HILIC	hydrophilic interaction liquid chromatography
HODE	hydroxyoctadecadienoic acid
HOTrE	hydroxyoctadecatrienoic acid
HTE	hexadeca-4*Z*,7*Z*,10*Z*,13*Z*-tetraenoic acid
IDA	information dependent acquisition
IMS	ion mobility spectrometry
IP3	inositol-1,4,5-trisphosphate
IPA	isopropanol
IS	internal standard
ITC	ion transmission control
KHT	12-keto-5*Z*,8*E*,10*E*-heptadecatrienoic acid
LA	linoleic acid
LC	liquid chromatography
LIPID MAPS	Lipid Metabolites and Pathways Strategy
LIT	linear ion trap
LOWESS	locally weighted scatterplot smoothing
LOX	lipoxygenase
LPC	lysophosphatidylcholine
LPE	lysophosphatidylethonolamine
LPI	lysophosphatidylinositol
LPS	lysophosphatidylserine
LTB4	leukotriene B4
MALDI	matrix-assisted laser desorption/ionisation
MCP	microchannel plate
MeOH	methanol

MG	monoglyceride
MS	mass spectrometer or mass spectrometry
MS/MS	tandem mass spectrometry
NOS	nitric oxide-synthase
NPLC	normal phase liquid chromatography
PBS	Dulbecco’s phosphate-buffered saline
PC	phosphatidylcholine
PE	phosphatidylethonolamine
PG	prostaglandin
PI	phosphatidylinositol
PKC	protein kinase C
PL	phospholipase
ppm	parts per million
PRM	parallel reaction monitoring
PS	phosphatidylserine
PUFA	polyunsaturated fatty acid
Q	quadrupole
QC	quality control
QqQ	triple quadrupoles
QTOF	quadrupole-time-of-flight
RF	alternating current voltage at radio frequency
ROS	reactive oxygen species
RPLC	reversed phase liquid chromatography
RT	retention time
RvD	resolvin D
sEH	soluble epoxide hydrolase
SFC	supercritical fluid chromatography
sGC	soluble guanylyl cyclase
SIM	selected ion monitoring
SM	sphingomyelins
SRM	selected reaction monitoring
STIM1	stromal interaction molecule 1
SWATH	sequential window acquisition of all theoretical fragment ion mass spectra
TDC	time-to-digital converter
TG	triglyceride
TOF	time-of-flight
TXA2	thromboxane A2
TXB2	thromboxane B2
TXS	thromboxane synthetase
UHPLC	ultra-high performance liquid chromatography
vWF	von Willebrand factor

INTRODUCTION

1. Introduction to lipids

Lipids are a diverse group of biomolecules, and because of their diversity, it is difficult to create a simple, but meaningful definition of a lipid, one which would clearly define all lipids, and at the same time easily distinguish them from molecules, which are not lipids. The most general and simple description, but least excluding, says that lipids are organic compounds insoluble in water and soluble in nonpolar solvents. [1]

Another commonly accepted definition refers to lipid structure: 'Lipids are fatty acids and their derivatives, and substances related biosynthetically or functionally to these compounds.'[2]

In 2003 an international consortium called Lipid Metabolites and Pathways Strategy (LIPID MAPS) gathered experts in chemistry of lipids to unify lipid classification and nomenclature, as well as to create a database and tools for lipid research. The lipid definition used by LIPID MAPS refers to their origin and says that 'lipids are defined as hydrophobic or amphipathic small molecules that may originate entirely or in part by carbanion based condensations of ketoacyl thioesters and/or by carbocation based condensations of isoprene units.' [3] LIPID MAPS recognizes 8 main lipid categories and the condensation of thioesters leads to 6 categories: fatty acyls, glycerolipids, glycerophospholipids, sphingolipids, saccharolipids and polyketides, while condensation of isoprene units creates lipids from 2 categories: prenol and sterol lipids [4, 5] (Figure 1).

Lipids are essential molecules which create life together with proteins, nucleic acids and saccharides. They play various roles in organisms: from structural function (building membranes), through energy storage to signalling. A changing composition of lipids might indicate a progressive disease and therefore lipids might be used as biomarkers for health status. The concept of 'lipidomics' is to analyse lipids in a comprehensive way and through comparison learn about a biochemical status of a cell or an organism.

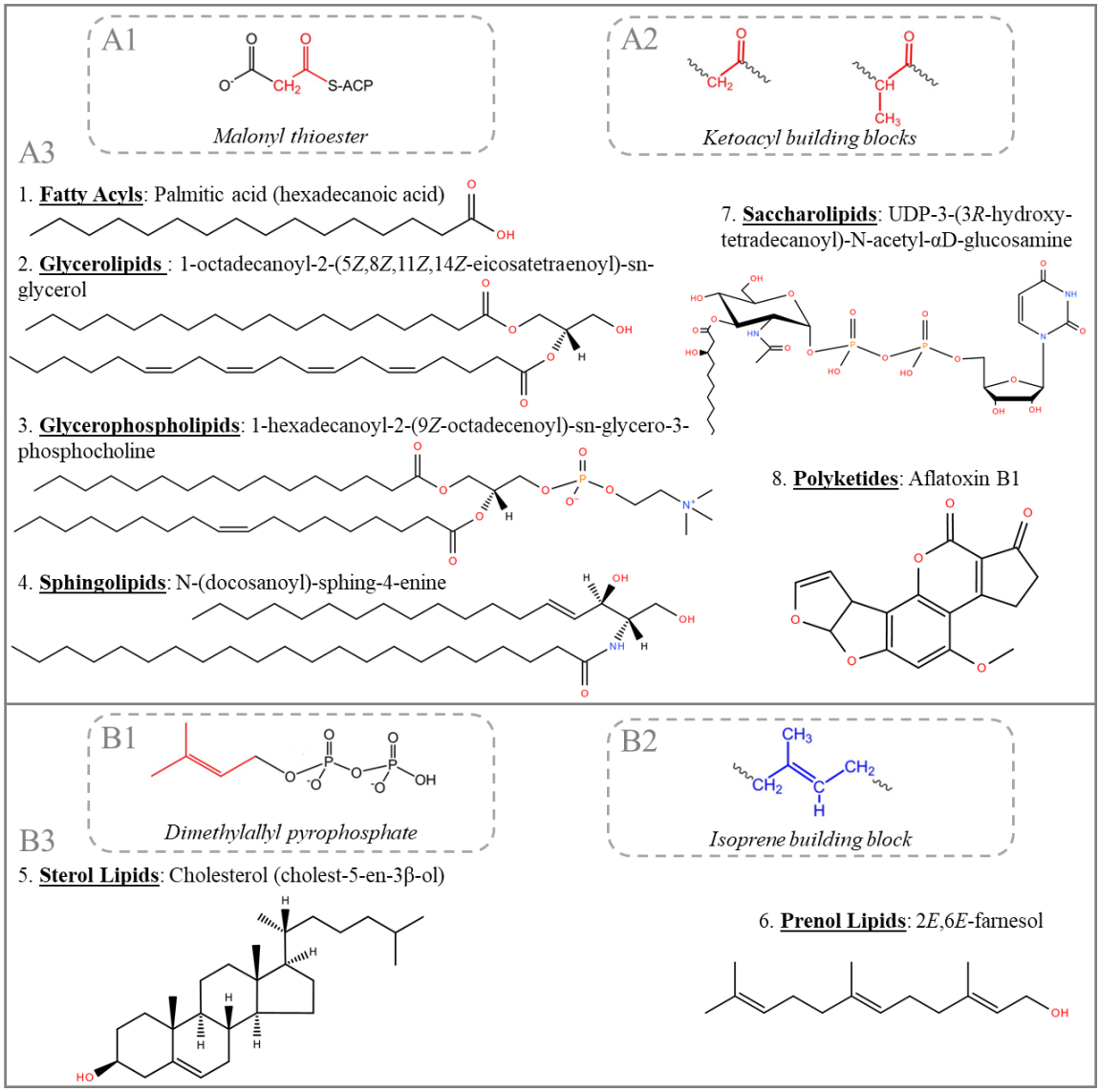

Figure 1*. Lipid categories according to LIPID MAPS (numbering of groups is kept as in the original source).* ***A1:*** *Malonyl thioester as the example of a thioester used in lipid biosynthesis,* ***A2****: acetyl and propionyl as the resulting building blocks,* ***A3****: examples of lipids belonging to 6 groups biosynthesised by condensations of ketoacyl thioesters.* ***B1****: Dimethylallyl pyrophosphate as an example of a isoprene unit in lipid biosynthesis,* ***B2****: isoprene as the resulting building block,* ***B3****: examples of lipids belonging to 2 groups biosynthesised by condensations of isoprene units.[3]*

1.1 Lipid short annotation

Each of 8 main lipid categories proposed by LIPID MAPS divides farther into lipid classes and subclasses. To simplify lipid reporting for large, comprehensive studies a short annotation of lipids has been proposed [4]. It contains a short few letter code holding the information about the head group, so about the class to which this lipid belongs and information about number of carbon atoms and double bonds in fatty acyl chains. Table 1

shows the letter code for lipids analysed in the studies described in this thesis, and it includes lipids from 5 main categories. Other lipid categories were not analysed in my studies.

Table 1. *Lipid classes and subclasses analysed in this research together with their short annotation and names.*

Main category in LIPID MAPS	**Class**		**Sub-class**	**Common name**
	Short annotation	Name in LIPID MAPS		
Fatty Acyls	FA	Fatty Acids	-	-
	ACar	Fatty acylcarnitines	-	Acylcarnitines
Glycerolipids	MG	Monoradylglycerolipids	-	Monoglycerides
	DG	Diradylglycerolipids	-	Diglycerides
	TG	Triradylglycerolipids	-	Triglycerides
Glycerophospholipids	PC	Glycerophosphocholines	LPC	Lysophosphatidylcholines
			PC	Phosphatidylcholines
			ePC	Etherphosphatidyl-cholines (O-PC or P-PC)
	PE	Glycerophospho-ethanolamines	LPE	Lysophosphatidyl-ethanolamines
			PE	Phosphatidyl-ethanolamines
			ePE	Etherphosphatidylethanol-amines (O-PE or P-PE)
	PI	Glycerophosphoinositols	LPI	Lysophosphatidylinositols
			PI	Phosphatidylinositols
	PS	Glycerophosphoserines	LPS	Lysophosphatidylserines
			PS	Phosphatidylserines
Sphingolipids	Cer	Ceramides	-	-
	Various	Glycosphingolipids	HexCer	Hexosylceramides
	SM	Sphingomyelins	-	-
Sterol Lipids	CE	Sterol esters	-	Cholesteryl esters

A cell lipidome describes all lipids contained in a cell. It consists of many isobaric lipids, which include (among others) positional isomers (e.g. the same fatty acyl chains, but connected opposite in the sn1 and sn2 positions), isomers with different positions of double bonds, geometric isomers with different *cis-trans* configuration and stereoisomers with different *R-S* configuration (Figure 2). These isobaric compounds often possess very similar physicochemical properties and are difficult to distinguish with the commonly used analytical methods for lipidomics. Incorrect annotation and lipid reporting could though cause erroneous biological interpretation of collected data. Conventional separation methods (see chapter 3 of this introduction) and detection techniques (see chapter 2 of this

introduction) cannot provide all structural information about each lipid in an analysed lipidome. Therefore, the aim of lipid researchers is to judge the level of structural details obtained with the used experimental method (so-called structural resolution) and to report the detected lipids accordingly, rather than to completely characterize every single lipid molecule. [6]

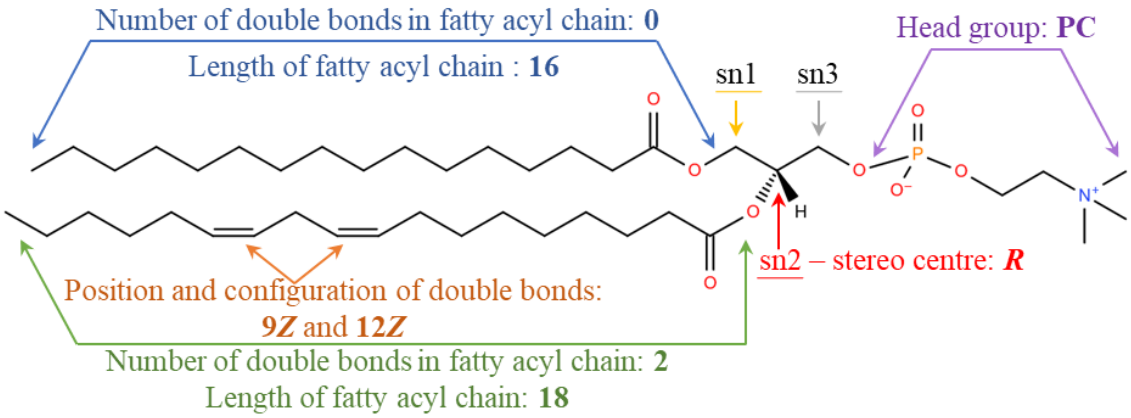

***Figure 2**. Structure of 1-hexadecanoyl-2-(9Z,12Z-octadecadienoyl)-sn-glycero-3-phosphocholine.*

***Table 2**. Different annotations of 1-hexadecanoyl-2-(9Z,12Z-octadecadienoyl)-sn-glycero-3-phosphocholine based on the different degree of structural resolution. The colours in annotations refer to the components shown in Figure 2. [6]*

Degree	Structural resolution	Annotation
1	Carbons and double bonds	**PC(34:2)**
2	Fatty acyl constituents	**PC(16:0_18:2)**
3	Positional isomers	**PC(16:0/18:2)**
4	Double bond position	**PC(16:0/18:2(9,12))**
5	Double bond *cis-trans*	**PC(16:0/18:2(9Z,12Z))**
6	Stereochemistry	**PC(16:0/18:2(9Z,12Z)[R])**

The most basic way of lipid annotation is to provide information of the lipid class together with the total number of carbon atoms and the total number of double bonds in the fatty acyl chains (Table 2, degree 1). This approach is common for classes, where fragmentation by mass spectrometry (MS) is related only to lipid head groups, e.g. sphingomyelins. When fragments associated to fatty acyls are observed, the fatty acyl chains should be indicated in the annotation (Table 2, degree 2). Without further biochemical analysis or biological assumptions this level is usually the limitation for conventional liquid chromatography coupled to tandem mass spectrometry (LC-MS/MS) analysis used in lipidomics. The

underscore sign '_' between fatty acyl chains in the annotation means that the positions in which the fatty acyl chains are connected to the glycerol backbone are not known. This is in opposition with the next degree of structural resolution (Table 2, degree 3) where these positions are defined and indicated with the slash sign '/'. The fatty acyl connected at sn1 position is written on the left, while sn2 on the right side. Degree 4 defines all positions of double bonds in the fatty acyl chains, and degree 5 shows its *cis-trans* configurations. With degree 6 all stereochemical centres in the molecule are defined with proper *R-S* annotation and the compound's structure is fully characterized.

The correct lipid annotation contains also information about linkages, i.e. types of bonds which connect fatty chain with the head group. No special indication means that an ester bond is present. Another common linkage is by an ether group and there are 2 different types of this connection. Letter 'P' in front of a chain indicates the vinyl linkage (C=C double bond directly neighbouring the oxygen in the ether connector) and letter 'O' shows a simple ether bond without neighbouring double bonds (Figure 3). This convention might cause some confusion, as positions of double bonds are not always easily defined with conventional analytical methods. In this work I used letter 'e' in front of a chain to indicate any type of an ether connection.

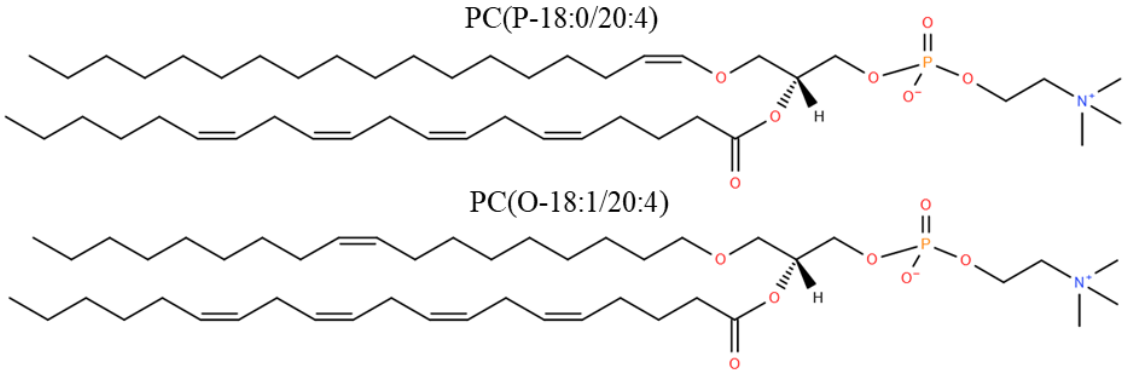

Figure 3. *Two ether phosphatidylcholines with a different ether linkage. The double bond included in the vinyl connector is not added to the total number of double bonds in the short annotation. In this work both phosphatidylcholines would be called PC(e18:1_20:4) to properly show the structural resolution.*

Sphingolipids do not have a glycerol backbone, but their annotation is similar to glycerolipids and glycerophospholipids. The first place in the short annotation (like sn1 for glycerophospholipids) is occupied by a sphingoid base – an aliphatic amino alcohol. The sphingoid base annotation includes one of 3 prefixes: 'm', which means a monohydroxy

base, ‘d’ that refers to a 1,3-dihydroxy base or ‘t’, which stands for a 1,3,4-trihydroxy base, whereas the total number of carbons and double bonds in the sphingoid base chain are shown in the same way as for other lipid groups. The most common sphingolipids in mammalian cells consist of 2-amino-1,3-diols, and are marked with the prefix ‘d’. Then the fatty acid which is linked by an amide bond to the amino alcohol is annotated similarly to the sn2 position of glycerophospholipids [7]. In case of glycosphingolipids the sugar moiety should be also defined in the annotation. The most common glycosphingolipids contain glucose; however, it is difficult to analytically distinguish it from other monosaccharides, e.g. galactose. That is why in this work glycosphingolipids are defined in the more general way as hexosylceramides (HexCer).

1.2 Oxylipins

Another distinctive, but also structurally various lipid group are oxylipins. They belong to fatty acyls and include subclasses like eicosanoids, docosanoids or octadecanoids. Oxylipins are oxidized polyunsaturated fatty acids (PUFAs), where other functionalities are introduced during the oxidation process e.g. hydroxyl or hydroperoxyl groups, epoxide or ketone moieties or many others. LIPID MAPS include already nearly 3,000 structures of oxylipins. Most of them are highly bioactive and they play numerous biological roles [8]. For many of them, however, the exact mechanisms of action or even their biological roles remain still unknown. Recognizing the biological functions of oxylipins is very challenging due to their short in vivo life span, and because of overlapping, interconnected or even opposite roles [9]. They are also important for regulation of platelet biochemistry, as they mediate intraplatelet signalling as autocrine (within cell signalling: an effect is caused to the same cell that a signalling agent comes from) and paracrine agents (cell-to-cell signalling: an effect is caused to a nearby cell to the one from which a signalling agent comes).

Most of the oxylipins are chemically unstable and they are metabolized quickly. Therefore they are not stored in cells, but synthetized de novo at the place of their action [10]. The enzymatic pathway of oxylipin synthesis includes the release of polyunsaturated fatty acids (PUFA) from membrane phospholipids. The main enzyme responsible for this role is cytosolic phospholipase A2 (PLA2), which cleaves phospholipids at the sn2 position.

Further on, released PUFAs are oxidized by proteins belonging to one of 3 families of enzymes: lipoxygenases (LOX), cyclooxygenases (COX) or cytochromes P450 (CYP450) [11]. LOX might have one of 3 forms: 5-, 12- and 15-LOX (the presence of the 12-LOX in platelets is confirmed, and the other are under debate [8]), COX is expressed in 2 forms: COX-1 and COX-2 (in platelets only the first type is present) and CYP450 is a large family of enzymes, but 2 most important for production of oxylipins are CYP2J and CYP2C [12]. The initially synthetized oxylipins might be further converted by other enzymes: e.g. soluble epoxide hydrolase (sEH) changes epoxides to dihydroxy compounds [13] or thromboxane-A synthase is necessary for production of thromboxane A2 (TXA2), one of the best described signalling molecules in platelet biochemistry [14].

Oxylipins can be also produced in non-enzymatic oxidation. In-vivo oxidative stress, caused by imbalance between antioxidants and free radicals, leads to non-specific oxidation of PUFA to oxylipins by reactive oxygen species (ROS). In-vitro autoxidation appears when PUFA are exposed to oxygen or other oxidants [15].

2. MS in lipid research

MS is a technique which creates, separates and detects ions in gas phase and records their *m/z* ratio. The first MS instruments in early 20th century were used to measure masses of atoms and therefore allowed researchers to discover the existence of isotopes. It took decades, however, until chemists started to use this technique to identify unknown compounds. McLafferty's work on MS fragmentation patterns and Biemann's research on identifying structures of peptides and alkaloids (50s and 60s of 20th century) introduced MS to the field of natural sciences. Further development of mass spectrometers, especially inventions of electrospray ionisation (ESI) and matrix-assisted laser desorption/ionisation (MALDI) techniques, which both happened nearly simultaneously in 1988, resulted that MS has become the gold-standard detection method in proteomics, metabolomics and lipidomics, where complex biological samples are analysed and thousands of compounds can be detected in a single run [16].

2.1 Types of MS used in lipid research

Every MS consists of 3 main parts, which are: ion source, mass analyser and detector. Some MS are also equipped with a collision cell, where ions are fragmented, so that additional information about compound structure can be obtained.

2.2 ESI ion source

The ion source is a device, which creates ions in gas phase. The most commonly used sources in lipid research are ESI and atmospheric pressure chemical ionisation (APCI), both of them operate under atmospheric pressure, which allows their easy coupling to LC. Another common technique is MALDI, which is predominantly used in MS imaging.

In this thesis solely ESI was used as ion source. In ESI, a sample is introduced to the MS as a solution and directed towards the source through a narrow needle (Figure 4A). A high potential is applied to the needle and it causes the formation of an electrostatic field. In this field the solution coming out from the needle is polarized and forms a Taylor cone (Figure 4B, point 1). Multiply charged droplets are torn out from the cone and create a spray. The spray formation may be supported additionally by a gas flow (nebulizer gas). Further on, the solvent is evaporated from the droplets (Figure 4B, point 2), which is controlled by high temperature produced in heaters and by the heater gas, which distributes the heat over the ion source. The charged droplets get smaller in size due to the solvent evaporation and their surface charge density increases until the moment they reach the Rayleigh limit (Figure 4B, point 3) – at this point the surface tension does not compensate anymore for Coulombic repulsion forces and the droplets explode into several smaller droplets with lower surface charge density. This phenomenon is called Coulombic explosion (Figure 4B, point 4). These processes repeat until all the solvent is evaporated and gas phase analyte ions are formed (Figure 4B, point 5). The ions are then guided to the mass analyser through openings of cones, which are called for AB Sciex instruments curtain plate and orifice [17]. The orifice plays several roles in the ESI source. Additional voltage called declustering potential is applied to its surface, which helps to destroy remaining solvent-analyte clusters before they enter the mass analyser. The orifice creates also a barrier between atmospheric pressure in the ESI source and vacuum in other parts of MS.

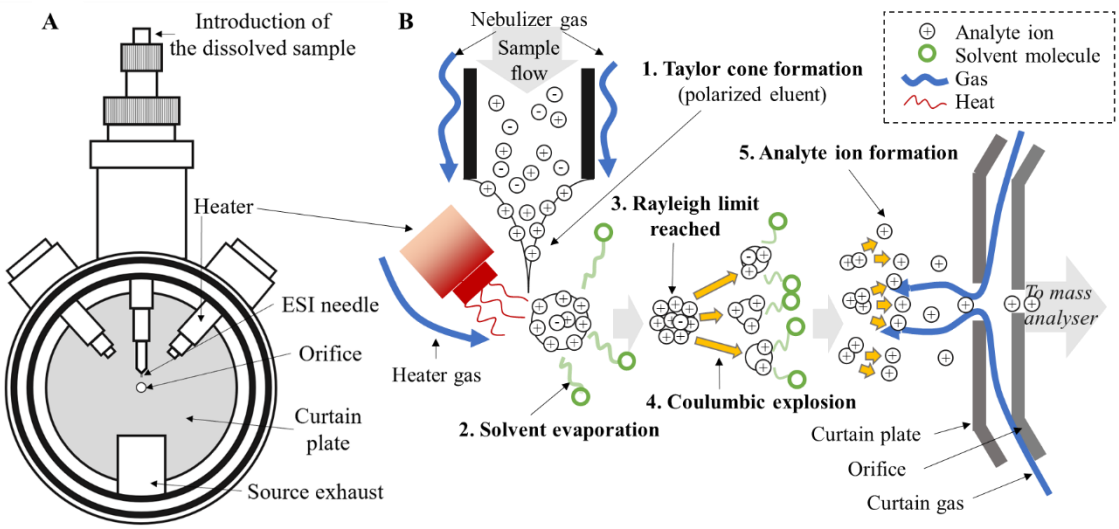

Figure 4. A: *Components of ESI.* ***B:*** *Scheme of the working principle of ESI [17].* ***A*** *and* ***B*** *based on AB Sciex instrumentation.*

To prevent contamination in form of non-ionised molecules, which could enter the mass analyser, the exit of the ESI needle and the opening in the orifice are positioned orthogonally to each other (Figure 4A and B). In this way only charged ions, which are attracted by counter potential in mass analyser, find the way through the orifice. Additionally, a counter flow of curtain gas blows out non-ionised substances (Figure 4B). The ESI source is connected to a supply of dry gas (usually N_2 or synthetic air), which is later divided into nebulizer gas, heater gas and curtain gas flows.

ESI is a soft ionisation method and it is a suitable method for lipid ionisation, as even neutral lipids can form adducts with small cations or anions with this technique and hence can be detected. Therefore, nearly all non-volatile lipids can be ionised without significant in-source fragmentation [18]. In ESI usually pseudo-molecular ions are created: $[M+H]^+$ in positive mode and $[M-H]^-$ in negative mode. However, depending on nature of the analyte and the additives used in the mobile phase, other adducts can also be formed, for example $[M+NH_4]^+$ or $[M+HCOO]^-$. Table 3 shows typical adducts created by different lipid classes when ammonium formate is added to the mobile phase. Most of the lipids form single-charged ions in ESI, however, large molecules, like cardiolipins can also create multiple charged ions [19].

ESI sensitivity, differently to most other sources, depends on concentration rather than on the total amount of an analyte. That is why increased sensitivity is achieved, when injecting a larger volume of sample into ESI (but only when this sample is pre-concentrated in the chromatographic system before it enters the ESI source) while keeping the flow rate constant, but also when keeping the injection volume the same while reducing the flow rate. The reduction of flow rate also reduces the amount of buffer, salts and contamination introduced to the source, and provides easier and faster fine droplet formation. Based on this principle modern modifications of ESI ionisation technique have been invented: µESI and nano-ESI, which are characterized by exceptionally high sensitivity [20, 21]. However, to achieve satisfying results with these methods a proper capillary LC column and narrow ESI needle need to be utilized.

Table 3. *Selection of adducts for precursor ions depending on lipid class in ESI ionisation with ammonium formate used in the mobile phase.*

C	Positive mode	Negative mode
FA	not ionised	$[M-H]^-$
LPC	$[M+H]^+$	$[M+HCOO]^-$
PC	$[M+H]^+$	$[M+HCOO]^-$
ePC	$[M+H]^+$	$[M+HCOO]^-$
LPE	$[M+H]^+$	$[M-H]^-$
PE	$[M+H]^+$	$[M-H]^-$
ePE	$[M+H]^+$	$[M-H]^-$
LPI	$[M+H]^+$	$[M-H]^-$
PI	$[M+NH_4]^+$	$[M-H]^-$
LPS	$[M+H]^+$	$[M-H]^-$
PS	$[M+H]^+$	$[M-H]^-$
MG	$[M+H]^+$	not ionised
DG	$[M+NH_4]^+$	$[M+HCOO]^-$
TG	$[M+NH_4]^+$	not ionised
ACar	$[M+H]^+$	$[M+HCOO]^-$
Cer	$[M+H]^+$	$[M+HCOO]^-$
HexCer	$[M+H]^+$	$[M+HCOO]^-$
SM	$[M+H]^+$	$[M+HCOO]^-$
CE	$[M+NH_4]^+$	not ionised
oxylipins	not ionised	$[M-H]^-$
cholesterol	$[M-H_2O+H]^+$	not ionised
sphingoid bases	$[M+H]^+$	not ionised

The ESI ionisation might suffer from serious matrix effects, when complex, biological samples are introduced to the source. The matrix effect is a change in an analyte signal in presence of co-eluting components of a matrix. The change might be observed as an increase in the response (comparing to a standard solution of the analyte in a pure solvent), and then it is called ion enhancement. However, most of the time the signal intensity gets lower due to the matrix effect and then it is called ion suppression [22].

2.3 Mass analysers

Nowadays a researcher can choose between several types of mass analysers used in commercially available MS. The choice is made based on the nature of analysis and purpose of study. Various mass analysers differ significantly in their working principles and construction, and therefore they show very different performance. There are 5 main parameters which characterize the analytical performance of a mass analyser [18, 19, 23, 24].

Mass resolving power also called resolution explains how well ions with different *m/z* are separated from each other. Its value is usually reported as full width at half maximum (FWHM), and its mathematical explanation is the ratio of *m/z* of an ion to its peak width (measured at half of the peak height). The smaller FWHM is, the better separation of ions with different *m/z* is achieved by the mass analyser.

Mass accuracy refers to the measurement error – the difference of true (theoretical) and measured *m/z* values. It is usually reported as parts per million (ppm). In practice, instruments with better resolving power give results with higher mass accuracy and therefore allow researcher to easier find the elemental composition of an analyte and faster identify its structure. Mass accuracy depends also on stability and quality of instrument calibration.

Another important parameter, especially when macromolecules are analysed, is the mass range. It refers to the highest *m/z* value that can be detected by a mass analyser.

Linear dynamic range describes the range, within which the signal of an ion is directly proportional to the concentration of the analyte. It is important for purpose of absolute and relative quantification.

Spectrum acquisition speed refers to the time needed to acquire a complete scan of *m/z* spectrum from the moment ions are generated to their detection. Usually the time needed to produce ions in the source is orders of magnitude lower than the time they travel through the mass analyser. Therefore the acquisition speed mostly depends on the operation mode for static-field mass analysers, e.g. time-of-flight (TOF) and Fourier-transform ion cyclotron resonance (FT-ICR), or on scanning speed for dynamic-field mass analysers, e.g. quadrupole (Q) and linear ion trap (LIT). Spectrum acquisition speed is usually reported as frequency and its unit is Hz.

The main types of analysers used in lipid research are quadrupole, LIT, TOF, orbitrap and FT-ICR. They are all available commercially from different manufactures and their exact parameters will differ depending on specifications. Table 4 compares typical parameters of different mass analysers.

Table 4. *Overview of typical analytical characteristics of different mass analysers* [18, 23, 24].

Type of mass analyser	**Resolving power***	**Mass accuracy*** [ppm]	**Upper limit for *m/z* range** [*m/z*]	**Acquisition speed** [Hz]	**Linear dynamic range**
Quadrupole	1,000	100 – 1,000	4,000	10 – 20	10^5
LIT	10,000	50 – 100	2,000	10 – 30	$10^2 – 10^5$
Orbitrap	150,000	1 – 5	6,000	10 – 40	$10^2 – 10^5$
FT-ICR	1,000,000	0.1 – 1	10,000	0.5 – 2	$10^3 – 10^4$
TOF	40,000	2 – 50	unlimited	10 – 100	10^4

* at *m/z* 1,000

Nowadays, hybrid MS, which combine two or more mass analysers in one instrument, are frequently used. In lipid research triple quadrupoles (QqQ) or QTraps (combined quadrupoles and linear ion traps) are commonly utilized for quantitative studies, whereas QTOF (combined quadrupoles and TOF) and Orbitraps combined with linear ion traps are generally used in untargeted analysis.

In the presented studies 3 different MS instruments were used: QqQ AB SCIEX API 4000, QTrap Sciex 4500 and QTOF Sciex 5600^{+} (all: AB SCIEX, Ontario, Canada). The next paragraphs will explain working principles of mass analysers used in these instruments.

2.3.1 Quadrupole and LIT

Quadrupole mass analyser is built of 4 hyperbolic or circular shaped rods (Figure 5A). Direct current (DC) potential of the same polarity is applied to opposite rods. Additionally to DC an alternating current voltage at radio frequency (RF) is superimposed to the rods. Combine DC and RF define ion trajectories. Ions with stable trajectories pass the mass analyser, while those with unstable trajectories are neutralised by hitting a quadrupole rod.

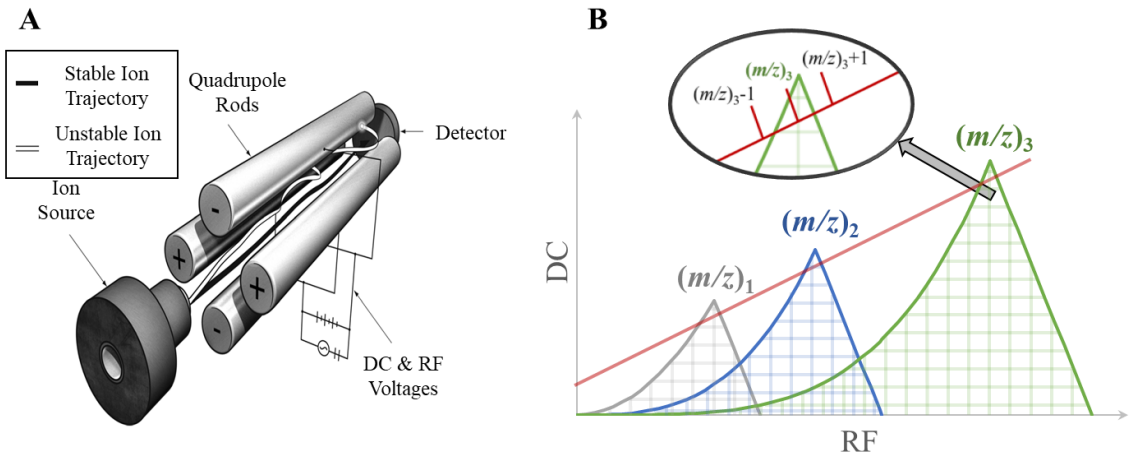

***Figure 5. A**: Basic components of a quadrupole* [23]. ***B:** Stability diagrams for $(m/z)_1$, $(m/z)_2$ and $(m/z)_3$, where $(m/z)_1 < (m/z)_2 < (m/z)_3$* [25, 26].

Mathieu's differential equation describes mathematically how ions travel in the electromagnetic field of a quadrupole. Its result can be visualised by stability diagrams (Figure 5B) [26]. Each ion shows a stability area (gridded), which is a combination of RF and DC voltages which provide this ion with a stable trajectory. Ions with higher *m/z* show larger stability area due to their slower reaction to variations in the electromagnetic field. To change the *m/z* which can pass the quadrupole, constant ratio of RF and DC is used, but their magnitude is changed (red line in Figure 5B). Quadrupole resolution might be modulated by adjusting the scanning line, however, higher resolution often causes loss in signal intensity. By setting DC to 0 (so the ratio of DC and RF also to 0), resolution of quadrupole is reduced to 0 and the quadrupole is passed by all ions [17].

A quadrupole mass analyser can be used in 3 different modes. Full-scan mode changes DC and RF with preserving their constant ratio along a scanning line, as shown with red line in Figure 5B. In this mode, ions with different *m/z* within a given range are passing the quadrupole one by one and their abundance is recorded. Selected-ion monitoring (SIM) mode allows only one selected *m/z* to cross the quadrupole. In this mode the quadrupole serves as a mass filter. Exceptional sensitivity might be reached with SIM as all the ions of the selected kind reach a detector. Open (transmission) mode (also called RF-only mode) reduces DC potential to 0 and supports all ions to pass through. Here the quadrupole is a device to transport and focus ions with different *m/z*.

In the open mode, the quadrupole can be also changed into a collision cell. Ions travelling through a quadrupole in an 'open mode' are accelerated by the electric field and collide with neutral gas (e.g. N_2). Kinetic energy of ions is converted into internal energy and causes breakage of covalent bonds and ion fragmentation. This process is called collision-induced dissociation (CID). The degree of fragmentation depends strongly on kinetic energy of travelling ions, which might be modulated by introducing additional potential called collision energy [27].

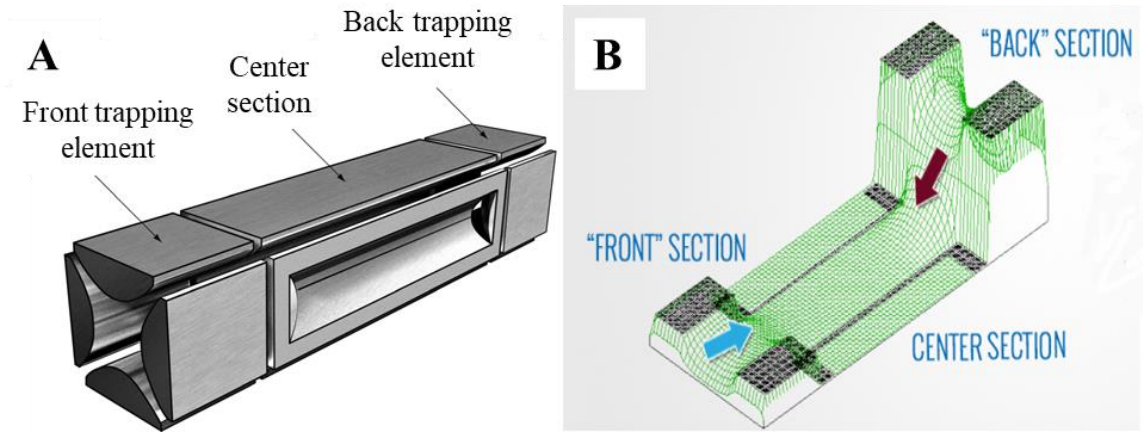

Figure 6. A: *Basic components of LIT* [23]. ***B****: Electric field along the long axis of LIT [28].*

In LIT, similarly to quadrupoles, an ion trajectory is defined by changing DC and RF potentials. LIT is able not only to guide ions through, but also to trap them in 3 dimensions. The trapping is done by combined DC and RF fields: two-dimensional RF voltage is applied to rods of LIT and it traps ions radially (along the rods), while DC voltage applied

to the back trapping element (Figure 6A) reflects ions back to the central section and therefore traps them axially.

Figure 6B shows the trapping electric field inside the LIT along the trap's long axis. The blue arrow indicates that ions enter LIT with low kinetic energy and they are slightly accelerated to the centre section of the analyser, until they approach the back section with high potential of the same polarity as the analysed ions. This potential reflects ions back towards the centre section (red arrow). Ions lose their kinetic energy when they traverse the trap, so they are not able to overcome the potential of the front barrier of LIT.

Trapped ion can be then excited by additional low amplitude RF voltage applied between opposite rods. If the frequency of this additional RF matches ion's frequency of motion (which is dependent on *m/z*), this ion will pick up energy. The gained energy allows the ion to cross the DC potential barrier applied to the back trapping element – the ion is ejected from the trap and moves to a detector. In another operating mode the gained energy can be converted into ion's internal energy and cause its fragmentation inside LIT [29].

2.3.2 TOF

The working principle of TOF analysers is to accelerate ions by an electric field and provide all ions with the identical kinetic energy. The kinetic energy depends on mass and velocity, so when different ions obtain the same portion of the kinetic energy, those which have lower *m/z* travel faster compared to ions with higher *m/z*. Ions with different *m/z* are separated inside the TOF analyser and the time they need to cross it is recorded with high precision, which results in the high mass resolving power of TOF analysers.

Ions entering TOF are accelerated by potential and they travel through the drift region (Figure 7A), which is a potential free region. The time, which ions need to cross the drift region and arrive to a detector depends on their *m/z*, but also on the length of the drift region and on the potential applied to the ions in the acceleration unit. These parameters are known and in the theory the same for all the ions during the analysis time, however, they might be affected by changes in temperature (the drift region length) and the power supply output (the potential). To compensate for possible fluctuations in the laboratory temperature where

TOF is located, this analyser should be frequently calibrated (e.g. once an hour, when for comparison the calibration of a quadrupole is necessary once in 6 – 12 months) [30].

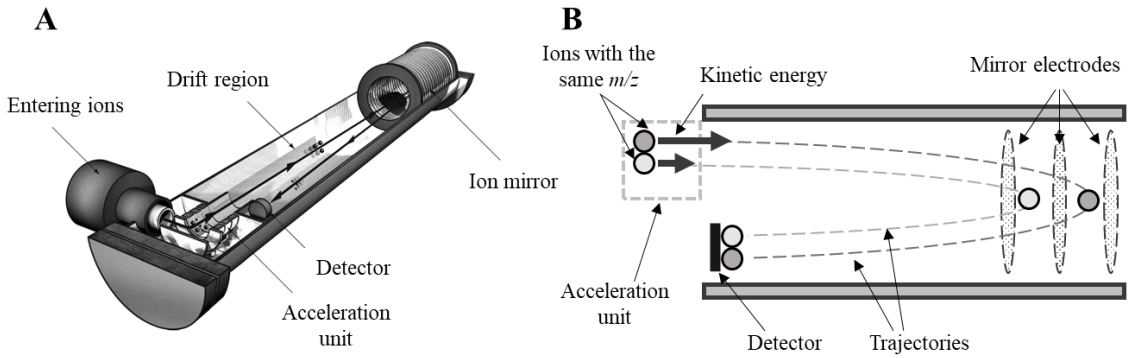

Figure 7. A: *Basic components of TOF* [23]. ***B****: Schematic working principle of an ion mirror* [17].

To equip TOF with extraordinary resolution, the analyser needs to compensate for the spatial and velocity spread of ions with the equal *m/z*. This is provided in 3 steps: by the orthogonal ion acceleration, the delayed pulsed extraction and by using an ion mirror [19, 23, 25].

TOF analysers work in pulses, which means that a portion of ions is collected in the acceleration unit and then accelerated together towards the drift region (Figure 7A). This way avoids the situation that ions with different *m/z*, which travel with different speed, but entered the analyser at a different time, arrive to a detector together. The ions are accelerated orthogonally to the direction they enter TOF and the ions which have longer way to the detector, are actually located in the acceleration unit closer to the pulse source, and therefore they experience slightly stronger acceleration (this technique is called delayed pulsed extraction). Later on in the drift region these ions join the ions with the same *m/z*, which obtained little lower acceleration during the pulse.

Modern TOFs are V-shaped and have an ion mirror, which is a series of electrodes that create electric field to reflect ions (Figure 7B). Ion mirrors unify arrival time to the detector of ions with the same *m/z*, but with slightly different kinetic energies. Ions with higher kinetic energy penetrate the mirror deeper and have longer trajectories compared to the ions with the identical *m/z*, but a lower kinetic energy.

2.4 Detectors

Detector systems convert ions into a signal, which can be interpreted and stored by computers. The most widely used detector in MS is the electron multiplayer. Single ions, which reach the detector, create only a very low current, so in order to achieve a good instrument sensitivity, this signal needs to be multiplied. In the first step of detection, ions coming from the mass analyser are accelerated by a high counter potential. They strike the detector surface and release several secondary particles. In case of negative mode analysis, the secondary particles are positive ions, and in case of positive mode analysis the created particles are electrons. This starts the cascade of impacts, as secondary particles (both: positive ions or electrons) collide again with the surface and release additional electrons. The cascade continues and multipliers typically enrich the signal 10^6 times. The electron current can be then easily measured.

The QqQ and QTrap instruments from Sciex, which have been used in my research, are equipped with continuous electron multiplier (CEM). This type of multiplier is a curved tube with good secondary emission properties. The released electrons travel through the tube hitting its wall and releasing more and more electrons (Figure 8A). At the exit of the tube the multiplied current is measured [20, 31].

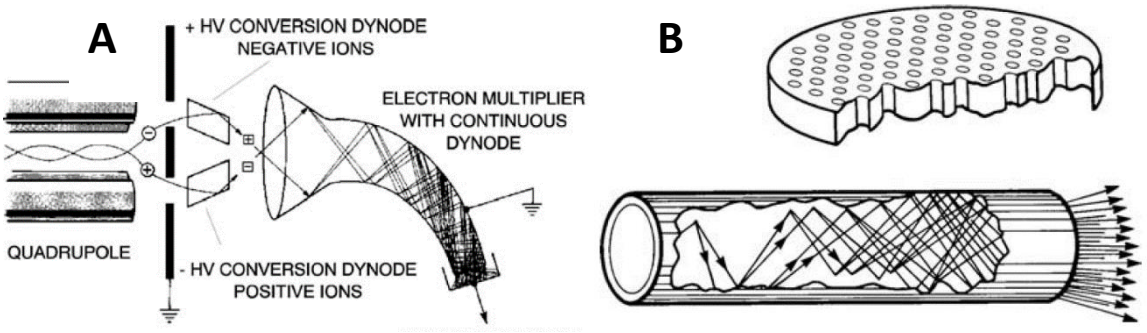

***Figure 8. A**: CEM used in QqQ and QTrap. **B**: MCP used in QTOF. Lines show movement and multiplication of electrons [20].*

TOF analysers require detectors, which are able to very precisely determine ion arrival time. Microchannel plate (MCP) is the type of electron multiplier, which is typically used with this analyser (it is also installed in QTOF instrument from AB Sciex). MCP is a small plate with parallel channels drilled through it (Figure 8B, top). Inside each channel electrons are multiplied similarly to CEM (Figure 8B, bottom). Ions with different *m/z*

reach the plate at different spots and enter different channels. At the end of each channel the electron current is measured, simultaneously and separately for all the channels. This type of multiplier is very fast, because of the short electron path and large detection area. Another advantage of MCP is its ability to simultaneously measure ions with different *m/z*. The drawback of this detector is its fragility and high price [19, 20, 31, 32].

The final step of ion detection is the conversion of electron current signal into computer data. This part is done by a converter. QqQ and QTrap use traditional analogue-to-digital converter (ADC). This type of converter has wide linear dynamic range [20].

The Sciex QTOF instrument is equipped with time-to-digital converter (TDC), which operate in pulse mode. The signal from the multiplier is forwarded to the discriminator and if it reaches a certain threshold its signal is received by TDC. This detector is a time counting device, and if several ions of the same *m/z* reach the detector at the same time, they will be counted as only one ion. The counting dead time of TDC is in the range of several nanoseconds, when the detector cannot register another ion. This is why TDC easily gets saturated and show poor linear dynamic range. To overcome this problem multiple TDC converters with equal probability to receive a signal from an ion are installed (multi-channelling). Another approach to extend linear dynamic range of this detector is by using ion transmission control (ITC). Here, lenses are installed before the mass analyser, which reduce ion load, if the signal gets too high. The QTOF instrument from AB Sciex has 4 TDC channels and is equipped with the ITC system [20, 32].

3. Separation techniques used in lipidomics

Lipids can be analysed by direct injection of their extract to the MS instrument or by separation of species prior to the MS detection [33]. The first approach is called direct infusion or shotgun analysis. The main advantages of shotgun lipidomics are high sample throughput [34] and straightforward compound normalization with an internal standard (IS) [35]. On the other hand, this analytical technique might suffer from a significant matrix effect when a complex biological sample is injected, and what is more, isobaric compounds with similar fragmentation pattern cannot be distinguished by this method [36].

To avoid the mentioned pitfalls many researchers decide to simplify sample complexity by separation of lipids prior to detection. Separation techniques use differences in physicochemical properties e.g. molecule sizes or surface area, hydrophilicity, pKa, etc. to separate different compounds in space. Separation acts also as a pre-concentration step and focuses compounds before entering to MS, which eases their detection. What is more, some isobaric compounds might be separated with well-chosen separation techniques and therefore they can be individually analysed with MS detectors.

Several types of separation techniques are used in lipidomics, most commonly chromatography. Gas chromatography (GC) was one of the first techniques that coupled chromatography with MS detection [37]. GC-MS analysis requires analytes that are thermally stable and volatile, which is not the case for many lipids [38]. Therefore, lipids need to be derivatized prior to the GC-MS analysis in order to increase their volatility and minimize adsorption effects on a GC column. The most common approach to remove polar functionalities of lipid molecules is by methylation of FA and transesterification of more complex lipids. These reactions result in transforming all lipids into fatty acid methyl esters (FAME), which are volatile. The final result of the GC-MS analysis is qualitative and quantitative information about all fatty acyl chains included in all lipids from a sample [39].

Fiehn and Cajka conducted studies in 2014, which compared analytical techniques used in lipid research by different groups. The studies revealed that the most common chromatographic technique was reversed-phase liquid chromatography (RPLC) followed by normal phase liquid chromatography (NPLC) and hydrophilic interaction liquid chromatography (HILIC) (Figure 9). A less common method was supercritical fluid chromatography (SFC) [40]. All these techniques are described in more details in the next chapters of this introduction.

Non-chromatographic methods for lipid separation include capillary electrophoresis and recently introduced ion mobility spectrometry (IMS) [41]. IMS is a gas-phase electrophoretic method, where ionised analytes are separated in a pressurized chamber filled with buffered gas (e.g. nitrogen). Ions collide to the gas in the chamber and different ions separate, because they need different time (called drift time) to cross the chamber to a detector. The drift time is related to ion size, shape and charge [42]. IMS can often differentiate between structural isomers and conformers [43]. The separation by IMS

occurs in the millisecond scale, which makes it suitable as an additional dimension to the LC-MS analysis [42].

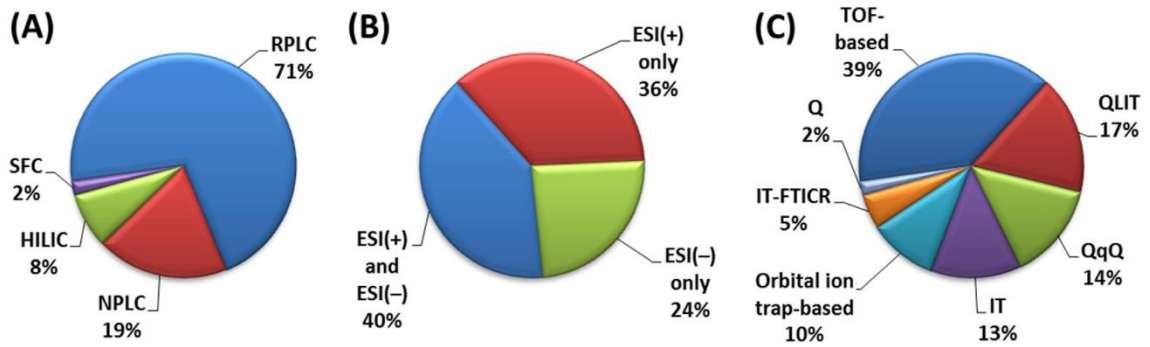

Figure 9. *Frequency of usage of **A**: different chromatographic systems, **B**: various MS ionisation modes and **C**: mass analyser types in publications based on LC-MS lipidomics research [40]. IT – ion trap.*

3.1 RPLC

In RPLC nonpolar stationary phase consists of silica particles functionalized with hydrophobic ligands. There is a number of ligands to choose from, with C18 alkyl chain being the most often used. Other common options are C8 and C30 chains as well as phenyl and cyano derivatives [44]. Mobile phases used in RPLC are polar mixtures of water and water miscible organic solvent e.g. acetonitrile (ACN), methanol (MeOH) or isopropanol (IPA). Lipids elute from an RPLC column in order of increasing hydrophobicity.

The widely accepted retention mechanism for RPLC is the so called hydrophobic effect, which is an entropy driven process [45]. The lipid extract is injected into the column, which contains a relatively water-rich mobile phase. The high entropy of such a system comes mostly from the mobility of the water molecules and the highly dynamic hydrogen bonds [46]. Nonpolar fatty acyl chains of lipids restrict the water movement and, hence to keep the entropy of the entire chromatographic system high, they are ‘pushed away’ and partitioned into the stationary phase. The minor driving force for RPLC retention is the London dispersive interactions between chains of stationary phase ligands and lipid molecules [47]. The higher organic solvent content in the mobile phase, the higher the lipid partitioning into the mobile phase is. This results in release of analytes from the stationary phase, their elution from the column and final detection.

The retention time of a lipid in RPLC depends on the length of the fatty acyl chains, the number of double bonds and their polar head. The longer the fatty acyls are, the more hydrophobic the molecule is, and the longer the retention time is. Double bonds on the contrary increase the polarity of the molecule as they contain π electrons, which increase the dipole moment of the compound [44]. This shows that the dipole-dipole and dipole-induced-dipole interactions are also important in the RPLC retention mechanism [47]. Double bonds in a molecule cause decrease in its retention time. Lipid species with different head group, so belonging to different classes might co-elute with RPLC, but lipids within once class separate in a very characteristic order according to their number of carbon atoms and double bonds (Figure 10) [48]. Because of this phenomenon the retention time of lipid species can be used as additional criteria for lipid identification.

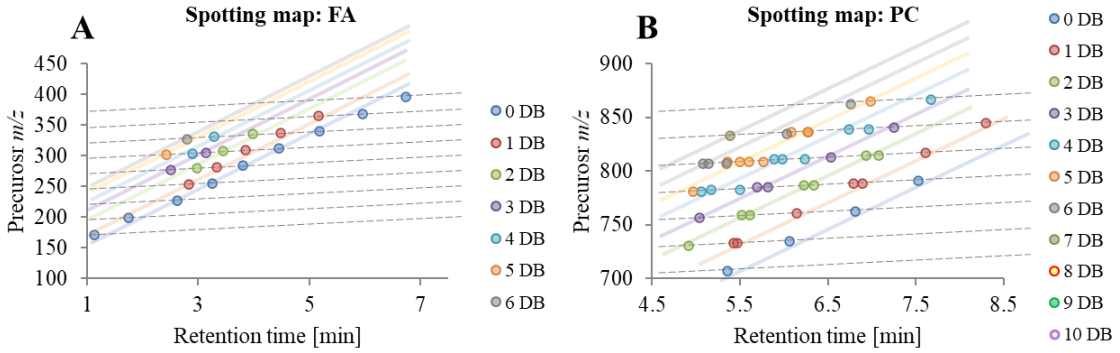

***Figure 10**. Spotting maps of **A**: fatty acids and **B**: phosphatidylcholines showing the relation of elution order of lipids within one class with RPLC to their precursor m/z. Dots with the same colour show lipids with equal number of double bonds (DB).*

Lipid separation with RPLC can be optimized by choosing a proper column (column dimensions as well as the packing material are important). Nowadays, ultra-high performance liquid chromatography (UHPLC) columns with fully porous sub-2 µm particles are preferred, because they provide highly effective separation [49]. Another commonly used packing material is solid core silica particles. It shows similar separation efficiency to the fully porous silica even for higher particle diameter and at the same time it provides lower backpressure [50]. Another often preferential feature of a column for lipidomics is silica end-capping, which removes or restricts access to residual silanol groups and therefore minimalizes hydrophilicity of the stationary phase [51].

Once the column is chosen the mobile phase needs to be optimized. This includes solvent components and gradient profile or isocratic parameters. Mobile phase components are

water and organic solvent, which for lipids is very often IPA or its mixture with ACN. IPA provides good elution of highly nonpolar lipids like triglycerides (TG) and cholesteryl esters (CE). Additives to mobile phase include formic or acetic acids or their ammonium salts. Different additives are often used as a mixture, usually in low concentration up to 10 mM for salts and up to 0.2% for acids. These additives improve LC separation, and also increase ionisation in the MS source [52].

Main drawbacks of RPLC for lipid analysis are the poor solubility of analytes in water-rich solvents and the lack of coelution of analytes and IS. Lipid extracts are poorly soluble in highly aqueous solvents, which are often the starting conditions for gradient elution [53]. In the result lipids are injected as a solution in organic solvent, which causes mismatch to the LC conditions and which might influence peak shape, especially for polar, early eluting lipids [54]. The other drawback is chromatographic separation of lipids and an IS used for their normalization. In lipidomics it is not possible to add IS for each of hundreds lipid species detected. The common strategy is to use one IS per lipid class [55]. However, difference in retention of IS and the analyte means that the mobile phase composition at MS source is different, which influences ionisation efficiency. What is more, the matrix effect is different for these substances. This might result in inadequate normalization and incorrect lipid quantification [56].

3.2 NPLC, HILIC and SFC

NPLC, HILIC and SFC show many similarities when used in the lipid analysis. All of them separate lipids according to their polarity with hydrophobic compounds being eluted earlier and polar analyte later from the chromatographic system. The separation is performed according to polar head group and all lipids from the same class elute closely together (also IS) [40]. All 3 techniques utilize polar stationary phases and bare silica is the most commonly used for all of them. Other stationary phases include various silica modifications, like polyvinyl alcohol or dihydroxypropyl and many other [44].

The difference between these methods is in the mobile phase, which results also in different retention mechanism. NPLC uses highly nonpolar solvents (e.g. heptane or hexane) often mixed with relatively more polar liquids like IPA, ethyl acetate or chloroform. Retention

of lipids in NPLC is driven mainly by adsorption of analytes (their polar groups) on the stationary phase. Nonpolar fatty acyl chains play only minor role in the retention process (or none at all) [57].

Elution of analytes in NPLC is performed by replacement of adsorbed molecules by increased proportion of relatively polar solvent (e.g. IPA) in the mobile phase. Polar solvents might bind very strongly to the stationary phase, which results in long equilibration time between runs [44]. Another disadvantage of NPLC is the mismatch of the mobile phase with MS ionisation source. Organic solvents used in NPLC are incapable of accepting or donating protons to analytes, so the ionisation is highly suppressed. Furthermore, these solvents show low conductivity and do not support a stable spray for ESI ionisation. To overcome these problems post column mixing with protic solvents is used [58].

Because of the mentioned limitation of NPLC, HILIC separation is gaining more and more popularity in lipid research. The mobile phase in HILIC consists of water (at least 2.5%) and high amount of water-miscible organic solvent, usually ACN. Water molecules interact strongly with the polar stationary phase and create a stagnant water-rich layer on its surface. The composition of this layer is different to the bulk 'water-deficient' mobile phase and analytes partition between these 2 solvents [59]. Lipids, which partitioned into the polar layer, can further interact with the stationary phase by dipole-based or electrostatic forces. This leads to separation of analytes based on their polarity and charge [60]. HILIC mobile phase is easily combined with the ESI MS source and it shows even better ionisation efficiency compared to RPLC, due to high amount of ACN in the mobile phase [61]. The pitfall of HILIC is its disability to retain highly nonpolar lipids like TG and CE.

SFC techniques use CO_2 at high temperature and high pressure, to keep it under the supercritical state or close to it. The polarity of CO_2 is comparable with hexane, but it is fully miscible with polar organic solvents, especially with MeOH, which is a commonly used modifier for changing polarity of the mobile phase in SFC [62]. The mobile phase under the SFC conditions shows very high diffusivity and very low viscosity, when compared to any LC solvents. This causes that the equilibrium of the analyte partition between the stationary and mobile phases is reached very quickly even at high flow rates. As a result SFC can be used for fast and efficient lipid separation. It can retain apolar lipids

like TG and CE, which are eluted in the beginning of a chromatogram and are followed by more polar lipids. SFC can be easily coupled to MS [63]. The drawback of this method is the need of special chromatographic instruments able to pump liquid CO_2 and equipped in the back pressure regulator (BPR), which keeps the whole system under high pressure [64].

3.3 Other LC techniques

Other separation techniques used in lipid research are utilized for very specific purposes rather than for general lipid profiling. The most common are chiral chromatography and silver ion chromatography.

The first one applies chromatographic columns with chiral stationary phases to separate enantiomers. Modern chiral columns are compatible with wide variety of solvents including water-rich solvents easily applied for MS detection [65]. Chiral separation is most commonly used for oxylipin analysis, as these compounds gain additional stereoisomeric centres at carbon atoms connected to heteroatoms introduced in the process of FA oxidation [66]. The result of chiral analysis of oxylipins might reveal their origin. While pure enantiomers are produced enzymatically, racemic mixtures indicate accidental autoxidation during sample preparation or oxidative stress by ROS in a cell [67].

Silver ion chromatography is used to separate lipids with different number and configuration of double bonds. This technique utilizes the stationary phase, in which silica is derivatized with phenylsulfonic acid ligands and these are linked by ionic bonds to Ag^+ ions [68]. During chromatographic separation silver ions create weak reversible complexes with π-orbitals of double bonds. Compounds with more double bonds retain stronger on the column than analytes with fewer double bonds. A lesser effect to retention is caused by the distance between double bonds and their *cis-trans* configuration [69]. Silver ion chromatography can be used for separation of free fatty acids, FAME as well as more complex lipid classes [70]. It uses highly nonpolar solvents as mobile phase similarly to NPLC and therefore is not easily coupled to the MS detector.

4. MS analytical strategies

MS detection is nowadays a method of choice for lipid analysis. The commonly used hybrid MS instruments in lipid research, QqQ, QTrap, QTOF and orbitrap acquire data in cycles [29, 32, 71]. The cycle time, which is the time required to perform all MS and MS/MS experiments of an MS measurement cycle, is an important parameter for detection sensitivity – if it is too short, the signal of an analyte will not be distinguishable from noise [72]. Shotgun analysis do not highly restrict the cycle time, but the situation is different for LC-MS. Analytes elute from the LC system as 'chromatographic peaks' with certain width, which represents time, when an analyte can be detected. If the cycle time is too long it might be unsuitable for the LC method, as chromatographic peaks might be poorly defined or an analyte can even pass MS undetected (Figure 11). A rule of thumb says that there should be minimum 8 points per chromatographic peak for analyte qualitative analysis and at least 10 for quantification [73].

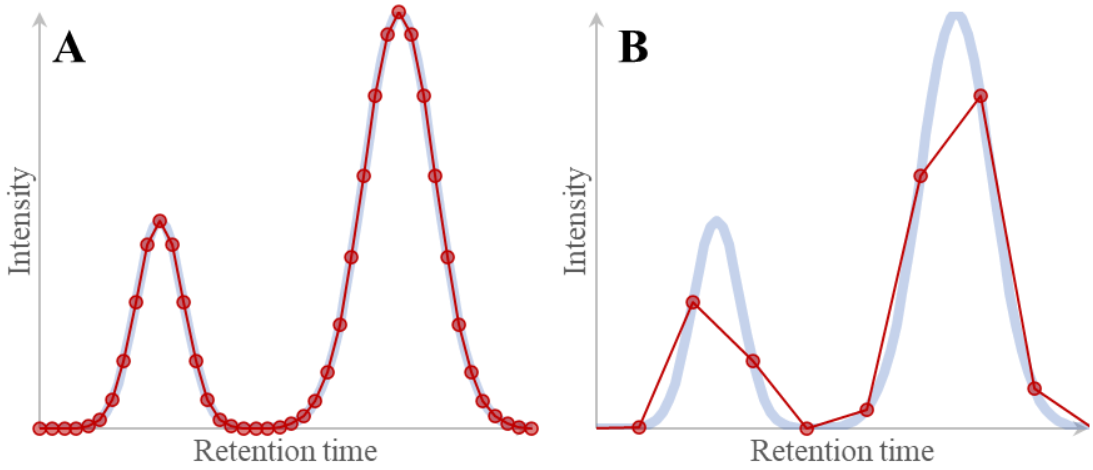

Figure 11. *Red dots represent point at which MS data was recorded. Red lines show recorded chromatogram; light blue lines show actual elution of analytes.* ***A****: proper cycle time provides good number of data points and peaks are well defined.* ***B****: too long cycle time causes that too less data points are recorded and peaks are not well defined.*

The peak width is related to a chromatographic method and might differ a lot. Commonly used C18 UHPLC columns in lipidomics provide peaks, which baseline width measures around 5 s. It means that cycle time should be no longer than 500 ms to provide at least 10 points per peak.

4.1 Targeted analysis

The principle for the targeted analysis is to define a hypothesis about the planned experiment together with a list of compounds, which will be detected with MS. After performing the experiment and collecting MS data, this predefined hypothesis is verified. The MS list of analytes might contain numerous targets, even hundreds, but hardly the whole lipidome. There will always be lipids that are not discovered at the time of the analysis and the information about them will be lost. These methods are usually highly sensitive and they are used for absolute quantification of lipids in samples. Quantitative targeted methods should be validated before analysing real samples. Validation proves that the method is not only sensitive enough, but also selective, that the analytes are within the linear detection range of the MS detector and that the analysis is reproducible in terms of accuracy and precision [74].

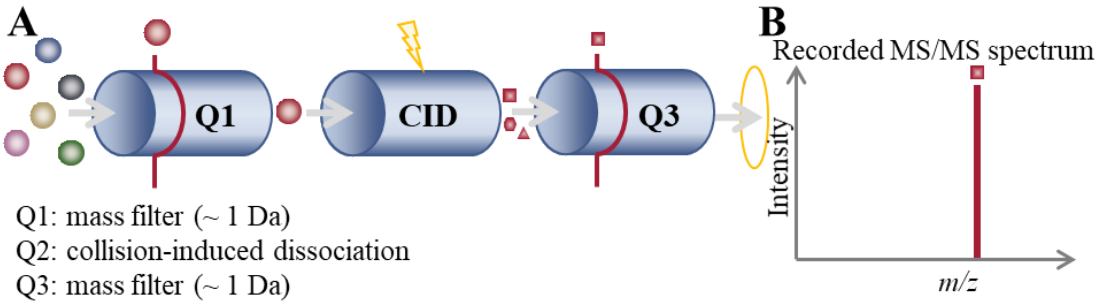

***Figure 12**. **A**: Schematic representation of an SRM experiment; **B**: MS/MS spectrum, which contains only one fragment.*

To provide high sensitivity for the targeted compounds, the data is usually acquired with low resolution MS – QqQ or QTrap with the selected reaction monitoring (SRM) mode. SRM switches Q1 and Q3 to SIM mode. The Q1 defines very narrow range of *m/z* (0.7 to 1 units), so only the selected precursor ion can pass it. Q2 is used as the collision cell. The targeted compound is fragmented with optimized collision energy and the fragments enter Q3. Q3 again defines a narrow 0.7-1 unit *m/z* range to allow only a characteristic fragment to reach the detector (Figure 12). SRM, when well optimized, provides high selectivity, as well as high sensitivity due to effective noise filtration by the 2 quadrupoles (Q1 and Q3).

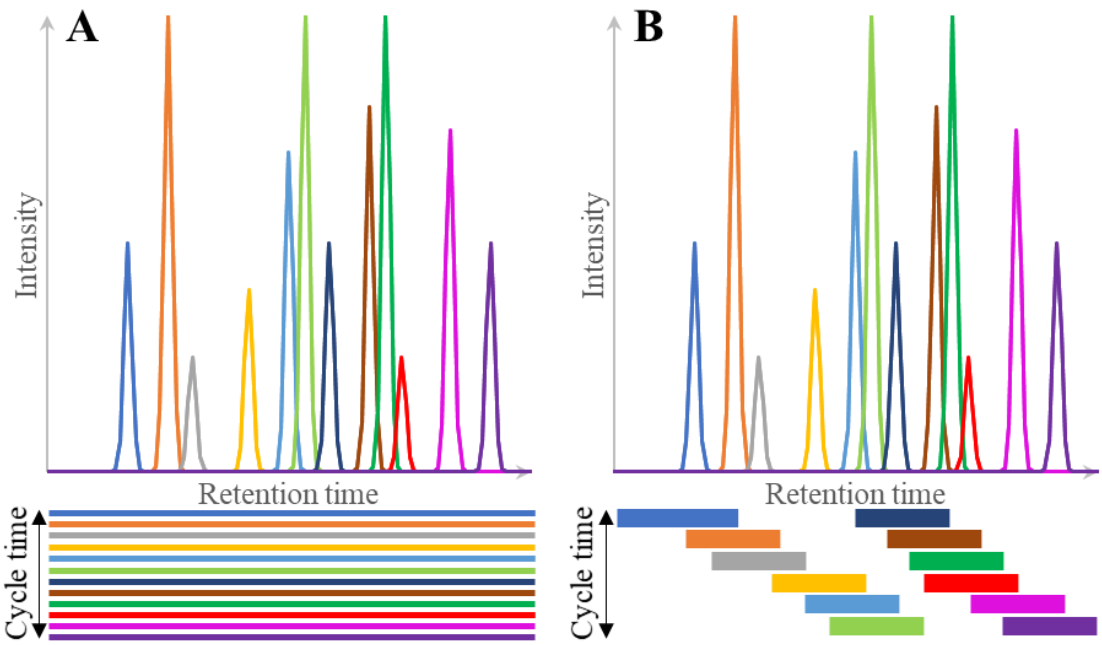

Figure 13. *Chromatograms acquired with **A**: SRM; **B**: scheduled SRM. Lines under chromatograms represent acquisition time of single SRM experiments, line thickness represents dwell time.*

SRMs might be defined for multiple compounds and analysed all together during one LC-MS run or during the same shotgun injection. The dwell times of all SRMs sum up to the cycle time (plus ca. 1 ms between each SRM, which is needed for quadrupoles to stabilize the electromagnetic field). In case of LC-MS analysis the cycle time is restricted, and dwell times of each SRM need to be short, if high number of compounds is analysed. To increase the dwell time of SRMs, and consequently to gain sensitivity for analytes [75], scheduled SRM was developed [76]. This algorithm enables intelligent planning of detection time windows for each SRM, so that SRMs are only acquired around the retention time, when their analytes elute from the chromatographic system and reach the MS detector (Figure 13, the shorter length of the lines under the B chromatogram compared to under the A chromatogram). As the result the cycle time at each point of the analysis is divided into smaller number of SRM experiments, so single SRMs can be recorded with the longer dwell time (Figure 13, the greater thickness of the lines under the B chromatogram compared to under the A chromatogram).

4.2 Untargeted analysis

Untargeted strategies generate new hypotheses and are used in lipid discovery. The principle of untargeted methods is to acquire all data within a wide range of *m/z* in order to record all detectable analytes, also unknowns, which further lead to discovery of new lipids and potential biomarkers. Untargeted methods provide global and comprehensive analysis of a lipidome. During untargeted analysis big amount of data is acquired, which needs to be processed and interpreted. These are usually the critical and most difficult steps. The identities of analytes are often not known and their identification is not trivial. Usually the collected data is compared to existing databases to find which lipids were in the sample. Most typically untargeted methods do not provide the exact concentrations of lipids, but the detected intensities are used for relative comparison of lipid levels in different samples. This, however, causes problems, when different laboratories with different MS instruments want to exchange their results. What is more, even measurements acquired at the same place, but on different days and as different batches, cannot be easily compared and combined. Currently new techniques to estimate absolute concentrations of analytes measured with untargeted methods are developing and are becoming more common [77, 78].

A

PG(18:1/18:1)
Exact mass: 774.5411
Formula: $C_{42}H_{79}O_{10}P$

B

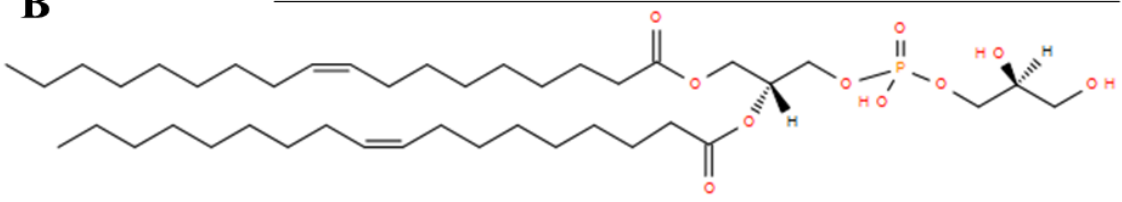

C

Measured *m/z*	Mass tolerance	Matching formulas	Number of findings in LIPID MAPS
774.5	+/- 1.0	18	122
774.54	+/- 0.10	6	32
774.541	+/- 0.01	1	17

Figure 14*. **A**: An example of a lipid with its short annotation, theoretical exact mass and formula; **B**: its chemical structure. **C**: Table showing number of matching formulas depending on how accurate the measured m/z is defined and the number of findings in the LIPID MAPS database.*

In the case of untargeted analysis, the lipid identification is done during data processing, post-acquisition. The main parameters used to identify a compound are: its exact mass,

isotope pattern and the information about compound fragmentation. Additionally, the retention pattern obtained with a chromatographic system might provide information about a lipid class or fatty acyl composition (see chapter 3 of this introduction).

MS instruments can acquire the *m/z* ratio of a precursor ion (e.g. $[M+H]^+$ or $[M+NH_4]^+$, see Table 3 for more examples). However, for the lipid identification the measured accurate precursor *m/z* needs to be re-calculated into the theoretical exact mass of the neutral compound. The theoretical exact mass is strictly connected to compound's chemical composition, so knowing one, the other can be calculated. The better defined the measured accurate *m/z* is, the easier it is to find the theoretical exact mass, so also the proper chemical formula (Figure 14). This is why for untargeted lipid profiling high resolution MS instruments like QTOF, Orbitrap and FT-ICR are utilized [79] – they provide high mass accuracy, so the measured accurate mass is a close match to the theoretical exact mass (low mass error; < 5 ppm).

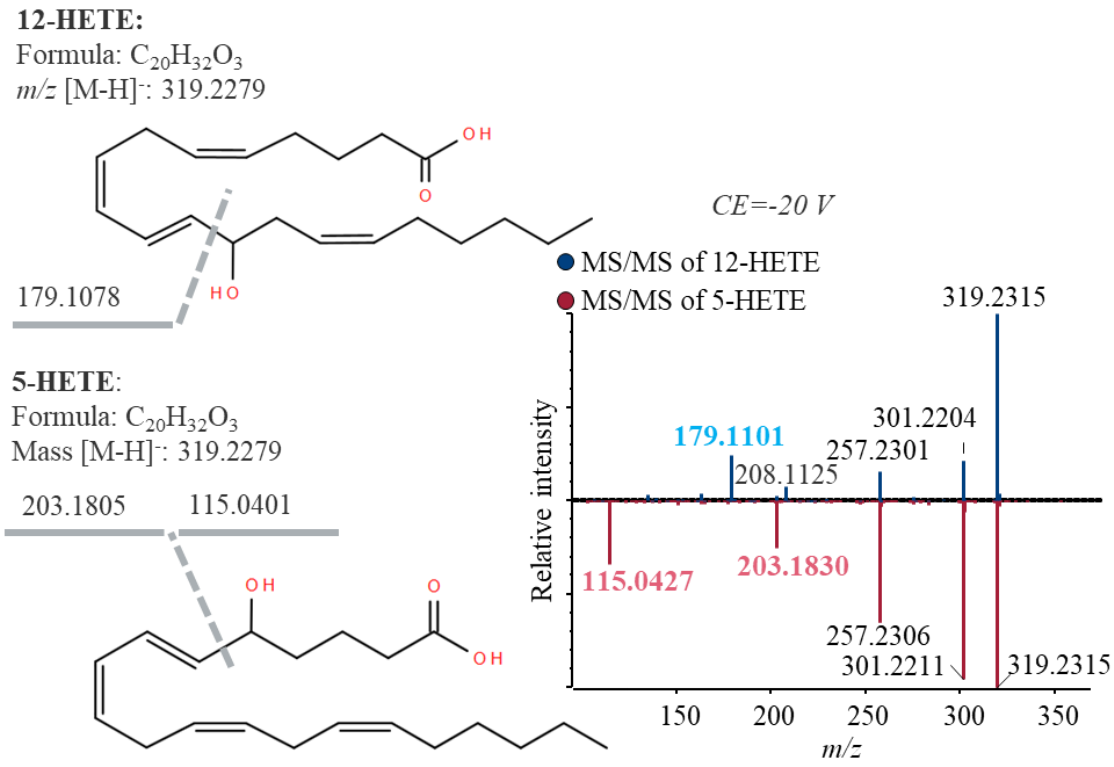

***Figure 15**. Example of 2 isomeric lipids, which can be distinguished with the MS/MS analysis.*

The lipidome comprises many isomers with identical exact masses (as an example: last line in Figure 14C). To distinguish between them the MS/MS data with compound

fragmentation needs to be collected. Currently there are 3 available ways to acquire MS/MS information for untargeted analysis: data dependent acquisition (DDA), data independent acquisition (DIA) and parallel reaction monitoring (PRM) (also called high resolution multiple reaction monitoring: MRM^{HR}).

4.2.1 Untargeted analysis: DDA

DDA analysis can be described as a dynamic product ion scan. This analysis requires to parallelly perform 2 types of MS experiments: full MS scan (Figure 15A and B) and product ion scan (Figure 15C and D). The full MS scan records precursor ions *m/z*, while the product ion scan collects information about compound fragmentation. The decision about which compounds to fragment is made automatically and it entirely depends on the full MS scan. The data from the scan is collected and then it is immediately computed and the most abundant ions are selected for their instantaneous fragmentation. The narrow, unit mass isolation window for the precursor ion provides high quality of the MS/MS spectra [80].

DDA methods can be personalized to the conducted research: an exclusion list can be formed, which contains common impurities, an inclusion list with most critical analytes can be added, as well as sensible thresholds for triggering the precursors might be defined. It is also advised to temporarily exclude each precursor after its first fragmentation – this avoids the situation when a highly concentrated analyte is triggered over and over again during its elution. Due to the temporal exclusion, bigger variability of compounds can be fragmented and it gives the opportunity for lower abundant compounds to be analysed. A good practice is to exclude the precursor only for about half time of its chromatographic peak width, as in this way each compound is triggered once when it reaches the threshold and the second time around its peak maximum, which gives high certainty in good quality of the collected MS/MS data.

The number of MS/MS spectra, which can be recorded per MS cycle depends on the acquisition frequency and is limited to 10-20 for QTOF and 4-5 for an orbitrap [81]. Thus theoretically, during each cycle time 20 new MS/MS spectra can be recorded, which can sum up to thousands of analytes being recorded from each sample.

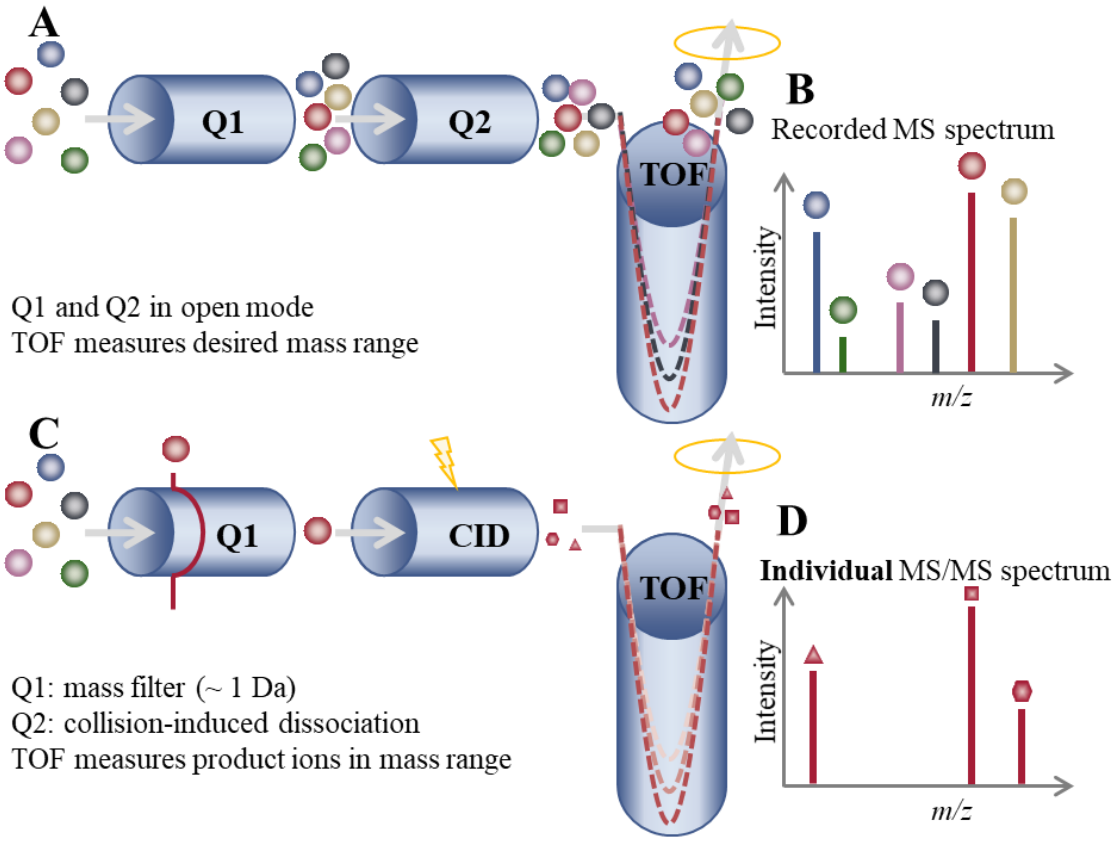

Figure 16*. **A**: Schematic representation of full MS scan experiment; **B**: MS spectrum recorded by the full MS scan. **C**: Schematic representation of product ion scan experiment used to obtain MS/MS data in DDA; **D**: MS/MS spectrum recorded by the product ion scan.*

The disadvantage of DDA approach is that still not all the lipids are fragmented, so identification of very low abundant species might be impossible.

4.2.2 Untargeted analysis: DIA

In the DIA approach a full MS scan of precursor ions is recorded and followed by instantaneous fragmentation of all analytes without any preselection, so no information about any of the analytes is lost.

There are three approaches to fragment all the analytes during the analysis run time. The first one uses one very broad Q1 isolation window and fragments all precursor ions

together. It is called all ion fragmentation (AIF) and it results in very complex MS/MS spectrum [82].

With the second approach, called MS/MS^{ALL}, fragmentation spectra are collected by discrete stepping of narrow unit mass isolation windows and analytes are fragmented one by one [83]. Here high quality MS/MS spectra are recorded, similarly to DDA. It, however, requires extremely long cycle time, therefore it is not suitable for LC-MS hyphenation and it is only limited to shotgun lipidomics [84].

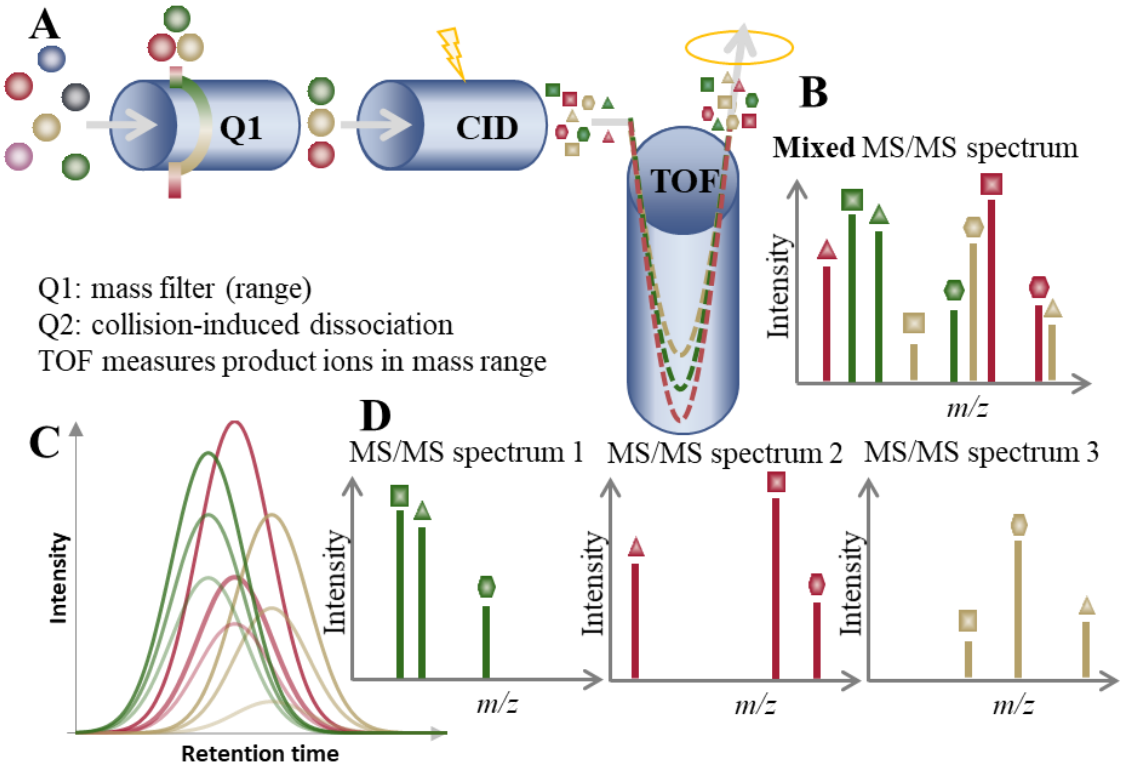

Figure 17. ***A****: Schematic representation of SWATH experiment;* ***B****: MS/MS spectrum recorded by SWATH.* ***C****: Small differences in retention times of coeluting compounds used for MS/MS spectra deconvolution;* ***D****: resulting deconvoluted MS/MS spectra.*

The last approach utilizes multiple Q1 isolation windows of intermediate sizes (e.g. each one 100 Da). These windows can be acquired stepwise to obtain fragmentation of broad range of ions. This DIA approach is called sequential window acquisition of all theoretical fragment ion mass spectra (SWATH) [85, 86] and it gives mixed fragmentation MS/MS spectra of intermediate complexity (Figure 17A and B). In the SWATH analysis it is advised to overlap neighbouring windows by 1 Da. This way avoids losing a precursor,

whose *m/z* lays on the edge of a window, as Q1 ion transmission efficiency for the edge *m/z* tends to be low during Q1 window switching.

Fragmentation spectra obtained by SWATH and AIF need to be deconvoluted to assign fragments to their precursors. This is supported by chromatographic separation of analytes and small differences in the retention times are used to refer fragments to different, but co-eluting compounds (Figure 17C and D) [87].

All DIA approaches collect MS/MS data comprehensively through the whole LC-MS run time and therefore they give the opportunity to quantify compounds using not only the precursor *m/z* (as in the case of DDA) but also their fragments. Quantitative analysis by fragment *m/z* is often more selective and sometimes more sensitive [85].

4.2.3 Untargeted analysis: PRM

PRM collects the full MS scan and records comprehensive data about the precursor ions, but only preselected targeted compounds are fragmented. The listed targets are acquired and their MS/MS of high quality is recorded. This method, however, does not provide comprehensive MS/MS data for all lipids in a sample. Similarly to DIA fragment ions can be used for compound quantification as their fragmentation is recorded throughout the whole analysis time [88].

5. Platelet structure and functions

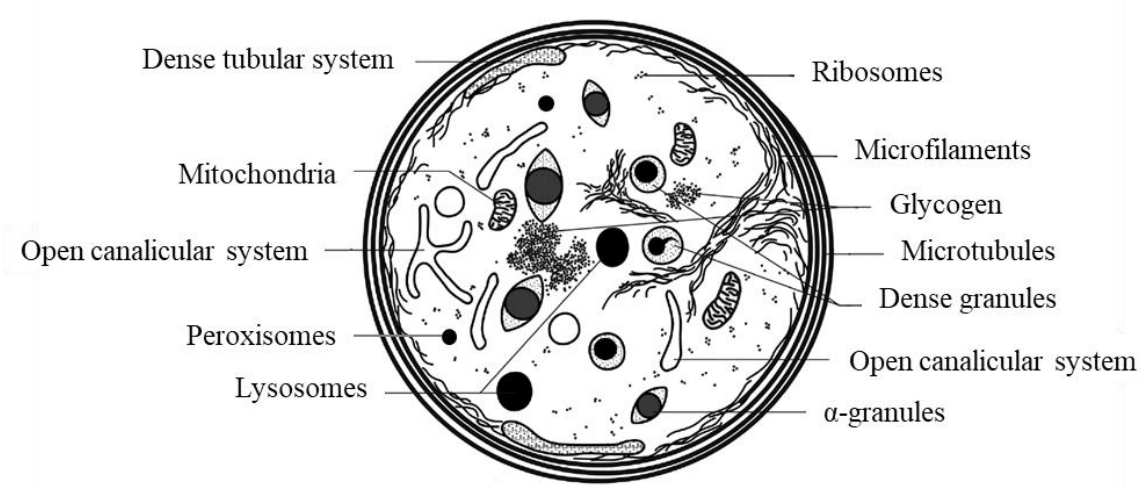

***Figure 18**. Schematic structure of a platelet showing most important features [89, 90].*

Platelets, also called thrombocytes, are small cellular components of blood, with discoid shape (resting platelets) and 2 to 4 μm in the longest diameter and around 1 μm thick [90]. They are quite numerous in blood – 150,000 up to 400,000 per mm^3 [91].

Platelets are highly specialized cells with their primary role in blood clogging. They lack a nucleus and therefore they are incapable of cell division and multiplication (cell mitosis). Platelet cell structure (Figure 18) include lipid bilayer membrane, which is asymmetric (Figure 19), with phosphatidylcholines (PC) being the major lipid group in the outer layer and aminophospholipids (phosphatidylethonolamines (PE) and phosphatidylserine (PS)) creating most of the inner layer (in the resting state) [92]. Platelets contain mitochondria and 4 types of granules: α-granules, dense granules, lysosomes and peroxisomes [90, 93]. Granules are secretory organelles and they store active substances, which might be released upon specific biochemical signals.

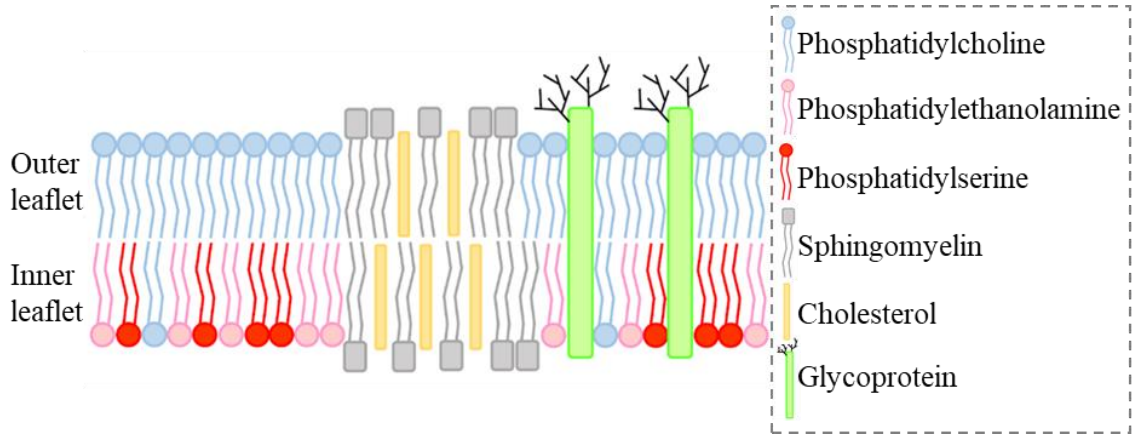

***Figure 19**. Structure of asymmetric plasma membrane in resting platelets [92].*

The most abundant type of granules is α-granules. There are around 50 to 80 α-granules in one platelet, and with the diameter varied from 200 to 500 nm, they make up to 10% of total platelet volume. The structure of an α-granule includes multiple types of membrane proteins and soluble cargo. α-granules contain many factors like coagulant and anticoagulant agents as well as fibrinolytic proteins (e.g. plasminogen, factor V and factor X); adhesion proteins (including fibrinogen and von Willebrand factor (vWF)); chemokines (e.g. CXCL4, CXCL12); angiogenic factors (promoting blood vessel growth) and angiogenic inhibitors; immune mediators and growth factors. Many of these agents play opposite biological roles to each other (like pro-inflammatory and anti-inflammatory

mediators) and it is still not well understood how α-granules efficiently mediate their biochemical functions [90, 93].

Dense granules are a sub-type of lysosome-related organelles. They are much fewer in platelets (typically only 5 to 8 dense granules in the platelet cell). The diameter of dense granules is around 150 nm. They contribute to around 1% of total platelet volume (around 10 times less then α-granules). They play a crucial role in blood clogging, as they possess factors as adenosine diphosphate (ADP) and Ca^{2+} cations, which act as autocrine and paracrine stimulants. Moreover, dense granules contain also other cations (e.g. Mg^{2+}); other nucleotides ((e.g. adenosine triphosphate (ATP)); bioactive amines (mostly serotonin, but also histamine); and polyphosphates [90, 93].

Lysosomes in platelets, similarly as in other cell types, have acidic pH and contain proteases as well as other enzymes needed for protein and generally cell degradation. Their size is between α-granules and dense granules: 200 – 250 nm. The content of platelet lysosomes can be also released upon platelet activation, similarly to α- and dense granules, however it requires grater stimuli [94]. Platelets contain also few small peroxisomes (90 nm in diameter), which are referred to in some publications as 'microperoxisomes', because of their small size compared to peroxisomes in other cell types. They are oxidative organelles with catalase activity. Their main function is the metabolism of very long chain fatty acids, which is done through beta oxidation [95].

Platelets have a quite unique membrane structure, which is created by the dense tubular system (DTS) and open canalicular system. DTS is a closed-channel system built as narrow, membrane-like tubules. It consists of a high concentration on Ca^{2+}, which is released during platelet activation. It is also believed to play an important role in prostaglandin synthesis.

The open canalicular system is a complex internal network of membrane channels connected to the outer cell membrane. The channels tunnel the interior of the platelet, and they differ in the diameter and length. On average channels of the open canalicular system occupy around 4% of platelet volume. Lipid composition of the open canalicular system is identical to the cell membrane and also the surface glycoproteins are present at similar level in both membranes. Its main function is to transport substances in and out of a platelet.

Platelets have very limited possibilities for protein synthesis, so they intake a number of proteins from plasma, including fibrinogen. The open canalicular system also plays an important role in releasing substances from platelets, as during activation, α- and dense granules fuse to the channels and release their content. Another important role of the open canalicular system is to provide a reservoir of additional membrane, which is necessary for the platelet shape change during activation (surface area of a fully spread platelet after activation is nearly 4 times higher than this of a resting platelet (Figure 20) [96].

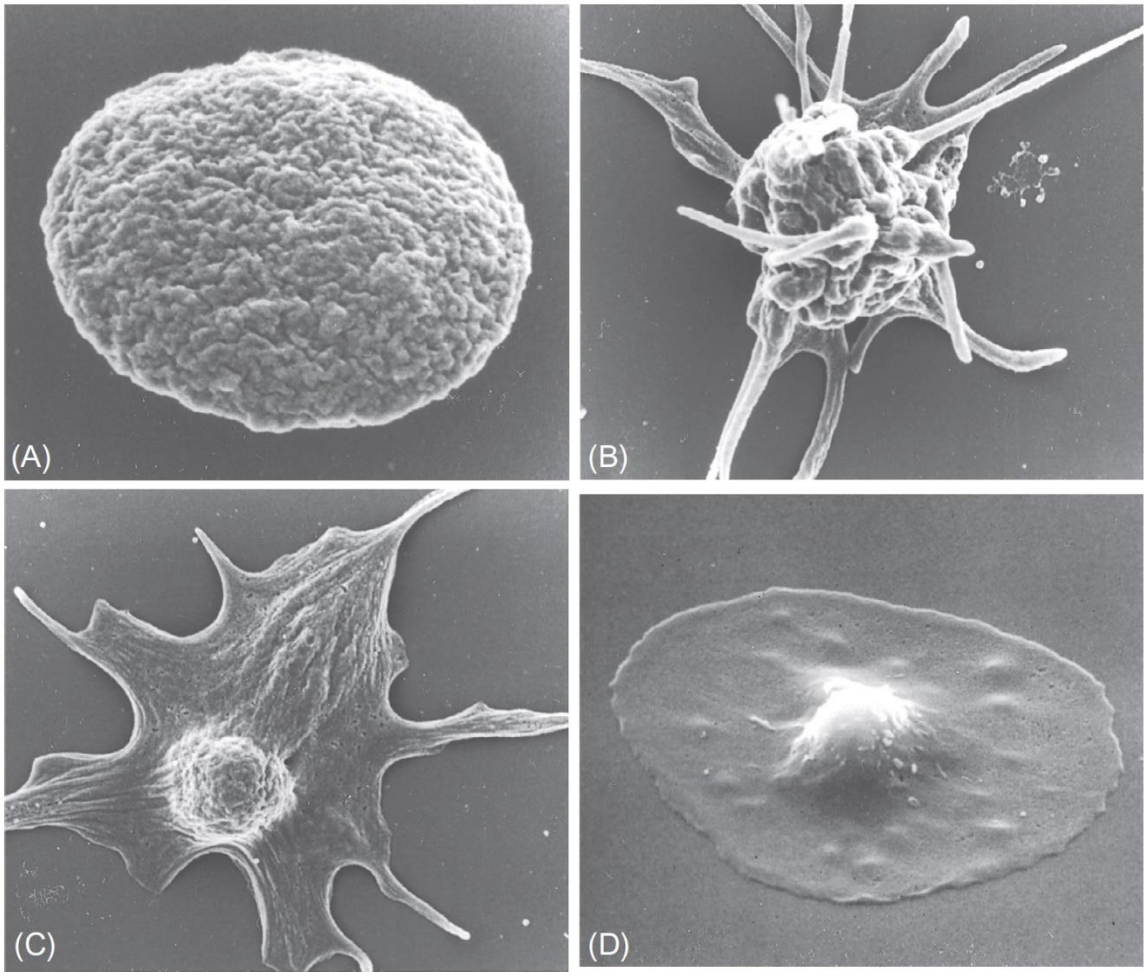

Figure 20*. Scanning electron micrographs illustrating changes in platelet shape during activation.* ***A****: A resting platelet;* ***B****: Early spreading of an activated platelet;* ***C****: The advanced stage of an activated platelet;* ***D****: A fully spread platelet.[92]*

Platelet discoid shape in the resting state is supported by microtubules. They are situated close to the cell wall and they are formed by two nonidentical subunits of a protein: α– and β-tubulin, which create together a coil. Microtubules disassemble during platelet activation, which results in the shape change.

Platelets originate from bone marrow. The process of their production is called thrombopoiesis. They are formed by segmentation of the cytoplasm of megakaryocytes, which are the largest cells of the marrow. Platelet production is controlled by a hormone-like substance thrombopoietin. It is believed to be a mediator, which regulates a number of platelets in blood, as it stimulates growth of megakaryocytes [97, 98].

Platelets are eliminated from blood in 2 main ways. They might be 'consumed' after their hemostasis. Others die when they reach their life span, which is around 10 days for human platelets (different researchers report different life span: 7-10 days [99], 9.5 ± 0.6 days [100], 10 days [101] or 8 – 12 days [102]). After that they are removed by reticuloendothelial cells in spleen and liver [91, 97].

5.1 Hemostasis

Platelets' primary role is hemostasis (also spelled haemostasis), which is a response to blood vessel injury and bleeding. It results in forming blood clot and stopping bleeding.

At the same time, platelets are also responsible for a pathological condition called thrombosis, during which a blood clot is formed inside a blood vessel. This usually happens when platelets aggregate around raptured atherosclerotic plaques. Thrombosis causes problems with proper blood circulation and might result in heart attack and stroke.

The other important roles of platelets are modulation and maintaining inflammation, because they are a source of pro-inflammatory mediators, and enhancing immune response, because they, next to leukocytes, are involved in combating microbial infections [93].

In case of injury and breakage of a blood vessel wall, platelets immediately attach to this injured surface in a large number and then to each other to create a blood clot called thrombus. The whole process can be divided into 3 main stages, however, it should be mentioned, that these stages can overlap each other. The first stage is called adhesion. Here platelets get immobilized from the blood flow, as they attach to the vessel wall next to the injury side. This triggers a signalling cascade inside immobilized platelets, which leads to the second stage: platelet activation. The activation is mediated by tyrosine kinases and G-

protein coupled receptors. The result of this stage is the release of secretory granule contents to the outer space, which starts the final stage: aggregation of platelets. During the aggregation platelets interact with each other to create procoagulant surface and hemostatic plug.

5.1.1 Hemostasis step 1: adhesion

When the vascular vessel is injured it exposes subendothelial extracellular matrix (inner layer of blood vessel wall, which is normally not in contact with flowing blood). This matrix has many ligands for platelet receptors, from which the most commonly described are: collagen (type I and III) and vWF. Platelet adhesion depends on synergistic actions between different receptors.

Fast circulating platelets bind reversibly to vWF through glycoprotein (GP) Ibα, which is a part of the GPIb/IX/V complex. This process, called platelet tethering, slows down the cells and allows them to establish other interactions, like binding collagen through platelet GPVI and α2β1 receptors (Figure 21).

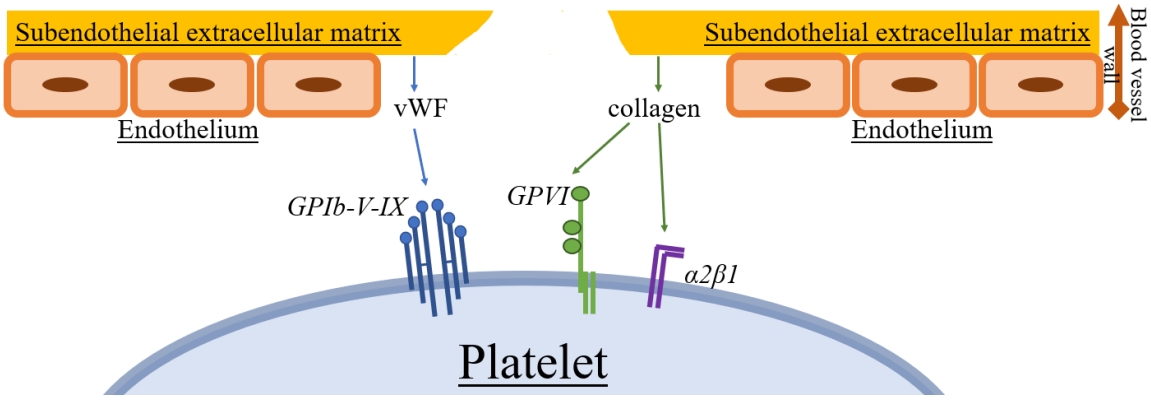

***Figure 21**. Schematic overview of platelet adhesion to injured blood vessel.*

5.1.2 Hemostasis step 2: activation

Binding collagen to its receptors in platelets: GPVI and α2β1 results in activation of phospholipase (PL) Cγ2, which then hydrolyses phosphatidylinositol-4,5-bisphosphate to inositol-1,4,5-trisphosphate (IP_3) and diacylglycerol (DG) (Figure 22).

IP_3 binds to its receptor IP_3R on the membrane of DTS. IP_3R receptor is a membrane calcium-selective channel, and once activated by IP_3 causes transfer of calcium cations Ca^{2+} from inside of DTS to platelet cytoplasm. Lower level of Ca^{2+} in DTS causes relocation of one of its transmembrane proteins: stromal interaction molecule 1 (STIM1) to the plasma membrane, where it associates with the calcium channel Orai1. This is followed by an opening of the Orai1 channel, uptake of calcium ions from plasma and further increase of cytosolic Ca^{2+} level.

Combined action of high concentration of Ca^{2+} and DG in cytoplasm causes a number of changes in the platelet: translocation and activation of serine/threonine protein kinase C (PKC); activation of PLA2, granule secretion and change in platelet shape (Figure 20).

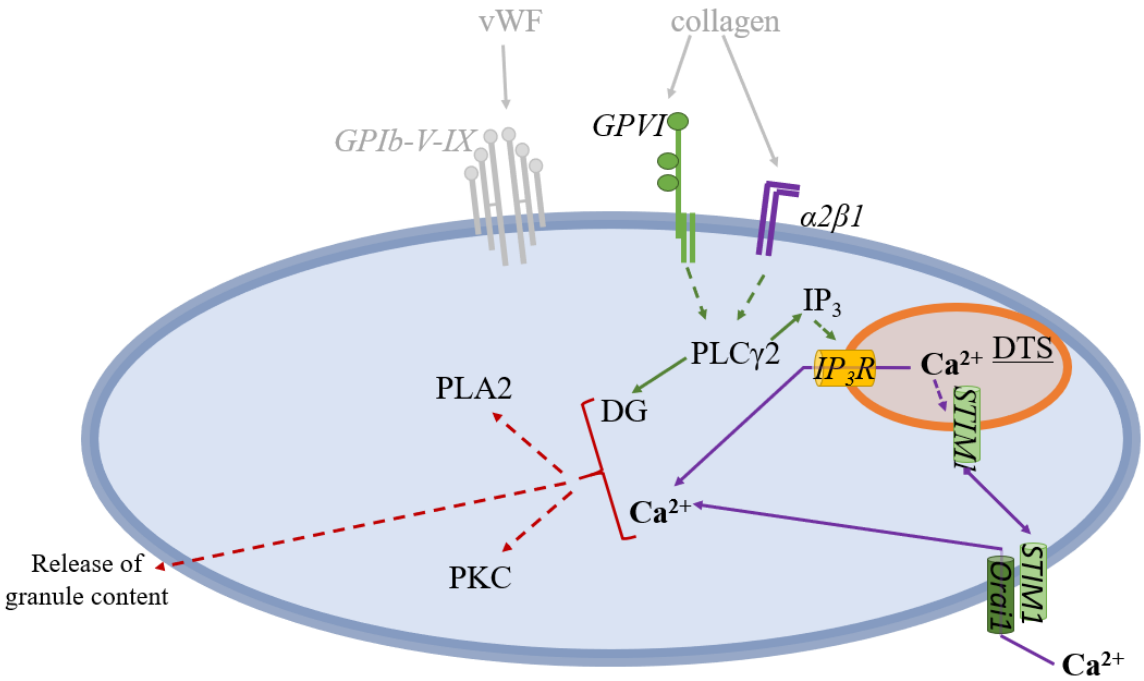

***Figure 22**. Schematic overview of platelet biochemical reactions during the first phase of activation.*

Upon platelet activation many other signals are transmitted which cause changes in biochemical behaviour of nearby platelets. The final result is the activation of many platelets and later their aggregation.

Activated PLA2 cleaves phospholipids at the sn2 position to release polyunsaturated fatty acids, amongst others arachidonic acid (AA). AA is a substrate for COX-1 and it is

transformed into prostaglandin (PG) G2 and further to PGH2, which is then converted by thromboxane synthase to TXA2. TXA2 activates other platelets through their membrane TP receptor. The main effector protein derived from activation of TP receptor is PLCβ2, which, similarly to PLCγ2, causes increase in cytosolic Ca^{2+} level (Figure 23).

Platelets release granule content to the extracellular space during activation. ADP is stored in big amounts in dense granules and it is released upon activation. It binds to platelet membrane receptor $P2Y_1$. This action results in production of PLCβ2. Another important compound, serotonin, is also stored and released from dense granules. It is believed to bind to 5HT2A-receptor and, similarly to ADP, and hence amplify platelet response.

The α-granules contain many factors, important for platelet activation, for example adhesive proteins. The vWF and fibrinogen, which are stored inside α-granules, are critical factors for platelet aggregation. The α-granules provide also important membrane receptors, as the membrane of α-granules fuses to the plasma membrane, and in this way receptors, which are normally only located on the α-granules, are now exposed on the platelet surface.

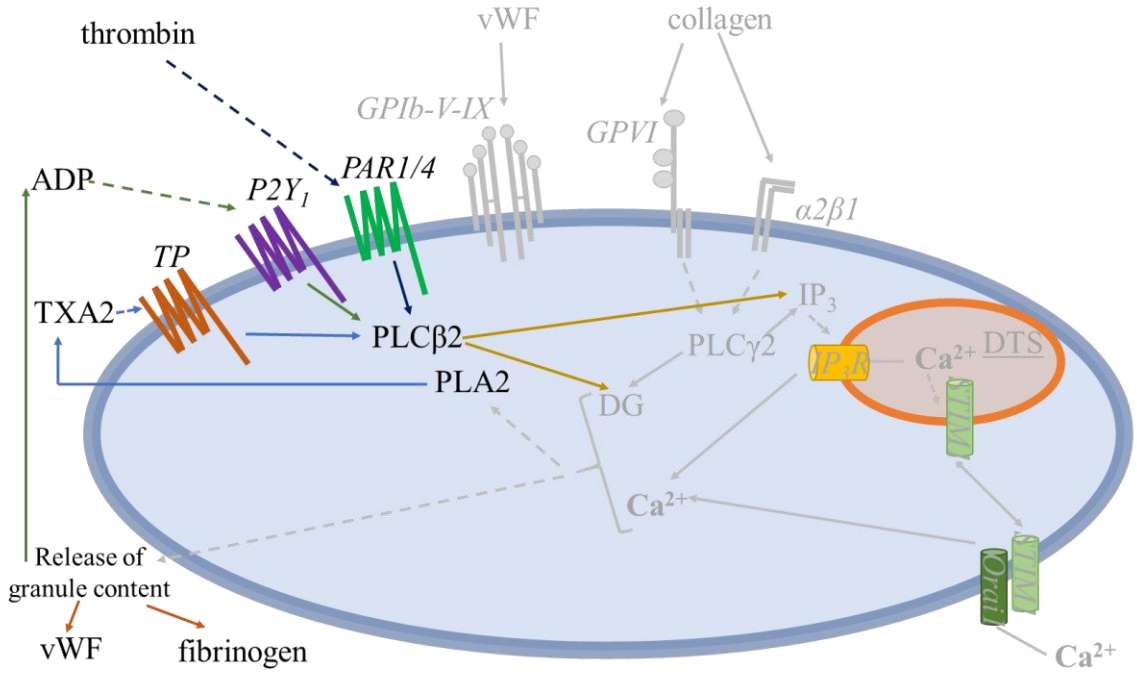

***Figure 23**. Schematic overview of platelet biochemical reactions during the second phase of activation.*

Platelet activation is associated with so called ‘flip-flop’ changes in plasma membrane: PC are moved into the inner leaflet and PE and PS are exposed in the outer leaflet. This change creates catalytic surface for production of thrombin, which is generated on the surface of vascular and blood cells.

Thrombin can activate other platelets through their surface PAR-1 and PAR-4 receptors.

5.1.3 Hemostasis step 3: aggregation

Increased level of calcium ions causes activation of guanosine triphosphate (GTP) binding protein Rap1b. Rap1b interacts with its adaptor molecules RIAM and talin, which results in a protein complex. This complex changes the conformation of the membrane integrin αIIbβ3, which after activation, can bind fibrinogen and vWF (Figure 24). A resting platelet presents tens of thousands of the αIIbβ3 integrins on its surface. After stimulation even more of these protein complexes come to the cell membrane by fusion of granule membranes. Fibrinogen, a symmetric molecule, can crosslink 2 platelets with active αIIbβ3 and aggregate them. Under high shear (high blood flow) also vWF can bridge 2 platelets through the activated αIIbβ3 integrin.

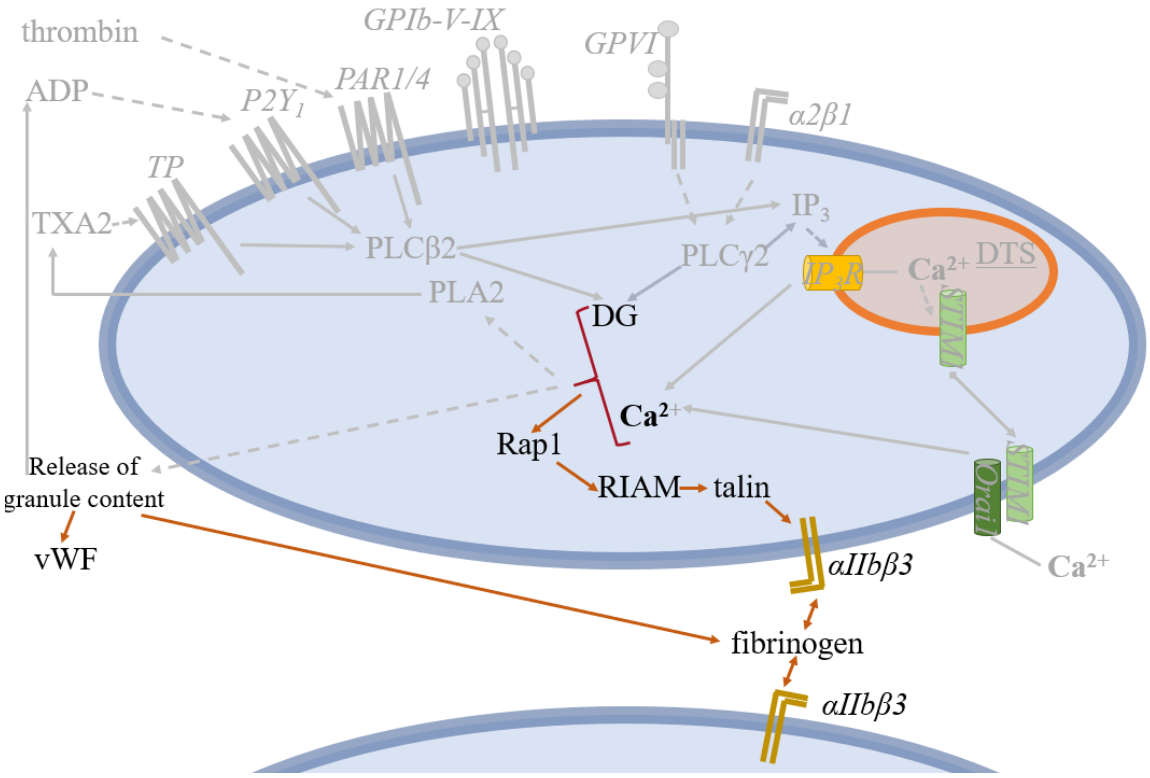

***Figure 24**. Schematic overview of platelet biochemical reactions during aggregation.*

Thrombin plays also a crucial role in forming a thrombus, as its second role (next to platelet activation through PAR receptors) is to convert soluble fibrinogen into insoluble fibrin. This then leads to stable fibrin clot formation.

5.1.4 Factors limiting platelet activation and aggregation

Thrombus growth should be limited to the site of vascular injury and there are factors, which prevent from undesirable continuous platelet activation and aggregation. The main signalling molecules in this inhibitory process are prostaglandin I2 (PGI2) (also called prostacyclin) and nitric oxide (NO).

NO originates from arginine and it is formed by oxidation of this amino acid by nitric oxide-synthases (NOS) in the endothelial cells. It is a unique signalling molecule, because of its small size, which allows it to easily diffuse through the platelet cell membrane. Inside a platelet it binds to the soluble guanylyl cyclase (sGC) and increases its activity. The sGC produces the secondary messenger: cyclic guanosine monophosphate (cGMP).

PGI2 is also produced in the endothelial cells through oxidation of AA by COX-2 and then prostacyclin synthase. PGI2 stimulates adenylate cyclase, which then increases production of another secondary messenger: cyclic adenosine monophosphate (cAMP).

High concentration of these messengers (cGMP and cAMP) influence Ca^{2+} channels in platelets and causes a decrease in cellular concentration of Ca^{2+} cations, as well as a drop in IP_3 synthesis. Consequently, platelet activation and aggregation are reduced.

5.2 CXCR7 receptor in platelets

Platelets express on their surface several types of chemokine receptors (CXCR) among others: CXCR4 and CXCR7. Natural ligands for these receptors are chemokines proteins (CXCL) that are small signalling proteins. Upon ligation of a CXCL protein to a chemokine receptor, the receptors become activated and mediate various cellular responses, which depend on the type of receptor as well as on the type of ligand [103].

Chemokines are stored in granules in resting platelets. During platelet activation the granule membrane fuses to the cellular membrane and the vehicle content is released to the intercellular space. Only then CXCL proteins are available for binding to the chemokine receptors on the platelet surface. The binding leads either to increase in platelet activation, cell aggregation and then platelet death (e.g. when CXCL12 binds to CXCR4 receptor) or to platelet survival (e.g. when CXCL12 binds to CXCR7 receptor) [104].

As the CXCR7 receptor promotes platelets pro-survival response and acts against increase in activation, it is currently investigated as a possible new therapeutic target against cardiovascular diseases. The hope is that therapeutic activation of this receptor could lead to reduced thrombosis in patients [105].

AIM OF THE WORK

The main aim of my research performed at University of Tübingen was to develop new methods and improve existing workflows for the analysis of lipids. The developed methods were then applied to analyse the lipidome of human platelets. My work was divided into 4 main analytical projects, and for 3 of them, the goals were to develop new LC-MS/MS methods and the aim of the 4th part was to improve post-acquisition data processing for comprehensive analysis of a total cell lipidome. My research also included analysis of several sets of real samples – platelet pellets (cellular lipidome) and platelet releasates (secretory lipidome).

The aim of the first analytical project was to combine untargeted profiling with quantitative targeted analysis. The main reason to marge these 2 analytical approaches was to obtain maximum information in one analytical run and with only one injection of each precious biological sample. The new LC-MS/MS method was developed for analysis of fatty acids and oxylipins and it was optimized and then validated to show good sensitivity for targeted compounds and wide coverage of other sample components.

The second study was aiming to analyse oxylipins with RPLC in a micro scale separation. Oxylipins are present in biological matrices at very low concentrations and highly sensitive methods are needed for their detection. The μLC combined with optimized ESI parameters provides increased sensitivity over conventional UHPLC methods. The new method was developed and validated for large number of distinct oxylipins using complex biological matrix of concentrated plasma.

The goal of the third analytical project was to develop a chiral method for separation and quantitation of single enantiomers of oxylipins. The research included comparison of new generation of highly efficient sub-2μm particle polysaccharide chiral columns and optimizing LC-MS/MS parameters for the most promising separation.

The platelet projects aimed in broadening the knowledge about platelet activation and in understanding the role of the platelet CXCR7 receptor. For this reason, samples with different in-vitro treatments were prepared: resting platelets, activated with thrombin and (in case of the last project) also treated with a selective CXCR7 agonist (with and without thrombin). The platelet samples were analysed with a general method for lipid profiling, as well as with newly developed methods for oxylipin and FA analysis. The goal was to obtain a comprehensive picture of platelet lipidome and to understand biochemical pathways by observing changes in lipids caused by different treatments.

RESULTS AND DISCUSSION

1. Publication I: analysis of (oxidized) fatty acids released upon platelet activation

Simultaneous targeted and untargeted UHPLC-ESI-MS/MS method with data-independent acquisition for quantification and profiling of (oxidized) fatty acids released upon platelet activation by thrombin

Malgorzata Cebo[a], Jörg Schlotterbeck[a], Meinrad Gawaz[b], Madhumita Chatterjee[b]*, Michael Lämmerhofer[a]*

[a] University of Tübingen, Institute of Pharmaceutical Sciences, Pharmaceutical (Bio-)Analysis, Auf der Morgenstelle 8, 72076 Tübingen, Germany

[b] Department of Cardiology and Angiology, University Hospital Tübingen, Otfried-Müller-Strasse 10, 72076 Tübingen, Germany

Analytica Chimica Acta

Volume 1094, 15 January 2020, Pages 57-69

DOI: 10.1016/j.aca.2019.10.005

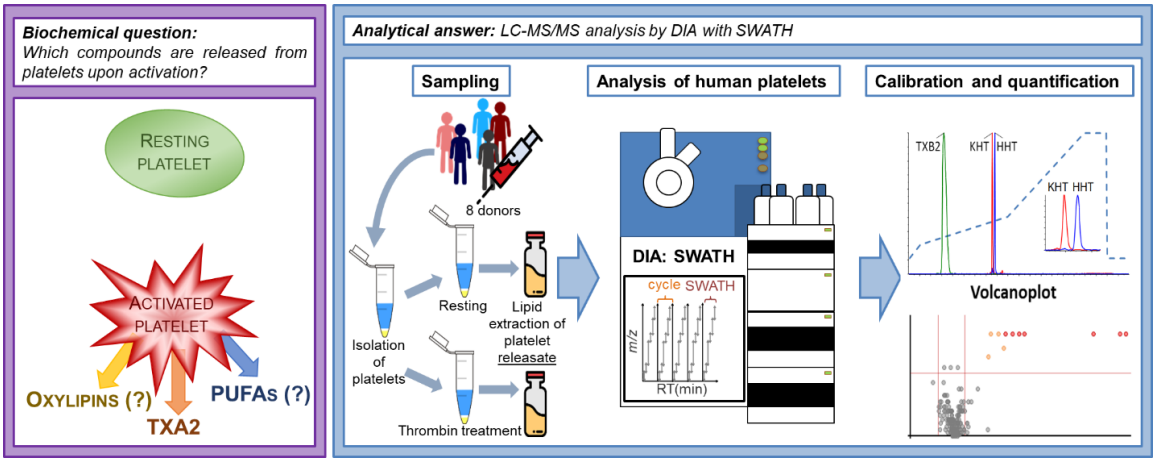

***Figure 25**. Graphical abstract for Publication I*

Keywords: Intercellular platelet signalling, platelet activation, lipidomics, SWATH, oxylipins, lipid mediators

Highlights

• New combined targeted/untargeted UHPLC-ESI-QTOF-MS/MS lipidomics assay developed.

• Data-independent acquisition with SWATH enables comprehensive profiling at MS and MS/MS level.

• Method for standard synthesis of keto-analogues of hydroxylated lipids with double bonds proposed.

• Oxidized and polyunsaturated fatty acids upregulated in releasates of thrombin-activated platelets.

• On average 13 ± 7 attomols thromboxane released per platelet upon thrombin-activation.

Abstract

In this study, a combined targeted/untargeted UHPLC-ESI-QTOF-MS/MS method for the targeted quantitative analysis of the primary platelet lipid mediators thromboxane B2 (TXB2), 12*S*-hydroxy-5*Z*,8*E*,10*E*-heptadecatrienoic acid (HHT) and its oxidation product 12-keto-5*Z*,8*E*,10*E*-heptadecatrienoic acid (KHT) was developed, which allowed simultaneous untargeted profiling for the detection of other lipid biomarkers such as other oxylipins and fatty acids (FAs) in platelet releasates. A general procedure for the synthesis of keto-analogues from hydroxylated polyunsaturated FAs (PUFAs) using Dess-Martin periodinane oxidation reagent was proposed for the preparation of KHT standard. MS detection was performed in data independent acquisition (DIA) mode with sequential window acquisition of all theoretical fragment ion mass spectra (SWATH) in the range of 50–500 Da with variable window sizes. The LC-MS/MS assay was validated for the targeted analytes and applied for analysis of supernatants derived from resting platelets and from platelets treated with thrombin. The targeted analytes KHT, HHT and TXB2 were found at highly elevated levels in the activated platelet releasates. On average, 13 ± 7, 15 ± 9, and 0.6 ± 0.2 attomols per platelet were released upon thrombin-activation. Furthermore, the simultaneous untargeted profiling (n = 8 in each group) revealed that these oxylipins are released with a pool of other (significantly upregulated) oxidized (12-HETE, 12-HEPE) and non-oxidized PUFAs. All these compounds can be considered additional biomarkers of platelet activation complementing the primary platelet activation marker thromboxane B2. The other lipids may support platelet activation or trigger other biological actions with some potential implications in thromboinflammation.

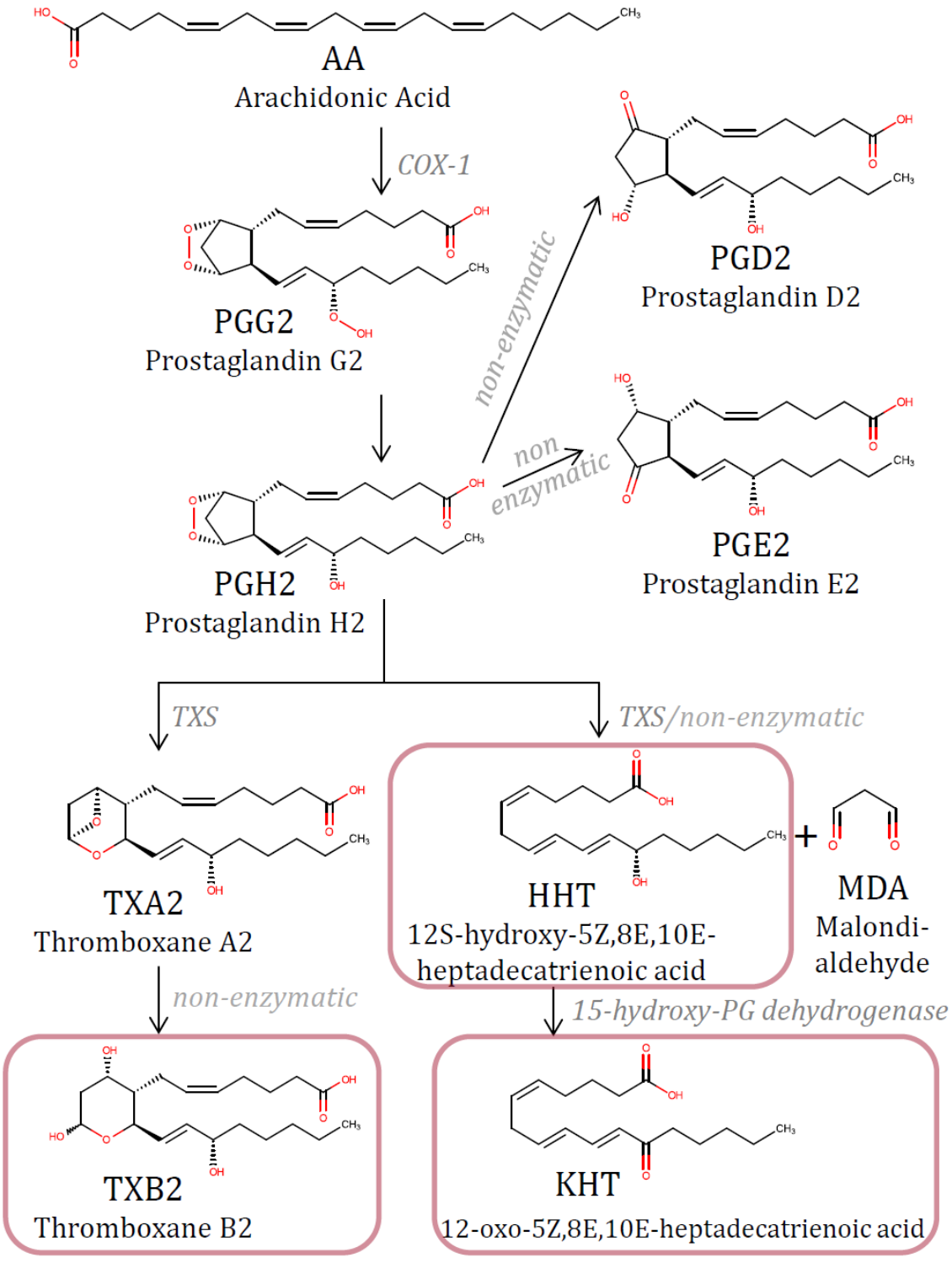

***Figure 26**. Selected pathway of the arachidonic acid metabolism in platelets during their activation [106, 107].*

Lipids play an important role in membrane integrity signalling processes and procoagulant functions of platelets. They are converted enzymatically to bioactive molecules like fatty acids, prostaglandins and other eicosanoids, 1,2-diacyglycerol, lysophosphatidic acid, lysophospholipids and phosphatidylinositides during platelet activation [106, 108]. Most importantly, in the early phase of platelet activation upon receiving external stimuli a number of phospholipases are activated [109]. They cause hydrolysis of membrane phospholipids to release free fatty acids; predominant of which are arachidonic acid (AA), eicosapentaenoic acid (EPA) and docosahexaenoic acid (DHA) [110-112]. Among these AA can be oxidized via different pathways to various bioactive products (for example HETEs, EETs, LTB4) [113]. One of the important pathways leading to platelet activation involves cyclooxygenase-1 (COX-1); it catalyses the synthesis of PGG2, which is further converted to PGH2. Thromboxane synthetase (TXS) catalyses the formation of thromboxane A2 (TXA2) from its substrate PGH2 (Figure 26) [106, 107]. TXA2 is an autocrine platelet activator acting via its TP receptor following its release during platelet activation [14]. TXA2 is a very unstable compound and is converted rapidly into TXB2 which is more stable and therefore analysed in this form. TXA2 synthesis is accompanied by the formation of 12*S*-hydroxy-5*Z*,8*E*,10*E*-heptadecatrienoic acid (HHT) through cleavage of malondialdehyde (MDA). TXA2 and HHT are synthesized by the same pathways, but they have different biological activities and functions. The biological role of HHT was unknown for a long time. Recently it was reported that HHT activates BLT2 (leukotriene B(4) receptor-2) [114]. HHT can be further oxidized to its keto-form by 15-hydroxy-PG dehydrogenase, the product of this reaction is KHT [107, 115]. Not much is known about KHT function in cells. KHT has been reported recently to introduce resistance to cancer treatment with commonly used platinum based chemotherapeutic agents [116].

Platelet activation is a very complex process which involves many intricate signalling pathways, and both positive and negative feedback loops to regulate it. Literature widely describes platelet communication with the external microenvironment which leads to clot formation. TXA2 and adenosine diphosphate (ADP) are named as the main autocrine mediators. It is also known that intracellularly platelets produce a number of free fatty acids and oxylipins as described above [14, 107, 110-113]. However, there is little knowledge which of these compounds are released to the intercellular niche influencing other platelets or cells in the vicinity. Several studies have reported the comprehensive characterization of the platelet lipidome, however, they focused primarily on the cellular lipidome of

isolated platelet pellets [77, 86, 117, 118]. The releasate obtained upon platelet activation is also of physiological significance due to their potential action on other cells and platelets themselves. However, the lipids, in particular (oxidized) fatty acids, released by platelets have rarely been profiled with newer analytical technologies in a more comprehensive manner, which addressed in our work. Very recently, vesicles from stored platelet concentrates which were supposed to be used for therapeutic purposes have been analysed regarding changes in lipid profiles and lipid mediators during storage [119]. Such studies are of vital importance in the context of transfusion medicine. Further characterization of platelet derived lipids are needed which might influence their physiological function and efficacy when platelets or platelet lysates are used as therapeutics.

From analytical perspective, early research on oxylipins has usually been performed with GC-MS method as e.g. reported for HHT and KHT [120]. Nowadays, oxylipins including TXB2 are usually analysed by targeted assays with triple quadrupole instruments or quadrupole-linear ion trap (QTRAP) instruments using selective reaction monitoring (SRM) acquisition [12, 77, 108, 121-124]. These assays are highly sensitive, have wide linear range and are robust. However, the targeted analytes need to be known in advance and the selective SRM transitions programmed prior data acquisition. As a consequence, valuable information may be missed if lipids undergoing significant regulation are not on the target list.

For this reason, comprehensive lipidomics profiling methods by high resolution-mass spectrometry (FT-ICR-MS, Orbitrap and QTOF instruments) with direct infusion (shotgun lipidomics) [77, 125] and hyphenated to liquid chromatography in product ion acquisition mode (known as MRM^{HR} or PRM) [88, 126], data dependent [34, 127-129] and data independent acquisition modes [75, 86, 130-133], respectively, are becoming more and more of interest for such biomedical research on lipids. MRM^{HR}/PRM provides comprehensive profiling at MS level through an MS survey scan followed by targeted acquisition of product ions with narrow precursor isolation windows for selected lipids. It, therefore, does not provide a comprehensive picture at the MS/MS level. For this reason, untargeted lipidomics mostly uses information dependent acquisition (IDA; synonymous for DDA) in which only the most abundant species are triggered for fragmentation. Hence, MS/MS data are of confirmative nature only and may not be available for all detected precursors. MS/MS chromatograms of fragment ions, on the other hand, cannot be

extracted. DIA, by sharp contrast, acquires comprehensive MS and MS/MS data which allows extraction of EICs for fragment ions as well. It can be performed with broad band isolation of precursors (MS^E, AIF) or in a stepwise manner with intermediate sized windows (sequential window acquisition of all fragment ion mass spectra, SWATH). The latter should be advantageous in terms of assay specificity compared to former DIA approaches.

DIA with SWATH used herein fills the gap between targeted assays and comprehensive profiling by combining these two acquisition modes [130, 131]. In this paper a new LC-MS/MS method based on DIA with SWATH is presented for the quantitative analysis of the major lipid mediators of platelet activation TXB2, HHT, and its oxidation product KHT in platelet supernatants (releasate), which is until now a poorly described matrix. The supernatants are derived from resting and thrombin-activated human platelets. The current investigation also aimed to explore other lipid biomarkers of the fatty acid class are potentially regulated and released upon thrombin activation and for this untargeted scientific objective a DIA method with SWATH covering the mass range from 50 to 500 Da was devised. It has the potential of simultaneous untargeted profiling of other oxylipins and fatty acids in the platelet derived supernatant samples. A new efficient synthesis procedure for the preparation of KHT lipid standard, applicable to other keto-fatty acids as well, is presented here. The uniqueness of the new combined targeted/untargeted LC-MS/MS assay are discussed in detail.

1.2. Materials and methods

1.2.1. Materials

The standard substances 12*S*-hydroxy-5*Z*,8*E*,10*E*-heptadecatrienoic acid (HHT), thromboxane B2 (TXB2), 5*Z*,8*Z*,11*Z*,14*Z*-eicosatetraenoic-5,6,8,9,11,12,14,15-d8 acid (deuterated arachidonic acid, AA-d8), (4*Z*,7*Z*,10*Z*,13*Z*)-hexadeca-4,7,10,13-tetraenoic-15,15',16,16,16-d5 acid (HTE-d5), 9-oxo-11α,15*S*-dihydroxy-prosta-5*Z*,13*E*-dien-1-oic-3,3,4,4-d4 acid (deuterated prostaglandin E2, PGE2-d4) and 9*S*,11,15*S*-trihydroxy-thromboxa-5*Z*,13*E*-dien-1-oic-3,3,4,4-d4 acid (deuterated thromboxane B2, TXB2-d4)

were purchased from Cayman Chemical (Ann Arbor, MI, USA). The standards 2,2,3,3,4,4,5,5,6,6,7,7,8,8,9,9,10,10,10-nonadecadeuteriodecanoic acid (deuterated decanoic acid: C10:0-d19) and undecanoic acid (C11:0) were from Merck (Sigma Aldrich) (Munich, Germany) (for structures of internal standards see also Suppl. Materials Figure 34). If not stated otherwise, the shorthand notation for lipids suggested by Liebisch et al. from ref. [7] was applied. LC-MS-grade solvents (acetonitrile, ACN; 2-propanol, IPA; methanol, MeOH) were obtained from Carl Roth (Karlsruhe, Germany). Dichloromethane (DCM) GC grade was purchased from Carl Roth. Methyl *tert*-butylether (MTBE), Dess-Martin periodinane, ammonium acetate, citric acid, glucose, sodium chloride were from Sigma Aldrich, sodium bicarbonate, potassium chloride from Merck, and sodium citrate from AppliChem (Darmstadt, Germany). Ultrapure water for LC-MS was produced by Elga Purelab Ultra (Celle, Germany).

Blood from healthy donors were used to isolate the platelets for the study and collected at the Department of Cardiology and Angiology in accordance with ethical guidelines.

1.2.2. Synthesis of KHT

12-Keto-5*Z*,8*E*,10*E*-heptadecatrienoic acid (KHT) was synthesized from HHT following the Dess-Martin procedure [134]. 5 µL of C11:0 fatty acid internal standard (10 µg mL^{-1} in MeOH) was placed in a 300 µL glass micro vial. Then, 5µL of HHT solution (0.1 mg mL^{-1} in EtOH) was added. MeOH and EtOH were evaporated under a gentle stream of N_2. 60 µL of DCM and 15 µL of Dess-Martin reagent solution (0.3 M in DCM) were added. After 5 min, the mixture was transferred to a 1.5 mL glass vial. DCM was evaporated under a stream of N_2 and the residue was dissolved in 1000 µL of MeOH. The sample was filtered through a 0.2 µm syringe membrane filter and placed in an autosampler vial. The resultant stock solution had a concentration of 0.45 ± 0.03 µg mL^{-1} of KHT (see Suppl. materials - Section 1.5.2 for more details).

1.2.3. Sample preparation

1.2.3.1.Platelet isolation and separation of platelet supernatant (releasate)

Blood from 8 healthy donors was collected in 2 batches (each with 4 donors). The blood was collected in acid-citrate-dextrose (ACD) buffer as anticoagulant (12.5 g sodium citrate,

6.82 g of citric acid, 10 g glucose, 500 mL distilled water, adjusted to pH 4.69 with NaOH) (40 mL in total, ACD anticoagulant:blood 1:4, v/v) and then centrifuged (430xg for 20 min without acceleration and deceleration). Obtained platelet-rich plasma was mixed with Tyrodes-HEPES buffer (2.5 mM HEPES, 150 mM NaCl, 1mM KCl, 2.5 mM $NaHCO_3$, 0.36 mM NaH_2PO_4, 5.5 mM glucose, 1 mg mL^{-1} BSA, pH 6.5) and centrifuged (900 x g for 10 min without acceleration and deceleration). The platelet pellet was re-suspended in PBS supplemented with calcium and divided into aliquots (with 3 x 10^8 platelets in each one) for individual experimental treatments. One of the aliquots was activated with platelet activating stimulus thrombin (*defined as thrombin activated platelets in this manuscript*). A final concentration of 0.1 U mL^{-1} of thrombin was used and the sample was kept for 15 min at room temperature. In another experimental set platelets (*defined as resting platelets in this manuscript*) were kept untreated. At the end of the treatment period, the samples were centrifuged (550 x g, 5 min at 4°C) in a microcentrifuge tube. The supernatants were separated from the platelet pellets by careful aspiration without touching the platelet pellet [135] and used for lipid extraction.

1.2.3.2.Lipid extraction

Platelet supernatant was divided into 2 aliquots and to one of them 4 µL of internal standard solution (C10:0-d19, TXB2-d4, PGE2-d4, HTE-d5, AA-d8, 3 µg mL^{-1} of each compound in MeOH) were added at a final concentration of 120 ng mL^{-1} of each internal standard. Then, 750 µL of MeOH and 2.5 mL of MTBE were added. Samples were vortexed and left for 1h at room temperature. Next, 625 µL of water was added and the samples were centrifuged (3,500 x g, 10 min without acceleration and deceleration). The upper phase was collected and the lower phase was re-extracted with 1 mL of the upper phase of the following mixture: MTBE/MeOH/H_2O (10:3:2.5; v/v/v). The samples were centrifuged again. The upper phases were combined and dried with an EZ2 evaporator from GeneVac (Ipswich, UK) under nitrogen protection. The residues were dissolved in 100 µL of MeOH and stored at -20°C before analysis [136].

1.2.3.3.Preparation of solutions for calibration and method validation

Matrix-matched calibration was performed. Thus, calibrants were prepared by spiking blank matrix (supernatant from *resting platelets*) with different concentrations of the four

analytes (10 to 200 ng mL^{-1}, 7 levels). Internal standards were added at the same concentrations as in the samples (1.2.3.2). Three quality control samples for the targeted analysis (QC_t) (QC_t low, QC_t mid and QC_t high) were prepared in the same way, but the analyte concentrations were equal to 10, 30 and 180 ng mL^{-1}. Calibrants and QC_t samples were processed like the samples, i.e. by lipid extraction with MTBE and MeOH, as described above in section 1.2.3.2.

Three sets of calibrants were prepared to determine extraction recovery, matrix effect and process efficiency [137]: pre-extraction spiked matrix (calibration set 1), post-extraction spiked matrix (calibration set 2) and spiked MeOH (calibration set 3). The first set (calibration set 1) was prepared the same way as the QC_t samples, but the concentration levels of the analytes were equal to 40, 80, 160 and 200 ng mL^{-1}, and the internal standards: each at 120 ng mL^{-1}. To prepare the second set (calibration set 2), 400 µL of resting platelet supernatant was used for lipid extraction (neither analytes nor internal standards were spiked into the matrix). After lipid extraction (procedure described in 1.2.3.2), the resultant lipid extract was divided into aliquots and then spiked with analytes at four different concentrations (40, 80, 160 and 200 ng mL^{-1}) and internal standards were added at equal concentrations (120 ng mL^{-1}). In the third set (calibration set 3), MeOH was spiked with internal standards (120 ng mL^{-1}) and analytes (40, 80, 160 and 200 ng mL^{-1}). Methanol solutions of different concentrations (1 ng mL^{-1} to 10 µg mL^{-1} for KHT and 1 ng mL^{-1} to 80 µg mL^{-1} for HHT and TXB2) were prepared to check for detector linearity range and instrument detection limits.

A QC sample for untargeted analysis (QC_u) was obtained by mixing equal volumes of each platelet supernatant extract (internal standards concentration: 120 ng mL^{-1} each).

1.2.4. UHPLC-ESI-QTOF-MS/MS method

UHPLC-ESI-QTOF-MS/MS analysis was performed on an Agilent 1290 Infinity binary UHPLC system (Agilent, Waldbronn, Germany) coupled to the PAL-HTX xt DLW autosampler (CTC Analytics AG, Switzerland) and the SCIEX TripleTOF 5600+ mass spectrometer with DuoSpray Source (SCIEX, Ontario, Canada). An ACQUITY UPLC CSH C18 column (dimensions: 100 mm × 2.1 mm; particle size: 1.7 µm; Waters

Corporation, Millford, MA, USA) with precolumn (1.7 µm, 5 mm x 2.1 mm) was used for chromatographic separation. The solvent A was aqueous 9.5 mM ammonium acetate and the solvent B was a mixture of IPA, ACN and water (10:10:1; v/v/v) containing 9.5 mM ammonium acetate. The following gradient was used: the method started with 10% of B rising to 20% B in 1 min, then to 40% B in the following 8 min; next it increased to 100% B in 7 min followed by a 2 min hold at 100% B and finally 2 min re-equilibration with 10% B. The flow rate was 600 µL min^{-1} and the oven temperature was set to 60°C. The injection volume was 3 µL.

The MS platform was used in the negative ion mode with ion spray voltage equal to -4500 V and the source temperature set to 500°C. Curtain gas, nebulizer gas and heater gas pressures were used at 30, 50, 40 psi, respectively. Declustering potential was equal to -80 V. For data-independent MS/MS acquisition SWATH windows in high sensitivity mode were applied with cycle time equal to 780 ms (Table 5). The data were processed with PeakView and MultiQuant 3.0 (Sciex, Ontario, Canada) (targeted analysis) and MS-DIAL (ver. 2.84) (RIKEN Center for Sustainable Resource Science, Yokohama, Japan) [131] (untargeted analysis).

Table 5*. TOF-MS experiment and SWATH windows (with their m/z range, accumulation time and collision energy) used for MS analysis.*

Experiment	**Scan Type**	**Start**	**Stop**	**Acc. Time**	**CE**	**Experiment**	**Scan Type**	**Start**	**Stop**	**Acc. Time**	**CE**
		m/z	*m/z*	[ms]	[V]			*m/z*	*m/z*	[ms]	[V]
1	TOF-MS	50	1000	50	-10	11	SWATH	280	291	20	-20 +/-5
2	SWATH	50	170	20	-20 +/-5	12	SWATH	290	302	20	-20 +/-5
3	SWATH	169	200	20	-20 +/-5	13	SWATH	301	306	80	-20 +/-5
4	SWATH	199	216	20	-20 +/-5	14	SWATH	305	320	20	-20 +/-5
5	SWATH	215	231	20	-20 +/-5	15	SWATH	319	335	20	-20 +/-5
6	SWATH	230	246	20	-20 +/-5	16	SWATH	334	350	20	-20 +/-5
7	SWATH	245	250	80	-20 +/-5	17	SWATH	349	354	80	-20 +/-5
8	SWATH	249	263	20	-20 +/-5	18	SWATH	353	367	20	-20 +/-5
9	SWATH	262	277	20	-20 +/-5	19	SWATH	366	371	80	-20 +/-5
10	SWATH	276	281	80	-20 +/-5	20	SWATH	370	500	20	-20 +/-5

1.2.5. Validation of quantitative analysis of KHT, HHT and TXB2

Method validation was performed in accordance to the guideline of the U.S. Food and Drug Administration (FDA) [138] and the procedure of Matuszewski and coworkers [137]. Linearity, limit of detection (LOD), lower limit of quantification (LOQ), intra-assay and inter-day precision and accuracy, matrix effect, extraction recovery, process efficiency and compound stability were investigated.

LOD was determined as the lowest measured concentration, for which signal-to-noise (S/N) ratio was equal or higher than 3 (6 replicates) and similarly LOQ was equal to the concentration for which the S/N ratio was equal or higher than 10 (6 replicates). Accuracy and precision were determined with the 3 QC_t samples of known concentration of analytes measured repetitively within 3 consecutive days (6 times each day).

To determine extraction recovery, peak areas of pre-spiked samples to post-spiked samples were calculated for each concentration. The mean value in percentages was given as the extraction recovery. Similarly, matrix effect was established by comparison of peak areas from post-spiked matrix samples with spiked methanol, and the overall process efficiency was calculated from the peak areas of pre-spiked matrix and spiked MeOH.

The stability of the target compounds during standard laboratory procedures was determined. Four types of stability were analysed: i) long-term storage stability (blank matrix was spiked with analytes at 2 levels and stored at -80°C for 6 months); ii) freeze-thaw stability (2 spiked blank matrix samples were stored at -80°C for 24h and during this time they were 3 times frozen and unfrozen); iii) bench-top stability (2 spiked blank matrix samples were kept at room temperature for 6h); and iv) processed sample stability i.e. of the lipid extract (see below). All these samples (except for the processed samples) were analysed by the UHPLC-ESI-QTOF-MS/MS method and compared with freshly prepared QCs. In the end, the fresh QCs were left for 24h in autosampler (4°C) to determine processed sample stability

1.2.6. UHPLC-MS/MS analysis of samples

Samples were analysed in 2 batches as explained in paragraph 1.2.3.1. The order was randomized. QC_u was analysed 3 times directly before the samples from each set and 3

times directly after each set. For quantitative analysis a set of calibration samples was run before the real samples. QC_t (3 different levels) run before the calibration set, then after it (before the samples) and the third time after the real samples.

1.2.7. Data analysis

Quantitative analysis was based on area ratios of fragment ion EICs of target analytes to precursor ion EICs of internal standards (Table 6). All the EICs (both fragment and precursor ions; for MS/MS spectra see Suppl. Materials Figure 36 and Figure 37) were extracted from the respective SWATH windows (including the internal standards) with the accuracy window of ± 10 mDa. Quantitative analysis was performed using MultiQuant 3.0 software with the following parameters: baseline subtraction, 2 min; Gaussian smoothing, 1 point (2 points for TXB2 and TXB2-d4); peak splitting, 2 points (6 points for TXB2 and TXB2-d4). For further quantification the following software packages were utilized: SPSS Statistics 23 (IBM, Armonk, NY, USA) and Excel 2007 (Microsoft, Redmond, WA, USA). Untargeted analysis was performed with MS-DIAL [131] (for details on MS-DIAL parameters used for untargeted profiling see Suppl. Materials Section 1.5.9.1), MultiQuant 3.0 and R (version i386 3.4.2; R-project for statistical computing) and SIMCA-P+ 12.0 (Umetrics, Sartorius AG, Göttingen, Germany).

Table 6. *Analysis of targeted compounds.*

	Compound	Ion species	Precursor ion mass *m/z*	SWATH window range *m/z*	Fragment chosen for quantification *m/z*	Internal standard
Analytes	HHT	[M-H]-	279.1965	276 - 281	179.1078	PGE2-d4
	KHT	[M-H]-	277.1809	276 - 281	233.1915	PGE2-d4
	TXB2	[M-H]-	369.2283	366 - 371	169.0870	TXB2-d4
Internal standards	PGE2-d4	[M-H]-	355.2428	353 - 367	precursor*	-
	TXB2-d4	[M-H]-	373.2534	370 - 500	precursor*	-

**Precursor ions were still present in SWATH windows (because of incomplete fragmentation at given CE) and they were used for quantification.*

1.3. Results and discussion

1.3.1. Synthesis of KHT

The targeted compound KHT was not commercially available and was therefore synthesized by mild oxidation of commercially available HHT. The Dess-Martin oxidation was selected for this purpose. The reaction scheme is depicted in Figure 27.

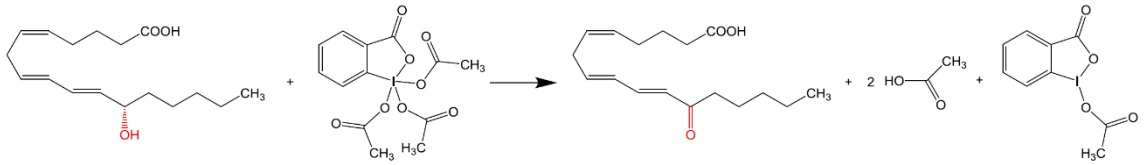

Figure 27. *Reaction scheme for the synthesis of KHT.*

This oxidation reaction makes use of the Dess-Martin reagent, periodinane (1,1,1-triacetoxy-1,1-dihydro-1,2-benziodoxol-3(1H)-one), which selectively oxidizes secondary hydroxyl groups to ketones or primary alcohols to aldehydes. It does not affect double bonds and reacts quantitatively under mild conditions. The reaction is fast at room temperature and consequently the sensitive polyunsaturated fatty acid educt and product are not exposed to extreme conditions [134].

Since the reaction was quantitative (see Suppl. materials Section 1.5.2 for details), the KHT solution was used as prepared without further chromatographic isolation and purification of KHT to avoid further loss of the minute quantities of KHT available. After quantitative reaction, the excess of the reagent, however, was quenched with methanol, in order to avoid oxidation of other analytes when KHT solution was used to prepare mixed calibrants. The sample with the reaction product was analysed by UHPLC-ESI-QTOF-MS/MS in IDA mode to verify quantitative conversion, absence of HHT and to get clean MS/MS spectra for structural verification of the reaction product i.e. of KHT. Product formation was confirmed by accurate mass and isotope pattern of the precursor ion $[M-H]^-$ (experimental *m/z*, 277.1810; theoretical *m/z* 277.1809, error: 0.36 ppm) as well as by the MS/MS spectrum (Figure 28). Only minute quantity of HHT and no significant side products were detected in the reaction mixture, and thus it was confirmed that KHT was obtained in

quantitative yields (98.4% yield). The final concentration of KHT was calculated as 0.45 ± 0.03 µg mL^{-1} (see Suppl. materials Section 1.5.2).

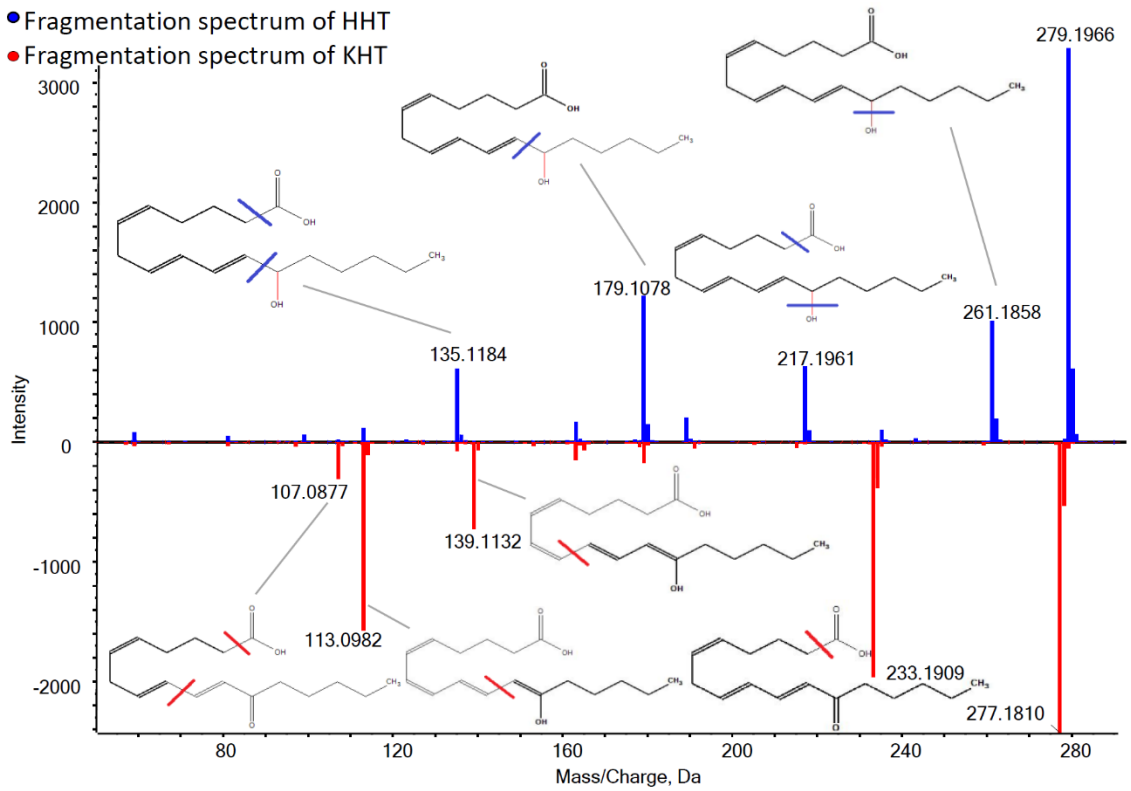

Figure 28. *Comparison of fragmentations by MS/MS spectra of purchased HHT (blue, top) and synthesized KHT (red, bottom) acquired by IDA; bolded part of structure symbolizes fragment ion and non-bolded: the loss.*

The resultant MS/MS spectrum of KHT was compared to the one of HHT (Figure 28) in order to figure out which of the KHT signals is the most suitable one for specific quantitative analysis being sufficiently sensitive. Tentative structural assignments of fragments are indicated in Figure 28 (details see Suppl. materials Table 10). The precursor ion of KHT shows a 2 Da mass shift compared to the educt HHT, as expected. Some of the fragments can be explained by keto-enol tautomerism of KHT of which the one with *m/z* 139.1128 is characteristic for KHT and was not observed in HHT.

1.3.2. LC-MS/MS method

Supernatants collected from experiments in which platelets were either kept under resting conditions or activated with thrombin stimulus were used as samples for efficient two-

phase lipid extraction with MTBE (Matyash) protocol [136, 139]. Internal standards were added before extraction to compensate for loss in the course of the extraction procedure and for instrument variances. The upper organic phase (MTBE) was collected, evaporated and reconstituted in MeOH for UHPLC-ESI-QTOF-MS/MS analysis.

Special attention had to be paid to the development of a selective LC method. Oxylipins released by platelets may consist of a number of isomers (e.g. HETE) and isotopic interferences due to M+2 isotopologues of compounds with an additional double bond or keto/hydroxy pairs may challenge assay specificity. In the current targeted assay for HHT and KHT the M+2 isotopologue of KHT ($[M-H]^-$ + 2 Da) may interfere with HHT quantitation based on precursor ion. Similarly, the HHT fragment with *m/z* 179.1078 is found to a minor extent in the KHT spectrum as well. Hence, chromatographic separation is recommended. Furthermore, more polar oxidized fatty acids must be sufficiently retained in order not to elute too close to t_0 where quantitative analysis is error prone.

Under these considerations, a selective RPLC method was developed. Two columns, Acquity UPLC CSH C18 1.7 µm and Kinetex C8 2.6 µm were evaluated with two different additives to the mobile phase (ammonium formate and ammonium acetate) and different (acetonitrile) gradient conditions were tested (see Suppl. materials Section 1.5.5 for more details). The CSH C18 column was finally chosen because of better peak shape. Ammonium acetate provided better sensitivity. With the final optimized method, as described in chapter 1.2.4., KHT and HHT were fully baseline resolved (resolution equal to 1.9) in the second gradient step (20 – 40%B in 8 min) (Figure 29, insert). Furthermore, TXB2 and other oxidized fatty acids were sufficiently retained. Unlike the other targets and (oxidized) fatty acids, the TXB2 peak is relatively broad, because of interconversion between its two hemiacetal forms that give slightly different retention times [140].

MS detection was performed by ESI-QTOF-MS/MS in data-independent acquisition mode with SWATH. The SWATH design is shown in Table 5. Each MS cycle consisted of a full scan MS experiment (TOF-MS) over a mass range of *m/z* 50-1000 followed by a series of MS/MS experiments with intermediate wide, variable Q1 precursor isolation windows sequentially stepped through the mass range of *m/z* 50-500. In the mass range between *m/z* 169 and 395 (in which most of the common fatty acids and oxylipins were expected) narrower windows were chosen. For the three target compounds (HHT, KHT and TXB2),

which were accurately quantified, the SWATH windows were narrowed down to 5 Da Q1 isolation width to increase assay selectivity [86], on the one hand, and to improve sensitivity through extended accumulation times (80 instead of 20 ms), on the other. Collision energies, which could be customized for each SWATH window as well, were adjusted generally to -20 V with a collision energy spread (CES) of ±5 V. For other targets this MS method can be easily adjusted through changes in SWATH window sizes and accumulation times to lower detection limits of these particular compounds. A total cycle time of 780 ms ensured enough data points across the chromatographic peaks for accurate quantitation.

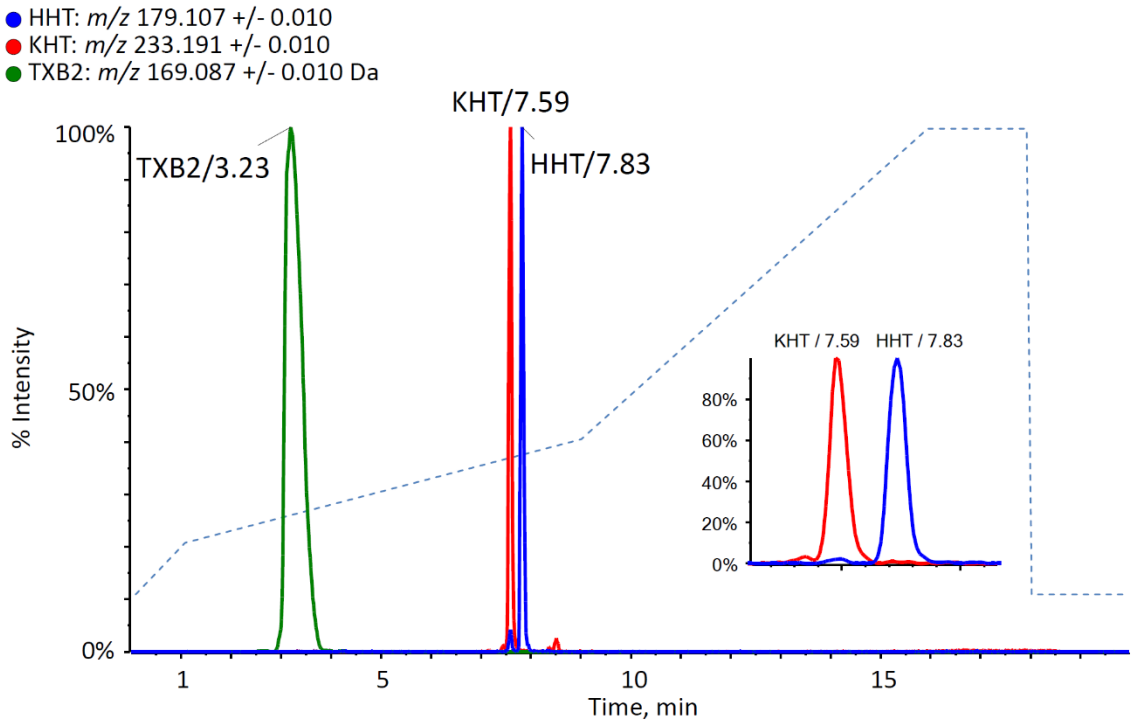

Figure 29. *Chromatogram of the targeted compounds (EICs of their specific fragments extracted from their respective SWATH windows). Dotted line shows changes in mobile phase (percentage of B). Zoom in clearly shows the baseline separation of HHT and KHT.*

1.3.3. Peculiarities and potential of SWATH acquisition

The above described DIA with SWATH provides, besides precursor ion information from MS experiments, also fully comprehensive MS/MS data for the selected *m/z* range across the entire chromatogram and for all samples. This digital map of precursor and product ions makes it possible to select post-acquisition the most appropriate signals for quantitative

analysis by criteria such as sensitivity and assay specificity. For detected analytes, peak group chromatograms can be extracted from the respective SWATH window whereby the individual EICs of the peak group result from recorded unfragmented precursor ion and fragment ions, as exemplified in Figure 30 for KHT. As a consequence, there is a possibility to quantify compounds using their precursor (from MS or MS/MS experiment) or fragment ions. Since all signals are available throughout all samples, other signals can be used for cross-validation (of assay specificity). Oftentimes, interferences with other compounds and the noise level can be minimized with carefully chosen fragment ion.

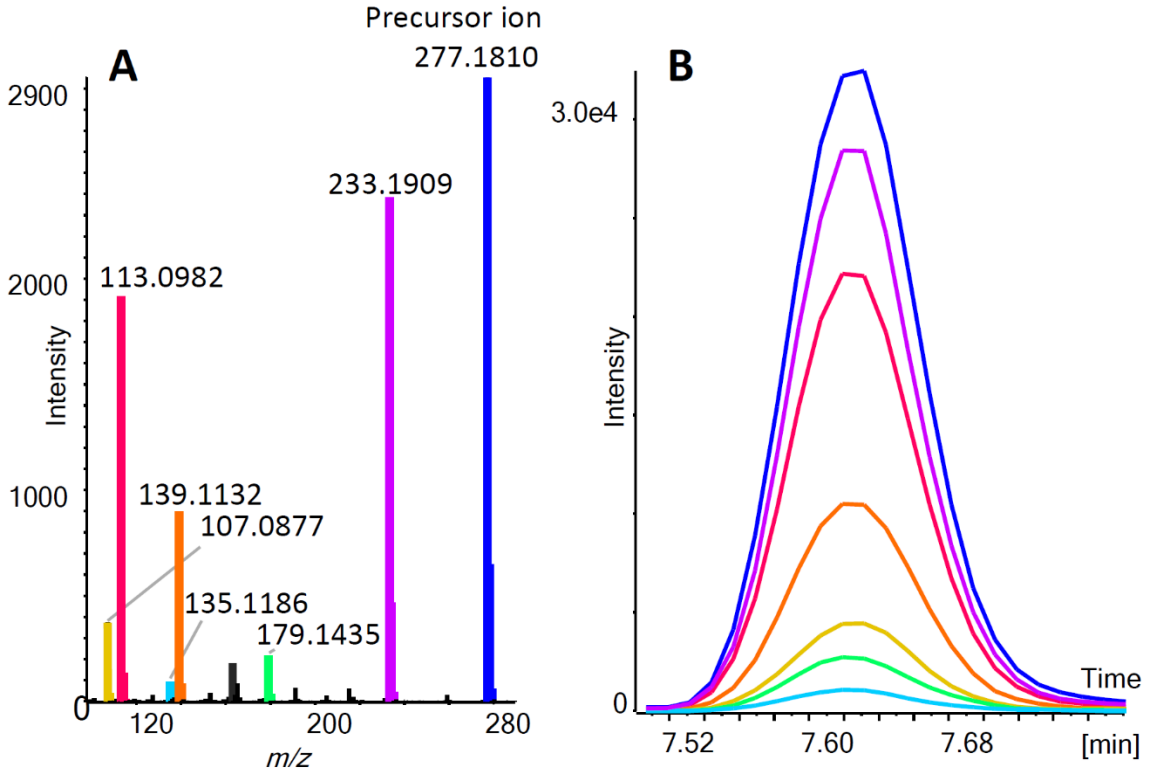

Figure 30. A: *KHT MS/MS spectrum;* ***B****: Peak group chromatogram as obtained by EICs of different fragments extracted from the SWATH window with KHT precursor ion, colours match the fragment masses in the fragmentation spectrum in* ***A****.*

For all the targeted compounds EICs of precursor peaks and abundant fragment peaks were compared to find out the most sensitive ion trace with adequate assay selectivity, being devoid of potential interferences. First, the EICs, which showed the lowest interference level, were chosen. Then, the collision energy was adjusted for gaining the highest intensity of the signal. In each case -20 ± 5 V showed good results for the targeted compounds. This energy was applied to all the SWATH windows as it provided good fragmentation spectra of oxylipins, however, fatty acids remained mostly unfragmented.

Figure 31 demonstrates as an example the improved sensitivity when quantification was based on properly selected fragment ion EIC. The chromatogram in Figure 31A was obtained by extraction of the KHT precursor ion with *m/z* 277.1809 from the TOF-MS experiment (Experiment 1,Table 5). In spite of the high signal intensity an unfavorable signal-to-noise (S/N) ratio of 3.5 (as calculated by PeakView software) resulted in this MS experiment due to a high noise level. When the EIC of the same precursor ion *m/z* was extracted from the respective SWATH window (Table 5, experiment 10), S/N increased to 22 (Figure 31B). The accumulation time was increased in the corresponding SWATH-MS/MS experiment compared to TOF-MS run (80 vs. 50 ms). However, since sensitivity increases roughly proportional to the accumulation time, as shown earlier [75], the rise in S/N by a factor of 6 cannot be fully explained by the factor 1.6 increase in accumulation time alone. Further increase in S/N (to 49) can be obtained by extraction of the EIC by use of the characteristic fragment ion of KHT with *m/z* 233.1909 from the respective SWATH window (Figure 31C). When Q1 precursor isolation is restricted to a small range, less background ions arrive at the detector in MS/MS mode and the lower noise level may contribute to a better S/N ratio (for more examples see Suppl. materials Figure 43 and Figure 44).

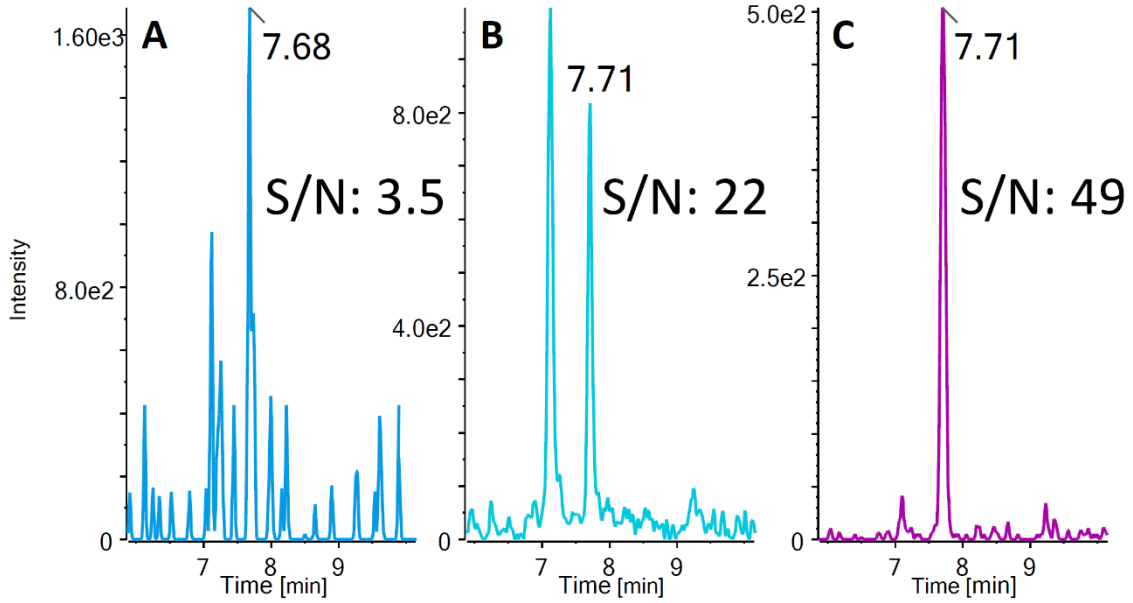

Figure 31. *EIC chromatograms extracted from the same run (matrix spiked with KHT in the concentration 15 ng mL-1).* ***A****: EIC of precursor ion (m/z 277.181) extracted from TOF MS experiment;* ***B****: EIC of precursor ion (m/z 277.181 extracted from the respective SWATH window) and* ***C****: EIC of fragment ion (m/z 233.191) extracted from the SWATH window (i.e. MS/MS experiment).*

This example demonstrates the advantage of quantification by SWATH-MS/MS (as compared to TOF-MS). In this study, the targeted compounds HHT, KHT and TXB2 were quantified based on fragment ion EICs (Table 6) mainly for the reason of higher sensitivity and lower limits of detection, respectively.

1.3.4. Validation of quantitative analysis of targets

Assay specificity, LOD, LOQ, linearity, intra-assay and inter-day accuracy and precision as well as stability were validated for the three targeted compounds following largely the FDA guideline [138]. Extraction recovery and matrix effects were investigated in accordance to the protocol suggested by Matuszewski and coworkers [137]. As blank matrix, a pool of the supernatants from non-activated resting platelets, in which the targeted compounds were not detected, was used. Matrix-matched calibrants and quality controls were prepared from this blank matrix. The results of method validation are summarized in Table 7.

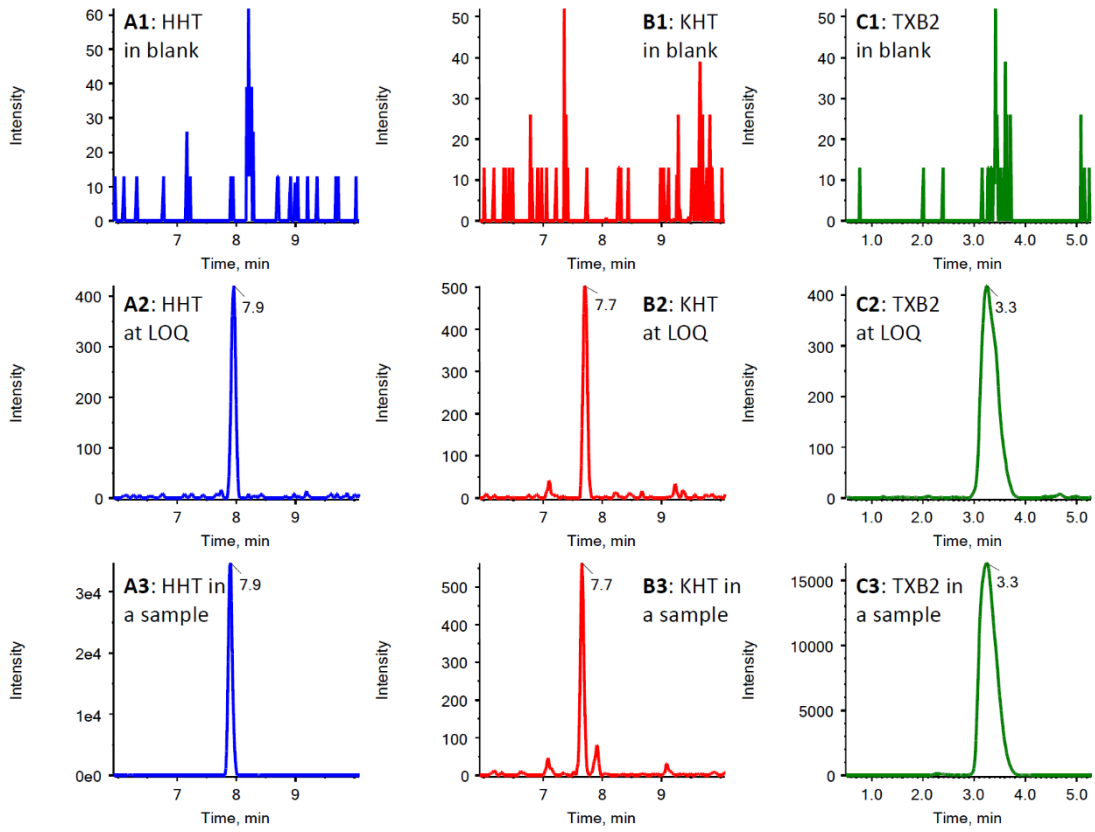

Figure 32. *Chromatograms of the targeted compounds. EICs as given in Table 6. Row 1 (**A1**, **B1**, **C1**): matrix; Row 2 (**A2**, **B2**, **C2**): matrix spiked with analytes at LOQ level. Row 3 (**A3**, **B3**, **C3**): an example of a real sample (thrombin-treated from donor 3) (note, S/N as calculated with PeakView).*

Table 7. *Summary of validation.*

Analyte		**HHT**			**KHT**			**TXB2**		
LOD	µM	0.0036			0.0036			0.0027		
LOQ	µM	0.036			0.036			0.027		
linearity range (determined in MeOH)	µM	0.036 - 45			0.036 – 28.7			0.027 – 10.8		
	r	0.997			0.998			0.998		
calibration range weighting: $1/x^2$	µM	0.036 – 0.72			0.036 - 0.72			0.027 – 0.54		
	r	0.996	0.994	0.994	0.992	0.994	0.993	0.993	0.991	0.989
Within-run accuracy [%]	QC low	109.7	101.8	89.4	102.2	108.9	82.8	111.4	99.6	110.2
	QC mid	98.4	101.3	87.0	95.2	101.6	96.8	102.3	103.2	109.3
	QC high	98.5	101.6	95.0	95.8	102.6	99.3	92.3	95.4	87.0
Within-run precision [%]	QC low	4.27	10.85	6.39	14.46	9.95	2.54	5.90	11.92	3.25
	QC mid	7.10	9.84	1.56	8.65	10.11	4.28	8.93	10.08	2.94
	QC high	10.99	6.25	7.87	10.67	8.24	8.25	8.63	9.07	4.63
Between runs accuracy [%]	QC low	100.3			98.0			107.1		
	QC mid	95.6			97.9			104.9		
	QC high	98.4			99.2			91.6		
Between runs precision [%]	QC low	8.33			11.31			4.95		
	QC mid	6.29			2.85			3.06		
	QC high	2.75			2.90			3.78		
Matrix effect	[%]	108.6			108.4			101.2		
Extraction recovery	[%]	95.2			96.4			76.9		
Process Efficiency	[%]	102.9			104.0			77.2		
Long storage stability - accuracy [%]	QC low	113.3			102.9			93.2		
	QC high	94.0			92.8			92.4		
Freeze-thaw stability - accuracy [%]	QC low	116.2			112.6			94.2		
	QC high	80.4			110.6			111.5		
Bench-top stability - accuracy [%]	QC low	104.5			84.0			80.1		
	QC high	85.7			109.7			99.4		
Processed sample stability - accuracy [%]	QC low	111.2			119.5			119.8		
	QC high	111.5			108.2			110.0		
		day 1	day 2	day 3	day 1	day 2	day 3	day 1	day 2	day 3

Briefly, assay specificity was evaluated by analysing blank matrix (platelet supernatants) from three different donors, checking for absence of signals in the ion traces of the target analytes and internal standards. Furthermore, absence of analyte signals in internal standards and signals from internal standards in analytes was verified as well. As all signals (EICs of precursor and fragment ions) were recorded comprehensively during method

validation and sample analysis, assay specificity could be verified by internal cross-validation of the results using other ion signals for calculation of the quantitative results [75]. LODs and LOQs were determined as 1 and 10 ng mL^{-1}, respectively, for all three targeted compounds. Matrix-matched calibrants were prepared from blank matrix (supernatants of resting platelets) with spiking levels of targeted analytes in the range between 10 ng mL^{-1} and 200 ng mL^{-1} (Figure 32). Calibrants with higher concentrations were not prepared because there was not enough blank matrix available. The entire linearity range was established by standard solutions of the target analytes in methanol. As can be seen from Table 7, the detector response was linear over a much wider concentration range (ca. 3 orders of magnitude). Intra-assay and inter-day accuracy (determined as % recovery) and precision (measured as % RSD) fulfilled the FDA acceptance criteria for bioanalytical method validation. The matrix effects, as determined from the response ratios of calibration set 2 divided by calibration set 3 x 100 [%], were acceptable (mean values ranged between 101% and 108%). Extraction recoveries were determined from the response ratios of calibration set 1 divided by calibration set 2 x 100 [%]. They were above 90% for HHT and KHT, and 77% for TXB2. Process efficiency, as calculated from the response ratios of calibration set 1 divided by calibration set 3 x 100 [%], ranged between 77 and 104 %. Stability tests showed that the compounds are sufficiently stable under the standard laboratory procedures (Table 7).

1.3.5. Results of quantitative analysis of HHT, KHT and TXB2

The validated combined targeted/untargeted LC-MS/MS assay with SWATH was applied to samples of supernatants from resting platelets (non-activated controls) and thrombin-activated platelet supernatant samples of 8 donors. Thrombin-activated platelet samples were prepared at two dilution levels (without dilution and diluted 20 times) because of the expected high concentration of some analytes exceeding the calibration range. All samples were measured in triplicates and the results are summarized in Table 8.

The target analytes could not be detected (< LOD) or the concentration was very small (< LOQ) in the samples from resting platelets which indicates that no accidental activation of platelets occurred during sample preparation. On contrary, in the thrombin-activated platelet supernatants high concentration levels of TXB2 and HHT between 0.6 and 4.5 µM

were found, corresponding to release of about 4-30 attomol per platelet. KHT was present in all cases at much lower concentrations (20 to 300-fold lower concentrations) in the supernatants of the thrombin-activated platelet samples.

Table 8. *Quantitative analysis of targeted compounds. Data shown as molar concentrations in supernatant and as average release (in mol) per one platelet (n = 8 in each group).*

		TXB2 Amount ± st. dev.		**HHT** Amount ± st. dev.		**KHT** Amount ± st. dev.	
		[µM]	[attomol per platelet]	[µM]	[attomol per platelet]	[nM]	[attomol per platelet]
		LOD = 0.0027	LOD = 0.018	LOD = 0.0036	LOD = 0.024	LOD = 3.6	LOD = 0.024
	Donor	LOQ = 0.027	LOQ = 0.180	LOQ = 0.036	LOQ = 0.24	LOQ = 36	LOQ = 0.24
Resting platelets	1	< LOD		< LOD		< LOD	
	2	< LOD		< LOD		< LOD	
	3	< LOD		< LOD		< LOD	
	4	< LOD		< LOD		< LOD	
	5	< LOQ		< LOQ		< LOD	
	6	< LOD		< LOD		< LOD	
	7	< LOQ		< LOD		< LOD	
	8	< LOQ		< LOD		< LOD	
Thrombin treated platelets	1	1.71 ± 0.10	11.4 ± 0.7	2.04 ± 0.18	13.6 ± 1.2	69.0 ± 4.0	0.460 ± 0.026
	2	3.31 ± 0.24	22.1 ± 1.6	4.43 ± 0.64	29.6 ± 4.3	55.7 ± 0.7	0.371 ± 0.005
	3	0.66 ± 0.05	4.4 ± 0.3	1.00 ± 0.06	6.7 ± 0.4	< LOQ	
	4	1.43 ± 0.16	9.5 ± 1.0	1.53 ± 0.20	10.2 ± 1.3	93.0 ± 7.2	0.620 ± 0.048
	5	1.90 ± 0.23	12.7 ± 1.5	1.90 ± 0.18	12.7 ± 1.1	< LOQ	
	6	< LOQ		< LOD		< LOQ	
	7	3.13 ± 0.25	20.8 ± 1.7	3.67 ± 0.38	24.4 ± 2.5	122.5 ± 7.5	0.817 ± 0.050
	8	1.04 ± 0.11	7.0 ± 0.7	1.19 ± 0.15	7.9 ± 1.0	< LOQ	

1.3.6. Results of simultaneous untargeted profiling

In this study, the data from 16 platelet supernatant samples from 8 donors (thrombin treated and non-treated resting platelet supernatant of each donor) were subjected to untargeted data processing. MS-DIAL software (employing parameters as specified in Suppl. materials Section 1.5.9.1) was utilized for peak finding, deisotoping, adduct annotation, alignment, deconvolution, automated identification (via spectral matching of deconvoluted MS/MS spectra with in silico spectra of the LipidBlast database) and assessment of annotations via scoring functions [141]. MultiQuant was utilized for peak integration and data were exported as peak heights. Missing values were filled with 2/3 of the smallest

value for a given feature. Data were then normalized by use of internal standards (see Suppl. materials Table 13).

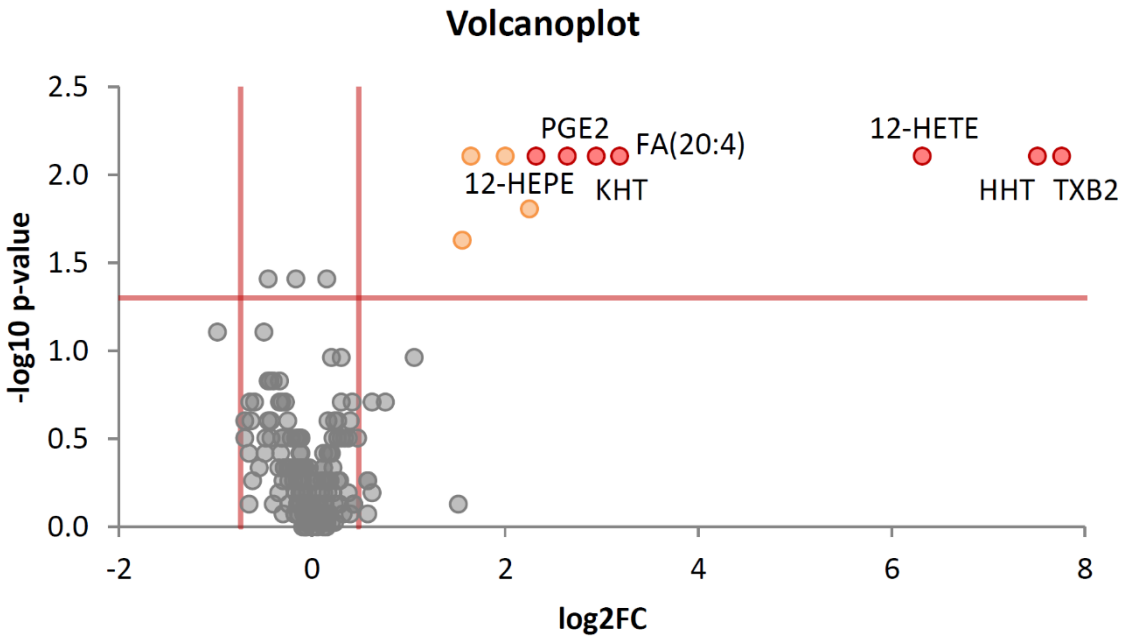

Figure 33. *Volcano plot showing the relation of p-values and fold changes for all features in untargeted analysis (n = 8 in each group). Only features with the largest distance to the (0,0) point are labelled for clarity.*

From the 408 initially detected and aligned features 187 remained after manual curation. Twenty-five could be annotated by MS-DIAL with a total score of > 800. The statistical program R and SIMCA-P+ were used for statistical evaluation of the data. Non-parametric paired Wilcoxon-signed rank test (*U*-test) was performed at significance level P = 0.05. Fold changes were also calculated in the paired manner to find significantly regulated lipids between the two groups of resting platelets and thrombin-treated samples (Figure 33). Eight compounds (in addition to the targeted ones) showed significantly altered relative concentrations in the two groups (Table 9). These compounds all belong to unsaturated FAs (FA 20 with 1-5 double bonds) or oxidized PUFAs (12-HETE, 12-HEPE, PGE2). Many of the former PUFAs are typically not included in the target list of targeted SRM assays and this finding would therefore have been missed like the information that other fatty acids like saturated FAs are not increased upon platelet activation in releasates. Their correct structural annotations were confirmed with purchased authentic standards by comparison of retention times, accurate masses, isotope patterns and MS/MS spectra (see Suppl. materials, in particular Table 13). Two of the confirmed significantly regulated

lipids, 12-HETE and FA(20:4) (AA), were of particular interest and quantified afterwards, as described in detail in Suppl. materials Section 1.5.10. The concentrations of 12-HETE in supernatants of resting platelets were always below LOQ but increased by a fold change of around 80 in thrombin-activated platelets (concentrations in releasates were in the range between 1 and 5 µM corresponding to 6-35 attomol released per platelet). AA was determined at concentration levels close to the LOQ in the supernatants of the resting platelets, but concentrations were elevated by a fold change around 9 in releasates of thrombin-activated platelets.

Table 9. *Compounds showing significant differences between resting platelets and thrombin-treated platelets, which were detected and identified in the untargeted analysis (targeted compounds are not included in this table; for details on confirmation of structural annotation see Suppl. materials Table 13).*

Name	**Abbreviation**	**Experimental** *m/z*	**Theoretical** *m/z*	**Error** ppm	**Retention time** [min]	**Precision in QC** [%]
eicosenoic acid	FA(20:1)	309.2780	309.2799	0.3	14.50	8.8
eicosadienoic acid	FA(20:2)	307.2639	307.2643	-1.3	13.94	10.7
eicosatrienoic acid	FA(20:3)	305.2478	305.2486	-2.6	13.42	18.2
eicosatetraenoic acid	FA(20:4)	303.2327	303.2330	-1.0	12.98	12.7
eicosapentaenoic acid	FA(20:5)	301.2171	301.2173	-0.7	12.40	13.8
12-hydroxyeicosatetraenoic acid	12-HETE	319.2284	319.2279	1.6	10.57	10.8
12-hydroxyeicosapentaenoic acid	12-HEPE	317.2118	317.2122	-1.3	9.77	20.0
Prostaglandin E2	PGE2	351.2181	351.2177	1.1	3.58	24.5

1.3.7. Biochemical interpretation

Oxylipins and PUFAs may differentially influence platelet responsiveness acting as autocrine mediators [142]; moreover, participate in diverse atherothrombotic vascular processes while acting on target cells, e.g. inflammatory leukocytes, vascular smooth muscle cells, as paracrine mediators. This work highlights the molecular diversity of lipid mediators derived through the COX-1 pathway in thrombin activated platelet releasate, adding to the wide range of protein mediators (e.g. chemokines, cytokines) from the platelet α-granules and nucleotides from δ-granules. These mediators propagate a pro-aggregatory

and pro-thrombotic microenvironment where platelets are activated, and subsequently lead to thromboischemic complications like myocardial infarction and cerebral stroke [8]. 12-HETE is the most dominant metabolite generated intracellularly during platelet activation induced by thrombin, collagen or calcium ionophore stimulation, while AA is channelled through 12-LOX instead of COX-1 [143]. Some previous studies have shown that 12-HETE can synergistically enhance aggregation triggered by collagen, ADP and protease activated receptor (thrombin receptor-PAR), but counteracts arachidonic acid induced responses [143]. Since expression of the 12-HETE receptor GPR31 on platelet remains elusive as compared to the definitive characteristics and intracellular signalling cascade triggered by the thromboxane receptor (TP), the actions of free 12-HETE remain vague. However, intraplatelet generation of 12-HETE on receiving thrombin, collagen or ionophore stimulation [144, 145], is rapidly followed by its esterification to membrane phospholipids (PLs), in particular PEs by Co-A dependent ligases (16:0p, 18:1p, 18:0p, 18:0a/12-HETE-PE) and PCs (16:0a, 18:0a/12-HETE-PC). Thus, the majority of 12-HETE remains platelet associated and not released into the extracellular space. Membrane tethered 12-HETE-PLs substantiate coagulation like other anionic PLs (PS and PE), by facilitating binding of calcium and coagulation factors [144, 145]. The clinical significance of this action is exemplified in anti-phospholipid syndrome patients who show enhanced levels of many (31) 12-HETE-PLs [146], accounting for their pro-thrombotic disposition. Herein, we could detect 12-HETE liberated in thrombin activated platelet supernatants. However, given the recently defined pathophysiological significance of PL-esterified 12-HETE, a thorough characterization of 12-HETE generation and flux to generate 12-HETE-PLs, plasmalogens, and additional biochemical adducts as a function of time in activated platelet lysate rather than supernatant would be worthwhile exploring.

Currently, we focused on the previously characterized autocrine platelet agonists derived in the COX-1 metabolic pathway demonstrating a quantitative UHPLC-MS/MS method for the targeted analysis of TXB2, HHT and its oxidized derivative KHT. Although TXA2 actions on platelet responsiveness are outlined in details, that of HHT and KHT is overlooked with only one article showing that synthetic KHT (within a concentration of 0.5-5 μM) can inhibit platelet aggregation [146]. Therefore, presence of KHT in thrombin activated platelet releasate may be considered as part of a negative regulatory feedback loop following activation.

Overall, our endeavors have set an example of an innovative approach for simultaneous targeted and untargeted detection of oxylipins that orchestrate platelet functions. A potential translational significance of our research might be appreciated in the context of clinical manifestations of cardiovascular diseases where COX-1 inhibition by aspirin still remains the first line of anti-platelet strategy [9].

1.4. Conclusions

The new LC-MS method was developed and is well suited for analysis of primary platelet-related oxylipins and fatty acids in resting and thrombin activated platelet supernatant samples. Data independent MS acquisition with SWATH windows allowed detection and quantification of targeted compounds (TXB2, HHT, KHT) in releasates, and at the same time detection of several other compounds significantly altered in the thrombin activated samples. High resolution mass analysis and fragmentation spectra for all detected features made it possible to identify these compounds.

The described method allowed tracking the release of eicosanoids. The COX-1 derived lipid mediator TXB2 features as one of the most effective pro-thrombotic lipid agonist in a positive feedback loop to synergistically substantiate response to other platelet activating stimuli [142]. Besides, we detected a pool of oxidized (12-HETE, 12-HEPE, PGE2, HHT, KHT) and non-oxidized polyunsaturated fatty acids (FA(20:2), FA(20:3), FA(20:4), FA(20:5)) released upon platelet activation by thrombin. These oxylipins and PUFAs may exert diverse biological functions depending on tissue of action and presence of enzymes. This work gives an indication of a wider molecular diversity of releasates than typically shown in pathway maps (e.g. KEGG) on platelet activation.

Declaration of conflict of interests

The authors declare no conflict of interests.

Acknowledgements

This project was funded by the Deutsche Forschungsgemeinschaft (DFG, German Research Foundation) – Project number 374031971 – TRR 240.

1.5. Supplementary materials

1.5.1. Internal standards

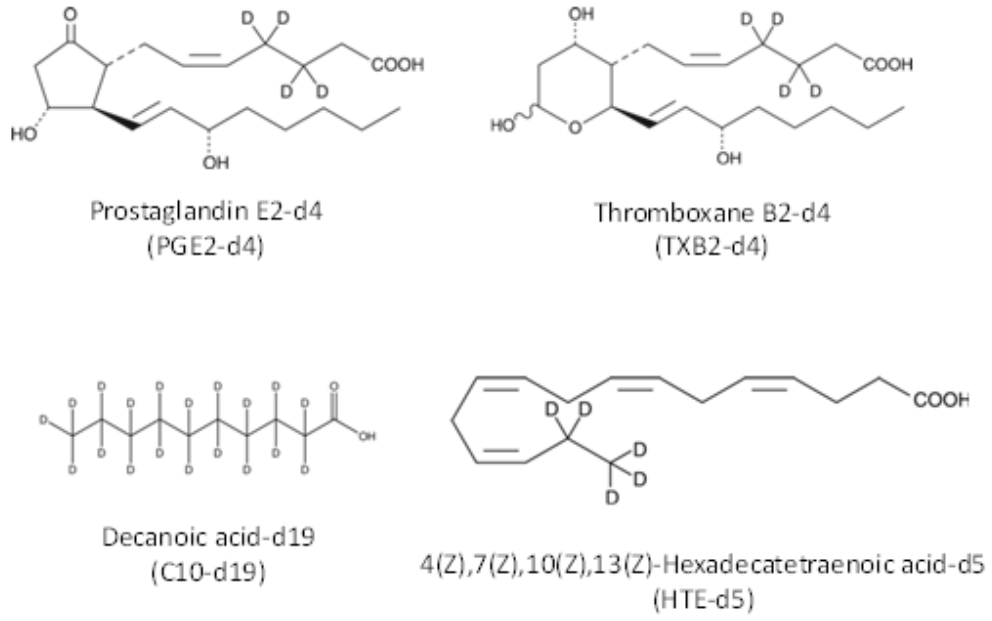

Figure 34. *Structures of internal standards.*

1.5.2. Synthesis of KHT

KHT was synthetized as described in the 'Materials and methods' section (1.2.2 in main document). The standard of HHT was analysed together with the *synthesis sample* to quantify residual HHT in the KHT reaction product. A stock solution of the HHT standard was prepared as follows: 1 µL of C11:0 internal standards was put into a glass 1.5 mL vial (10 µg/mL in MeOH), then 1 µL solution of HHT (0.1 mg/ml in EtOH) was added and the mixture was diluted with 198 µL of methanol. The *standard* had the same concentration of HHT, as the *synthesis sample*, just without Dess-Martin reagent.

The *synthesis sample* and the *standards* were analysed in pairs, each pair 3 times, by LC-MS/MS to calculate the yield of the reaction and final concentration of KHT. An equal

detector response was assumed for KHT and HHT. Losses due to transfer into new vials were compensated by the internal standard (C11:0) and residual HHT in the reaction mixture was subtracted. The reaction yield was 98.4%. Assuming an equal detector response for KHT and HHT, the KHT concentration in the KHT standard (stock) solution obtained after re-dissolution in MeOH was 0.45 ± 0.03 µg/mL.

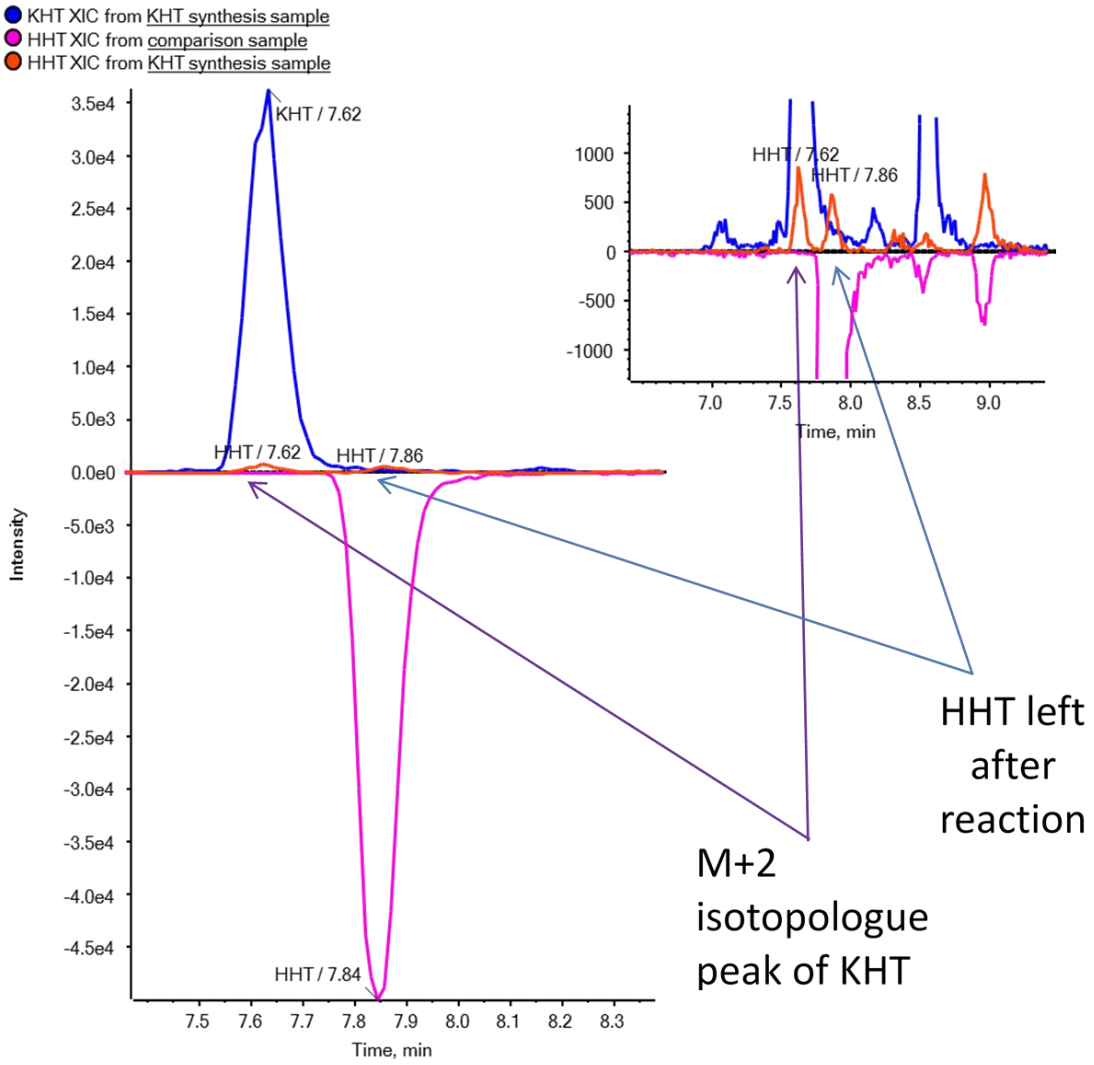

Figure 35. *Analysis of reaction product from KHT synthesis and HHT reference sample. Blue trace, EIC of KHT precursor ion [M-H]- (m/z 277.181 ± 0.01) after reaction. Red trace, EIC of HHT precursor ion [M-H]- (m/z 279.197 ± 0.01) after reaction; peak at 7.86 min corresponds to unreacted, residual HHT; peak at 7.62 corresponds to the M+2 isotopologue peak of KHT product. Pink trace, HHT reference EIC of HHT precursor ion [M-H]- (m/z 279.197 ± 0.01) of a reference sample prepared as HHT standard spiked to MeOH with the same concentration as in the reaction sample.*

Quenching of Dess Martin reagent

In order to avoid losses of precious KHT substance, the reaction mixture was not further purified but used directly as stock solution to prepare the standards. The excess of Dess Martin reagent in the reaction mixture was quenched by MeOH. In order to test for residual activity of the reagent, an aliquot of the KHT reaction product was spiked with HHT and the change of HHT area was monitored over time. The following sample was prepared.

Sample preparation: 30 µL of HHT solution (1 µg/mL in MeOH) was added to 100 µL of the *synthesis sample* (0.45 ± 0.03 µg/mL KHT, quenched with methanol).

The sample was then kept for 5 days at 4°C in the autosampler and analysed 4 times during this time. The residual activity of reagent was monitored as ratio of peak areas of KHT to HHT. It remained constant within 1.9% and did not increase over time which means that no residual activity of the reagent existed.

1.5.3. Identification of KHT by MS/MS spectrum and comparison with HHT fragmentation spectrum

The reaction product KHT was then characterized and identified by its MS (accurate mass, isotope pattern) and MS/MS spectra (Figure 28 of main document and accurate mass information in Suppl. Materials Table 10). For sake of convenience the corresponding data of HHT are given as well.

Table 10. *Accurate mass information of precursor and fragment ions of KHT and HHT.*

	Experimental *m/z*	Formula	Theoretical *m/z*	Error *ppm*
KHT	277.1810	$C_{17}H_{25}O_3^-$	277.1809	0.4
	233.1915	$C_{16}H_{25}O^-$	233.1911	1.7
	139.1128	$C_9H_{15}O^-$	139.1128	0.0
	113.0981	$C_7H_{13}O^-$	113.0972	8.0
	107.0879	$C_8H_{11}^-$	107.0866	12.1
HHT	279.1972	$C_{17}H_{27}O_3^-$	279.1966	2.1
	261.1866	$C_{17}H_{25}O_2^-$	261.1860	2.3
	217.1963	$C_{16}H_{25}^-$	217.1962	0.5
	179.1078	$C_{11}H_{15}O_2^-$	179.1078	0.0
	135.1182	$C_{10}H_{15}^-$	135.1179	2.2

1.5.4. MS/MS spectra of targeted compounds

Figure 36 shows the fragmentation of the targeted compounds, HHT, KHT and TXB2. The fragment ion used for quantification is indicated in red. The corresponding MS/MS spectra of the internal standards are depicted in Figure 37.

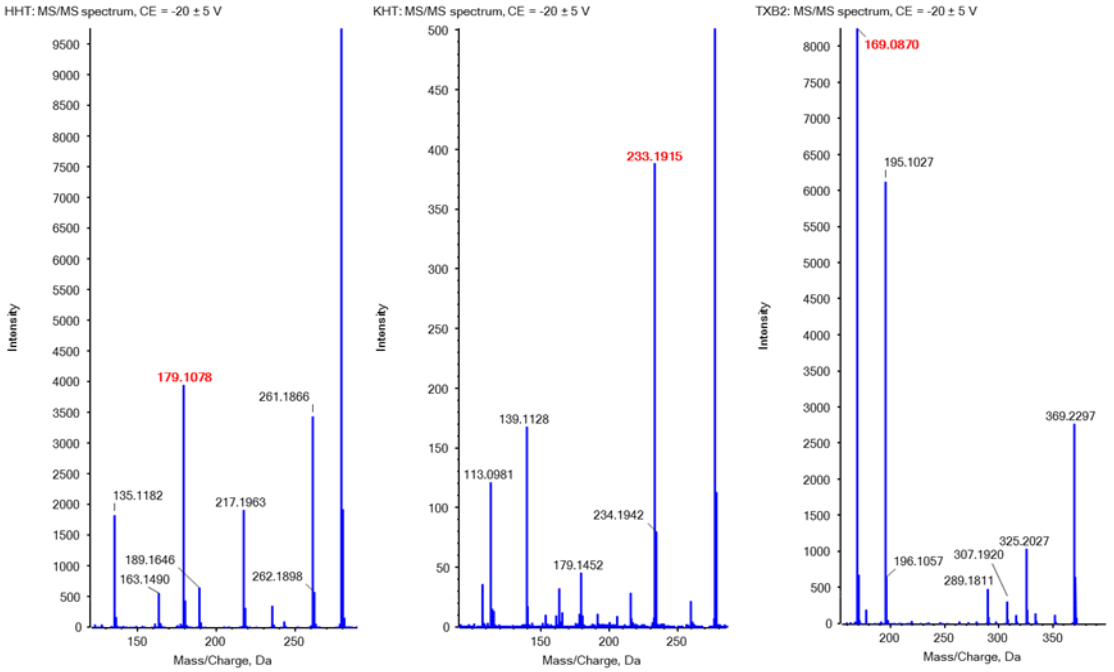

Figure 36. *MS/MS spectra of the targeted compounds. Fragment ion used for quantitation indicated in red.*

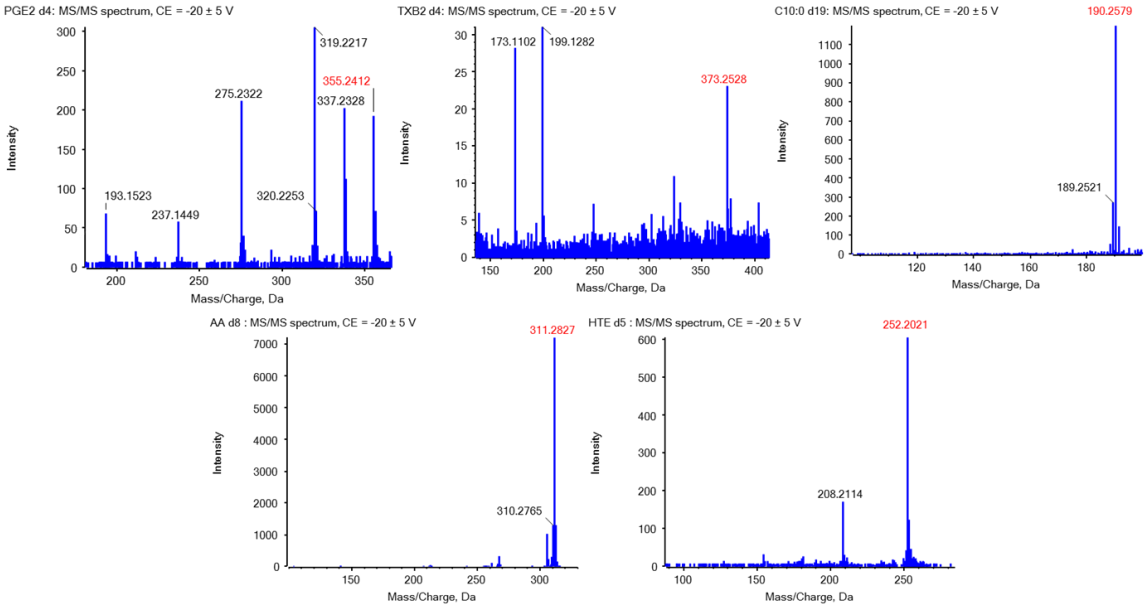

Figure 37. *Fragmentation of internal standards used. Precursor ion (marked red) was used for quantification.*

1.5.5. LC-MS method development

1.5.5.1. Column screening

Initially two different columns previously successfully employed in lipidomics analysis were screened for their capability to resolve KHT and HHT. One column was the ACQUITY UPLC CSH C18 (100 mm × 2.1 mm; 1.7 µm; Waters Corporation, Milford, MA, USA) and the other a Kinetex (150 mm × 2.1 mm; 2.6 µm core-shell particle; Phenomenex, Torrance, CA, USA). The comparison is shown in Figure 38. The Kinetex column gave broad beaks under conditions which are favourable in terms of ionisation efficiencies of fatty acids. In contrast, the Waters CSH C18 showed good peak shape and good peak resolution between HHT and KHT, so no further columns were evaluated.

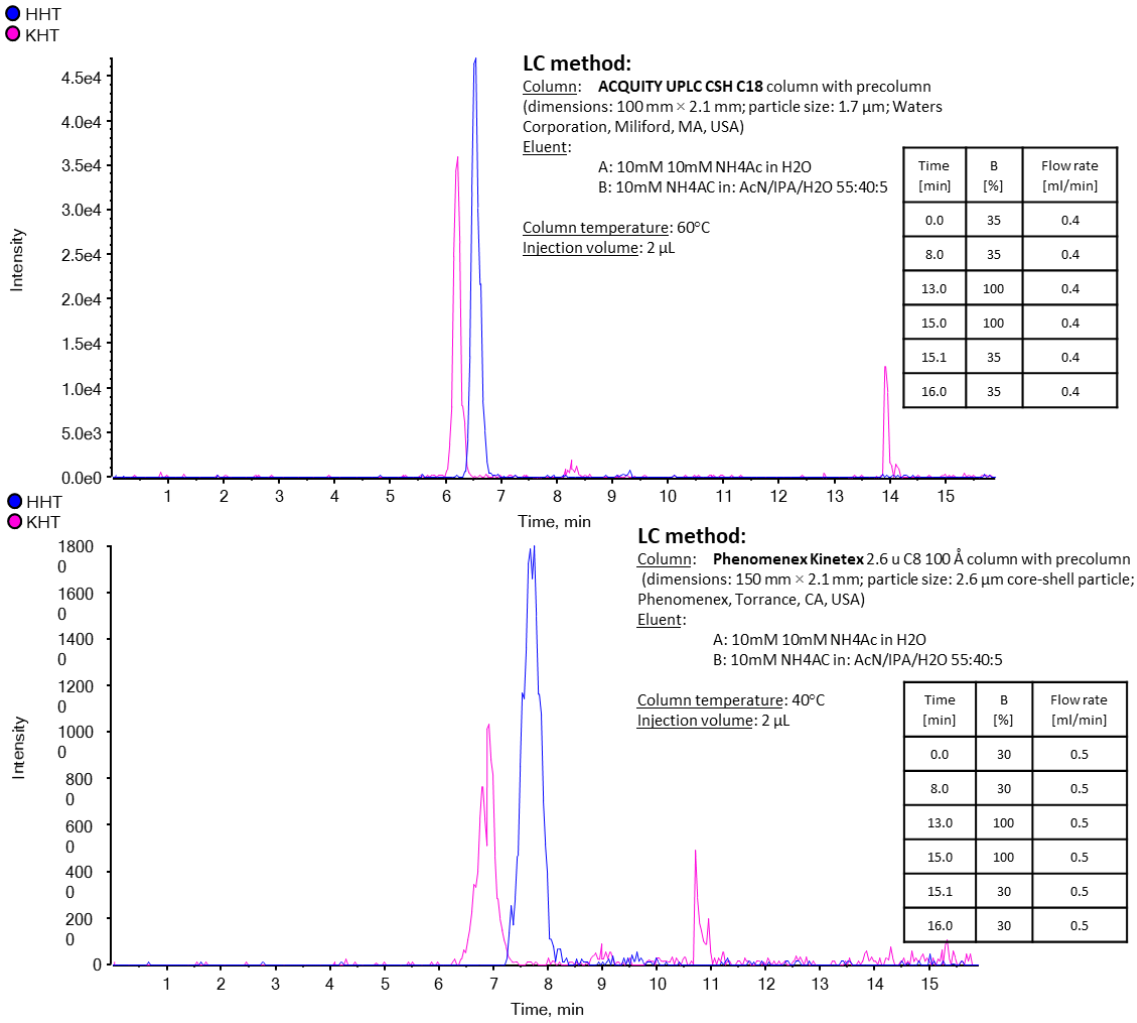

Figure 38. *Column screening. Comparison of KHT/HHT separations on fully porous sub-2µm particle column CSH C18 (top) and superficially porous 2.6 µm Kinetex C8 (bottom).*

1.5.5.2.Additive effect

Different additives (ammonium acetate, ammonium formate, as well as mixtures with corresponding acids) to the mobile phase (water, acetonitrile and isopropanol) were studied (Figure 39), in order to figure out which one provides better peak shapes and supports most effectively ESI ionisation efficiencies for obtaining good assay sensitivities for oxidized fatty acids. The results were evaluated in terms of peak areas and signal-to-noise ratios for HHT and TXB2 (Table 11). KHT behaved very similar to HHT.

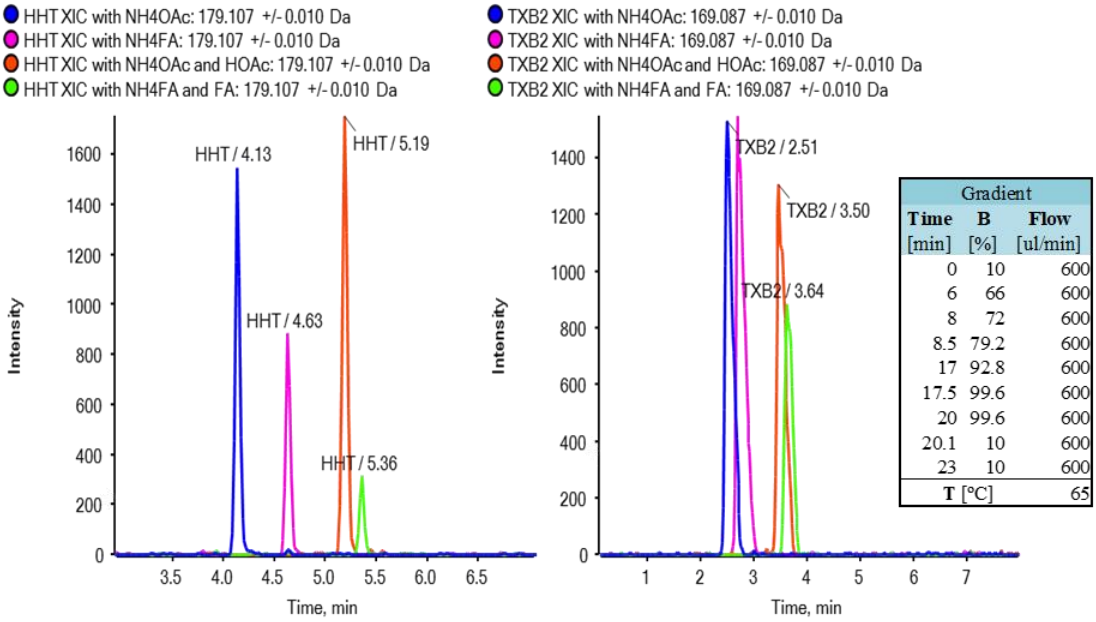

Figure 39. *Chromatograms of HHT and TXB2 with different additives to the mobile phase. Concentration of additive: 10 mM, concentration of acid (if present): 0.1%. A: H2O + additives, B: ACN/IPA/H2O (49:50:1; v/v/v) + additives. CE = -20 +/- 5 V. Colours show EICs obtained with different additives: NH_4OAc (blue), NH_4FA (pink), NH_4OAc and HOAc (dark orange), NH_4FA and FA (green).*

As can be seen from Table 11 and Figure 39, ammonium acetate (NH_4Ac) was chosen as the best compromise between the two analytes, which showed good results for both HHT and TXB2. Under these conditions the proton of the carboxylic group can be easily abstracted, favourably enhancing ionisation in the negative ESI mode.

Table 11. *Effect of additives on signal-to-noise ratio and peak areas.*

Additive	SIGNAL-TO-NOISE		PEAK AREA	
	HHT	TXB2	HHT	TXB2
NH_4Ac	184.7	638.0	5.12E+03	1.58E+04
NH_4FA	105.6	184.6	3.03E+03	1.74E+04
NH_4Ac/HOAc	206.6	156.2	6.26E+03	1.45E+04
NH_4FA/FA	37.9	105.6	1.05E+03	9.28E+03

1.5.5.3.MS parameters

After optimization of LC-conditions and selection of specific fragments for quantitative analysis of the targeted compounds, ion source parameters were optimized to maximize sensitivity. Amongst others, the collision energy (CE) was systematically optimized (Figure 41). As can be seen, an intermediate CE of -20 V gave the highest signal intensities in all cases and was selected for the final method.

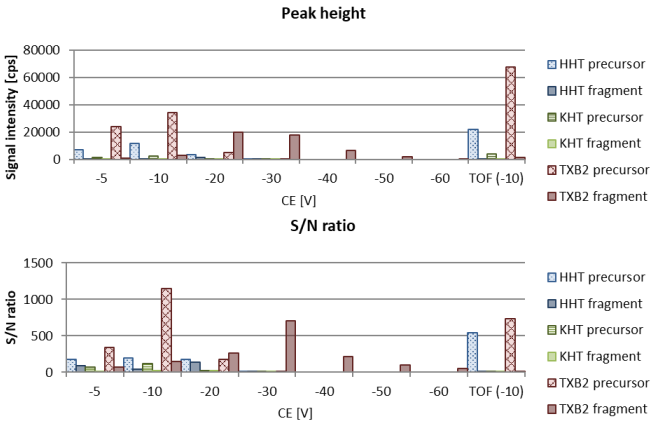

Figure 40*. Signal intensities (top) and signal-to-noise (S/N) (bottom) for precursor and fragment ions in TOF-MS and MS2 experiments in dependence on different collision energies (CEs). Accumulation time for MS2 experiments was equal to 100 ms, and for TOF experiment also to 100 ms; standards were dissolved in MeOH.*

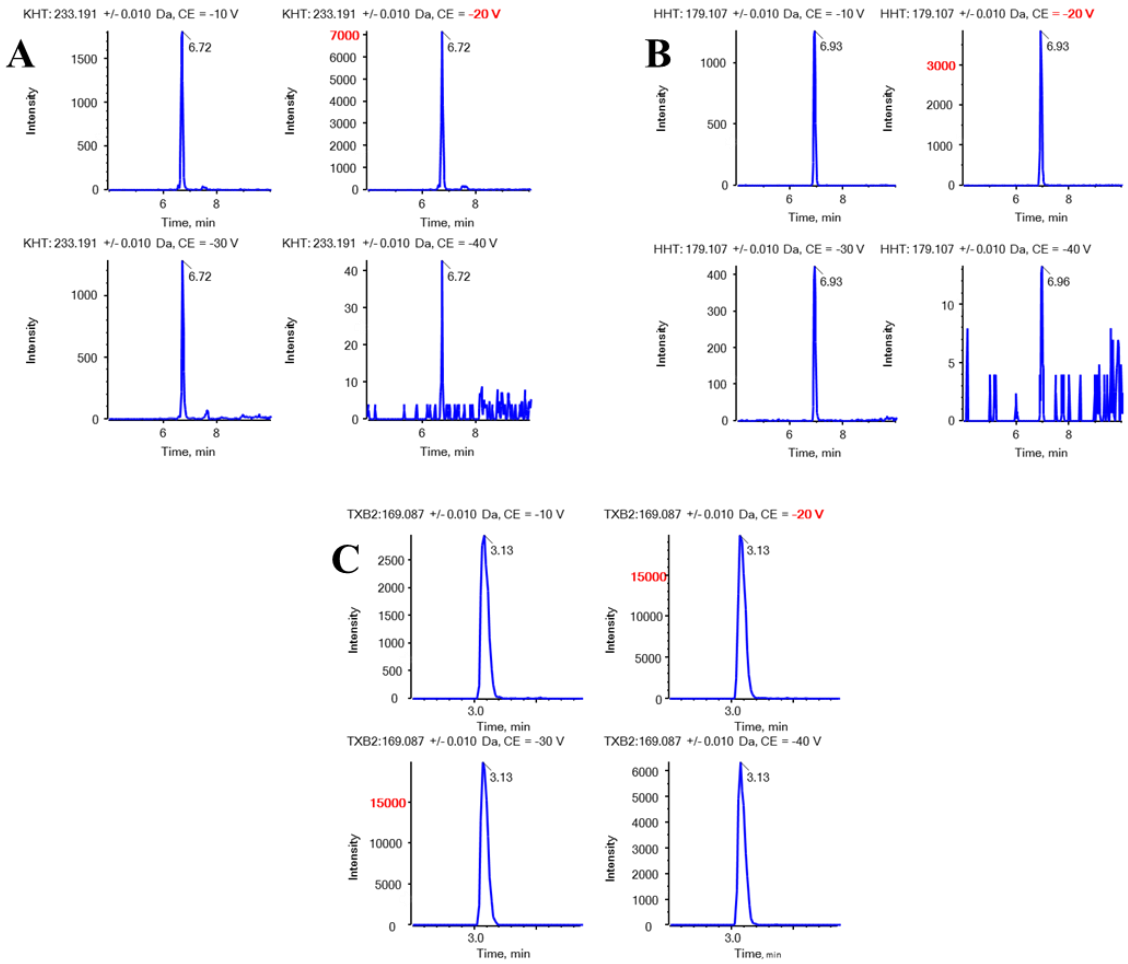

Figure 41. *Chromatograms from the study of the effect of CE on signal intensity for **A**: KHT, **B**: HHT and **C**: TXB2.*

1.5.6. Final LC-MS method: Cycle time, data points per peak and absence of targets in blank matrix

The final method was then examined whether a sufficient number of data points were available across the peaks for an accurate quantification (required at least 10 data points per peak). Figure 42 shows EIC chromatograms of the targeted compounds with MS data points (which depend on MS cycle time) indicated. Each data point stands for a full MS cycle consisting of the MS experiments summarized in Table 5 (1 full MS scan and 19 MS/MS experiments). The red traces in Figure 42 clearly document that there are enough data points across the peak (21 for KHT, 18 for HHT, 32 for TXB2). Figure 42 also depicts an overlay of the 10 ng/mL calibrants (lowest calibrants) (blue trace) and blank matrix (pink trace). It becomes evident that the target analytes were virtually absent in the blank

matrix. The lowest calibrant (at LOQ level) can be reasonably well detected at this concentration with a good signal to noise ratio.

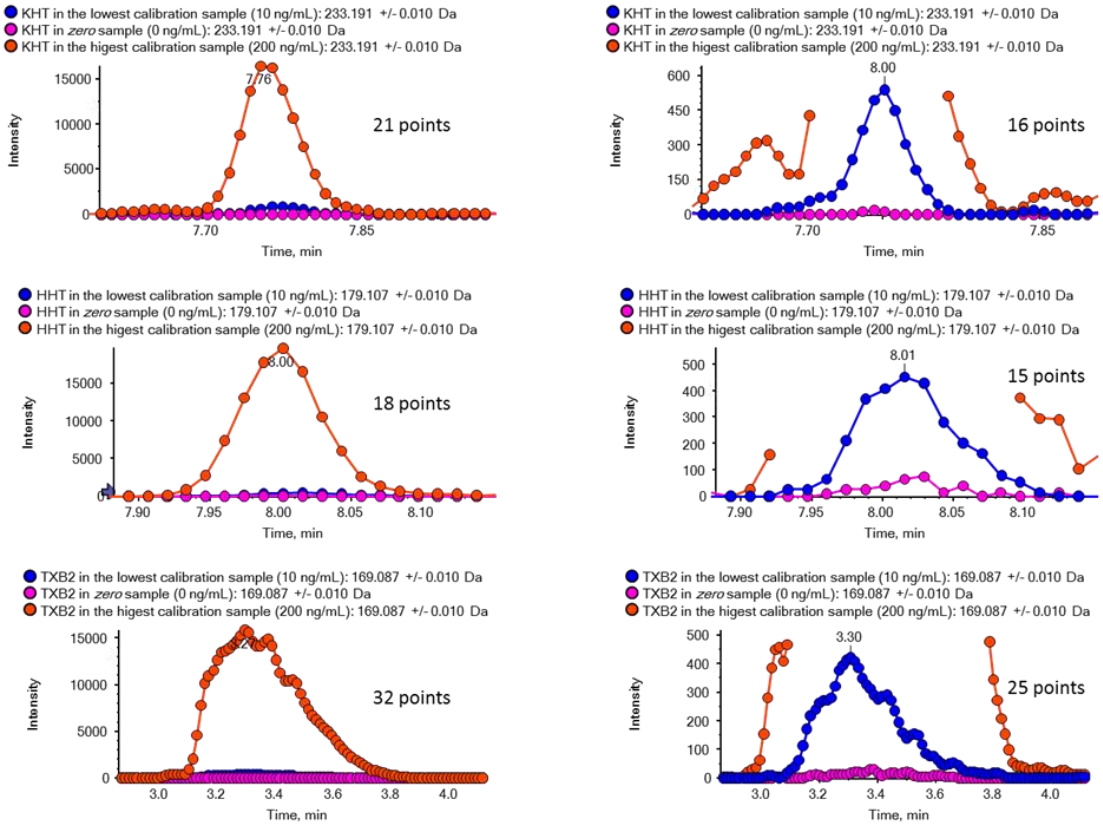

Figure 42. *Data points per peak for targeted compounds (KHT, top; HHT, middle; TXB2, bottom) and absence of targets in blank matrix. Red trace, highest calibrant with 200 ng/mL); pink trace, blank matrix (resting platelet supernatants) without spiking targeted compounds; blue trace, lowest calibrant with 10 ng/mL).*

1.5.7. Uniqueness peculiarities and potential of SWATH acquisition

It is already mentioned in the main document (part 1.3.3) that carefully chosen EIC might increase sensitivity of an analytical method when SWATH (together with TOF-MS) experiments are used. There is a choice of extracting precursor ion from TOF-MS or from SWATH or one of fragment ions from SWATH. There are many factors which will influence sensitivity for any EIC in an experiment, among others: accumulation time, mass range, collision energy, *m/z* extraction window, interferences in matrix. Each analyte should be approached individually for the best EIC.

In this paragraph 2 more examples are given, where method has gained sensitivity for oxylipins, because of switching to EIC of a fragment in SWATH. The difference to the example in 1.3.3 part of the main document is that accumulation time of SWATH is shorter than TOF-MS (20 vs. 50 ms) as the examples are given of not targeted compounds. However, to clarify the situation, EIC from precursor *m/z* might be more sensitive for other compounds, especially when a simpler matrix is used.

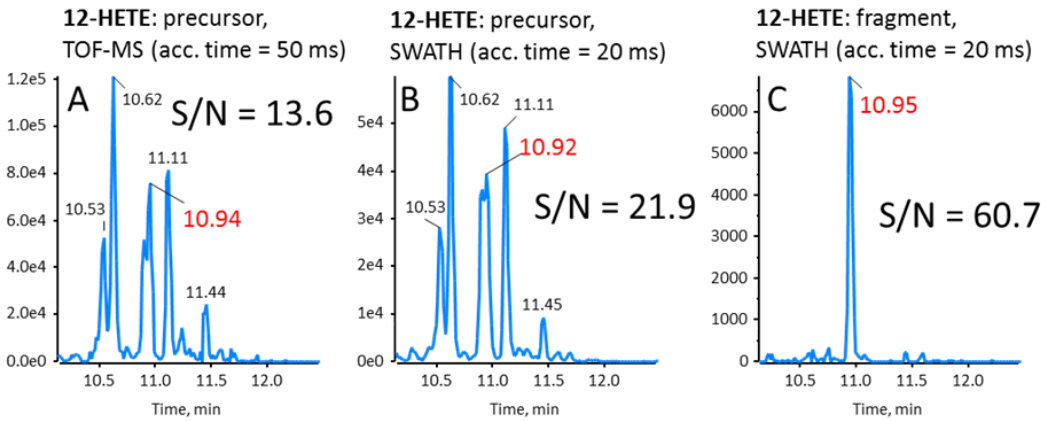

Figure 43*. EIC chromatograms extracted from the same run (sample from donor 2, thrombin treated).* ***A****: EIC of precursor ion (m/z 319.2250 ± 0.010) extracted from TOF MS experiment;* ***B*** *and* ***C****: EICs of precursor ion (m/z 319.2250 ± 0.010) and fragment ion (m/z 179.1080 ± 0.010), respectively, extracted from the SWATH window (i.e. MS/MS experiment). MS/MS spectrum of 12-HETE can be found in Figure 47 in this document.*

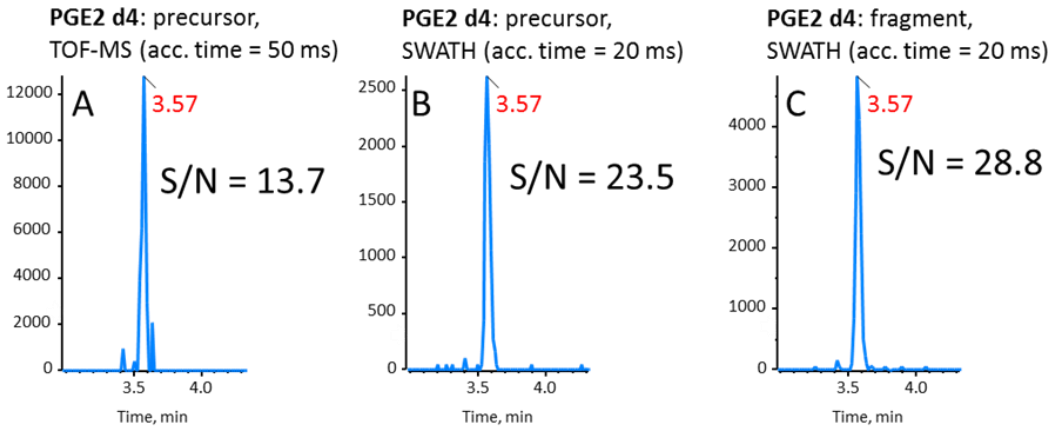

Figure 44. *EIC chromatograms extracted from the same run (sample from donor 2, thrombin treated, sample was spiked with internal standard PGE2 d4 at 120 µg/mL).* ***A****: EIC of precursor ion (m/z 355.241 ± 0.010) extracted from TOF MS experiment;* ***B*** *and* ***C****: EICs of precursor ion (m/z 355.241 ± 0.010) and fragment ion (m/z 319.221 ± 0.010), respectively, extracted from the SWATH window (i.e. MS/MS experiment). MS/MS spectrum of PGE2 d4 can be found in Figure 37 in this document.*

1.5.8. Matrix effect, extraction recovery, process efficiency

Matrix effect (ME), extraction recovery (RE) and process efficiency (PE) were calculated according to the Matuszewski protocols:

$$ME = \frac{B}{A} \cdot 100\ [\%] \qquad RE = \frac{C}{B} \cdot 100\ [\%] \qquad PE = \frac{C}{A} \cdot 100\ [\%]$$

A is the peak area (not normalized) in standards spiked to MeOH, B is the peak area in the post-spiked samples (standards spiked to extracted matrix just before LC-MS analysis) and C is the peak area in the pre-spiked samples (analytes added to matrix before extraction).

Table 12. *Results of determination of matrix effect, extraction recovery and process efficiency for targeted compounds.*

Compound concentration [ng/mL]	**Matrix effect** [%]			**Extraction recovery** [%]			**Process efficiency** [%]		
	TXB2	HHT	KHT	TXB2	HHT	KHT	TXB2	HHT	KHT
40	96.3	103.7	104.1	85.5	104.4	97.6	82.4	108.3	101.7
80	108.8	113.5	121.2	68.2	88.4	84.3	74.2	100.4	102.2
160	113.4	120.8	117.6	72.8	89.5	102.4	82.5	108.2	120.4
200	86.1	96.3	90.5	80.9	98.4	101.4	69.7	94.7	91.7
Mean [%]:	**101.2**	**108.6**	**108.4**	**76.9**	**95.2**	**96.4**	**77.2**	**102.9**	**104.0**
Standard dev. [%]:	10.7	9.4	12.1	6.8	6.6	7.2	5.5	5.7	10.3
CV [%]:	10.6	8.6	11.2	8.8	6.9	7.5	7.1	5.6	9.9

1.5.9. Untargeted analysis

1.5.9.1.MS-DIAL parameters

General:

MS-DIAL parameters used for untargeted analysis:
Ionisation type: Soft ionisation
Method type: Data independent MS/MS
Data type (MS1): Profile data
Data type (MS/MS): Profile data
Ion mode: Negative ion mode
Targeted omics: Lipidomics

Data collection

Retention time begin: 0.5 min
Retention time end: 20 min
Mass range begin: 50 Da
Mass range end: 500 Da
MS1 tolerance: 0.01 Da
MS2 tolerance: 0.025 Da
Maximum charged number: 2
Number of threads: 1

Peak detection

Smoothing method: Linear weighted moving average
Smoothing level: 3 scan
Minimum peak width: 5 scan
Minimum peak height: 500 amplitude
Mass slice width: 0.1 Da

MS2Dec

Sigma window value: 0.5
MS/MS abundance cut off: 0 amplitude
Exclude after precursor ion: yes
Keep the isotopic ions until: 0.5 Da
Keep the isotopic ions w/o MS2Dec: no

Identification:

Solvent type: CH_3COONH_4
Collision type: CID
Lipid classes: all
Accurate mass tolerance (MS1): 0.01 Da
Accurate mass tolerance (MS2): 0.05 Da
Identification score cut off: 80 %
Use retention information for scoring: no

Adducts: $[M-H]^-$, $[M+Hac-H]^-$

Alignment:

Reference file: one of the QCs
Retention time tolerance: 0.5 min
MS1 tolerance: 0.015 Da
Retention time factor: 0.2
MS1 factor: 0.8
Peak count filter: 0 %
N% detected in at least one group: 51 %
Detected in all QCs: no

1.5.9.2.Confirmation of structural annotations with authentic standards

Structural annotations of MS-DIAL were confirmed by purchased authentic standards. Standards used for identification were purchased from Cayman Chemical (Ann Arbor, MI, USA): 5*Z*,14*Z*-eicosadienoic acid (FA(20:2)), dihomogammalinolenic acid (FA(20:3)), arachidonic acid (FA(20:4)), 5*Z*,8*Z*,11*Z*,14*Z*,17*Z*-eicosapentaenoic acid (FA(20:5)), prostaglandin E2, 12-HETE and 12-HEPE. 11*Z*-Eicosenoic acid was bought from Merck (Sigma Aldrich) (Munich, Germany). Additionally, to show method specificity prostaglandin D2 (PGD2), alpha-linolenic acid (ALA) and gamma-linolenic acid (GLA) were purchased from Cayman Chemical. Standard solution, sample (donor 5) and standards spiked to sample were injected.

Compounds were considered identified if at least 3 of 5 criteria were passed:
1. Retention time match: less than 2 s (0.03 min) difference between compound found in sample and standard.
2. Match of accurate mass of precursor ion from experiment 1 (Table 5): less than 5 mDa difference (*m/z* difference smaller than 0.005) between sample and standard.
3. Match of accurate mass of precursor ion from SWATH window: less than 5 mDa difference (*m/z* difference smaller than 0.005) between sample and standard.
4. Match of accurate mass of 2^{nd} and 3^{rd} isotopic peak from experiment 1: less than 5 mDa difference (*m/z* difference smaller than 0.005) between sample and standard.
5. Match of accurate mass of 3 main fragment *m/z* (different than precursor) from SWATH window: less than 5 mDa difference (*m/z* difference smaller than 0.005) between sample and standard.

Different criteria were used, because of different MS properties of compounds: fatty acids do not fragment well, so fragmentation information could not be used. On the other hand, oxylipins, present in the samples at low concentration, are not easily detected in the TOF-MS experiment 1, which lacks specificity.

Table 13 shows also relative distribution of peak heights (always compared to the first isotopic peak of precursor ion). These are additional information and were not used for compound identification. It should also be noted that mass accuracies may be lower if the compound is present at low concentrations close to LOQ.

Table 13. *Identification of significantly altered compounds found in untargeted analysis, based on comparison with bought standards.*

Compounds	Precursor ions and isotopic distribution					Fragment ions (CE = 20 +/- 5)					Retention time		
	m/z			Relative height		m/z			Relative height				
	Standard in MeOH	Sample	Difference (*sample - standard in MeOH*)	Standard in MeOH	Sample	Standard in MeOH	Sample	Difference (*sample - standard in MeOH*)	Standard in MeOH	Sample	Standard in MeOH	Sample	Difference (*sample - standard in MeOH*)
	Da	*Da*	*mDa*			*Da*	*Da*	*mDa*			*min*	*min*	*s*
FA(20:1)	309.2767	309.2776	0.89	100	100	309.2770	309.2784	1.41	100	100	14.571	14.571	0.00
	310.2808	310.2813	0.46	25.0	24.0								
	311.2832	311.2829	-0.28	2.9	2.0								
FA(20:2)	307.2609	307.2635	2.61	100	100	307.2613	307.2630	1.75	100	100	14.000	14.006	0.28
	308.2636	308.2621	-1.49	24.0	39.8	255.2310			4.3				
	309.2653	309.2727	7.34	2.2	2.1								
FA(20:3)	305.2450	305.2460	0.93	100	100	305.2453	305.2463	1.07	100	100	13.488	13.497	0.54
	306.2486	306.2545	5.87	23.5	39.1								
	307.2524	307.2551	2.72	3.1	11.3								
FA(20:4)	307.2609	307.2635	2.61	100	100	303.2298	303.2317	1.95	100	100	13.046	13.050	0.24
	308.2636	308.2621	-1.49	24.0	39.8	259.2405	259.241	0.43	7.0	7.8			
	309.2653	309.2727	7.34	2.2	2.1								
FA(20:5)	301.2144	301.2134	-0.96	100.0	100.0	301.2147	301.2146	-0.09	100.0	100.0	12.482	12.454	-1.68
	302.2172	302.2181	0.85	23.5	30.5	257.2250	257.2246	-0.39	23.4	24.3			
	303.2207	303.2169	-3.81	3.3	4.6	203.1790	203.1766	-2.37	4.8	6.9			
12-HETE	319.2245	319.2255	1.03	100.0	100.0	319.2245	319.226	1.51	100	100	10.645	10.650	0.32
	320.2276	320.2278	0.19	26.5	44.3	301.2139	301.2175	3.52	94.4	94.4			
	321.2306	321.2271	-3.48	3.3	9.3	257.224	257.2237	-0.30	80.6	80.6			
						208.1090	208.1092	0.20	65.2	65.2			
						179.1061	179.1075	1.31	56.1	56.1			
12-HEPE	317.2088	317.2089	0.11	100	100	317.2093	317.2085	-0.81	100	100	9.870	9.873	0.18
	318.2124	318.2125	0.13	19.9	21.4	299.1977	299.1975	-0.16	94.3	94.3			
	319.2137	319.2165	2.86	3.6	16.1	255.2089	255.2039	-5.00	80.5	80.5			
						208.1078	208.1082	0.46	65.6	65.6			
						179.1058	179.1069	1.12	56.5	56.5			
PGE2						351.2145	351.2188	4.35	100	100	3.658	3.671	0.78
						333.2039	333.199	-4.89	198.0	155.6			
						315.1935	315.1946	1.09	240.1	291.3			
						271.2041	271.2015	-2.59	212.4	243.4			
						233.1158			40.8				
						189.1266	189.1281	1.55	68.2	103.6			

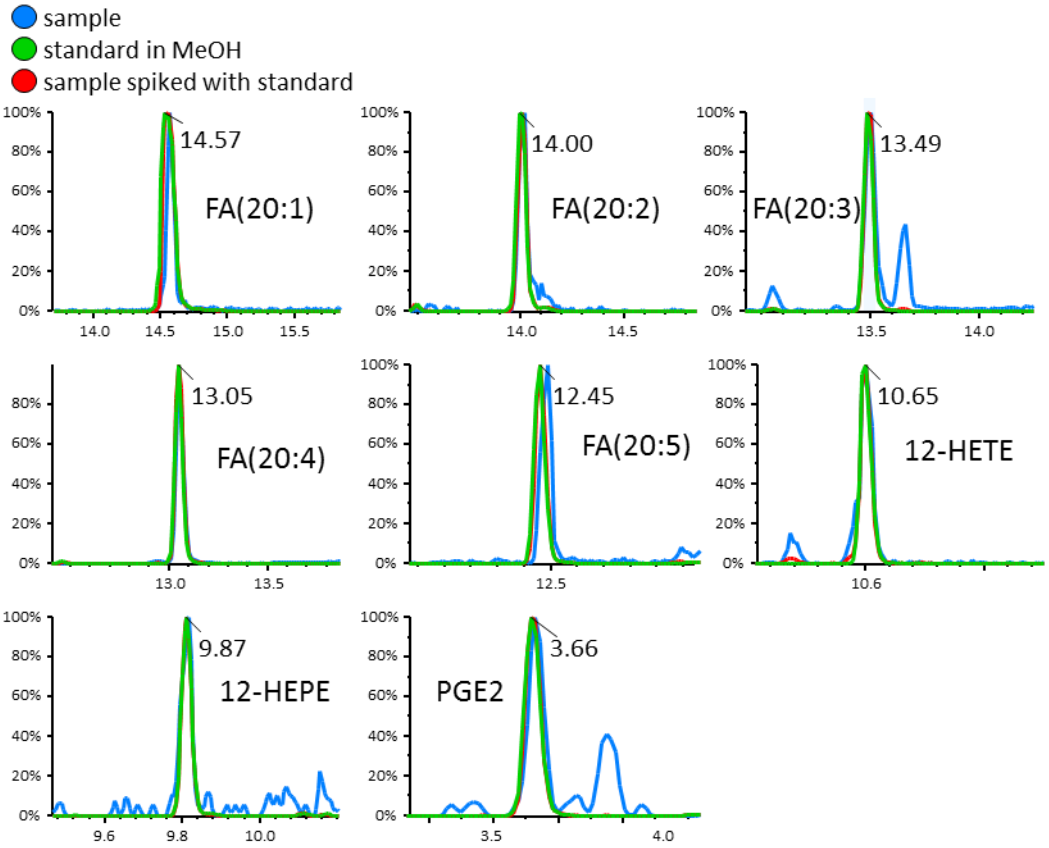

Figure 45. *Comparison of retention times between standard, sample, and sample spiked with standard for structurally annotated compounds found by untargeted analysis and data processing with MS-DIAL. Blue: EIC of precursor m/z from analysed sample (donor 5, thrombin treatment); green: the same EIC from standards dissolved in MeOH; red: EIC from sample (donor 5, thrombin treatment) additionally spiked with standards.*

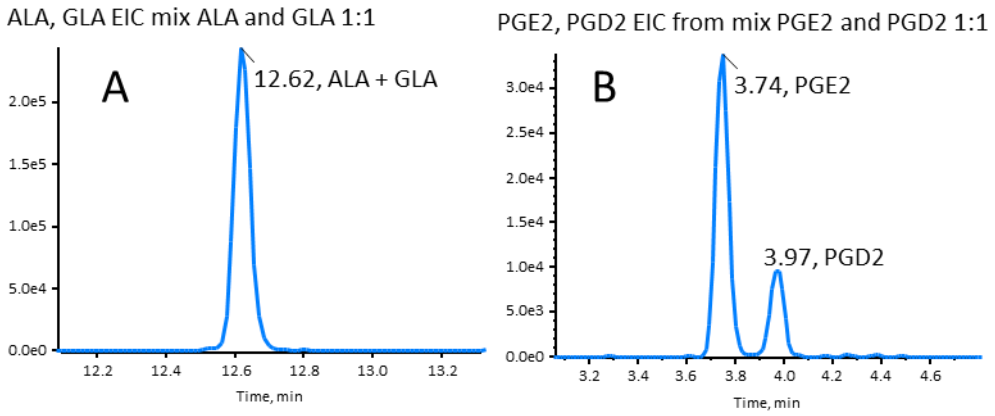

Figure 46. A*: EICs of precursor of FA(18:3) (m/z 277.217 ± 0.010) from experiment 1 showing no separation of isomeric fatty acids, which differ with double bond positions;* ***B****: EICs of precursor m/z of prostaglandins E2 and D2 (351.218 ± 0.010) from experiment 1 showing good separation of these compounds. Mixtures were prepared as standards dissolved in MeOH.*

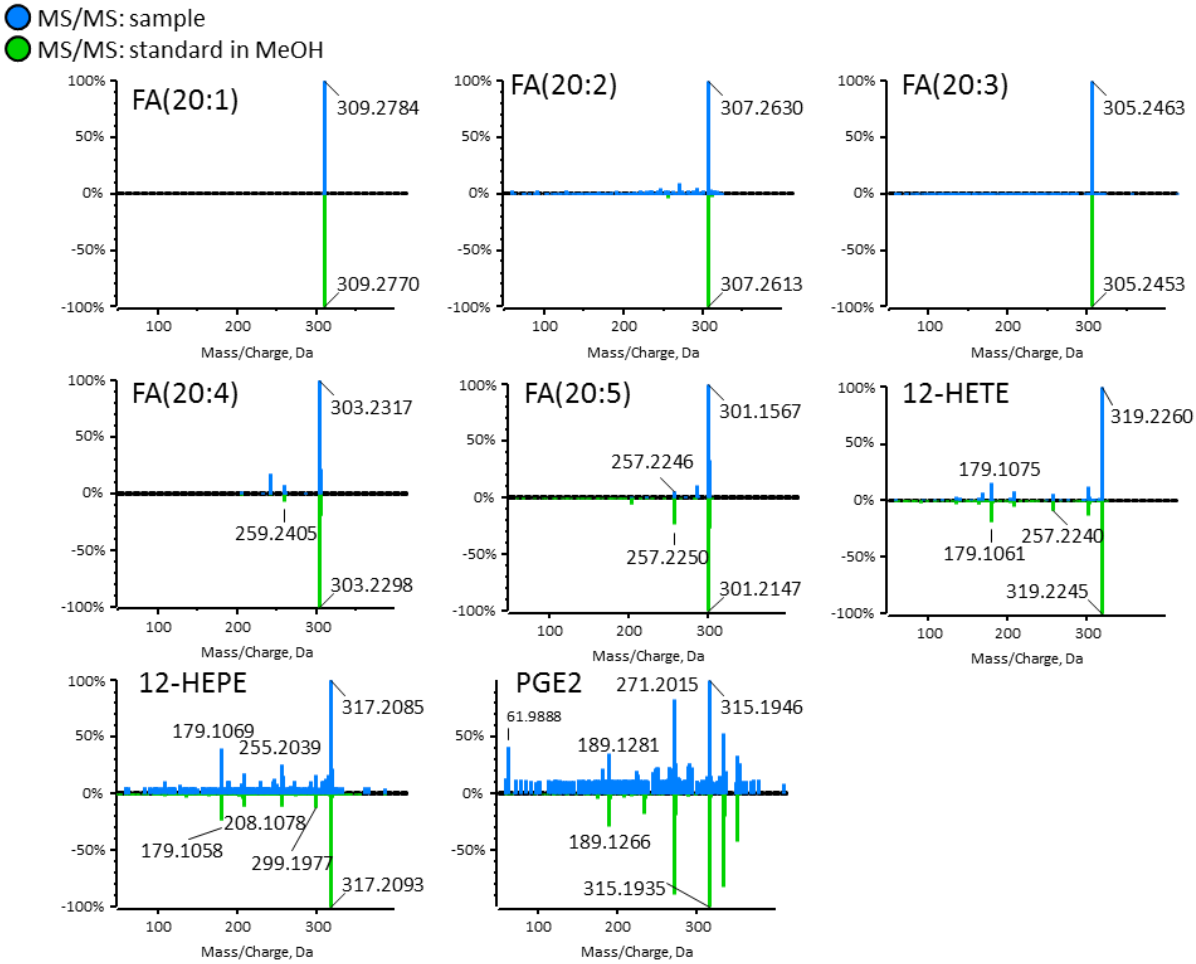

Figure 47. *Comparison of MS/MS spectra for structurally annotated compounds found by untargeted analysis. Blue: Raw spectrum from analysed sample (donor 5, thrombin treatment); green: spectrum from standard dissolved in MeOH. CE = -20 ± 5.*

Table 14. *List of all features (precision lower than 30 %) found by untargeted analysis, n = 8 for each group.*

Name or alignment number	Mass [M-H]⁻ *m/z*	Retention time [min]	Internal standard used for normalization	Precision in QCs [%]	Paired *p*-value	Paired fold change	Suggested identification by MS-Dial
Identified compounds (confirmed by authentic standards)							
KHT	277.197	7.59	C10 d19	28.4	0.008	7.69	Unknown
HHT	279.197	7.83	AA d8	14.9	0.008	217.30	Unknown
FA(20:5)	301.217	12.40	HTE d5	13.8	0.008	4.00	FA(20:5)
FA(20:4)	303.233	12.98	HTE d5	12.7	0.008	9.09	FA(20:4)
FA(20:3)	305.248	13.42	AA d8	18.2	0.008	3.13	FA(20:3)
FA(20:2)	307.264	13.94	AA d8	10.7	0.016	4.76	FA(20:2)
FA(20:1)	309.280	14.50	AA d8	8.8	0.023	2.94	FA(20:1)
12-HEPE	317.212	9.77	HTE d5	20.0	0.008	5.00	Unknown
12-HETE	319.228	10.57	C10 d19	10.8	0.008	79.76	Unknown
PGE2	351.218	3.58	AA d8	24.5	0.008	6.25	Unknown
TXB2	369.228	3.23	HTE d5	8.0	0.008	182.40	Unknown
Unknown compounds							
1	84.993	1.56	HTE d5	14.6	0.844	1.04	Unknown
2	84.993	2.70	HTE d5	10.8	0.945	0.97	Unknown
3	101.062	0.63	AA d8	19.5	0.742	1.18	Unknown
4	115.077	0.96	C10 d19	10.2	0.461	0.85	FA(6:0)
5	118.993	0.68	HTE d5	10.7	0.383	1.14	Unknown
6	121.029	0.58	C10 d19	27.8	0.641	0.92	Unknown
7	121.030	1.16	HTE d5	18.7	0.742	1.05	Unknown

8	129.093	1.65	AA d8	10.9	0.742	0.90	Unknown
9	134.964	0.80	HTE d5	13.5	1.000	0.95	Unknown
10	134.988	1.67	HTE d5	15.5	0.641	1.30	Unknown
11	135.046	1.38	TXB2 d4	17.7	0.945	1.00	Unknown
12	138.020	1.71	TXB2 d4	29.1	0.461	0.85	Unknown
13	143.107	2.03	HTE d5	15.9	0.195	1.33	Unknown
14	143.107	2.91	AA d8	16.6	0.250	0.73	FA(8:0)
15	145.086	0.94	TXB2 d4	15.1	0.547	0.90	Unknown
16	157.123	4.76	HTE d5	8.8	0.742	0.98	Unknown
17	157.123	14.20	TXB2 d4	19.0	0.844	1.11	Unknown
18	159.103	1.44	TXB2 d4	22.8	0.078	0.51	Unknown
19	162.982	0.68	HTE d5	16.6	0.547	1.14	Unknown
20	168.464	1.22	HTE d5	13.8	0.383	1.12	Unknown
21	168.990	1.22	HTE d5	11.5	0.641	1.12	Unknown
22	171.138	7.00	HTE d5	17.4	0.313	0.93	Unknown
23	171.139	7.15	AA d8	14.4	0.547	0.91	FA(10:0)
24	178.952	0.78	PGE2 d4	20.4	0.148	0.76	Unknown
25	185.154	9.20	HTE d5	20.1	0.461	0.90	Unknown
26	187.133	2.51	AA d8	27.6	0.313	1.39	Unknown
27	190.258	6.83	C10 d19	23.4	0.945	1.00	Unknown
28	194.988	0.82	TXB2 d4	19.4	0.195	0.79	Unknown
29	199.170	10.84	AA d8	14.1	0.547	1.08	FA(12:0)
30	201.148	4.02	TXB2 d4	18.5	0.844	1.14	Unknown
31	212.312	1.22	HTE d5	12.1	0.461	1.09	Unknown
32	213.186	11.68	PGE2 d4	12.4	0.195	0.83	Unknown
33	215.163	5.88	PGE2 d4	27.6	0.742	0.85	Unknown
34	218.985	2.24	HTE d5	13.9	0.945	1.18	Unknown
35	221.081	1.52	TXB2 d4	28.4	0.195	0.66	Unknown
36	225.109	2.86	C10 d19	22.8	0.945	0.99	Unknown
37	227.201	12.41	HTE d5	18.9	0.461	1.09	FA(14:0)
38	228.948	1.39	HTE d5	21.6	0.383	0.71	Unknown
39	228.973	1.55	HTE d5	24.9	0.844	0.96	Unknown
40	229.181	7.78	TXB2 d4	20.9	0.844	0.97	Unknown
41	239.128	4.33	AA d8	22.6	0.461	0.68	Unknown
42	241.216	12.82	HTE d5	11.8	0.641	1.06	Unknown
43	242.175	14.20	TXB2 d4	12.1	0.641	1.54	Unknown
44	242.175	2.47	TXB2 d4	12.5	1.000	0.95	Unknown
45	243.196	9.57	TXB2 d4	22.2	0.742	1.05	Unknown
46	252.200	10.28	TXB2 d4	20.8	0.945	1.15	Unknown
47	253.217	12.73	C10 d19	9.2	0.313	0.86	FA(16:1)
48	254.965	1.22	HTE d5	15.7	0.250	1.20	Unknown
49	255.233	13.51	HTE d5	9.6	0.547	1.11	FA(16:0)
50	262.975	2.24	PGE2 d4	16.4	0.547	0.93	Unknown
51	267.231	13.27	AA d8	29.4	0.742	1.22	Unknown
52	269.247	13.93	HTE d5	18.3	0.547	1.12	FA(17:0)
53	270.127	12.23	PGE2 d4	15.6	0.742	1.04	Unknown
54	271.226	11.14	PGE2 d4	21.9	0.461	0.95	Unknown
55	271.226	11.84	C10 d19	28.8	0.641	0.93	Juniperic acid
56	274.979	1.25	AA d8	13.0	0.547	1.03	Unknown
58	277.217	12.46	C10 d19	10.0	0.313	0.81	FA(18:3)
59	278.189	13.56	TXB2 d4	23.0	0.945	1.01	Unknown
60	278.919	2.16	HTE d5	25.3	0.313	1.27	Unknown
61	278.969	2.70	PGE2 d4	10.9	0.148	0.79	Unknown
63	279.233	13.08	AA d8	7.5	0.250	1.12	FA(18:2)
64	281.172	10.78	AA d8	19.9	0.844	0.88	Unknown
65	281.248	13.72	HTE d5	9.2	0.039	1.11	FA(18:1)
66	283.095	7.36	HTE d5	17.4	0.547	1.49	Unknown
67	283.117	1.55	HTE d5	20.6	0.313	1.23	Unknown
68	283.264	14.37	HTE d5	7.8	0.547	1.10	FA(18:0)
69	294.980	1.22	AA d8	9.5	0.383	1.09	Unknown
70	295.190	12.36	PGE2 d4	28.6	0.313	1.20	Unknown
71	297.048	10.93	C10 d19	26.7	0.844	0.94	Unknown
72	297.279	14.72	HTE d5	20.1	0.844	1.04	FA(19:0)
73	299.201	12.17	TXB2 d4	15.4	0.461	0.84	Unknown
74	299.258	11.56	HTE d5	27.5	0.844	0.91	Unknown
79	309.203	12.37	AA d8	18.8	0.844	0.97	Unknown
80	309.270	12.91	HTE d5	23.9	0.195	1.23	Unknown
82	311.282	12.90	HTE d5	15.9	0.313	0.93	Unknown
83	311.293	14.68	AA d8	17.9	0.945	0.96	Unknown
84	311.295	15.11	HTE d5	12.3	0.945	1.05	FA(20:0)
87	321.209	12.76	AA d8	12.2	0.945	1.10	Unknown
88	323.218	13.47	HTE d5	19.4	0.109	1.23	Unknown
89	323.219	12.95	HTE d5	16.9	0.547	1.02	Unknown

90	325.310	15.36	TXB2 d4	22.8	0.250	0.75	FA(21:0)
91	327.233	12.77	PGE2 d4	19.4	0.742	2.86	FA(22:6)
92	329.248	13.22	AA d8	12.1	0.109	2.08	FA(22:5)
93	329.267	14.35	AA d8	21.8	0.250	1.32	Unknown
94	335.050	9.53	TXB2 d4	13.1	0.547	0.88	Unknown
95	337.235	13.47	C10 d19	12.8	0.742	1.03	Unknown
96	339.327	15.68	PGE2 d4	13.3	0.313	0.75	FA(22:0)
97	341.172	11.99	HTE d5	19.5	0.945	1.11	Unknown
98	341.174	12.57	TXB2 d4	19.4	0.742	0.96	Unknown
99	341.269	13.42	AA d8	25.5	0.844	1.09	Unknown
100	343.136	1.53	HTE d5	19.4	0.250	1.18	Unknown
101	343.185	11.10	TXB2 d4	28.3	0.383	0.93	Unknown
102	347.216	13.04	TXB2 d4	18.7	0.742	0.99	Unknown
103	349.237	13.66	TXB2 d4	20.1	0.195	0.64	Unknown
105	351.218	13.47	C10 d19	10.5	1.000	0.93	Unknown
106	351.250	14.35	AA d8	16.5	0.547	1.02	Unknown
107	351.250	13.94	AA d8	17.7	0.641	1.09	Unknown
108	353.341	15.84	TXB2 d4	11.2	0.461	0.89	Unknown
109	355.224	13.27	C10 d19	28.6	0.742	0.93	Unknown
110	355.241	3.53	TXB2 d4	12.5	0.844	0.81	Unknown
111	355.320	13.53	TXB2 d4	27.0	0.742	1.35	Unknown
112	358.293	13.53	PGE2 d4	21.7	0.078	0.71	Unknown
113	361.234	13.03	C10 d19	19.4	1.000	1.00	Unknown
114	363.250	13.68	AA d8	12.7	0.945	1.11	Unknown
115	365.265	14.35	C10 d19	10.5	0.742	0.92	Unknown
116	365.339	15.67	TXB2 d4	27.1	0.547	0.93	Unknown
117	367.156	4.19	C10 d19	24.0	0.313	0.62	Unknown
118	367.358	16.12	TXB2 d4	9.6	0.461	0.93	FA(24:0)
120	370.965	1.22	HTE d5	22.3	0.742	1.10	Unknown
121	374.188	13.59	TXB2 d4	14.4	0.844	1.06	Unknown
122	377.059	10.69	TXB2 d4	28.1	0.148	0.73	Unknown
123	379.229	13.69	AA d8	22.2	0.547	1.20	Unknown
124	379.250	14.36	C10 d19	17.9	0.844	0.88	Unknown
125	381.372	16.24	TXB2 d4	17.9	0.461	0.79	Unknown
126	390.315	15.32	TXB2 d4	23.2	0.945	1.00	Unknown
127	391.112	12.41	TXB2 d4	12.5	0.844	1.02	Unknown
128	391.287	14.52	TXB2 d4	28.3	0.547	0.65	Unknown
129	393.374	16.12	TXB2 d4	26.2	0.945	1.09	Unknown
130	395.389	16.47	TXB2 d4	12.8	0.461	0.89	FA(26:0)
131	396.345	15.05	TXB2 d4	14.5	0.844	1.25	Unknown
132	397.329	14.80	HTE d5	20.3	0.313	0.91	Unknown
133	399.252	12.93	TXB2 d4	20.1	0.383	0.80	Unknown
134	399.252	13.48	HTE d5	23.2	0.742	0.96	Unknown
135	405.217	13.58	TXB2 d4	17.9	0.641	0.97	Unknown
136	405.266	13.74	C10 d19	10.3	0.742	0.64	Unknown
137	419.236	13.47	AA d8	14.6	0.547	1.14	Unknown
138	421.225	11.80	AA d8	19.5	0.641	0.93	Unknown
139	421.298	14.41	C10 d19	16.0	0.945	0.97	Unknown
140	421.327	15.63	TXB2 d4	23.8	0.383	0.92	Unknown
141	421.403	16.45	TXB2 d4	24.2	0.461	0.82	Unknown
142	423.420	16.77	TXB2 d4	21.3	0.461	0.92	FA(28:0)
143	425.354	15.26	TXB2 d4	29.6	0.313	0.91	Unknown
144	425.619	1.22	HTE d5	11.4	0.313	1.16	Unknown
145	429.332	11.76	C10 d19	21.6	0.313	0.72	Unknown
146	431.236	13.68	TXB2 d4	26.7	0.547	0.88	Unknown
147	433.253	14.35	HTE d5	17.7	0.195	1.54	Unknown
148	433.315	13.75	TXB2 d4	20.7	0.844	1.32	Unknown
149	436.319	15.31	PGE2 d4	28.9	0.461	0.93	Unknown
150	440.276	13.47	AA d8	28.6	0.313	1.30	Unknown
151	441.063	14.21	TXB2 d4	25.7	0.844	0.96	Unknown
152	444.403	13.44	C10 d19	22.2	0.742	0.76	Unknown
153	445.182	7.41	TXB2 d4	28.5	0.195	0.81	Unknown
154	445.184	6.49	TXB2 d4	19.7	0.250	0.62	Unknown
155	445.253	13.68	HTE d5	21.1	0.383	1.15	Unknown
156	445.265	15.68	TXB2 d4	24.2	0.148	0.74	Unknown
157	446.377	15.73	TXB2 d4	26.0	0.461	0.95	Unknown
158	447.269	14.35	AA d8	19.6	0.313	1.20	Unknown
159	447.330	14.50	HTE d5	29.1	0.195	1.69	Unknown
160	448.946	1.22	HTE d5	15.0	0.461	1.16	Unknown
161	450.336	15.31	TXB2 d4	26.4	0.742	0.98	Unknown
162	451.038	6.07	TXB2 d4	23.9	0.250	0.84	Unknown
163	453.367	10.90	PGE2 d4	26.5	1.000	1.11	Unknown
164	457.364	12.78	AA d8	12.3	0.313	0.89	Unknown

165	460.945	10.98	TXB2 d4	15.4	0.461	0.98	Unknown
166	461.092	8.20	AA d8	29.8	0.547	1.49	Unknown
167	461.097	6.66	PGE2 d4	23.1	0.461	0.82	Unknown
168	461.230	13.00	TXB2 d4	24.5	1.000	0.96	Unknown
169	464.921	1.22	HTE d5	14.6	0.109	1.15	Unknown
170	465.302	14.08	HTE d5	11.8	0.945	1.06	Unknown
171	466.296	13.69	AA d8	20.0	0.742	1.35	Unknown
172	468.313	14.35	C10 d19	18.1	0.742	0.99	Unknown
173	473.038	10.31	C10 d19	29.9	0.641	1.16	Unknown
174	473.284	12.82	PGE2 d4	19.1	0.547	0.81	Unknown
175	473.298	16.10	TXB2 d4	27.9	0.641	0.79	Unknown
176	475.017	11.12	C10 d19	26.7	0.547	1.22	Unknown
177	475.027	14.05	TXB2 d4	26.6	0.039	0.89	Unknown
178	475.300	15.06	TXB2 d4	27.4	0.547	0.85	Unknown
179	477.027	14.10	TXB2 d4	28.8	0.383	0.64	Unknown
180	479.066	5.77	TXB2 d4	28.2	0.313	0.81	Unknown
181	479.373	15.60	C10 d19	19.1	0.844	1.49	Unknown
182	480.308	13.79	HTE d5	27.6	0.039	0.73	Unknown
183	480.309	12.92	HTE d5	22.9	0.742	1.10	Unknown
184	485.016	1.22	HTE d5	19.5	0.641	0.89	Unknown
185	485.392	13.64	C10 d19	26.2	0.250	0.65	Unknown
186	487.400	15.78	AA d8	29.8	1.000	1.09	Unknown
187	496.966	13.89	TXB2 d4	27.7	1.000	1.04	Unknown

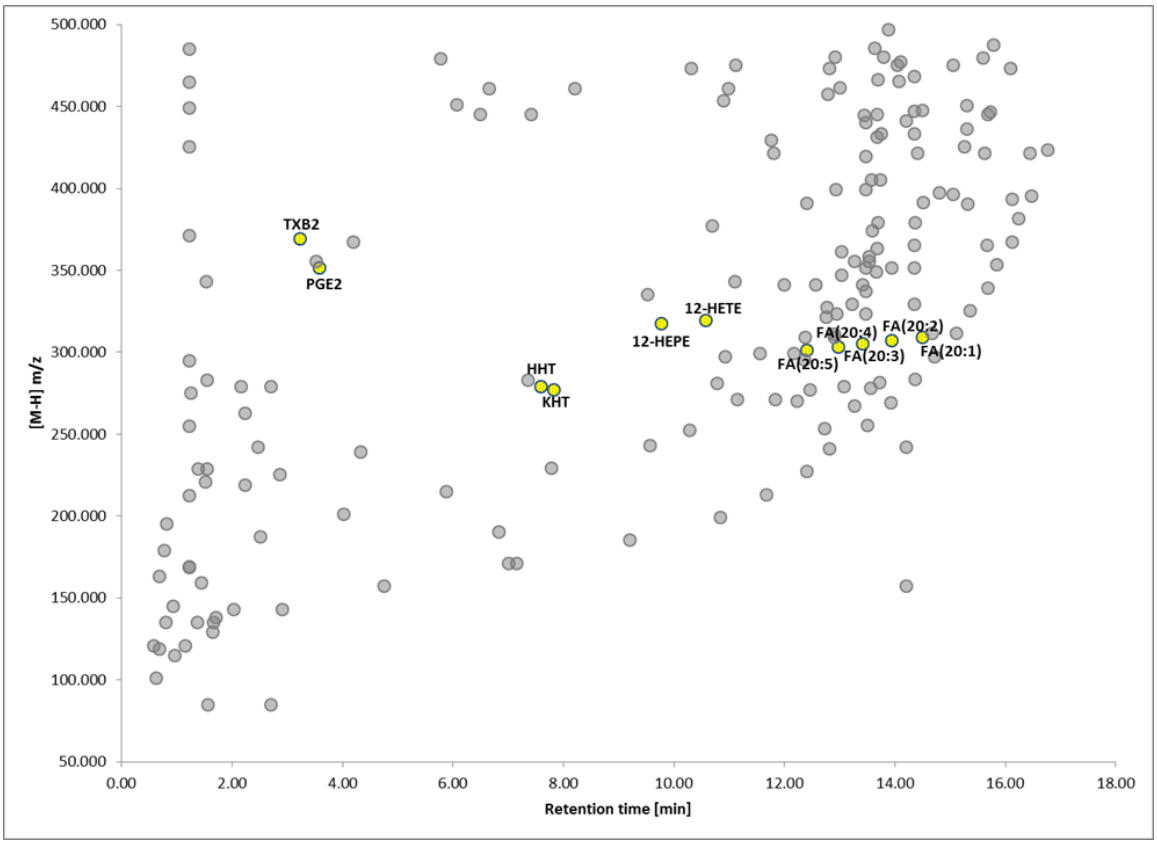

Figure 48. *Scatter plot showing the relation of retention time and m/z for all 187 found features, grey dots: unknown, yellow and labelled dots: identified; n = 8 for each group.*

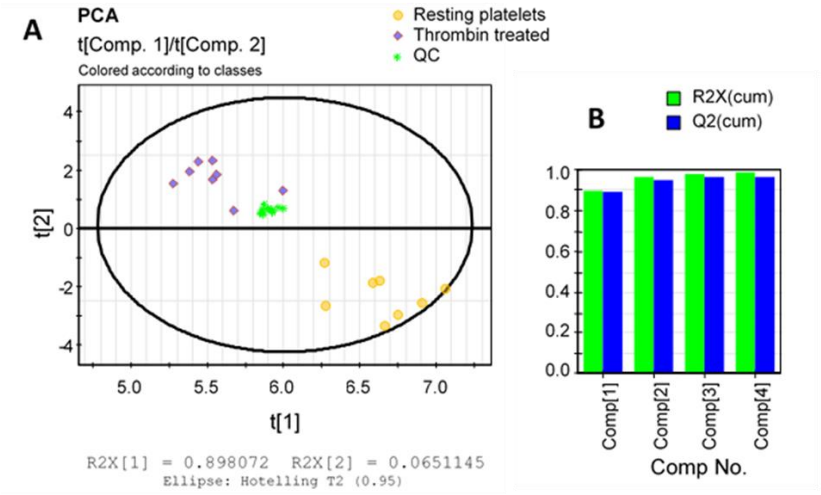

Figure 49. *Principal component analysis (PCA), unsupervised of all identified features showing grouping of the samples depending on the treatment (yellow: resting platelets, blue: thrombin treated). Green stars: quality control (QC) samples. Weighting: logarithmic, scaling: Pareto without centring.* ***A****: PCA,* ***B****: Model overview, n = 8 for each group.*

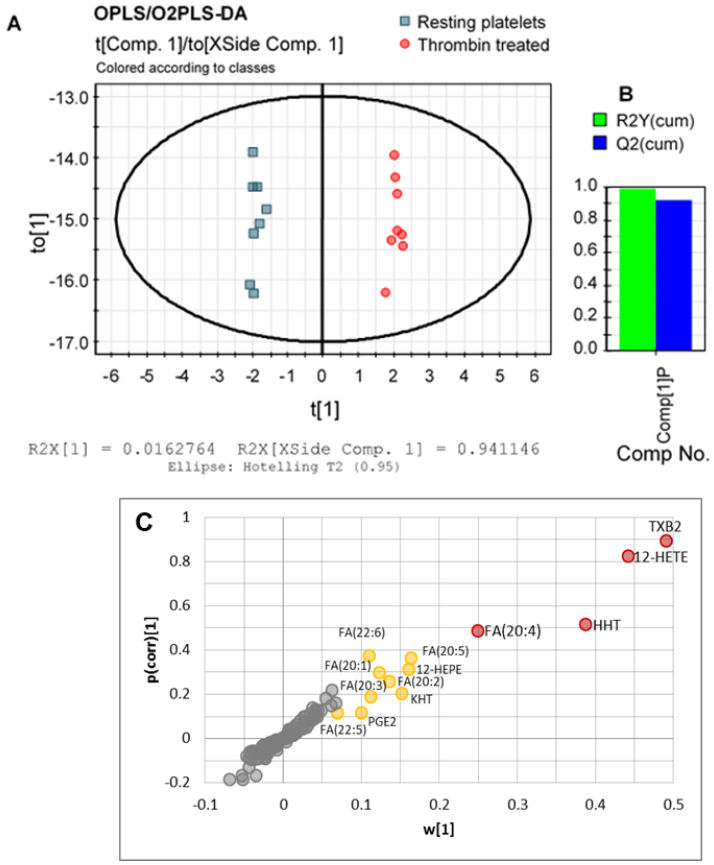

Figure 50. *OPLS-DA for all found features showing grouping of the samples depending on the treatment (blue: resting platelets, red: thrombin treated). Weighting: logarithmic, scaling: Pareto without centring.* ***A****: OPLS,* ***B****: Model overview,* ***C****: S-plot, n = 8 for each group.*

1.5.10. Additional quantification of 12-HETE and FA(20:4)

Two compounds (12-HETE and FA(20:4)), which were found significantly altered in activated platelet supernatants in the untargeted data processing, were of significant interest and thus subsequently additionally quantified. These 2 compounds are highly important for platelet metabolism and they seem to be released to intra-platelet environment. This was unexpected and discovered during untargeted analysis as a new finding.

1.5.10.1. Sample preparation and LC-MS analysis

Standards of 12-HETE and arachidonic acid (AA, FA(20:4)) were obtained from Cayman Chemical as described in chapter 1.5.9.2 of this document. Eight calibrants (30, 60, 100, 150, 250, 500, 850 and 1000 ng mL^{-1}) and 3 QC samples (80, 225, 800 ng mL^{-1}) were prepared as follows: standards of 12-HETE and AA were spiked to Tyrodes-HEPES buffer (HEPES 60 mg, NaCl 880 mg, KCl 10 mg, $NaHCO_3$ 20 mg, $NaH_2PO_4*H_2O$ 5 mg, glucose 100 mg, bovine serum albumin (BSA) 100 mg, H_2O 100 mL). No platelet supernatant was used in this case, because of unavailability and expected endogenous levels. It was the same buffer, which was used for preparation of platelet supernatant (see: paragraph 1.2.3.1 in the main document).

In the next step the mixture of internal standards (C10:0-d19, TXB2-d4, PGE2-d4, HTE-d5, AA-d8) was added and lipids were extracted with Matyash protocol as described in the chapter 1.2.3.2 of the main document. After the extraction, samples were measured with UHPLC-ESI-QTOF-MS/MS with exactly the same method as described in the 1.2.4 paragraph of the main document. Together with the calibration samples the platelet supernatant extracts were analysed (previously stored in -20°C).

The following fragments and internal standards were chosen for compound quantification:

- 12-HETE: *m/z* 179.106; HTE d5;
- FA(20:4): *m/z* 259.240; AA d8.

1.5.10.2. Calibration and pre-validation

Note: At this point no full validation was performed for these compounds.

Table 15. *Calibration data for 12-HETE and FA(20:4)*

Analyte		**12-HETE**	**FA(20:4)**
Calibration range weighting: $1/x^2$	µM	0.094 – 3.12	0.099 – 3.28
	r	0.997	0.998
Within-run accuracy [%]	QC low	104.8	101.8
	QC mid	102.4	102.3
	QC high	100.8	103.6
Within-run precision [%]	QC low	3.7	2.4
	QC mid	4.9	6.1
	QC high	3.5	4.5

1.5.10.3. Results: Concentrations of 12-HETE and FA(20:4) in samples

Table 16. *Concentrations of 12-HETE and FA(20:4) in samples*

		12-HETE		**FA(20:4)**	
		[µM]	[attomol per platelet]	[µM]	[attomol per platelet]
	Donor	LOQ = 0.094	LOQ = 0.62	LOQ = 0.099	LOQ = 0.66
Resting platelets	1	< LOQ		< LOQ	
	2	< LOQ		< LOQ	
	3	< LOQ		0.134	0.89
	4	< LOQ		< LOQ	
	5	< LOQ		< LOQ	
	6	< LOQ		< LOQ	
	7	< LOQ		0.10	0.68
	8	< LOQ		0.136	0.91
Thrombin treated platelets	1	2.49	16.6	0.173	1.15
	2	5.00*	33.3*	0.132	0.88
	3	1.01	6.7	1.153	7.69
	4	2.18	14.5	0.826	5.51
	5	1.27	8.4	1.82	12.2
	6	4.08*	27.2*	3.82*	25.5*
	7	0.58	3.9	0.492	3.28
	8	0.89	5.9	1.395	9.30

*Extrapolated results: exceeding calibration line.

2. Publication II: analysis of oxylipins in plasma and platelets

Micro-UHPLC-MS/MS method for analysis of oxylipins in plasma and platelets

Malgorzata Cebo[a], Xiaoqing Fu[a], Meinrad Gawaz[b], Madhumita Chatterjee[b], Michael Lämmerhofer[a]*

[a] University of Tübingen, Institute of Pharmaceutical Sciences, Pharmaceutical (Bio-) Analysis, Auf der Morgenstelle 8, 72076 Tübingen, Germany

[b] Department of Cardiology and Angiology, University Hospital Tübingen, Otfried-Müller-Strasse 10, 72076 Tübingen, Germany

Journal of Pharmaceutical and Biomedical Analysis

Volume 189, 10 September 2020, 113426

DOI: 10.1016/j.jpba.2020.113426

Highlights

• A micro-UHPLC-ESI-QqQ-MS/MS method for quantification of 42 oxylipins developed.

• Superficially porous (2.7 μm) particle capillary column (50 × 0.5 mm ID).

• Fast analysis in 10 min per run with low flow rate of 30 μL/min compatible with ESI.

• SPE with Bond Elut Certify II and 5 μL injections provided LOQs between 30 and 150 pg/mL.

• Method suitability documented for plasma and platelets.

Keywords: Capillary HPLC-ESI-MS/MS, Bioanalysis, Superficially porous particle capillary column, Platelet, Lipid mediator, Thromboinflammation

Abstract

Oxylipins play an important role in cell signalling and they act as auto- and paracrine factors. There are numerous reports on the analysis of oxylipins in biofluids, especially in plasma. Only a limited number of studies addressed the analysis of oxylipins in platelets using modern, sensitive LC-MS methods, even though these compounds have a huge impact on platelet functions and thrombo-inflammation. In this work, a new method based on superficially porous particle (2.7 μm) capillary column (0.5 mm ID) and micro-liquid chromatography coupled to tandem mass spectrometry (μUHPLC-ESI-QqQ-MS/MS) has been developed, optimized and validated. It has finally been successfully applied for human plasma and platelet analysis. The method allows the precise and accurate simultaneous quantification of 42 oxylipins with 13 deuterated internal standards. Solid phase extraction with Bond Elut Certify II provides good extraction recoveries (on average around 75 %). The μUHPLC-MS/MS method is selective, sensitive (LOQs between 30 and 150 pg/mL) and shows good linearity. Limits of detections for most of the compounds are between 2 and 250 fmol on column. Twenty-three oxylipins have been detected in plasma and 19 in non-activated (resting) platelets (all samples were from healthy donors). The μUHPLC-MS/MS method uses very low volume of mobile phase (less than 250 μL of organic solvents in mobile phase per analysis), and therefore is considered environmentally friendly. It also turned out to be robust enough for routine analysis.

2.1.Introduction

Oxylipins are oxidized polyunsaturated fatty acids (PUFAs) which are highly bioactive and play numerous important biological functions [8]. Most of the oxylipins are either chemically unstable or are metabolized very quickly. They are synthesized from PUFAs that are released from membrane phospholipids by cleavage at the sn2 position by cytosolic phospholipase A2 (cPLA2) [8, 11]. Then, free PUFAs are metabolized to oxylipins by 3 different families of enzymes: by cyclooxygenase (COX), lipoxygenase (LOX) or by cytochrome P450 (CYP450) [8, 11] (Figure 51). Oxylipins might also result from in-vivo or in-vitro non-enzymatic autoxidation.

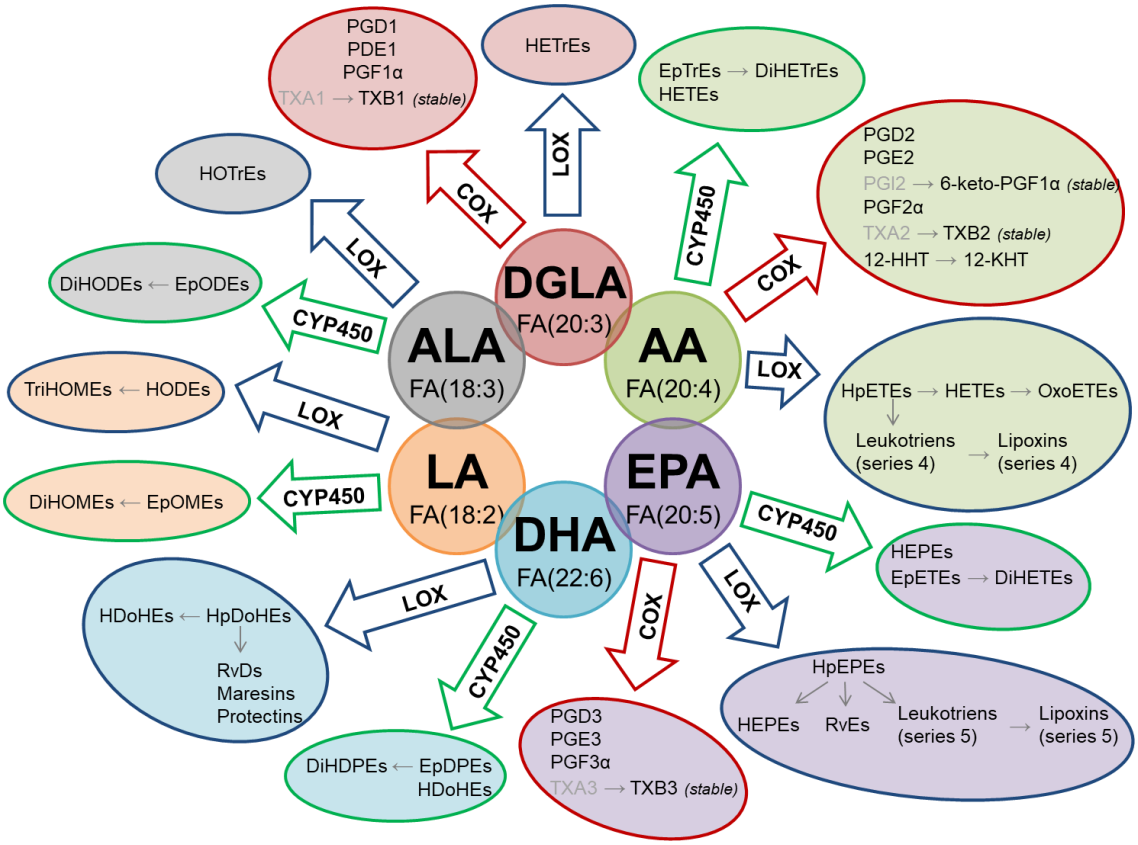

Figure 51. *Overview of enzymatic biosynthesis of oxylipins originating from the 6 most common PUFAs [108, 124, 147].*

The comprehensive quantitative analysis of oxylipins in biofluids, cells and tissues is of major importance as it might provide better insights into the biochemical changes associated with pathophysiological states [11, 77]. However, analysis of oxylipins is challenging [148]. These compounds are typically present at very low concentrations in biological samples; and what is more, concentration of highest and lowest abundant analytes may differ a lot (in some cases over 10^3 fold). Also, the concentration of a particular analyte might be very different in healthy and disease state. This requires a wide linear range of detection. Some oxylipins might be unstable and usually light protection and inhibitors of further oxidation (i.e. antioxidants) are used during sample preparation; furthermore, the samples need to be stored and processed at low temperatures [149]. Many oxylipins, even if they play very different biochemical roles, have highly similar structures, hence method specificity is of high importance, but might be challenging [12, 148]. Another issue is availability of standards and isotopically labelled analogues used as internal standards (IS). Their quality including purity, exact concentration (if purchased as solution) or mass (if supplied as solid material) and stability is very important for method validation and correct quantification [150]. However, in many cases suppliers of oxylipin

standards provide insufficient information regarding these parameters and lot-to-lot variations may be another concern.

In the past, oxylipins were analysed, after derivatization, with gas chromatography (GC) coupled to MS, but these GC assays were largely substituted by liquid chromatographic methods (LC) combined with tandem MS (MS/MS), which allows the analysis of oxylipins in their underivatized form [151]. Nowadays, ultra-high performance liquid chromatography (UHPLC) with reversed-phase (RP) stationary phases combined with triple quadrupole (QqQ) instruments, which feature very high sensitivity and wide linear range [147, 152] or quadrupole linear ion traps (QTrap) with enhanced scan functions are most popular instrumentations for multiplexed oxylipin assays analysing simultaneously up to 200 targets [11, 123, 153-157]. High resolution MS with QTOF [158] and Orbitrap gained also popularity recently and allow untargeted profiling of oxylipins. Supercritical fluid chromatography (SFC) coupled to MS is also slowly emerging in oxylipin analysis [159]. Recently, ion mobility (IMS) hyphenated to QTOF-MS has been utilized in oxylipin analysis, as it provides an additional dimension for separation of isomers [160]. In order to get a full picture of bioactivities, the chirality of oxylipins has to be considered as well. Very often only one enantiomeric form is biologically active, so it is of high importance to distinguish between racemic mixtures and pure enantiomers. MS instruments, as achiral detector, are not able to differentiate between enantiomers and only chiral separation prior to MS detection provides insight into enantiomeric composition of a sample. Nowadays, there are efficient enantioselective LC-MS/MS assays available for this purpose [161, 162]. However, chiral columns give typically broader peaks and therefore might provide lower sensitivity compared to RP chromatographic methods. For this reason, in this work we describe an achiral LC-MS/MS assay for oxylipins.

There is a limited number of studies on oxylipins in platelets, even though they are highly important for platelet biochemistry [77, 158]. In our studies, we established a new *ecofriendly* and robust miniaturized LC-MS method for accurate analysis of oxylipins. It utilizes µUHPLC for oxylipin separation. The method is sensitive, as the narrow column (inner diameter equal to 0.5 mm) packed with core-shell particles provides very narrow peaks with good peak resolution and enhanced signal-to-noise (S/N) ratio due to efficient ionisation at low flow rates (30 µL/min). It is robust enough for routine analysis of hundreds of samples per day at significantly lower solvent costs and environmental impact.

The new method has been validated for complex matrix, viz. plasma, incorporating an SPE enrichment step and was also applied to analyse platelet oxylipins.

2.2.Materials and methods

2.2.1. Materials

Arachidonic acid (AA), decanoic-2,2,3,3,4,4,5,5,6,6,7,7,8,8,9,9,10,10,10-d19 acid (FA(10:0)-d19) and undecanoic acid were purchased from Sigma Aldrich (*Merck*, Munich, Germany). All the other analytes and internal standards were obtained from Cayman Chemical (Ann Arbor, MI, USA): 5-hydroxy-6*E*,8*Z*,11*Z*,14*Z*-eicosatetraenoic acid (5-HETE), 8-hydroxy-5*Z*,9*E*,11*Z*,14*Z*-eicosatetraenoic acid (8-HETE), 9-hydroxy-5Z,7E,11Z,14Z-eicosatetraenoic acid (9-HETE), 11-hydroxy-5*Z*,8*Z*,12*E*,14*Z*-eicosatetraenoic acid (11-HETE), 12-hydroxy-5Z,8Z,10E,14Z-eicosatetraenoic acid (12-HETE), 15-hydroxy-5*Z*,8*Z*,11*Z*,13*E*-eicosatetraenoic acid (15-HETE), 20-hydroxy-5*Z*,8*Z*,11*Z*,14*Z*-eicosatetraenoic acid (20-HETE), 5-hydroxy-6*E*,8*Z*,11*Z*,14*Z*,17*Z*-eicosapentaenoic acid (5-HEPE), 8-hydroxy-5*Z*,9*E*,11*Z*,14*Z*,17*Z*-eicosapentaenoic acid (8-HEPE), 12-hydroxy-5*Z*,8*Z*,10*E*,14*Z*,17*Z*-eicosapentaenoic acid (12-HEPE), 15-hydroxy-5*Z*,8*Z*,11*Z*,13*E*,17*Z*-eicosapentaenoic acid (15-HEPE), 18-hydroxy-5*Z*,8*Z*,11*Z*,14*Z*,16*E*-eicosapentaenoic acid (18-HEPE), 14(15)-epoxy-5Z,8Z,11Z,17Z-eicosatetraenoic acid (14(15)-EpETE), 5,6-dihydroxy-7*E*,9*E*,11*Z*,14*Z*-eicosatetraenoic acid (5,6-DiHETE), 10-hydroxy-4*Z*,7*Z*,11*E*,13*Z*,16*Z*,19*Z*-docosahexaenoic acid (10-HDoHE), 14-hydroxy-4*Z*,7*Z*,10*Z*,12*E*,16*Z*,19*Z*-docosahexaenoic acid (14-HDoHE), 17-hydroxy-4*Z*,7*Z*,10*Z*,13*Z*,15*E*,19*Z*-docosahexaenoic acid (17-HDoHE), 9-hydroxy-10*E*,12*Z*-octadecadienoic acid (9-HODE), 13-hydroxy-9Z,11E-octadecadienoic acid (13-HODE), 12-hydroxy-5*Z*,8*E*,10*E*-heptadecatrienoic acid (12-HHT), 8R-hydroxy-4*Z*,6*E*,10*Z*-hexadecatrienoic acid (T-12-HETE), 12-hydroxy-5*Z*,8*Z*,12*Z*-eicosatrienoic acid (12-HETrE), 13-hydroxy-9*Z*,11*E*,15*Z*-octadecatrienoic acid (13-HOTrE), 5-oxo-6*E*,8*Z*,11*Z*,14*Z*-eicosatetraenoic acid (5-OxoETE), Resolvin D1 (RvD1), Resolvin D2 (RvD2), Resolvin D3 (RvD3), Resolvin D4 (RvD4), Resolvin D5 (RvD5), Resolvin E1 (RvE1), Maresin 1 (Mar1), Maresin 2 (Mar2), Lipoxin A4 (LXA4), Leukotriene B4 (LTB4), Prostaglandin D1 (PGD1), Prostaglandin E1 (PGE1), Prostaglandin D2 (PGD2), Prostaglandin E2 (PGE2), 6-keto-Prostaglandin F1α (6-keto-PGF1α), Prostaglandin F2α

(PGF2α), Thromboxane B2 (TXB2), 4*Z*,7*Z*,10*Z*,13*Z*,16*Z*,19*Z*-docosahexaenoic acid (DHA), 7*Z*,10*Z*,13*Z*,16*Z*,19*Z*-docosapentaenoic acid (DPA), 7*Z*,10*Z*,13*Z*,16*Z*-docosatetraenoic acid (adrenic acid, ADA), 5*Z*,8*Z*,11*Z*,14*Z*,17*Z*-eicosapentaenoic acid (EPA), arachidonic acid (AA) and 8*Z*,11*Z*,14*Z*-eicosatrienoic acid (DGLA). Internal standards were also purchased from Cayman Chemical: 6*Z*,8*E*,10*E*,14*Z*,16*E*-eicosapentaenoic-6,7,14,15-d4 acid (RvE1-d4), 7*S*,8*R*,17*S*-trihydroxy-4*Z*,9*E*,11*E*,13*Z*,15*E*,19*Z*-21,21',22,22,22-d5 docosahexaenoic acid (RvD1-d5), 9-oxo-11alpha,15*S*-dihydroxy-prosta-5*Z*,13*E*-dien-1-oic-3,3,4,4-d4 acid (PGE2-d4), 15*S*-dihydroxy-11-oxo-prosta-5*Z*,13*E*-dien-1-oic-17,17,18,18,19,19,20,20,20-d9 acid (PGD2-d9), 9alpha,11,15*S*-trihydroxy-thromba-5*Z*,13*E*-dien-1-oic-3,3,4,4-d4 acid (TXB2-d4), 9alpha,11alpha,15*S*-trihydroxy-prosta-5*Z*,13*E*-dien-1-oic-3,3,4,4-d4 acid (PGF2α-d4), 13*R*,14*S*-dihydroxy-4*Z*,7*Z*,9*E*,11*Z*,16*Z*,19*Z*-docosahexaenoic-21,21,22,22,22-d5 acid (Mar2-d5), 5*S*,12*R*-dihydroxy-6*Z*,8*E*,10*E*,14*Z*-eicosatetraenoic-6,7,14,15-d4 acid (LTB4-d4), 5*S*-hydroxy-6*E*,8*Z*,11*Z*,14*Z*-eicosatetraenoic-5,6,8,9,11,12,14,15-d8 acid (5-HETE-d8), 12*S*-hydroxy-5*Z*,8*Z*,10*E*,14*Z*-eicosatetraenoic-5,6,8,9,11,12,14,15-d8 acid (12-HETE-d8), 20-hydroxy Arachidonic Acid-d6, 20-hydroxy-5*Z*,8*Z*,11*Z*,14*Z*-eicosatetraenoic-16,16,17,17,18,18-d6 acid (20-HETE-d6), 4*Z*,7*Z*,10*Z*,13*Z*-hexadecatetraenoic-15,15,16,16,16-d5 acid (HTE-d5), 5*Z*,8*Z*,11*Z*,14*Z*-eicosatetraenoic-16,16,17,17,18,18,19,19,20,20,20-d11 acid (AA-d11), 8*Z*,11*Z*,14*Z*-eicosatrienoic-8,9,11,12,14,15-d6 acid (DGLA-d6), 4*Z*,7*Z*,10*Z*,13*Z*,16*Z*,19*Z*-docosahexaenoic-21,21,22,22,22-d5 acid (DHA-d5) and 5*Z*,8*Z*,11*Z*,14*Z*,17*Z*-eicosapentaenoic-19,19,20,20,20-d5 acid (EPA-d5). All standards were utilized as provided and with concentrations as specified by the supplier assuming appropriate quality of the supplied standard solutions and correctness of their concentrations. Validation of the quality of supplied non-certified standards and corrections for inadequate standard concentrations as suggested by N.H. Schebb and co-workers are recommended when interlaboratory studies are performed or for interstudy comparisons [150].

Solvents: methanol (MeOH), acetonitrile (ACN) and isopropanol (IPA) of LC-MS grade as well as dichloromethane (DCM) of GC grade were purchased from Carl Roth (Karlsruhe, Germany). Dess-Martin periodinane, *N*-[1-(1-Oxopropyl)-4-piperidinyl]-*N*'-[4-(trifluoromethoxy)phenyl]urea (TPPU), butylated hydroxytoluene (BHT), acetic acid (HAc), formic acid (FA), ammonium acetate (NH_4Ac), ammonium formate (NH_4FA) and

sodium acetate were from Sigma Aldrich (*Merck*). Ultrapure water was produced by Elga Purelab Ultra (Celle, Germany).

Bond Elut Certify II solid phase extraction cartridges (3 mL / 200 mg) were obtained from Agilent (Waldbronn, Germany).

2.2.2. Synthesis of 12-KHT

12-Oxo-5*Z*,8*E*,10*E*-heptadecatrienoic acid (12-KHT) was synthesized from 12-HHT as described before [158]. Briefly, 50 µL of 12-HHT (100 µg/mL in ethanol) was placed together with 5 µL of undecanoic acid (100 µg/mL) as internal standard in a glass vial. Solvents were evaporated and 60 µL of DCM and 15 µL of Dess-Martin reagent solution (0.3 M in DCM) were added. The reaction was allowed to proceed at room temperature for 5 min. After that solvent was evaporated and the reaction was quenched with 500 µL MeOH. The sample was left at -80°C for 24 h and then filtrated. The final concentration of the stock solution was determined as 8.9 µg/mL.

2.2.3. Sample preparation

2.2.3.1. Collection of plasma and platelet samples

Plasma samples were collected from the peripheral blood of healthy male donors at the Department of Medical Psychology and Behavioral Neurobiology, University Hospital Tübingen, Germany, and platelet samples were obtained from the peripheral blood of healthy donors at the Dept. of Cardiology and Angiology, University Hospital Tübingen, according to ethical guidelines and approved by regional authorities. Resting platelets were isolated from blood, as described previously [158], and samples with platelet count 2 x 10^8 were prepared. At the last stage of the reported protocol, phosphate-buffered saline (PBS buffer) supplemented with calcium ions was not removed. Plasma and platelets (suspended in PBS) were kept at -80°C until extraction.

2.2.3.2. Oxylipin and fatty acid extraction from plasma, preparation of calibrants and quality control samples

To perform the oxylipin and fatty acid extraction, plasma was slowly thawed on ice for about 2h. For preparation of matrix-matched calibrants and QCs, plasma was pooled and solutions of BHT as antioxidant and TPPU as soluble epoxide hydrolase (sEH) inhibitor were added: 20 µL of the mixed stock solution (200 µg/mL of each compound in MeOH, final concentration after extraction: 20 µg/mL) were added per 1 mL of plasma. Pooled plasma was then divided into 500 µL aliquots and spiked with 40 µL of internal standard (IS) mix stock solution (TXB2-d4, PGF2α-d4, PGE2-d4, PGD2-d9, RvD1-d5, RvE1-d4, Mar2-d5, LTB4-d4, 5-HETE-d8, 12-HETE-d8, 20-HETE-d6, FA(10:0)-d19, HTE-d5: each 25 ng/mL resulting in a final concentration of 10 ng/mL; except for 13-HODE-d4, DHA-d5, DGLA-d6, EPA-d5, AA-d11 for which a 2.5 µg/mL solution was added resulting in a final concentration of 1 µg/mL).

Calibrants and quality controls (QC) were prepared from above stock solutions. Calibrants were prepared at 12 different concentrations to cover sufficiently wide concentration ranges of the different analytes: oxylipin range (except 9- and 13-HODE) - 50 pg/mL of plasma to 25 ng/mL; calibrants of 9- and 13-HODE were in the range of 500 pg/mL to 250 ng/mL and fatty acids between 5 ng/mL to 2.5 µg/mL. QC samples were prepared at 3 different levels: oxylipins except 9- and 13-HODE – 160 pg/mL, 1.6 ng/mL and 4 ng/mL; 9- and 13-HODE: 16 ng/mL, 40 ng/mL and 160 ng/mL; fatty acids: 16 ng/mL, 160 ng/mL and 400 ng/mL.

Then, 1 mL of buffer pH 6 (1 M CH_3COONa in the mixture of water/MeOH (95:5; v/v) adjusted to pH 6 with HAc) was added to each sample. The samples were centrifuged (4,000 x g, 4°C, 5 min) in order to remove possible precipitants and solid particles from the solution, which could plug the SPE cartridge (proteins were not precipitated at this point, as only 5% of organic solvent - MeOH were too low to cause it).

The Bond Elut Certify II SPE cartridges were pre-conditioned with 2 mL of a mixture of ethyl acetate/n-hexane/HAc (75:24:1; v/v/v), followed by 2 mL MeOH and in the last step with 2 mL of the 1 M CH_3COONa buffer pH 6. Then samples were loaded and washed 2 times with 2.5 mL H_2O/MeOH (4:1; v/v) mixture. Until this step, the cartridges were

prevented from drying. After the second washing step the cartridges were dried for 5 min. Then the samples were eluted with 2 times 1 mL mixture of ethyl acetate/n-hexane/HAc (75:24:1; v/v/v)

Eluates were evaporated with GeneVac (Ipswich, UK) under nitrogen protection. Evaporation time was around 1h. After that, samples were re-dissolved in 40 µL of MeOH and 60 µL water were added. Samples were vortexed and centrifuged (4,000 x g, 4°C, 5 min) and transferred to autosampler vials for immediate LC-MS analysis.

2.2.3.3.Determination of matrix effects and extraction recoveries

Determination of matrix effects and extraction recoveries was performed according to Matuszewski's protocol [137]. Three sets of samples were prepared: pooled plasma spiked with standards and ISs before extraction (pre-extraction spike) (as described in the paragraph 2.2.2); pooled plasma spiked with standards and ISs after extraction, i.e. standards and ISs added with the reconstitution solvent to dried extracts; solvent (H_2O/MeOH (3:2; v/v)) spiked with standards and ISs (standard solutions). The theoretical concentration in each set was the same. ISs were spiked, as described above for QCs with the following concentrations: 10 ng/mL for TXB2-d4, PGF2α-d4, PGE2-d4, PGD2-d9, RvD1-d5, RvE1-d4, Mar2-d5, LTB4-d4, 5-HETE-d8, 12-HETE-d8, 20-HETE-d6, FA(10:0)-d19, HTE-d5, and 1 µg/mL for 13-HODE-d4, DHA-d5, DGLA-d6, EPA-d5, AA-d11. Standards were added at 3 different levels: 1.6 ng/mL, 4 ng/mL and 16 ng/mL for all oxylipins except of 9- and 13-HODE for which the concentrations were 16 ng/mL, 40 ng/mL and 160 ng/mL. For fatty acids, the concentrations were 160 ng/mL, 400 ng/mL and 1.6 µg/mL. Matrix effect was calculated as ratio of peak areas in post-extraction spiked samples and corresponding standard solution (spiked solvent). Extraction recovery was determined as ratio of peak areas in pre-extraction spiked samples and corresponding post-extraction spiked samples.

2.2.3.4.Oxylipin and fatty acid extraction from platelets

IPA was added to frozen platelets suspended in PBS buffer to obtain the ratio IPA/H_2O (9:1; v/v). BHT and TPPU stock solutions were added (10 µL, 200 µg/mL of each

compound in MeOH). Samples were kept for 80 min in a shaker at 4°C for thawing, protein precipitation and lipid extraction. Then, ISs were added (TXB2-d4, PGF2α-d4, PGE2-d4, PGD2-d9, RvD1-d5, RvE1-d4, Mar2-d5, LTB4-d4, 5-HETE-d8, 12-HETE-d8, 20-HETE-d6, FA(10:0)-d19, HTE-d5 at a final concentration of 10 ng/mL; 13-HODE-d4, DHA-d5, DGLA-d6, EPA-d5, AA-d11 at a final concentration of 1 µg/mL). Samples were vortexed (10 s) and sonicated (5 times, each time 2 min, samples were cooled for minimum 10 min in between). Afterwards, the samples were centrifuged (4,000 x g, 4°C, 5 min) in order to remove precipitated proteins and cell residues, and the supernatants were transferred to fresh falcon tubes. Each supernatant was diluted with 2 mL of buffer pH 6 (1 M CH_3COONa in water/MeOH (95:5;v/v) adjusted to pH 6 with HAc) and loaded onto preconditioned Bond Elut Certify II SPE cartridges, as described for plasma in the Section 2.3.2. After sample loading, the cartridges were washed 2 times with 2.5 mL H_2O/MeOH (4:1; v/v) and dried for 5 min. Samples were eluted into fresh falcon tubes with (2 times 1 mL) ethyl acetate/n-hexane/HAc (75:24:1; v/v/v). The solvent was evaporated with GeneVac under nitrogen protection. The samples were reconstituted with 20 µL MeOH and then 30 µL of water was added. The samples were vortexed (10 s), centrifuged (4,000 x g, 4°C, 5 min) and transferred to autosampler vials. A QC sample was prepared by pooling 20 µL of each sample in a separate vial. It was used to assure good quality of µLC-MS analysis and to prepare calibrants. The samples were analysed by µUHPLC-MS/MS immediately after their preparation. The order of analysis was randomized and the QC sample was injected before, after and in between the samples.

2.2.3.5.Calibrants for platelets

The QC pool was divided into 6 aliquots and 5 of them were spiked with standards at different levels to prepare matrix-matched external calibration. Calibration ranges of oxylipins covered concentrations from 50 pg/mL to 25 ng/mL except of 9- and 13-HODE for which concentrations ranged from 0.5 ng/mL up to 250 ng/mL. Moreover, fatty acids were calibrated at concentrations from 5 ng/mL to 2.5 µg/mL. Calibrants were analysed in the same batch with the platelet samples and QC.

2.2.4. µUHPLC-MS/MS method

µUHPLC-MS/MS analysis was performed with an Eksigent µLC 200 Plus System (Sciex, Ontario, Canada) coupled to a QTrap 4500 MS instrument (Sciex) equipped with a Turbo

V source and 50 µm ID hybrid electrodes – made of PEEKsil, with a 1 cm stainless steel tip. An Eksigent HALO C18 (Sciex) column (dimension 50 mm × 0.5 mm; particle size 2.7 µm, 90 Å) was used for the chromatographic separation. The column was kept at 50°C during the analysis. The injection volume was 5 µL. Mobile phase A was H_2O with 0.1% HAc (v/v) and mobile phase B was ACN with 0.1% HAc (v/v). Gradient elution started with 15% B, followed by a linear gradient to 99% B in 9 min and subsequent hold at 99% B for 1 min. The flow rate at this stage was equal to 30 µL/min (Table 17). At the end of this gradient a 'solvent plug' of 5 µL IPA was injected to wash the column and remove contaminations of more apolar lipids. During this injection 99% mobile phase B and 1% mobile phase A were pumped through the column with reduced flow rate (10 µL/min); this step lasted 2 min. Then, the eluent composition was quickly changed (in 0.1 min) to 15 % B and the flow rate was raised to 30 µL/min to re-equilibrate the column for the next analysis (0.9 min equilibration time) (Table 17).

Table 17. *Binary gradient profile with eluent composition (%B) and flow rate as well as column washing program.*

LC GRADIENT		
During data acquisition: injection of 5 µL of sample		
Time [min]	B [%]	Flow rate [µL/min]
0.0	15	30
9.0	99	30
10.0	99	30
Wash and re-equilibration: injection of 5 µL IPA		
0.0	99	10
2.0	99	10
2.1	15	30
3.0	15	30

MS analysis was performed with ESI in negative mode. The source voltage was -4,000 V and the source temperature was 400°C. Nebulizer gas, heater gas and curtain gas pressures were set to 25 psi, 20 psi and 25 psi, respectively. The entrance potential was set to -10 V. The collision gas was used at medium pressure. Q1 and Q3 resolution was set to unit. SRMs were optimized individually for each analyte and are summarized in Table 18. Scheduled MRM mode was used with the cycle time equal to 300 ms.

Table 18. *SRMs (start and end RT specify the period in which the respective SRM transition was acquired).*

Name	Q1 *m/z*	Q3 *m/z*	Expected RT [min]	Start RT [min]	End RT [min]	CE [V]	CXP [V]	DP [V]
PGF2a	353.1	309.2	2.57	2.3	10.0	-27	-12	-80
PGE1 and PGD1	353.1	317.1	2.73 and 2.77	2.5	3.5	-18	-12	-60
TXB2	369.2	195.0	2.35	2.0	3.7	-19	-10	-80
6-keto-PGF1a	369.2	163.0	1.92	0.0	2.6	-35	-10	-65
PGE2 and PGD2	351.2	315.2	2.65 and 2.76	2.3	3.7	-18	-12	-80
10-HDoHE	343.1	153.0	5.24	5.0	5.9	-20	-8	-70
14-HDoHE	343.1	205.0	5.23	4.9	5.9	-18	-10	-60
17-HDoHE	343.1	201.0	5.14	4.9	5.9	-20	-10	-80
5-HETE	319.1	114.9	5.4	5.1	6.1	-18	-8	-80
8-HETE	319.1	154.9	5.27	5.0	6.0	-20	-12	-75
9-HETE	319.1	151.0	5.33	5.1	6.0	-21	-8	-40
11-HETE	319.1	167.0	5.18	4.9	5.9	-22	-8	-75
12-HETE	319.1	208.0	5.27	5.0	6.0	-21	-10	-80
15-HETE	319.1	219.0	5.07	4.8	5.8	-17	-10	-40
20-HETE	319.1	245.0	4.66	4.4	5.4	-22	-10	-80
5-HEPE	317.1	114.9	4.91	4.6	5.6	-20	-8	-75
8-HEPE	317.1	154.8	4.79	4.5	5.5	-20	-12	-70
12-HEPE	317.1	179.0	4.81	4.5	5.5	-18	-8	-75
15-HEPE	317.1	219.0	4.71	4.4	5.4	-18	-10	-95
18-HEPE	317.1	215.1	4.56	4.3	5.3	-18	-10	-65
14(15)-EpETE	317.1	207.0	5.26	5.0	6.0	-16	-10	-60
5,6-DiHETE	335.1	144.9	4.19	3.9	4.9	-22	-9	-20
5-OxoETE	317.1	203.0	5.53	5.3	6.3	-24	-10	-85
12-OxoETE	317.1	153.0	5.41	5.1	6.4	-24	-10	-80
9-HODE	295.2	171.0	4.95	4.7	5.7	-25	-8	-80
13-HODE	295.2	195.0	4.91	4.6	5.6	-26	-8	-80
LXA4	351.1	114.9	3.01	2.7	3.7	-23	-8	-70
12-HHT	279.1	179.0	4.24	4.0	5.0	-17	-8	-80
12-KHT	277.2	113.0	4.46	4.2	5.2	-20	-11	-80
LTB4	335.2	195.0	3.87	3.6	4.6	-22	-8	-80
T-12-HETE	265.1	109.0	4.13	3.9	4.8	-18	-8	-50
RvD1	375.1	121.1	3.05	2.8	3.8	-35	-8	-80
RvD2	375.1	277.1	2.84	2.6	3.6	-20	-8	-70
RvD3	375.1	147.0	2.75	2.5	3.5	-25	-8	-40
RvD4	375.1	100.9	3.30	3.0	4.0	-26	-8	-80
RvD5	359.2	199.1	3.82	3.6	4.6	-21	-10	-40
RvE1	349.1	194.9	2.00	1.7	2.7	-22	-11	-65
Mar1	359.2	297.2	3.82	3.5	4.5	-22	-10	-75
Mar2	359.2	221.0	4.12	3.9	4.8	-16	-10	-60
12-HETrE	321.4	181.0	5.47	5.2	6.2	-24	-7	-40
13-HOTrE	293.0	224.0	4.54	4.3	5.2	-18	-9	-40
FA(20:4)	303.0	259.0	6.90	6.6	7.6	-20	-12	-80
FA(20:5)	301.0	257.0	6.40	6.1	7.1	-15	-12	-80
FA(20:2)	307.3	307.3	7.77	7.5	8.5	-10	-14	-80
FA(22:4)	331.3	287.0	7.54	7.3	8.2	-20	-12	-80
FA(20:3)	305.2	261.0	7.26	7.0	8.0	-25	-12	-80
FA(22:6)	327.0	283.0	6.79	6.5	7.5	-15	-12	-80
FA(22:5)	329.0	329.0	7.27	7.0	7.9	-5	-8	-80
PGE2-d4	355.2	319.2	2.64	2.4	3.3	-17	-12	-80
TxB2-d4	373.3	173.1	2.34	2.0	3.7	-24	-8	-80
12-HETE-d8	327.3	184.0	5.23	5.0	5.9	-20	-8	-80
13-HODE-d4	299.1	198.0	4.89	4.6	5.6	-24	-10	-90
RvD1-d5	380.3	140.9	3.02	2.7	3.7	-20	-8	-40
PGD2-d9	360.2	280.2	2.74	2.5	3.5	-24	-10	-80
FA(10:0)-d19	190.3	190.3	4.26	4.0	5.0	-10	-11	-70
PGF2a-d4	357.2	169.1	2.56	2.3	3.3	-35	-8	-80
HTE-d5	252.2	208.2	5.25	5.0	6.0	-20	-11	-80
AA-d11	314.2	270.1	6.87	6.6	7.5	-19	-12	-90
20-HETE-d6	325.1	281.2	4.63	4.4	5.4	-20	-13	-90
5-HETE-d8	327.1	115.9	5.36	5.1	6.1	-18	-7	-50
DHA-d5	332.1	288.1	6.77	6.5	7.5	-14	-11	-50
EPA-d5	306.0	262.0	6.38	6.1	7.1	-16	-11	-60
LTB4-d4	339.1	196.9	3.85	3.6	4.6	-22	-9	-70
Mar2-d5	364.1	221.0	4.11	3.8	4.8	-16	-9	-40
RvE1-d4	353.1	196.9	1.98	1.7	2.7	-22	-7	-40
DGLA-d6	311.2	267.2	7.23	7.0	7.9	-25	-11	-80

2.2.5. Validation of method for plasma

Instrument linearity (analytes dissolved in solvent) and linearity in matrix, as well as within-batch and between-batch precision and accuracy, limit of detection (LOD) and limit of quantification (LOQ) were investigated.

Within-batch accuracy and precision was calculated based on 6 measurements of each from 3 QCs, prepared on the same day and measured in the same batch.

Between-batch accuracy and precision were calculated from results obtained for QCs prepared and measured on 3 different days.

LOQ and LOD were calculated from matrix-matched calibration curve. LOQ was equal to 10 times the ratio of uncertainty in calculation of peak area ratio to calibration curve (10*sigma/slope). LOD was equal to 3 times this ratio (3*sigma/slope).

Linearity, both in solvent and in matrix, was characterized as coefficient of determination (R^2) for the linear range of the calibration function.

2.2.6. Data analysis

Data analysis was performed with MultiQuant 3.0 (Sciex) using the algorithm MQ4. The Gaussian smooth width was set to 1.0 points, retention time half window was 5.0 s, minimal peak width was 3 points and minimum peak height was established individually for each SRM, but usually set to 500. Integration parameters included noise percentage (set to 40%), baseline subtraction window (0.20 min) and peak splitting (usually 1 point). MultiQuant was used for peak finding and integration, as well as calculation of the calibration function by weighted linear regression (weighting was set to $1/x^2$ for all compounds). Further calculations were done with Excel 2007 (Microsoft, Redmond, WA, USA) and R (version i386 3.4.2, R-project for statistical computing).

Calibration functions were obtained by plotting peak area ratios against concentrations, except for TXB2, for which peak height ratio was used, because of the double peak caused

by interconversion of hemiacetal forms. The 2 peaks of TXB2, with a plateau in between were hard to integrate accurately by peak area, but well defined by peak height. The higher, first eluted peak of TXB2 was used for calculations. The ratio of the 2 peaks was well conserved during the analysis.

2.3.Results and discussion

2.3.1. Method development

2.3.1.1.Optimization of µUHPLC method

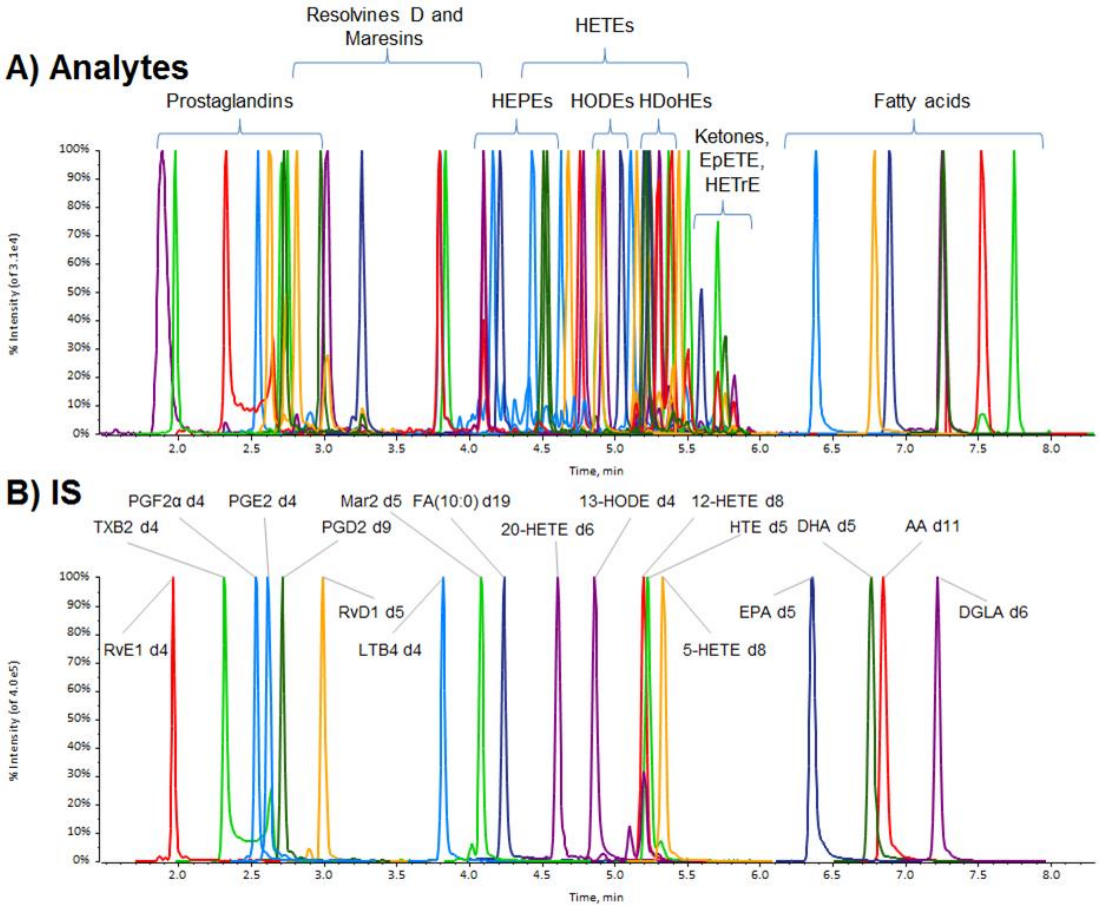

Figure 52. *Normalized chromatograms (extracted EIC) of:* ***A****) all analytes of indicated compound classes; and* ***B****) all ISs with compounds names/abbreviations.*

Specificity of oxylipin assays can be easily compromised by numerous isobaric and isomeric interferences, if they are not properly separated. Hence, great attention was paid

to the optimization of chromatographic separation to avoid coelution of oxylipins which cannot be distinguished by specific SRM transitions or get compromised due to interference from similar fragmentation pattern (Suppl. materials Table 31). On the other hand, assay sensitivity is an issue as baseline concentrations of oxylipins in plasma and resting platelets may be quite low (pg/mL to ng/mL range). While most of the reported HPLC-MS/MS assays were based on standard flow LC, in this work we selected µUHPLC. Its lower volumetric flow rates are deemed to be favourable in terms of ESI efficiency and sensitivity, respectively, while robustness is not affected significantly. To cope with high throughput requirements of clinical studies, the run time was kept short (13 min). The utilized µUHPLC system has a pressure range up to 10,000 psi (68.9 MPa). This comparably narrow pressure range limits its flexibility for use of sub-2µm particle columns. Anyway, it was shown that 2.7µm core-shell particle columns have a better performance/speed/back pressure compromise. They typically provide faster separations at about the same efficiency with lower back pressure as compared to sub-2 µm particle columns. Hence, a Halo C18 2.7 µm superficially porous particle column (50 mm x 0.5 mm ID) was employed in this study.

Different mobile phases were tested in order to find the most sensitive and selective chromatographic method. Mobile phase A was always water with additive and mobile phase B was 5% of water and 95% of either ACN or MeOH (v/v) or a mixture of both; an additive was always added also to the mobile phase B, viz. the same one and at the same final concentration as in the mobile phase A. There were 6 different additives tested: NH_4FA, NH_4Ac, FA, HAc, NH_4FA with FA and NH_4Ac with HAc (see Suppl. material chapter 1.1 for more details).

Two standard solutions of oxylipins (each one 100 pg/mL and 1 ng/mL, respectively) were injected in triplicates with each of the mobile phases. The S/N ratios were calculated for each compound to evaluate method sensitivity. Resolution of isomeric substances like PGE2-PGD2 served to evaluate method selectivity (these 2 isomeric compounds cannot be distinguished by MS only and consequently need to be resolved chromatographically).

Generally, MeOH (especially with buffer salts as additives) provided good sensitivity; however, the peaks were much broader than with ACN. Therefore, resolution of PGE2 and PGD2 was poor with MeOH. ACN gave narrower peaks and HAc as additive was

favourable in terms of detection sensitivity. As a consequence, the final mobile phase was established as: B – 100 % ACN with 0.1% HAc (v/v) and A – 100 % H_2O with 0.1% HAc (v/v). The gradient profile of the final method is specified in Table 17 along with flow rates and column regeneration program. S/N ratios improved with lower flow rates (tested between 20 and 50 µL/min), yet at the expense of longer run times. 30 µL/min was finally selected as the best compromise. The best chromatographic efficiencies could be achieved at the highest column temperature tested (50°C) which represents the upper limit according to recommendations of column supplier (Suppl. materials chapter 2.5.1.2).

In order to assure good retention time repeatability, a column regeneration step was implemented. For this purpose, a 5 µL 2-propanol (IPA) plug was injected after the end of the gradient. IPA has high elution strength for lipids and allows efficient cleaning of the column. With this column wash and subsequent re-equilibration, the method was stable and no problems with pressure increase, retention time drifts or sensitivity loss in the course of longer analysis sequences were experienced during validation and sample analysis.

The sensitivity gain of µUHPLC is based on the fact that MS with ESI source behaves like a concentration-dependent detector and can be maximized by maintaining a high injection volume and low volumetric flow rate. Therefore, a large injection volume of 5 µL was selected. Due to this large injection volume the composition of the sample diluent was of utmost importance. With 100% MeOH as sample diluent peaks were distorted. When the sample diluent consisted of 40% MeOH and 60% water (v/v), the sample zones were efficiently refocused during gradient elution (Suppl. materials Figure 55).

2.3.1.2.MS method development

Assay specificity of LC-MS/MS methods for oxylipins is a critical parameter and requires besides adequate chromatographic selectivity, also selection of proper SRM transitions. Distinct isomeric oxylipins may share common fragment ions and only the combination of selective LC, selective Q1 precursor isolation, and specific Q3 product ion selection may guarantee adequate assay specificity. Thus, SRMs were first established by automatic compound optimization provided by Sciex' analytical software Analyst (optimization of precursor and fragment ion, DP, CE and CXP). Each compound was prepared as single

solution of 1 µg/mL in MeOH and then diluted (around 1:1, v/v) with the mobile phase A in a syringe and sprayed directly to MS by direct infusion. For each compound the 3 most sensitive SRMs were chosen and then checked for selectivity by the LC-MS method. For this purpose, single standards were injected into µUHPLC-MS/MS at the highest concentration of the calibration ranges and all SRMs were recorded. The ion trace, which gave a selective signal at the expected retention time (as determined by single standard injection) for the respective analyte only was eventually chosen (Table 18). For the majority of the targets, selective SRM transitions could be found (Suppl. materials Table 31). FA(20:2) did not exhibit significant fragmentation and hence a pseudo-SRM transition was recorded i.e. the precursor ion with m/z 307.3 was selected in Q3 as well. As stated above, the isomer pairs PGE1 and PGD1 as well as PGE2 and PGD2 could not be distinguished by MS and required chromatographic separation which was accomplished by the described µUHPLC method (Suppl. materials Table 31).

2.3.1.3.Extraction protocol

Efficient extraction of targeted oxylipins with high recoveries, expedient enrichment and effective removal of interfering matrix components is of importance, especially for the current µUHPLC method. The large injection volume supports high sensitivity but at the same time amplifies the risk of matrix interferences and matrix effects. Dedicated sample preparation protocols are therefore mandatory. At the moment there is no common protocol for extraction of oxylipins, and different groups use different SPE cartridges and protocols, like Oasis HLB [147], Bond Elut Certify II [154, 155], Oasis MAX [108], Strata-X [123]. One protocol reports the use of liquid-liquid extraction (with MtBE) for extraction of oxylipins from platelets [77].

Following the comparison of different extraction protocols [163] Oasis HLB was initially evaluated regarding its performance for oxylipin extraction. The results, however, were quite disappointing; especially in terms of matrix effects (strong ion suppression was observed for most compounds). Therefore, other SPE cartridges: InertSep C18, Chromabond C18 ec, Strata-X and Oasis HLB Prime (as reversed phase stationary phases), as well as Oasis MAX and Bond Elut Certify II (as mixed-mode with strong anion exchanger stationary phases) were compared with each other and with the general

monophasic lipid extraction protocol with IPA. The latter lipid extraction protocol (comprising protein precipitation) gave high extraction yields but also exhibited strong matrix effects; therefore, it was not a viable option. The most promising results were obtained with Strata-X (average process efficiency equal to 35.9%) and Bond Elut Certify II (average process efficiency 37.7%) (for more details see Suppl. materials Table 32 and Table 33). The latter one was selected as SPE cartridge for the final extraction method. It is an anion exchange/mixed-mode SPE sorbent which allows capture of oxylipins by both ionic and hydrophobic interactions.

Besides, different sample pre-processing methods such as no protein precipitation, protein precipitation with $ZnSO_4$ and with ACN were tested as well (for more details see Suppl. materials Table 34 and Table 35). However, it was found that the simplest method, the one without protein precipitation prior to SPE, gave reasonable results and was used for the final method. It seems that plasma protein-bound oxylipins are sufficiently liberated during the SPE process.

2.3.2. Calibration and validation

Method validation largely followed the guideline of the Food and Drug Administration (FDA) [164]. Some adaptations were made in view of the given application and due to absence of analyte-free matrix.

For calibration three distinct approaches were initially evaluated (all containing ISs): i) External calibration prepared in sample diluent: H_2O/MeOH; 3:2, v/v (spiked solvent). ii) Standard-addition to plasma sample [165] (pre-extraction-spiked standard addition series), and iii) standard addition to extracted plasma sample (post-extraction spiked standard addition series). The slopes of these calibration curves were compared to each other, in order to assess the quality of each type of calibration to compensate for matrix effects and analyte losses during extraction. It was found that the slopes of spiked solvent and pre-extraction-spiked standard addition series matched very well for those analytes for which a compound-specific stable isotope analogue was available (e.g. RvD1 with RvD1-d5 as IS, see Suppl. materials Figure 57). Analytes, for which no compound-specific stable isotope labelled ISs were available, showed a significant difference between slopes of

standard solution and standard addition series (e.g. RvD2) (Suppl. materials Figure 57). It was therefore concluded that external calibration with standard solution is not adequate for the oxylipin assay in plasma, but that matrix-matched calibration is required.

The lack of blank matrix dictates more uncommon matrix-matched calibration approaches. Surrogate calibration [75] could be an option or standard addition [165]. Surrogate calibration is difficult to establish for a multiplexed assay like herein. A classical standard addition approach is not a viable option for a large clinical cohort, as samples have to be aliquoted and series of different levels of standards added to each sample have to be measured. It can be done for a limited number of samples with high accuracy requirements, but generates way too much expenditure for a clinical study. Therefore, an alternative matrix-matched standard addition approach was evaluated. A plasma pool was prepared, extracted as described in 2.2.3.2, and aliquots of this extract were fortified with standards at different levels affording a post-extraction spiked standard addition series (post-spiked matrix). Endogenous levels were obtained by extrapolation to the abscissa (-1×(x-intercept)). Correction of standard addition series for endogenous levels gave the working matrix-matched calibration which is suitable for quantification of a larger number of samples in an analysis sequence. This approach minimizes the expenditure for calibration and can also be carried out with cells for which matrix is limited (e.g. platelets, see below). It turned out that this 'post spiked matrix' calibration matched quite well with the one of classical standard addition corrected for endogenous levels (pre-extraction-spiked standard addition series) (Suppl. materials Figure 57). Forty (40) out of 41 analytes provided a deviation of the slope of the post-extraction spiked standard addition of less than 15% from the classical standard addition series (see Suppl. materials Figure 58). Hence, it was concluded that it is a viable option to use this simpler strategy of matrix-matched calibration. Notwithstanding, for plasma the classical standard addition approach corrected for endogenous levels was selected for calibration. However, for platelets (limited matrix available) the simplified approach of post-extraction spiked standard addition was utilized.

The method was then validated for plasma. Selectivity of the method was checked as absence of interferences from the other targeted analytes as described in 2.3.1.2. LOD and LOQ were calculated for each compound from the standard-addition calibration curve in plasma, based on the ratio of standard error to predict y-value (area ratio) to slope (s/S)

with LOD and LOQ defined as 3 and 10 times s/S. Only the 3 calibrants with concentrations closest to (but higher than) the intrinsic level of an analyte were considered for these calculations. In most of the cases LODs were lower than 40 pg/mL of plasma and LOQs were typically 100 pg/mL of plasma or lower (Table 19).

Table 19. *Summary of detection and quantification limits, linearity and range for oxylipin analysis in plasma.*

Analyte	Internal standard	Sensitivity		Linearity range		Calibration			
		LOD in plasma	LOQ in plasma			range	R		
		[ng/mL of plasma]		[ng/mL of solvent]	R	[spiked: ng/mL of plasma]	day1	day2	day3
PGF2a	PGF2a-d4	0.038	0.12	0.05 - 200	0.995	0.1 - 20	0.994	0.994	0.993
PGE1 and PGD1	PGD2-d9	0.010	0.03	0.05 - 200	0.995	0.01 - 20	0.997	0.996	0.996
TXB2	TXB2-d4	0.032	0.11	0.05 - 200	0.998	0.05 - 20	0.995	0.994	0.994
6-keto-PGF1a	RvE1-d4	0.010	0.03	0.05 - 200	0.999	0.02 - 20	0.998	0.997	0.998
PGE2	PGE2-d4	0.010	0.03	0.05 - 200	0.997	0.01 - 20	0.995	0.996	0.997
PGD2	PGD2-d9	0.010	0.03	0.05 - 200	0.994	0.01 - 20	0.996	0.998	0.996
10-HDoHE	12-HETE-d8	0.042	0.14	0.05 - 200	0.998	0.15 - 20	0.991	0.993	0.990
14-HDoHE	12-HETE-d8	0.015	0.06	0.05 - 200	0.996	0.05 - 20	0.995	0.995	0.993
17-HDoHE	12-HETE-d8	0.047	0.15	0.05 - 200	0.996	0.1 - 20	0.991	0.994	0.994
5-HETE	5-HETE-d8	0.010	0.03	0.05 - 200	0.994	0.02 - 20	0.992	0.996	0.989
8-HETE	13-HODE-d4	0.040	0.13	0.05 - 200	0.997	0.15 - 20	0.996	0.998	0.991
9-HETE	20-HETE-d6	0.055	0.18	0.05 - 200	0.997	0.15 - 20	0.993	0.986	0.999
11-HETE	12-HETE-d8	0.040	0.12	0.05 - 200	0.998	0.15 - 20	0.995	0.997	0.992
12-HETE	12-HETE-d8	0.038	0.13	0.05 - 200	0.998	0.15 - 20	0.997	0.998	0.993
15-HETE	13-HODE-d4	0.043	0.14	0.05 - 200	0.994	0.1 - 20	0.991	1.000	0.994
20-HETE	20-HETE-d6	0.010	0.03	0.05 - 200	0.995	0.01 - 20	0.993	0.996	0.994
5-HEPE	13-HODE-d4	0.010	0.03	0.05 - 200	0.990	0.05 - 20	0.997	0.994	0.997
8-HEPE	13-HODE-d4	0.011	0.04	0.05 - 200	0.995	0.01 - 20	0.988	0.994	0.995
12-HEPE	13-HODE-d4	0.010	0.03	0.05 - 200	0.997	0.05 - 20	0.997	0.997	0.996
15-HEPE	13-HODE-d4	0.021	0.06	0.05 - 200	0.996	0.02 - 20	0.997	0.987	0.987
18-HEPE	13-HODE-d4	0.080	0.27	0.05 - 200	0.994	0.2 - 20	0.997	0.996	0.995
14(15)-EpETE	HTE-d5	0.015	0.05	0.05 - 200	0.996	0.02 - 20	0.992	0.995	0.994
5,6-DiHETE	20-HETE-d6	0.022	0.07	0.25 - 200	0.996	0.15 - 20	0.994	0.983	0.993
5-OxoETE	LTB4-d4	0.010	0.03	0.05 - 200	0.998	0.01 - 20	0.992	0.997	0.996
9-HODE	13-HODE-d4	0.990	3.03	0.5 - 500	0.992	2 - 200	0.998	0.994	0.995
13-HODE	13-HODE-d4	0.921	3.08	0.5 - 500	0.997	2 - 200	0.997	0.996	0.998
LXA4	RvD1-d5	0.012	0.04	0.05 - 200	0.998	0.01 - 20	0.995	0.997	0.994
12-HHT	Mar2-d5	0.010	0.04	0.05 - 200	0.994	0.1 - 20	0.994	0.993	0.996
12-KHT	LTB4-d4	0.010	0.03	0.05 - 200	0.996	0.01 - 20	0.996	0.997	0.995
LTB4	LTB4-d4	0.010	0.03	0.05 - 200	0.999	0.01 - 20	0.997	0.996	0.996
T-12-HETE	LTB4-d4	0.040	0.12	0.05 - 200	0.999	0.05 - 20	0.996	0.997	0.993
RvD1	RvD1-d5	0.010	0.03	0.05 - 200	0.998	0.01 - 20	0.996	0.996	0.995
RvD2	RvD1-d5	0.024	0.08	0.05 - 200	0.998	0.1 - 20	0.994	0.993	0.992
RvD3	RvD1-d5	0.021	0.07	0.05 - 200	0.998	0.01 - 20	0.992	0.996	0.996
RvD4	RvD1-d5	0.013	0.04	0.05 - 200	0.997	0.01 - 20	0.995	0.995	0.995
RvD5	LTB4-d4	0.010	0.03	0.05 - 200	0.999	0.01 - 20	0.996	0.995	0.995
RvE1	RvE1-d4	0.010	0.03	0.05 - 200	0.999	0.01 - 20	0.997	0.998	0.996
Mar1	LTB4-d4	0.027	0.09	0.05 - 200	0.997	0.05 - 20	0.997	0.994	0.992
Mar2	Mar2-d5	0.014	0.05	0.05 - 200	0.998	0.01 - 20	0.996	0.996	0.994
12-HETrE	HTE-d5	0.010	0.03	0.05 - 200	0.998	0.02 - 20	0.994	0.994	0.990
13-HOTrE	13-HODE-d4	0.013	0.04	0.05 - 200	0.992	0.02 - 20	0.996	0.997	0.997

The instrument linearity range was checked with standards dissolved in H_2O/MeOH (3:2; v/v). For most of the oxylipins standard solutions up to 200 ng/mL were prepared. Higher concentrations were not used, as they were considered irrelevant for biological samples.

An additional reason was also the high price and restricted availability of oxylipin standards. Only 9- and 13-HODE were prepared in higher concentrations, up to 2 µg/mL. For all the oxylipins concentrations between 0.05 – 200 ng/mL were within the instrument linearity range. In case of the HODEs the instrument linearity range was up to 500 ng/mL (Table 19).

Table 20. *Validation of extraction recoveries and matrix effects in plasma (mean and standard deviation of three distinct levels).*

Analyte	**Extraction recovery** [%]		**Matrix effect** [%]	
	mean	sd	mean	sd
PGF2a	87.4	3.3	41.2	3.4
PGE1 and PGD1	83.7	11.7	35.0	4.6
TXB2	88.1	8.8	47.4	2.4
6-keto-PGF1a	93.1	11.2	80.2	27.2
PGE2	96.1	14.0	55.9	7.5
PGD2	82.6	7.1	34.5	1.6
10-HDoHE	67.1	7.6	44.8	7.2
14-HDoHE	81.8	5.5	44.1	8.2
17-HDoHE	75.3	8.4	31.4	0.7
5-HETE	102.9	7.4	53.5	11.9
8-HETE	69.6	6.4	48.5	7.5
9-HETE	79.2	12.8	37.3	4.7
11-HETE	72.9	7.9	33.3	4.7
12-HETE	66.7	8.8	54.3	0.5
15-HETE	84.1	6.6	38.3	3.1
20-HETE	44.1	4.6	48.8	3.7
5-HEPE	73.7	3.2	45.4	1.9
8-HEPE	59.7	5.7	45.8	7.0
12-HEPE	77.3	5.2	54.2	2.0
15-HEPE	69.5	3.5	40.5	2.9
18-HEPE	53.0	2.8	49.5	4.8
14(15)-EpETE	61.5	3.3	50.7	7.3
5,6-DiHETE	84.2	9.6	79.2	11
5-OxoETE	61.2	8.5	44.1	3.3
9-HODE	73.1	9.7	43.9	3.4
13-HODE	74.5	9.9	54.1	1.8
LXA4	71.8	9.5	38.7	5.2
12-HHT	95.1	5.3	31.1	1.1
12-KHT	66.4	2.1	42.5	2.4
LTB4	76.5	7.3	60.9	14.7
T-12-HETE	88.6	9.2	37.4	5.3
RvD1	69.6	9.7	47.9	5.2
RvD2	78.5	7.3	26.4	7.1
RvD3	67.0	0.5	54.3	4.0
RvD4	82.8	6.2	59.1	11.1
RvD5	75.1	5.1	55.2	10
RvE1	92.4	13.0	45.4	2.3
Mar1	74.1	6.2	40.1	8.7
Mar2	81.8	8.4	52.0	6.3
12-HETrE	38.3	4.7	58.6	3.8
13-HOTrE	68.9	6.7	50.3	7.1

Extraction recoveries and matrix effects were determined for all analytes (Table 20) and also internal standards (Suppl. materials Table 33). For this purpose, QCs in plasma spiked before and after extraction, respectively, with 1.6, 5 and 16 ng per 1 mL of plasma, and 10 times more for HODEs were prepared. Extraction recoveries and matrix effects were determined according to the protocol of Matuszewski [137]. Extraction recoveries of

oxylipins were mostly above 70% (mean over all oxylipins 75.3 ± 13.3%) (Table 20). Significant ion suppression, despite SPE purification, was observed for the majority of analytes, most probably due to the large injection volume. Matrix effect was around 40-50% (mean 47.2 ± 11.2) (Table 20). To compensate for high matrix effect a large number of isotope-labelled ISs was included. For those compounds, for which no stable isotope labelled IS was available, the proper IS was carefully assigned.

Table 21. *Between batch precision and accuracy for plasma.*

	Between batch accuracy			Between batch precision		
Analyte	**QC low**	**QC mid**	**QC high**	**QC low**	**QC mid**	**QC high**
PGF2a	94.7	102.6	101.4	2.5	6.0	6.9
PGE1 and PGD1	98.0	107.6	99.5	11.8	7.3	11.4
TXB2	101.3	104.8	96.3	3.6	5.7	4.5
6-keto-PGF1a	89.9	95.4	94.4	7.9	8.5	11.4
PGE2	95.0	103.7	95.8	7.1	7.5	8.1
PGD2	94.3	106.8	99.0	4.6	5.3	6.9
10-HDoHE	96.6	105.5	92.9	2.1	10.2	2.4
14-HDoHE	106.7	105.7	96.9	3.9	12.7	11.6
17-HDoHE	99.8	103.0	93.6	5.2	10.3	6.0
5-HETE	98.6	100.9	95.8	13.2	10.0	9.9
8-HETE	88.7	110.3	93.2	3.7	12.0	5.3
9-HETE	104.5	102.9	98.0	5.1	10.0	6.4
11-HETE	92.7	101.5	93.2	6.5	7.5	7.0
12-HETE	105.2	99.3	96.2	21.1	2.0	8.2
15-HETE	97.9	109.9	103.8	11.3	2.3	7.0
20-HETE	92.9	97.4	91.2	5.6	15.5	4.7
5-HEPE	102.0	99.7	102.9	5.1	12.4	7.0
8-HEPE	89.6	101.3	92.5	3.4	6.1	2.2
12-HEPE	87.1	90.4	89.3	4.3	2.8	3.9
15-HEPE	96.4	93.9	95.0	4.2	11.4	9.2
18-HEPE	103.5	102.4	93.3	9.1	3.3	10.2
14(15)-EpETE	100.1	104.6	94.3	12.2	9.1	2.0
5,6-DiHETE	114.7	93.8	98.4	21.8	6.3	11.8
5-OxoETE	87.9	110.2	90.9	7.5	6.2	9.2
9-HODE	94.8	103.7	93.2	8.8	5.8	8.4
13-HODE	104.5	104.4	96.1	9.8	3.6	6.3
LXA4	94.1	101.9	96.0	9.7	9.4	9.2
12-HHT	94.4	101.6	89.9	11.2	5.1	1.3
12-KHT	93.2	109.3	97.4	7.3	2.8	7.0
LTB4	91.6	103.2	95.6	6.2	5.3	1.8
T-12-HETE	92.4	106.3	100.3	8.4	4.2	5.4
RvD1	103.2	108.5	104.1	12.2	1.5	10.4
RvD2	101.2	97.1	93.6	11.6	7.2	4.7
RvD3	106.0	106.7	106.1	2.5	11.0	6.9
RvD4	101.3	103.6	101.7	10.2	3.2	7.2
RvD5	90.1	100.4	90.9	4.8	2.4	4.5
RvE1	92.2	103.5	95.4	3.7	3.8	2.1
Mar1	94.1	103.3	94.8	4.2	5.6	2.8
Mar2	92.0	105.4	98.7	5.6	5.3	3.4
12-HETrE	84.0	92.3	85.1	7.8	20.4	9.9
13-HOTrE	102.3	100.0	92.6	2.8	10.1	14.0

Finally, within-batch and between-batch precision and accuracy were validated using matrix-matched calibration corrected for endogenous levels and obtained by pre-extraction standard addition approach. The results for within batch precision and accuracy are given

in Suppl. materials Table 38 and the results for between batch precision and accuracy are summarized in Table 21. It can be seen in Table 21 that the employed internals standards adequately corrected for losses during extraction and matrix effects so that the results passed the requirements of FDA, which state that precision (as determined by % RSD) and accuracy (as assessed by % bias) should be less than 15%. The assay performance should therefore be adequate, if LOQs are adequate.

Here it should be mentioned that the quality of the supplied standards was not validated, as suggested by N.H. Schebb [150], but labelled concentrations of the supplied standards were assumed to be correct. For inter-laboratory and inter-study comparisons it is, however, advised to assure the correct concentrations of supplied non-certified standard solutions by protocols as suggested.

2.3.3. Concentration of oxylipins in biological samples

2.3.3.1. Results for plasma

The validated multi-target µUHPLC-ESI-MS/MS assay was employed to determine the concentrations of the targeted oxylipins in pooled human EDTA plasma. The results are summarized in Table 22. It can be seen that several oxylipins, in particular lipoxin A4, resolvins, maresins, some less abundant HETE and HEPE constitutional isomers could not be detected (<LOD), as expected. The highest concentrations were found for 9- and 13-HODE (3.3 and 4.4 ng/mL). TXB2, 14HDoHE, 12-HETE, 15-HETE, 5,6-diHETE, 12-HHT, 12-HETrE, and 13-HOTrE were detected in a concentration range between 100 and 400 pg/mL. Other oxylipins such as PGE2, PGD2, 5-HETE, 20-HETE, 5-HEPE, and 12-HEPE were found in the range between LOQ and 100 pg/mL. Evidently, for many oxylipins LOQs were adequate to allow quantification of these important lipid mediators in plasma samples of healthy donors. These findings clearly document the practical applicability of the newly developed µUHPLC-ESI-MS/MS assay.

Table 22. *Concentration (with standard deviation) of oxylipins in pooled plasma.*

Analyte	Concentration [pg/mL of plasma]	sd	Analyte	Concentration [pg/mL of plasma]	sd
PGF2a	< LOD		14(15)-EpETE	< LOD	
PGE1 and PGD1	< LOD		5,6-DiHETE	236	82
TXB2	131	17	5-OxoETE	< LOD	
6-keto-PGF1a	< LOD		9-HODE	3331	419
PGE2	38	3	13-HODE	4210	436
PGD2	33	2	LXA4	< LOD	
10-HDoHE	< LOQ		12-HHT	133	17
14-HDoHE	139	11	12-KHT	< LOD	
17-HDoHE	< LOQ		LTB4	< LOD	
5-HETE	61	6	T-12-HETE	< LOQ	
8-HETE	< LOQ		RvD1	< LOD	
9-HETE	< LOD		RvD2	< LOD	
11-HETE	< LOQ		RvD3	< LOD	
12-HETE	353	39	RvD4	< LOD	
15-HETE	184	23	RvD5	< LOD	
20-HETE	29	11	RvE1	< LOD	
5-HEPE	40	4	Mar1	< LOD	
8-HEPE	< LOD		Mar2	< LOD	
12-HEPE	45	2	12-HETrE	107	13
15-HEPE	< LOQ		13-HOTrE	142	5
18-HEPE	< LOQ				

2.3.3.2.Results for platelets

The ultimate goal of this study was to establish a targeted lipidomics workflow to accurately measure oxylipins in platelets. Thus, the method which was first developed for readily available plasma was adapted for platelets isolated from peripheral blood. Some adjustments in sample preparation had to be made. Oxylipins were first extracted from platelets with IPA and then subjected to SPE. Due to limited amounts of matrix in case of platelets, matrix-matched calibration was done by post-extraction spiked standard addition series as described above. For this purpose, the platelet samples of 5 donors (each 2×10^8 platelets) were extracted with IPA and then aliquoted for calibrant and (spiked and non-spiked) QC preparation (see Suppl. materials chapter 6 for more details); one aliquot of each sample was kept for analysis of oxylipins concentrations in the platelet samples under resting (non-activated) state from 5 healthy donors. Endogenous levels of oxylipins in the pooled platelet extract were obtained from the x-intercept of the standard addition series. Matrix-matched calibration functions for platelets were then constructed and used to

determine endogenous concentration of oxylipins in samples from each donor, as well as method LOD and LOQ (in the same way as described above for plasma). The non-spiked QC injections allowed deriving information on the precision of the µUHPLC-MS/MS method for this matrix. The results of this preliminary validation are summarized in Suppl. materials Table 39.

Table 23. *Concentrations of oxylipins in non-activated (resting) platelets (targeted analytes, which are not found in the table, were not detected in the samples).*

Analyte	Donor				
	D1	D2	D3	D4	D5
	Estimated concentration [ng/1 x 108 platelets]				
TXB2	11.95	8.36	2.47	2.43	12.97
PGE2	< LOQ	0.69	< LOD	< LOD	< LOQ
10-HDoHE	< LOQ	0.98	< LOQ	< LOQ	< LOQ
14-HDoHE	< LOQ	33.44	< LOQ	< LOD	< LOD
17-HDoHE	0.39	1.22	< LOD	< LOD	< LOD
8-HETE	0.05	0.36	0.09	< LOD	< LOD
9-HETE	< LOQ	6.71	< LOQ	< LOQ	< LOQ
11-HETE	0.38	0.63	< LOQ	< LOQ	0.36
12-HETE	< LOQ	44.58	< LOQ	< LOD	< LOQ
15-HETE	< LOQ	0.37	< LOD	< LOD	< LOQ
12-HEPE	3.34	23.59	2.73	< LOQ	< LOQ
15-HEPE	< LOQ	0.72	0.57	0.32	0.44
9-HODE	< LOQ	4.22	< LOQ	< LOQ	< LOQ
13-HODE	6.06	18.33	5.94	4.46	4.52
12-HHT	54.34	16.98	5.28	6.39	15.1
12-KHT	1.2	< LOD	< LOD	< LOD	0.35
T-12-HETE	0.09	2	< LOD	< LOD	< LOD
12-HETrE	< LOD	11.9	< LOQ	< LOD	< LOD
13-HOTrE	0.27	1.83	0.3	< LOQ	< LOQ

The concentrations of oxylipins measured in non-activated (resting) platelet samples from 5 distinct donors are given in Table 23. It can be seen that the baseline levels of many oxylipins are very low, in many cases undetectable. However, some donors clearly show elevated baseline concentrations, e.g. donor 2 (D2). Resolvins, maresins, and lipoxin A4 were not detected. The major platelet activation factor Thromboxan A2 (analysed as the more stable analogue TXB2) was found above LOQ in the platelet samples of all donors (between 2 and 15 ng/100 Mio platelets corresponding to about 20-150 atto gram per platelet). The assay was found to be suitable and will be utilized to determine oxylipin concentrations in experimental platelet samples of a pharmacolipidomics project as well as in patients of a clinical CAD cohort.

2.3.4. Discussion of assay performance

Some recent reviews discussed the general performance of assays for oxylipins in biofluids, particularly in plasma [12, 124, 148]. In any case, most of the LC-MS/MS assays employed SPE to extract and enrich oxylipins, in order to reach required LOQs down to the low pg/mL range. Gladine et al. reported a summary of LC-MS/MS assays, which is quite useful to assess the performance of our assay in comparison to previously published works (see Table 2 of ref [148] and in Suppl. materials Table 41). LOQs were typically in the range of 0.5-600 fmol injected on-column [123, 147, 148, 166]. In our work, these values were between 2.0 and 250 fmol on-column for plasma and between 0.7 and 8.4 fmol on-column for standard solution (Suppl. materials Table 40). It allowed to quantitate important oxylipins down to the low pg/mL range, e.g. PGE2 and PGD2 down to 30 pg/mL (LOQ) corresponding to 0.085 nM in plasma. On the other hand, run times were typically between 10 and 30 min in those reported assays. Our µUHPLC-ESI-MS/MS assay eluted all target compounds within 8 min and took only 13 min together with column regeneration and re-equilibration. While other assays partly cover more analytes (up to 175 oxylipins), the coverage of the current method is reasonable, in particular for its application to platelets. Overall, the current µUHPLC-MS/MS assay for oxylipins compares fairly well with recently published assays using standard flow HPLC and UHPLC format.

2.4. Conclusions

A new sensitive and highly economic µUHPLC-ESI-MS/MS assay for oxylipin analysis in terms of solvent usage (less than 250 µL of organic solvent in the mobile phase per sample) has been developed. It has been validated for plasma and documented its suitability to analyse baseline levels in plasma and platelets as real biological test samples. The assay covers 42 oxylipins. It shows good precision and accuracy for quantitative analysis in plasma and platelets. The microflow regime may be a good compromise between nano-HPLC with its higher sensitivity due to reduced volumetric flow rates in the nL/min range and standard HPLC with its robustness in several 100 µL/min flow regime. The current µUHPLC assay may also be regarded as eco-friendly. If implemented in routine analysis in clinical laboratories, limited use of toxic acetonitrile of the mobile phase may help to reduce organic waste.

Acknowledgements

This project was funded by the Deutsche Forschungsgemeinschaft (DFG, German Research Foundation) – Project number 374031971 – TRR 240.

Declaration of conflict of interests

The authors declare no conflict of interests.

2.5.Supplementary materials

2.5.1. LC-MS method development

2.5.1.1.Comparison of mobile phases

Table 24. *Preparation of mobile phases for the first round of comparison.*

Mobile phase		H_2O	ACN	MeOH	200 mM NH_4Ac in H_2O	200 mM NH_4FA in H_2O	HAc	FA
		mL	mL	mL	mL	mL	µL	µL
A	1	97.5			2.5			
B	1	2.5	95		2.5			
A	2	97.5				2.5		
B	2	2.5	95			2.5		
A	3	97.5			2.5		100	
B	3	2.5	95		2.5		100	
A	4	97.5				2.5		100
B	4	2.5	95			2.5		100
A	5	100					100	
B	5	5	95				100	
A	6	100						100
B	6	5	95					100
A	7	97.5			2.5			
B	7	2.5		95	2.5			
A	8	97.5				2.5		
B	8	2.5		95		2.5		
A	9	97.5			2.5		100	
B	9	2.5		95	2.5		100	
A	10	97.5				2.5		100
B	10	2.5		95		2.5		100
A	11	100					100	
B	11	5		95			100	
A	12	100						100
B	12	5		95				100

Different mobile phases were tested to figure out which one will give the best sensitivity (assessed by the S/N ratio for selected oxylipins) and the best selectivity (i.e. resolution between PGE2 and PGD2).

In the first round, ACN and MeOH were compared as mobile phase B (mobile phase B consisted of 95% of organic solvent and 5% of water (v/v)). Six different types of additives were added: 5 mM NH_4FA, 5 mM NH_4Ac, 0.1% FA (v/v), 0.1% HAc (v/v), 5 mM NH_4FA with 0.1% FA (v/v) and 5 mM NH_4Ac with 0.1% HAc (v/v). Mobile phase A was prepared separately for each type of mobile phase B and it consisted of water with the same additive in the same concentration as in the matching mobile phase B. Preparation of each mobile phase is shown in Table 24.

A short 3.5 min chromatographic method with linear gradient from 10% to 50% B when ACN was used and 40% to 80% when MeOH was used was programmed to compare the performances of the mobile phases.

Table 25. *Comparison of S/N ratios for 3 prostaglandins with different mobile phases. The best result for each compound is marked with dark green background and the second-best result with light green.*

Mobile phase	**PGE2** (100 pg/mL)		**PGD2** (100 pg/mL)		**PGF2a** (1 ng/mL)	
	S/N	*st. dev.*	*S/N*	*st. dev.*	*S/N*	*st. dev.*
1	10.9	1.6	6.1	1.4	16.9	6.0
2	9.2	4.9	5.7	1.7	14.3	2.7
3	14.6	2.1	6.3	0.3	16.0	3.5
4	8.8	0.5	6.0	2.7	15.5	2.7
5	22.2	5.5	9.1	1.5	11.2	3.1
6	10.8	1.7	4.5	1.6	12.9	1.7
7	23.9	4.8	11.9	3.5	26.4	3.1
8	Not separated				21.0	4.1
9	Not separated				25.6	1.5
10	Not separated				16.7	2.1
11	Not separated				13.8	2.3
12	Not separated				3.7	4.4

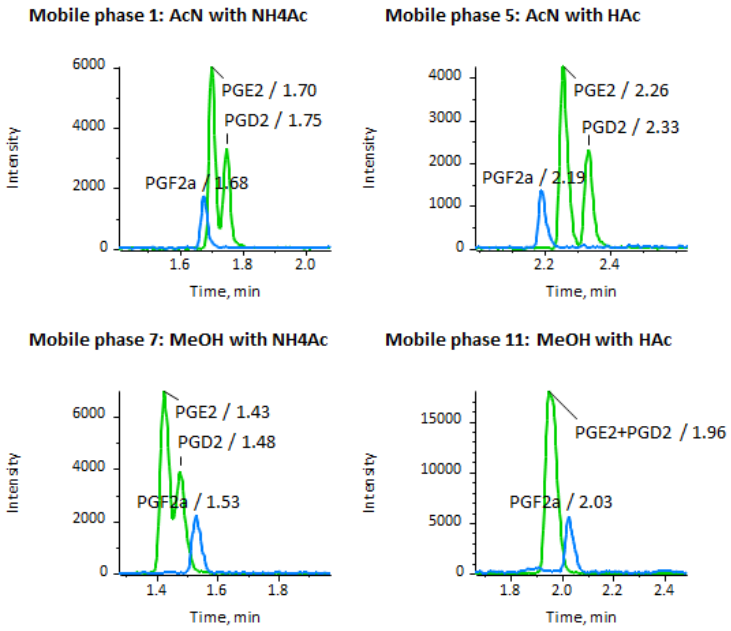

***Figure 53**. EIC of 3 prostaglandins with 4 selected methods.*

***Table 26.** Preparation of mobile phases for the second round of comparison.*

Mobile phase			H_2O	ACN	MeOH	200 mM NH_4OAc in H_2O	200 mM NH_4FA in H_2O	HAc	FA
			mL	mL	mL	mL	mL	µL	µL
A	13		95			5			
B	13	a		95		5			
B	13	b		70	25	5			
B	13	c		50	45	5			
A	14		95			5		100	
B	14	a		95		5		100	
B	14	b		70	25	5		100	
B	14	c		50	45	5		100	
A	15		95					100	
B	15	a		95				100	
B	15	b		70	25			100	
B	15	c		50	45			100	
A	16		95				5		
B	16	a		95			5		
B	16	b		70	25		5		
B	16	c		50	45		5		
A	17		100				5		100
B	17	a	5	95			5		100
B	17	b	5	70	25		5		100
B	17	c	5	50	45		5		100
A	18		100						100
B	18	a	5	95					100
B	18	b	5	70	25				100
B	18	c	5	50	45				100

Two mixtures of selected prostaglandins (PGE2, PGD2 and PGF2a) in H_2O/MeOH 3:2 (v/v) were prepared, one with concentration of 100 pg/mL of each prostaglandin and the

other 1 ng/mL of each prostaglandin. The mixtures were injected in triplicates with each mobile phase. PGE2 and PGD2 gave higher peaks and therefore the lower concentration (100 pg/mL) was used for comparison. PGF2a, which gave smaller peaks, was compared at higher concentration (1 ng/mL). The comparison of the sensitivity for the different mobile phases is shown in Table 25.

These preliminary results showed that the best sensitivity was obtained with MeOH with salt (in particular 5 mM ammonium acetate, eluent 7) as additive (also acids with salts gave good results). However, mobile phases containing MeOH gave also quite broad peaks with worse separation of PGE2 and PGD2, when compared to ACN (examples are shown in Figure 53).

Table 27. *Comparison of S/N ratios for oxylipins at concentration* ***1 ng/mL*** *with different mobile phases. The best result for each compound is marked with dark green background and the second-best result with light green.*

Mobile phase	PGE2		PGD2		PGF2a		HHT		5-HETE		12-HETE		9-HODE		13-HODE	
	S/N	*Sd*	*S/N*	*sd*	*S/N*	*sd*	*S/N*	*sd*	*S/N*	*sd*	*S/N*	*sd*	*S/N*	*sd*	*S/N*	*sd*
13a	25	3	36	4	46	3	22	2	73	10	210	16	167	11	126	3
13b	23	1	38	6	40	7	22	4	90	8	273	17	198	10	173	12
13c	23	1	35	2	47	4	50	8	146	9	475	9	329	13	330	12
14a	31	2	60	7	71	13	40	3	93	5	318	33	268	3	269	2
14b	41	7	80	3	73	3	65	6	147	14	504	30	410	25	388	16
14c	48	5	97	7	118	8	70	5	153	10	534	19	441	7	407	23
15a	220	17	601	10	368	11	284	13	489	39	1764	101	1662	73	1581	54
15b	168	25	527	44	254	29	267	23	485	40	1638	51	1556	18	1357	107
15c	207	7	569	39	580	118	188	20	431	35	1230	75	1333	50	1208	142
16a	34	6	34	6	41	10	12	2	45	8	118	17	99	14	98	10
16b	40	5	40	5	52	13	31	3	68	4	236	14	185	9	186	23
16c	58	3	58	3	59	8	33	4	83	7	238	21	186	10	191	13
17a	31	2	55	5	56	8	22	2	65	10	193	17	158	2	147	8
17b	39	3	79	2	95	10	31	3	95	6	277	10	199	13	199	18
17c	99	8	99	8	129	5	28	9	105	16	276	28	186	2	191	17
18a	94	16	203	24	229	20	83	14	315	23	781	91	608	38	559	29
18b	128	13	264	21	291	40	118	9	369	13	1277	54	745	53	703	31
18c	143	13	309	42	342	28	108	17	350	18	985	25	729	8	697	13

The second round of comparison involved mixtures of ACN and MeOH to check if it is possible to obtain narrow peaks (as for ACN) with great sensitivity of MeOH (Table 26). The LC gradient for this comparison was as follows: 10% to 70% B in 5 min. More

compounds were added at this point to obtain broader knowledge about sensitivity (2 mixtures in H_2O/MeOH 3:2 (v/v): 100 pg/mL of each compound and 1 ng/mL of each compound; PGE2, PGD2, PGF2a, HHT, 5-HETE, 12-HETE, 9-HODE and 13-HODE).

Table 28. *Comparison of S/N ratios for oxylipins at concentration* ***100 pg/mL*** *with different mobile phases. The best result for each compound is marked with dark green background and the second-best result with light green.*

Mobile phase	PGE2		PGD2		PGF2a		HHT		5-HETE		12-HETE		9-HODE		13-HODE	
	S/N	*Sd*	*S/N*	*sd*	*S/N*	*sd*	*S/N*	*sd*	*S/N*	*sd*	*S/N*	*sd*	*S/N*	*sd*	*S/N*	*sd*
13a									7.2	1.1	21.7	4.6	26.7	0.3	21.5	0.5
13b									11.6	3.4	34.0	6.2	27.3	2.5	26.2	2.1
13c									15.9	3.7	46.0	3.0	37.0	2.0	57.2	4.7
14a									14.5	4.0	39.0	2.0	35.7	4.5	34.3	5.3
14b									18.5	7.8	48.5	2.1	48.5	3.5	49.5	2.1
14c									18.2	3.8	62.7	10.0	53.7	7.1	55.8	8.0
15a	30.1	0.6	55.3	3.5	56.8	2.0	26.4	7.3	61.0	3.6	200.9	11.8	212.0	12.9	199.8	4.8
15b	21.6	1.5	47.0	1.0	36.0	2.7	30.5	4.1	59.8	3.0	188.5	5.5	187.6	11.7	189.7	13.9
15c	18.7	7.6	42.3	3.1	203.1	42.4	25.8	3.0	59.8	11.5	183.0	9.0	184.4	9.2	172.7	21.7
16a	5.3	2.5	5.3	2.5	5.6	0.9			7.9	2.1	11.7	1.5	14.3	1.2	16.6	2.2
16b	6.3	1.2	6.3	1.2	8.4	1.6			11.6	4.5	27.0	4.0	34.0	1.7	37.7	7.5
16c	7.7	1.5	7.7	1.5	11.3	4.5			13.0	3.0	30.3	3.1	32.3	7.5	40.3	4.2
17a	8.0	5.2	8.0	5.2	9.2	3.8			9.4	1.2	24.7	3.2	19.7	2.9	21.7	2.1
17b	9.0	1.7	9.0	1.7	12.9	0.9			13.7	3.0	32.0	5.2	25.0	4.4	32.0	5.0
17c	11.3	2.1	11.3	2.1	18.7	3.1			16.9	4.7	27.7	2.3	28.3	4.2	30.0	9.5
18a	10.3	0.6	24.0	2.6	28.2	3.3	8.9	0.9	38.3	10.2	85.3	13.1	76.7	8.6	63.5	4.0
18b	18.0	2.0	28.7	1.5	33.9	4.7	12.5	1.9	44.2	9.3	140.7	1.5	91.7	9.8	88.3	6.7
18c	16.7	5.1	37.0	0.0	55.1	16.3	14.2	1.4	37.1	1.8	98.0	3.0	94.7	5.5	93.2	2.3

The best results were obtained when 0.1% HAc was used (Table 27 and Table 28). As earlier shown, peaks were broader when more MeOH was in the mobile phase (Figure 54). In the next step, different gradient methods were evaluated for mobile phases 15a, 15b and 15c (data not shown). The best results in terms of sensitivity and PGE2-PGD2 resolution were obtained with ACN and without addition of MeOH.

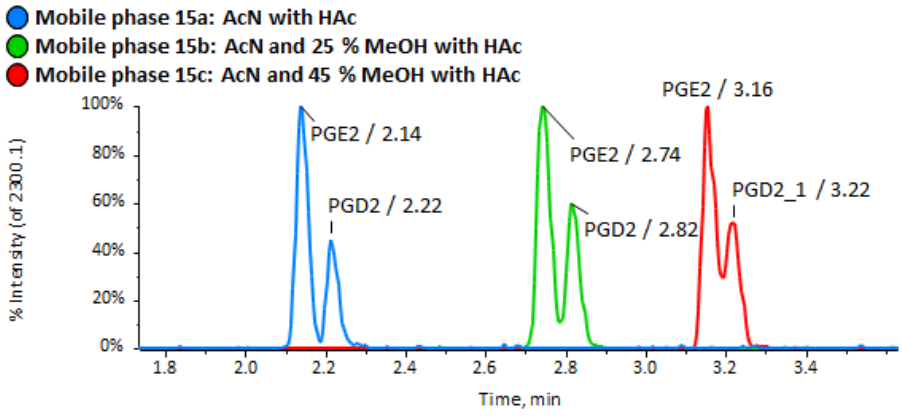

Figure 54*. EIC of PGE2 and PGD2 with 3 selected mobile methods.*

The final mobile phase was chosen as: A – 100% H_2O with 0.1% HAc and B – 100% ACN with 0.1% HAc.

2.5.1.2.Adjustment of column temperature and flow rate

Table 29. *Comparison of S/N ratio for oxylipins at concentration 100 pg/mL with different flow rates. The best result for each compound is marked with dark green background and the second-best result with light green.*

Flow rate [uL/min]	PGE2		PGD2		PGF2a		HHT		5-HETE		12-HETE		9-HODE		13-HODE	
	S/N	*sd*	*S/N*	*sd*	*S/N*	*sd*	*S/N*	*sd*	*S/N*	*sd*	*S/N*	*sd*	*S/N*	*sd*	*S/N*	*sd*
20	36.3	2.3	61.7	4.7	130.7	21.0	38.6	4.2	22.7	0.6	94.0	7.9	151.0	1.7	158.7	14.0
25	30.3	4.0	65.3	9.9	132.2	14.7	36.3	3.8	42.0	9.2	149.7	12.7	167.1	12.6	157.1	27.2
30	29.7	3.2	52.7	4.2	118.2	9.9	31.0	3.5	45.0	7.0	139.3	9.7	178.3	22.3	175.6	14.9
35	21.7	1.2	47.7	4.0	90.2	2.4	26.3	4.0	46.7	7.0	143.3	8.6	166.4	4.1	147.6	23.0
40	22.0	2.0	41.3	5.1	81.9	6.3	23.0	1.7	43.0	3.6	124.4	9.8	158.0	11.5	139.7	5.9
45	21.3	3.1	39.3	1.5	78.5	8.0	19.7	2.5	45.7	3.5	124.3	8.1	132.2	1.8	125.9	13.2
50	19.0	0.0	42.7	3.8	69.8	11.4	16.7	1.5	40.7	4.6	125.0	2.0	122.6	23.1	118.2	9.5

Seven different flow rates between 20 and 50 µL/min were tested to compare sensitivity (S/N) (Table 29). For most of the compounds the sensitivity was the best when a low flow rate was used (20 – 35 µL/min). The flow rate for the final method was chosen as 30 µL/min as a compromise between efficiency and run time.

Table 30. *Comparison of S/N ratio for oxylipins at concentration 100 pg/mL with different temperatures. The best result for each compound is marked with dark green background and the second-best result with light green.*

Temperature [°C]	PGE2		PGD2		PGF2a		HHT		5-HETE		12-HETE		9-HODE		13-HODE	
	S/N	*sd*	*S/N*	*sd*	*S/N*	*sd*	*S/N*	*sd*	*S/N*	*sd*	*S/N*	*sd*	*S/N*	*sd*	*S/N*	*sd*
30	37.3	5.1	55.7	3.2	132.6	7.8	51.7	8.1	64.7	8.0	208.7	3.2	249.0	14.1	206.6	3.0
35	36.7	1.5	65.0	6.1	147.0	4.1	58.7	2.1	64.3	4.5	243.7	14.5	275.4	36.0	239.7	18.7
40	41.7	6.5	67.7	7.8	147.0	6.1	51.9	3.0	82.0	5.3	261.7	8.3	290.5	31.1	253.9	12.0
45	36.7	8.5	67.0	12.8	143.7	3.9	52.5	6.4	79.7	6.0	290.3	9.1	303.2	40.8	294.7	36.7
50	40.7	2.5	65.7	7.6	152.4	6.4	57.5	6.5	83.7	1.2	301.7	17.6	316.8	21.2	301.1	51.2

In the next step the column temperature was adjusted. Five different temperatures between 30 and 50°C were compared. As always, higher S/N was used as parameter for the decision.

The highest temperature gave the best results for most of the compounds. No temperature higher than 50°C was tested, because of the column usage guideline discourages use of higher temperatures.

The temperature 50°C was used in the final method.

2.5.1.3.Comparison of injection solvents

Standards solutions of oxylipins in different injection solvents with different H_2O-MeOH ratios were prepared. On the one hand, the injection solvent should match well with the gradient starting conditions i.e. it should not have higher elution strength and, on the other hand, it should provide good solubility of analytes. The first requirement is better fulfilled with high water content (the RP method starts with 15% ACN in H_2O). For the second requirement more MeOH is better, especially when common lipid extraction protocols are used, as apolar lipids extracted with such procedures might not be fully soluble in high water content solvents.

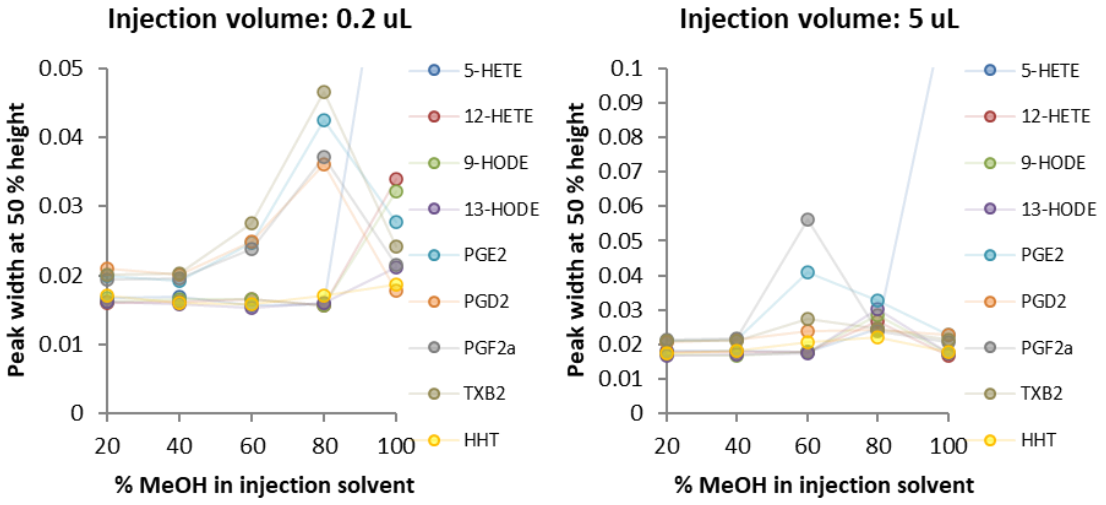

Figure 55. *Comparison of peak width (at 50% of peak height) with different injection solvents for 2 injection volumes (left: 0.2 µL and right: 5 µL) and 9 oxylipins.*

It is especially important for µLC to carefully select the injection solvent as the injected sample volume, here 5 µL, is quite large. This large injection volume was selected in favour

of high sensitivity of the method. It means that the column is filled to a significant extent with the sample plug and efficient refocusing on the stationary phase is mandatory to avoid extra peak broadening which is possible only with a weakly eluting sample solvent (diluent).

Peaks, especially early eluted ones, showed significant peak broadening when solvent with high MeOH content was used for sample reconstitution. No negative effects were observed for low MeOH contents. However, poor solubility of real extracts was giving some problems. The final method used therefore a H_2O/MeOH (3:2; v/v) mixture as injection solvent as a good compromise (Figure 55).

2.5.1.4.Selectivity of the final µUHPLC-MS/MS method

Table 31 (parts 1 and 2) describes peak resolution of each peak pairs calculated as $R = 1.18 \cdot (RT_2 - RT_1)/(W_1 + W_2)$, where RT_1 and RT_2 are retention times of earlier and later eluted peaks, respectively, and W_1 and W_2 are peak width (at 50% of peak height) of earlier and later eluted peaks, respectively. Colours indicate MS/MS selectivity.

The most critical pairs in terms of MS/MS selectivity are PGE1/PGD1 and PGE2/PGD2, as these isomeric compounds share all fragments and it is impossible to find a selective SRM. Unfortunately, PGE1 and PGD1 show also very similar chromatographic behaviour and they elute closely together. Resolution 0.7 is not enough to well separate these compounds, and therefore they were integrated together and their concentration in samples was reported as a sum. Alternatively, quantitation by peak height is recommended for insufficiently resolved peak pairs. The other pair: PGE2 and PGD2 was well separated chromatographically with baseline separation and resolution equal to 2.2.

Other compounds, which had to be separated chromatographically for achieving good method selectivity were Mar1 and Mar2, as Mar2 gave interfering signal to the SRM of Mar1. There were also interferences seen to signals of RvD1 given by isomeric RvD2 and RvD4. The oxylipin 14(15)-EpETE showed interferences to 12-HEPE and 9-HETE to 11-HETE. All these compounds were well separated by the µUHPLC method.

Table 31 Part 1. *Chromatographic resolution between each pair of peaks. Green colour indicates that an analyte B gives no MS interference to an analyte A, while yellow and red colours mean minor and serious interferences introduced by the analyte B, respectively.*

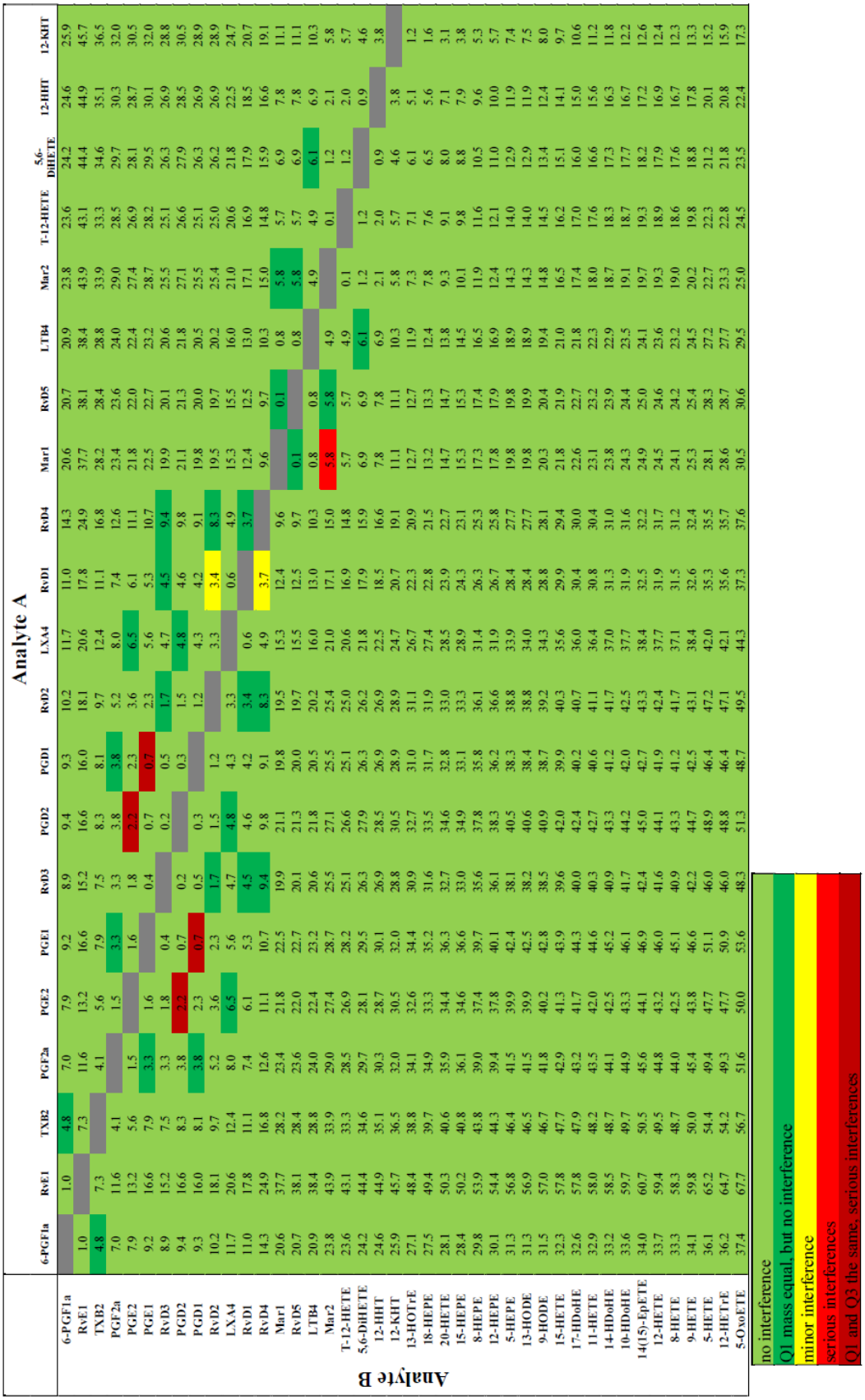

Table 31 Part 2

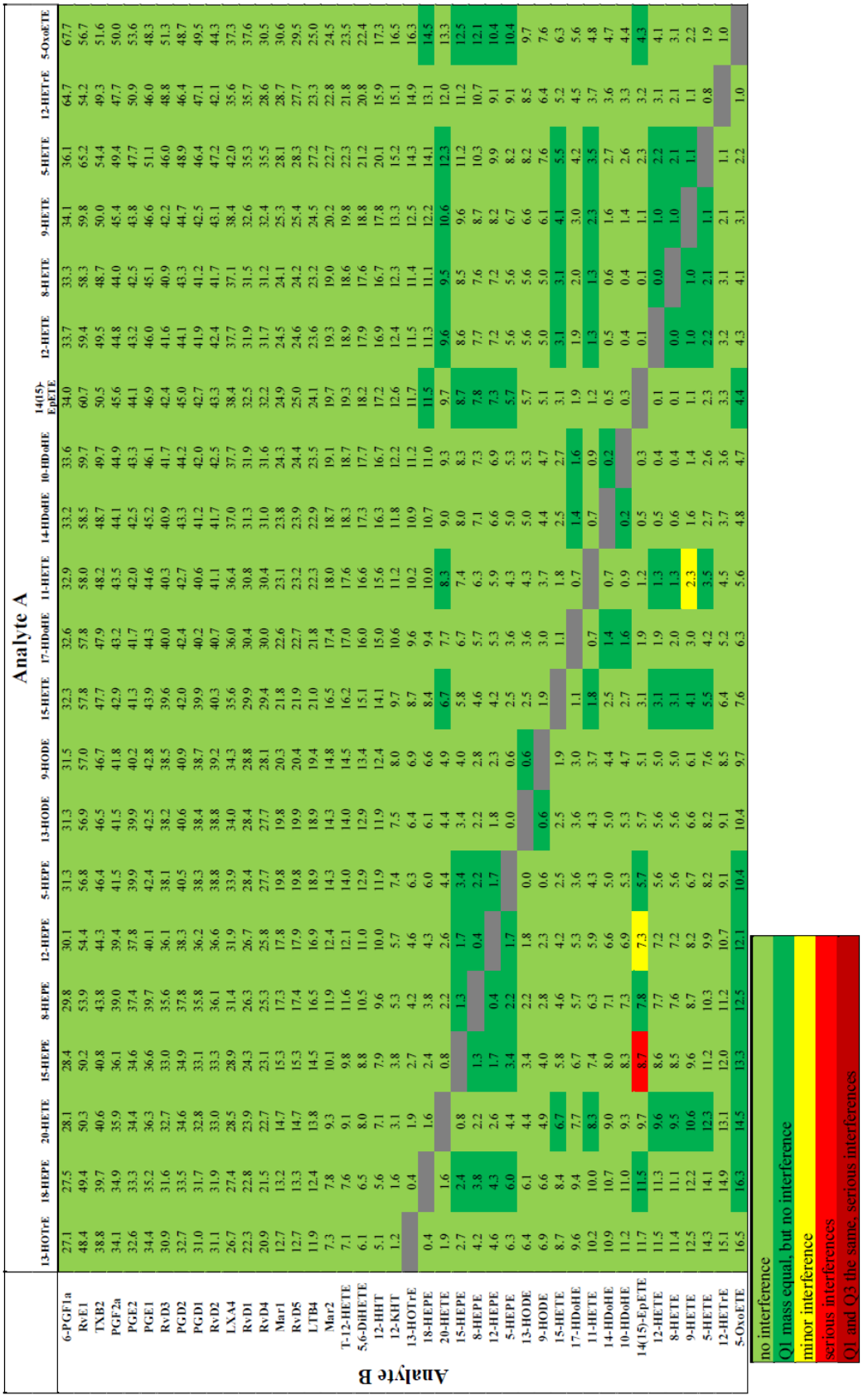

2.5.2. Extraction protocol

2.5.2.1. Comparison of different SPE protocols and liquid extraction

Extraction efficiency was compared for different SPE methods studying both matrix effects and extraction recoveries as performance parameters. For this purpose, 3 sets of samples were prepared: pre-extraction spiked, post-extraction spiked and standards spiked to H_2O/MeOH (3:2; v/v) (standard solutions). Deuterated oxylipins were used for this purpose as standards, because they do not appear naturally in plasma, which was the matrix in this study. Seven compounds were used for these experiments (PGE2-d4, PGD2-d9, PGF2a-d4, TXB2-d4, 12-HETE-d8, 13-HODE-d4 and AA-d11). Six different reversed phase or mixed mode SPEs were tested: InertSep C18, Chromabond C18 ec, Strata X, Oasis HLB Prime, Oasis Max and Bond Elut Certify II. Also monophasic liquid extraction with 90% (v/v) IPA in water was used for comparison.

The employed protocol was unified for all SPE cartridges. EDTA plasma from different donors was pooled and BHT and TPPU solutions were added (10 µL, 200 µg/mL of each compound in MeOH). Then, the plasma was aliquoted (250 µL) to falcon tubes. For pre-extraction spiked samples, deuterated oxylipins were added. The plasma was diluted 1:1 (v/v) with the final solvent for SPE conditioning (Table 32). The samples were centrifuged at 4°C and the supernatant was loaded onto pre-conditioned SPE cartridges (Table 32). Afterwards, the charged SPE cartridges were washed and then analytes were eluted to clean falcon tubes (as described in detail in Table 32). The eluates were dried with a Gene-Vac (2-3 h) under nitrogen protection. For post-extraction spiked samples deuterated oxylipins were added after the extraction procedure at the same concentrations. All samples were reconstituted by H_2O/MeOH (3:2; v/v). For mere standard solutions, the deuterated oxylipins were spiked at the same concentrations to H_2O/MeOH (3:2; v/v). All 3 sets were analysed immediately by µUHPLC-MS/MS in randomized sample order.

Table 32. *Overview of extraction methods with different SPE cartridges and liquid extraction.*

	SPE cartridge	Size	SPE conditioning	SPE wash	SPE elution
Reversed phase	InertSep C18	3 mL / 200 mg	MeOH **2.5 mL**	MeOH/H_2O/HAc 20:80:0.1	MeOH
	Chromabond C18 ec	3 mL / 200 mg	H_2O **2.5 mL**		
	Strata-X	3 mL / 200 mg	MeOH/H_2O/HOAc 5:95:0.1	2 x **2.5 mL**	**2 x 2 mL**
	Oasis HLB Prime	3 cc / 60 mg	**2.5 mL**		
Mixed mode anion exchanger	Oasis MAX	3 cc / 60 mg	MeOH **2.5mL** H_2O **2.5 mL**	2 % NH_4OH in water **2.5 mL** H_2O/MeOH 4:1 **2.5 mL**	MeOH/FA 95:05:00 2 x **2 mL**
	Bond Elut Certify II	3 mL / 200 mg	MeOH **2.5mL** 1 M NaAc in water Adjusted to pH 6 **2.5 mL**	H_2O/MeOH 4:1 2 x **2.5 m** Dried: 5 min	Hexane/ethyl acetate/HAc 25:75:1 2 x **2 mL**
Liquid extraction	IPA/H_2O 9:1 (v/v)	2.5 mL			

Monophasic liquid extraction using IPA was performed as described previously [139]. Plasma was pooled, BHT and TPPU (as specified in main document) were added and samples were divided into 250 µL aliquots For pre-extraction spiked samples deuterated oxylipins were added. 2.25 mL of IPA was added to each sample (final extraction solvent: IPA/H_2O 9:1 (v/v)). Samples were shaken for 20 min at 4°C and then centrifuged. The supernatants were transferred to fresh falcon tubes and samples were dried with a Gene-Vac. The dried lipid extract was reconstituted in MeOH, because it was not possible to dissolve it in H_2O/MeOH (3:2; v/v) (most probably because of a high content of apolar TGs and CEs). For the post-extraction spiked set and the set in MeOH deuterated oxylipins were spiked either to matrix (plasma extracted with IPA protocol and dried) or MeOH. All samples were analysed immediately after preparation in randomized order

Table 33. *Results of extraction recoveries and matrix effects for different extraction methods.*

	Extraction recovery [%]						
SPE	**PGE2-d4**	**PGD2-d9**	**PGF2a-d4**	**TXB2-d4**	**12-HETE-d8**	**13-HODE-d4**	**AA-d11**
InertSep C18	104.8	32.1	102.2	84.9	5.7	15.6	3.1
Chromabond C18 ec	107.6	138.9	102.7	80.2	64	111.8	14.1
Strata X	70.8	61.2	76	68.8	132.3	67.6	56.7
Oasis HLB Prime	83.5	82	104.1	58.4	13.8	21.1	23
Oasis Max	36	6.6	72.2	58.8	50.7	31.5	12.2
Bond Elut Certify II	83	88.7	82.5	95.2	67.7	69.5	14.8
IPA (liquid extraction)	100.6	30	109	109.5	104.1	108.4	114.6
	Matrix effect [%]						
SPE	**PGE2-d4**	**PGD2-d9**	**PGF2a-d4**	**TXB2-d4**	**12-HETE-d8**	**13-HODE-d4**	**AA-d11**
InertSep C18	41.8	53.5	46.2	61.6	46	26.3	25.2
Chromabond C18 ec	36.9	21.4	46.3	49.3	47.5	16.8	15.4
Strata X	61.6	71.2	60.7	63.4	24.2	34.8	32.5
Oasis HLB Prime	24.6	27.2	23.5	23.7	49.6	40.2	3.2
Oasis Max	63.9	52.2	61	44.7	48.3	55.1	46.7
Bond Elut Certify II	50.2	57.8	50.3	40.2	50.8	62.6	88
IPA (liquid extraction)	27	19.4	13.4	30.1	28.5	32.7	33.6
	Process efficiency [%]						
SPE	**PGE2-d4**	**PGD2-d9**	**PGF2a-d4**	**TXB2-d4**	**12-HETE-d8**	**13-HODE-d4**	**AA-d11**
InertSep C18	43.8	17.2	47.2	52.3	2.6	4.1	0.8
Chromabond C18 ec	39.7	29.7	47.6	39.5	30.4	18.8	2.2
Strata X	43.6	43.6	46.1	43.6	32.0	23.5	18.4
Oasis HLB Prime	20.5	22.3	24.5	13.8	6.8	8.5	0.7
Oasis Max	23.0	3.4	44	26.3	24.5	17.4	5.7
Bond Elut Certify II	41.7	51.3	41.5	38.3	34.4	43.5	13.0
IPA (liquid extraction)	27.2	5.8	14.6	33.0	29.7	35.4	38.5

The biggest problem for all SPE protocols was a serious matrix effect with strong ion suppression (Table 33). In this regard, Bond Elut Certify II showed the best results with a mean value for matrix effect of 57.1%. The strongest matrix effect was obtained with Oasis HLB Prime, especially for late eluted AA-d11, and also liquid extraction with 90% IPA. The best extraction recoveries were obtained with Chromabond C18 ec, Strata X, Bond Elut Certify II and also liquid extraction. Overall most promising results were obtained with Bond Elut Certify II and Strata X, and the first one was chosen as the final extraction method.

2.5.2.2.Different methods of protein precipitation

Furthermore, protein precipitation prior to extraction was examined as a possibility to improve extraction results. Three different methods were compared: no protein precipitation, precipitation with aqueous $ZnSO_4$ solution and with ACN. These experiments were done at the early stage of SPE testing with Oasis HLB, and later repeated (only no precipitation and precipitation with ACN) with Bond Elut Certify II.

Table 34. *Results of extraction recoveries and matrix effects for different extraction methods – oxylipin internal standards.*

	Extraction recovery [%]						
SPE	**PGE2-d4**	**PGD2-d9**	**PGF2a-d4**	**TXB2-d4**	**12-HETE-d8**	**13-HODE-d4**	**AA-d11**
Oasis HLB Prime	83.5	82	104.1	58.4	13.8	21.1	23
Oasis HLB Prime ZnSO4	50.6	74.1	95.6	64.5	15.8	19.9	20.6
Oasis HLB Prime ACN	74.7	68.4	54.5	45.4	98	89.5	111.8
Bond Elut Certify II	74.3	34.9	77	90.5	45.2	50.9	11.6
Bond Elut Certify II ACN	3	3.2	3	1.6	22.1	17.1	35.8
	Matrix effect [%]						
SPE	**PGE2-d4**	**PGD2-d9**	**PGF2a-d4**	**TXB2-d4**	**12-HETE-d8**	**13-HODE-d4**	**AA-d11**
Oasis HLB Prime	24.6	27.2	23.5	23.7	49.6	40.2	3.2
Oasis HLB Prime ZnSO4	57.1	15.2	26.3	22.7	67	70.5	26.6
Oasis HLB Prime ACN	56.3	27.8	44.2	20.8	21.7	32.3	10.8
Bond Elut Certify II	55.6	50.3	47.7	45.6	55.8	62.6	80.5
Bond Elut Certify II ACN	57.5	47.2	48	48.6	21.8	22.5	20.5
	Process efficiency [%]						
SPE	**PGE2-d4**	**PGD2-d9**	**PGF2a-d4**	**TXB2-d4**	**12-HETE-d8**	**13-HODE-d4**	**AA-d11**
Oasis HLB Prime	20.5	22.3	24.5	13.8	6.8	8.5	0.7
Oasis HLB Prime ZnSO4	28.9	11.3	25.1	14.6	10.6	14.0	5.5
Oasis HLB Prime ACN	42.1	19.0	24.1	9.4	21.3	28.9	12.1
Bond Elut Certify II	41.3	17.6	36.7	41.3	25.2	31.9	9.3
Bond Elut Certify II ACN	1.7	1.5	1.4	0.8	4.8	3.8	7.3

The experiment without protein precipitation was done as described above. The protocol for protein precipitation with $ZnSO_4$ was as follows: plasma was diluted 2.5 times with $ZnSO_4$ water solution (56 mg/mL). The samples were shaken on ice for 20 min and then centrifuged. The supernatant was loaded onto SPE and the general protocol described in the former paragraph was followed. To precipitate proteins with ACN, plasma samples were diluted 9 times with ACN (250 µL of plasma with 2,250 µL of ACN) and stored at -

20°C for 30 min. After centrifugation the supernatant was transferred to a new falcon tube and was diluted with the solution of the final step of SPE conditioning (Table 32): 8.75 mL of the solution was added to each sample. Then, diluted samples were loaded (stepwise) to SPE cartridges.

The method without protein precipitation was chosen (with Bond Elut Certify II as SPE cartridge), as it gave good results and was the simplest procedure, hence presumably the least error-prone to perform in larger clinical studies.

Additionally, a comparison of peak intensities of endogenous oxylipins was performed (Table 35 and Figure 56). These compounds exist naturally in plasma and they might bind to plasma proteins.

Comparable results with protein precipitation by ACN and without protein precipitation were obtained, which means that there was no loss of oxylipins due to their binding to proteins. Oxylipin – protein interactions are probably interrupted at the stage of loading to SPE or washing and eluting steps. During these steps bonded oxylipins are released and can be extracted together with free oxylipins.

Table 35. *Comparison of peak areas with protein precipitation (with ACN) and without protein precipitation. Result 1.00 means that the peak areas were equal with both extraction methods. Result lower than 1.00 indicates that analyte concentration was higher when no protein precipitation was used.*

Analyte	Ratio of peak intensity: extraction with protein precipitation by ACN to this without protein precipitation
PGE2	0.15
PGD2	0.26
14-HDoHE	0.96
5-HETE	1.11
12-HETE	0.87
15-HETE	0.98
20-HETE	1.01
5-HEPE	1.00
12-HEPE	1.03
9-HODE	0.91
13-HODE	0.72
12-HHT	0.78

In case of prostaglandins even worse results (lower intensity) were obtained with protein precipitation. This might be caused by compound instability during longer extraction protocol, or because of poor loading in presence of residual amount of organic solvent. Prostaglandins are relatively polar compounds and elute from SPE already with low concentration of organic solvent.

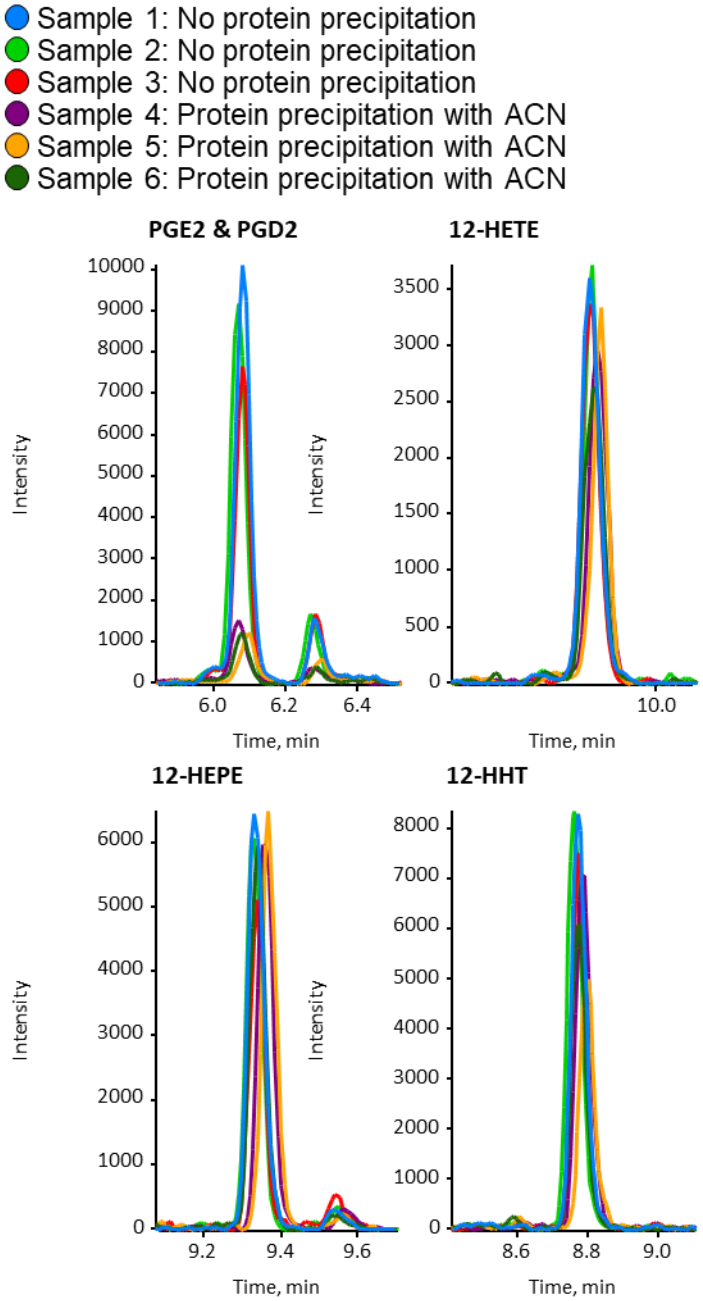

Figure 56. *Comparison of 6 separately prepared samples: 3 without protein precipitation and 3 with ACN used for protein precipitation.*

2.5.3. Calibration

Table 36. *Accuracies as determined by the slope ratios of post-spiked matrix and spiked solvent vs. pre-extraction spiked standard addition (classical standard addition) (slope ratio*100 assuming that the standard addition represents 100% of the true value). Blue background indicates compounds for which their deuterated real analogues ware used as IS.*

Accuracy of slope in:					
Compound	**Post-spiked matrix**	**Spiked solvent**	**Compound**	**Post-spiked matrix**	**Spiked solvent**
PGF2a	99.8	98.1	14(15)-EpETE	86.5	115.6
PGE1 and PGD1	92.3	149.9	5,6-DiHETE	89.1	89.6
TXB2	97.5	104.7	5-OxoETE	100.2	160.8
6-keto-PGF1a	96.0	52.0	9-HODE	93.7	110.7
PGE2	94.0	87.3	13-HODE	92.5	97.7
PGD2	96.3	121.6	LXA4	104.9	119.8
10-HDoHE	100.6	107.7	12-HHT	109.4	173.6
14-HDoHE	103.7	111.4	12-KHT	95.4	158.8
17-HDoHE	107.2	181.4	LTB4	104.0	102.1
5-HETE	85.8	75.1	T-12-HETE	90.2	157.9
8-HETE	104.0	100.0	RvD1	107.5	100.4
9-HETE	96.4	157.6	RvD2	103.4	155.2
11-HETE	108.6	150.9	RvD3	90.9	77.4
12-HETE	110.7	111.8	RvD4	99.8	71.8
15-HETE	85.7	130.8	RvD5	103.4	117.9
20-HETE	96.6	97.2	RvE1	90.0	109.3
5-HEPE	93.1	105.6	Mar1	103.8	107.7
8-HEPE	107.6	166.0	Mar2	109.7	95.8
12-HEPE	105.2	106.3	12-HETrE	125.4	174.9
15-HEPE	98.9	125.4	13-HOTrE	102.4	92.6
18-HEPE	109.0	105.4			

Three distinct calibration sets were prepared and compared to each other in terms of their performance to compensate for losses and matrix effect: i) pre-extraction spiked standard addition in plasma (post-spiked matrix), ii) post-extraction-spiked standard addition to plasma (classical standard addition approach), and iii) standards in plain solvent (H_2O/MeOH 3:2 (v/v)) (spiked solvent). Endogenous analyte concentrations in the employed plasma matrix employed for pre- and post-extraction spiked standard addition were calculated from the x-intercept of the standard addition calibration functions (-1(x-intercept)). Respective matrix-matched calibration functions corrected for endogenous levels were then prepared and used for this study.

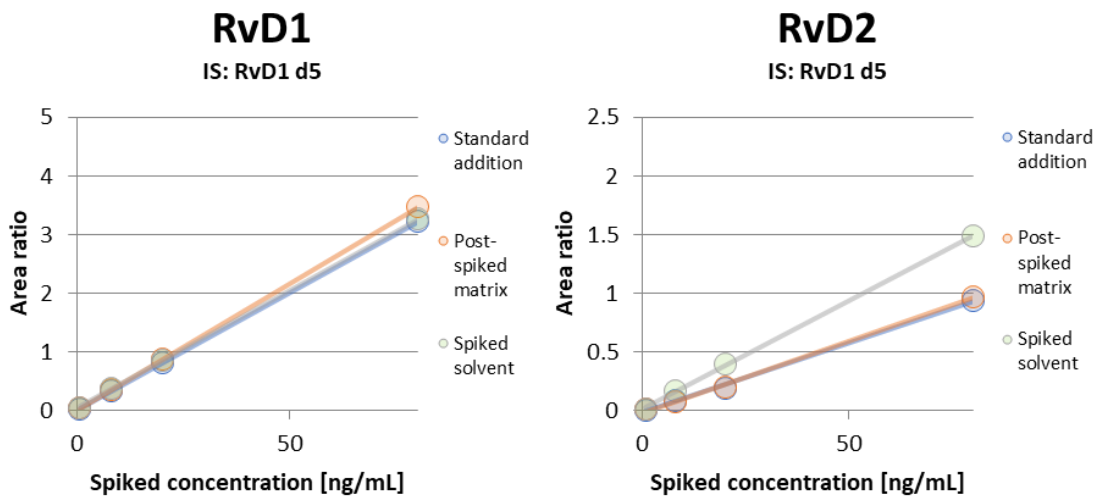

Figure 57. *Comparison of calibration curves for different methods. Left plot: RvD1, which uses its deuterated analogue for normalization (RvD1-d5) and right: RvD2, which lacks its deuterated analogue. Standard addition means pre-extraction-spiked standard addition series, and post-spiked matrix means post-extraction spiked standard addition series. Spiked solvent means standards dissolved in H_2O/MeOH 3:2 (v/v).*

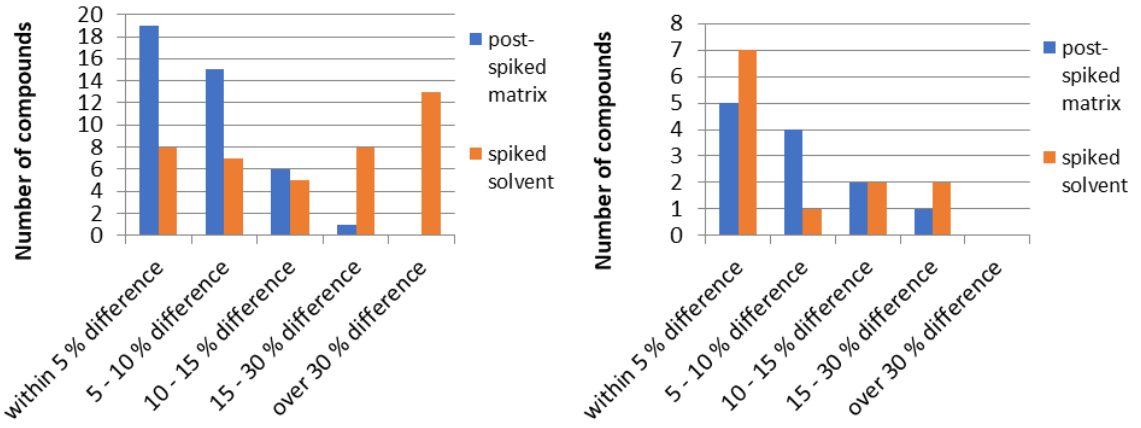

Figure 58. *Bias of calibration by post-extraction-spiked standard addition series (post-spiked matrix) (blue bars) and standard solutions (spiked solvent) (red bars) as compared to pre-extraction-spiked standard addition series. Left graph: All compounds including those for which no compound-specific stable isotope labelled IS was available. Right graph: Only compounds considered for which compound-specific stable isotope labelled IS (deuterated analogues) were available. 'Within 5% difference' means accuracy between 95 and 105% (or bias between -5 and 5%), assuming that the classical pre-extraction-spiked standard addition series gives fully accurate results (100%). Bias (%) was calculated from the slopes of the distinct calibration functions, i.e. (slope ratio of post-extraction-spiked standard addition series and pre-extraction-spiked standard addition series – 1)*100 (%) as well as (slope ratio of standard solution series and pre-extraction-spiked standard addition series – 1)*100 (%).*

The method using spiked solvent is straightforward and does not need any additional biological samples. However, this method failed for compounds, which did not have their real compound-specific isotopically labelled analogues. The post-extraction spiked standard addition method has the advantage over the classical 'standard addition method', because it does not require high volume of precious biological matrix and generates much less samples for extraction and LC-MS analysis. The approach with post-spiked samples was devised, because it is possible to apply it later for platelet cell pellets. If there is not enough matrix (like for platelet cell pellets) to prepare calibration curves, the real samples might be extracted and after extraction small aliquots of each extract can be pooled together. Then, the pooled extract can be aliquoted and used for calibrant preparation. The 'post-spiked matrix' method showed good results with slopes well matching the ones from the classical 'standard addition' approach (pre-extraction spiked standard addition assumed to be the most accurate way of calibration).

2.5.4. Extraction recovery and matrix effect for IS with the final method

Table 37. *Extraction recovery and matrix effect for ISs obtained with the final method (mean and standard deviation of three levels investigated; 1.6, 5 and 16 ng per 1 mL of plasma).*

	Extraction recovery [%]		Matrix effect [%]	
	mean	sd	mean	sd
PGF2a-d4	83.4	12.5	46.9	6.7
PGE2-d4	82.0	11.1	53.1	7.3
PGD2-d9	79.8	13.2	37.4	3.9
TXB2-d4	97.1	8.3	41.4	3.1
5-HETE-d8	71.2	20.5	35.7	5.2
12-HETE-d8	69.2	9.3	47.9	2.4
20-HETE-d6	56.3	23.2	41.0	6.8
13-HODE-d4	71.8	14.0	60.6	6.0
LTB4-d4	86.4	19.6	29.7	3.2
RvD1-d5	72.5	10.0	28.3	3.3
RvE1-d4	91.9	4.5	34.7	5.1
Mar2-d5	85.1	10.4	47.0	5.1
FA(10:0)-d19	46.3	7.2	29.9	8.9
HTE-d5	49.9	12.6	62.4	7.7
DGLA-d6	2.7	0.4	89.1	8.4
AA-d11	13.0	0.9	87.3	26.4
EPA-d5	27.6	3.1	72.5	10.6
DHA-d5	14.7	2.2	104.2	30.9

The extraction recovery and matrix effect for ISs were also determined with the final method during the method validation. The results are summarized in Table 37.

The extraction recovery showed good results for oxylipins, as for most of them it exceeded 70%. The results were much worse for fatty acids, for all of them the recovery was below 50% and for DGLA-d6 the result was only 2.7%. This suggests that the current SPE method is not adequate for fatty acids. They were therefore not further considered as they are covered by another assay.

The results for the matrix effect indicated high ion suppression for oxylipins (around 50%, but sometimes even lower than 30%). The matrix effect was much better for fatty acids, probably because matrix components of similar polarity and similar retention time were poorly removed from SPE.

2.5.5. Validation of within batch precision and accuracy for plasma

Table 38 Part 1. *Within batch precision and accuracy for plasma.*

	Within batch accuracy								
Analyte	**QC low**			**QC mid**			**QC high**		
	day 1	**day 2**	**day 3**	**day 1**	**day 2**	**day 3**	**day 1**	**day 2**	**day 3**
PGF2a	92.1	96.6	95.4	108.3	103.6	96.0	94.2	108.1	102
PGE1/PGD1	86.7	109.9	97.5	109.4	114.4	99.0	94.2	112.5	91.8
TXB2	97.1	102.9	103.9	103.4	111.3	99.6	94.1	101.3	93.5
6-keto-PGF1a	91.7	82.1	96.0	103.2	87.1	95.9	100.4	82.0	100.9
PGE2	87.5	100.5	96.9	105.9	110.2	95.1	90.9	104.7	91.8
PGD2	90.3	98.9	93.8	110.7	109.3	100.3	97.5	106.4	93.0
10-HDoHE	95.3	95.5	98.9	114.6	108.3	93.7	91.9	95.5	91.3
14-HDoHE	102.2	110.3	107.7	114.5	112.3	90.3	94.3	109.3	87.2
17-HDoHE	97.8	95.8	105.7	112.1	105.7	91.3	87.2	97.2	96.5
5-HETE	83.7	105.0	107.2	106.8	106.6	89.3	86.3	105.2	95.8
8-HETE	87.3	86.4	92.5	124.8	107.3	98.9	89.9	98.9	90.9
9-HETE	108.6	98.5	106.5	110.2	91.1	107.5	94.4	94.3	105.2
11-HETE	89.9	99.6	88.6	106.8	104.9	92.8	98.2	95.7	85.8
12-HETE	90.4	94.4	130.7	98.0	101.5	98.3	87.5	98.5	102.7
15-HETE	85.8	100.2	107.6	112.8	108.3	108.5	97.3	111.6	102.6
20-HETE	88.5	91.5	98.6	114.9	88.4	89.0	91.3	86.9	95.5
5-HEPE	96.2	103.8	106.1	107.8	105.8	85.5	103.9	109.6	95.3
8-HEPE	86.1	91.3	91.4	107.9	100.4	95.6	94.8	91.0	91.8
12-HEPE	86.2	83.9	91.3	93.0	87.9	90.4	91.4	85.3	91.2
15-HEPE	98.2	99.2	91.7	105.8	90.9	85.1	104.6	92.8	87.5
18-HEPE	112.8	103.7	94.0	103.5	105.1	98.6	89.3	104.2	86.5
14(15)-EpETE	88.5	98.9	112.8	102.9	114.9	96.1	93.5	96.5	92.9
5,6-DiHETE	102.0	98.6	143.5	98.6	87.2	95.6	100.2	86.0	108.9
5-OxoETE	80.3	91.1	92.2	114.7	102.4	113.5	81.3	96.4	94.9
9-HODE	100.7	98.5	85.3	108.2	106.1	96.9	88.7	88.6	102.2
13-HODE	113.3	106.9	93.3	103.3	108.6	101.4	93.2	92.1	103.1
LXA4	85.0	103.3	94.1	105.5	109.2	91.1	94.5	105.5	88.1
12-HHT	86.8	106.4	89.9	104.1	105.1	95.6	90.0	91.0	88.7
12-KHT	85.4	96.3	97.8	110.7	105.8	111.5	89.6	102.4	100.3
LTB4	85.9	91.6	97.2	107.7	104.7	97.1	95.2	97.5	94.1
T-12-HETE	85.0	91.6	100.5	111.4	104.7	102.8	96.8	97.5	106.5
RvD1	88.8	109.1	111.8	106.6	109.6	109.2	91.6	109.6	111.0
RvD2	107.8	87.6	108.2	98.6	89.5	103.3	93.8	89.1	97.9
RvD3	108.5	106.4	103.2	112.3	114.7	93.2	99.2	113.8	105.2
RvD4	100.4	91.4	112.0	100.6	102.9	107.2	94.1	102.3	108.8
RvD5	86.2	89.4	94.7	102.6	100.7	97.9	86.3	94.2	92.2
RvE1	88.2	94.5	93.8	106.9	104.3	99.2	94.1	97.7	94.4
Mar1	93.8	90.3	98.2	110.0	100.0	99.9	93.4	97.9	93.2
Mar2	86.4	96.5	93.1	110.4	106.4	99.4	95.2	101.8	99.2
12-HETrE	76.4	87.8	87.8	75.1	89.3	112.4	81.2	79.3	94.7
13-HOTrE	99.3	102.6	105.1	104.1	107.5	88.5	96.9	102.9	78.0

Table 38 Part 2.

Analyte	Within batch precision								
	QC low			QC mid			QC high		
	day 1	day 2	day 3	day 1	day 2	day 3	day 1	day 2	day 3
PGF2a	7.4	7.8	6.7	6.1	4	8.8	6.1	3.9	6.3
PGE1/PGD1	1.8	4.6	5.7	7.2	0.3	8.6	6.2	1.1	6.3
TXB2	9.1	8.8	1.9	3.2	1.9	2.0	3.3	3.8	8.2
6-keto-PGF1a	5.3	2.1	6.4	3.6	1.5	6.8	3.7	1.0	11
PGE2	7.8	5.0	6.0	2.8	1.9	6.8	12.2	5.6	5.4
PGD2	4.9	10.1	7.0	3.7	5.8	7.4	3.3	5.8	3.5
10-HDoHE	12.3	14.2	12.6	2.5	3.9	4.6	8.2	4.1	6.6
14-HDoHE	7.9	6.6	12.7	0.2	4.7	3.5	4.1	1.1	11.4
17-HDoHE	10.4	12.0	3.7	8.8	2.8	7.6	7.3	6.0	9.4
5-HETE	6.3	5.8	10.2	3.9	1.6	7.4	2.8	4.1	6.4
8-HETE	7.5	13.5	12.8	2.5	6.1	8.6	6.0	6.8	14.1
9-HETE	2.9	13.1	4.4	3.4	12.5	8.4	6.0	10.5	6.1
11-HETE	10.2	9.7	7.0	2.6	13.2	5.6	8.7	4.9	7.7
12-HETE	22.7	11.2	18.8	7.3	5.6	3.9	6.4	8.1	7.3
15-HETE	18.6	6.5	4.4	7.0	3.1	7.3	6.3	7.0	9.3
20-HETE	6.6	11.4	7.4	2.9	12.3	8.5	5.6	7.7	14
5-HEPE	8.1	6.0	19.8	4.6	4.2	4.5	4.6	4.6	10.4
8-HEPE	7.5	8.3	12.6	8.4	5.0	6.2	4.6	9.2	6.9
12-HEPE	5.3	8.1	12.5	6.2	5.7	7.8	7.5	9.9	3.1
15-HEPE	12.6	6.8	13.5	9.2	5.8	4.1	7.8	7.8	4.3
18-HEPE	10.8	2.4	11.2	5.5	5.1	9.3	4.2	7.5	5.3
14(15)-EpETE	12.7	10.6	3.2	3.5	1.9	11.5	5.0	5.3	11.1
5,6-DiHETE	8.2	9.4	60.5	10.7	9.2	14.7	6.6	11.5	7.9
5-OxoETE	3.9	9.4	10.7	3.9	3.2	7.4	4.3	9.2	8.0
9-HODE	8.2	5.1	8.0	4.4	5.5	11.1	5.6	8.3	14.3
13-HODE	7.0	4.0	4.2	2.2	2.2	9.4	3.5	3.7	4.2
LXA4	8.2	7.6	7.3	8	3.5	7.6	9.9	5.3	4.5
12-HHT	12.8	8.2	7.2	5.7	2.8	6.9	5.3	8.2	7.1
12-KHT	4.1	10.1	11.1	3.7	3.5	1.8	3.6	6.8	8.4
LTB4	0.7	3.4	7.9	3.7	2.3	6.3	2.9	3.2	12.1
T-12-HETE	5.9	3.4	12.0	7.9	2.3	11.4	5.7	3.2	12.2
RvD1	4.5	2.7	6.7	5.6	2.4	4.0	4.5	3.6	3.1
RvD2	8.5	8.0	8.3	9.6	8.4	9.4	8.1	10.2	12.3
RvD3	10.6	10.5	11.4	8.3	1.9	9.7	8.3	3.6	9.5
RvD4	5.2	4.0	9.4	6.1	3.9	7.0	6.7	3.7	3.3
RvD5	1.1	3.3	8.6	7.3	2.9	8.1	1.7	1.8	10.9
RvE1	4.1	2.2	9.0	4.9	4.6	6.1	3.3	2.9	6.7
Mar1	4.6	2.2	7.6	3.5	4.9	8.8	4.7	4.9	9.9
Mar2	1.5	5.0	10.0	4.2	2.9	4.0	3.4	6.8	5.0
12-HETrE	7.1	4.2	13.7	2.3	5.1	2.5	1.6	8.7	10.3
13-HOTrE	14.4	10.3	12.3	10.2	2.7	7.8	1.9	5.8	7.8

2.5.6. Estimated concentrations of oxylipins in platelets

Table 39 shows the results of linearity and sensitivity for the quantification of oxylipins in platelets (calibration performed in pooled QC by post-extraction standard addition). To document adequate performance of the method for platelets, a pooled, non-spiked QC sample was prepared and was injected before and after the sequence as well as within the sequence. Precision of the results were calculated for these multiple injections of the same sample and are also included in the Table 39. In several instances, the target oxylipins were

not detected and in several cases at low concentrations resulting in lower precision, e.g. 9-HETE, 15-HEPE, 12-KHT. When concentration levels were above LOQ, the precisions were well in the acceptance range of common validation guidelines. Spiked QCs were injected only once due to limited sample amounts. Accuracies, calculated as percent recovery, were with a few outliers always within the acceptance ranges of guidelines

Table 39. *Sensitivity, linearity and precision for platelet samples.*

Analyte	LOD	LOQ	Linearity	Precision in QC
	[ng / 1 x 10^8 platelets]		[R]	[%]
PGF2a	1.101	3.67	0.9989	N/A
PGE1	0.206	0.69	0.9989	N/A
PGD1	2.635	8.78	0.9986	N/A
TXB2 peak 1	0.305	1.02	0.9990	6.2
6-keto-PGF1a	0.888	2.96	0.9997	N/A
PGE2	0.104	0.35	0.9997	12.5
PGD2	0.254	0.85	0.9988	N/A
10-HDoHE	0.089	0.30	1.0000	15.4
14-HDoHE	2.357	7.86	0.9920	4.7
17-HDoHE	0.073	0.24	0.9999	19.9
5-HETE	0.089	0.30	0.9995	N/A
8-HETE	0.003	0.01	0.9988	11.0
9-HETE	0.500	1.67	0.9995	27.3
11-HETE	0.098	0.33	1.0000	11.6
12-HETE	4.709	15.70	0.9461	4.2
15-HETE	0.072	0.24	1.0000	15.8
20-HETE	0.130	0.43	0.9999	N/A
5-HEPE	0.214	0.71	0.9999	N/A
8-HEPE	0.082	0.27	0.9998	N/A
12-HEPE	0.589	1.96	0.9996	4.5
15-HEPE	0.073	0.24	0.9996	24.0
18-HEPE	0.079	0.26	1.0000	N/A
14(15)-EpETE	0.075	0.25	0.9987	N/A
5,6-DiHETE 20 hete	0.497	1.66	1.0000	N/A
5-OxoETE	0.417	1.39	0.9999	N/A
9-HODE	1.328	4.43	0.9985	8.9
13-HODE	0.878	2.93	0.9996	6.4
LXA4	0.044	0.15	0.9981	N/A
12-HHT	0.102	0.34	0.9984	7.6
12-KHT	0.118	0.39	0.9991	20.4
LTB4	0.051	0.17	0.9998	N/A
T-12-HETE	0.011	0.04	0.9995	7.0
RvD1	0.095	0.32	0.9996	N/A
RvD2	0.108	0.36	0.9993	N/A
RvD3	0.060	0.20	0.9983	N/A
RvD4	0.048	0.16	0.9996	N/A
RvD5	0.033	0.11	0.9998	N/A
RvE1	0.041	0.14	0.9989	N/A
Mar1	1.054	3.51	0.9989	23.4
Mar2	0.060	0.20	0.9995	N/A
12-HETrE	1.583	5.28	0.9978	7.2
13-HOTrE	0.024	0.08	0.9990	8.5

2.5.7. Assay performance

Table 40 describes LOQ (as fmol on column) for different matrices used in this study. It can be directly compared to recent oxylipin method comparison by Cécile Gladine at al. [148]. Table 2 from Gladine *et al.* has been adapted and implemented here as Table 41. Gladine's comparison has been reduced to methods which used LC-MS/MS quantification of oxylipins in plasma with stated LOQ values for different analytes. Additionally, the information about MS instrument has been added. It can be seen that our new method (line 1 in Table 41) provides comparable results in terms of method sensitivity to other contemporary methods, even though we used MS instrument of lower sensitivity (higher number next to the AB Sciex QTrap name indicates higher instrument sensitivity). We believe that the lower sensitivity of our instrument is compensated by excellent sensitivity gain due to narrow peaks provided by µUHPLC system. Further sensitivity gain could be obtained by replacing the MS instrument using instruments with wider orifice (QTRAP 5500, QTRAP 6500).

Table 40. *LOQ in solvent, plasma and platelets*

	LOQ as fmol on column				LOQ as fmol on column		
	solvent	plasma	platelets		solvent	plasma	platelets
PGF2a	0.7	8.5	52	**14(15)-EpETE**	0.8	3.9	3.9
PGE1 and PGD1	0.7	2.1	9.7	**5,6-DiHETE**	3.7	5.2	25
TXB2	0.7	7.4	14	**5-OxoETE**	0.8	2.4	21.8
6-keto-PGF1a	0.7	2.0	40.0	**9-HODE**	8.4	255.7	75
PGE2	0.7	2.1	5	**13-HODE**	8.4	260.0	49.5
PGD2	0.7	2.1	12.1	**LXA4**	0.7	2.8	2
10-HDoHE	0.7	10.2	4	**12-HHT**	0.9	3.6	6.1
14-HDoHE	0.7	4.4	114.2	**12-KHT**	0.9	2.7	7
17-HDoHE	0.7	10.9	3	**LTB4**	0.7	2.2	2.5
5-HETE	0.8	2.3	4.7	**T-12-HETE**	0.9	11.3	1
8-HETE	0.8	10.2	0	**RvD1**	0.7	2.0	4.3
9-HETE	0.8	14.1	26.1	**RvD2**	0.7	5.3	5
11-HETE	0.8	9.4	5	**RvD3**	0.7	4.7	2.7
12-HETE	0.8	10.2	245.2	**RvD4**	0.7	2.7	2
15-HETE	0.8	10.9	4	**RvD5**	0.7	2.1	1.5
20-HETE	0.8	2.3	6.7	**RvE1**	0.7	2.1	2
5-HEPE	0.8	2.4	11	**Mar1**	0.7	6.2	48.7
8-HEPE	0.8	3.1	4.2	**Mar2**	0.7	3.5	3
12-HEPE	0.8	2.4	31	**12-HETrE**	0.8	2.3	81.9
15-HEPE	0.8	4.7	3.8	**13-HOTrE**	0.9	3.4	1
18-HEPE	0.8	21.2	4				

Table 41. *Comparison of available methods for oxylipins quantification, adapted from*: *[148]*

Laboratory	MS	Column dimensions	Run time [min]	LOQ range; fmol on column	No. Analytes	No. IS
Lämmerhofer, 2020	**AB Sciex QTrap 4500**	**50 mm × 0.5 mm; 2.7 µm**	**13**	**2-260**	**42**	**13**
Schebb, 2019	AB Sciex QTrap 6500	150 × 2.1 mm; 1.8 µm	32	0.5–200	175	20
Holčapek, 2019	AB Sciex QTrap 6500	150 × 2.1 mm; 1.7 µm	20	7.5–70	63	14
Dennis, 2018	AB Sciex QTRap 6500	100 × 2.1 mm; 1.7 µm	7	0.3–810	158	26
Ceglarek, 2013	AB Sciex Qtrap 5500	100 × 2.1 mm; 2.6 µm	13	5.4–620	94	22
Vreeken, 2012	Agilent 6460	150 × 2.1 mm; 2.7 µm	26	1.5–510	104	11
Ramsden, 2018	AB Sciex QTrap 5500	100 × 4.6 mm; 1.8 µm	35	2.7–17	57	9
Nording, 2015	Waters triple quadrupole MS	150 × 2.1 mm; 2.5 µm	25	0.0016–11	37	5
Nicolaou, 2013	Waters triple quadrupole MS	150 × 2.0 mm; 5 µm	30	3–600	20	1
Zhu, 2015	AB Sciex QTrap 5500	100 × 2.1 mm, 1.7 µm	18	0.35–12	65	10

3. Publication III: enantioselective analysis of oxylipins

Enantioselective ultra-high performance liquid chromatography-tandem mass spectrometry method based on sub-2µm particle polysaccharide column for chiral separation of oxylipins and its application for the analysis of autoxidized fatty acids and platelet releasates

Malgorzata Cebo[a], Xiaoqing Fu[a], Madhumita Chatterjee[b], Meinrad Gawaz[b], Michael Lämmerhofer[a]*

[a] University of Tübingen, Institute of Pharmaceutical Sciences, Pharmaceutical (Bio-) Analysis, Auf der Morgenstelle 8, 72076 Tübingen, Germany

[b] Department of Cardiology and Angiology, University Hospital Tübingen, Otfried-Müller-Strasse 10, 72076 Tübingen, Germany

Journal of Chromatography A

Volume 1624, 2 August 2020, 461206

DOI: 10.1016/j.chroma.2020.461206

Highlights

• Enantioselective UHPLC-MS/MS method for chiral oxylipins developed.

• Chiral separation of HODEs, HETEs, HEPEs, HDoHEs, HETrEs, HOTrEs, DiHETEs, Resolvins D1.

• Screening of different methods with sub-2µm Chiralpak IA-U and IC-U columns.

• Quantification of racemic mixtures from PUFA autoxidation.

• Analysis of platelet releasates from resting and thrombin activated platelets.

Keywords: Chiral separation, Oxylipin enantiomer, Targeted lipidomics, Polyunsaturated fatty acid, Autoxidation, Chiral stationary phase

Abstract

Oxylipins, the oxidation products of polyunsaturated fatty acids, are important signalling molecules in living organisms. Some of them have pro-inflammatory properties, while others act as pro-resolving agents. Oxylipins also play a major role in platelet biology and the progression of thrombo-inflammation. Depending on their structure, they may be pro-thrombotic or anti-thrombotic. For an unbiased biological interpretation, a detailed analysis of a broad spectrum of oxylipins including their stereoisomers is necessary. In our work, we developed for the first time an enantioselective UHPLC-ESI-MS/MS assay which allows quantifying individual oxylipin enantiomers. The assay made use of a sub-2µm particle-based amylose-(3,5-dimethylphenylcarbamate) chiral stationary phase (Chiralpak IA-U) under MS-compatible reversed-phase conditions. It covered 19 enantiomeric pairs of oxylipins and one diasteromeric pair of a lipid mediator: 2 pairs of hydroxyoctadecadienoic acids (HODE), 6 pairs of hydroxyeicosatetraenoic acids (HETE), 5 pairs of hydroxyeicosapentaenoic acids (HEPE), 3 pairs of hydroxydocosahexaenoic acids (HDoHE) and one pair of each: resolvins D1, hydroxyeicosatrienoic acid (HETrE), hydroxyoctadecatrienoic acid (HOTrE) and dihydroxyeicosatetraenoic acid (DiHETE). The new method is fast and showed outstanding peak resolution for most of the isomeric pairs. Excellent method sensitivity (average LOD was equal to 2.7 pg on column) was obtained by using a triple quadrupole instrument as a detector in a targeted, selected reaction monitoring (SRM) mode. The applicability of the method was verified by preliminary validation. It was then applied to analyse oxylipins produced by autoxidation of polyunsaturated fatty acids (PUFA) in air. Multiple oxylipins were found in each of the samples as racemic mixtures and served as reference substances for identification. Finally, the new enantioselective UHPLC method was applied to analyse releasates from platelets in resting state, and following activation with thrombin. The highest abundant oxylipin in the platelet releasate was 12(*S*)-HETE, but many other oxylipins were found in the thrombin activated samples, usually as single enantiomers (e.g. 12(*S*)-HEPE, 11(*R*)-HETE, 9(*R*)-HODE, 13-(*S*)-HODE, 14(*S*)-HDoHE). The latter was detected at about similar concentration in resting platelet releasates as well. 15-HETE showed elevated levels for both *R*-and *S*-enantiomers in releasates of thrombin-activated platelets. 12-HETrE was found presumably as both enantiomers, however, retention time inconsistencies indicate that the *R*-enantiomer is actually a different compound, maybe another constitutional isomer with different double-bond configuration.

3.1.Introduction

Oxylipins, the oxidation products of polyunsaturated fatty acids (PUFA), play a crucial role in several pathophysiological conditions e.g. metabolic disorders, cardiovascular diseases or cancer, regulating inflammatory processes [167]. They are also important regulators of platelet functions, whereby their autocrine and paracrine mode of actions and intraplatelet signalling is mediated by members of this class of compounds [86, 158, 168]. Oxylipins are major players of thrombo-inflammation and have influence on the progression of cardiovascular disease (CVD) risk and thrombosis [10, 118]. It is well-known that some members of the oxylipin class are pro-inflammatory, while others are anti-inflammatory [8]. As a consequence, the full understanding of thrombo-inflammatory processes requires a detailed analysis of these lipid mediators.

In general, oxylipins can originate from autoxidation of PUFAs, oxidative stress and enzymatic synthesis. Autoxidation and lipid oxidation by reactive oxygen species (ROS) due to oxidative stress are non-stereospecific and therefore lead to racemic mixtures of products [169]. Enzymatic production of oxylipins occurs by 3 main families of enzymes: cyclooxygenases (COXs), lipoxygenases (LOXs) and cytochrome P450 (CYP450). These enzymatic reactions proceed enantioselectively due to the chiral nature of the enzymes and they result in production of pure enantiomers.

The stereochemical differences of products from autoxidation/oxidative stress, and enzymatic reactions (i.e. racemate vs. pure enantiomer) might be used to determine the level of oxidative stress in tissues. Moreover, non-enzymatically derived oxylipins might serve as markers of autoxidation or biomarkers of oxidative stress [170].

The biological activity of oxylipins is most often related to only one enantiomeric form. To get unbiased insight into biochemical processes, it is advisable to perform the analysis of oxylipins in biological samples by enantioselective assays. However, routine analysis of oxylipins typically use achiral reversed-phase ultra- high performance liquid chromatography (UHPLC) [11, 77, 108, 124, 155, 158] or, less commonly, achiral supercritical fluid chromatography (SFC) [159]. These chromatographic methods coupled to a mass spectrometer (MS) provide concentrations of 10s to 100s for oxylipins with high

sensitivity. However, they are unable to separate enantiomers, so the information about enantiomeric composition of oxylipins in the samples is lost.

Such information about individual oxylipin enantiomers can be obtained by enantioselective liquid chromatography. There are many chiral stationary phases (CSP) available for enantioselective liquid chromatographic separation [162, 171].

Chiral separations of short-chain and long-chain hydroxycarboxylic acids have been reported with quinine- and quinidine carbamate-derived brush-type CSPs [172-174]. The selectivity of these CSPs turned out to depend on the hydroxycarboxylic acid structure, especially on the position of the OH group with respect to the carboxylic acid group. Good chiral recognition and enantiomer separation could be obtained for 2- and 3-hydroxy carboxylic acids. Hydroxy carboxylic acid enantiomer separations for such compounds have also been reported for macrocyclic antibiotic CSPs [175].

However, in the case of oxylipins, the position of the hydroxy group is farther away from the carboxylic acid group than α and β, and it varies from compound to compound. Therefore, a more generally applicable method with enantioselectivity for a variety of distinct hydroxy fatty acids is required. In the recent decades, the polysaccharide-based CSPs have gained enormous popularity, because of their versatility. These CSPs can be used in various elution modes, most commonly in normal- phase LC, reversed-phase LC and supercritical fluid chromatography mode, but also in polar organic LC, and hydrophilic interaction liquid chromatography (HILIC) mode [176, 177]. Chromatographic separations with polysaccharide-based CSPs are nowadays the most common methods for enantiomer separation of oxylipins and especially the columns with tris(methylbenzoate) and tris(3,5-dimethylphenylcarbamate) derivatives of cellulose [178, 179] and amylose [180-182] have been widely used. Most of the recent chiral separations of oxylipins have been reviewed by Mesaros et al. [183], and more recently by Ianni et al. [162].

The commercially available polysaccharide-based CSPs were originally produced as polysaccharide-coated CSPs [176, 177]. These columns are less flexible where the usage of mobile phases is concerned, as some solvents cause dissolution or swelling of the chiral selector. The newer generation of columns is the immobilized type of columns with the chiral selector covalently bonded to silica. They can be safely used with extended set of

solvents and conveniently switched between elution modes [184, 185]. Oxylipin enantiomer separations on polysaccharides were initially performed mainly in normal-phase mode due to excellent enantioselectivities [186]. However, normal-phase LC is not very well compatible with electrospray ionisation (ESI) and therefore reversed-phase mode HPLC separations dominate the field of bioanalytical applications with mass spectrometric detection [187]. The columns employed are typical standard HPLC columns based on 5 μm, or more recently also 3 μm, particle based polysaccharide CSPs.

Herein, we report the first UHPLC enantiomer separations of oxylipins on polysaccharide-type sub-2μm particle columns which can be used for fast UHPLC separations. We used them to develop a selective and sensitive enantioselective UHPLC-MS/MS method for chiral separation of multiple oxylipins of different types in biological samples. The method utilized the newest generation of polysaccharide-based CSP columns, in particular Chiralpak IA-U with sub-2μm particles and immobilized amylose tris(3,5- dimethyl-phenylcarbamate) as the chiral selector. The new enantioselective UHPLC-MS/MS method was then successfully employed for the analysis of oxylipins in autoxidized PUFA samples and in platelet releasates after thrombin activation.

3.2.Materials and methods

3.2.1. Materials

All the oxylipins, fatty acid standards and deuterated internal standards (IS) (5(*S*)-HETE-d8, 12(*S*)-HETE-d8 and 13(*S*)-HODE-d4) were purchased from Cayman Chemical (Ann Arbor, MI, USA). Their structures, IUPAC and common names are displayed in the Suppl. materials (section 3.5.1). Acetonitrile (ACN) and methanol (MeOH) of LC-MS grade were obtained from Carl Roth (Karlsruhe, Germany). Acetic acid (HAc), formic acid (FA), sodium acetate, butylated hydroxytoluene (BHT), Dulbecco's phosphate-buffered saline (PBS buffer) as well as solvents of HPLC grade (MeOH, ethyl acetate and n-hexane) were all purchased from Sigma Aldrich (Merck, Munich, Germany). Purified water was produced by Elga Purelab Ultra (Celle, Germany).

The preparation of the autoxidation samples is reported in Suppl. materials (section 3.5.2.1). Platelet releasates were from a previous study [158] and were prepared from blood collected from healthy donors at the Department of Cardiology and Angiology, University Hospital Tübingen in accordance with ethical guidelines. The extraction procedure of oxylipins from platelet releasates is described in detail in Suppl. material (section 3.5.2.2).

3.2.2. Test mixtures

Two mixtures of standards were prepared in order to test the chromatographic enantiomer separation of the compounds. The mixtures were comprised of 15 pairs of enantiomeric monohydroxy fatty acids, 2 pairs of positional isomers (2 pairs of prostaglandins) and 1 pair of diastereoisomers (2 resolvins).

The mixture A (Mix A) contained (±)9-HODE, (±)13-HODE, (±)5-HETE, (±)8-HETE, (±)11-HETE, (±)12-HETE, (±)15-HETE, (±)5- HEPE, (±)12-HEPE, (±)15-HEPE, (±)18-HEPE, (±)10-HDoHE, (±)17-HDoHE, RvD1, 17(*R*)-RvD1, PGD1, PGE1, PGD2 and PGE2 (for structures see Suppl. materials, section 3.5.1.1).

The mixture B (Mix B) contained 9(*S*)-HODE, 13(*S*)-HODE, (±)9-HETE, (±)8-HEPE, 17(*R*)-RvD1, PGE1 and PGE2.

The concentration of each substance in the mixtures was 50 ng/mL and the compounds were dissolved in MeOH.

3.2.3. LC methods

3.2.3.1.Screening methods

All the measurements were done with an Agilent 1290 Infinity UHPLC system (Agilent, Waldbronn, Germany) comprised of a binary pump, degasser and column oven and coupled to CTC PAL HTS autosampler (CTC Analytics AG, Switzerland).

Two immobilized polysaccharide UHPLC columns with sub-2μm particles were used for method screening to find suitable conditions for enantiomer separation, namely Chiralpak IA-U and Chiralpak IC-U (Daicel, Osaka, Japan) with identical dimensions of 3.0 mm x 100 mm and identical particle size of 1.6 μm.

Four different gradient methods with different mobile phases were used. Each mobile phase consisted of water with 0.1% (v/v) of acid as the component A. The component B was organic solvent (either ACN or MeOH) with 0.1% (v/v) of the same acid as in A. HAc and FA were used as the acid additives.

The gradient method for screening with ACN as the B component of the mobile phase started with 50% B and the percentage of B was raised to 95% in 5 min, followed by a hold at 95% for the next 2.5 min, then %B quickly dropped to 50% (in 0.1 min) and it stayed at this level for the last 2.4 min for column re-equilibration.

Due to a weaker elution strength, the gradient methods with MeOH started with 90% B and the fraction of B increased to 100% in 5 min, then it was kept at this level for 2.5 min, followed by re-equilibration for 2.4 min.

For all the screening methods the flow rate was equal to 0.3 mL/min, column temperature was kept at 25 °C and the injection volume was 10 μL.

3.2.3.2.Final method

The final method thus developed utilized the Chiralpak IA-U column (3.0 mm x 100 mm, 1.6 μm). The mobile phase was composed of water with 0.1% (v/v) HAc as the component A and ACN with 0.1% (v/v) HAc as the component B. Gradient elution was performed from 50% B to 100% B in 5 min, followed by a hold at 100%%B for 5 min. Then, the B level was decreased to 50% in 0.1 min and kept at 50% for the next 1.9 min. The flow rate was 0.3 mL/min and column temperature was kept at 40 °C. Injection volume was always 10 μL.

3.2.4. MS method

For detection, an AB SCIEX API 4000^{TM} MS/MS mass spectrometer with TurboIonSpray (SCIEX, Ontario, Canada) was utilized. Selected reaction monitoring (SRM) ion pairs were individually optimized for each compound and checked for possible interferences. The list of SRMs of the components of Mix A and Mix B is displayed in Table 42.

Table 42. *SRMs for components of Mix A and Mix B. The selected pre- cursor ions in quadrupole 1 (Q1 m/z) and chosen fragment ion (Q3 m/z) as well as collision energy (CE) and decluster- ing potential (DP) for each compound is shown.*

Name	Q1 *m/z*	Q3 *m/z*	CE [V]	DP [V]
9-HODE	295.2	171.2	-24	-85
13-HODE	295.2	195.1	-27	-90
5-HETE	319.2	115.1	-20	-70
8-HETE	319.2	155.0	-19	-70
9-HETE	319.2	151.0	-20	-60
11-HETE	319.2	167.2	-24	-70
12-HETE	319.2	179.2	-20	-70
15-HETE	319.2	219.4	-19	-70
5-HEPE	317.2	115.1	-22	-70
8-HEPE	317.2	161.1	-26	-70
12-HEPE	317.2	179.2	-19	-70
15-HEPE	317.2	219.4	-19	-65
18-HEPE	317.2	259.5	-19	-70
10-HDoDE	343.2	153.0	-22	-60
17-HDoDE	343.2	201.0	-20	-40
RvD1	375.1	215.1	-27	-40
PGD1 & PGE1	353.0	317.2	-22	-40
PGD2 & PGE2	351.0	271.1	-25	-80

All the measurements were done with ESI in negative polarity mode. Cell exit potential was set to –15 V, entrance potential was -10 V, source voltage was equal to -4,000 V, source temperature was kept at 400 °C, heater gas pressure and nebulizer gas pressure were both equal to 50 psi, curtain gas pressure was 35 psi and the collision gas pressure was set to medium. Dwell time for each SRM in Table 42 was 20 ms and the total cycle time was 378 ms. These parameters were identical for the screening methods and the final method.

The parameters used for the extended set of oxylipins are summarized in the Suppl. materials (Table 50).

3.2.5. Data processing

The data were processed with PeakView 2.1 and MultiQuant 3.0 (both from Sciex, Ontario, Canada). The following parameters were used for peak integration: Gaussian smooth

width: 1 point, minimum peak width: 3 points, minimum peak height: 100, noise percentage: 40%, baseline subtraction window: 0.5 min. Peak splitting points were adjusted individually depending on peak shape and how close the isomers eluted to each other, but usually was set to 1 point.

Microsoft Office 2010 (Microsoft, Redmond, WA, USA) and R (version i386 3.4.2; R-project for statistical computing) were used for further calculations and figure preparation.

Chromatographic resolution Rs was calculated by the peak width at half height method.

3.3.Results and discussion

3.3.1. Screening of methods

Column selection is the most critical factor in analytical process development for enantioselective methods. Rational column selection based on prediction of chiral recognition mechanisms has turned out illusive. Consequently, method development in enantioselective chromatography typically starts with the screening of a number of distinct promising chiral stationary phases with broad selectivity using a variety of different mobile phases [188, 189]. For the current application, MS detection was mandatory and hence columns with MS compatibility (reversed-phase elution mode) were prioritized. Polysaccharide CSPs have the broadest application spectra and since recently are available as stable-bonded phases with immobilized selectors on sub-2µm particle basis. Two members of this family (one amylose, one cellulose based CSP) with complementary enantioselectivity profiles were tested: Chiralpak IA-U, based on amylose tris(3,5-dimethylphenylcarbamate), and Chiralpak IC-U (cellulose tris(3,5-dichlorophenylcarbamate). Eighteen pairs of structural isomers were analysed with different screening methods using these two columns. The resolution values between each pair of corresponding isomers were calculated and they are summarized in Table 43 . The obtained chromatograms are illustrated in Figure 59.

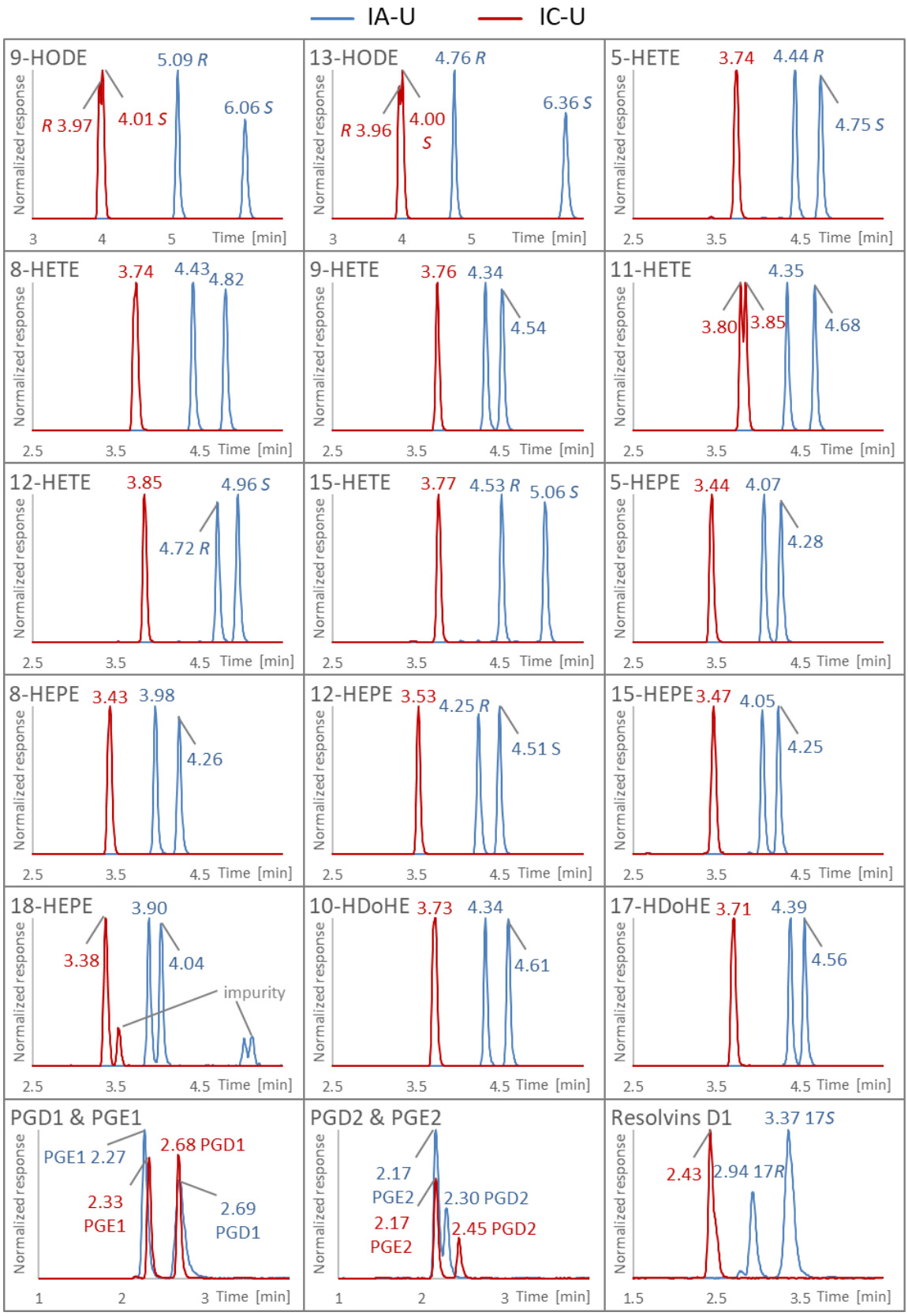

Figure 59. *Comparison of chromatograms obtained with Chiralpak IA-U column (blue) and Chiralpak IC-U column (red). Chromatographic conditions: A: H_2O + 0.1% (v/v) HAc, B: ACN + 0.1% (v/v) HAc, 50-95% B in 5 min, 95% B for 2.5 min, 95-50% B in 0.1 min, 50% for 2.4 min; flow rate: 0.3 mL/min; column temperature 25 °C.*

Overall, better results in terms of resolution between isomers were obtained with the IA-U column (i.e. with amylose based CSP) for all of the compounds except for prostaglandins (PGD1/E1 and PGD2/E2). These two constitutional isomer pairs can be separated by RPLC with C18 phase but are actually often poorly resolved in RPLC, especially the PGD1/E1 isomer pair. As can be seen from Figure 59 , the IC-U column (with the cellulose CSP) gives exceptional resolution values (> 3.0) when ACN was used as organic modifier. However, in the current studies the main focus was on separation of enantiomeric mono- and polyhydroxycarboxylic acids and the IA-U column was chosen for further method development. Prostaglandins were removed from further comparisons and discussions.

Table 43. *Resolution between isomeric peak pairs obtained with different screening methods (for corresponding values of Chiralpak IC-U see Suppl. materials Table 46 and for corresponding retention times see Suppl. materials Table 47).*

Compounds	Column IA-U				Column IC-U			
	ACN + HAc	ACN + FA	MeOH + HAc	MeOH + FA	ACN + HAc	ACN + FA	MeOH + HAc	MeOH + FA
9-HODE	9.53	9.63	5.48	5.61	0.50	0.50	0.00	0.00
13-HODE	14.97	14.69	11.70	11.76	0.50	0.52	0.00	0.00
5-HETE	3.55	3.57	7.50	7.46	0.00	0.00	0.00	0.00
8-HETE	4.35	4.42	6.39	6.36	0.00	0.00	0.00	0.00
9-HETE	2.36	2.52	3.01	2.93	0.00	0.00	0.00	0.00
11-HETE	4.07	4.06	4.17	4.12	0.60	0.59	0.00	0.00
12-HETE	2.73	2.83	4.99	4.84	0.00	0.00	0.00	0.00
15-HETE	5.96	6.21	8.73	8.82	0.00	0.00	0.00	0.00
5-HEPE	2.44	2.49	6.57	6.45	0.00	0.00	0.00	0.00
8-HEPE	3.35	3.42	5.79	5.65	0.00	0.00	0.00	0.00
12-HEPE	2.94	3.04	4.95	4.87	0.00	0.00	0.00	0.00
15-HEPE	2.34	2.45	5.92	5.70	0.00	0.00	0.00	0.00
18-HEPE	1.81	1.95	3.76	3.44	0.00	0.00	0.00	0.00
10-HDoDE	3.29	3.51	5.33	5.32	0.00	0.00	0.00	0.00
17-HDoDE	2.08	2.09	5.28	5.12	0.00	0.00	0.00	0.00
Resolvins D1	2.59	2.65	2.63	2.55	0.00	0.00	0.00	0.00
PGD1 and PGE1	2.67	2.73	1.70	1.72	3.94	4.10	1.13	1.18
PGD2 and PGE2	1.12	1.14	0.00	0.00	3.00	3.04	0.80	0.74

In terms of organic solvent comparison, both ACN and MeOH provided resolution over 1.5, so baseline separations were achieved for all the isomer pairs except for PGD2/PGE2. Generally, higher resolution values were obtained with MeOH mainly due to larger separation factors (Suppl. materials Figure 68). However, peaks were broader with MeOH (Suppl. materials Table 48), which was considered disadvantageous with regard to

detection sensitivities. Moreover, methods with MeOH were considered less flexible in terms of adjustments of mobile phase elution strengths (the gradient started already with 90% B) and flow rate (higher backpressure in the system was observed with MeOH; a comparison is provided in the Suppl. materials Figure 67). Therefore, ACN was chosen for final method fine tuning.

Last but not the least, the type of acid additive (acetic vs. formic acid) was examined as it could show some effect on isomer resolution, but also on detection sensitivity. It was found that the acid additive did not exert a strong influence neither on the retention time, nor peak shape, and therefore resolution as well. Method sensitivity was then compared for these 2 acids and the results were also very similar with slightly better sensitivity obtained with HAc (data provided in the Suppl. materials Table 49). Therefore, this acid was selected for the final method adjustment.

3.3.2. Final method adjustment (fine tuning of gradient profile)

The final gradient profile of the method was adjusted for obtaining good isomer separations, avoiding interferences from structurally related oxylipins in order to secure satisfactory assay specificity, and finally assuring complete elution of other possible components of the oxidized PUFAs and the platelet releasate samples. Had they accumulated on the column, problems with assay specificity and method ruggedness might have occurred.

The final gradient was slightly steeper with channel B varying from 50 to 100% B (instead of to 95% B as in the screening method) in 5 min. Then the washing step of 100% B was extended to 5 min in order to elute possible other more lipophilic compounds (for example fatty acids) from the column, which might show stronger retention. For the same reason, the column temperature was increased to 40 °C.

At this point, different MS source parameters were also tested by automated optimization with flow injection, but the initial conditions performed very well and were not changed for the final method. The fully optimized final method is given in the experimental section.

***Table 44**. Preliminary validation results for quantification of oxylipins from autoxidation of PUFAs.*

Corresponding PUFA	Compound	LOD [pg on column]	LOQ [pg on column]	Range [pg per 1 µg of PUFA]	R	Accuracy [%] QC lower	Accuracy [%] QC higher	Precision [%] QC lower	Precision [%] QC higher
LA	9(*R*)-HODE	2.5	5	50-5,000	0.989	114.1	98.3	1.2	5.0
	9(*S*)-HODE	2.5	5	50-5,000	0.991	107.7	97.7	8.0	10.7
	13(*R*)-HODE	2.5	5	50-5,000	0.985	111.1	104.2	0.9	3.2
	13(*S*)-HODE	2.5	5	50-5,000	0.990	108.1	102.5	2.0	9.3
AA	5(*S*)-HETE	0.5	5	50-5,000	0.991	112.2	105.7	7.0	5.2
	5(*R*)-HETE	0.5	5	50-5,000	0.983	113.3	105.2	9.1	4.2
	8-HETE p1	2.5	5	50-5,000	0.991	115.0	104.6	2.6	6.7
	8-HETE p2	2.5	5	50-5,000	0.988	112.6	102.5	3.1	2.3
	9-HETE p1	2.5	5	50-5,000	0.990	113.9	101.8	5.4	1.3
	9-HETE p2	2.5	5	50-5,000	0.987	110.5	102.8	1.5	1.0
	11-HETE p1	0.25	5	50-5,000	0.99	114.8	101.8	6.2	3.1
	11-HETE p2	0.25	5	50-5,000	0.988	114.2	105.8	11.5	7.4
	12(*R*)-HETE	2.5	5	50-5,000	0.991	114.1	105.2	6.3	2.6
	12(*S*)-HETE	2.5	5	50-5,000	0.990	114.0	104.4	6.0	8.9
	15-HETE p1	2.5	5	50-5,000	0.992	113.9	100.7	8.8	5.7
	15-HETE p2	2.5	5	50-5,000	0.993	112.6	102.6	5.7	3.9
EPA	5-HEPE p1	2.5	5	50-5,000	0.983	112.3	110.4	7.7	6.6
	5-HEPE p2	2.5	5	50-5,000	0.992	111.9	101.7	0.3	5.0
	8-HEPE p1	2.5	5	50-5,000	0.993	112.0	102.6	3.4	4.3
	8-HEPE p2	2.5	5	50-5,000	0.991	114.4	101.1	6.0	3.8
	12(*R*)-HEPE	2.5	5	50-5,000	0.994	110.2	99.3	0.2	5.5
	12(*S*)-HEPE	2.5	5	50-5,000	0.993	114.7	100.3	3.7	4.5
	15-HEPE p1	2.5	5	50-5,000	0.989	111.6	102.7	0.1	3.4
	15-HEPE p2	2.5	5	50-5,000	0.994	110.7	97.0	3.7	0.6
	18-HEPE p1	5	25	250-5,000	0.997	97.4	99.9	6.2	0.2
	18-HEPE p2	5	25	250-5,000	0.993	87.7	92.4	6.1	0.2
DHA	10-HDoHE p1	0.5	5	50-5,000	0.991	114.9	100.3	2.8	6.7
	10-HDoHE p2	0.5	5	50-5,000	0.991	113.4	103.3	1.2	7.2
	17-HDoHE p1	5	25	250-5,000	0.995	94.6	97.4	8.1	6.3
	17-HDoHE p2	5	25	250-5,000	0.995	86.8	95.7	5.0	7.4
	RvD1	5	25	250-5,000	0.986	113.6	94.8	7.2	9.8
	17(*R*)-RvD1	5	25	250-5,000	0.986	113.6	94.8	7.2	9.8
ALA	13(*R*)-HOTrE	1	10	100-10,000	0.989	N/A	N/A	N/A	N/A
	13(*S*)-HOTrE	1	10	100-10,000	0.878	113.0	103.3	3.5	5.9
DGLA	12(*R*)-HETrE	1	10	100-10,000	0.989	N/A	N/A	N/A	N/A
	12(*S*)-HETrE	1	10	100-10,000	0.989	114.9	99.2	4.0	6.4
DHA	14(*R*)-HDoHE	1	10	100-10,000	0.990	N/A	N/A	N/A	N/A
	14(*S*)-HDoHE	1	10	100-10,000	0.990	113.5	101.5	2.6	2.1
EPA	5,6-DiHETE p1	10	50	500-5,000	0.987	95.3	102.1	3.6	13.0
	5,6-DiHETE p2	10	50	500-5,000	0.992	108.9	99.1	11.2	1.4

3.3.3. Preliminary validation for quantification of oxylipins from autoxidation of PUFAs

Several parameters were determined in the pre-validation studies to prove that the method can give reliable results when real samples are analysed. For this reason, instrumental limit of detection (LOD) as the lowest concentration of an analyte (dissolved in MeOH), which gives signal-to-noise (S/N) ratio of minimum 3 was determined. Similarly, the desired lower limit of quantification (LOQ) was confirmed to give S/N ratio of at least 10. Method linearity in the calibration range was determined, as well as intra- assay method accuracy and precision for 2 independent concentration levels was measured: 2.5 ng/mL and 12.5 ng/mL for all the analytes except of 14(*S*)-HDoHE, 12(*S*)-HETrE and 13(*S*)-HOTrE, for which the spiked concentration was two times higher (5.0 and 25.0 ng/mL) The results were satisfying and are displayed in Table 44.

3.3.4. Results of autoxidation of PUFAs

Six different PUFAs (LA , AA , EPA , DHA , ALA , DGLA) were oxidized in air at 3 different time points: 18 h, 24 h and 48 h. All the compounds used for method development were monitored in this experiment: 2 pairs of HODEs, 6 pairs of HETEs, 5 pairs of HEPEs, 2 pairs of HDoHEs and a pair of resolvins D1. Additionally, 4 more SRMs were added to monitor 3 other hydroxy fatty acids, viz. 12 HETrE, 13-HOTrE and 14-HDoHE (pure *S* enantiomers were used as standards, but no *R* nor racemic mixture were available for comparison) as well as 5,6-DiHETE (the standard was a racemic mixture of the two *cis* -enantiomers, but not all 4 stereoisomers were available). The results of the oxidation are shown in Figure 60 (compounds above LOQ) and a table with all the results is displayed in the Suppl. materials (Suppl. materials Table 51).

As shown in Figure 60 several compounds were found in the oxidized samples. Oxidation of AA produced high amounts of 15-HETE and lower concentrations of other HETEs. For all HETEs the maximal amount was observed at 24 h of oxidation and it dropped or was not detected anymore when the arachidonic acid was oxidized for 48 h. It seems that these compounds are further degraded to secondary oxidation products. As expected, the two

enantiomers were always produced in equal quantities (within the error limits) and no stereoselectivity was observed due to the absence of chiral catalyst.

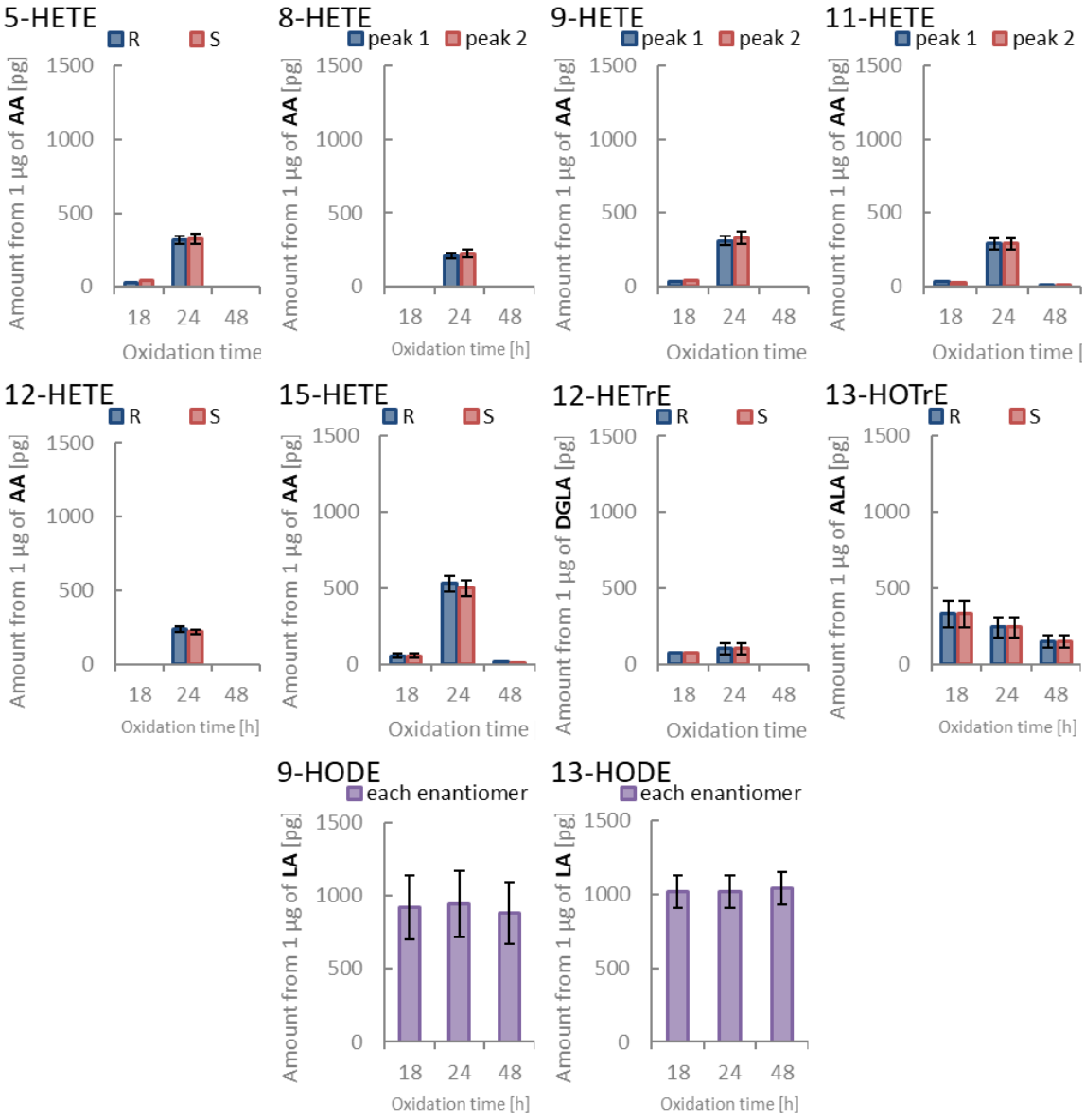

Figure 60. *Bar graphs showing mass [in pg] of hydroxy fatty acids produced by oxidation of 1 µg of a corresponding PUFA. Compounds were analysed at 3 different time points of oxidation: exposure to air for 18, 24 and 48 h. Blue bars show the amount of the first eluted enantiomer (specified in legend as R or S if identified), and the red bars display the later eluted enantiomer; In case of HODEs the purple bar graphs show amount of the R enantiomer and the S enantiomer is assumed to be equal. The y scale is unified for all the bar graphs to 1,500 pg.*

HEPEs, which are products of EPA oxidation, were found at minute amounts, always below LOQ. Similarly to HETEs, they usually appeared after 24 h of oxidation and were

not detected anymore in the sample after 48 h of oxidation. 5,6-DiHETE, which also originates from EPA, was not detected in air-oxidized samples.

HODEs, oxylipins originating from LA, were found in high amounts around 1 ng of each enantiomer of the hydroxy fatty acid from 1 µg of the PUFA (LA). They were highly abundant already after 18 h of oxidation and their levels remained more or less constant throughout the oxidation experiments. We have reported amounts of oxidation only for the *R* enantiomers as there were interfering signals eluting close to the *S* enantiomers. Due these interferences correct quantification of these enantiomers is cumbersome and some further chromatographic optimization is recommended. However, as it is shown for other autoxidation products, equal amounts of *S* and *R* enantiomers were expected and accurate quantification of one enantiomer allowed conclusion on the second one.

No oxidation products of DHA with selected SRMs were found above the LOQ levels and only minor amounts of 10-HDoHE and 14-HDoHE close to LOD were detected.

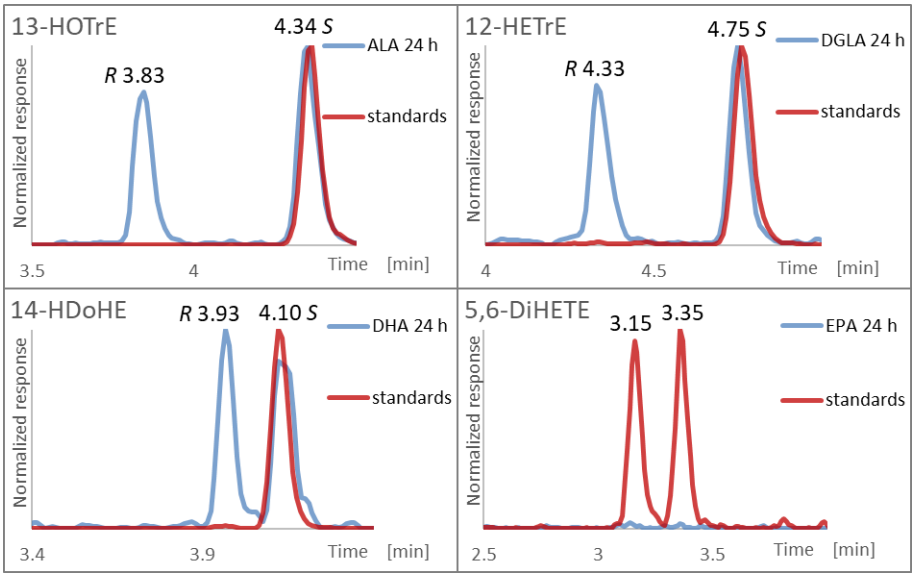

Figure 61. *Separation of enantiomers of 13-HOTrE, 12-HETrE, 14-HDoHE and 5,6-DiHETE. Blue line shows chromatogram from a corresponding oxidized PUFA and red trace shows chromatogram from a pure standard (in case of 13-HOTrE, 12-HETrE and 14-HDoHE standards were pure S enantiomers and 5,6-DiHETE was a racemic mixture of cis- enantiomers).*

12-HETrE and 13-HOTrE, which are formed from DGLA and ALA respectively, were observed in the corresponding samples. 12- HETrE reached the maximum level at 24 h and was not detected after 48 h of oxidation. 13-HOTrE showed the highest abundance already

after 18 h of oxidation. The calibration function was only available for the *S* enantiomers, but equal concentration of *R* enantiomers can be validly assumed in the absence of a chiral catalyst as supported by equal peak area ratios.

All of the newly added compounds - 12-HETrE, 13-HOTrE, 14- HDoHE and 5,6-DiHETE, were well separated, which shows that the method can be conveniently extended to other mono and polyhydroxy fatty acids. Three of the compounds (12-HETrE, 13-HOTrE and 14-HDoHE) were found as pairs of enantiomers (with similar area ratio *R* to *S* enantiomer in the respective samples) in the corresponding autoxidized PUFAs. 5,6-DiHETE was not detected in the oxidation samples, but the standard was a pair of *cis*-enantiomers, which were well separated. The chromatograms are showed in Figure 61.

3.3.5. Preliminary validation for the quantification of oxylipins in platelet releasates

Released hydroxy fatty acids from resting and thrombin-activated platelets were extracted and analysed by UHPLC-MS/MS using a matrix-matched calibration and three stable isotope labelled internal standards. The analytical method was extended by addition of 12-HETrE, 13-HOTrE, 14-HDoHE and 5,6-DiHETE (compared to the screening method).

Similarly to previously described quantification, the analysis of platelet releasates was also pre-validated to show that the method gives satisfying results and can be used for quantification of the analytes in platelet supernatant studies. Instrumental LOD (as analytes dissolved in MeOH, not in matrix because of lack of an analyte-free-matrix for all compounds) was established with minimal value of S/N as 3. LOQ was determined in matrix with minimal S/N ratio equal to 10. Calibration functions were established using area ratios (peak area of an analyte divided by peak area of an internal standard), by weighted linear regression using $1/x^2$. Good linearity was confirmed over the calibration range specified in Table 45 by correlation coefficients $R > 0.98$. Intra-assay accuracy and precision were determined for two independent concentration levels: platelet release spiked with 2.5 ng/mL and 12.5 ng/mL of all analytes accept of 14(*S*)-HDoHE, 12(*S*)-HETrE and

13(*S*)-HDoHE, which were spiked with 2 times higher concentration. The final results are presented in Table 45.

Table 45. *Preliminary validation results for quantification of oxylipins in platelet releasates.*

Compound	IS	LOD [pg on column]	LOQ [pg on column]	Range [fg/1e6 platelets]	R	Accuracy [%] QC lower	Accuracy [%] QC higher	Precision [%] QC lower	Precision [%] QC higher
9(*R*)-HODE	13(*S*)-HODE d4	2.5	6	20-1500	0.987	85.8	93.0	3.5	5.0
9(*S*)-HODE	13(*S*)-HODE d4	2.5	6	20-1500	0.982	110.9	90.5	12.6	2.0
13(*R*)-HODE	13(*S*)-HODE d4	2.5	6	20-1500	0.986	86.6	88.2	3.8	8.3
13(*S*)-HODE	13(*S*)-HODE d4	2.5	6	20-1500	0.987	87.6	91.5	3.8	14.5
5(*S*)-HETE	5(*S*)-HETE d8	0.5	5	20-1500	0.991	91.4	97.4	8.0	5.5
5(*R*)-HETE	5(*S*)-HETE d8	0.5	5	20-1500	0.992	87.1	98.3	11.2	1.7
8-HETE p1	12(*S*)-HETE d8	2.5	6	20-1500	0.996	86.1	96.2	3.3	2.6
8-HETE p2	12(*S*)-HETE d8	2.5	6	20-1500	0.997	85.1	93.9	6.1	3.9
9-HETE p1	12(*S*)-HETE d8	2.5	6	20-1500	0.998	91.4	93.5	11.6	7.5
9-HETE p2	12(*S*)-HETE d8	2.5	6	20-1500	0.986	88.0	99.1	5.2	4.6
11-HETE p1	12(*S*)-HETE d8	0.25	5	20-1500	0.991	86.6	90.0	4.8	2.0
11-HETE p2	12(*S*)-HETE d8	0.25	5	20-1500	0.995	87.4	91.9	3.9	1.1
12(*R*)-HETE	12(*S*)-HETE d8	2.5	6	20-1500	0.991	86.6	93.6	2.5	2.8
12(*S*)-HETE	12(*S*)-HETE d8	2.5	6	20-1500	0.993	88.9	93.8	2.1	5.4
15-HETE p1	12(*S*)-HETE d8	2.5	6	20-1500	0.990	86.8	87.0	4.6	2.0
15-HETE p2	12(*S*)-HETE d8	2.5	6	20-1500	0.993	92.8	89.1	9.0	6.7
5-HEPE p1	5(*S*)-HETE d8	2.5	6	20-1500	0.985	94.8	98.9	8.1	5.3
5-HEPE p2	5(*S*)-HETE d8	2.5	6	20-1500	0.984	86.0	91.9	2.1	7.8
8-HEPE p1	12(*S*)-HETE d8	2.5	6	20-1500	0.993	86.6	95.7	1.1	7.2
8-HEPE p2	12(*S*)-HETE d8	2.5	6	20-1500	0.987	86.4	90.7	7.0	1.8
12(*R*)-HEPE	12(*S*)-HETE d8	2.5	6	20-1500	0.992	85.8	91.3	3.6	2.4
12(*S*)-HEPE	12(*S*)-HETE d8	2.5	6	20-1500	0.991	88.6	91.3	5.0	4.6
15-HEPE p1	12(*S*)-HETE d8	2.5	6	20-1500	0.986	85.9	90.5	1.9	8.2
15-HEPE p2	12(*S*)-HETE d8	2.5	6	20-1500	0.989	86.5	90.9	4.3	4.2
18-HEPE p1	12(*S*)-HETE d8	5	25	90-1500	0.994	< LOQ	94.1	< LOQ	3.0
18-HEPE p2	12(*S*)-HETE d8	5	25	90-1500	0.996	< LOQ	85.6	< LOQ	3.3
10-HDoHE p1	12(*S*)-HETE d8	0.5	5	20-1500	0.983	85.0	94.6	4.7	3.6
10-HDoHE p2	12(*S*)-HETE d8	0.5	5	20-1500	0.992	88.3	91.5	7.2	4.1
17-HDoHE p1	12(*S*)-HETE d8	5	25	90-1500	0.989	< LOQ	87.7	< LOQ	8.6
17-HDoHE p2	12(*S*)-HETE d8	5	25	90-1500	0.969	< LOQ	94.9	< LOQ	11.4
RvD1	5(*S*)-HETE d8	5	25	90-1500	0.995	< LOQ	101.2	< LOQ	5.2
17(*R*)-RvD1	5(*S*)-HETE d8	5	25	90-1500	0.990	< LOQ	103.9	< LOQ	7.4
13(*R*)-HOTrE	13(*S*)-HODE d4	1	10	40-3000	0.999	N/A	N/A	N/A	N/A
13(*S*)-HOTrE	13(*S*)-HODE d4	1	10	40-3000	0.999	87.6	92.6	2.5	8.9
12(*R*)-HETrE	12(*S*)-HETE d8	1	10	40-3000	0.993	N/A	N/A	N/A	N/A
12(*S*)-HETrE	12(*S*)-HETE d8	1	10	40-3000	0.993	90.1	89.9	3.1	4.5
14(*R*)-HDoHE	12(*S*)-HETE d8	1	10	40-3000	0.987	N/A	N/A	N/A	N/A
14(*S*)-HDoHE	12(*S*)-HETE d8	1	10	40-3000	0.987	88.1	90.0	6.4	2.8
5,6-DiHETE p1	12(*S*)-HETE d8	10	50	200-1500	0.972	< LOQ	92.2	< LOQ	3.7
5,6-DiHETE p2	12(*S*)-HETE d8	10	50	200-1500	0.995	< LOQ	87.0	< LOQ	0.4

3.3.6. Results of the analysis of platelet releasates

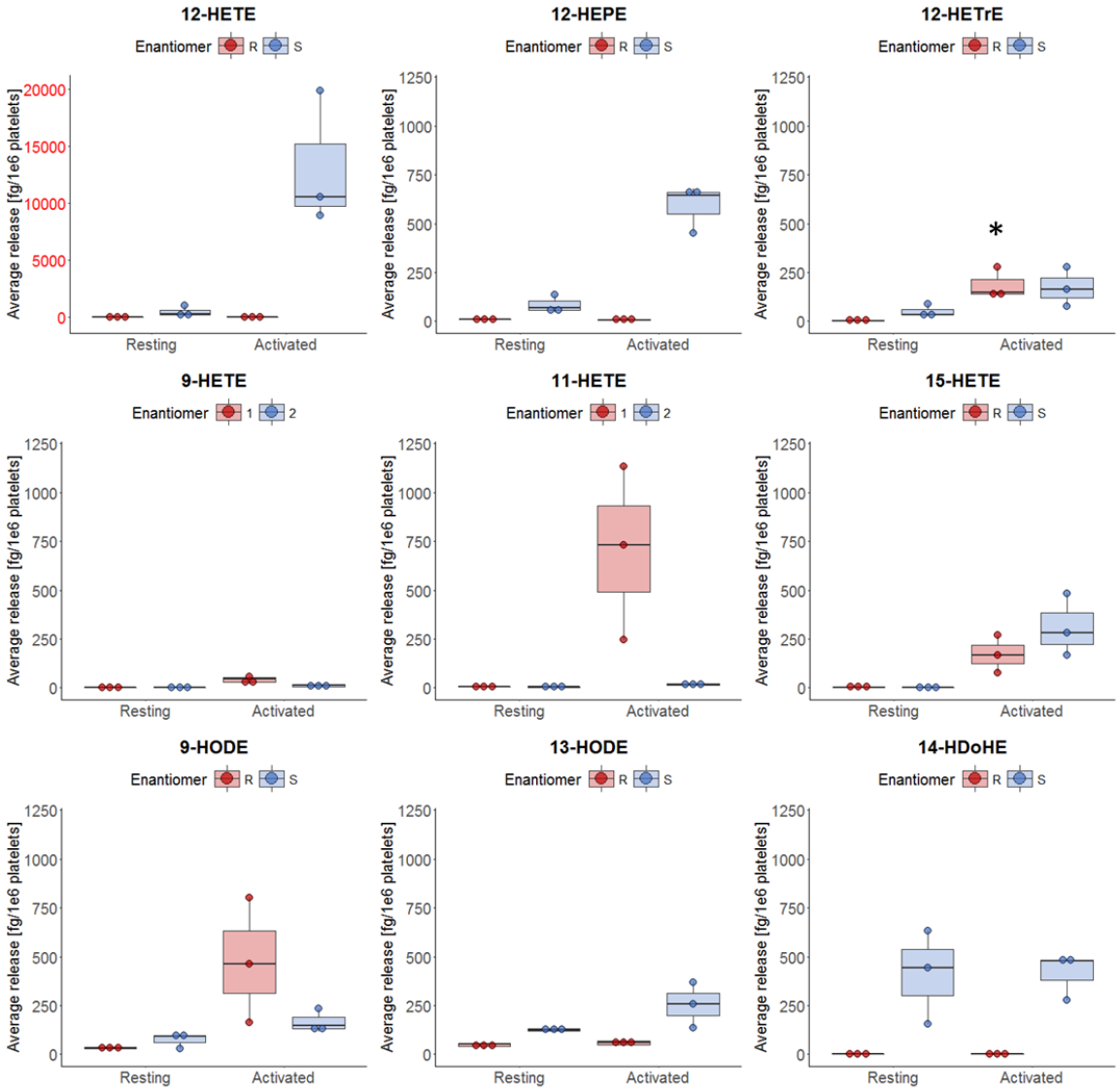

Figure 62. *Box bots of the average release (n = 3) of oxylipins [in fg] from 1 million platelets (estimated release for 12-HETE, whose concentration highly exceeded ULOQ). Red colour shows levels of the first eluted peak and blue colour represents the second eluted peak (R and S annotation is present if enantiomers are identified). The y-axis scale is unified for all the compounds except 12-HETE. The left part of the plots represents release for resting platelets and the right part from thrombin-activated platelets. 12(R)-HETrE detected in activated platelets (∗) is most probably an isomer with different double bond composition.*

Several oxylipins were detected in the platelet releasates and for many of them an increased level in thrombin-activated platelets was observed. Importantly, in most of the cases one of the enantiomers was elevated, while the other was not detected or detected in minute concentrations, which is indicative for enzymatic oxidation. Box plots of the oxylipins with

concentrations higher than LOQ are illustrated in Figure 62, while all the results are summarized in the supplementary information (Suppl. materials Table 52).

The highest concentration of the hydroxy fatty acids released from activated platelets was that of 12(*S*)-HETE. This compound exceeded over 15 times the concentration of any other oxylipin analysed in this study. 12(*S*)-HETE was present in the releasate from resting platelets only at very minor concentrations and highly increased with thrombin activation. It is a product of 12-LOX activity and it is one of the main metabolites generated when platelets are activated by factors like thrombin, calcium or collagen. The role of free 12(*S*)-HETE remains unknown, but it has been shown that significant amounts of this hydroxy fatty acid are re-esterified into membrane phospholipids [143, 144].

The production of other 12-hydroxy fatty acids was also observed. 12-HEPE, which originates from EPA, was also detected as *S* enantiomer, while 12-HETrE from DGLA was seemingly present in both forms as *R* and *S* enantiomers (*vide infra*), and their concentration was very similar.

In case of 11-HETE the first eluted peak, which is supposed to be the *R* enantiomer, increased upon activation. Both enantiomers of 15-HETE were elevated in the samples of thrombin-activated platelets.

Opposite observations were made for 9- and 13-HODE: for 9- HODE mostly the *R* enantiomer increased upon activation, while 13-HODE was detected mostly as the *S* enantiomer in thrombin activated samples.

14(*S*)-HDoHE was present already in resting platelets and its level remained quite the same in activated platelets. The R enantiomer was not observed.

3.3.7. Practical implications of the current results and discussion on their biological effects

The vast majority of methods used nowadays for oxylipin analysis are non-enantioselective targeted assays (e.g. [157]). These assays often cover a wide variety of lipid mediators.

However, they do not give the entire picture of oxylipin synthesis in biological systems like platelets, as they cannot distinguish whether the products are originating from autoxidation, cellular ROS-triggered oxidation (which is undoubtedly faster than oxidation in air due to the reactive potential of the transiently generated radicals) or enzymatic biotransformation. Enantioselective assays are more powerful as they create additional information which allows for a more differentiated interpretation of the results in terms of biochemical pathways. The following discussion should document this for platelet activation, however, has been already reported for other biological questions on other columns (mostly Chiralpak AD-H) [190].

3.3.7.1. Distinction between autoxidation, oxidative stress and enzymatic biotransformation

One particular problem of PUFAs and PUFA-containing lipids is their ease of autoxidation. PUFA-autoxidation products cannot be distinguished from enzymatic PUFA metabolites by achiral LC-MS/MS assays. Enantioselective UHPLC-MS/MS does provide this information. For example, human platelet-type 12-lipoxygenase (12-LOX) plays an important role in the regulation of human platelet function. Autoxidation produces both enantiomers (Figure 63A1), while 12-LOX action generates the *S*-enantiomer of 12-HETE only (Figure 63A2). In Figure 63A2 we see that there was no 12(*R*)-HETE present in the activated platelet sample and therefore we could conclude that autoxidation was absent. If both enzymatic and autoxidation products had been present at the same time, non-racemic mixtures would have been the result and the enantiomeric excess of *S*-enantiomer (ee% = (*S* - *R*)/(*S* + *R*)) would have indicated the 12-LOX product while the *R*-enantiomer peak would have been considered as a marker of autoxidation. The same principal picture of enantiomer ratios as elaborated for autoxidation is expected for hydroxyl PUFA metabolites that are formed from oxidative stress due to cellular ROS which also generates the racemic mixture. Distinction between autoxidation (in course of sample preparation) and ROS-triggered oxidation becomes possible if the corresponding isotope labelled PUFA is added as an internal standard.

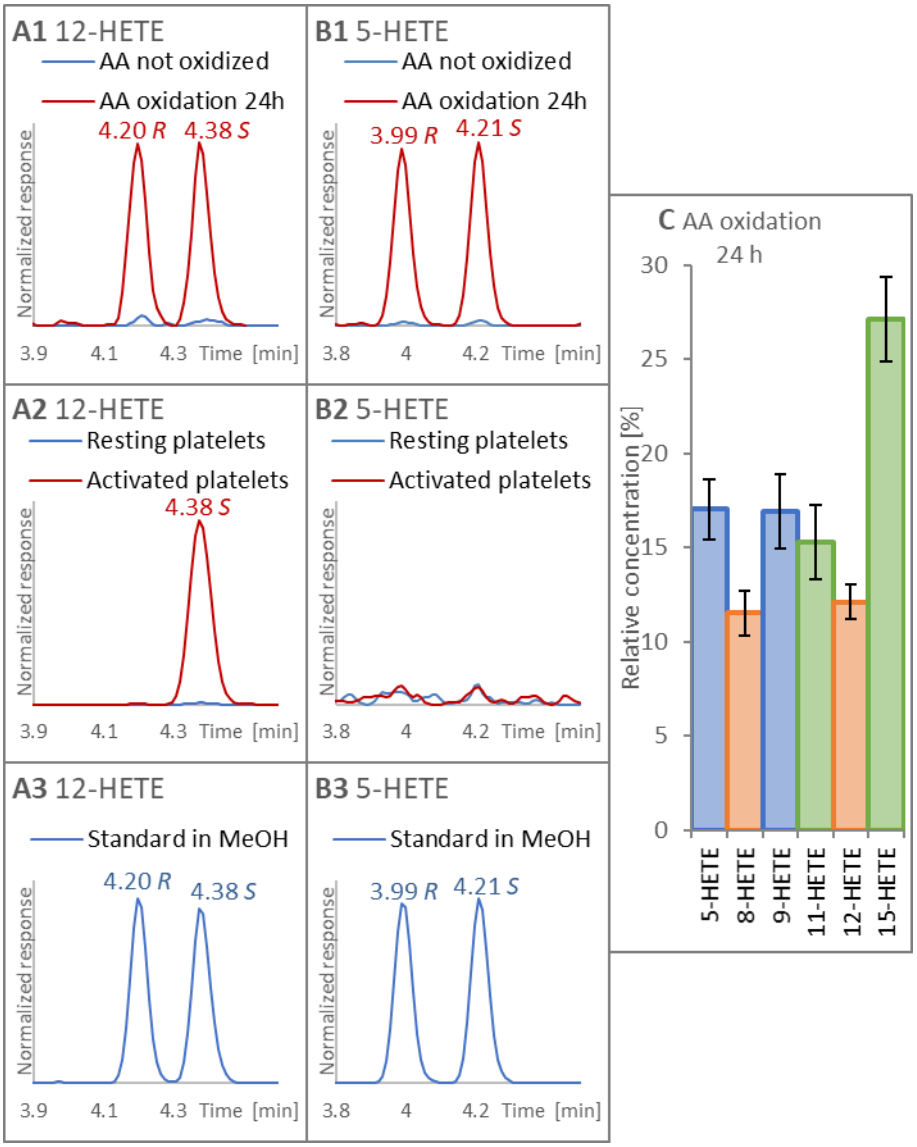

Figure 63. *Comparison of oxylipins from different origins. EIC of 12-HETE in oxidized PUFA (**A1**), platelets (**A2**) and standard solution (**A3**); EIC of 5-HETE in oxidized PUFA (**B1**), platelets (**B2**) and standard solution (**B3**); and a boxplot showing distribution of HETEs obtained after 24 h of AA oxidations (**C**), the same colours indicate the same initial position of a free radical. Analysed with the final method.*

3.3.7.2.Contamination of platelet isolate with leukocytes

A distinctive problem of the purity of isolated platelet preparations is their contamination with leukocytes. Leukocytes express 5-LOX, while platelets are deficient in 5-LOX [191]. 5-HETE, if present in platelet samples, is therefore due to autoxidation/ROS- oxidation (both enantiomers present at same concentration level), or if present as *S*-enantiomer (or as enantiomeric excess of *S*-enantiomer) might indicate leukocyte contamination. If

autoxidation was the problem the entire PUFA oxidation profile for AA is expected to be present in similar levels as shown in Figure 63C. If a single 5(*S*)-HETE enantiomer is detected, it might indicate leukocyte activity. It can be seen that in our platelet samples (both resting and thrombin–activated) 5-HETE is completely absent as expected (Figure 63B2). It documents a good quality of our platelet isolates.

3.3.7.3. 12-HETrE case

12-HETrE is the oxidation product of DGLA (Figure 61, top right chromatogram). In a recent study on substrate specificity of human platelet-type 12-LOX, it has been shown that DGLA is comparable as substrate to AA and EPA [192]. However, as can be seen from Figure 62, top row, the stereoselectivity pattern is different from that of AA (12-HETE as product) and EPA (12-HEPE as product). The product of DGLA formed by 12-LOX is 12(*S*)- hydroperoxy-8*Z*,10*E*,14*Z*-eicosatrienoic acid and its reduced form 12(*S*)-hydroxy-8*Z*,10*E*,14*Z*-eicosatrienoic acid (12(*S*)-HETrE). As can be seen in Figure 64A1, 12(*S*)-HETrE could be detected in thrombin- activated platelet releasates (peak at 4.75 min, also detected in 12(*S*)-HETrE standard (peak at 4.73 min, Figure 64A4) and in racemate from oxidized DGLA (peak at 4.73 min, Figure 64A3)). The *R*-enantiomer 12(*R*)-HETrE is eluted at 4.32 min (Figure 64A3). In the activated platelet sample, also a second peak was eluted before the *S*-enantiomer (peak at 4.44 min in Figure 64A1). This peak could be misleadingly identified as 12(*R*)-HETrE, but the retention time did not match with the one of the racemate from oxidized DGLA (0.12 min difference is too much to be within the experimental error of this enantioselective UHPLC method). Hence, MeOH was also evaluated as modifier in the mobile phase with the Chiralpak IA-U column (Figure 64B1-3) and the complementary enantioselective UHPLC column Chiralpak IC-U was tested as well by injection of the same samples (Figure 64C1- 3). Using the same elution conditions with AcN on the IC-U column, the racemate of 12-HETrE was not resolved; the two enantiomers eluted both at 3.92 min (Figure 64C3). However, in the thrombin-activated platelet releasate sample, a second peak was observed, which eluted slightly earlier (peak at 3.56 min in Figure 64C1). These results suggest that there is another compound formed which is structurally similar to 12(*R*)-HETrE. Indeed, it was reported earlier that besides platelet 12(*S*)-HETrE (with 8*Z*,10*E*,14*Z* double bond configurations) another HETrE, viz. 12(*R*)-hydroxy- 5*Z*,8*Z*,14*Z*-eicosatrienoic acid exists [192]. In fact, this compound differs

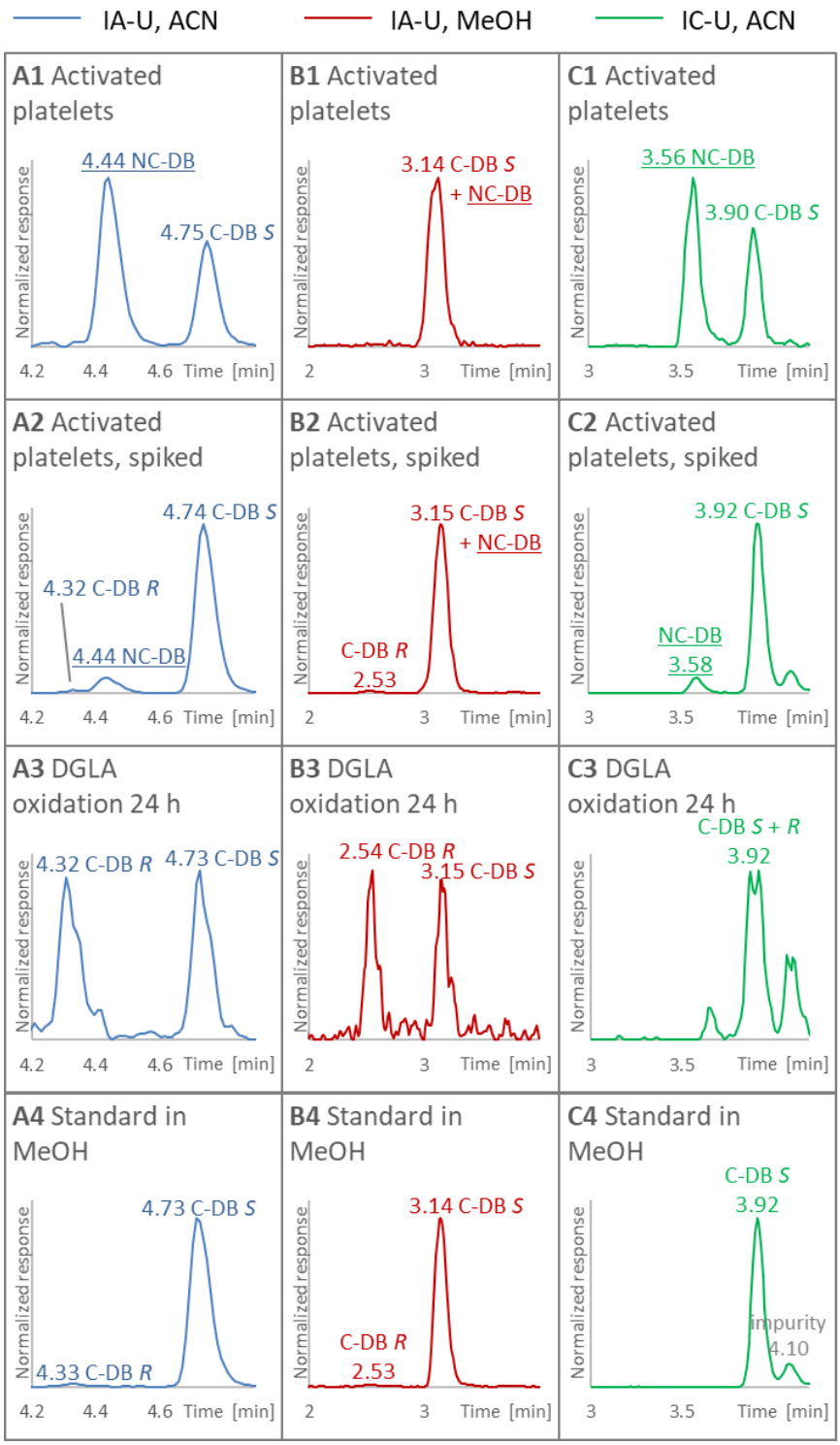

Figure 64. *Separation of 12-HETrEs: with conjugated double bonds (C-DB S and C-DB R) and with non-conjugated double bonds (NC-DB) with different chromatographic conditions.* ***A1-4*** *and* ***B1-4****: separation with IA-U column;* ***C1-4****: separation with IC-U column. Mobile phase A: H_2O + 0.1% HAc (v/v), B: ACN + 0.1% HAc (v/v) for* ***A1-4*** *and* ***C1-4*** *or MeOH + 0.1% HAc (v/v) for* ***B1-4****. Gradient for ACN methods: 50-100% B in 5 min, 100% for 5 min, 50 % for 1.9 min. Gradient for MeOH methods: 90-100% B in 5 min, 100% for 5 min, 90 % for 1.9 min. Column temperature: 40 °C, flow rate: 0.3 mL/min, injection volume: 10 µL. Concentration of 12-HETrE in the oxidized DGLA (****A3****,* ***B3*** *and* ***C3****) was very low, that is why the chromatograms showed poor quality.*

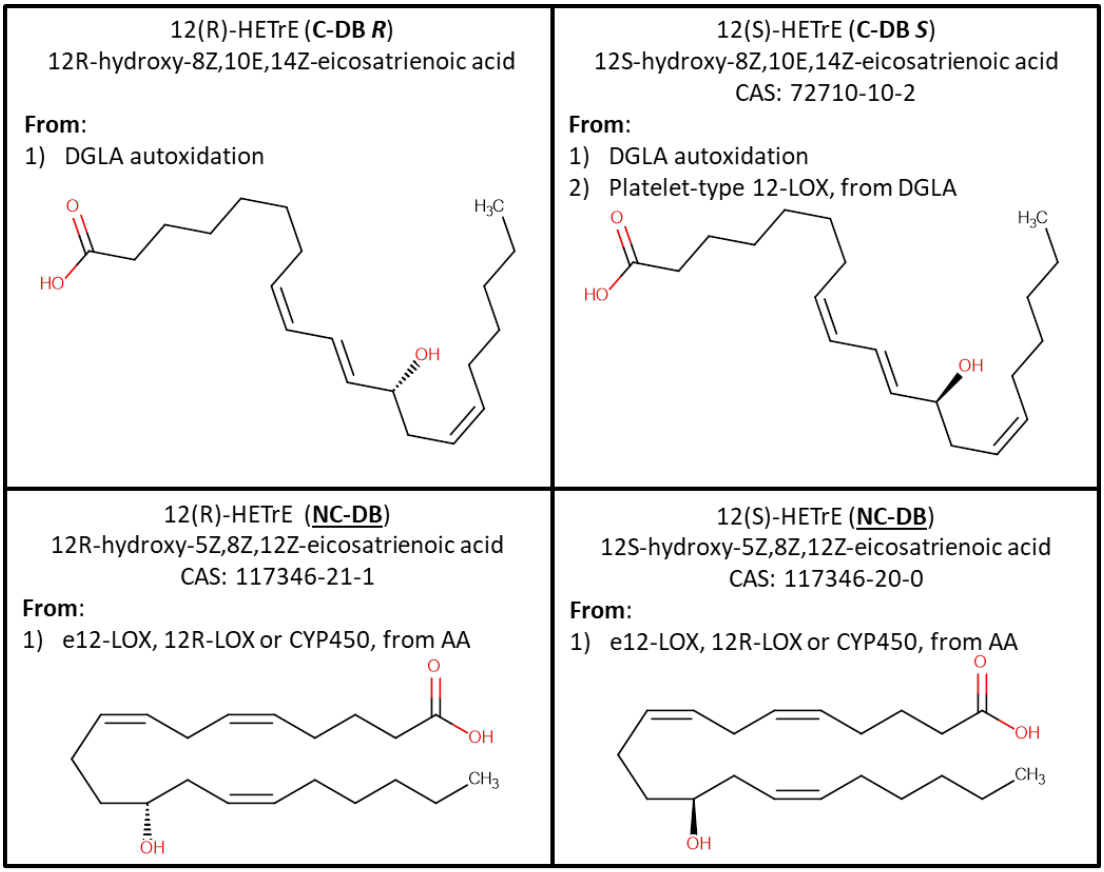

Figure 65. *Structures of 12-HETrEs and their origins. The coding next to names (e.g. C-DB R) is related to the peak naming in Figure 64.*

just by the position and configuration of double bonds (Figure 65) and may therefore show similar retention time as 12(*R*)-hydroxy- 8*Z*,10*E*,14*Z*-eicosatrienoic acid and the same SRM transitions (*m/z* 321.4 → 181.0). The slight shift in retention times on Chiralpak IA-U and IC-U columns could be explained by the different double bond positions and double bond configurations, respectively, and this shift therefore could be indicative for the other 12(*R*)-HETrEs (without conjugated double bonds). However, this compound has not been detected yet in platelets, but seems to be specific for epithelium cells [193]. To clarify this issue and inconsistency in structural assignment is of importance because the two 12(*R*)-HETrEs have not only different structure and different origin (DGLA and AA), but also elicit distinct biological actions. The 12-LOX metabolite of DGLA *i.e.* 12(*S*)-hydroxy-8*Z*,10*E*,14*Z*-eicosatrienoic acid has been shown to inhibit platelet activation and thrombosis [193]. The AA metabolite 12(*R*)-hydroxy-5*Z*,8*Z*,14*Z*-eicosatrienoic acid demonstrated biological activities that are typical for inflammatory mediators including increased membrane permeability, vasodilation, chemotaxis and angiogenesis [194].

Unfortunately, this compound is currently not available commercially, for which reason a full identification could not be provided at present and our hypothesis could not be proven in this manuscript. We are currently working, however, on its clarification to provide experimental evidence via custom synthesized standard and more selective chromatography.

3.3.7.4. 8-, 9-, and 11-HETE

For all of these three PUFA metabolites, the first eluted peak (presumably *R*-configuration) dominated, while the second eluted peak (presumably *S*) was present at much lower concentration or essentially absent (Suppl. materials Figure 73). From this we could conclude that these oxidation products were not generated by autoxidation or ROS, but were products of enzymatic reactions. 8- and 9-HETE were detected only at very low concentrations. However, 11-HETE was detected in the platelet releasates in significant concentrations (Figure 62 and Suppl. materials Figure 73C2). There is not much known about the 11-HETE stereochemistry in human platelets and their releasates. Our data indicate that 11(*R*)-HETE is formed upon platelet activation with thrombin. In a study with cultured bovine coronary artery endothelial cells it was reported previously that 11(*R*)-HETE is probably derived from cyclooxygenase [195]. This could explain the different stereochemistry with respect to 12-LOX but was not discussed hitherto for releasates from thrombin-activated platelets.

3.3.7.5. 15-HETE

The enantioselective analysis of 15-HETE in thrombin-activated releasates showed the presence of both enantiomers with a slight excess of the *S*-enantiomer (Suppl. materials Figure 73D2). In the work cited above on bovine coronary artery endothelial cells 15(S)-HETE was found predominantly formed by 15-LOX [195]. Platelets reportedly do not express 15-LOX or 5-LOX but have 12-LOX. Although we did not observe any autoxidation in our platelet samples throughout this work, lipid peroxidation is detected in activated platelets [191] which could account for the presence of 15-HETE. However, in this case a racemic mixture was expected. Previous studies have also detected these 15-

HETE enantiomers in whole blood in a similar enantiomeric ratio [157]. Thus, we hypothesize that the enantiomers of 15-HETE are formed through enzymatic contribution from either COX [196] or Cytochrome P450 [197] as reported previously. Further experimental studies are required to validate the exact source and mode of 15-HETE formation in platelets.

3.3.7.6. 9-HODE and 13-HODE

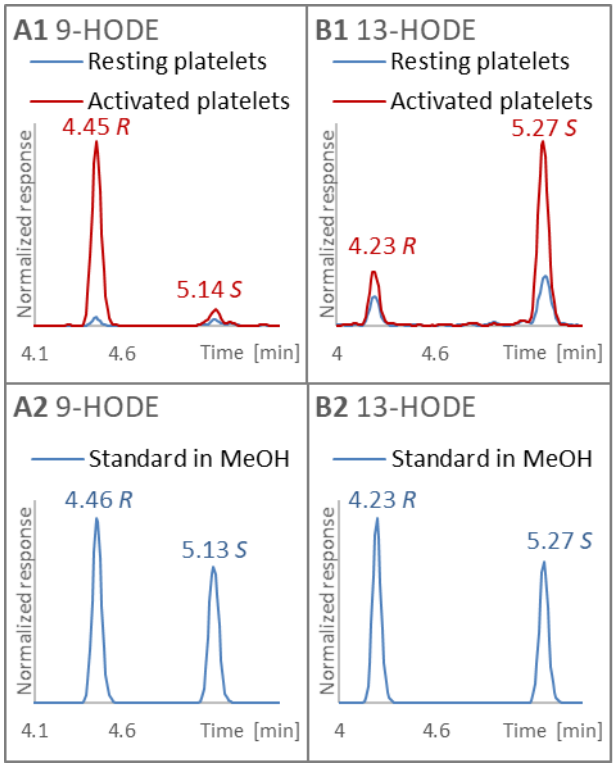

***Figure 66**. Stereoselectivity of 9- and 13-HODE formed upon platelet activation by thrombin as analysed in releasates and compared to resting platelets (**A1** and **B1**); and separation of 9- and 13-HODE enantiomers in racemic standard solution (**A2** and **B2**). Analysed with the final method.*

9- and 13-HODE are the oxidation products of LA. They show some peculiar stereochemistries. In releasates from thrombin-activated platelets, the *R*-enantiomer prevails for 9-HODE while the *S*-enantiomer is present in excess for 13-HODE. Little is known about the stereochemical preference of 9- and 13-HODE in platelets and their releasates. However, a few studies have investigated the stereochemical preference of LA biotransformation by 12-LOX. In a recent work, linoleic acid metabolism by intestinal

tissues of Min mice, an animal model for intestinal neoplasia, showed that LA was converted to an equal mixture of 9(*S*)- and 13(*S*)-HODE [198]. In another study, positional isomer selectivity and stereoselectivity of HODE oxidation by mouse 12(*S*)-lipoxygenase isoenzymes was investigated [199]. For 13-HODE mainly *S*-enantiomers were formed. For 9-HODE platelet- and epidermis-type isoenzymes generated the *R*-enantiomer while leukocyte-type 12(*S*)- lipoxygenase yielded the *S*-enantiomer. Our findings (Figure 66) agree well with the results of the platelet type isoenzymes of this study.

3.3.7.7. 14-HDoHE

10-, 14-, and 17-HDoHE are metabolites of DHA oxidation and were included in our stereoselective assay. 17-HDoHE was not detected at all and 10-HDoHE was detected below LOQ in activated platelet supernatants. However, 14-HDoHE was present in significant amounts in platelet supernatants and only the *S*-enantiomer was found (Suppl. materials Figure 73E2). Interestingly, the levels in releasates from non-activated resting platelets were essentially the same as in thrombin-activated platelets. Yet, it must be emphasized that this fact cannot be attributed to autoxidation because of the finding that only the *S*-enantiomer was present indicative of an enzymatic process. If autoxidation was the reason for 14-HDoHE, also other HDoHE isomers would have been formed and the racemic mixture would have been obtained for all of them.

3.4.Conclusions

Enantioselective UHPLC-ESI-MS/MS based on sub-2 μm particle- based polysaccharide CSPs using reversed-phase elution conditions was used for the first time to develop a highly selective and sensitive assay for analysing enantiomers and diastereoisomers of different types of oxylipins in platelet samples and autoxidized PUFAs. Autoxidation of PUFAs yielded racemic mixtures, as expected and provided reference samples of both enantiomers and regioisomers for method development. For several analytes the enantiomer elution order could be determined and seems to be preferentially *R*- before *S*-enantiomer on Chiralpak IA-U. The new method was finally utilized for enantioselective analysis of releasates from resting and thrombin-activated human platelets. In the majority of the cases,

single enantiomers of oxylipins were produced in thrombin-activated platelet samples by enzymatic oxidation, e.g. 12(*S*)-configuration in case of 12-LOX products (12(*S*)- HETE and 12-(*S*)-HEPE). Other oxylipins had *R*-configurations such as 11(*R*)-HETE. In several cases, both enantiomers were present, although not as racemic (50:50) mixtures. In any case, for a meaningful biological interpretation of oxylipin formation, enantioselective assays are indispensable and currently employed Chiralpak IA-U column has the performance to set the state-of-art in this field.

CRediT authorship contribution statement

Malgorzata Cebo: Investigation, Methodology, Formal analysis, Data curation, Visualization, Writing - original draft, Writing - review & editing. **Xiaoqing Fu**: Investigation, Data curation, Writing - review & editing. **Meinrad Gawaz**: Writing - review & editing, Funding acquisition. **Madhumita Chatterjee**: Investigation, Writing - review & editing, Funding acquisition. **Michael Lämmerhofer**: Conceptualization, Methodology, Supervision, Writing - review & editing, Resources, Funding acquisition.

Declaration of conflict of interests

The authors declare no conflict of interests.

Acknowledgements

This project was funded by the Deutsche Forschungsgemein- schaft (DFG, German Research Foundation) –Project number 374031971 –TRR 240. We would like to acknowledge support by the master students of the Univeristy of Tuebingen, Master in Phar- maceutical Sciences & Technologies, Florian Stahl, Jiayue Xu and Anita Bär.

3.5.Supplementary materials

3.5.1. Structures and names of standards and internal standards used in this study

3.5.1.1.Compounds in Mix A and Mix

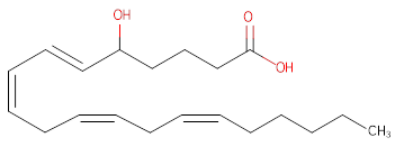

(±)5-HETE
5-hydroxy-6E,8Z,11Z,14Z-eicosatetraenoic acid

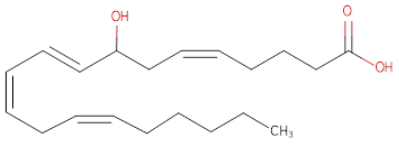

(±)8-HETE
8-hydroxy-5Z,9E,11Z,14Z-eicosatetraenoic acid

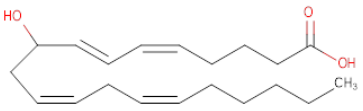

(±)9-HETE
9-hydroxy-5Z,7E,11Z,14Z-eicosatetraenoic acid

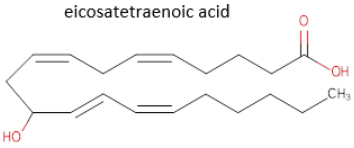

(±)11-HETE
11-hydroxy-5Z,8Z,12E,14Z-eicosatetraenoic acid

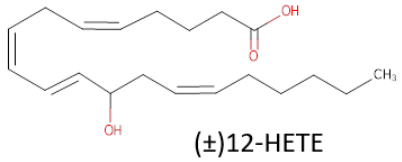

(±)12-HETE
12-hydroxy-5Z,8Z,10E,14Z-eicosatetraenoic acid

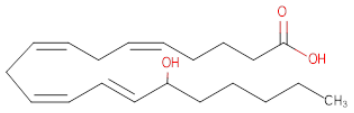

(±)15-HETE
15-hydroxy-5Z,8Z,11Z,13E-eicosatetraenoic acid

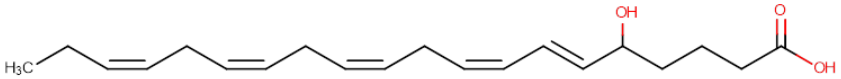

(±)5-HEPE
5-hydroxy-6E,8Z,11Z,14Z,17Z-eicosapentaenoic acid

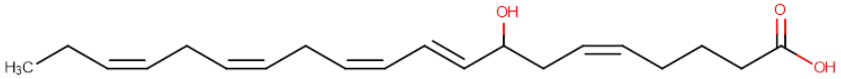

(±)8-HEPE
8-hydroxy-5Z,9E,11Z,14Z,17Z-eicosapentaenoic acid

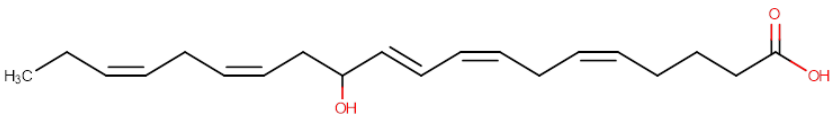

(±)12-HEPE
12-hydroxy-5Z,8Z,10E,14Z,17Z-eicosapentaenoic acid

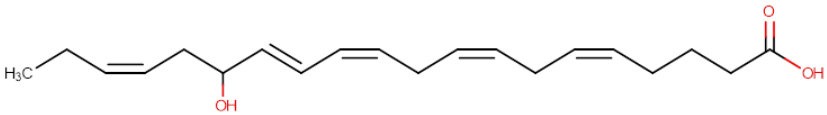

(±)15-HEPE
15-hydroxy-5Z,8Z,11Z,13E,17Z-eicosapentaenoic acid

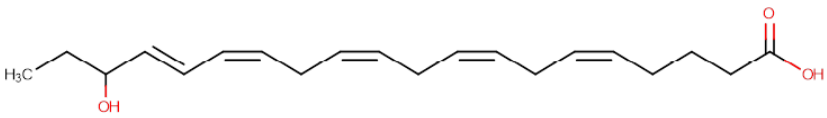

(±)18-HEPE
18-hydroxy-5Z,8Z,11Z,14Z,16E-eicosapentaenoic acid

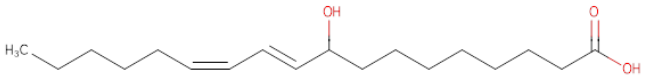

(±) 9-HODE
9-hydroxy-10E,12Z-octadecadienoic acid

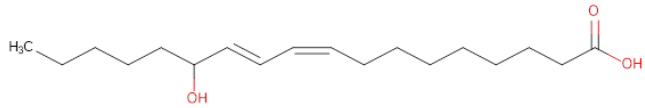

(±) 13-HODE
13-hydroxy-9Z,11E-octadecadienoic acid

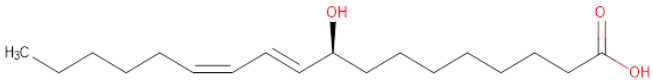

9(*S*)-HODE
9-hydroxy-10E,12Z-octadecadienoic acid

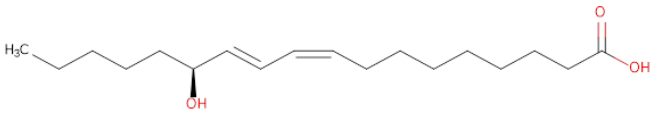

13(*S*)-HODE
13-hydroxy-9Z,11E-octadecadienoic acid

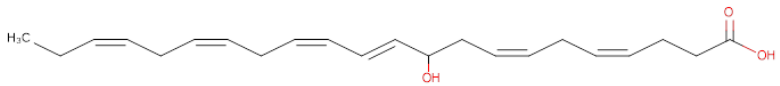

(±)10-HDoHE
10-hydroxy-4Z,7Z,11E,13Z,16Z,19Z-docosahexaenoic acid

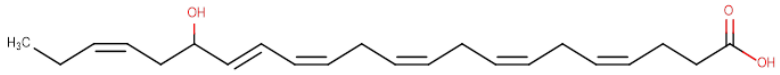

(±)17-HDoHE
17-hydroxy-4Z,7Z,10Z,13Z,15E,19Z-docosahexaenoic acid

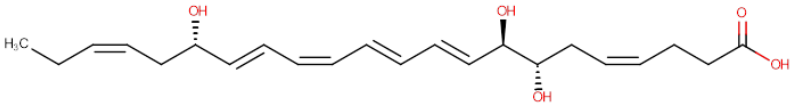

RvD1
Resolvin D1
7S,8R,17S-trihydroxy-4Z,9E,11E,13Z,15E,19Z-docosahexaenoic acid

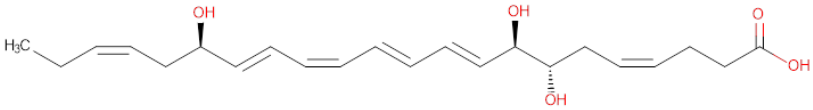

17(*R*)-RvD1
17(R)-Resolvin D1
7S,8R,17R-trihydroxy-4Z,9E,11E,13Z,15E,19Z-docosahexaenoic acid

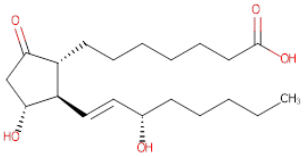

PGE1
Prostaglandin E1
9-oxo-11*R*,15*S*-dihydroxy-13E-prostaenoic acid

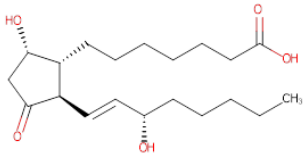

PGD1
Prostaglandin D1
9*S*,15*S*-dihydroxy-11-oxo-13E-prostaenoic acid

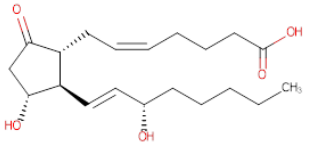

PGE2
Prostaglandin E2
9-oxo-11*R*,15*S*-dihydroxy-5Z,13E-prostadienoic acid

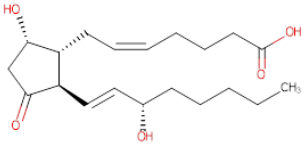

PGD2
Prostaglandin D2
9*S*,15*S*-dihydroxy-11-oxo-5Z,13E-prostadienoic acid

3.5.1.2.PUFAs used for autoxidation

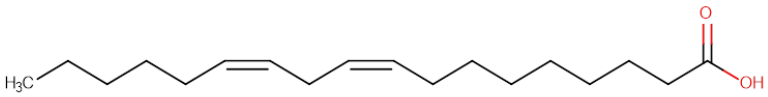

Linoleic acid (LA)
9Z,12Z-octadecadienoic acid

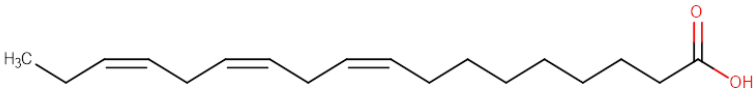

α-Linolenic acid (ALA)
9Z,12Z,15Z-octadecatrienoic acid

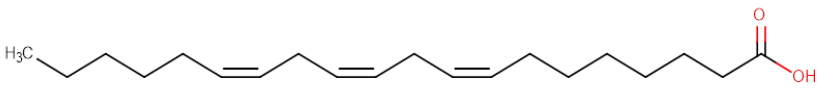

Dihomo-γ-linolenic acid (DGLA)
8Z,11Z,14Z-eicosatrienoic acid

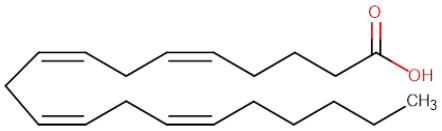

Arachidonic acid (AA)
5Z,8Z,11Z,14Z-eicosatetraenoic acid

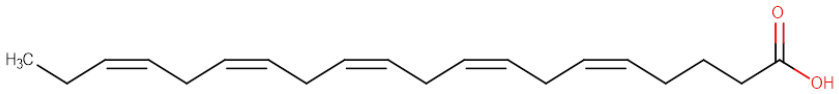

5Z,8Z,11Z,14Z,17Z-eicosapentaenoic acid (EPA)

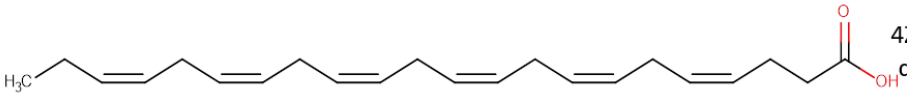

4Z,7Z,10Z,13Z,16Z,19Z-docosahexaenoic acid (DHA)

3.5.1.3.Additional oxylipins in the extended set

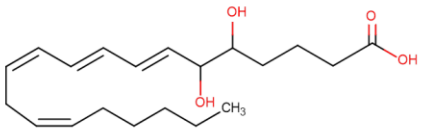

(±)5,6-DiHETE
cis-5,6-dihydroxy-7E,9E,11Z,14Z-eicosatetraenoic acid

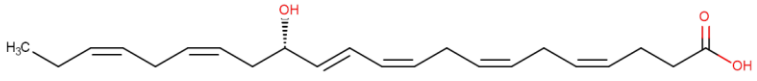

14(*S*)-HDoHE
14*S*-hydroxy-4Z,7Z,10Z,12E,16Z,19Z-docosahexaenoic acid

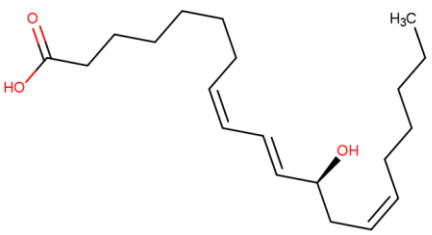

12(*S*)-HETrE
12*S*-hydroxy-5Z,8Z,12Z-eicosatrienoic acid

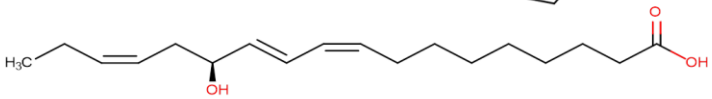

13(*S*)-HOTrE
13*S*-hydroxy-9Z,11E,15Z-octadecatrienoic acid

3.5.1.4.IS used in platelet releasate analysis

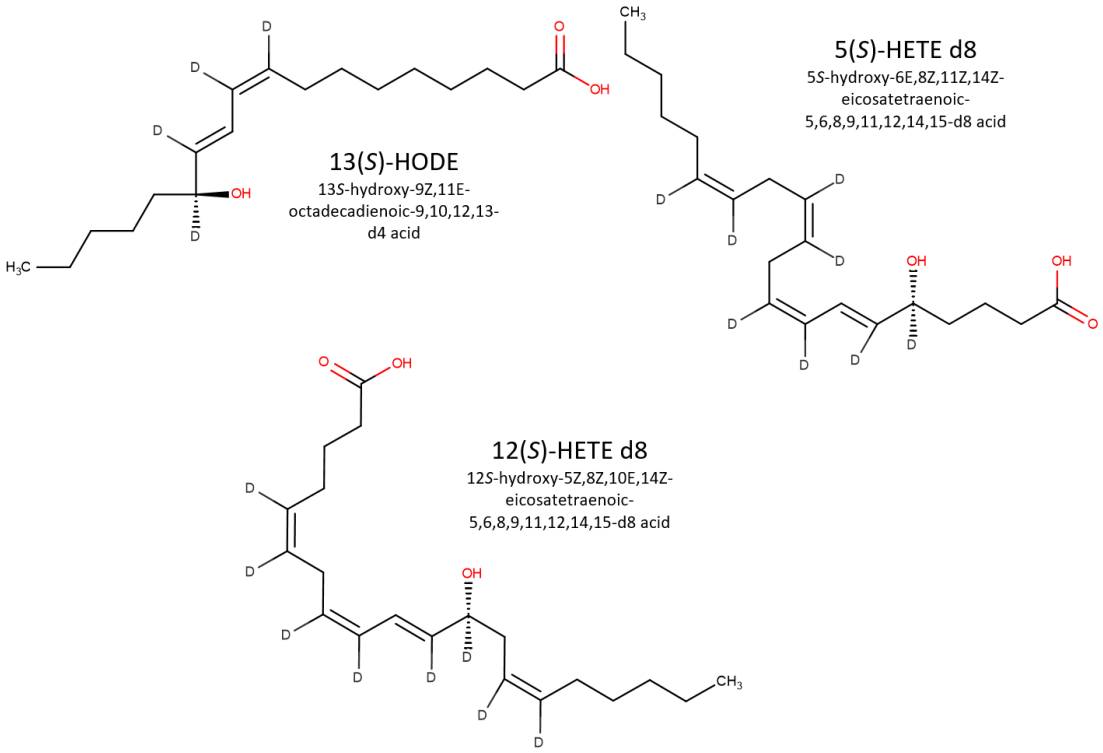

3.5.2. Sample preparation

3.5.2.1.Autoxidation of polyunsaturated fatty acids

Linoleic acid (LA), α-linolenic acid (ALA), dihomo-γ-linolenic acid (DGLA), arachidonic acid (AA), eicosapentaenoic acid (EPA) and docosahexaenoic acid (DHA) were separately autoxidized on air. For this purpose, stock solutions of each fatty acid was prepared with the concentration 100 µg/mL of each PUFA in MeOH. The stock solutions were aliquoted to 3-times 10 µL into 3 Eppendorf tubes for each acid. The aliquots were dried in a GeneVac EZ-2 (Ipswich, UK) evaporator and then left opened and exposed to air for oxidation. After certain time points (18 h, 24 h and 48 h), the samples were dissolved in 100 µL MeOH, briefly purged with nitrogen and placed in -20°C until LC-MS/MS analysis. A negative control was prepared as MeOH placed in Eppendorf and kept at room temperature for the same time length as the samples. No interferences were found in the negative control.

Calibration samples were prepared as mixed solutions of analytes dissolved in MeOH. The calibrants ranged from 0.5 to 50 ng/mL (for single enantiomers 14(*S*)-HDoHE, 12(*S*)-HETrE and 13(*S*)-HOTrE the concentration was twice higher in each calibration sample). Quality control (QC) samples were prepared in the same way as the calibrants, at 2 concentration levels: 2.5 ng/mL and 12.5 ng/mL (the concentration of 14(*S*)-HDoHE, 12(*S*)-HETrE and 13(*S*)-HOTrE was also twice higher in QCs). Peak area was used as measurement of compound response. A weighting of $1/x^2$ was applied for establishing the calibration curve.

3.5.2.2.Extraction of oxylipins from platelet releasate

Blood from 3 healthy donors was collected and platelets were isolated as described previously in [158] of the main document. Platelets were suspended in PBS buffer supplemented with calcium. Each sample was then aliquoted into two 3 x 10^8 platelet aliquots. One aliquot from each donor was treated with 0.1 U mL^{-1} of thrombin for 15 min at room temperature, which triggered platelet activation. The other aliquot was left untreated under resting condition for comparison; it is designated as resting platelets in this work. Next, platelets were centrifuged in microcentrifuge tubes (550 x g, 5 min at 4°C) and the supernatants were separated from the resting and thrombin-activated platelet pellets. In these study, the supernatant was used for oxylipin analysis.

An aliquot of 50 µL from each sample was taken for extraction; this amount corresponded to a releasate from around 3 x 10^7 platelets. Next, 500 µL of 1 M sodium acetate buffer adjusted to pH 6 with acetic acid (dissolved in water/MeOH; 95:5, v/v) was added to each sample. Then, 10 µL of a 20 ng/mL solution of antioxidant BHT in MeOH was pipetted to the samples and 12.5 µL of a mixed stock solution containing 3 internal standards (5(*S*)-HETE-d8, 12(*S*)-HETE-d8 and 13(*S*)-HODE-d4) in MeOH was added (concentration of each component in the stock solution was equal to 100 ng/mL).

At the same time, matrix-matched calibrants and QCs were prepared from pooled resting platelet supernatants. The pooled supernatant was aliquoted at 50 µL. The 1 M sodium acetate buffer (500 mL, prepared as specified above), BHT solution (10 µL, 20 ng/mL) and stock solution of internal standards (12.5 µL, 100 ng/mL) were added to each sample,

similarly as described in the previous paragraph. Then, different volumes of stock solution of oxylipin standards were spiked into these solutions to obtain final calibrants from 0.5 ng/mL to 50 ng/mL and 2 QCs at levels 2.5 ng/mL and 12.5 ng/mL (14(*S*)-HDoHE, 12(*S*)-HETrE and 13(*S*)-HDoHE were 2 times higher concentrated).

All the samples, calibrants and QCs were then treated in the same way: they were first vortexed for 6 s, then centrifuged (16,100 x g, 5 min, 4°C) and the supernatant was placed on pre-conditioned Bond Elute Certify II (3 mL / 200 mg) (Agilent, Waldbronn, Germany) solid phase extraction cartridges. Pre-conditioning was done in 3 steps: first with 1 mL of a mixture ethyl acetate/n-hexane/HAc (75:24:1; v/v/v), then with 2 mL of MeOH, and the last step was 2 mL 1 M sodium acetate buffer (prepared as specified above) pH 6. Then, loaded samples were washed twice with 2 mL H_2O/MeOH (4:1; v/v). Next, the cartridges were dried for 5 min, falcon tubes were exchanged and the extract was eluted with 2 mL of ethyl acetate/n-hexane/HAc (75:24:1; v/v/v). Samples were dried with GeneVac EZ-2 (under nitrogen atmosphere). The residues were dissolved with 50 µL of MeOH and immediately analysed by LC-MS/MS.

3.5.3. Screening methods

Polysaccharide CSPs can be used in different elution conditions, viz. normal-phase, polar organic, reversed-phase (RP) and SFC elution conditions. In this work, RP elution conditions were chosen. Two columns, 2 organic solvents used as mobile phase component B and 2 acidic additives were screened for finding a suitable method for separation of isomers of oxylipins. That gave all together 8 different separation conditions.

The results of the column screening with resolution values on Chiralpak IA-U were already discussed in the main document. Table 46 gives corresponding resolution values obtained with Chiralpak IC-U. Figure 68 shows the comparison of separations obtained with MeOH and ACN as organic modifiers on the preferable Chiralpak IA-U column. Table 49 displays sensitivities of methods as signal-to-noise ratio (S/N) with different acid additives (HAc vs. FA). The data for the IA-U column and ACN as organic component in the mobile phase were chosen for this comparison.

Table 46. *Resolution between isomeric peak pairs obtained with different screening methods on Chiralpak IC-U (for corresponding retention times see Table 47).*

Compounds	Column IC-U			
	ACN + HAc	ACN + FA	MeOH + HAc	MeOH + FA
9-HODE	0.50	0.50	0.00	0.00
13-HODE	0.50	0.52	0.00	0.00
5-HETE	0.00	0.00	0.00	0.00
8-HETE	0.00	0.00	0.00	0.00
9-HETE	0.00	0.00	0.00	0.00
11-HETE	0.60	0.59	0.00	0.00
12-HETE	0.00	0.00	0.00	0.00
15-HETE	0.00	0.00	0.00	0.00
5-HEPE	0.00	0.00	0.00	0.00
8-HEPE	0.00	0.00	0.00	0.00
12-HEPE	0.00	0.00	0.00	0.00
15-HEPE	0.00	0.00	0.00	0.00
18-HEPE	0.00	0.00	0.00	0.00
10-HDoDE	0.00	0.00	0.00	0.00
17-HDoDE	0.00	0.00	0.00	0.00
Resolvins D1	0.00	0.00	0.00	0.00
PGD1 and PGE1	3.94	4.10	1.13	1.18
PGD2 and PGE2	3.00	3.04	0.80	0.74

One of the arguments to choose ACN over MeOH as an organic modifier for the mobile phase of the final analytical method was the higher backpressure observed when MeOH was used. The backpressure was higher even though the gradient method always contained high amounts of the organic solvent (90-100% B). Figure 67 compares pressure profiles during gradient runs of the screening methods. If the MeOH method had contained higher amounts of water, the pressure would have been even higher.

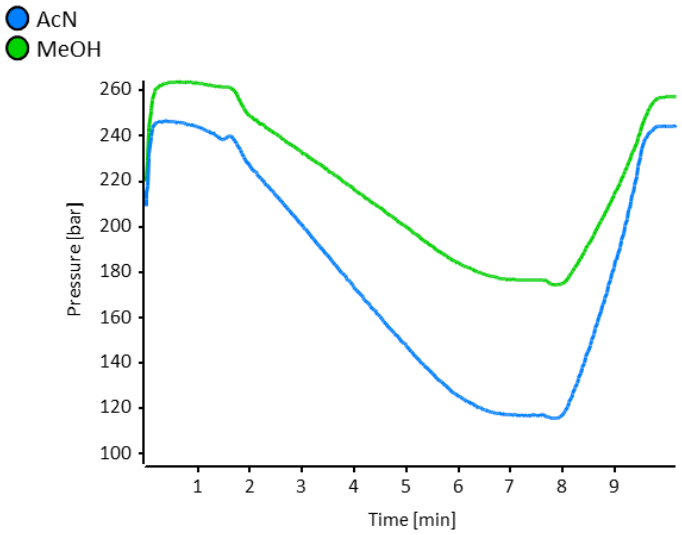

Figure 67. *Comparison of pressure profiles for gradient methods. Injection: 10 µL of MeOH in both cases. Mobile phase ACN or MeOH with 0.1% (v/v) HAc, and methods as described in paragraph 3.2.3.1. of the main document.*

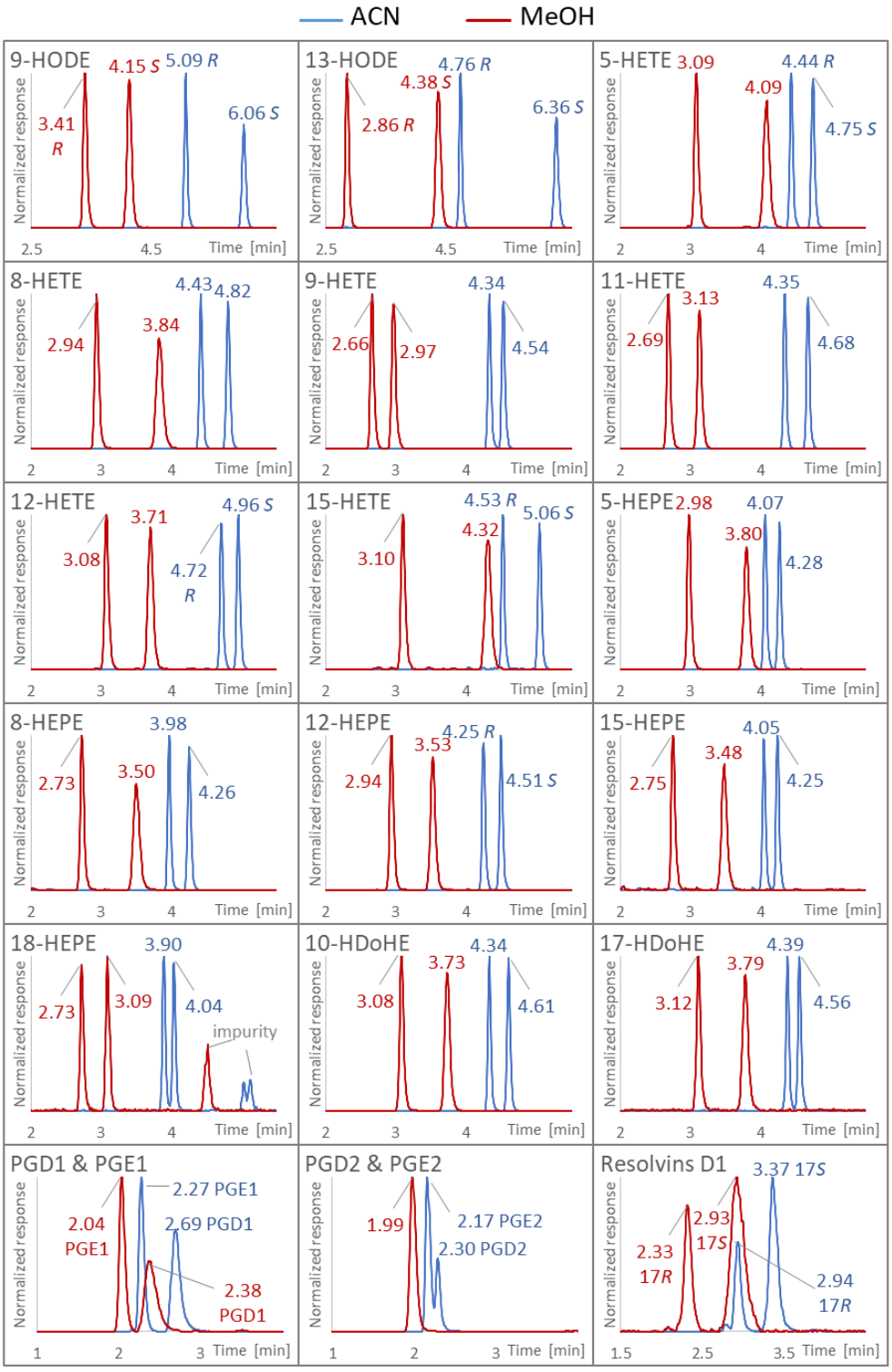

Figure 68. *Comparison of chromatograms obtained with ACN (blue) and MeOH (red). Chromatographic conditions: Column: Chiralpak IA-U, flow rate: 0.3 mL/min; column temperature 25°C; gradient for ACN: A: H_2O+0.1% (v/v) HAc, B: ACN+0.1% (v/v) HAc, 50-95% B in 5 min, 95% B for 2.5 min, 95-50% B in 0.1 min, 50% for 2.4 min; gradient for MeOH: A: H_2O+0.1% (v/v) HAc, B: MeOH+0.1% (v/v) HAc, 90-100% B in 5 min, 100% B for 2.5 min, 100-90% B in 0.1 min, 90% for 2.4 min.*

Table 47. *Retention times [min] of analytes obtained with screening methods.*

Compounds	Column IA-U				Column IC-U			
	ACN + HAc	ACN + FA	MeOH + HAc	MeOH + FA	ACN + HAc	ACN + FA	MeOH + HAc	MeOH + FA
9(*R*)-HODE	5.09	5.12	3.41	3.37	3.97	3.97	2.29	2.28
9(*S*)-HODE	6.06	6.10	4.15	4.11	4.01	4.01	2.29	2.28
13(*R*)-HODE	4.76	4.78	2.86	2.83	3.96	3.96	2.28	2.27
13(*S*)-HODE	6.36	6.39	4.38	4.34	4.00	4.01	2.28	2.27
5(*R*)-HETE	4.44	4.46	3.09	3.06	3.74	3.74	2.20	2.19
5(*S*)-HETE	4.75	4.78	4.09	4.04	3.74	3.74	2.20	2.19
8-HETE peak 1	4.43	4.45	2.94	2.91	3.74	3.74	2.18	2.17
8-HETE peak 2	4.82	4.84	3.84	3.77	3.74	3.74	2.18	2.17
9-HETE peak 1	4.34	4.36	2.66	2.66	3.76	3.75	2.17	2.18
9-HETE peak 2	4.54	4.56	2.97	2.96	3.76	3.75	2.17	2.18
11-HETE peak 1	4.35	4.37	2.69	2.67	3.80	3.80	2.20	2.20
11-HETE peak 2	4.68	4.71	3.13	3.10	3.85	3.85	2.20	2.20
12(*R*)-HETE	4.72	4.75	3.08	3.05	3.85	3.85	2.20	2.19
12(*S*)-HETE	4.96	4.99	3.71	3.66	3.85	3.85	2.20	2.19
15(*R*)-HETE	4.53	4.55	3.10	3.07	3.77	3.78	2.19	2.19
15(*S*)-HETE	5.06	5.08	4.32	4.26	3.77	3.78	2.19	2.19
5-HEPE peak 1	4.07	4.09	2.98	2.95	3.44	3.45	2.13	2.13
5-HEPE peak 2	4.28	4.30	3.80	3.76	3.44	3.45	2.13	2.13
8-HEPE peak 1	3.98	4.00	2.73	2.72	3.43	3.42	2.11	2.11
8-HEPE peak 2	4.26	4.29	3.50	3.47	3.43	3.42	2.11	2.11
12(*R*)-HEPE	4.25	4.27	2.94	2.92	3.53	3.53	2.13	2.12
12(*S*)-HEPE	4.51	4.53	3.53	3.48	3.53	3.53	2.13	2.12
15-HEPE peak 1	4.05	4.07	2.75	2.73	3.47	3.47	2.12	2.11
15-HEPE peak 2	4.25	4.27	3.48	3.43	3.47	3.47	2.12	2.11
18-HEPE peak 1	3.90	3.92	2.73	2.71	3.38	3.39	2.12	2.12
18-HEPE peak 2	4.04	4.06	3.09	3.06	3.38	3.39	2.12	2.12
10-HDoDE peak 1	4.34	4.36	3.08	3.05	3.73	3.73	2.19	2.19
10-HDoDE peak 2	4.61	4.64	3.73	3.68	3.73	3.73	2.19	2.19
17-HDoDE peak 1	4.39	4.41	3.12	3.09	3.71	3.71	2.19	2.18
17-HDoDE peak 2	4.56	4.58	3.79	3.73	3.71	3.71	2.19	2.18
17(*R*)-RvD1	2.94	2.95	2.33	2.32	2.43	2.44	1.84	1.85
RvD1	3.37	3.39	2.93	2.89	2.43	2.44	1.84	1.85
PGE1	2.27	2.28	2.04	2.03	2.33	2.34	2.20	2.17
PGD1	2.69	2.70	2.38	2.37	2.68	2.69	2.31	2.28
PGE2	2.17	2.17	1.99	1.99	2.17	2.18	2.04	2.03
PGD2	2.30	2.30	1.99	1.99	2.45	2.46	2.13	2.11

Table 48. *Peak width at 50% of peak height [min] obtained with screening methods.*

Compounds	Column IA-U				Column IC-U			
	ACN + HAc	ACN + FA	MeOH + HAc	MeOH + FA	ACN + HAc	ACN + FA	MeOH + HAc	MeOH + FA
9(*R*)-HODE	0.053	0.054	0.075	0.070	0.046	0.046	0.076	0.069
9(*S*)-HODE	0.067	0.066	0.084	0.085	0.050	0.050	0.076	0.069
13(*R*)-HODE	0.052	0.052	0.063	0.059	0.043	0.042	0.079	0.076
13(*S*)-HODE	0.075	0.078	0.091	0.092	0.052	0.053	0.079	0.076
5(*R*)-HETE	0.050	0.050	0.064	0.064	0.062	0.060	0.061	0.057
5(*S*)-HETE	0.053	0.054	0.094	0.091	0.062	0.060	0.061	0.057
8-HETE p1	0.050	0.050	0.064	0.061	0.073	0.073	0.060	0.060
8-HETE p2	0.055	0.055	0.102	0.098	0.073	0.073	0.060	0.060
9-HETE p1	0.049	0.047	0.055	0.056	0.048	0.047	0.052	0.054
9-HETE p2	0.051	0.047	0.065	0.065	0.048	0.047	0.052	0.054
11-HETE p1	0.047	0.047	0.057	0.055	0.051	0.052	0.072	0.070
11-HETE p2	0.049	0.051	0.068	0.067	0.052	0.052	0.072	0.070
12(*R*)-HETE	0.051	0.050	0.066	0.065	0.052	0.052	0.059	0.058
12(*S*)-HETE	0.053	0.052	0.083	0.083	0.052	0.052	0.059	0.058
15(*R*)-HETE	0.048	0.047	0.066	0.065	0.055	0.050	0.058	0.059
15(*S*)-HETE	0.056	0.053	0.098	0.093	0.055	0.050	0.058	0.059
5-HEPE p1	0.050	0.048	0.061	0.061	0.054	0.056	0.056	0.055
5-HEPE p2	0.050	0.050	0.087	0.086	0.054	0.056	0.056	0.055
8-HEPE p1	0.048	0.048	0.059	0.058	0.062	0.066	0.060	0.062
8-HEPE p2	0.053	0.051	0.099	0.097	0.062	0.066	0.060	0.062
12(*R*)-HEPE	0.051	0.049	0.062	0.061	0.048	0.048	0.057	0.054
12(*S*)-HEPE	0.050	0.050	0.078	0.077	0.048	0.048	0.057	0.054
15-HEPE p1	0.049	0.046	0.061	0.060	0.063	0.060	0.053	0.058
15-HEPE p2	0.049	0.049	0.085	0.084	0.063	0.060	0.053	0.058
18-HEPE p1	0.046	0.045	0.056	0.057	0.056	0.057	0.057	0.055
18-HEPE p2	0.049	0.044	0.060	0.064	0.056	0.057	0.057	0.055
10-HDoDE p1	0.048	0.046	0.063	0.061	0.069	0.068	0.061	0.059
10-HDoDE p2	0.051	0.048	0.082	0.078	0.069	0.068	0.061	0.059
17-HDoDE p1	0.049	0.048	0.063	0.063	0.064	0.065	0.056	0.052
17-HDoDE p2	0.049	0.049	0.087	0.085	0.064	0.065	0.056	0.052
17(*R*)-RvD1	0.081	0.084	0.096	0.095	0.064	0.057	0.281	0.271
RvD1	0.117	0.113	0.176	0.171	0.064	0.057	0.281	0.271
PGE1	0.067	0.068	0.074	0.072	0.053	0.051	0.058	0.054
PGD1	0.118	0.114	0.164	0.156	0.053	0.051	0.057	0.056
PGE2	0.066	0.066	0.081	0.080	0.054	0.053	0.064	0.070
PGD2	0.065	0.065	0.081	0.080	0.055	0.054	0.074	0.072

Table 49. *Comparison of S/N ratio obtained with HAc and FA as acid additives for 3 different concentrations of analytes: 10 ng/mL, 1 ng/mL and 0.1 ng/mL. Chromatographic conditions: column: IA-U, flow rate: 3 mL/min; column temperature 25°C; A: H_2O+0.1% (v/v) acid, B: ACN+0.1% (v/v) acid, 50-95% B in 5 min, 95% B for 2.5 min, 95-50% B in 0.1 min, 50% for 2.4 min.*

Concentration [ng/mL]:	10		1		0.1	
Compound	HAc	FA	HAc	FA	HAc	FA
9(*R*)-HODE	297.0	297.0	42.5	21.3	4.3	6.5
9(*S*)-HODE	566.1	327.5	52.7	21.3	6.8	6.5
13(*R*)-HODE	105.6	96.8	25.7	23.1	7.3	5.3
13(*S*)-HODE	325.0	129.7	34.4	28.4	10.3	4.5
5(*S*)-HETE	311.7	311.7	65.0	65.0	13.0	4.3
5(*R*)-HETE	721.2	357.0	133.5	71.0	28.0	6.7
8-HETE p1	293.7	176.2	30.0	120.0	4.3	8.5
8-HETE p2	681.3	197.6	56.4	160.0	6.8	6.0
9-HETE p1	370.3	309.7	64.5	62.0	8.8	6.0
9-HETE p2	878.9	350.3	117.4	72.0	19.2	6.2
11-HETE p1	276.0	193.2	138.0	69.0	13.5	13.5
11-HETE p2	619.2	206.1	255.5	73.3	29.5	15.5
12(*R*)-HETE	765.0	765.0	60.0	40.0	10.0	2.0
12(*S*)-HETE	1849.7	875.0	108.5	38.7	26.0	1.8
15(*R*)-HETE	205.0	102.5	29.5	16.0	3.0	1.5
15(*S*)-HETE	523.0	116.0	33.0	17.0	5.5	1.3
5-HEPE p1	124.0	93.0	17.7	26.5	4.3	7.0
5-HEPE p2	342.1	102.8	32.0	29.0	4.7	11.0
8-HEPE p1	86.2	101.0	21.3	39.5	7.1	5.3
8-HEPE p2	215.4	110.9	40.5	44.4	10.1	7.5
12(*R*)-HEPE	113.4	189.0	40.0	80.0	14.0	7.5
12(*S*)-HEPE	252.4	206.7	81.5	92.0	20.0	10.0
15-HEPE p1	21.2	20.9	6.2	12.1	3.0	1.5
15-HEPE p2	51.6	23.1	8.1	12.3	5.5	1.5
18-HEP p1E	21.0	12.0	2.5	1.7	1.0	1.5
18-HEPE p2	28.0	12.0	4.5	2.0	1.5	0.5
10-HDoHE p1	746.0	149.2	89.5	46.0	3.3	5.0
10-HDoHE p2	1690.6	165.8	91.5	51.5	9.0	10.0
17-HDoHE p1	38.1	54.2	2.5	8.2	0.6	1.7
17-HDoHE p2	94.6	63.3	4.8	7.0	1.4	1.8
RvD1	12.9	15.2	2.5	4.2	1.6	1.2
17(*R*)-RvD1	31.8	19.3	4.2	3.7	1.9	0.8

3.5.4. MS method for extended set of oxylipins

All the SRMs used for analysis are shown in Table 50.

Table 50. *SRMs for extended set of analytes. The ion transitions with precursor ion selection in quadrupole 1 (Q1 m/z) and chosen fragment ion (product ion) (Q3 m/z) as well as collision energy (CE) and declustering potential (DP) for each compound are shown.*

Name	Q1 *m/z*	Q3 *m/z*	CE [V]	DP [V]
10-HDoHE	343.1	153.0	-20	-70
14-HDoHE	343.1	205.0	-18	-60
17-HDoHE	343.1	201.0	-20	-80
5-HETE	319.1	114.9	-18	-80
8-HETE	319.1	154.9	-20	-75
9-HETE	319.1	151.0	-21	-40
11-HETE	319.1	167.0	-22	-75
12-HETE	319.1	208.0	-21	-80
15-HETE	319.1	219.0	-17	-40
5-HEPE	317.1	114.9	-20	-75
8-HEPE	317.1	154.8	-20	-70
12-HEPE	317.1	179.0	-18	-75
15-HEPE	317.1	219.0	-18	-95
18-HEPE	317.1	215.1	-18	-65
5,6-DiHETE	335.1	144.9	-22	-20
9-HODE	295.2	171.0	-25	-80
13-HODE	295.2	195.0	-26	-80
RvD1	375.1	121.1	-35	-80
12-HETrE	321.4	181.0	-24	-40
13-HOTrE	293.0	224.0	-18	-40
12-HETE-d8	327.3	184.0	-20	-80
13-HODE-d4	299.1	198.0	-24	-90
5-HETE-d8	327.1	115.9	-18	-50

3.5.5. Autoxidation of PUFAs

3.5.5.1.Results of autoxidation of PUFAs

Table 51 shows detailed results of autoxidation of PUFAs. Limit of detection (LOD), lower limit of quantification (LOQ) and upper limit of quantification (ULOQ) are summarized together with oxylipin amount observed at each time point of PUFA oxidation.

Table 51. *Results of PUFA autoxidation.*

		Amount from 1 µg of PUFA [pg]					
		Limits			Oxidation time [h]		
Corresponding PUFA	Compound	LOD	LOQ	ULOQ	18	24	48
LA	9(*R*)-HODE	25	50	5000	920 ± 220	945 ± 225	881 ± 210
	9(*S*)-HODE	25	50	5000	N/A	N/A	N/A
	13(*R*)-HODE	25	50	5000	1020 ± 110	1018 ± 110	1038 ± 110
	13(*S*)-HODE	25	50	5000	N/A	N/A	N/A
AA	5(*S*)-HETE	5.0	50	5000	< LOQ	321 ± 25	< LOD
	5(*R*)-HETE	5.0	50	5000	< LOQ	325 ± 35	< LOD
	8-HETE p1	25	50	5000	< LOD	211 ± 20	< LOD
	8-HETE p2	25	50	5000	< LOD	227 ± 25	< LOD
	9-HETE p1	25	50	5000	< LOQ	312 ± 30	< LOD
	9-HETE p2	25	50	5000	< LOQ	332 ± 45	< LOD
	11-HETE p1	2.5	50	5000	< LOQ	290 ± 35	< LOQ
	11-HETE p2	2.5	50	5000	< LOQ	291 ± 40	< LOQ
	12(*R*)-HETE	25	50	5000	< LOD	240 ± 20	< LOD
	12(*S*)-HETE	25	50	5000	< LOD	220 ± 15	< LOD
	15(*R*)-HETE	25	50	5000	55 ± 2	530 ± 50	< LOQ
	15(*S*)-HETE	25	50	5000	55 ± 3	500 ± 35	< LOQ
EPA	5-HEPE p1	25	50	5000	< LOD	< LOQ	< LOD
	5-HEPE p2	25	50	5000	< LOD	< LOQ	< LOD
	8-HEPE p1	25	50	5000	< LOD	< LOQ	< LOD
	8-HEPE p2	25	50	5000	< LOD	< LOQ	< LOD
	12(*R*)-HEPE	25	50	5000	< LOQ	< LOQ	< LOD
	12(*S*)-HEPE	25	50	5000	< LOQ	< LOQ	< LOD
	15-HEPE p1	25	50	5000	< LOD	< LOQ	< LOD
	15-HEPE p2	25	50	5000	< LOD	< LOQ	< LOD
	18-HEPE p1	50	250	5000	< LOD	< LOQ	< LOD
	18-HEPE p2	50	250	5000	< LOD	< LOQ	< LOD
DHA	10-HDoHE p1	5.0	50	5000	< LOQ	< LOQ	< LOQ
	10-HDoHE p2	5.0	50	5000	< LOQ	< LOQ	< LOQ
	17-HDoHE p1	50	250	5000	< LOD	< LOD	< LOD
	17-HDoHE p2	50	250	5000	< LOD	< LOD	< LOD
	RvD1	50	250	5000	< LOD	< LOD	< LOD
	17(*R*)-RvD1	50	250	5000	< LOD	< LOD	< LOD
ALA	13(*R*)-HOTrE	10	100	10000	331 ± 90	243 ± 65	148 ± 40
	13(*S*)-HOTrE	10	100	10000	331 ± 90	243 ± 65	148 ± 40
DGLA	12(*R*)-HETrE	10	100	10000	< LOQ	102 ± 40	< LOD
	12(*S*)-HETrE	10	100	10000	< LOQ	102 ± 40	< LOD
DHA	14(*R*)-HDoHE	10	100	10000	< LOQ	< LOQ	< LOQ
	14(*S*)-HDoHE	10	100	10000	< LOQ	< LOQ	< LOQ
EPA	5,6-DiHETE p1	100	500	5000	< LOD	< LOD	< LOD
	5,6-DiHETE p2	100	500	5000	< LOD	< LOD	< LOD

Corresponding PUFA	Compound	Oxidation time [h] 18	24	48
LA	9-HODE			
	13-HODE			
AA	5-HETE			
	8-HETE			
	9-HETE			
	11-HETE			
	12-HETE			
	15-HETE			
EPA	5-HEPE			
	8-HEPE			
	12-HEPE			
	15-HEPE			
	18-HEPE			
	5,6-DiHETE			
DHA	10-HDoHE			
	14-HDoHE			
	17-HDoHE			
	RvD1			
ALA	13-HOTrE			
DGLA	12-HETrE			

Concentration [pg from 1µg of PUFA]
1000
500
250
< LOQ
< LOD

Figure 69. *Heat map showing abundance of compounds created during PUFAs autoxidation.*

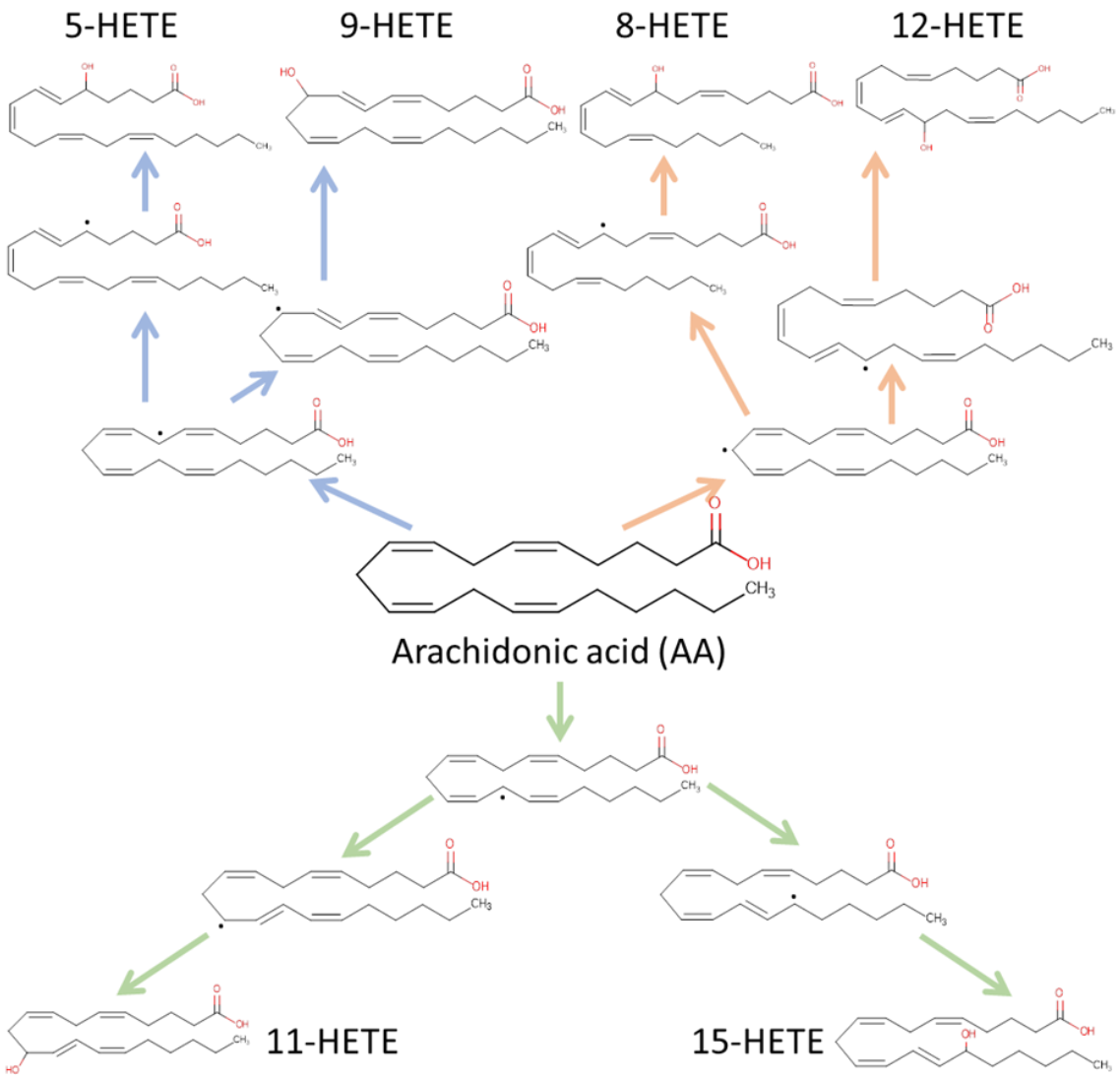

Figure 70*. Scheme of autoxidation of AA to monohydroxy fatty acids.*

3.5.5.2.Interference in 9- and 13-HODE

Potential interferences, which partially co-eluted with 9(*S*)-HODE and 13(*S*)-HODE were detected in oxidized LA. None of these interferences were present in standards and in the extracts from platelet releasates.

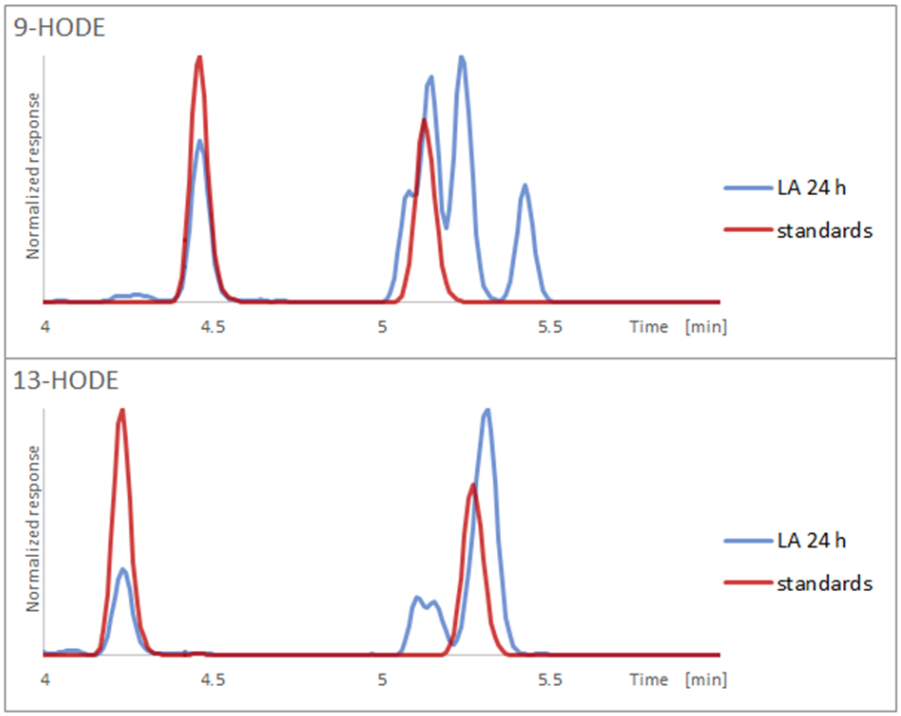

Figure 71. *Extracted ion chromatograms of SRM for 9-HODE (top) and 13-HODE (bottom). Blue line shows the signals in oxidized LA in which potential interferences to the S enantiomers were detected. Red line displays the signals for standard solution.*

3.5.6. Results from the analysis of platelet releasate

Table 52. *Results of platelet releasates.*

	Release [fg/1e6 platelets]								
	Limits			Resting			Thrombin activated		
Compound	LOD	LOQ	ULOQ	Donor 1	Donor 2	Donor 3	Donor 1	Donor 2	Donor 3
9(*R*)-HODE	9	20	1500	32 ± 4	42 ± 6	23 ± 4	163 ± 25	801 ± 120	463 ± 70
9(*S*)-HODE	9	20	1500	90 ± 8	101 ± 9	31 ± 3	115 ± 10	236 ± 21	149 ± 13
13(*R*)-HODE	9	20	1500	58 ± 7	51 ± 6	28 ± 4	59 ± 8	78 ± 10	41 ± 5
13(*S*)-HODE	9	20	1500	123 ± 9	140 ± 9	116 ± 7	137 ± 11	368 ± 25	259 ± 20
5(*S*)-HETE	2	20	1500	< LOD	< LOD	< LOD	< LOD	< LOD	< LOD
5(*R*)-HETE	2	20	1500	< LOD	< LOD	< LOD	< LOD	< LOD	< LOD
8-HETE p1	9	20	1500	< LOD	< LOD	< LOD	< LOQ	< LOQ	< LOQ
8-HETE p2	9	20	1500	< LOD	< LOD	< LOD	< LOD	< LOD	< LOD
9-HETE p1	9	20	1500	< LOD	< LOD	< LOD	< LOQ	58 ± 1	44 ± 1
9-HETE p2	9	20	1500	< LOD	< LOD	< LOD	< LOD	21 ± 1	< LOQ
11-HETE p1	1	20	1500	< LOQ	< LOQ	< LOQ	247 ± 47	1134 ± 215	732 ± 139
11-HETE p2	1	20	1500	< LOQ	< LOQ	< LOQ	< LOQ	25 ± 5	< LOQ
12(*R*)-HETE	9	20	1500	< LOD	< LOD	< LOD	< LOQ	47 ± 3	< LOD
12(*S*)-HETE	9	20	1500	302 ± 12	187 ± 7	1041 ± 41	10,000*	20,000*	10,000*
15(*R*)-HETE	9	20	1500	< LOQ	< LOD	< LOD	78 ± 3	270 ± 13	167 ± 8
15(*S*)-HETE	9	20	1500	< LOQ	< LOQ	< LOD	166 ± 8	484 ± 24	281 ± 14
5-HEPE p1	9	20	1500	< LOD	< LOD	< LOD	< LOD	< LOD	< LOD
5-HEPE p2	9	20	1500	< LOD	< LOD	< LOD	< LOD	< LOD	< LOD
8-HEPE p1	9	20	1500	< LOQ	< LOD	< LOD	< LOD	< LOD	< LOD
8-HEPE p2	9	20	1500	< LOD	< LOD	< LOD	< LOD	< LOD	< LOD
12(*R*)-HEPE	9	20	1500	< LOQ	< LOQ	< LOD	< LOD	< LOD	< LOQ
12(*S*)-HEPE	9	20	1500	136 ± 5	44 ± 2	71 ± 3	643 ± 25	678 ± 27	452 ± 18
15-HEPE p1	9	20	1500	< LOD	< LOD	< LOD	< LOD	< LOD	< LOD
15-HEPE p2	9	20	1500	< LOD	< LOD	< LOD	< LOD	< LOD	< LOD
18-HEPE p1	20	90	1500	< LOD	< LOD	< LOD	< LOD	< LOD	< LOD
18-HEPE p2	20	90	1500	< LOD	< LOD	< LOD	< LOD	< LOD	< LOD
10-HDoHE p1	2	20	1500	< LOQ	< LOQ	< LOQ	< LOQ	< LOQ	< LOQ
10-HDoHE p2	2	20	1500	< LOQ	< LOQ	< LOQ	< LOQ	< LOQ	< LOQ
17-HDoHE p1	20	90	1500	< LOD	< LOD	< LOD	< LOD	< LOD	< LOD
17-HDoHE p2	20	90	1500	< LOD	< LOD	< LOD	< LOD	< LOD	< LOD
RvD1	20	90	1500	< LOD	< LOD	< LOD	< LOD	< LOD	< LOD
17(*R*)-RvD1	20	90	1500	< LOD	< LOD	< LOD	< LOD	< LOD	< LOD
13(*R*)-HOTrE	4	40	3000	< LOD	< LOD	< LOD	< LOD	< LOD	< LOD
13(*S*)-HOTrE	4	40	3000	< LOD	< LOD	< LOD	< LOD	< LOQ	< LOD
12(*R*)-HETrE	4	40	3000	< LOD	< LOD	< LOQ	132 ± 10	277 ± 22	149 ± 11
12(*S*)-HETrE	4	40	3000	< LOQ	< LOQ	88 ± 7	76 ± 6	277 ± 22	165 ± 13
14(*R*)-HDoHE	4	40	3000	< LOD	< LOD	< LOD	< LOD	< LOD	< LOD
14(*S*)-HDoHE	4	40	3000	444 ± 25	157 ± 9	633 ± 35	278 ± 16	483 ± 28	480 ± 28
5,6-DiHETE p1	40	200	1500	< LOD	< LOD	< LOD	< LOD	< LOD	< LOD
5,6-DiHETE p2	40	200	1500	< LOD	< LOD	< LOD	< LOD	< LOD	< LOD

* estimated value

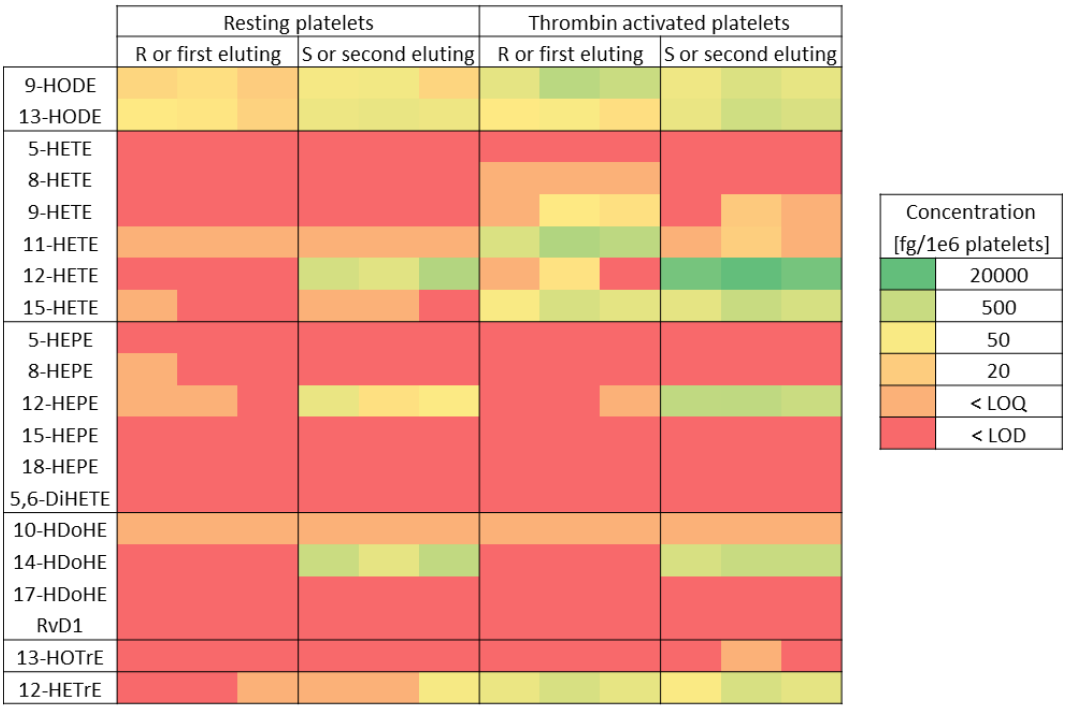

Figure 72. *Heat map showing release of oxylipins from platelets in resting and activated states, logarithmic scale.*

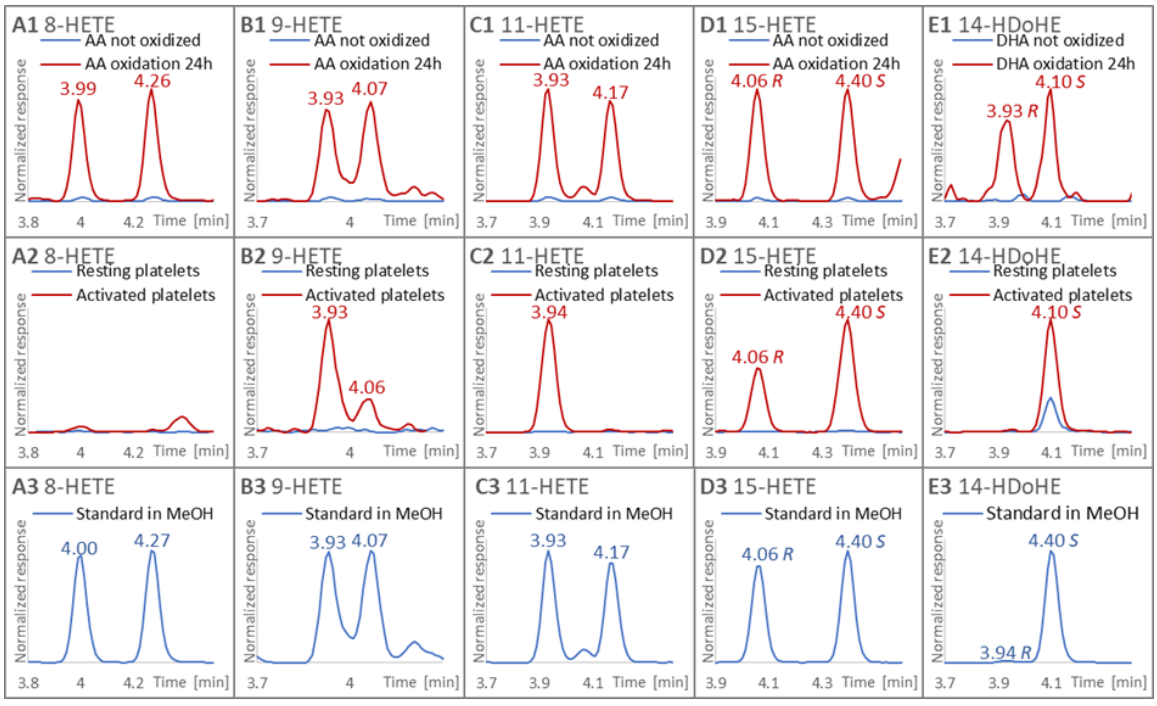

Figure 73. *Comparison of oxylipins from different sources. EIC of 8-HETE in oxidized PUFA (**A1**), platelets (**A2**) and standard solution (**A3**); EIC of 9-HETE in oxidized PUFA (**B1**), platelets (**B2**) and standard solution (**B3**); EIC of 11-HETE in oxidized PUFA (**C1**), platelets (**C2**) and standard solution (**C3**); EIC of 15-HETE in oxidized PUFA (**D1**), platelets (**D2**) and standard solution (**D3**); EIC of 14-HDoHE in oxidized PUFA (**E1**), platelets (**E2**) and standard solution (**E3**). Analysed with the final method.*

4. Publication IV: untargeted analysis of platelet lipidome

Untargeted UHPLC-ESI-QTOF-MS/MS analysis with improved lipid identification and quantification for describing total platelet lipidome and its changes upon thrombin-activation and treatment with a platelet inhibitor

Malgorzata Cebo[a], Jörg Schlotterbeck[a], Carlos Calderón Castro[a], Meinrad Gawaz[b], Madhumita Chatterjee[b], Michael Lämmerhofer[a]*

[a] University of Tübingen, Institute of Pharmaceutical Sciences, Pharmaceutical (Bio-)Analysis, Auf der Morgenstelle 8, 72076 Tübingen, Germany

[b] Department of Cardiology and Angiology, University Hospital Tübingen, Otfried-Müller-Strasse 10, 72076 Tübingen, Germany

Manuscript ready for submission.

Keywords: Lipidomics, platelet lipidome, platelet activation, SWATH, lipid identification

Abstract

Lipids play a major role in platelet signalling and activation. In this study we analysed the platelet lipidome in untargeted manner by reversed-phase UHPLC for lipid species separation coupled to high-resolution QTOF-MS/MS in data-independent acquisition mode with sequential window acquisition of all theoretical fragment ion mass spectra (SWATH) for compound detection. Lipid identification and peak picking was supported by the characteristic elution pattern of lipids from the same class. It was primarily based on post-acquisition targeted feature extraction from the SWATH data. Multiple extracted ion chromatograms (EICs) from SWATH data of diagnostic ions on MS1 and MS2 level from positive and negative mode allowed distinguishing between poorly resolved isomeric lipids based on their distinct fragment ions which could be used for relative quantification on the molecular lipid species level. This approach provides higher assay specificity for lipid analysis compared to conventional quantification with precursor ions such as in data-dependent acquisition methods. This advanced approach was used to analyse platelet samples. Absolute concentrations of lipids from some classes were estimated by one-point calibration using stable isotope-labelled internal standards as single level calibrants. The lipidome of platelets in the resting state is described by showing the distribution and relative abundances of lipid species within each class in terms of unsaturation level and length of fatty acid chains. The improved data processing method was also used to analyse platelets treated with a platelet inhibitor GPCR (CXCR7 chemokine receptor) pharmacological agonist. The results show that the platelet inhibitor significantly reduced platelet activation stimulated by thrombin, as most of the changes caused by activation like increased concentration of oxylipins and lysophosphatidylinositol were suppressed. The agonist also seems to cause changes in acylcarnitines and diglycerides.

4.1.Introduction

Platelet activation and following aggregation and adhesion to the blood vessel is essential for hemostasis, and lipids are major players in this process [91]. On the other hand, the same biochemical reactions might lead to pathophysiological conditions of thrombosis which could cause ischemic stroke or myocardial infarction [118]. The comprehensive analysis of the platelet lipidome and its alterations upon platelet activation might bring a

deeper understanding of this process and might lead to the development of new therapeutic strategies against diseases, in which platelets are involved [200]. The platelet lipidome has been explored in the last years by various modern MS and LC-MS techniques, which brought about important findings on absolute quantification of lipids [77], changes in lipidome during platelet activation [117, 158, 201, 202], platelet biochemistry [109] and changes in platelet lipids in various diseases [86, 106, 203].

The analysis of the whole lipidome in lipidomics, is most commonly realized by untargeted lipid profiling with high resolution MS like QTOF, Orbitrap or FT-ICR-MS instruments [79]. High mass resolution and additional information about compound fragmentation by tandem MS/MS is necessary for post-acquisition lipid identification. For this purpose, MS/MS data can be acquired in 3 different ways. The first one is data dependent acquisition (DDA), in which only the highest abundant precursor ions of an MS full scan experiment are fragmented providing usually good quality MS/MS spectra due to narrow (unit mass) precursor isolation window [80, 128]. The second approach is data independent acquisition (DIA), in which all precursor ions are fragmented without information from the MS full scan experiment. Due to limitations in terms of acquisition rates of high-resolution mass spectrometers, precursor ion selection with narrow (unit mass) isolation width is not possible. Instead, DIA can use one broad quadrupole 1 (Q1) isolation window for all precursors, an acquisition mode which is called all ion fragmentation (AIF), or multiple intermediate-wide Q1 windows acquired in a stepwise manner, an approach which is called sequential window acquisition of all theoretical fragment ion mass spectra (SWATH) [158] [86]. The third acquisition mode of high-resolution MS instruments for obtaining MS/MS information in lipidomics is parallel reaction monitoring (PRM) or multiple reaction monitoring (MRM^{HR}), which acquires comprehensive data about precursor ions in an MS full scan, but fragments only preselected targeted compounds [126]. PRM (MRM^{HR}) is thus not providing comprehensive MS/MS data. DIA acquisition modes have the advantage that no information about lower abundant species is lost and that it allows quantification of compounds not only on MS level but also MS/MS level with their fragments. However, AIF may lead to complex composite spectra. Spectral quality may be better with SWATH due to narrower precursor isolation windows, which also leads to more efficient filtering of noise and enhanced S/N ratios in MS/MS quantification [158].

In general, lipid analysis might be done by direct-infusion of the lipid extract of a sample to the MS (shotgun lipidomics) [34, 77], or by chromatographic separation prior to MS detection [40, 132, 133]. The advantage of the first approach is high sample throughput, but on the other hand, this analysis might suffer from high matrix effects and interferences due to isomeric and/or isobaric lipid species. Chromatographic separation before the detection simplifies sample complexity and therefore reduces matrix effects. There are multiple chromatographic methods to choose from for lipid analysis, the most common are reversed phase (RP) liquid chromatography (LC) methods [75, 127, 130], hydrophilic interaction liquid chromatography (HILIC) [128, 204, 205], or supercritical fluid chromatography (SFC) [64, 206, 207]. RPLC separates single lipid species of the same class [208]. On contrary, HILIC differentiates lipids by their polar head groups, i.e. lipid classes are separated from each other, but all the lipid species within one class elute very closely to each other. The elution pattern of SFC is similar to the one of HILIC, but it gives better performance for highly apolar neutral lipids. An additional dimension for lipid species separation might be provided by ion mobility which can be due to its separation in ms-time scale well integrated into LC-MS/MS analysis schemes [42, 209, 210].

Analysis of both DDA and DIA lipidomics data requires retrospective feature extraction and structural annotation post acquisition and a variety of vendor-specific and open source software tools are nowadays available, in particular for DDA data [211]. What concerns raw data processing of DIA data in untargeted lipidomics, two general strategies can be distinguished: i) structural annotation of features by database search, and ii) targeted feature extraction. Amongst the former, the most popular approach is based on untargeted peak finding with spectral deconvolution followed by structural annotation through database matching such as implemented in MS-DIAL software [131, 212]. Following the latter approach, Hopfgartner and co-workers used a research version of LipidView Method Exporter tool to create a lipid target list and quantification methods for vendor software [213]. In general, for targeted feature extraction no specific software is required. Since the building blocks of lipids are known, an in silico target list can be easily created. Fragmentation rules of the common lipid classes are also well known from the literature and hence multiple confirmative EICs for precursor and fragment level ions of each lipid can be defined in a straightforward manner by simple spread sheet programs like excel. Such targeted data processing on SWATH data allowed the identification and quantification of 611 lipid species from 21 different lipid classes in keratinocytes [208]. In

this publication, we focus on the latter approach of targeted feature extraction on untargeted lipidomics data obtained by data-independent SWATH acquisition. The consolidated approach implements prediction of retention time (RT) of lipids and relative quantification at MS/MS level. Then, we used the improved approach to successfully describe in qualitative and quantitative way the lipidome of platelets in their resting state and upon activation with thrombin. Moreover, we provide detailed information about changes in the platelet lipidome upon treatment with a pharmacological GPCR agonist - platelet inhibitor (also as absolute estimation of lipid concentration), which shows a novel approach for evaluating the anti-platelet efficacy of a compound by evaluating its effect on the platelet lipidome [118].

4.2.Materials and methods

4.2.1. Materials

SPLASH® LIPIDOMIX® Mass Spec Standard was purchased from Avanti Polar Lipids (Alabaster, AL, USA). Isopropanol (IPA), acetonitrile (ACN) and methanol (MeOH), all in Ultra LC-MS grade were obtained from Carl Roth (Karlsruhe, Germany). Ammonium formate, formic acid and IPA in HPLC grade were purchased from Merck (Darmstadt, Germany). Water was obtained from Elga Purelab Ultra ultrapure water purification system (Celle, Germany). Platelet inhibitor GPCR agonist VUF11207 (RDC-1 Agonist, GPR159 Agonist: (E)-N-(3-(2-fluorophenyl)-2-methylallyl)-3,4,5-trimethoxy-N-(2-(1-methyl-pyrrolidin-2-yl)ethyl)benzamide) was procured from Calbiochem [214].

Platelets were obtained from 11 healthy donors who gave informed consent to this study. They were collected at the University Hospital Tübingen in accordance to the ethics committee of the Medical Faculty, University of Tübingen.

4.2.2. Platelet isolation

Platelets were isolated as described elsewhere [158]. Briefly, the blood was collected in acid-citrate-dextrose buffer (ACD) (in total 60 mL) so that blood was diluted 5 times with

the ACD buffer and then centrifuged. Platelet-rich plasma was then washed with Tyrodes-HEPES buffer and centrifuged. The next step was re-suspension of the platelet pellet in phosphate-buffered saline (PBS) supplemented with calcium. At this point samples were aliquoted for equal platelet count.

Platelets from 11 different donors were aliquoted into samples with 3 x 10^8 cells. Four aliquots were obtained from each donor, which resulted in 44 samples. The four aliquots from each donor were treated in 4 different ways: the first aliquot (named *resting platelets*) was kept untreated; the second aliquot was activated with thrombin (0.1 U/mL of thrombin added to platelets and kept for 15 min at room temperature); the third aliquot was treated with platelet inhibitor and thrombin for 15 min at room temperature; and the last aliquot was treated with the platelet inhibitor only (15 min, room temperature). After incubation, the samples were centrifuged at 4^{o}C to avoid further platelet activation during centrifugation, the supernatant was discarded and the platelet pellet was used for lipid extraction and stored at -80^{o}C until further analysis.

4.2.3. Lipid extraction

Lipid extraction was performed using a monophasic extraction method following the isopropanol/water protocol reported elsewhere [139]. Dry platelet pellets were suspended in 5 mL IPA/H_2O 9:1 (v/v). The samples were vortexed (10 s) and sonicated (2 min). Then, 50 µL of 10 times diluted internal standard (IS) mix (MeOH was used as the dilution solvent) was added to each sample. Samples were shaken on ice for 1 h followed by centrifugation (3,500 x g, 10 min without acceleration and deceleration). Supernatant (lipid extract) was moved to fresh falcon tubes and dried with GeneVac EZ2 evaporator (Ipswich, UK) with nitrogen protection. The samples were then reconstituted in 100 µL MeOH, and after vortexing (10 s), sonication (2 min) and centrifugation (3,500 x g, 10 min without acceleration and deceleration) the methanol solutions were transferred to autosampler vials.

A pooled quality control (QC) sample was prepared by mixing together 15 µL aliquots of each re-constituted sample.

An IS solution was prepared in MeOH with the same concentration as in the samples (calculated as if extraction recovery was 100%).

The samples were placed in the autosampler at 4°C and analysed straight after the extraction.

4.2.4. UHPLC-ESI-QTOF-MS/MS method

The analyses were performed with an Agilent 1290 Infinity UHPLC system (Agilent, Waldbronn, Germany) equipped with a binary pump and a PAL-HTX xt DLW autosampler (CTC Analytics AG, Switzerland). The UHPLC system was coupled to a SCIEX TripleTOF 5600+ QTOF mass spectrometer with a DuoSpray Source (SCIEX, Ontario, Canada).

The ACQUITY UPLC CSH C18 column (100 mm × 2.1 mm; particles: 1.7 µm; Waters Corporation, Millford, MA, USA) with precolumn (5 mm x 2.1 mm; 1.7 µm particles) was used for chromatographic separation [131]. Eluent A was H_2O/ACN 2:3 (v/v) containing 10 mM ammonium formate and 0.1% formic acid (v/v), B was IPA/ACN/H_2O 90:9:1 (v/v/v) containing 10 mM ammonium formate and 0.1% formic acid (v/v). Gradient elution started with 15% B, followed by increase to 30% B in 2 min, then to 48% B in 0.5 min, further to 82% B at 11 min, then reached 99% B in the next 0.5 min, and stayed at this level for another 0.5 min. Afterwards, the percentage of B quickly dropped (in 0.1 min) to 15% to re-equilibrate the column for the next injection for 2.9 min (Table 55 in Suppl. materials). The flow rate was 600 µL/min. The column temperature was equal to 65°C. The injection volume was 3 µL for positive mode and 5 µL for negative mode.

LC-ESI-MS/MS experiments were first run in positive polarity mode and then in negative polarity mode. For MS full scan experiments a mass range between *m/z* 50-1250 was selected. MS/MS experiments were acquired by SWATH. More details on MS and MS/MS experiments are given in Table 53. The ion source temperature was set to 350°C, curtain gas, nebulizer gas and heater gas pressures were equal to 35 psi, 60 psi and 60 psi, respectively. The ion spray voltage was set to 5500 V in the positive mode and -4500 V in

negative mode. The declustering potential was adjusted to 80 V and -80 V for positive and negative polarity mode, respectively. The MS cycle time was always 750 ms.

Table 53. *Data independent acquisition (DIA) with SWATH windows. The table shows the m/z range for each individual experiment, its accumulation time (Acc. time) and collision energy.*

			Positive			Negative		
Experiment	**Type**	**Acc. time [ms]**	**Start *m/z***	**Stop *m/z***	**Collision energy [V]**	**Start *m/z***	**Stop *m/z***	**Collision energy [V]**
1	MS Full SCAN	80	50.0	1250.0	10	50.0	1250.0	-10
2	SWATH	31	50.0	214.6	45±15	49.5	342.2	-45±15
3	SWATH	31	213.6	281.8	45±15	341.2	453.6	-45±15
4	SWATH	31	280.8	390.7	45±15	452.6	480.8	-45±15
5	SWATH	31	389.7	480.4	45±15	479.8	507.8	-45±15
6	SWATH	31	479.4	509.0	45±15	506.8	532.3	-45±15
7	SWATH	31	508.0	536.5	45±15	531.3	566.8	-45±15
8	SWATH	31	535.5	610.6	45±15	565.8	617.4	-45±15
9	SWATH	31	609.6	677.1	45±15	616.4	687.1	-45±15
10	SWATH	31	676.1	709.0	45±15	686.1	715.0	-45±15
11	SWATH	31	708.0	735.1	45±15	714.0	744.1	-45±15
12	SWATH	31	734.1	759.1	45±15	743.1	755.1	-45±15
13	SWATH	31	758.1	773.1	45±15	754.1	776.0	-45±15
14	SWATH	31	772.1	790.2	45±15	775.0	794.6	-45±15
15	SWATH	31	789.2	811.2	45±15	793.6	807.6	-45±15
16	SWATH	31	810.2	827.2	45±15	806.6	830.3	-45±15
17	SWATH	31	826.2	856.2	45±15	829.3	840.1	-45±15
18	SWATH	31	855.2	884.3	45±15	839.1	859.2	-45±15
19	SWATH	31	883.3	915.9	45±15	858.2	889.1	-45±15
20	SWATH	31	914.9	983.7	45±15	888.1	924.6	-45±15
21	SWATH	31	982.7	1250.0	45±15	923.6	1050.5	-45±15

The sample order was randomized. The IS solution was injected 3 times in the beginning of the sequence. The QC was injected 3 times after IS solution and before the samples, then every 5th sample and then again 3 times after the samples.

4.2.5. Lipid identification and quantification

4.2.5.1. Step 1: Identification based on different MS and MS/MS signals

Twenty lipid classes were investigated in the course of this study: FAs, monoglycerides (MGs), DGs, triglycerides (TGs), lysophosphatidylcholines (LPCs), phosphatidylcholines (PCs), ether phosphatidylcholines (ePCs), lysophosphatidylethanolamines (LPEs),

phosphatidylethanolamines (PEs), ether phosphatidylethanolamines (ePEs), lysophosphatidylinositols (LPIs), phosphatidylinositols (PIs), lysophosphatidylserines (LPSs), phosphatidylserines (PSs), acylcarnitines (ACars), cholesteryl esters (CEs), ceramides (Cers), hexosylceramides (HexCers), sphingomyelins (SM) and oxylipins. Fatty acid chains with even number of carbons (from 8 to 26 carbon atoms) and with 0 to 6 double bonds were considered. For sphingolipids dihydroxy sphingoid bases with 17 and 18 carbon atoms and with 0, 1 and 2 double bonds were taken in account for lipid searching.

Lipids were pre-identified by using a target list approach with characteristic MS and MS/MS signals. Which of the signals is more sensitive and more selective strongly depends on the lipid class. Even though some lipid classes show multiple signals in positive and negative mode, in current studies we always chose a maximum of 4 signals for each lipid. This seemed to be an acceptable compromise between increasing data complexity with each additional processed signal and high confidence in obtained data as well as structural annotations. The same types of signals were chosen for all lipids within one class. Generally, a few rules were obeyed to select signals, if multiple signals were available. First, if the compound was detectable in both positive and negative modes, a signal from each mode was chosen. Second, at least one of the signals was a precursor mass from TOF MS full scan experiment (experiment 1 in Table 53) and if possible, at least one fragment from the corresponding SWATH window was also selected. Third, if there were several different fragments available, at least one signal was chosen, which gives the best selectivity to determine the FA composition of a lipid; signal sensitivity was in this case of second importance. The final selection of signals for each lipid class is shown in Table 54. Additionally, structures of fragments are proposed in the supplementary information (Suppl. materials Figure 81 to Figure 84).

In the next step, all extracted ion chromatograms (EICs) were generated for each lipid using MultiQuant 3.0 software (Sciex) with the *m/z* tolerance of ± 0.010 of the theoretical value. The threshold was set to 1000 cps. Obtained retention times for different signals of the same lipid were compared. To classify a lipid species as pre-identified, the retention times from at least 50% of signals had to match (2 out of 3, or 2 out of 4, or 1 in case of 1 to 2 signals in total). The retention times were considered the same if the difference within one polarity (the same LC run) was less than 0.05 min and between different polarities (which required 2 separate LC runs) - less than 0.1 min (Figure 74. Point 1).

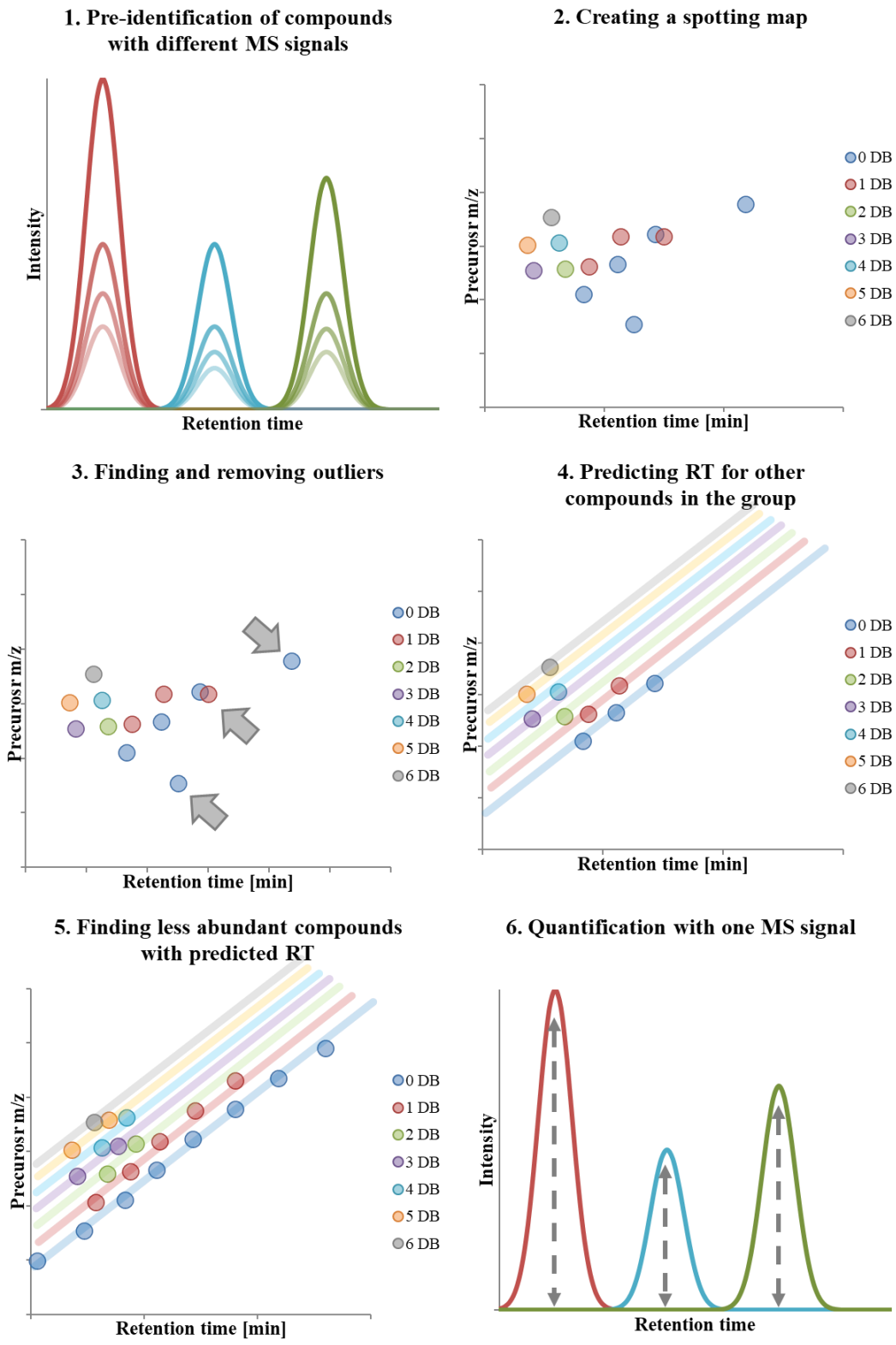

Figure 74. *Steps in qualitative and quantitative analysis of lipids for each lipid class (as described in chapters 4.2.4.1 – 4.2.4.3)*

4.2.5.2.Step 2: Identification with a retention time prediction model

In reversed phase chromatography the different lipid species of the same class elute with regular highly characteristic order (homology principle). As a consequence, retention time prediction models can be utilized to confirm lipid identification which was the next step of our approach. The retention time prediction model used herein was based on two main observations. First, lipids of the same class with the same number of double bonds in the FAs elute in order of increasing carbon number (as sum of carbon atoms in FA chains). Secondly, lipids of the same class and the same number of carbons in FA chains elute in order of decreasing double bond number.

All lipid classes were analysed separately. In each class, lipids were divided into groups with the same number of double bonds. For each class, a spotting map, i.e. a plot of *m/z* of precursor ions versus retention times was prepared (Figure 74. point 2). Then, the empirical correlation of the given *m/z* and RT was calculated for each group. A correlation coefficient > 0.95 was required to consider that all the found lipids were correctly identified. However, if the correlation coefficient was lower or elution order was not correct, outliers were removed (Figure 74 point 3).

In the next step, functions correlating *m/z* to RT for each group were described, based on the identified lipids. It was considered that the correlation lines for groups with different number of unsaturation should be parallel to each other within a lipid class, and that there should be similar distances between the lines (however, it was often a case, that with higher number of double bonds, the lines were getting closer to each other). Based on these correlations the retention times for all theoretical lipids in the class were predicted. If no lipids were identified in a group, an average slope of other groups and average difference in intercept were calculated and a new function for a missing group was predicted (Figure 74 point 4).

Then, EICs for theoretical lipids in the class with lower threshold were extracted. Usually, the threshold was set to 250 cps for a TOF experiment and 50 cps for SWATH, but sometimes the thresholds were raised, if there were high levels of noise. The predicted RT with the window of 0.5 min was used for searching the lipids.

This procedure allowed more findings, often of low abundant lipids. In the next step, the matching retention times of different signals for newly found lipids were confirmed, in the same way as explained in the paragraph 4.2.4.1. All the findings – already identified and freshly added ones were again plotted in a spotting map and correlation coefficient within each group of the lipids with the same unsaturation level was calculated (Figure 74 point 5). If the criteria for correlation coefficient (> 0.95) together with the 2 main assumptions of the elution model were met, all the lipids in the group were considered identified. If not, outliers were removed.

4.2.5.3.Step 3: Relative quantification

Table 54. describes types of signals (diagnostic ions) used for step 1 in the lipid identification for all lipid classes, but also for lipid quantification. M means precursor molecule and RCO_2 means a fatty acid anion (for structures of fragments see Suppl. materials Figure 81 to Figure 84). In case of most lipids R means alkyl or alkenyl chains and does not include carbonyl C atom nor heteroatoms from ester, ether or amide bonds).

Table 54. *Types of signals used lipid identification. Green background indicates signals chosen for relative lipid quantification. Bold green letters indicate the precursor ion signal chosen for absolute estimation of concentration. Gray background means that no more signals were available.*

	Precursor or fragment ion			
	1	**2**	**3**	**4**
FA	**TOF- / $[M-H]^-$**			
LPC	**TOF+ / $[M+H]^+$**	SWATH+ / $[RC_4H_6O_3]^+$	TOF- / $[M+HCOO]^-$	SWATH- / $[RCO_2]^-$
PC	**TOF+ / [M+H]+**	**SWATH+ / $[M-ROH]^+$**	TOF- / [M+HCOO]-	SWATH- / $[RCO_2]^-$
ePC	**TOF+ / $[M+H]^+$**	TOF- / $[M+HCOO]^-$	**SWATH- / $[M-CH_3]^-$**	
LPE	**TOF+ / [M+H]+**	SWATH+ / $[RC_4H_6O_3]^+$	**TOF- / $[M-H]^-$**	SWATH- / $[RCO_2]^-$
PE	**TOF+ / $[M+H]^+$**	TOF- / $[M-H]^-$	**SWATH- / $[RCO_2]^-$**	SWATH- / $[RCO_2]^-$
ePE	**TOF+ / [M+H]+**	TOF- / [M-H]-	**SWATH+ / $[RC_4H_6O_3]^+$**	SWATH- / $[RCO_2]^-$
LPI	TOF+ / $[M+H]^+$	SWATH+ / $[RC_4H_6O_3]^+$	**TOF- / $[M-H]^-$**	SWATH- / $[RCO_2]^-$
PI	TOF+ / $[M+NH_4]^+$	**SWATH+ / $[M-C_6H_{12}O_9P]^+$**	**TOF- / $[M-H]^-$**	SWATH- / $[RCO_2]^-$
LPS	TOF+ / $[M+H]^+$	SWATH+ / $[M-C_3H_8O_6NP]^+$	**TOF- / $[M-H]^-$**	SWATH- / $[RCO_2]^-$
PS	TOF+ / $[M+H]^+$	**SWATH+ / $[M-C_3H_8O_6NP]^+$**	**TOF- / $[M-H]^-$**	SWATH- / $[RCO_2]^-$
MG	**TOF+ / $[M+H]^+$**	TOF+ / $[M+NH_4]^+$		
DG	**TOF+ / $[M+NH_4]^+$**	**SWATH+ / $[RC_4H_6O_3]^+$**	SWATH+ / $[RC_4H_6O_3]^+$	TOF- / $[M+HCOO]^-$
TG	**TOF+ / [M+NH4]+**	SWATH+ / $[M+H]^+$		
ACar	**TOF+ / $[M+H]^+$**	SWATH+ / $[RC_5H_6O_4]^+$	TOF- / $[M+HCOO]^-$	SWATH- / $[RCO_2]^-$
Cer	TOF+ / $[M+H]^+$	**SWATH+ / $[RC_3H_5N]^+$**	SWATH+ / $[RC_2H_3]^+$	**TOF- / $[M+HCOO]^-$**
Hex-Cer	TOF+ / $[M+H]^+$	SWATH+ / $[RC_3H_7ON]^+$	SWATH+ / $[M-C_6H_{13}O_5]^+$	**TOF- / $[M+HCOO]^-$**
SM	TOF+ / $[M+H]^+$	SWATH+ / $[M-H_2O]^+$	**TOF- / $[M+HCOO]^-$**	SWATH- / $[M-CH_3]^-$
CE	**TOF+ / $[M+NH_4]^+$**	SWATH+ / 369.3523		
oxylipins	TOF- / $[M-H]^-$			
cholesterol	TOF+ / $[M-H_2O+H]^+$			
sphingoid bases	TOF+ / $[M+H]^+$			

The relative quantification of lipids was done with one of the signals used for the identification (Figure 74 point 6). The criterium to choose the signal was first selectivity and then sensitivity. The same type of signal was chosen for all lipids in one class. The chosen signals are shown in Table 54 with the green background.

4.2.6. Data analysis

Preliminary information about the data was obtained with PeakView (Sciex). Then EICs for each lipid class were chosen as described in the previous chapter. EICs were processed and peak heights were used for relative quantification and absolute quantification based on one-point calibration with lipid class specific IS by MultiQuant 3.0 software (Sciex).

R (ver. i386 3.4.2; R-project for statistical computing) and Excel 2007 (Microsoft, Redmond, WA, USA) were used for statistical evaluation and preparation of figures.

4.3.Results and discussion

4.3.1. Lipid identification

Automated untargeted raw data analysis by software tools like MS-DIAL is convenient to achieve structural annotation of a large number of features with minimal efforts [86, 131]. Typically, 10-20 % of all features can be annotated by matching deconvoluted MS/MS spectra to LipidBlast in silico spectral database. However, a certain percentage of structural identifications represent misannotations and must be manually curated. It was found that a targeted feature extraction approach from SWATH-MS data with multiple confirmative EICs may be more reliable and more robust with less misidentifications at expense of a lower total number of structural assignments though [208]. For this reason, we focus herein on a refined and consolidated targeted feature extraction process on SWAH-MS data of platelet lipidomics studies.

Lipid identification was based on two pillars: i) The use of sets of diagnostic ions from MS1 and MS2 level which are characteristic for both lipid class and molecular lipid species levels, and ii) retention time mapping based on carbon and double bond numbers of fatty acyl side chains (homology principle). Initially, a target lipid list was prepared and the peak

searched by targeted feature extraction in the QC-sample which is representative for the study samples as it represents a mixture of a small aliquot of all study samples. Its correct identification was verified by comparing the overlap of various EICs from precursor ion of TOF-MS full scan as well as precursor ions and fragment ions from MS/MS in respective SWATH windows in each positive and negative polarity mode (Figure 75). For this purpose, known fragmentation patterns as depicted in Suppl. materials Figure 81 to Figure 84 for the distinct lipid classes have been employed. The ions that were found to be most suitable for the purpose of identification are summarized in Table 54. Unlike to DDA that allows to generate EICs only on the MS1 level, SWATH acquisition has the advanced option of comprehensively collecting both MS and MS/MS data within the selected mass range over the entire chromatogram in all samples. It allows to extract several EICs of which some are characteristic for the lipid class (lipid class specific fragments) while others may be specific for the molecular lipid species level (molecular lipid species fragment). In any case, this together with the availability of (convoluted) MS/MS spectra (from intermediate wide precursor isolation windows) may give more confidence for correct identification than single EICs from DDA with stochastically triggered MS2.

Theses structural assignments of the most abundant lipids were then confirmed by inspection of peak spotting plots of *m/z* vs. RT (Suppl. materials Figure 85 to Figure 87). Lipid species of the distinct lipid classes elute in regular patterns in accordance to their homology principle; lipids with more double bonds elute earlier while lipids with longer acyl chains elute later always shifted by regular increments per structural repeat element. Hence, the construction of simple empirical correlations may be very helpful to identify misidentifications and extend structural assignments to less abundant lipids increasing lipid coverage. Retention time of less abundant lipids can be predicted by the empirical correlations and peak finding based on precursor and fragment EIC can then focus on this specific retention time window. This simple combined approach of retention maps with multiple EICs for confirmation is quite powerful and a helpful tool to improve data quality. Indeed, it is according to our experience more powerful than retention time prediction tools and allows quick spotting of misidentifications from other software used for automated identification by spectral match with databases. It is also easily transferable from one RP system to another. The RT of lipids can be predicted for any RP conditions based on the most abundant, easily identified lipids in a class, or on added internal standards [215].

Using this targeted feature extraction methodology, 453 lipids from 20 lipid classes have been identified and were used for statistical evaluation.

A

Peak	Lipid species	$[M+H]^+$	$[M-RO+H]^+$	RT [min]
1	PC(20:4_18:2)	806.5703	520.3405	5.07
2	PC(20:5_18:1)	806.5703	522.3562	5.14
3	PC(22:6_16:0)	806.5703	496.3405	5.35
4	PC(20:3_18:2)	808.5860	520.3405	5.36
5	PC(22:5_16:0)	808.5860	496.3405	5.50
6	PC(20:4_18:1)	808.5860	522.3562	5.60
7	PC(20:5_18:0)	808.5860	524.3719	5.76
8	PC(20:3_18:1)	810.6017	522.3562	5.89
9	PC(22:4_16:0)	810.6017	496.3405	5.98
10	PC(20:4_18:0)	810.6017	524.3719	6.24
11	PC(20:3_18:0)	812.6173	524.3719	6.53
12	PC(20:1_18:1)	814.6330	522.3562	6.93
13	PC(18:2_20:0)	814.6330	552.4032	7.08
14	PC(18:1_20:0)	816.6486	552.4032	7.61

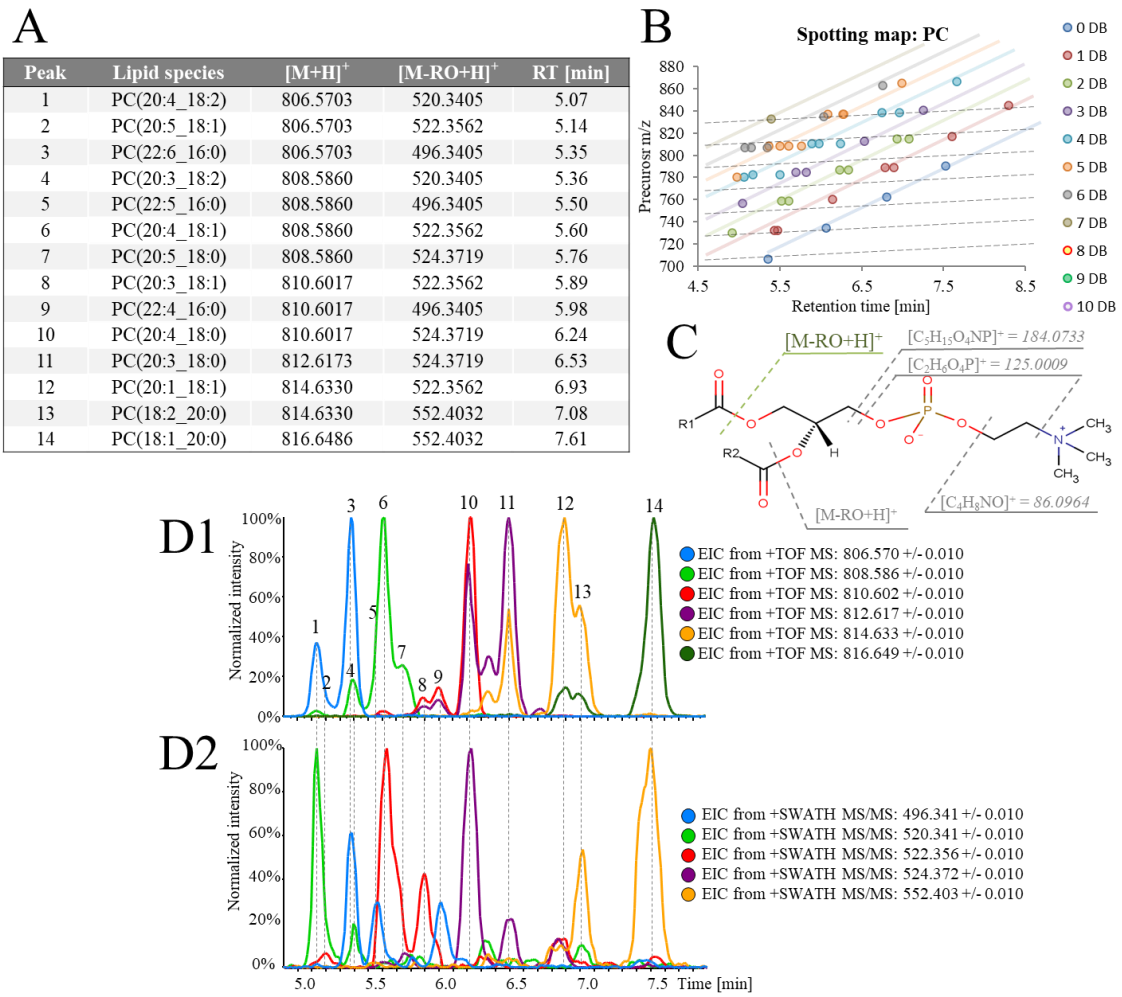

Figure 75. *Lipid identification as an example of PC (for simplification only positive mode).* ***A****: Targeted list of exemplary 14 PCs with precursor m/z from 806 to 816;* ***B****: Spotting map of all identified PCs;* ***C****: Proposed fragmentation of PC;* ***D****: EIC of* ***D1****: precursor m/z of the 14 PCs and* ***D2****: fragment m/z of the 14 PC; numbers above the peaks show identification as in* ***A****.*

4.3.2. Relative lipid quantification

Isomeric lipid species of the same class show very similar retention behaviour in RPLC. Therefore, they are often poorly separated, in particular when methods with short run times are used that are necessary in view of high throughput in clinical studies. As they share the same precursor ion mass, it is not possible to distinguish them at the MS1 level. Hence, if

not chromatographically resolved it is not possible to quantify them as different molecular lipid species using the precursor *m/z*.

When untargeted analysis with SWATH is used all the lipids are fragmented over the whole LC run time. The EICs of fragments, similarly to precursor signals, have enough data points to well define a chromatographic peak and might be used not only for lipid identification, but also for quantitative analysis [158]. An example showing how quantification with a fragment from SWATH might increase selectivity (and sometimes also sensitivity) compared to analysis with precursor from TOF-MS full scan experiment is shown in Figure 76 and additional examples are given in the Suppl. materials (Figure 88 and Figure 89).

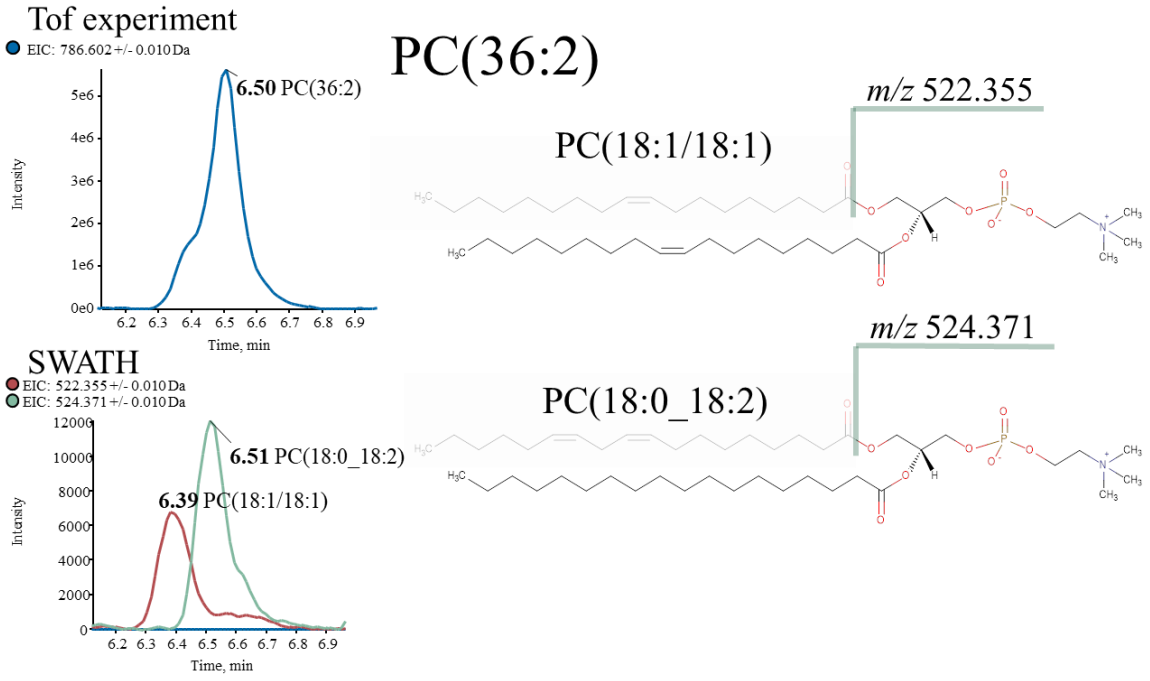

Figure 76. *TOF-MS and SWATH signals for 2 isomeric lipids: PC(18:0_18:2) and PC(18:1/18:1) with proposed fragmentation for shown signals in SWATH. Quantification with TOF would be only possible as the sum of these compounds (sum composition).*

In differential lipidomics, it may be quite misleading to monitor lipids at the lipid sum level. For example, it can happen and has happened that two distinct coeluted lipid species which are isomeric at the MS1 level and thus indistinguishable by DDA behave oppositely, one is upregulated while the other is down regulated between two study groups. These opposite fold-changes might (partially) cancel out each other and the information gets lost. Therefore, our aim for relative lipid quantification was to obtain the highest possible

selectivity. For most lipid classes it was possible to define all acyl chains. There were a few exceptions for classes which do not provide characteristic, selective fragments like ePC and SM (see their fragmentations in Suppl. materials Figure 81 and Figure 84). The type of signal used for quantification was chosen according to the following criteria: first, the most selective, and secondly, the most sensitive EIC. In case of all simple lipid classes which have only one acyl chain, the precursor ion gave equal selectivity, but better sensitivity than SWATH signals, and therefore it was chosen. Also lipid classes with 2 different possibilities for the acyl chain position (sn-1 or sn-2 positions) like LPC or LPE show full LC separation of these isomeric species; therefore, they could be quantified separately with the TOF-MS signal. The situation was different for more complex lipids, which have 2 acyl chains in their structure. Here, fragment signals from SWATH were more selective. For some (lower abundant) lipid species they were not available; thus, the identification level was lowered to the sum of carbon atoms and sum of double bonds in all acyl chains (lipid sum composition; MS1 level). This approach was also used for the class of TG, were structural complexity (3 acyl chains) made it very challenging to properly identify the composition of acyl chains. This class was identified (and quantified) at the level of total number of carbon atoms and sum of double bonds (lipid sum composition), even though fragments were available for analysis.

4.3.3. Estimation of absolute lipid concentrations

The drawback of using MS/MS signals for data processing is their less consistent detector response factor related to the corresponding IS as compared to precursor ion signals which has some implications in absolute quantification for quantitative lipidomics. The currently most common strategy to define lipid concentrations in untargeted analysis is based on added non-endogenous odd-chain or isotope labelled IS through one point calibration or with external calibration [77, 208]. Single lipid class specific IS are commonly used as calibrants for all species of this lipid class. Thereby, it is assumed that the head group (representative for the backbone or general structure of the lipids of this class) dominates the ionisation behaviour and all lipids within one class give the same response factor. Although it is not totally correct, it is commonly accepted as a reasonable first estimate of absolute lipid concentrations in samples allowing comparisons between studies [78]. If ISs are selected which are in the middle of the acyl side chain distribution, acceptable results have been obtained for many lipid classes with such quantitation by precursor ions. If

quantitation is based on fragment ions, identical fragmentation efficiency in the collision cell would be required between all lipids species of the class and the selected IS besides identical ionisation efficiency. It has been shown that response factors between lipids and IS deviate more strongly on the MS/MS level [78]. Still, other ways of absolute quantification with real standards [158] or with surrogate calibrants [78] are possible for defining lipid concentrations with fragments from SWATH.

In this work, we used relative quantification for comparison of study groups, for profiling of lipid classes for which no appropriate internal standard was available, and for the distinction of coeluted isomeric lipid species with different acyl side chains.

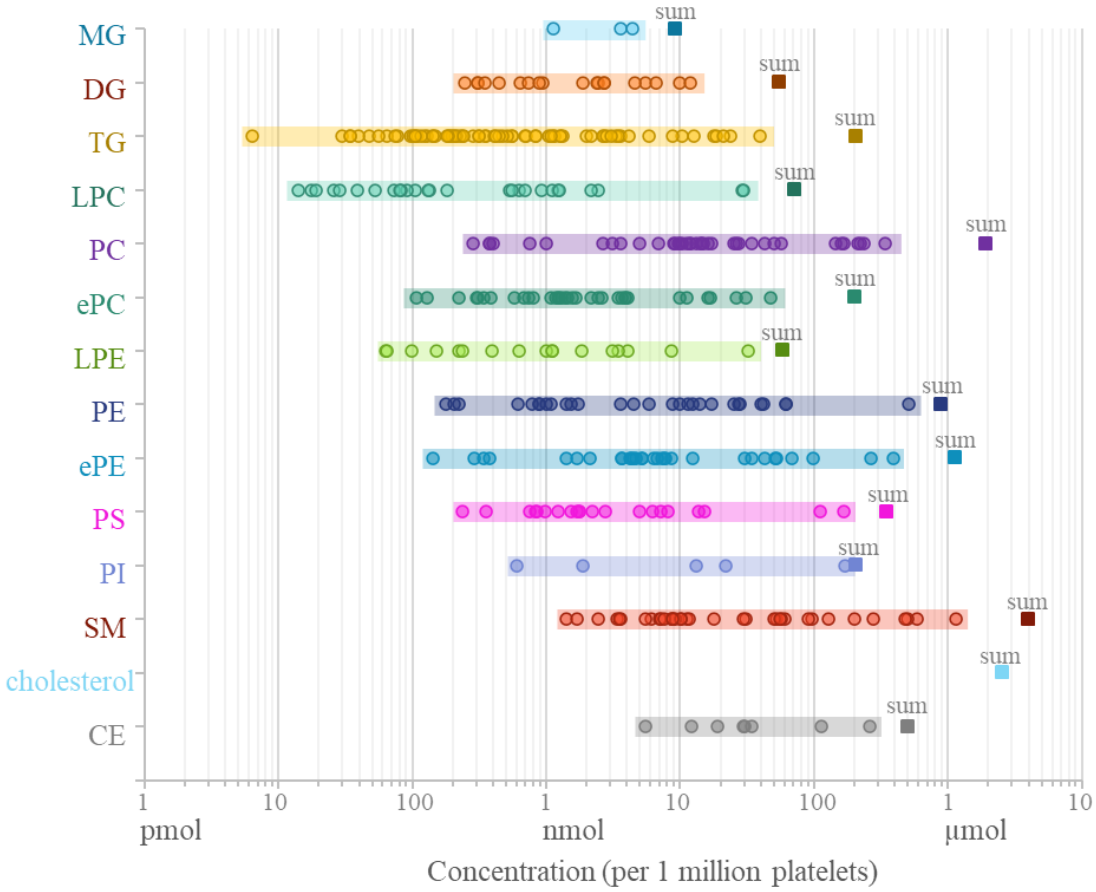

Figure 77. *Estimated concentration of lipid species detected in platelets. Circles indicate single lipids (as sum composition) and squares depict the sum of all lipids within a class. Mean values of 11 resting platelet samples.*

Besides relative quantification, absolute lipid concentrations were calculated to support inter-laboratory and inter-study comparisons. For this purpose, the precursor ions (as

specified in Table 54) were utilized and lipid concentrations were estimated using one-point calibration with lipid class specific IS. Only lipids of classes, for which a lipid class-specific internal standard was added to the samples, were estimated including MG, DG, TG, LPC, PC, ePC (deuterated PC was used as standard), LPE, PE, ePE (deuterated PE was used as standard), PI, PS, SM and CE (Figure 77). This method was less selective compared to our relative quantification and considers only sum compositions, but it allows better comparison of results between different laboratories. The quantitative results given in nmol/1x10^6 platelets are summarized in Suppl. materials Table 58 to Table **63**. Lipid concentrations were then used to create heatmaps illustrating distributions of fatty acid length and unsaturation in every lipid class. For lipid classes, which lacked a class-specific IS to estimate their absolute concentrations, relative intensities of precursor ion signals (peak height) were employed to generate heat maps of side chain distributions. The heat maps are shown in Figure 78.

The most abundant free fatty acid in platelets at resting state is palmitic acid (FA(16:0)) followed by stearic acid (FA(18:0)) and oleic acid (FA(18:1)) (Figure 78). PUFAs can be detected but are not highly abundant in resting platelets. To large extent, the fatty acyl profile of acyl carnitines (ACar), the fatty acid shuttle into mitochondria, reflects the free fatty acid distribution with exception of PUFAs with more than 3 DBs which are essentially missing. LPC, LPE, and LPI are three important lipid classes which are characterized by significantly different fatty acyl profiles. In LPCs, FA(16:0) and FA(18:0) are the dominant acyl residues while others are detected only at low levels. In sharp contrast, the fatty acyl profile is significantly shifted towards PUFA in the LPEs with LPE(20:4) being the most abundant of its class. LPI shows a narrow range of acyl moieties, with the LPI(18:0) being the most abundant. LPI(20:4) is the only one with PUFA side chain and present at relatively low levels only. Solely a few MGs with acyls from the group of saturated FAs (SFAs) or monounsaturated FAs (MUFAs) were detected in resting platelets. On contrary, CEs have mainly PUFAs as side chains with CE(18:2) and CE(20:4) as the most abundant ones. These specific acyl profiles (mean of n=11) may reflect their particular functional roles in cellular energy metabolism (FAs, ACar, MGs with dominance of saturated and monounsaturated FAs), membrane function, substrates for membrane remodelling and membrane function coupled to signalling processes (LPC, LPE, LPI).

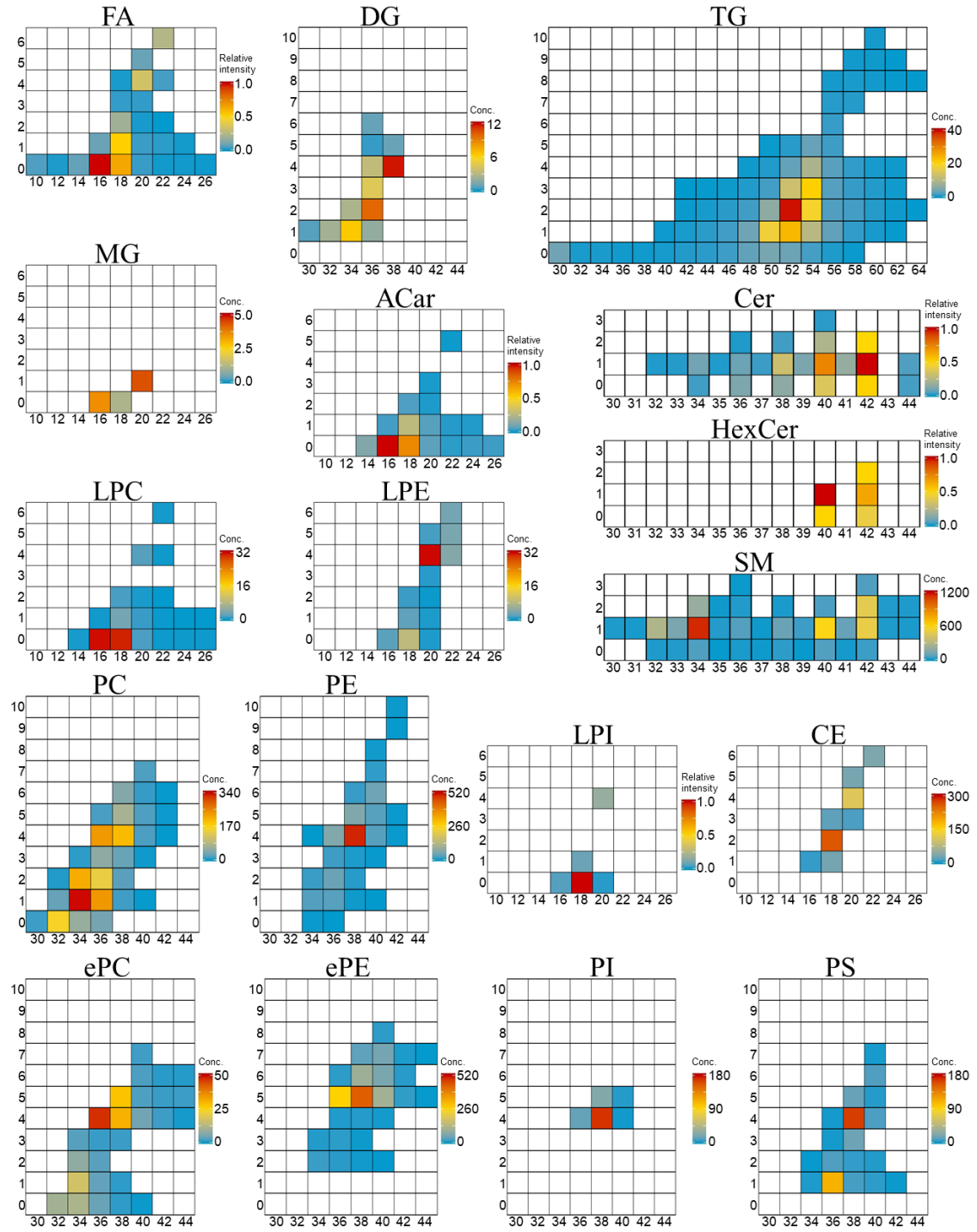

Figure 78. *Snapshot of the platelet lipidome: Heat maps showing intensities of lipids with different number of carbon atoms in acyl chains (sum of carbon atoms is shown on the x-axis) and with different total number of double bonds in fatty acyl chains (y-axis). Red colour indicates high intensity and blue low intensity; white fields present lipids which were not detected. Mean values of 11 resting platelet samples.*

DGs seem to have two global maxima, one for PUFA-DGs (in particular DG(38:4) resulting from FA(18:0) and FA(20:4) acyl side chains) and another one for MUFA-DGs (DG(34:1) and DG(36:2)), being indicative for their distinct biological roles as products of PLC signalling and building blocks of TGs as well as phospholipids (Figure 78). PCs and PEs mirror the fatty acyl maps of the corresponding LPCs and LPEs, described above. PCs are enriched in the outer leaflet of the platelet membrane and are rich in SFAs and MUFAs while also a certain percentage of PUFAs are found as constituents. Abundance maxima are found for PC(34:1) and PC(36:4). PEs, on the other hand, exhibit a single abundance maximum for PE(38:4) representative for the functional role of this lipid class as membrane constituents in the inner leaflet and substrates for enzymes like cPLA2. Interestingly, for the corresponding ether lipids (ePC and ePE) similar fatty acyl maps can be observed with a slight shift to (higher) unsaturation (with abundance maxima for ePC(36:4) and ePE(38:5)). It is also striking that ePEs are almost as abundant as PEs while ePCs are a factor of around 5 less abundant than PCs, speaking in gross terms (Figure 77 and Figure 78). The fatty acyl map of the PS lipid class resembles the one of PE. PS shares its functional role with PE as membrane constituent of the inner leaflet; they are externalized by platelet activation, aging or apoptosis. It appears that functional similarity coincides with structural similarity what the fatty acyl side chains is concerned. PIs have a very narrow distribution of fatty acyls (with 36, 38, or 40 carbons) and high degree of unsaturation (4 or 5 double bonds) that was anticipated from their functional role as substrates for cPLA2. The TG acyl map is dominated by medium chain FAs preferably with MUFAs; the most abundant lipid sum composition of TGs is observed for TG(52:2). Sphingolipids show the highest intensities with 1 double bond, most probably due to a sphingosine base (18:1) connected to a saturated fatty acyl chain. For Cer and HexCer lipids the acyl map shows the highest abundance for C40 followed by C42, while for SMs only a global maximum is found at these carbon numbers yet the global maximum with C34 (C16 fatty acyl and sphingosine base).

These fatty acyl maps for the major lipid classes are illustrative for the distribution of fatty acids and allow to anticipate some correlation to the functional roles of the distinct lipid classes.

4.3.4. Final results of 44 platelet samples with 4 different treatments

The final set of samples contained 44 platelet isolates stemming from 11 donors each with 4 different treatments as explained in the materials and methods section. Lipids were identified and quantified as described in paragraphs 4.2.4.1 to 4.2.4.3. In total 457 lipids were identified in the samples. LOWESS normalization was applied to check for improvement in data quality. The CV of IS across all the samples and QC was checked, as the theoretical concentration of IS was the same in all of them. The final outcome was that 9 IS showed improved CV after normalization and 3 showed worse. The average CV decreased from 18.02% to 15.20% after normalization (Suppl. materials Table 56). The data was then processed with the LOWESS normalized values.

The CV of lipids in QC was calculated and 4 compounds were removed due to CV exceeding 30% (Suppl. materials Figure 90). The final set used for statistical analysis contained 453 identified lipids. The missing values were replaced with 2/3 of the smallest recorded value for a given feature.

The score plot of PCA was checked for unsupervised sample groupings and outliers. One outlier was discovered: the sample of resting platelets from the 3rd donor (Suppl. materials Figure 99). This sample was removed and the finally obtained PCA is shown in Figure 79A. The samples clearly cluster by donor rather than treatment. The QC samples, on the other hand, are closely grouped together, what confirms adequate quality of LC-MS data.

The data was further curated. Each 4 samples stemming from the same donor were normalized by z-scores to reduce the influence of the donor. A new PCA with the normalized data was calculated (Figure 79B) and it shows good clustering of the samples according to the treatment used (QC samples were removed). It confirms significant changes in lipid profiles due to different sample treatments.

In the next step the paired Wilcoxon test was used to recognize which lipids were changed with the treatments. Three comparisons were made: resting platelets vs. thrombin treated to discover which lipids are involved in platelet activation; thrombin vs. thrombin and platelet inhibitor, to see if and how the addition of the agonist influences the platelet

activation; and finally resting vs. platelet inhibitor treatment, to see if the compound causes difference in platelet lipidome. Samples from the same donor were paired for comparison of matched samples to reduce the influence of biological variations between individuals. The q-values were calculated by correction of p-values in accordance to the concept of the false discovery rate [216]. The significance level for q-values was set to 0.05. The obtained results are presented as volcano plots in Figure 80 and the significant findings are listed in Suppl. materials Table 65. The comparison of thrombin-activated vs. resting platelets revealed that oxylipins are significantly increased in the thrombin-activated samples, as expected (Figure 80A). At the same time some of the PUFAs decrease (FA(20:4), FA(20:5), FA(22:6)), indicating their further metabolic processing by enzymatic oxidation and conversion to oxylipins. All LPIs show a significant increase after thrombin-activation. It may be explained by the cleavage of unsaturated PIs to PUFAs and LPIs. PUFAs, as already mentioned, are further metabolized during the activation, but LPIs remain in the platelets. We have not observed a significant decrease in PIs, but their initial concentrations are expected to be much higher than those of LPIs [77]. As a consequence, it is much easier to detect changes in the low abundant LPIs. Some other lyso-forms of lipids show significant changes, probably also due to phospholipase activity. Exemplary boxplots are presented in the Suppl. materials Figure 103.

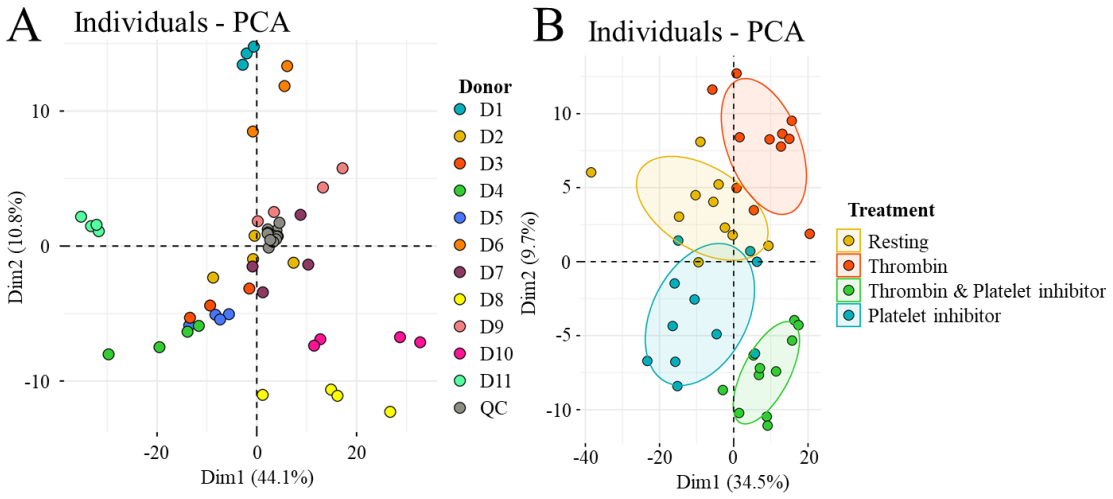

Figure 79. *Unsupervised PCA;* ***A****: for raw data, clustering is due to the donor;* ***B****: for z-scaled (for each donor) data; clustering is due to the treatment type.*

The comparison of platelets exposed to thrombin with and without the platelet inhibition strategy clearly shows that platelet activation is reduced by the inhibitory action (Figure

80B). The concentrations of oxylipins and LPIs, which increased upon activation, are now lowered. ACar are raised while the concentration of DGs are decreased in the samples incubated with both thrombin and the platelet inhibitor.

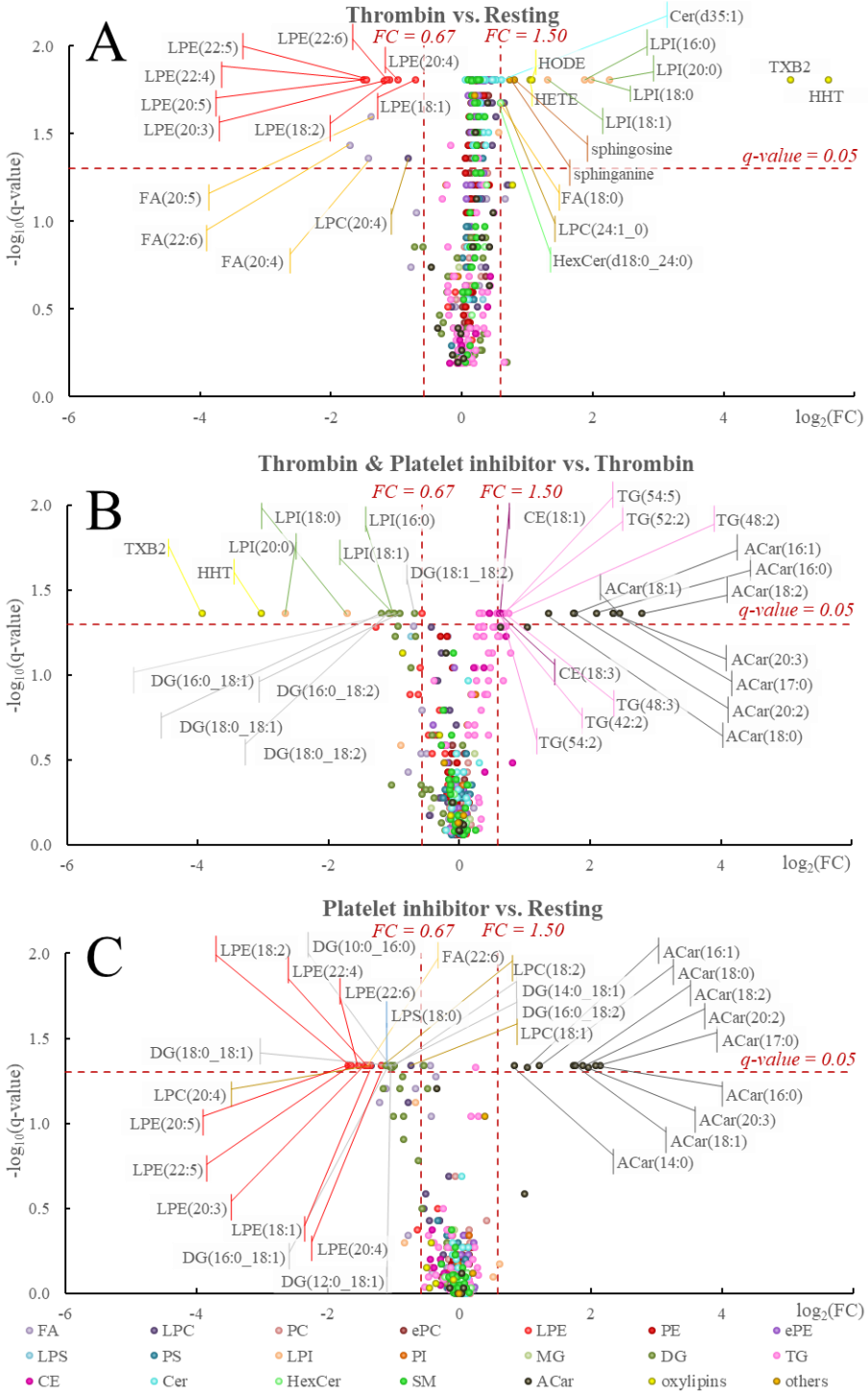

Figure 80. *Volcano plots for the 3 comparisons, A: resting vs. thrombin, B: thrombin vs. thrombin and platelet inhibitor and C: resting vs. platelet inhibitor. The labelled points present results significantly changed in terms of q-value and FC. The same colour means that the lipids belong to the same class. Red lines indicate levels of significance.*

Comparison between resting platelets and the samples treated with the platelet inhibitor shows that all ACars are significantly increased in the treated samples, and some DGs and LPEs are decreased (Figure 80C). This is similar behaviour observed when samples were treated with the agonist and thrombin.

4.4.Conclusions

The improved approach for lipid finding and identification based on targeted feature extraction supported by peak spotting plots and multiple EICs provided robust data sets for analysing lipids in platelets. The comprehensive data was collected and the total platelet lipidome has been described with 457 lipid species from 21 different lipid classes. What is more, absolute concentration of lipids has been estimated for 14 classes based on the one-point calibration approach with the class matched IS used as calibrants.

The method was then successfully applied for studies of alterations of the platelet lipidome in an ex-vivo pharmacolipidomics study. Our results clearly demonstrate that the platelet lipidome is subject of significant alterations upon activation and pharmacological inhibition. Analytical strategies like the currently elaborated will aid in validating the efficacy of potential anti-platelet agents in controlling the generation of lipid metabolites with pathological implications in thrombosis and thrombo-inflammation. Consequently, this might aid in developing a new generation of antiplatelet drugs.

Declaration of conflict of interests

The authors declare that there is no conflict of interests.

Acknowledgements

This project was funded by the German Research Foundation (DFG, Deutsche Forschungsgemeinschaft), project number 374031971-TRR 240.

4.5.Supplementary materials

4.5.1. Analytical conditions

Table 55 shows the gradient elution program and the change of mobile phase component B during the gradient elution, respectively. Component A was H_2O/AcN 2:3 (v/v) + 10 mM ammonium formate + 0.1 % formic acid (v/v), and B was IPA/AcN/H_2O 90:9:1 (v/v/v) + 10 mM ammonium formate + 0.1 % formic acid (v/v).

Table 55. *Gradient method for LC separation.*

Time [min]	% B
0	15
2	30
2.5	48
11	82
11.5	99
12	99
12.1	15
15	15

4.5.2. Lipid identification based on different MS and MS/MS signals

Figure 81 to Figure 84 show lipid fragmentation in positive and negative ion mode with collision energy 45 ± 15 V (positive mode) and -45 ± 15 V (negative mode). Fragmentation of all analysed lipid classes (FA, oxylipins, MG, DG, TG, LPC, PC, ePC, LPE, PE, ePE, LPI, PL, LPS, PS, ACar, CE, Cer, HexCer and SM) was investigated. If there are no fragments described for a lipid class or for one of the two MS polarity modes, it means that lipids of this class did not provide characteristic fragments with the used collision energy. An exception is the class of TGs, which gives good fragmentation, but the interpretation of fragments and proper lipid identification is more complicated due to their structure with 3 acyl chains.

For most lipids ‘R’ in Figure 81 to Figure 84 means alkyl or alkenyl groups and it does not include carbonyl C atoms nor heteroatoms like O or N from ester, ether or amide bonds.

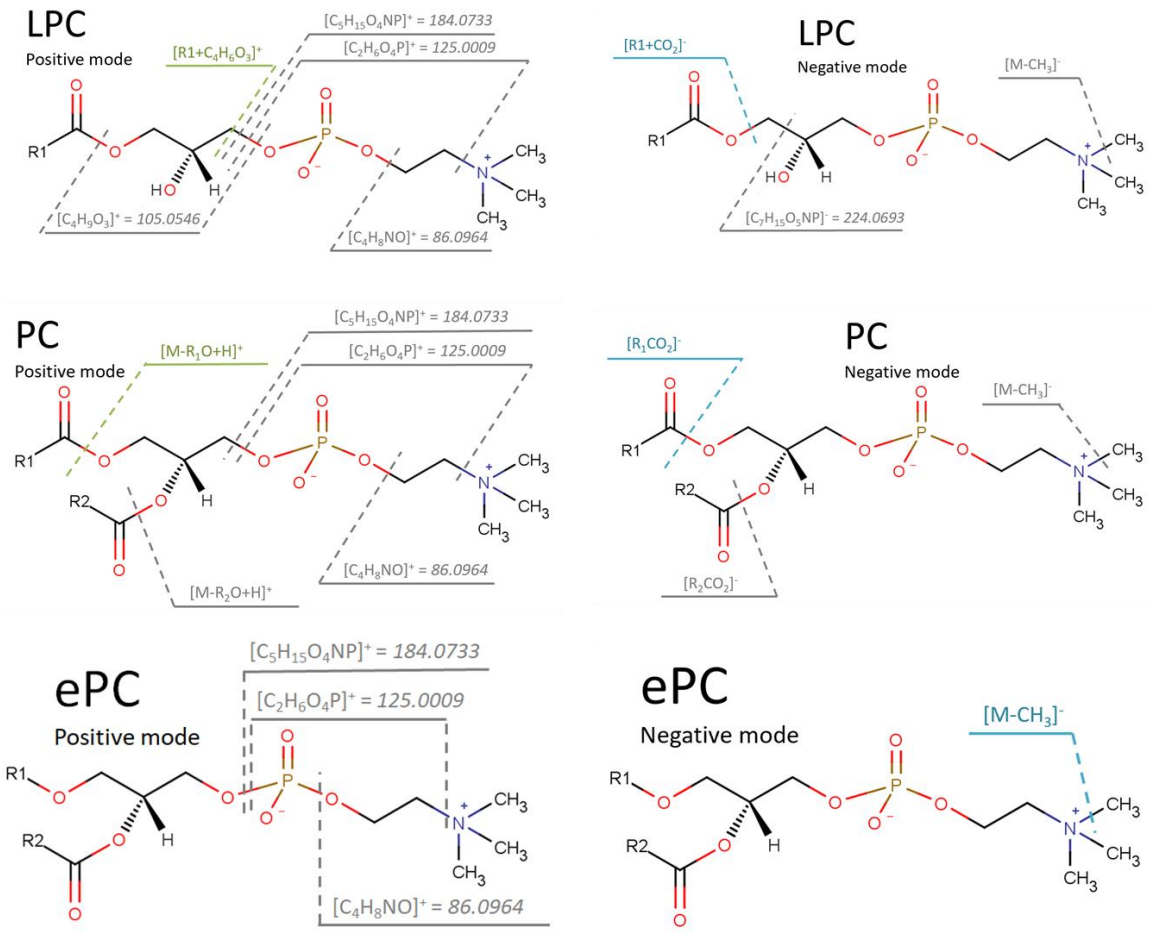

Figure 81. *Fragmentation of LPC, PC and ePC; coloured (green and blue) fragments were used for lipid identification (as in Table 54 of the main text), and grey fragments are given as additional information and were not used for identification nor for quantification.*

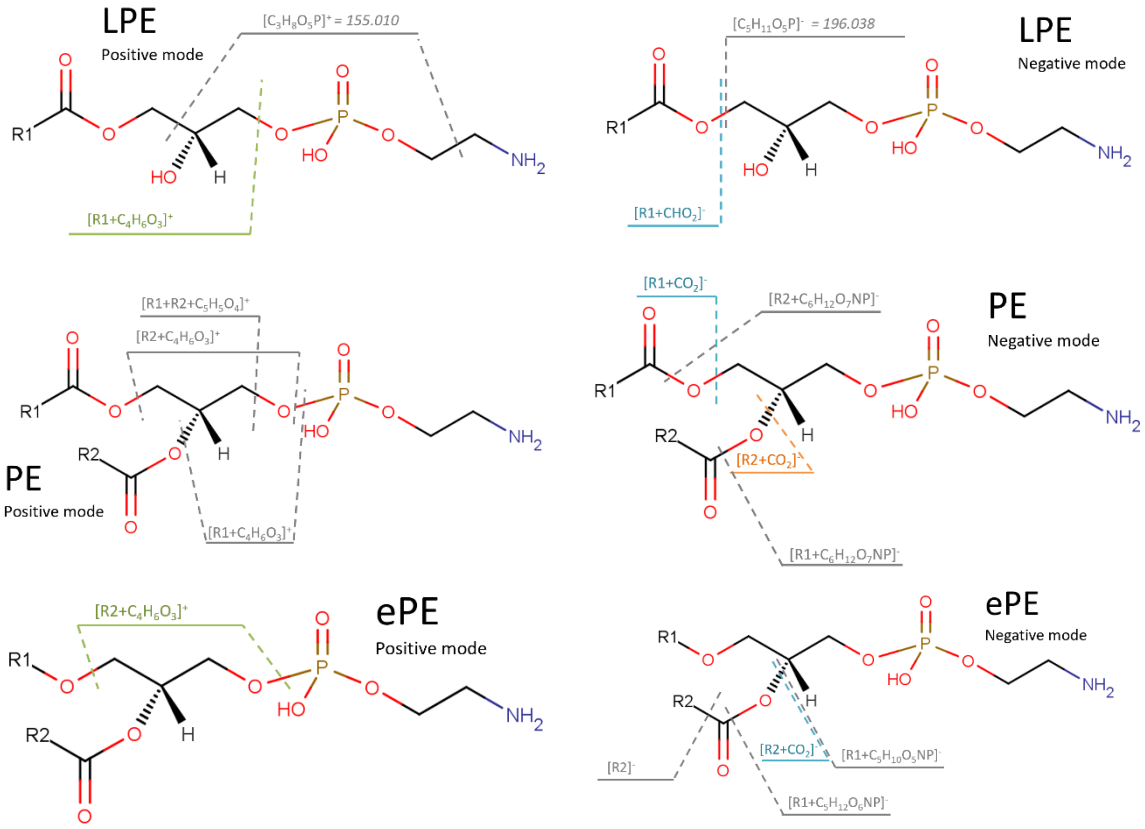

Figure 82. *Fragmentation of LPE, PE and ePE; coloured (green, blue and orange) fragments were used for lipid identification (as in Table 54 of the main text), and grey fragments are given as additional information and were not used for identification nor for quantification.*

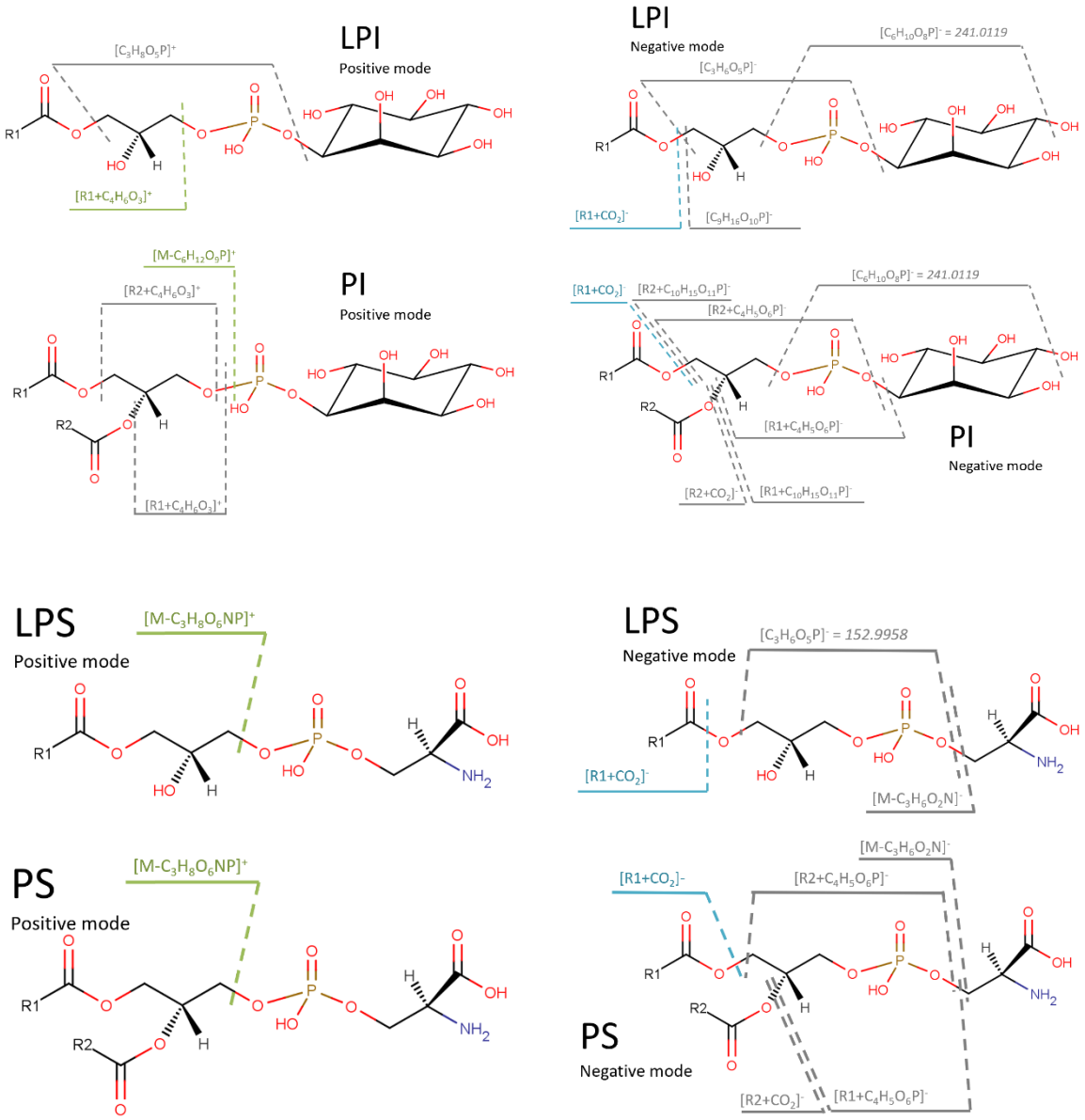

Figure 83. *Fragmentation of LPI, PI, LPS and PS; coloured (green and blue) fragments were used for lipid identification (as in Table 54 of the main text), and grey fragments are given as additional information and were not used for identification nor for quantification.*

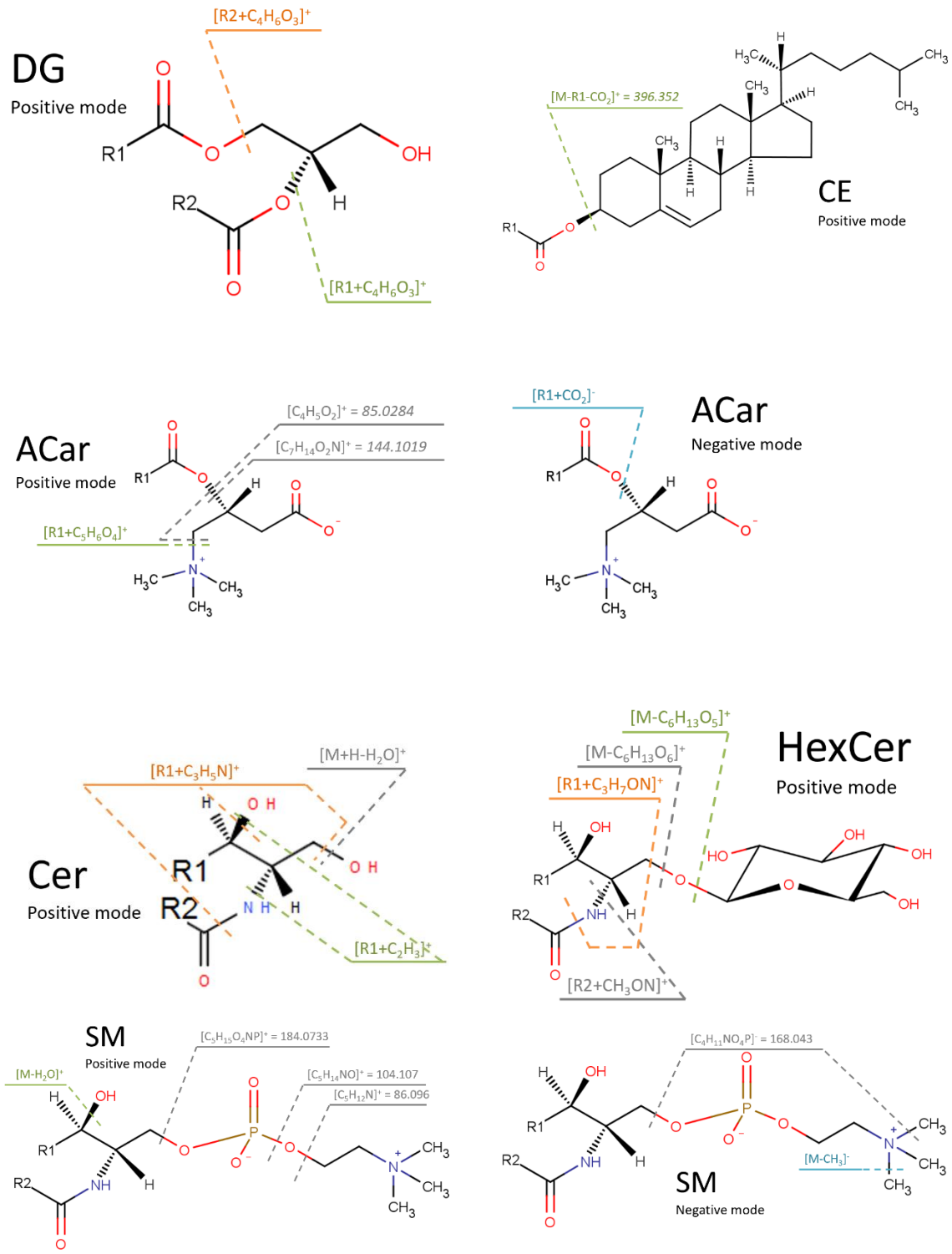

Figure 84. *Fragmentation of DG, CE, ACar, Cer, HexCer and SM; coloured (green, blue and orange) fragments were used for lipid identification (as in Table 54 of the main text), and grey fragments are given as additional information and were not used for identification nor for quantification.*

4.5.3. Lipid identification with empirical retention time prediction model

Figure 85 to Figure 87 present plots of *m/z* of precursor ion vs. retention time (peak spotting maps) for all lipid classes except of oxylipins. Oxylipins have more diverse structure than other lipid classes, so the retention time prediction model would possibly not work correctly for this class.

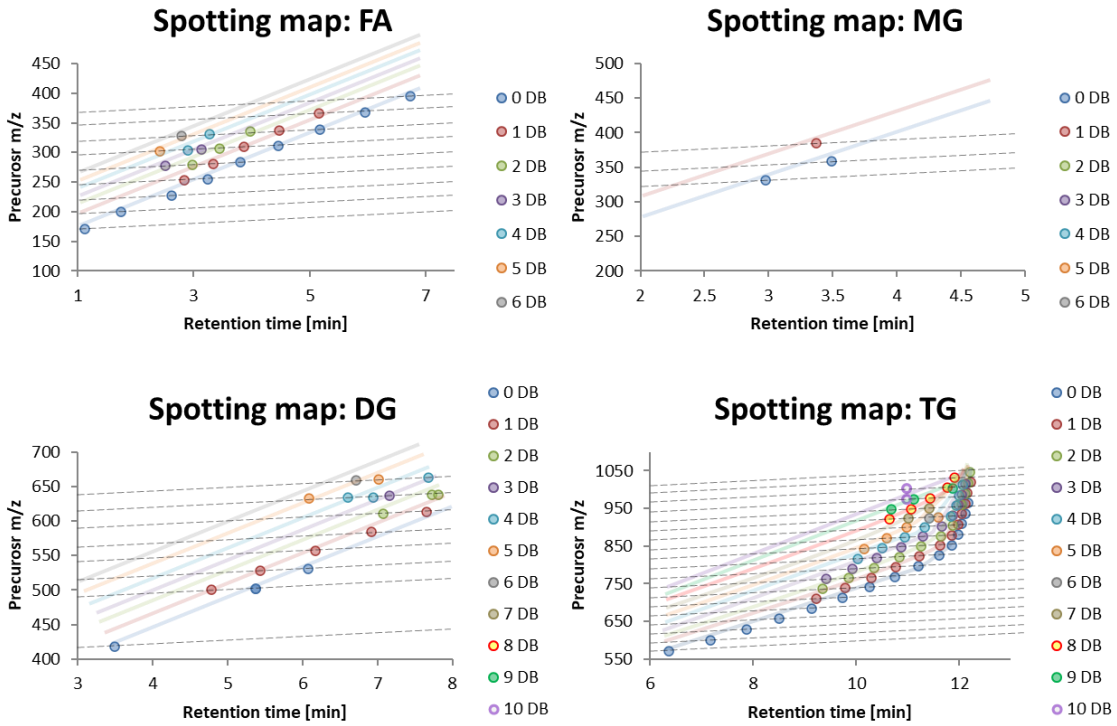

Figure 85. *Spotting maps showing relationship of precursor m/z and RT for 4 different lipid classes: FA, MG, DG and TG. The same symbols represent lipids with the same number of double bonds.*

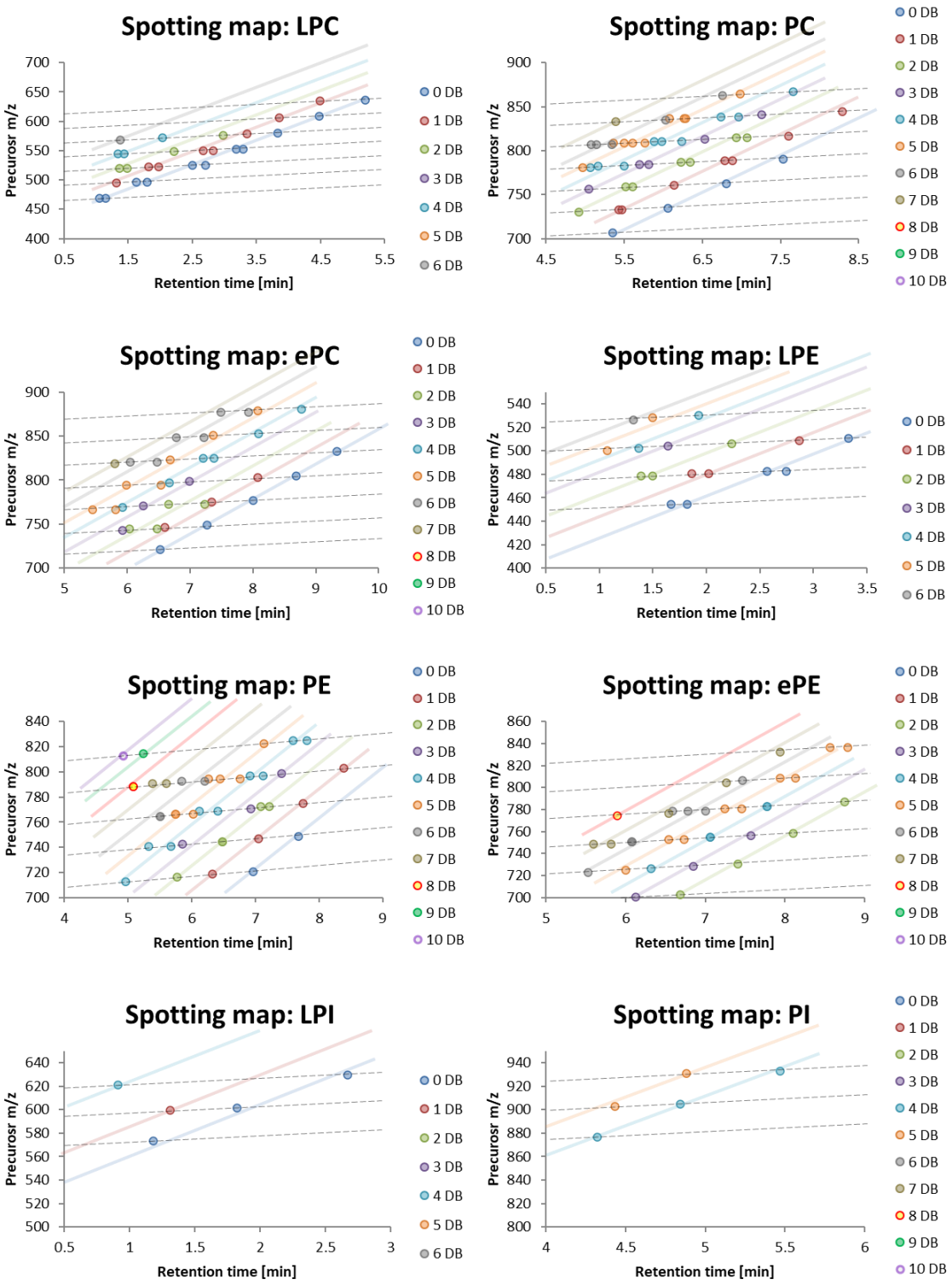

Figure 86. *Spotting maps showing relationship of precursor m/z and RT for 8 different lipid classes: LPC, PC, ePC, LPE, PE, ePE, LPI and PI. The same symbols represent lipids with the same number of double bonds.*

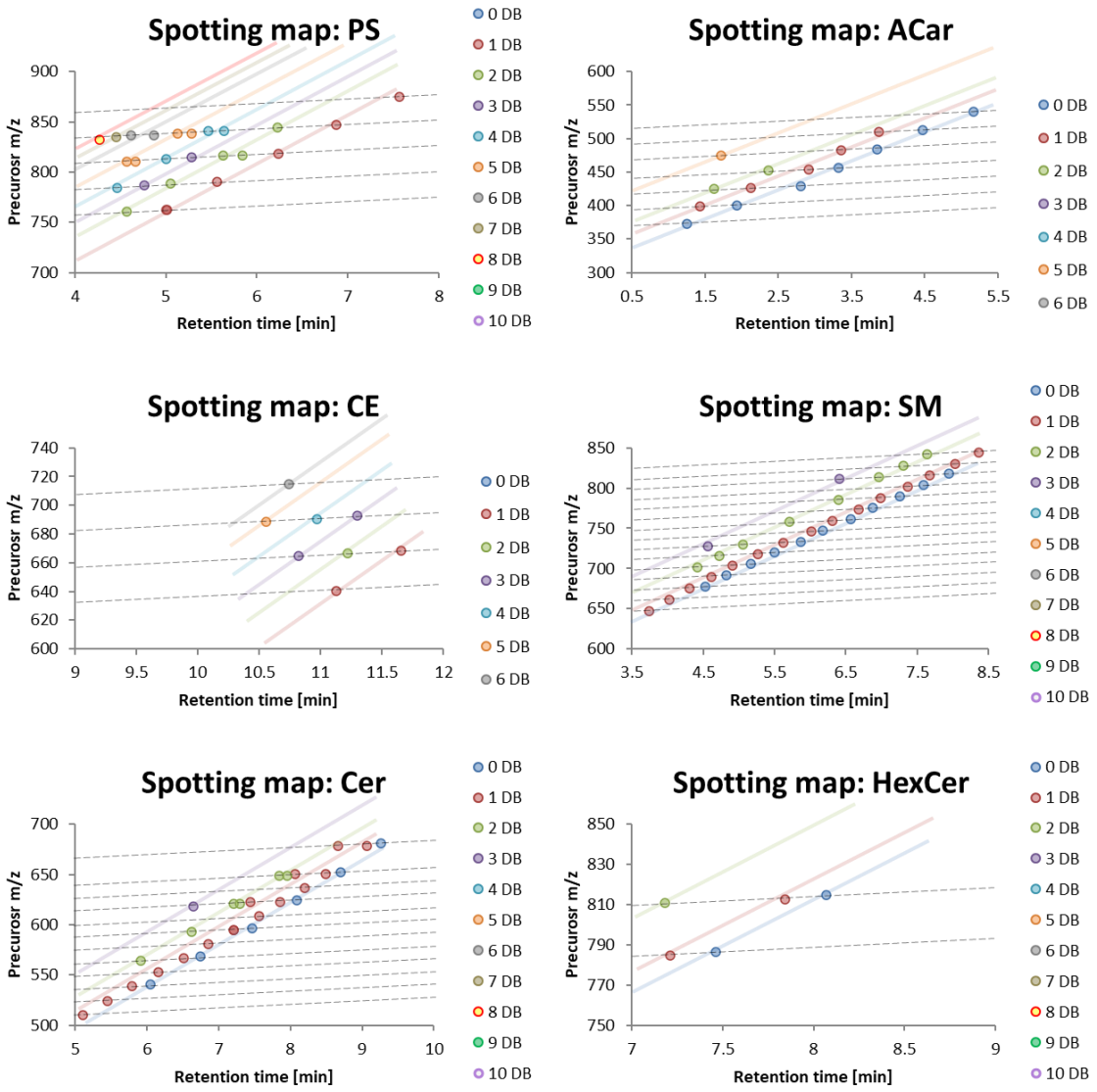

Figure 87. *Spotting maps showing the relationship of precursor m/z and RT for 7 different lipid classes: PS, ACar, CE, Cer, HexCer and SM. The same symbols represent lipids with the same number of double bonds.*

4.5.4. Lipid quantification

In the present studies, we aimed at identification and (relative) quantification of lipids in the most selective way possible with our LC-MS method targeting characterization of the lipidome at the molecular lipid species level. Many isomeric lipids from the same class are poorly separated on the LC column (because run times were kept short to allow high throughput in clinical studies and this was accompanied by a compromise in isomer selectivity). Their (relative) quantification as different lipid species is only possible with

characteristic fragment ions from SWATH. Such cases are exemplified in Figure 88 and Figure 89 as well as in Figure 76 of the main document.

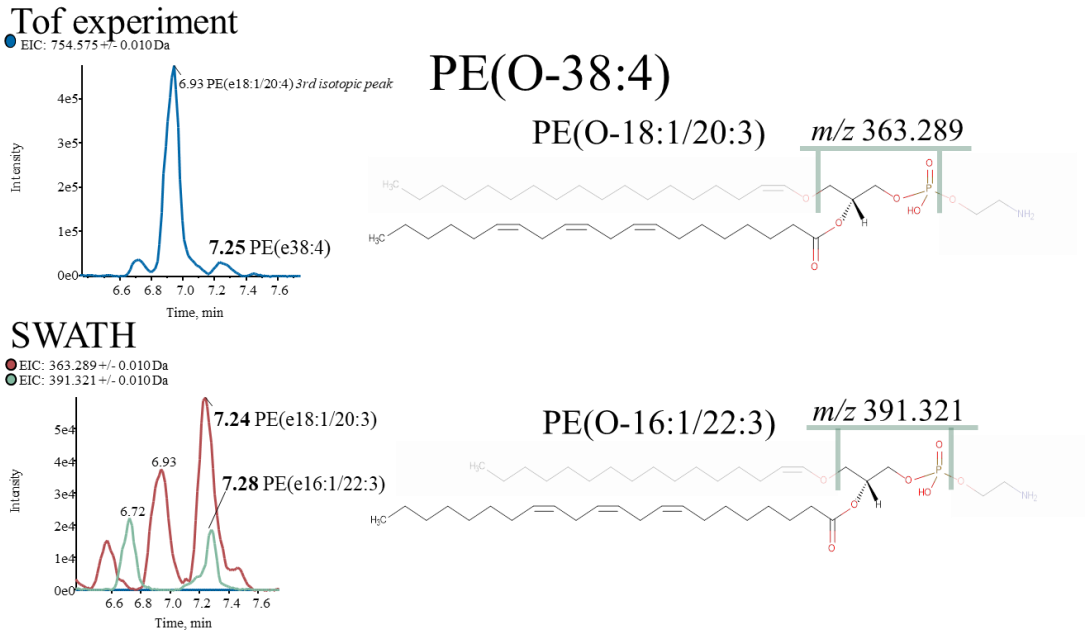

Figure 88. *Tof and SWATH signals for 2 isomeric lipids: PE(O-18:1/20:3) and PE(O-16:1/22:3) with proposed fragmentation for shown signals in SWATH. Quantification with TOF would be only possible as the sum of these compounds.*

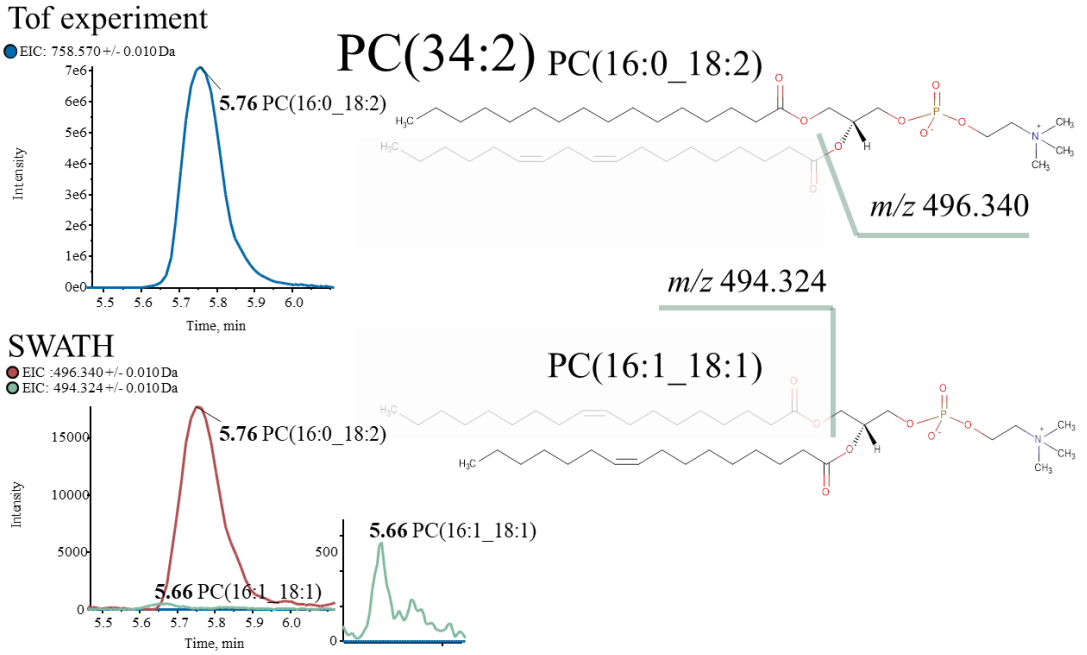

Figure 89. *TOF-MS and SWATH signals for 2 isomeric lipids: PC(16:0_18:2) and PC(16:1_18:1) with proposed fragmentation for shown signals in SWATH. Quantification with TOF would cause loss of information about the lower abundant lipid (PC(16:1_18:1)).*

4.5.5. Final results of 44 platelet samples with 4 different treatments – results of LC-MS analysis

Table 56. *CV (in %) of results for IS across all 44 samples and all QCs with and without LOWESS normalization. Green colour indicates the better results.*

CV (%)	without LOWESS	with LOWESS
PS(15:0_18:1d7)	13.2	11.7
TG(15:0_15:0_18:1d7)	18.3	12.4
LPC(18:1d7)	8.4	7.6
CE(18:1d7)	28.3	19.4
MG(18:1d7)	18.8	18.9
DG(15:0_18:1d7)	13.1	11.5
PI(15:0_18:1d7)	12.7	12.2
PC(15:0_18:1d7)	13.8	13.9
SM(d18:1_18:1d9)	25.9	27.3
LPE(18:1d7)	12.8	8.7
PE(15:0_18:1d7)	33.9	29.1
PG(15:0_18:1d7)	17.1	9.7

Data with normalized values were used for statistical analysis.

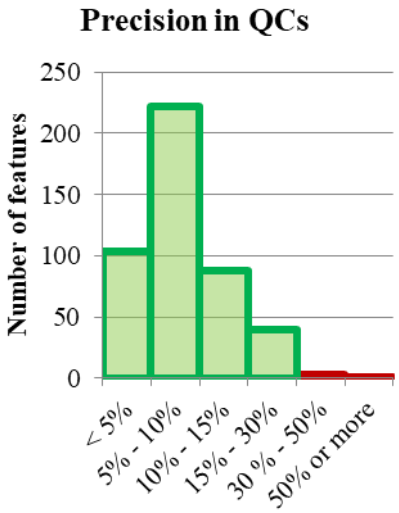

Figure 90. *Distribution of CVs for all the identified lipids in QCs; green bars show acceptable CV < 30% and red bars show data which were removed, because of CV > 30%.*

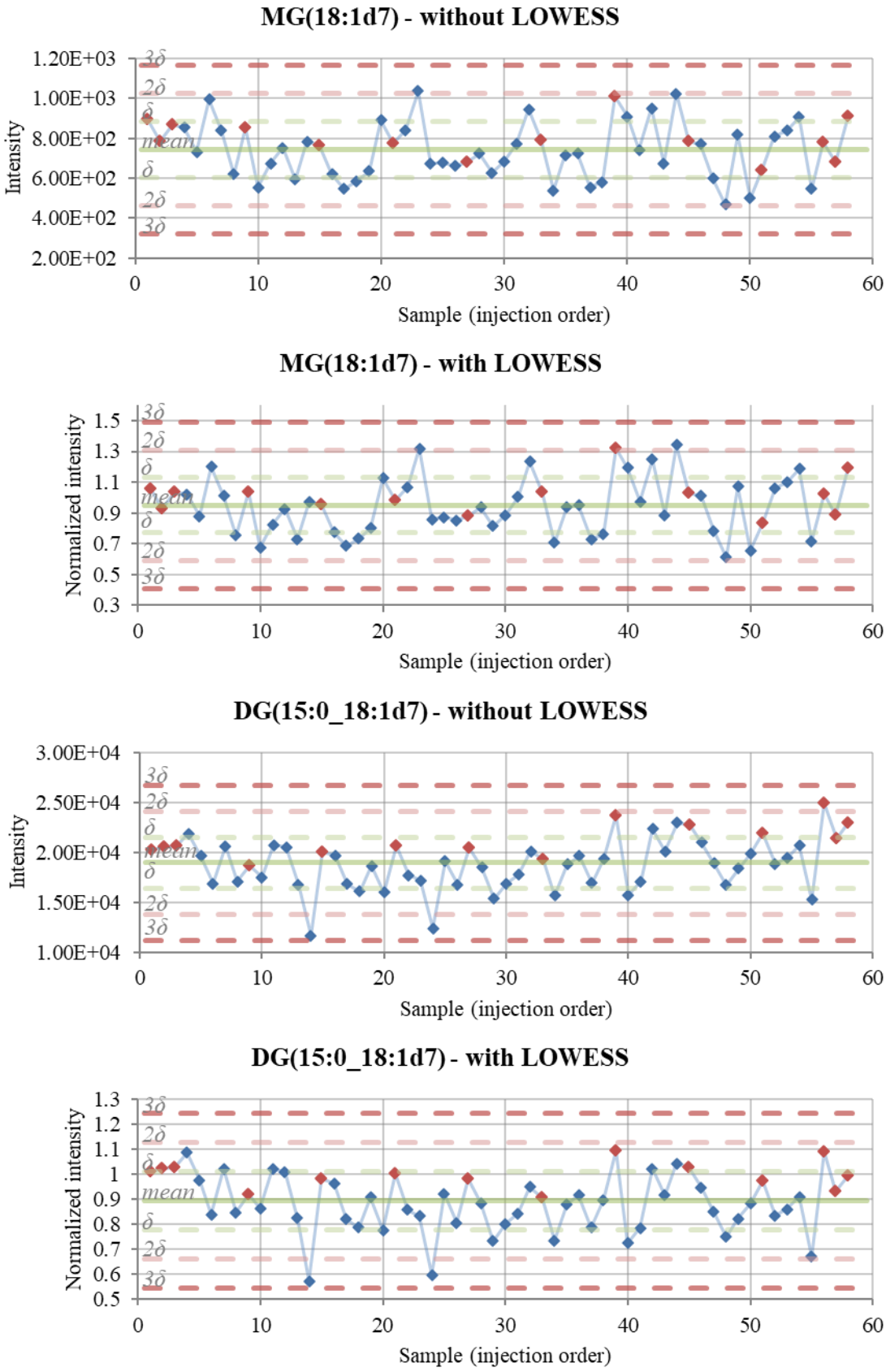

Figure 91. *Control charts of IS (MG and DG) proving good quality of the LC-MS analysis Blue points present results for samples and red points results for QC.*

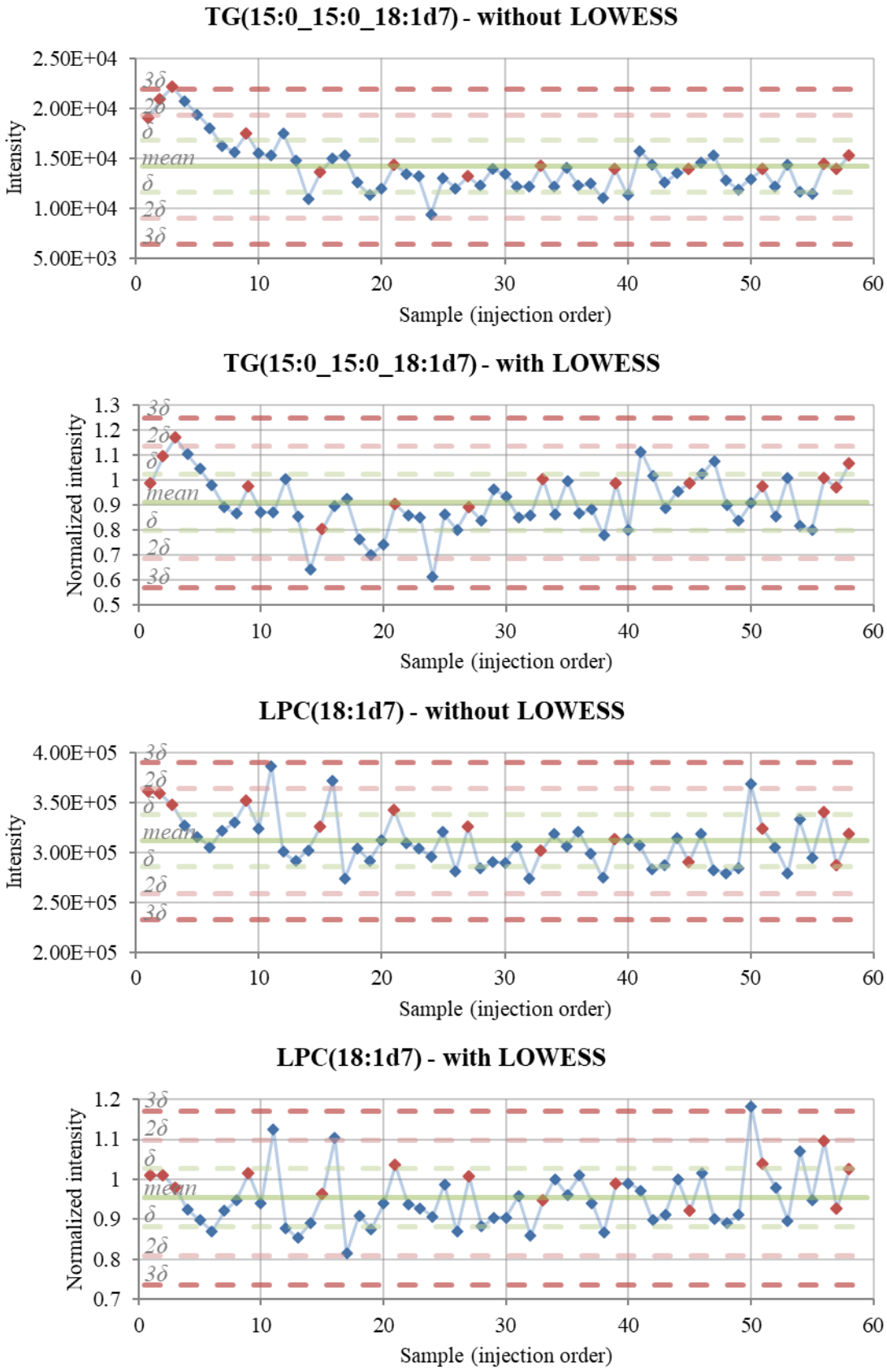

Figure 92. *Control charts of IS (TG and LPC) proving good quality of the LC-MS analysis. Blue points present results for samples and red points results for QC.*

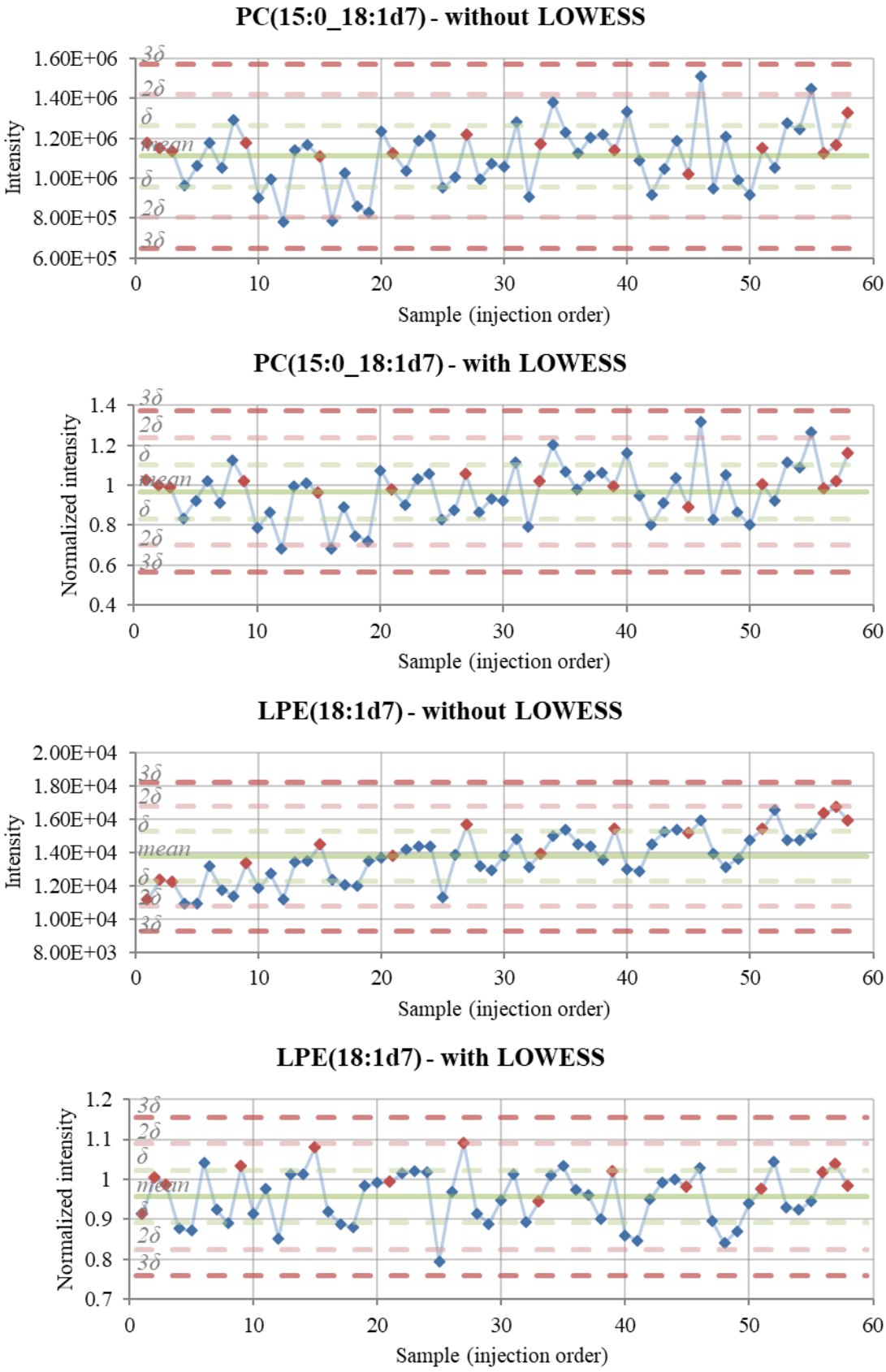

Figure 93. *Control charts of IS (PC and LPE) proving good quality of the LC-MS analysis. Blue points present results for samples and red points results for QC.*

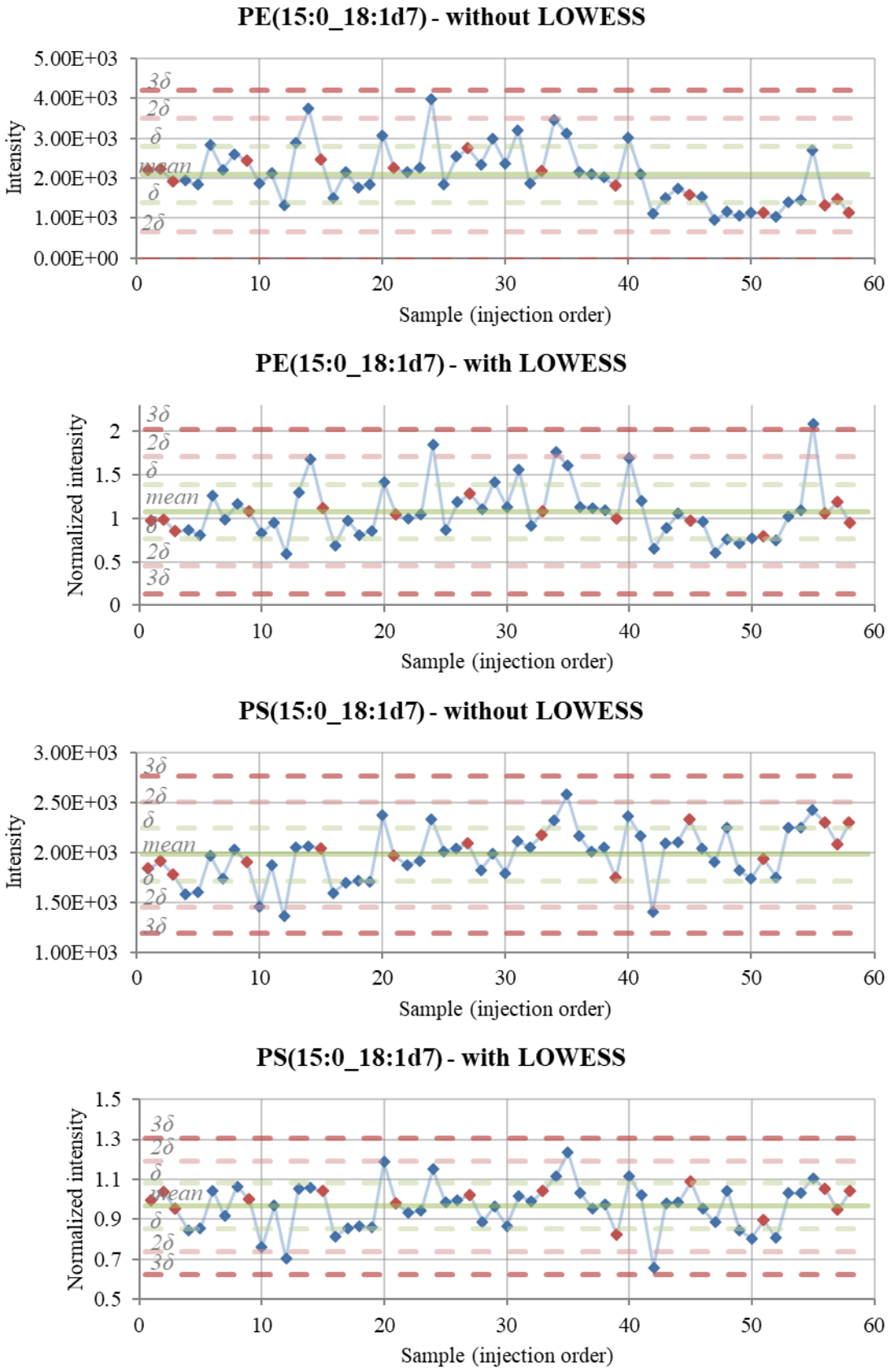

Figure 94. *Control charts of IS (PE and PS) proving good quality of the LC-MS analysis. Blue points present results for samples and red points results for QC.*

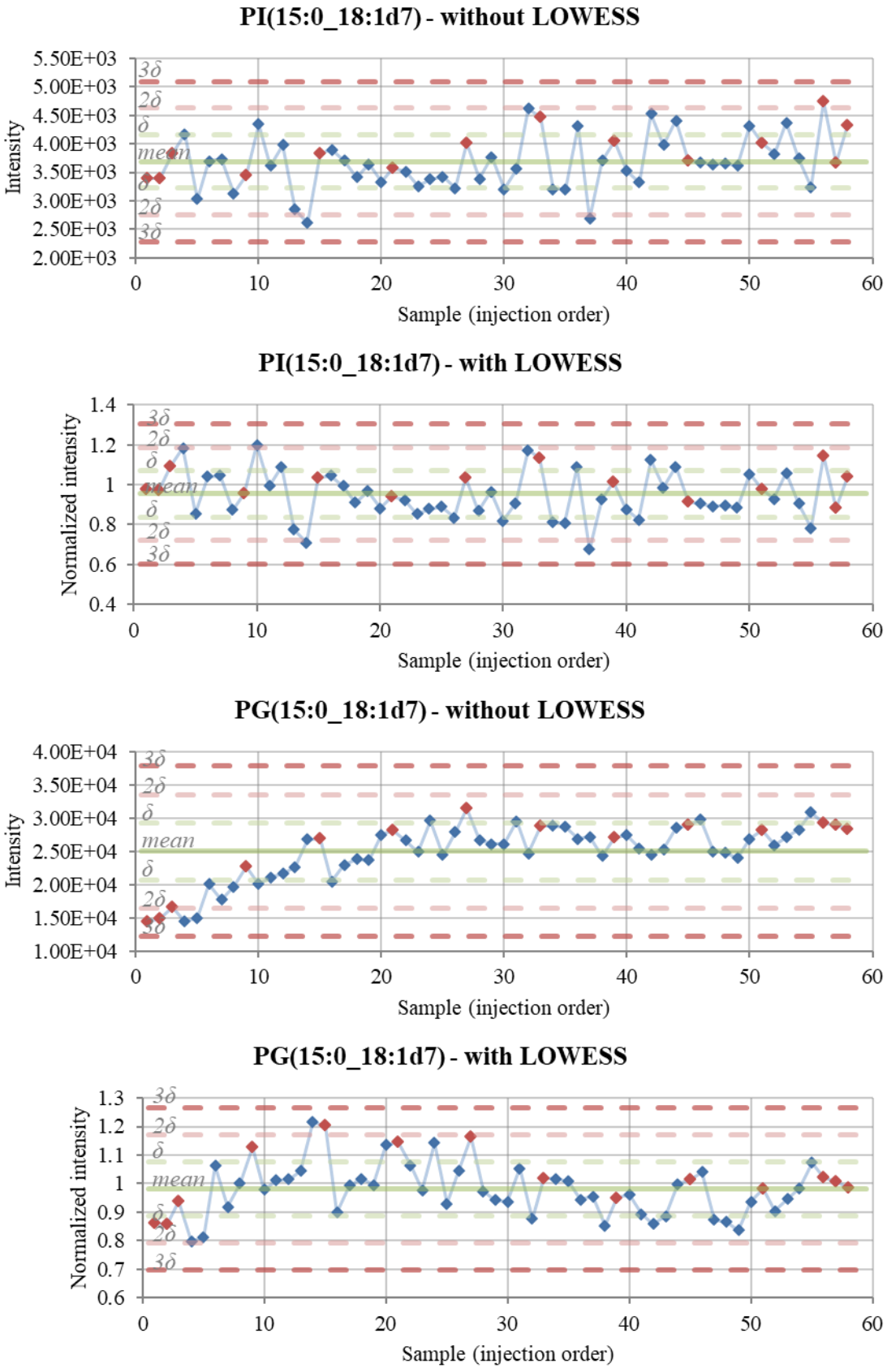

Figure 95. *Control charts of IS (PI and PG) proving good quality of the LC-MS analysis. Blue points present results for samples and red points results for QC.*

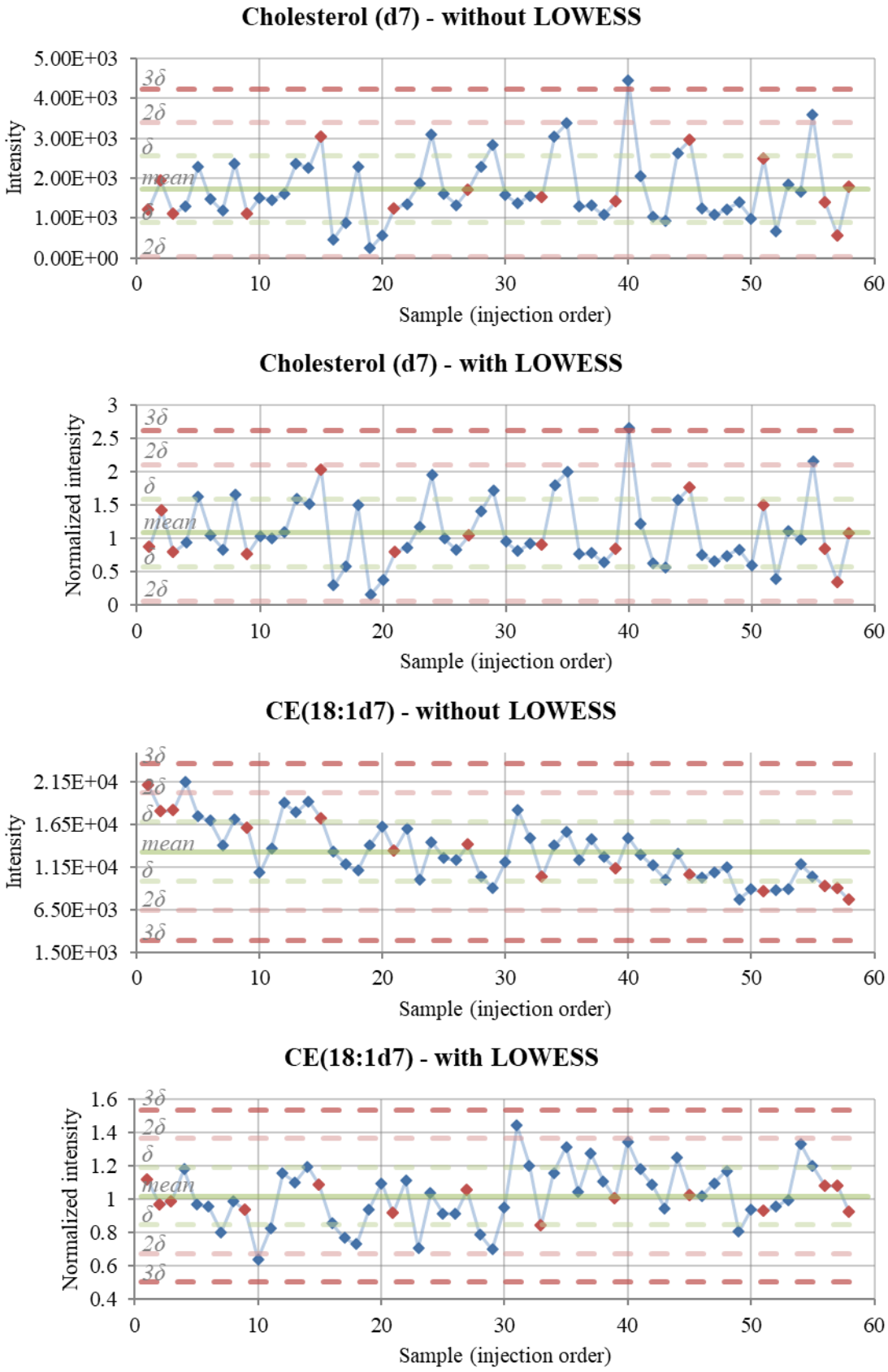

Figure 96. *Control charts of IS (cholesterol and CE) proving good quality of the LC-MS analysis. Blue points present results for samples and red points results for QC.*

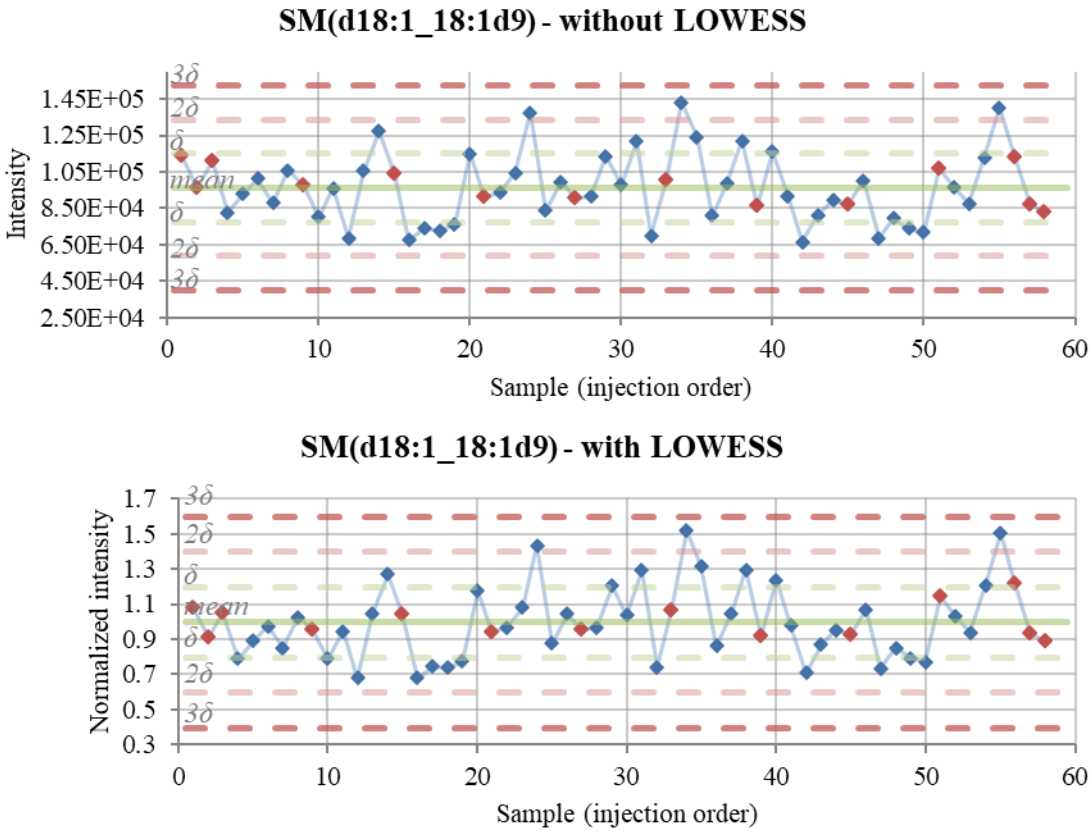

Figure 97. *Control charts of IS (SM) proving good quality of the LC-MS analysis. Blue points present results for samples and red points results for QC.*

Table 57 part 1. *List of all found lipids. Letters in the lipid names mean isomeric compounds which were separately quantified, but it was not possible to identify them at the level which would differentiate these compounds. All m/z used for identification are shown (as in Table 54 in the main document) as well as RT.*

Class	Lipid species	*m/z* 1	*m/z* 2	*m/z* 3	*m/z* 4	RT [min]
MG	MG(16:0)	331.2850	348.3116			2.98
	MG(18:0)	359.3163	376.3429			3.49
	MG(20:1)	385.3320	402.3586			3.37
	MG IS	364.3440	381.3700			3.06
LPC	LPC IS	529.3994	346.3333	573.3892	288.2912	1.96
	LPC(14:0)	468.3092	285.2431	512.2990	227.2012	1.15
	LPC(14:0)b	468.3092	285.2431	512.2990	227.2012	1.05
	LPC(16:1)	494.3249	311.2588	538.3147	253.2169	1.32
	LPC(16:0)	496.3405	313.2744	540.3304	255.2326	1.79
	LPC(16:0)b	496.3405	313.2744	540.3304	255.2326	1.63
	LPC(18:2)	520.3405	337.2744	564.3304	279.2326	1.48
	LPC(18:2)b	520.3405	337.2744	564.3304	279.2326	1.36
	LPC(18:1)	522.3562	339.2901	566.3460	281.2482	1.98
	LPC(18:1)b	522.3562	339.2901	566.3460	281.2482	1.82
	LPC(18:0)	524.3719	341.3058	568.3617	283.2639	2.70
	LPC(18:0)b	524.3719	341.3058	568.3617	283.2639	2.50
	LPC(20:4)	544.3405	361.2744	588.3304	303.2326	1.44
	LPC(20:4)b	544.3405	361.2744	588.3304	303.2326	1.34
	LPC(20:2)	548.3719	365.3058	592.3617	307.2639	2.21
	LPC(20:1)	550.3875	367.3214	594.3773	309.2795	2.83
	LPC(20:1)b	550.3875	367.3214	622.4087	337.3109	2.67
	LPC(20:0)	552.4032	369.3371	596.3930	311.2952	3.29
	LPC(20:0)b	552.4032	369.3371	596.3930	311.2952	3.18
	LPC(22:6)	568.3405	385.2744	612.3304	327.2326	1.38
	LPC(22:4)	572.3719	389.3058	616.3617	331.2639	2.03
	LPC(22:2)	576.4032	393.3371	620.3930	335.2952	2.98
	LPC(22:1)	578.4188	395.3527	622.4087	337.3109	3.35
	LPC(22:0)	580.4345	397.3684	624.4243	339.3265	3.83
	LPC(24:1)	606.4502	423.3841	650.4400	365.3422	3.85
	LPC(24:0)	608.4658	425.3997	652.4556	367.3578	4.48
	LPC(26:0)	636.4971	453.4310	680.4870	395.3892	5.20
	LPC(26:1)	634.4815	451.4154	678.4713	393.3735	4.49
CE	CE IS	675.6780	369.3523			11.63
	CE(18:1)	668.6350	369.3523			11.66
	CE(16:1)	640.6036	369.3523			11.13
	CE(18:3)	664.6036	369.3523			10.82
	CE(20:3)	692.6350	369.3523			11.30
	CE(20:4)	690.6193	369.3523			10.97
	CE(20:5)	688.6036	369.3523			10.56
	CE(22:6)	714.6193	369.3523			10.74
	CE(18:2)	666.6193	369.3523			11.22
DG	DG IS	605.5840	299.2589	346.3350	632.5490	7.26
	DG(20:4_18:1)	660.5570	361.2744	339.2901	701.5234	7.01
	DG(10:0_10:0)	418.3535	229.1805	229.1805	459.3198	3.49
	DG(16:0_10:0)	502.4474	313.2744	229.1805	543.4138	5.37
	DG(14:0_12:0)	502.4474	285.2431	257.2118	543.4138	5.37
	DG(18:1_10:0)	528.4631	339.2901	229.1805	569.4294	5.43
	DG(14:0_14:0)	530.4787	285.2431	285.2431	571.4451	6.08
	DG(18:1_14:0)	584.5257	339.2901	285.2431	625.4921	6.92
	DG(18:2_16:0)	610.5414	337.2744	313.2744	651.5077	7.07
	DG(18:1_12:0)	556.4944	339.2901	257.2118	597.4607	6.17
	DG(18:1_16:0)	612.5570	339.2901	313.2744	653.5234	7.65
	DG(18:3_18:2)	632.5257	335.2588	337.2744	673.4921	6.09
	DG(18:2_18:2)	634.5414	337.2744	337.2744	675.5077	6.60
	DG(20:4_16:0)	634.5414	361.2744	313.2744	675.5077	6.94
	DG(18:2_18:1)	636.5570	337.2744	339.2901	677.5234	7.16
	DG(18:1_18:1)	638.5727	339.2901	339.2901	679.5390	7.72
	DG(18:1_18:0)	640.5884	339.2901	341.3058	681.5547	8.34
	DG(18:2_18:0)	638.5727	337.2744	341.3058	679.5390	7.81
	DG(22:6_16:0)	658.5414	385.2744	313.2744	699.5077	6.71
	DG(20:4_18:0)	662.5727	361.2744	341.3058	703.5390	7.68
	DG(8:0_10:0)	390.3221	201.1492	229.1805	431.2885	3.06
	DG(8:0_18:1)	500.4318	201.1492	339.2901	541.3981	4.78

Table 57 part 2.

Class	Lipid species	*m/z* 1	*m/z* 2	*m/z* 3	*m/z* 4	RT [min]
TG	IS TG	829.7980				11.20
	TG(30:0)	572.4893				6.37
	TG(32:0)	600.5206				7.18
	TG(34:0)	628.5520				7.87
	TG(36:0)	656.5833				8.51
	TG(38:0)	684.6146				9.15
	TG(40:0)	712.6459				9.74
	TG(42:0)	740.6772				10.27
	TG(44:0)	768.7086				10.75
	TG(46:0)	796.7399				11.20
	TG(48:0)	824.7712				11.61
	TG(50:0)	852.8025				11.86
	TG(52:0)	880.8338				11.98
	TG(54:0)	908.8652				12.06
	TG(56:0)	936.8965				12.12
	TG(58:0)	964.9278				12.18
	TG(40:1)	710.6303				9.22
	TG(42:1)	738.6616				9.79
	TG(44:1)	766.6929				10.30
	TG(46:1)	794.7242				10.78
	TG(48:1)	822.7555				11.22
	TG(50:1)	850.7869				11.63
	TG(52:1)	878.8182				11.86
	TG(54:1)	906.8495				11.98
	TG(56:1)	934.8808				12.06
	TG(58:1)	962.9121				12.12
	TG(60:1)	990.9435				12.16
	TG(62:1)	1018.9748				12.22
	TG(42:2)	736.6459				9.34
	TG(44:2)	764.6772				9.86
	TG(46:2)	792.7086				10.36
	TG(48:2)	820.7399				10.84
	TG(50:2)	848.7712				11.26
	TG(52:2)	876.8025				11.64
	TG(54:2)	904.8338				11.87
	TG(58:2)	960.8965				12.06
	TG(62:2)	1016.9591				12.17
	TG(64:2)	1044.9904				12.22
	TG(44:3)	762.6616				9.41
	TG(46:3)	790.6929				9.93
	TG(48:3)	818.7242				10.41
	TG(50:3)	846.7555				10.88
	TG(52:3)	874.7869				11.30
	TG(54:3)	902.8182				11.67
	TG(56:3)	930.8495				11.88
	TG(58:3)	958.8808				11.99
	TG(60:3)	986.9121				12.06
	TG(62:3)	1014.9435				12.12
	TG(48:4)	816.7086				10.03
	TG(50:4)	844.7399				10.51
	TG(52:4)	872.7712				10.95
	TG(54:4)	900.8025				11.33
	TG(56:4)	928.8338				11.84
	TG(58:4)	956.8652				11.94
	TG(60:4)	984.8965				12.00
	TG(62:4)	1012.9278				12.07
	TG(50:5)	842.7242				10.16
	TG(52:5)	870.7555				10.59
	TG(54:5)	898.7869				10.99
	TG(56:5)	926.8182				11.59
	TG(60:2)	988.9278				12.12
	TG(56:6)	924.8025				11.42
	TG(56:7)	922.7869				11.02
	TG(58:7)	950.8182				11.42
	TG(56:8)	920.7712				10.65
	TG(58:8)	948.8025				11.06
	TG(60:8)	976.8338				11.45
	TG(62:8)	1004.8652				11.78
	TG(64:8)	1032.8965				11.91
	TG(58:9)	946.7869				10.69
	TG(60:9)	974.8182				11.12
	TG(62:9)	1002.8495				11.87
	TG(60:10)	972.8025				10.99

Table 57 part 3.

Class	Lipid species	*m/z* 1	*m/z* 2	*m/z* 3	*m/z* 4	RT [min]
PE	PE IS	711.5660	709.5520	288.2905	288.2905	5.94
	PE(20:4_14:0)	712.4920	710.4764	227.2012	303.2326	4.96
	PE(18:0_16:0)	720.5547	718.5390	255.2326	283.2639	6.96
	PE(18:1_16:0)	718.5390	716.5234	255.2326	281.2482	6.33
	PE(18:2_16:0)	716.5234	714.5077	255.2326	279.2326	5.78
	PE(20:4_16:0)	740.5234	738.5077	255.2326	303.2326	5.68
	PE(22:4_16:0)	768.5547	766.5390	255.2326	331.2639	6.12
	PE(22:5_16:0)	766.5390	764.5234	255.2326	329.2482	5.75
	PE(22:6_16:0)	764.5234	762.5077	255.2326	327.2326	5.51
	PE(18:0_18:0)	748.5860	746.5703	283.2639	283.2639	7.67
	PE(18:1_18:0)	746.5703	744.5547	283.2639	281.2482	7.06
	PE(22:1_18:0)	802.6330	800.6173	283.2639	337.3109	8.38
	PE(18:2_18:0)	744.5547	742.5390	283.2639	279.2326	6.49
	PE(20:3_18:0)	770.5703	768.5547	283.2639	305.2482	6.93
	PE(22:3_18:0)	798.6017	796.5860	283.2639	333.2795	7.41
	PE(20:4_18:0)	768.5547	766.5390	283.2639	303.2326	6.41
	PE(22:4_18:0)	796.5860	794.5703	283.2639	331.2639	6.92
	PE(20:5_18:0)	766.5390	764.5234	283.2639	301.2169	6.03
	PE(22:5_18:0)	794.5703	792.5547	283.2639	329.2482	6.76
	PE(22:6_18:0)	792.5547	790.5390	283.2639	327.2326	6.21
	PE(18:1_20:0)	774.6017	772.5860	311.2952	281.2482	7.75
	PE(18:2_20:0)	772.5860	770.5703	311.2952	279.2326	7.22
	PE(20:4_20:0)	796.5860	794.5703	311.2952	303.2326	7.12
	PE(22:4_20:0)	824.6173	822.6017	311.2952	331.2639	7.60
	PE(20:4_22:0)	824.6173	822.6017	339.3265	303.2326	7.81
	PE(18:1_18:1)	744.5547	742.5390	281.2482	281.2482	6.49
	PE(20:1_18:1)	772.5860	770.5703	281.2482	309.2795	7.08
	PE(18:2_18:1)	742.5390	740.5234	281.2482	279.2326	5.86
	PE(20:4_18:1)	766.5390	764.5234	281.2482	303.2326	5.75
	PE(22:4_18:1)	794.5703	792.5547	281.2482	331.2639	6.26
	PE(22:6_18:1)	790.5390	788.5234	281.2482	327.2326	5.60
	PE(20:4_20:1)	794.5703	792.5547	309.2795	303.2326	6.44
	PE(20:4_22:1)	822.6017	820.5860	337.3109	303.2326	7.13
	PE(18:2_18:2)	740.5234	738.5077	279.2326	279.2326	5.33
	PE(20:4_18:2)	764.5234	762.5077	279.2326	303.2326	5.51
	PE(22:6_18:2)	788.5234	786.5077	279.2326	327.2326	5.08
	PE(20:4_20:2)	792.5547	790.5390	307.2639	303.2326	5.85
	PE(20:4_20:3)	790.5390	788.5234	305.2482	303.2326	5.39
	PE(20:4_20:4)	788.5234	786.5077	303.2326	303.2326	5.08
	PE(22:5_20:4)	814.5390	812.5234	303.2326	329.2482	5.24
	PE(22:6_20:4)	812.5234	810.5077	303.2326	327.2326	4.94
ePE	PE(e16:1/18:1)	702.5441	700.5285	339.2901	281.2482	6.68
	PE(e16:1/18:2)	700.5285	698.5128	337.2744	279.2326	6.12
	PE(e16:1/20:3)	726.5441	724.5285	363.2901	305.2482	6.32
	PE(e16:1/22:3)	754.5754	752.5598	391.3214	333.2795	7.06
	PE(e16:1/20:4)	724.5285	722.5128	361.2744	303.2326	6.00
	PE(e16:1/22:4)	752.5598	750.5441	389.3058	331.2639	6.53
	PE(e16:1/20:5)	722.5128	720.4971	359.2588	301.2169	5.53
	PE(e16:1/22:5)	750.5441	748.5285	387.2901	329.2482	6.07
	PE(e16:1/22:6)	748.5285	746.5128	385.2744	327.2326	5.81
	PE(e18:1/18:1)	730.5754	728.5598	339.2901	281.2482	7.41
	PE(e18:1/18:2)	728.5598	726.5441	337.2744	279.2326	6.85
	PE(e18:1/20:3)	754.5754	752.5598	363.2901	305.2482	7.06
	PE(e18:1/22:3)	782.6068	780.5911	391.3214	333.2795	7.77
	PE(e18:1/20:4)	752.5598	750.5441	361.2744	303.2326	6.74
	PE(e18:1/22:4)	780.5911	778.5754	389.3058	331.2639	7.25
	PE(e18:1/20:5)	750.5441	748.5285	359.2588	301.2169	6.07
	PE(e18:1/22:5)	778.5754	776.5598	387.2901	329.2482	6.78
	PE(e18:1/22:6)	776.5598	774.5441	385.2744	327.2326	6.54
	PE(e18:2/20:4)	750.5441	748.5285	361.2744	303.2326	6.07
	PE(e18:2/22:4)	778.5754	776.5598	389.3058	331.2639	6.59
	PE(e18:2/20:5)	748.5285	746.5128	359.2588	301.2169	5.60
	PE(e18:2/22:6)	774.5441	772.5285	385.2744	327.2326	5.89
	PE(e20:1/18:1)	758.6068	756.5911	339.2901	281.2482	8.10
	PE(e20:1/18:2)	756.5911	754.5754	337.2744	279.2326	7.57
	PE(e20:1/20:3)	782.6068	780.5911	363.2901	305.2482	7.77
	PE(e20:1/20:4)	780.5911	778.5754	361.2744	303.2326	7.46
	PE(e20:1/22:4)	808.6224	806.6068	389.3058	331.2639	7.94
	PE(e20:1/20:5)	778.5754	776.5598	359.2588	301.2169	7.01
	PE(e20:1/22:5)	806.6068	804.5911	387.2901	329.2482	7.47
	PE(e20:1/22:6)	804.5911	802.5754	385.2744	327.2326	7.26
	PE(e22:1/18:1)	786.6381	784.6224	339.2901	281.2482	8.75
	PE(e22:1/20:4)	808.6224	806.6068	361.2744	303.2326	8.13
	PE(e22:1/22:4)	836.6537	834.6381	389.3058	331.2639	8.56
	PE(e22:1/22:6)	832.6224	830.6068	385.2744	327.2326	7.94
	PE(e24:1/20:4)	836.654	834.638	361.274	303.233	8.79

Table 57 part 4.

Class	Lipid species	*m/z* 1	*m/z* 2	*m/z* 3	*m/z* 4	RT [min]
PC	PC(18:1_16:0)	760.5860	804.5758	496.3405	281.2482	6.14
	PC(16:0_14:0)	706.5390	750.5288	468.3092	255.2326	5.36
	PC(14:0_14:0)	678.5077	722.4975	468.3092	227.2012	4.67
	PC(16:1_16:0)	732.5547	776.5445	496.3405	253.2169	5.47
	PC(16:0_16:0)	734.5703	778.5602	496.3405	255.2326	6.06
	PC(18:2_14:0)	730.5390	774.5288	468.3092	279.2326	4.92
	PC(18:1_14:0)	732.5547	776.5445	468.3092	281.2482	5.43
	PC(18:2_16:0)	758.5703	802.5602	496.3405	279.2326	5.61
	PC(18:2_16:1)	756.5547	800.5445	494.3249	279.2326	5.04
	PC(18:1_16:1)	758.5703	802.5602	494.3249	281.2482	5.52
	PC(18:0_16:0)	762.6017	806.5915	496.3405	283.2639	6.81
	PC(20:5_16:0)	780.5547	824.5445	496.3405	301.2169	5.06
	PC(20:4_16:0)	782.5703	826.5602	496.3405	303.2326	5.50
	PC(20:3_16:0)	784.5860	828.5758	496.3405	305.2482	5.82
	PC(20:1_16:0)	788.6173	832.6071	496.3405	309.2795	6.79
	PC(18:2_18:0)	786.6017	830.5915	524.3719	279.2326	6.34
	PC(18:1_18:0)	788.6173	832.6071	524.3719	281.2482	6.89
	PC(18:1_18:1)	786.6017	830.5915	522.3562	281.2482	6.23
	PC(18:2_18:1)	784.5860	828.5758	522.3562	279.2326	5.69
	PC(18:2_18:2)	782.5703	826.5602	520.3405	279.2326	5.17
	PC(20:4_16:1)	780.5547	824.5445	494.3249	303.2326	4.97
	PC(20:0_16:0)	790.6330	834.6228	496.3405	311.2952	7.53
	PC(22:6_16:0)	806.5703	850.5602	496.3405	327.2326	5.35
	PC(22:5_16:0)	808.5860	852.5758	496.3405	329.2482	5.50
	PC(22:4_16:0)	810.6017	854.5915	496.3405	331.2639	5.98
	PC(20:5_18:0)	808.5860	852.5758	524.3719	301.2169	5.76
	PC(20:4_18:0)	810.6017	854.5915	524.3719	303.2326	6.24
	PC(20:4_18:1)	808.5860	852.5758	522.3562	303.2326	5.60
	PC(20:3_18:1)	810.6017	854.5915	522.3562	305.2482	5.89
	PC(20:5_18:1)	806.5703	850.5602	522.3562	301.2169	5.14
	PC(20:4_18:2)	806.5703	850.5602	520.3405	303.2326	5.07
	PC(20:3_18:2)	808.5860	852.5758	520.3405	305.2482	5.36
	PC(20:3_18:0)	812.6173	856.6071	524.3719	305.2482	6.53
	PC(18:2_20:0)	814.6330	858.6228	552.4032	279.2326	7.08
	PC(18:1_20:0)	816.6486	860.6385	552.4032	281.2482	7.61
	PC(20:1_18:1)	814.6330	858.6228	522.3562	309.2795	6.93
	PC(22:6_18:0)	834.6017	878.5915	524.3719	327.2326	6.03
	PC(22:5_18:0)	836.6173	880.6071	524.3719	329.2482	6.28
	PC(22:4_18:0)	838.6330	882.6228	524.3719	331.2639	6.74
	PC(20:4_20:0)	838.6330	882.6228	552.4032	303.2326	6.96
	PC(20:3_20:0)	840.6486	884.6385	552.4032	305.2482	7.25
	PC(18:1_22:0)	844.6800	888.6698	580.4345	281.2482	8.29
	PC(22:6_18:1)	832.5860	876.5758	522.3562	327.2326	5.39
	PC(22:4_18:1)	836.6173	880.6071	522.3562	331.2639	6.08
	PC(20:4_20:1)	836.6173	880.6071	550.3875	303.2326	6.27
	PC(22:6_20:0)	862.6330	906.6228	552.4032	327.2326	6.76
	PC(22:5_20:0)	864.6486	908.6385	552.4032	329.2482	6.99
ePC	PC(20:4_22:0)	866.6643	910.6541	580.4345	303.2326	7.67
	PC(e32:0)	720.5911	764.5809	704.5598		6.52
	PC(e34:0)	748.6224	792.6122	732.5911		7.28
	PC(e34:1)	746.6068	790.5966	730.5754		6.61
	PC(e34:2)a	744.5911	788.5809	728.5598		6.04
	PC(e34:2)b	744.5911	788.5809	728.5598		6.49
	PC(e34:3)	742.5754	786.5653	726.5441		5.93
	PC(e36:0)	776.6537	820.6436	760.6224		8.01
	PC(e36:1)	774.6381	818.6279	758.6068		7.34
	PC(e36:2)a	772.6224	816.6122	756.5911		6.67
	PC(e36:2)b	772.6224	816.6122	756.5911		7.24
	PC(e36:3)	770.6068	814.5966	754.5754		6.26
	PC(e36:4)	768.5911	812.5809	752.5598		5.93
	PC(e36:5)a	766.5754	810.5653	750.5441		5.45
	PC(e36:5)b	766.5754	810.5653	750.5441		5.82
	PC(e38:0)	804.6851	848.6749	788.6537		8.69
	PC(e38:1)	802.6694	846.6592	786.6381		8.08
	PC(e38:3)	798.6381	842.6279	782.6068		7.00
	PC(e38:4)	796.6224	840.6122	780.5911		6.67
	PC(e38:5)a	794.6068	838.5966	778.5754		5.99
	PC(e38:5)b	794.6068	838.5966	778.5754		6.54
	PC(e40:0)	832.7164	876.7062	816.6851		9.33
	PC(e40:4)a	824.6537	868.6436	808.6224		7.38
	PC(e40:4)b	824.6537	868.6436	808.6224		7.20
	PC(e40:5)	822.6381	866.6279	806.6068		6.69
	PC(e40:6)a	820.6224	864.6122	804.5911		6.05
	PC(e40:6)b	820.6224	864.6122	804.5911		6.47
	PC(e40:7)	818.6068	862.5966	802.5754		5.81
	PC(e42:4)	852.6851	896.6749	836.6537		8.09
	PC(e42:5)	850.6694	894.6592	834.6381		7.37
	PC(e42:6)a	848.6537	892.6436	832.6224		6.79
	PC(e42:6)b	848.6537	892.6436	832.6224		7.22
	PC(e44:4)	880.7164	924.7062	864.6851		8.77
	PC(e44:5)	878.7007	922.6905	862.6694		8.07
	PC(e44:6)a	876.6851	920.6749	860.6537		7.49
	PC(e44:6)b	876.6851	920.6749	860.6537		7.93

Table 57 part 5.

Class	Lipid species	*m/z* 1	*m/z* 2	*m/z* 3	*m/z* 4	RT [min]
ACar	ACar(14:0)	372.3116	313.2380	416.3014	227.2012	1.26
	ACar(16:0)	400.3429	341.2694	444.3327	255.2326	1.94
	ACar(16:1)	398.3272	339.2537	442.3171	253.2169	1.43
	ACar(18:0)	428.3742	369.3007	472.3640	283.2639	2.81
	ACar(18:1)	426.3586	367.2850	470.3484	281.2482	2.13
	ACar(18:2)	424.3429	365.2694	468.3327	279.2326	1.62
	ACar(20:0)	456.4055	397.3320	500.3954	311.2952	3.32
	ACar(20:1)	454.3899	395.3163	498.3797	309.2795	2.91
	ACar(20:2)	452.3742	393.3007	496.3640	307.2639	2.36
	ACar(20:3)	450.3586	391.2850	494.3484	305.2482	1.88
	ACar(22:0)	484.4369	425.3633	528.4267	339.3265	3.85
	ACar(22:1)	482.4212	423.3477	526.4110	337.3109	3.36
	ACar(22:5)	474.3586	415.2850	518.3484	329.2482	1.72
	ACar(24:0)	512.4682	453.3946	556.4580	367.3578	4.47
	ACar(24:1)	510.4525	451.3790	554.4423	365.3422	3.88
	ACar(26:0)	540.4995	481.4260	584.4893	395.3892	5.17
SM	SM IS	738.6470	720.6400	782.6380	722.6138	5.01
	SM(d30:1)	647.5131	629.5026	691.5029	631.4818	3.74
	SM(d31:1)	661.5288	643.5182	705.5186	645.4975	4.03
	SM(d32:0)	677.5601	659.5495	721.5499	661.5288	4.53
	SM(d32:1)	675.5444	657.5339	719.5343	659.5131	4.31
	SM(d33:0)	691.5758	673.5652	735.5656	675.5444	4.83
	SM(d33:1)	689.5601	671.5495	733.5499	673.5288	4.61
	SM(d34:0)	705.5914	687.5809	749.5812	689.5601	5.17
	SM(d34:1)	703.5758	685.5652	747.5656	687.5444	4.91
	SM(d34:2)	701.5601	683.5495	745.5499	685.5288	4.41
	SM(d35:0)	719.6071	701.5965	763.5969	703.5758	5.50
	SM(d35:1)	717.5914	699.5809	761.5812	701.5601	5.26
	SM(d35:2)	715.5758	697.5652	759.5656	699.5444	4.73
	SM(d36:0)	733.6227	715.6122	777.6126	717.5914	5.86
	SM(d36:1)	731.6071	713.5965	775.5969	715.5758	5.62
	SM(d36:2)	729.5914	711.5809	773.5812	713.5601	5.06
	SM(d36:3)	727.5758	709.5652	771.5656	711.5444	4.56
	SM(d37:0)	747.6384	729.6278	791.6282	731.6071	6.18
	SM(d37:1)	745.6227	727.6122	789.6126	729.5914	6.01
	SM(d38:0)	761.6541	743.6435	805.6439	745.6227	6.57
	SM(d38:1)	759.6384	741.6278	803.6282	743.6071	6.31
	SM(d38:2)	757.6227	739.6122	801.6126	741.5914	5.71
	SM(d39:0)	775.6697	757.6592	819.6595	759.6384	6.87
	SM(d39:1)	773.6541	755.6435	817.6439	757.6227	6.68
	SM(d40:0)	789.6854	771.6748	833.6752	773.6541	7.26
	SM(d40:1)	787.6697	769.6592	831.6595	771.6384	6.99
	SM(d40:2)	785.6541	767.6435	829.6439	769.6227	6.40
	SM(d41:0)	803.7010	785.6905	847.6909	787.6697	7.59
	SM(d41:1)	801.6854	783.6748	845.6752	785.6541	7.36
	SM(d42:0)	817.7167	799.7061	861.7065	801.6854	7.94
	SM(d42:1)	815.7010	797.6905	859.6909	799.6697	7.67
	SM(d42:2)	813.6854	795.6748	857.6752	797.6541	6.96
	SM(d42:3)	811.6697	793.6592	855.6595	795.6384	6.40
	SM(d43:1)	829.7167	811.7061	873.7065	813.6854	8.03
	SM(d43:2)	827.7010	809.6905	871.6909	811.6697	7.31
	SM(d44:1)	843.7324	825.7218	887.7222	827.7010	8.36
	SM(d44:2)	841.7167	823.7061	885.7065	825.6854	7.64
PS	PS(18:1_16:0)	762.5288	577.5199	760.5132	281.2482	5.00
	PS(18:2_16:0)	760.5132	575.5043	758.4975	279.2326	4.57
	PS(20:4_16:0)	784.5132	599.5043	782.4975	303.2326	4.47
	PS(16:1_18:0)	762.5288	577.5199	760.5132	253.2169	5.01
	PS(18:1_18:0)	790.5602	605.5512	788.5445	281.2482	5.56
	PS(20:2_18:0)	816.5758	631.5669	814.5602	307.2639	5.84
	PS(20:3_18:0)	814.5602	629.5512	812.5445	305.2482	5.29
	PS(20:4_18:0)	812.5445	627.5356	810.5288	303.2326	5.00
	PS(20:5_18:0)	810.5288	625.5199	808.5132	301.2169	4.67
	PS(22:4_18:0)	840.5758	655.5669	838.5602	331.2639	5.47
	PS(22:5_18:0)	838.5602	653.5512	836.5445	329.2482	5.28
	PS(22:6_18:0)	836.5445	651.5356	834.5288	327.2326	4.87
	PS(18:1_20:0)	818.5915	633.5826	816.5758	281.2482	6.23
	PS(18:1_22:0)	846.6228	661.6139	844.6071	281.2482	6.87
	PS(18:1_24:0)	874.6541	689.6452	872.6385	281.2482	7.56
	PS(20:4_20:0)	840.5758	655.5669	838.5602	303.2326	5.64
	PS(20:5_20:0)	838.5602	653.5512	836.5445	301.2169	5.13
	PS(18:1_18:1)	788.5445	603.5356	786.5288	281.2482	5.05
	PS(18:2_18:1)	786.5288	601.5199	784.5132	279.2326	4.77
	PS(20:1_18:1)	816.5758	631.5669	814.5602	309.2795	5.63
	PS(22:1_18:1)	844.6071	659.5982	842.5915	337.3109	6.23
	PS(20:4_18:1)	810.5288	625.5199	808.5132	303.2326	4.57
	PS(22:6_18:1)	834.5288	649.5199	832.5132	327.2326	4.45
	PS(20:4_20:2)	836.5445	651.5356	834.5288	303.2326	4.62
	PS(20:4_20:4)	832.5132	647.5043	830.4975	303.2326	4.28
	PS IS	755.5560	570.5471	753.5420	241.2147	4.66

Table 57 part 6.

Class	Lipid species	*m/z* 1	*m/z* 2	*m/z* 3	*m/z* 4	RT [min]
LPS	LPS(18:0)	526.3147	341.3058	524.2990	437.2670	1.90
LPE	LPE IS	487.3520	346.3324	485.3380	288.2908	2.00
	LPE(16:0)	454.2936	313.2744	452.2779	255.2326	1.82
	LPE(16:0)b	454.2936	313.2744	452.2779	255.2326	1.67
	LPE(18:0)	482.3249	341.3058	480.3092	283.2639	2.75
	LPE(18:0)b	482.3249	341.3058	480.3092	283.2639	2.57
	LPE(18:1)	480.3092	339.2901	478.2936	281.2482	2.02
	LPE(18:1)b	480.3092	339.2901	478.2936	281.2482	1.86
	LPE(18:2)	478.2936	337.2744	476.2779	279.2326	1.50
	LPE(18:2)b	478.2936	337.2744	476.2779	279.2326	1.39
	LPE(20:1)	508.3405	367.3214	506.3249	309.2795	2.87
	LPE(20:2)	506.3249	365.3058	504.3092	307.2639	2.24
	LPE(20:3)	504.3092	363.2901	502.2936	305.2482	1.64
	LPE(20:4)	502.2936	361.2744	500.2779	303.2326	1.37
	LPE(20:5)	500.2779	359.2588	498.2622	301.2169	1.07
	LPE(20:0)	510.3562	369.3371	508.3405	311.2952	3.33
	LPE(22:4)	530.3249	389.3058	528.3092	331.2639	1.93
	LPE(22:5)	528.3092	387.2901	526.2936	329.2482	1.50
	LPE(22:6)	526.2936	385.2744	524.2779	327.2326	1.32
LPI	LPI(16:0)	573.3042	313.2744	571.2885	255.2326	1.18
	LPI(18:1)	599.3198	339.2901	597.3042	281.2482	1.31
	LPI(18:0)	601.3355	341.3058	599.3198	283.2639	1.82
	LPI(20:4)	621.3042	361.2744	619.2885	303.2326	0.91
	LPI(20:0)	629.3668	369.3371	627.3512	311.2952	2.67
PI	PI IS	847.6040	570.5479	828.5620	288.2861	4.50
	PI(20:4_18:0)	904.5919	627.5356	885.5497	283.2639	4.84
	PI(20:4_16:0)	876.5606	599.5043	857.5183	255.2326	4.32
	PI(20:4_20:0)	932.6232	655.5669	913.5810	311.2952	5.47
	PI(20:4_20:1)	930.6075	653.5512	911.5653	309.2795	4.88
	PI(20:4_18:1)	902.5762	625.5199	883.5340	281.2482	4.43
Cer	Cer(d17:1/16:0)	524.5046	222.2349	250.2536	568.4944	5.45
	Cer(d17:1/18:0)	552.5359	222.2349	250.2536	596.5257	6.16
	Cer(d17:1/20:0)	580.5672	222.2349	250.2536	624.5570	6.86
	Cer(d17:1/22:0)	608.5985	222.2349	250.2536	652.5884	7.57
	Cer(d17:1/24:0)	636.6299	222.2349	250.2536	680.6197	8.20
	Cer(d18:0/16:0)	540.5359	238.2662	266.2850	584.5257	6.05
	Cer(d18:0/18:0)	568.5672	238.2662	266.2850	612.5570	6.75
	Cer(d18:0/20:0)	596.5985	238.2662	266.2850	640.5884	7.47
	Cer(d18:0/20:1)	594.5829	238.2662	266.2850	638.5727	7.21
	Cer(d18:0/22:0)	624.6299	238.2662	266.2850	668.6197	8.09
	Cer(d18:0/22:1)	622.6142	238.2662	266.2850	666.6040	7.44
	Cer(d18:0/24:0)	652.6612	238.2662	266.2850	696.6510	8.70
	Cer(d18:0/24:1)	650.6455	238.2662	266.2850	694.6353	8.06
	Cer(d18:0/26:0)	680.6925	238.2662	266.2850	724.6823	9.26
	Cer(d18:0/26:1)	678.6768	238.2662	266.2850	722.6667	8.66
	Cer(d18:1/14:0)	510.4889	236.2506	264.2693	554.4787	5.11
	Cer(d18:1/16:0)	538.5202	236.2506	264.2693	582.5101	5.80
	Cer(d18:1/18:0)	566.5516	236.2506	264.2693	610.5414	6.52
	Cer(d18:1/18:1)	564.5359	236.2506	264.2693	608.5257	5.92
	Cer(d18:1/20:0)	594.5829	236.2506	264.2693	638.5727	7.21
	Cer(d18:1/22:0)	622.6142	236.2506	264.2693	666.6040	7.86
	Cer(d18:1/22:1)	620.5985	236.2506	264.2693	664.5884	7.21
	Cer(d18:1/24:0)	650.6455	236.2506	264.2693	694.6353	8.49
	Cer(d18:1/24:1)	648.6299	236.2506	264.2693	692.6197	7.84
	Cer(d18:1/26:0)	678.6768	236.2506	264.2693	722.6667	9.07
	Cer(d18:2/20:0)	592.5672	234.2349	262.2536	636.5570	6.62
	Cer(d18:2/22:0)	620.5985	234.2349	262.2536	664.5884	7.29
	Cer(d18:2/22:1)	618.5829	234.2349	262.2536	662.5727	6.65
	Cer(d18:2/24:0)	648.6299	234.2349	262.2536	692.6197	7.96
HexCer	HexCer(d18:0/22:0)	786.6827	606.6193	284.2955	830.6725	7.46
	HexCer(d18:0/24:0)	814.7140	634.6506	284.2955	858.7039	8.07
	HexCer(d18:1/22:0)	784.6671	604.6036	282.2799	828.6569	7.21
	HexCer(d18:1/24:0)	812.6984	632.6350	282.2799	856.6882	7.84
	HexCer(d18:1/24:1)	810.6827	630.6193	282.2799	854.6725	7.18
FA	FA(10:0)	171.1386				1.12
	FA(12:0)	199.1699				1.74
	FA(14:0)	227.2012				2.63
	FA(16:0)	255.2326				3.25
	FA(16:1)	253.2169				2.83
	FA(18:0)	283.2639				3.81
	FA(18:1)	281.2482				3.33
	FA(18:2)	279.2326				2.98
	FA(18:3)	277.2169				2.51
	FA(20:0)	311.2952				4.45
	FA(20:1)	309.2795				3.86
	FA(20:2)	307.2639				3.44
	FA(20:3)	305.2482				3.13
	FA(20:4)	303.2326				2.90
	FA(20:5)	301.2169				2.42
	FA(22:0)	339.3265				5.18
	FA(22:1)	337.3109				4.48
	FA(22:2)	335.2952				3.98
	FA(22:4)	331.2639				3.28
	FA(22:6)	327.2326				2.79
	FA(24:0)	367.3578				5.95
	FA(24:1)	365.3422				5.16
	FA(26:0)	395.3892				6.74
cholesterol	cholesterol	369.3516				5.32
	cholesterol IS	376.3960				5.25

4.5.6. Estimation of absolute lipid concentrations

Table 58. *Results of estimation of absolute lipid concentrations for MG, DG and TG in resting and thrombin-activated platelets. Results are shown as average amount (nmol) per 1 million platelets.*

	Resting											Thrombin										
Donor:	*1*	*2*	*3*	*4*	*5*	*6*	*7*	*8*	*9*	*10*	*11*	*1*	*2*	*3*	*4*	*5*	*6*	*7*	*8*	*9*	*10*	*11*
MG(16:0)	1E+00	4E-01	4E+01	7E-01	5E-01	5E-01	4E-01	2E-01	3E-01	2E-01	2E-01	3E-01	3E-01	3E-01	3E-01	1E+00	3E-01	6E-01	3E-01	2E+00	4E-01	3E-01
MG(18:0)	7E-01	6E-01	8E+00	6E-01	5E-01	4E-01	5E-01	2E-01	4E-01	3E-01	2E-01	2E-01	4E-01	3E-01	4E-01	2E+00	3E-01	3E-01	4E-01	7E-01	3E-01	3E-01
MG(20:1)	8E-02	4E-01	0E+00	2E-01	2E-01	2E-01	6E-02	1E+01	2E+01	9E+00	9E+00	4E-02	8E-01	2E-01	5E-02	6E-02	6E-02	3E-01	1E+01	8E+00	9E+00	1E+01
DG(18:0)	2E-01	6E-02	6E+01	6E-02	3E-02	2E-01	6E-02	5E-02	9E-02	5E-02	9E-02	4E-02	1E-02	2E-02	4E-02	0E+00	6E-02	1E-01	7E-02	1E+00	1E-01	1E-01
DG(20:0)	1E-01	3E-02	3E+01	4E-02	6E-02	2E-01	7E-02	1E-02	3E-02	2E-02	3E-02	4E-02	2E-02	2E-02	6E-02	2E-02	5E-02	2E-01	8E-02	4E-01	6E-02	6E-02
DG(26:0)	5E-02	1E-01	4E+00	4E-02	7E-02	1E-01	2E-01	1E-01	6E-02	2E-02	5E-02	8E-02	3E-02	5E-02	6E-02	5E-02	6E-02	2E-01	1E-01	2E-01	4E-02	9E-02
DG(28:0)	9E-02	7E-02	3E+00	8E-02	7E-02	8E-02	1E-01	8E-02	3E-02	3E-02	7E-02	7E-02	8E-02	1E-01	5E-02	3E-02	8E-02	2E-01	1E-01	2E-01	5E-02	2E-01
DG(26:1)	2E-02	2E-02	3E+00	2E-02	4E-02	2E-02	5E-02	1E-02	2E-02	2E-02	3E-02	3E-02	1E-02	0E+00	3E-02	2E-02	2E-02	4E-02	2E-02	2E-02	1E-02	0E+00
DG(28:1)	7E-02	3E-02	3E+00	4E-02	2E-01	1E-01	2E-01	1E-01	1E-01	4E-02	6E-02	8E-02	9E-02	3E-02	2E-02	4E-02	5E-02	7E-02	6E-02	1E-01	2E-02	2E-02
DG(30:1)	8E-02	6E-02	6E+00	3E-01	1E-01	1E-01	2E-01	2E-01	1E-01	6E-02	2E-01	6E-02	2E-01	1E-01	4E-02	9E-02	7E-02	2E-01	1E-01	2E-01	1E-01	2E-01
DG(32:1)	5E-01	4E-01	2E+01	4E-01	4E-01	6E-01	1E+00	6E-01	7E-01	3E-01	3E-01	6E-01	4E-01	5E-01	5E-01	2E-01	4E-01	9E-01	6E-01	1E+00	5E-01	4E-01
DG(34:1)	3E+00	2E+00	4E+01	2E+00	2E+00	4E+00	8E+00	3E+00	3E+00	2E+00	1E+00	5E+00	2E+00	3E+00	2E+00	1E+00	4E+00	6E+00	3E+00	6E+00	4E+00	2E+00
DG(36:1)	1E+00	8E-01	1E+01	8E-01	8E-01	1E+00	3E+00	1E+00	9E-01	1E+00	5E-01	2E+00	1E+00	1E+00	8E-01	6E-01	2E+00	2E+00	1E+00	2E+00	2E+00	1E+00
DG(34:2)	2E+00	8E-01	1E+01	1E+00	1E+00	2E+00	4E+00	2E+00	2E+00	2E+00	6E-01	3E+00	1E+00	2E+00	9E-01	8E-01	2E+00	3E+00	2E+00	3E+00	3E+00	1E+00
DG(36:2)	5E+00	2E+00	7E+01	2E+00	3E+00	5E+00	1E+01	3E+00	4E+00	3E+00	2E+00	1E+01	2E+00	3E+00	2E+00	1E+00	4E+00	6E+00	2E+00	7E+00	3E+00	3E+00
DG(36:3)	4E+00	9E-01	1E+01	2E+00	2E+00	3E+00	1E+01	4E+00	4E+00	3E+00	2E+00	8E+00	1E+00	2E+00	2E+00	1E+00	2E+00	4E+00	2E+00	7E+00	3E+00	2E+00
DG(36:4)a	2E+00	3E-01	2E+01	7E-01	6E-01	1E+00	3E+00	7E-01	1E+00	8E-01	4E-01	3E+00	3E-01	8E-01	6E-01	2E-01	5E-01	1E+00	6E-01	2E+00	8E-01	5E-01
DG(36:4)b	6E-01	8E-01	1E+00	4E-01	9E-01	6E-01	5E-01	1E+00	6E-01	1E+00	3E-01	7E-01	1E+00	6E-01	4E-01	4E-01	2E+00	8E-01	1E+00	1E+00	2E+00	3E-01
DG(38:4)	1E+01	1E+01	1E+01	6E+00	2E+01	1E+01	8E+00	2E+01	2E+01	1E+01	5E+00	2E+01	1E+01	8E+00	3E+00	3E+00	1E+01	1E+01	2E+01	1E+01	1E+01	4E+00
DG(36:5)	4E-01	4E-02	9E-01	3E-01	1E-01	1E-01	5E-01	1E-01	1E-01	6E-02	5E-02	6E-01	3E-02	1E-01	7E-02	4E-02	3E-02	2E-01	1E-01	2E-01	3E-02	3E-02
DG(38:5)	9E-01	7E-01	2E+00	5E-01	1E+00	1E+00	7E-01	1E+00	1E+00	9E-01	4E-01	7E-01	1E+00	7E-01	4E-01	2E-01	9E-01	6E-01	8E-01	1E+00	1E+00	3E-01
DG(36:6)	1E+00	7E-01	4E+00	2E-01	3E-01	1E+00	5E-01	6E-01	7E-01	2E-01	5E-01	1E+00	6E-01	3E-01	2E-01	1E-01	8E-01	4E-01	4E-01	8E-01	6E-01	8E-01
TG(30:0)	7E-01	2E-01	4E+01	2E-01	0E+00	6E-01	2E-01	7E-02	9E-02	1E-01	5E-02	1E-01	0E+00	0E+00	1E-01	0E+00	8E-02	4E-01	1E-01	2E+00	4E-01	2E-01
TG(32:0)	6E-02	3E-02	2E+00	2E-02	1E-02	5E-02	3E-01	3E-02	4E-02	2E-02	2E-02	4E-02	1E-02	2E-02	3E-02	3E-02	7E-02	2E-01	4E-02	7E-02	4E-02	3E-02
TG(34:0)	4E-02	3E-02	2E+00	2E-02	3E-02	1E-01	3E-01	5E-02	5E-02	3E-02	1E-02	4E-02	2E-02	1E-02	2E-02	4E-02	6E-02	3E-01	7E-02	7E-02	5E-02	3E-02
TG(36:0)	5E-02	5E-02	8E-01	3E-02	4E-02	1E-01	3E-01	9E-02	8E-02	4E-02	4E-02	8E-02	2E-02	3E-02	5E-02	5E-02	1E-01	3E-01	1E-01	1E-01	6E-02	3E-02
TG(38:0)	7E-02	5E-02	5E-01	3E-02	4E-02	2E-01	2E-01	2E-01	1E-01	3E-02	5E-02	5E-02	5E-02	3E-02	4E-02	6E-02	2E-01	3E-01	2E-01	1E-01	6E-02	4E-02
TG(40:0)	1E-01	8E-02	5E-01	4E-02	9E-02	3E-01	3E-01	3E-01	2E-01	6E-02	5E-02	8E-02	6E-02	5E-02	8E-02	7E-02	3E-01	3E-01	3E-01	2E-01	8E-02	5E-02
TG(42:0)	2E-01	2E-01	5E-01	9E-02	2E-01	7E-01	4E-01	7E-01	5E-01	1E-01	2E-01	2E-01	2E-01	7E-02	1E-01	2E-01	8E-01	4E-01	9E-01	5E-01	1E-01	1E-01
TG(44:0)	3E-01	3E-01	5E-01	2E-01	4E-01	1E+00	5E-01	1E+00	9E-01	3E-01	3E-01	2E-01	3E-01	1E-01	2E-01	3E-01	1E+00	7E-01	1E+00	1E+00	3E-01	2E-01
TG(46:0)	8E-01	6E-01	7E-01	3E-01	8E-01	2E+00	9E-01	3E+00	2E+00	6E-01	4E-01	4E-01	5E-01	3E-01	4E-01	7E-01	2E+00	2E+00	2E+00	2E+00	6E-01	5E-01
TG(48:0)	2E+00	1E+00	2E+00	1E+00	3E+00	3E+00	2E+00	6E+00	3E+00	5E+00	1E+00	1E+00	2E+00	1E+00	8E-01	2E+00	4E+00	6E+00	4E+00	6E+00	3E+00	2E+00
TG(50:0)	3E+00	2E+00	4E+00	3E+00	7E+00	3E+00	1E+00	6E+00	5E+00	9E+00	3E+00	4E+00	4E+00	2E+00	3E+00	3E+00	3E+00	9E+00	8E+00	7E+00	4E+00	4E+00
TG(52:0)	2E+00	9E-01	4E+00	4E+00	7E+00	1E+00	8E-01	3E+00	4E+00	5E+00	4E+00	5E+00	3E+00	1E+00	3E+00	2E+00	2E+00	6E+00	5E+00	4E+00	2E+00	4E+00
TG(54:0)	7E-01	3E-01	2E+00	2E+00	3E+00	5E-01	3E-01	8E-01	2E+00	9E-01	2E+00	3E+00	7E-01	6E-01	2E+00	6E-01	6E-01	3E+00	1E+00	1E+00	6E-01	2E+00
TG(56:0)	2E-01	5E-02	3E-01	4E-01	8E-01	9E-02	6E-02	2E-01	4E-01	1E-01	6E-01	9E-01	1E-01	2E-01	3E-01	2E-01	2E-01	6E-01	2E-01	3E-01	1E-01	5E-01
TG(58:0)	5E-02	2E-02	7E-02	1E-01	2E-01	0E+00	3E-02	5E-02	9E-02	7E-02	2E-01	3E-01	3E-02	5E-02	8E-02	4E-02	4E-02	1E-01	5E-02	7E-02	2E-02	2E-01
TG(40:1)	3E-02	3E-02	5E-01	2E-02	3E-02	1E-01	8E-02	1E-01	8E-02	3E-02	2E-02	0E+00	3E-02	2E-02	0E+00	3E-02	1E-01	7E-02	7E-02	8E-02	2E-02	2E-02
TG(42:1)	1E-01	5E-02	9E-01	3E-02	1E-01	2E-01	2E-01	3E-01	3E-01	5E-02	7E-02	6E-02	6E-02	4E-02	6E-02	1E-01	3E-01	2E-01	3E-01	3E-01	9E-02	6E-02
TG(44:1)	3E-01	2E-01	1E+00	1E-01	4E-01	9E-01	5E-01	9E-01	9E-01	2E-01	2E-01	2E-01	2E-01	1E-01	2E-01	4E-01	9E-01	5E-01	9E-01	9E-01	2E-01	2E-01
TG(46:1)	6E-01	7E-01	3E+00	4E-01	8E-01	1E+00	1E+00	2E+00	2E+00	5E-01	5E-01	4E-01	5E-01	2E-01	3E-01	6E-01	2E+00	1E+00	2E+00	1E+00	4E-01	4E-01
TG(48:1)	3E+00	2E+00	6E+00	9E-01	2E+00	4E+00	5E+00	7E+00	5E+00	2E+00	1E+00	9E-01	2E+00	9E-01	1E+00	2E+00	6E+00	5E+00	4E+00	5E+00	2E+00	1E+00
TG(50:1)	1E+01	2E+01	1E+01	6E+00	2E+01	2E+01	4E+01	3E+01	2E+01	2E+01	4E+00	8E+00	1E+01	6E+00	4E+00	1E+01	2E+01	3E+01	1E+01	2E+01	2E+01	8E+00
TG(52:1)	2E+01	3E+01	2E+01	9E+00	2E+01	3E+01	4E+01	3E+01	2E+01	3E+01	8E+00	1E+01	2E+01	1E+01	1E+01	2E+01	4E+01	4E+01	2E+01	3E+01	3E+01	8E+00
TG(54:1)	1E+01	9E+00	8E+00	5E+00	8E+00	1E+01	2E+01	1E+01	1E+01	2E+01	6E+00	1E+01	1E+01	5E+00	7E+00	8E+00	1E+01	2E+01	1E+01	1E+01	2E+01	5E+00
TG(56:1)	3E+00	2E+00	2E+00	1E+00	2E+00	3E+00	3E+00	3E+00	4E+00	4E+00	2E+00	4E+00	2E+00	2E+00	3E+00	3E+00	4E+00	3E+00	3E+00	3E+00	4E+00	1E+00
TG(58:1)	8E-01	5E-01	6E-01	4E-01	8E-01	7E-01	5E-01	7E-01	1E+00	9E-01	8E-01	1E+00	3E-01	6E-01	7E-01	8E-01	9E-01	1E+00	9E-01	9E-01	7E-01	5E-01
TG(60:1)	2E-01	2E-01	2E-01	1E-01	2E-01	2E-01	1E-01	2E-01	4E-01	2E-01	2E-01	4E-01	1E-01	2E-01	2E-01	2E-01	2E-01	3E-01	3E-01	3E-01	2E-01	2E-01
TG(62:1)	6E-02	3E-02	4E-02	4E-02	6E-02	5E-02	5E-02	4E-02	6E-02	4E-02	6E-02	1E-01	3E-02	2E-02	6E-02	6E-02	5E-02	4E-02	5E-02	5E-02	5E-02	5E-02
TG(42:2)	5E-02	2E-02	2E-01	2E-02	4E-02	8E-02	1E-01	1E-01	8E-02	2E-02	3E-02	2E-02	2E-02	8E-03	3E-02	2E-02	8E-02	8E-02	1E-01	8E-02	3E-02	2E-02
TG(44:2)	1E-01	7E-02	7E-01	4E-02	1E-01	2E-01	2E-01	2E-01	3E-01	7E-02	8E-02	7E-02	4E-02	4E-02	6E-02	8E-02	2E-01	2E-01	3E-01	3E-01	8E-02	6E-02
TG(46:2)	3E-01	2E-01	1E+00	1E-01	3E-01	6E-01	6E-01	8E-01	8E-01	3E-01	2E-01	1E-01	2E-01	1E-01	1E-01	3E-01	8E-01	5E-01	7E-01	8E-01	3E-01	1E-01
TG(48:2)	8E-01	8E-01	3E+00	4E-01	8E-01	1E+00	2E+00	2E+00	2E+00	7E-01	4E-01	4E-01	7E-01	3E-01	5E-01	8E-01	2E+00	1E+00	2E+00	2E+00	7E-01	4E-01
TG(50:2)	7E+00	5E+00	7E+00	2E+00	4E+00	5E+00	9E+00	1E+01	8E+00	6E+00	2E+00	2E+00	3E+00	2E+00	2E+00	4E+00	8E+00	1E+01	5E+00	9E+00	6E+00	2E+00
TG(52:2)	5E+01	4E+01	6E+01	1E+01	3E+01	3E+01	8E+01	4E+01	5E+01	3E+01	7E+00	2E+01	3E+01	2E+01	1E+01	3E+01	4E+01	7E+01	2E+01	5E+01	4E+01	1E+01
TG(54:2)	3E+01	1E+01	3E+01	8E+00	9E+00	2E+01	4E+01	2E+01	2E+01	2E+01	7E+00	1E+01	1E+01	7E+00	1E+01	9E+00	2E+01	3E+01	1E+01	2E+01	2E+01	6E+00
TG(58:2)	2E+00	7E-01	3E+00	6E-01	7E-01	1E+00	2E+00	9E-01	2E+00	1E+00	8E-01	1E+00	6E-01	6E-01	1E+00	1E+00	1E+00	1E+00	1E+00	2E+00	1E+00	5E-01
TG(62:2)	1E-01	4E-02	1E-01	5E-02	1E-01	1E-01	1E-01	6E-02	1E-01	2E-01	8E-02	2E-01	5E-02	7E-02	7E-02	9E-02	9E-02	9E-02	8E-02	1E-01	1E-01	5E-02
TG(64:2)	4E-02	2E-02	2E-02	3E-02	2E-02	3E-02	4E-02	3E-02	4E-02	2E-02	4E-02	5E-02	1E-02	2E-02	2E-02	2E-02	1E-02	3E-02	2E-02	3E-02	2E-02	2E-02
TG(42:3)	1E-02	0E+00	7E-03	0E+00	8E-03	0E+00	7E-03	3E-02	0E+00	4E-03	0E+00	4E-03	6E-03	7E-03	4E-03	0E+00	8E-03	3E-02	0E+00	2E-02	7E-03	0E+00
TG(44:3)	3E-02	1E-02	1E-01	2E-02	3E-02	3E-02	4E-02	6E-02	6E-02	2E-02	2E-02	2E-02	2E-02	1E-02	2E-02	3E-02	5E-02	5E-02	6E-02	7E-02	2E-02	1E-02
TG(46:3)	8E-02	4E-02	2E-01	4E-02	7E-02	1E-01	1E-01	2E-01	3E-01	5E-02	6E-02	5E-02	3E-02	3E-02	7E-02	9E-02	2E-01	1E-01	2E-01	2E-01	5E-02	4E-02
TG(48:3)	3E-01	2E-01	5E-01	1E-01	2E-01	3E-01	5E-01	5E-01	6E-01	2E-01	1E-01	1E-01	1E-01	1E-01	2E-01	2E-01	6E-01	5E-01	5E-01	7E-01	2E-01	1E-01
TG(50:3)	2E+00	1E+00	1E+00	5E-01	8E-01	1E+00	2E+00	1E+00	3E+00	9E-01	4E-01	5E-01	8E-01	7E-01	7E-01	1E+00	2E+00	2E+00	1E+00	2E+00	1E+00	5E-01
TG(52:3)	3E+01	1E+01	9E+00	4E+00	6E+00	1E+01	2E+01	2E+01	2E+01	1E+01	3E+00	5E+00	7E+00	7E+00	5E+00	7E+00	2E+01	3E+01	7E+00	3E+01	2E+01	4E+00
TG(54:3)	3E+01	9E+00	7E+01	9E+00	9E+00	1E+01	3E+01	1E+01	3E+01	1E+01	5E+00	2E+01	6E+00	7E+00	8E+00	1E+01	2E+01	3E+01	1E+01	4E+01	2E+01	7E+00
TG(56:3)	4E+00	1E+00	2E+00	1E+00	1E+00	1E+00	2E+00	2E+00	3E+00	2E+00	1E+00	2E+00	1E+00	1E+00	1E+00	2E+00	2E+00	3E+00	1E+00	4E+00	3E+00	8E-01
TG(58:3)	2E+00	5E-01	8E-01	4E-01	5E-01	6E-01	1E+00	7E-01	1E+00	9E-01	7E-01	1E+00	5E-01	4E-01	6E-01	7E-01	8E-01	9E-01	6E-01	1E+00	9E-01	4E-01
TG(60:3)	7E-01	2E-01	4E-01	1E-01	2E-01	3E-01	4E-01	3E-01	6E-01	3E-01	3E-01	4E-01	1E-01	2E-01	3E-01	3E-01	3E-01	4E-01	2E-01	6E-01	4E-01	2E-01
TG(62:3)	1E-01	8E-02	1E-01	4E-02	7E-02	8E-02	9E-02	7E-02	2E-01	1E-01	4E-01	2E-01	4E-02	7E-02	7E-02	8E-02	1E-01	9E-02	1E-01	2E-01	2E-01	9E-02
TG(48:4)	8E-02	4E-02	3E-01	4E-02	6E-02	8E-02	2E-01	1E-01	2E-01	6E-02	5E-02	7E-02	4E-02	4E-02	7E-02	8E-02	1E-01	2E-01	2E-01	2E-01	7E-02	4E-02
TG(50:4)	4E-01	2E-01	4E-01	1E-01	2E-01	3E-01	5E-01	4E-01	7E-01	2E-01	9E-02	2E-01	1E-01	2E-01	3E-01	3E-01	4E-01	5E-01	4E-01	8E-01	3E-01	1E-01
TG(52:4)	4E+00	1E+00	6E+00	1E+00	1E+00	2E+00	5E+00	2E+00	6E+00	3E+00	8E-01	2E+00	1E+00	2E+00	2E+00	2E+00	5E+00	5E+00	2E+00	5E+00	3E+00	7E-01
TG(54:4)	2E+01	3E+00	9E+00	3E+00	3E+00	5E+00	1E+01	1E+01	2E+01	8E+00	2E+00	5E+00	2E+00	3E+00	4E+00	3E+00	7E+00	2E+01	4E+00	2E+01	9E+00	3E+00
TG(56:4)	2E+00	3E+00	9E-01	1E+00	2E+00	2E+00	2E+00	4E+00	1E+00	4E+00	8E-01	2E+00	3E+00	1E+00	2E+00	2E+00	3E+00	2E+00	3E+00	2E+00	5E+00	8E-01
TG(58:4)	8E-01	8E-01	5E-01	4E-01	7E-01	7E-01	7E-01	1E+00	5E-01	9E-01	4E-01	5E-01	9E-01	5E-01	6E-01	8E-01	8E-01	1E+00	9E-01	8E-01	1E+00	3E-01
TG(60:4)	3E-01	1E-01	2E-01	9E-02	2E-01	2E-01	2E-01	2E-01	3E-01	3E-01	2E-01	2E-01	2E-01	1E-01	2E-01	2E-01	2E-01	3E-01	2E-01	4E-01	4E-01	1E-01
TG(62:4)	1E-01	6E-02	5E-02	4E-02	6E-02	6E-02	8E-02	7E-02	2E-01	2E-01	4E-01	9E-02	8E-02	8E-02	5E-02	9E-02	9E-02	7E-02	1E-01	2E-01	3E-01	1E-01
TG(50:5)	8E-02	3E-02	2E-01	4E-02	3E-02	4E-02	1E-01	5E-02	2E-01	4E-02	2E-02	4E-02	3E-02	3E-02	5E-02	4E-02	7E-02	1E-01	6E-02	2E-01	5E-02	3E-02
TG(52:5)	8E-01	2E-01	6E-01	2E-01	2E-01	3E-01	9E-01	3E-01	1E+00	3E-01	1E-01	4E-01	2E-01	3E-01	3E-01	3E-01	5E-01	8E-01	4E-01	9E-01	4E-01	2E-01
TG(54:5)	5E+00	7E-01	6E+00	1E+00	9E-01	2E+00	5E+00	2E+00	7E+00	2E+00	1E+00	2E+00	6E-01	1E+00	2E+00	1E+00	3E+00	4E+00	2E+00	8E+00	3E+00	7E-01
TG(56:5)	1E+00	1E+00	6E-01	6E-01	1E+00	9E-01	1E+00	2E+00	1E+00	2E+00	3E-01	7E-01	1E+00	7E-01	6E-01	1E+00	2E+00	1E+00	1E+00	2E+00	2E+00	5E-01
TG(60:2)	7E-01	2E-01	9E-01	2E-01	3E-01	3E-01	3E-01	3E-01	6E-01	4E-01	3E-01	5E-01	2E-01	2E-01	3E-01	4E-01	5E-01	5E-01	3E-01	5E-01	3E-01	2E-01
TG(56:6)	2E+00	1E+00	5E-01	2E-01	4E-01	8E-01	4E-01	2E+00	5E-01	9E-01	4E-01	7E-01	1E+00	2E-01	2E-01	4E-01	1E+00	9E-01	8E-01	1E+00	1E+00	7E-01
TG(56:7)	1E+00	5E-01	7E-01	9E-02	1E-01	8E-01	2E-01	3E-01	5E-01	2E-01	3E-01	6E-01	5E-01	2E-01	2E-01	3E-01	1E+00	3E-01	4E-01	5E-01	4E-01	3E-01
TG(58:7)	1E+00	5E-01	5E-01	1E-01	2E-01	3E-01	3E-01	6E-01	3E-01	4E-01	2E-01	4E-01	4E-01	1E-01	2E-01	3E-01	6E-01	4E-01	3E-01	6E-01	5E-01	3E-01
TG(56:8)	5E-01	2E-01	3E-01	7E-02	6E-02	3E-01	9E-02	1E-01	2E-01	2E-01	9E-02	2E-01	2E-01	1E-01	9E-02	2E-01	6E-01	1E-01	2E-01	3E-01	2E-01	1E-01
TG(58:8)	8E-01	2E-01	3E-01	7E-02	8E-02	4E-01	1E-01	2E-01	3E-01	2E-01	1E-01	4E-01	2E-01	1E-01	2E-01	2E-01	6E-01	2E-01	2E-01	3E-01	2E-01	1E-01
TG(60:8)	3E-01	2E-01	2E-01	7E-02	1E-01	1E-01	1E-01	2E-01	1E-01	2E-01	5E-02	1E-01	2E-01	7E-02	1E-01	1E-01	2E-01	2E-01	1E-01	3E-01	3E-01	1E-01
TG(62:8)	1E-01	5E-02	2E-01	2E-02	3E-02	4E-02	5E-02	5E-02	4E-02	4E-02	3E-02	9E-02	4E-02	2E-02	4E-02	6E-02	9E-02	6E-02	5E-02	8E-02	6E-02	4E-02
TG(64:8)	8E-02	1E-02	1E-01	8E-03	2E-02	3E-02	6E-03	2E-02	3E-02	2E-02	3E-02	7E-02	2E-02	2E-02	1E-02	3E-02	5E-02	2E-02	2E-02	6E-02	3E-02	4E-02
TG(58:9)	4E-01	1E-01	1E-01	4E-02	5E-02	2E-01	7E-02	1E-01	2E-01	1E-01	8E-02	2E-01	1E-01	6E-02	9E-02	8E-02	3E-01	1E-01	1E-01	2E-01	2E-01	1E-01
TG(60:9)	1E-01	1E-01	7E-02	5E-02	7E-02	2E-01	8E-02	1E-01	1E-01	1E-01	7E-02	1E-01	1E-01	5E-02	8E-02	9E-02	3E-01	1E-01	1E-01	1E-01	1E-01	5E-02
TG(62:9)	8E-02	4E-02	4E-02	2E-02	2E-02	3E-02	2E-02	5E-02	2E-02	3E-02	2E-02	3E-02	3E-02	2E-02	2E-02	3E-02	5E-02	5E-02	3E-02	5E-02	4E-02	4E-02
TG(60:10)	4E-01	2E-01	6E-02	9E-02	1E-01	4E-01	8E-02	3E-01	2E-01	1E-01	1E-01	3E-01	3E-01	6E-02	1E-01	1E-01	6E-01	2E-01	3E-01	3E-01	2E-01	1E-01

Table 59. *Results of estimation of absolute lipid concentrations for MG, DG and TG in thrombin with the platelet inhibitor and inhibitor treated samples. Results are shown as average amount (nmol) per 1 million platelets.*

	Thrombin &Platelet Inhibitor											Platelet inhibitor										
Donor:	*1*	*2*	*3*	*4*	*5*	*6*	*7*	*8*	*9*	*10*	*11*	*1*	*2*	*3*	*4*	*5*	*6*	*7*	*8*	*9*	*10*	*11*
MG(16:0)	3E-01	3E-01	1E+00	3E-01	3E-01	2E-01	6E-01	4E-01	3E-01	4E-01	4E-01	3E-01	2E-01	3E-01	3E-01	2E-01	4E-01	5E-01	3E-01	3E-01	1E-01	3E-01
MG(18:0)	2E-01	2E-01	4E-01	3E-01	3E-01	1E-01	4E-01	2E-01	2E-01	2E-01	4E-01	3E-01	2E-01	2E-01	4E-01	3E-01	3E-01	5E-01	2E-01	2E-01	2E-01	2E-01
MG(20:1)	3E-01	1E-01	1E-01	4E-02	4E-01	6E-02	5E-02	1E+01	1E+01	9E+00	1E+01	5E-02	5E-02	6E-02	4E-02	1E-01	9E-02	7E-02	1E+01	6E+00	1E+01	1E+01
DG(18:0)	3E-02	2E-02	2E+00	5E-02	2E-02	2E-02	2E-01	3E-01	6E-02	6E-02	9E-02	0E+00	0E+00	2E-02	7E-02	6E-02	2E-02	1E-01	8E-02	1E-01	6E-02	1E-01
DG(20:0)	2E-02	3E-02	7E-01	3E-02	4E-02	4E-02	2E-01	1E-01	2E-02	7E-02	7E-02	2E-02	1E-02	2E-02	4E-02	3E-02	1E-02	6E-02	2E-02	1E-01	3E-02	3E-02
DG(26:0)	5E-02	3E-02	3E-01	5E-02	5E-02	7E-02	2E-01	9E-02	3E-02	5E-02	4E-02	3E-02	3E-02	7E-02	7E-02	2E-02	2E-02	2E-01	2E-02	9E-02	4E-02	6E-02
DG(28:0)	7E-02	4E-02	1E-01	2E-01	6E-02	2E-02	3E-02	6E-02	6E-02	5E-02	7E-02	2E-02	3E-02	1E-02	4E-02	7E-02	3E-02	2E-01	2E-02	8E-02	2E-02	5E-02
DG(26:1)	2E-02	2E-02	1E-01	2E-02	2E-02	2E-02	2E-02	4E-02	1E-02	1E-02	2E-02	2E-02	1E-02	2E-02	2E-02	0E+00	2E-02	3E-02	0E+00	2E-02	0E+00	2E-02
DG(28:1)	2E-02	2E-02	2E-01	4E-02	4E-02	5E-02	2E-02	5E-02	3E-02	2E-02	4E-02	6E-02	2E-02	5E-02	4E-02	7E-02	6E-02	6E-02	2E-02	5E-02	4E-02	2E-02
DG(30:1)	5E-02	3E-02	4E-01	5E-02	1E-01	1E-01	1E-01	9E-02	4E-02	4E-02	8E-02	6E-02	6E-02	9E-02	1E-01	4E-02	9E-02	7E-02	5E-02	1E-01	6E-02	1E-01
DG(32:1)	2E-01	2E-01	8E-01	2E-01	2E-01	6E-01	4E-01	3E-01	4E-01	3E-01	2E-01	3E-01	2E-01	3E-01	2E-01	3E-01	2E-01	7E-01	2E-01	3E-01	1E-01	2E-01
DG(34:1)	2E+00	1E+00	3E+00	8E-01	1E+00	2E+00	2E+00	2E+00	2E+00	2E+00	7E-01	3E+00	9E-01	2E+00	9E-01	1E+00	1E+00	3E+00	6E-01	1E+00	9E-01	8E-01
DG(36:1)	9E-01	5E-01	1E+00	5E-01	4E-01	8E-01	7E-01	9E-01	5E-01	8E-01	4E-01	9E-01	3E-01	7E-01	5E-01	5E-01	6E-01	1E+00	2E-01	5E-01	4E-01	4E-01
DG(34:2)	1E+00	5E-01	1E+00	6E-01	5E-01	1E+00	1E+00	1E+00	1E+00	1E+00	4E-01	2E+00	3E-01	2E+00	6E-01	7E-01	8E-01	2E+00	4E-01	9E-01	9E-01	5E-01
DG(36:2)	1E+00	2E+00	4E+00	1E+00	1E+00	2E+00	3E+00	2E+00	3E+00	2E+00	9E-01	6E+00	7E-01	2E+00	2E+00	2E+00	2E+00	5E+00	9E-01	2E+00	1E+00	1E+00
DG(36:3)	2E+00	7E-01	2E+00	1E+00	8E-01	2E+00	2E+00	2E+00	3E+00	2E+00	8E-01	5E+00	5E-01	3E+00	1E+00	1E+00	1E+00	4E+00	1E+00	2E+00	1E+00	1E+00
DG(36:4)a	7E-01	2E-01	2E+00	4E-01	3E-01	3E-01	7E-01	7E-01	8E-01	5E-01	2E-01	2E+00	1E-01	8E-01	7E-01	4E-01	6E-01	1E+00	3E-01	6E-01	5E-01	3E-01
DG(36:4)b	4E-01	4E-01	8E-01	2E-01	4E-01	5E-01	3E-01	1E+00	4E-01	1E+00	3E-01	5E-01	5E-01	5E-01	5E-01	4E-01	6E-01	4E-01	4E-01	5E-01	6E-01	4E-01
DG(38:4)	8E+00	7E+00	8E+00	2E+00	3E+00	4E+00	9E+00	4E+01	9E+00	3E+01	5E+00	1E+01	8E+00	8E+00	6E+00	7E+00	7E+00	8E+00	1E+01	1E+01	1E+01	6E+00
DG(36:5)	2E-01	9E-02	2E-01	2E-02	2E-02	3E-02	1E-01	6E-02	4E-02	2E-02	8E-02	5E-01	3E-02	2E-01	2E-01	8E-02	3E-02	2E-01	7E-02	1E-01	6E-02	2E-01
DG(38:5)	6E-01	5E-01	7E-01	2E-01	2E-01	5E-01	6E-01	1E+00	7E-01	2E+00	3E-01	8E-01	5E-01	7E-01	4E-01	5E-01	7E-01	7E-01	5E-01	7E-01	6E-01	3E-01
DG(36:6)	4E-01	4E-01	5E-01	1E-01	1E-01	5E-01	3E-01	4E-01	2E-01	4E-01	1E-01	8E-01	3E-01	5E-01	2E-01	3E-01	7E-01	6E-01	2E-01	2E-01	2E-01	4E-01
TG(30:0)	4E-02	1E-01	2E+00	2E-01	2E-01	9E-02	1E+00	5E-01	1E-01	2E-01	2E-01	0E+00	7E-02	5E-02	2E-01	9E-02	7E-02	4E-01	5E-02	5E-01	2E-01	9E-03
TG(32:0)	3E-02	3E-02	2E-01	2E-02	5E-02	7E-02	2E-01	4E-02	2E-02	4E-02	2E-02	2E-02	2E-02	6E-02	2E-02	3E-02	4E-02	4E-01	2E-02	4E-02	2E-02	2E-02
TG(34:0)	3E-02	3E-02	2E-01	3E-02	6E-02	7E-02	3E-01	9E-02	2E-02	6E-02	3E-02	2E-02	3E-02	5E-02	2E-02	3E-02	4E-02	4E-01	5E-02	7E-02	3E-02	3E-02
TG(36:0)	5E-02	4E-02	1E-01	5E-02	7E-02	1E-01	3E-01	1E-01	5E-02	6E-02	4E-02	3E-02	3E-02	7E-02	2E-02	3E-02	8E-02	5E-01	9E-02	8E-02	3E-02	6E-02
TG(38:0)	8E-02	4E-02	8E-02	4E-02	1E-01	2E-01	3E-01	2E-01	9E-02	7E-02	4E-02	7E-02	4E-02	7E-02	3E-02	6E-02	1E-01	4E-01	1E-01	9E-02	3E-02	5E-02
TG(40:0)	1E-01	6E-02	1E-01	7E-02	1E-01	3E-01	3E-01	5E-01	2E-01	1E-01	6E-02	8E-02	8E-02	7E-02	4E-02	1E-01	2E-01	3E-01	3E-01	2E-01	6E-02	8E-02
TG(42:0)	2E-01	2E-01	2E-01	1E-01	3E-01	5E-01	4E-01	1E+00	6E-01	2E-01	1E-01	2E-01	2E-01	1E-01	1E-01	3E-01	5E-01	4E-01	6E-01	5E-01	2E-01	1E-01
TG(44:0)	5E-01	3E-01	2E-01	3E-01	4E-01	1E+00	9E-01	2E+00	1E+00	3E-01	3E-01	3E-01	3E-01	2E-01	2E-01	4E-01	8E-01	6E-01	8E-01	9E-01	2E-01	3E-01
TG(46:0)	7E-01	7E-01	4E-01	7E-01	8E-01	2E+00	2E+00	2E+00	2E+00	8E-01	5E-01	7E-01	4E-01	3E-01	4E-01	6E-01	9E-01	1E+00	2E+00	2E+00	5E-01	5E-01
TG(48:0)	2E+00	2E+00	1E+00	2E+00	2E+00	3E+00	5E+00	2E+00	2E+00	3E+00	2E+00	1E+00	1E+00	1E+00	1E+00	9E-01	1E+00	2E+00	2E+00	4E+00	3E+00	2E+00
TG(50:0)	2E+00	3E+00	2E+00	3E+00	2E+00	3E+00	4E+00	1E+00	1E+00	3E+00	3E+00	3E+00	1E+00	2E+00	2E+00	9E-01	1E+00	1E+00	1E+00	5E+00	5E+00	4E+00
TG(52:0)	9E-01	2E+00	2E+00	3E+00	8E-01	1E+00	2E+00	2E+00	6E-01	3E+00	3E+00	3E+00	5E-01	4E+00	3E+00	5E-01	8E-01	4E-01	1E+00	4E+00	2E+00	4E+00
TG(54:0)	3E-01	7E-01	7E-01	1E+00	3E-01	4E-01	6E-01	8E-01	2E-01	1E+00	1E+00	9E-01	2E-01	1E+00	1E+00	3E-01	5E-01	2E-01	3E-01	1E+00	4E-01	2E+00
TG(56:0)	1E-01	1E-01	1E-01	2E-01	8E-02	9E-02	2E-01	2E-01	1E-02	3E-01	4E-01	2E-01	6E-02	4E-01	2E-01	9E-02	1E-01	1E-01	4E-01	3E-01	1E-01	4E-01
TG(58:0)	3E-02	4E-02	3E-02	5E-02	4E-02	4E-02	7E-02	5E-02	0E+00	6E-02	8E-02	0E+00	2E-02	9E-02	2E-02	2E-02	4E-02	2E-02	5E-02	1E-01	2E-02	2E-01
TG(40:1)	4E-02	2E-02	6E-02	2E-02	5E-02	1E-01	9E-02	2E-01	1E-01	3E-02	3E-02	3E-02	2E-02	1E-02	4E-02	5E-02	9E-02	1E-01	9E-02	9E-02	3E-02	3E-02
TG(42:1)	1E-01	1E-01	1E-01	8E-02	1E-01	2E-01	3E-01	6E-01	3E-01	8E-02	8E-02	1E-01	6E-02	5E-02	5E-02	1E-01	2E-01	3E-01	3E-01	2E-01	5E-02	8E-02
TG(44:1)	4E-01	4E-01	3E-01	2E-01	4E-01	7E-01	8E-01	2E+00	9E-01	3E-01	2E-01	3E-01	2E-01	2E-01	2E-01	6E-01	6E-01	6E-01	8E-01	9E-01	2E-01	2E-01
TG(46:1)	8E-01	7E-01	6E-01	5E-01	8E-01	2E+00	2E+00	3E+00	2E+00	6E-01	4E-01	5E-01	4E-01	3E-01	4E-01	9E-01	1E+00	1E+00	1E+00	2E+00	3E-01	5E-01
TG(48:1)	2E+00	3E+00	2E+00	2E+00	3E+00	6E+00	9E+00	6E+00	7E+00	4E+00	1E+00	2E+00	2E+00	1E+00	1E+00	3E+00	3E+00	6E+00	3E+00	4E+00	2E+00	1E+00
TG(50:1)	2E+01	2E+01	1E+01	1E+01	2E+01	3E+01	5E+01	2E+01	3E+01	4E+01	8E+00	9E+00	1E+01	9E+00	8E+00	1E+01	2E+01	4E+01	1E+01	2E+01	2E+01	8E+00
TG(52:1)	3E+01	3E+01	2E+01	2E+01	2E+01	4E+01	5E+01	3E+01	4E+01	4E+01	1E+01	2E+01	1E+01	1E+01	1E+01	2E+01	2E+01	5E+01	2E+01	3E+01	3E+01	1E+01
TG(54:1)	1E+01	1E+01	8E+00	1E+01	8E+00	1E+01	2E+01	1E+01	1E+01	2E+01	5E+00	1E+01	7E+00	9E+00	8E+00	6E+00	7E+00	2E+01	9E+00	1E+01	2E+01	6E+00
TG(56:1)	3E+00	2E+00	2E+00	2E+00	2E+00	2E+00	4E+00	3E+00	3E+00	4E+00	1E+00	4E+00	2E+00	2E+00	2E+00	2E+00	2E+00	3E+00	2E+00	3E+00	3E+00	2E+00
TG(58:1)	7E-01	6E-01	5E-01	7E-01	4E-01	5E-01	9E-01	6E-01	7E-01	8E-01	5E-01	1E+00	4E-01	5E-01	5E-01	4E-01	4E-01	7E-01	5E-01	9E-01	7E-01	5E-01
TG(60:1)	2E-01	1E-01	1E-01	2E-01	1E-01	1E-01	3E-01	1E-01	3E-01	2E-01	1E-01	4E-01	8E-02	1E-01	1E-01	1E-01	9E-02	1E-01	1E-01	4E-01	2E-01	3E-01
TG(62:1)	5E-02	3E-02	3E-02	4E-02	4E-02	3E-02	4E-02	6E-02	5E-02	7E-02	3E-02	8E-02	2E-02	4E-02	2E-02	2E-02	4E-02	7E-02	4E-02	8E-02	6E-02	4E-02
TG(42:2)	5E-02	4E-02	3E-02	3E-02	5E-02	8E-02	9E-02	1E-01	1E-01	5E-02	4E-02	3E-02	2E-02	2E-02	2E-02	4E-02	7E-02	8E-02	9E-02	9E-02	2E-02	3E-02
TG(44:2)	1E-01	8E-02	9E-02	5E-02	1E-01	2E-01	3E-01	5E-01	3E-01	1E-01	6E-02	1E-01	4E-02	5E-02	6E-02	1E-01	2E-01	3E-01	3E-01	3E-01	6E-02	8E-02
TG(46:2)	4E-01	2E-01	3E-01	2E-01	4E-01	6E-01	8E-01	1E+00	1E+00	4E-01	2E-01	3E-01	2E-01	1E-01	2E-01	5E-01	5E-01	7E-01	8E-01	9E-01	2E-01	2E-01
TG(48:2)	8E-01	1E+00	8E-01	7E-01	1E+00	2E+00	3E+00	3E+00	3E+00	1E+00	5E-01	7E-01	5E-01	5E-01	5E-01	1E+00	9E-01	2E+00	1E+00	2E+00	6E-01	6E-01
TG(50:2)	6E+00	9E+00	4E+00	5E+00	8E+00	1E+01	2E+01	7E+00	2E+01	1E+01	2E+00	4E+00	3E+00	3E+00	2E+00	5E+00	4E+00	1E+01	4E+00	7E+00	5E+00	2E+00
TG(52:2)	5E+01	6E+01	3E+01	3E+01	4E+01	5E+01	9E+01	4E+01	6E+01	5E+01	2E+01	3E+01	3E+01	2E+01	2E+01	3E+01	3E+01	8E+01	2E+01	4E+01	4E+01	2E+01
TG(54:2)	3E+01	2E+01	1E+01	2E+01	1E+01	2E+01	5E+01	2E+01	4E+01	2E+01	8E+00	2E+01	7E+00	9E+00	1E+01	1E+01	1E+01	4E+01	1E+01	2E+01	2E+01	1E+01
TG(58:2)	2E+00	8E-01	9E-01	9E-01	8E-01	1E+00	2E+00	1E+00	2E+00	1E+00	6E-01	2E+00	5E-01	7E-01	7E-01	9E-01	7E-01	1E+00	7E-01	2E+00	1E+00	8E-01
TG(62:2)	2E-01	6E-02	8E-02	6E-02	6E-02	9E-02	1E-01	9E-02	1E-01	1E-01	9E-02	2E-01	3E-02	7E-02	7E-02	1E-01	7E-02	1E-01	7E-02	1E-01	8E-02	1E-01
TG(64:2)	3E-02	1E-02	2E-02	2E-02	1E-02	2E-02	2E-02	4E-02	5E-02	3E-02	2E-02	4E-02	2E-02	1E-02	2E-02	2E-02	1E-02	3E-02	3E-02	3E-02	2E-02	3E-02
TG(42:3)	1E-02	3E-03	4E-03	7E-03	2E-02	2E-02	3E-02	3E-03	5E-02	0E+00	7E-03	9E-03	0E+00	7E-03	7E-03	4E-03	0E+00	7E-03	6E-03	2E-02	4E-03	7E-03
TG(44:3)	3E-02	2E-02	2E-02	2E-02	4E-02	3E-02	7E-02	7E-02	9E-02	2E-02	3E-02	3E-02	1E-02	1E-02	2E-02	3E-02	4E-02	7E-02	5E-02	7E-02	2E-02	3E-02
TG(46:3)	9E-02	6E-02	8E-02	5E-02	9E-02	1E-01	2E-01	3E-01	3E-01	7E-02	5E-02	7E-02	3E-02	4E-02	5E-02	1E-01	1E-01	2E-01	2E-01	3E-01	5E-02	6E-02
TG(48:3)	4E-01	3E-01	3E-01	3E-01	3E-01	5E-01	8E-01	9E-01	1E+00	3E-01	2E-01	2E-01	1E-01	1E-01	2E-01	3E-01	2E-01	7E-01	5E-01	6E-01	2E-01	2E-01
TG(50:3)	1E+00	2E+00	1E+00	1E+00	1E+00	2E+00	4E+00	2E+00	3E+00	2E+00	6E-01	1E+00	7E-01	7E-01	8E-01	1E+00	1E+00	2E+00	1E+00	3E+00	1E+00	5E-01
TG(52:3)	3E+01	2E+01	1E+01	1E+01	2E+01	3E+01	6E+01	1E+01	3E+01	3E+01	3E+00	1E+01	5E+00	6E+00	6E+00	9E+00	7E+00	3E+01	6E+00	1E+01	1E+01	4E+00
TG(54:3)	4E+01	9E+00	2E+01	2E+01	1E+01	2E+01	3E+01	1E+01	4E+01	2E+01	8E+00	3E+01	6E+00	9E+00	2E+01	1E+01	1E+01	3E+01	1E+01	3E+01	2E+01	1E+01
TG(56:3)	4E+00	2E+00	2E+00	2E+00	2E+00	2E+00	4E+00	2E+00	5E+00	4E+00	6E-01	3E+00	1E+00	1E+00	1E+00	1E+00	1E+00	3E+00	1E+00	3E+00	3E+00	1E+00
TG(58:3)	2E+00	6E-01	6E-01	8E-01	7E-01	7E-01	2E-01	9E-01	2E+00	3E-01	1E-01	2E+00	4E-01	6E-01	6E-01	1E+00	6E-01	1E+00	7E-01	1E+00	7E-01	7E-01
TG(60:3)	4E-01	2E-01	2E-01	3E-01	2E-01	2E-01	4E-01	2E-01	4E-01	4E-01	1E-01	1E-01	5E-02	5E-02	7E-02	7E-02	4E-02	8E-02	7E-02	1E-01	1E-01	3E-01
TG(62:4)	1E-01	5E-02	7E-02	7E-02	7E-02	7E-02	8E-02	1E-01	2E-01	2E-01	1E-01	6E-02	3E-02	2E-02	5E-02	7E-02	5E-02	1E-01	7E-02	2E-01	3E-02	3E-02
TG(50:5)	1E-01	5E-02	7E-02	8E-02	6E-02	6E-02	2E-01	1E-01	2E-01	7E-02	3E-02	8E-01	2E-01	2E-01	3E-01	4E-01	2E-01	1E+00	3E-01	1E+00	4E-01	2E-01
TG(52:5)	8E-01	4E-01	4E-01	4E-01	4E-01	5E-01	2E+00	6E-01	1E+00	5E-01	2E-01	8E-01	2E-01	2E-01	3E-01	4E-01	2E-01	1E+00	3E-01	1E+00	4E-01	2E-01
TG(54:5)	7E+00	1E+00	2E+00	3E+00	1E+00	2E+00	9E+00	3E+00	9E+00	4E+00	1E+00	5E+00	5E-01	1E+00	2E+00	2E+00	1E+00	6E+00	2E+00	7E+00	3E+00	1E+00
TG(56:5)	1E+00	2E+00	1E+00	1E+00	1E+00	2E+00	2E+00	2E+00	2E+00	3E+00	5E-01	8E-01	1E+00	9E-01	8E-01	7E-01	1E+00	1E+00	9E-01	1E+00	2E+00	7E-01
TG(60:2)	7E-01	2E-01	2E-01	3E-01	3E-01	3E-01	6E-01	4E-01	6E-01	5E-01	2E-01	9E-01	2E-01	2E-01	3E-01	3E-01	3E-01	5E-01	3E-01	6E-01	4E-01	3E-01
TG(56:6)	2E+00	1E+00	5E-01	5E-01	5E-01	2E+00	1E+00	1E+00	1E+00	2E+00	5E-01	1E+00	8E-01	3E-01	3E-01	3E-01	1E+00	6E-01	7E-01	6E-01	8E-01	7E-01
TG(56:7)	1E+00	7E-01	3E-01	2E-01	2E-01	1E+00	5E-01	5E-01	7E-01	5E-01	4E-01	1E+00	4E-01	2E-01	1E-01	3E-01	7E-01	2E-01	3E-01	6E-01	4E-01	3E-01
TG(58:7)	1E+00	4E-01	3E-01	4E-01	4E-01	1E+00	7E-01	4E-01	1E+00	9E-01	3E-01	7E-01	3E-01	2E-01	2E-01	5E-01	5E-01	3E-01	3E-01	3E-01	4E-01	4E-01
TG(56:8)	5E-01	3E-01	3E-01	9E-02	1E-01	4E-01	3E-01	2E-01	3E-01	1E-01	1E-01	4E-01	2E-01	8E-02	8E-02	1E-01	1E-01	2E-01	2E-01	2E-01	2E-01	2E-01
TG(58:8)	9E-01	2E-01	2E-01	1E-01	2E-01	5E-01	3E-01	3E-01	4E-01	3E-01	2E-01	7E-01	2E-01	1E-01	1E-01	2E-01	4E-01	2E-01	2E-01	3E-01	3E-01	2E-01
TG(60:8)	3E-01	2E-01	2E-01	3E-01	2E-01	4E-01	3E-01	2E-01	4E-01	4E-01	1E-01	2E-01	1E-01	9E-02	1E-01	1E-01	2E-01	2E-01	1E-01	2E-01	2E-01	1E-01
TG(62:8)	1E-01	6E-02	7E-02	5E-02	4E-02	1E-01	7E-02	6E-02	9E-02	7E-02	3E-02	1E-01	5E-02	3E-02	3E-02	4E-02	7E-02	5E-02	3E-02	6E-02	8E-02	4E-02
TG(64:8)	1E-01	1E-02	2E-02	3E-02	4E-02	9E-02	4E-02	2E-02	5E-02	2E-02	3E-02	6E-02	1E-02	1E-02	2E-02	1E-02	4E-02	2E-02	2E-02	6E-02	3E-02	4E-02
TG(58:9)	5E-01	1E-01	1E-01	9E-02	7E-02	3E-01	2E-01	2E-01	2E-01	2E-01	9E-02	4E-01	8E-02	8E-02	7E-02	6E-02	2E-01	9E-02	1E-01	2E-01	1E-01	9E-02
TG(60:9)	2E-01	2E-01	1E-01	1E-01	1E-01	3E-01	1E-01	2E-01	2E-01	2E-01	9E-02	1E-01	1E-01	6E-02	8E-02	9E-02	2E-01	1E-01	1E-01	1E-01	1E-01	8E-02
TG(62:9)	6E-02	3E-02	3E-02	4E-02	5E-02	7E-02	6E-02	5E-02	7E-02	8E-02	2E-02	3E-02	3E-02	2E-02	2E-02	2E-02	3E-02	3E-02	2E-02	4E-02	3E-02	3E-02
TG(60:10)	5E-01	3E-01	2E-01	1E-01	2E-01	5E-01	2E-01	4E-01	3E-01	3E-01	2E-01	4E-01	2E-01	1E-01	1E-01	1E-01	4E-01	1E-01	3E-01	3E-01	3E-01	2E-01

Table 60. *Results of estimation of absolute lipid concentrations for LPC, PC, ePC and PI in resting and thrombin-activated platelet samples. Results are shown as average amount (nmol) per 1 million platelets.*

	Resting											Thrombin										
Donor:	*1*	*2*	*3*	*4*	*5*	*6*	*7*	*8*	*9*	*10*	*11*	*1*	*2*	*3*	*4*	*5*	*6*	*7*	*8*	*9*	*10*	*11*
LPC(14:0)	1E-01	2E-01	1E-01	4E-02	6E-02	1E-01	1E-01	3E-01	2E-01	2E-01	6E-02	1E-01	3E-01	1E-01	9E-02	1E-01	3E-01	1E-01	3E-01	2E-01	3E-01	7E-02
LPC(14:0)b	2E-02	2E-02	3E-02	9E-03	1E-02	1E-02	2E-02	3E-02	2E-02	2E-02	2E-02	8E-03	3E-02	9E-03	7E-03	2E-02	3E-02	1E-02	2E-02	2E-02	2E-02	6E-03
LPC(16:1)	2E-01	1E-01	1E-01	4E-02	4E-02	1E-01	1E-01	1E-01	1E-01	2E-01	6E-02	8E-02	1E-01	1E-01	6E-02	8E-02	2E-01	9E-02	1E-01	1E-01	2E-01	4E-02
LPC(16:0)	4E+01	3E+01	2E+01	1E+01	1E+01	5E+01	3E+01	4E+01	3E+01	5E+01	1E+01	3E+01	5E+01	3E+01	2E+01	2E+01	7E+01	3E+01	4E+01	4E+01	6E+01	1E+01
LPC(16:0)b	3E+00	3E+00	2E+00	1E+00	1E+00	3E+00	3E+00	3E+00	3E+00	4E+00	1E+00	2E+00	3E+00	2E+00	1E+00	2E+00	5E+00	2E+00	3E+00	3E+00	4E+00	9E-01
LPC(18:2)	1E+00	4E-01	1E+00	2E-01	2E-01	6E-01	1E+00	5E-01	5E-01	7E-01	2E-01	5E-01	6E-01	1E+00	6E-01	9E-01	2E+00	1E+00	6E-01	7E-01	9E-01	2E-01
LPC(18:2)b	7E-01	4E-01	1E+00	3E-01	2E-01	5E-01	6E-01	3E-01	4E-01	5E-01	7E-01	3E-01	3E-01	4E-01	2E-01	3E-01	8E-01	4E-01	3E-01	3E-01	4E-01	2E-01
LPC(18:1)	3E+00	2E+00	2E+00	8E-01	8E-01	3E+00	2E+00	2E+00	3E+00	3E+00	7E-01	2E+00	3E+00	3E+00	2E+00	2E+00	5E+00	3E+00	2E+00	4E+00	4E+00	8E-01
LPC(18:1)b	1E+00	9E-01	1E+00	4E-01	4E-01	1E+00	9E-01	8E-01	1E+00	1E+00	8E-01	6E-01	8E-01	7E-01	3E-01	5E-01	1E+00	7E-01	7E-01	8E-01	1E+00	3E-01
LPC(18:0)	4E+01	4E+01	2E+01	1E+01	1E+01	4E+01	3E+01	4E+01	4E+01	4E+01	1E+01	3E+01	4E+01	3E+01	2E+01	2E+01	6E+01	3E+01	4E+01	5E+01	4E+01	1E+01
LPC(18:0)b	1E+00	1E+00	1E+00	5E-01	5E-01	2E+00	1E+00	2E+00	2E+00	2E+00	5E-01	1E+00	2E+00	1E+00	9E-01	8E-01	2E+00	1E+00	2E+00	2E+00	2E+00	5E-01
LPC(20:4)	5E-01	3E-01	6E-01	2E-01	1E-01	3E-01	4E-01	4E-01	3E-01	5E-01	2E+00	2E-01	4E-01	4E-01	3E-01	2E-01	6E-01	4E-01	4E-01	4E-01	5E-01	1E-01
LPC(20:4)b	6E-01	8E-01	4E+00	7E-01	5E-01	5E-01	7E-01	5E-01	6E-01	6E-01	2E+00	3E-01	4E-01	5E-01	3E-01	2E-01	7E-01	3E-01	4E-01	4E-01	5E-01	3E-01
LPC(20:2)	2E-01	2E-01	2E-01	9E-02	9E-02	2E-01	2E-01	3E-01	3E-01	3E-01	6E-02	2E-01	2E-01	2E-01	1E-01	1E-01	3E-01	2E-01	3E-01	3E-01	4E-01	6E-02
LPC(20:1)	8E-01	7E-01	6E-01	3E-01	4E-01	8E-01	7E-01	8E-01	1E+00	1E+00	2E-01	7E-01	8E-01	7E-01	5E-01	5E-01	1E+00	7E-01	9E-01	1E+00	1E+00	2E-01
LPC(20:1)b	2E-02	2E-02	2E-02	5E-03	1E-02	3E-02	2E-02	1E-02	4E-02	3E-02	7E-03	2E-02	3E-02	1E-02	1E-02	1E-02	3E-02	2E-02	2E-02	3E-02	3E-02	3E-03
LPC(20:0)	1E+00	1E+00	1E+00	6E-01	7E-01	1E+00	2E+00	2E+00	2E+00	2E+00	5E-01	1E+00	2E+00	1E+00	1E+00	8E-01	2E+00	1E+00	2E+00	2E+00	2E+00	6E-01
LPC(20:0)b	3E-02	4E-02	4E-02	2E-02	4E-02	4E-02	5E-02	5E-02	6E-02	5E-02	2E-02	4E-02	5E-02	3E-02	3E-02	4E-02	6E-02	3E-02	4E-02	6E-02	6E-02	2E-02
LPC(22:6)	4E-01	1E-01	1E-01	3E-02	3E-02	2E-01	8E-02	1E-01	1E-01	1E-01	1E-01	2E-01	1E-01	9E-02	5E-02	5E-02	3E-01	7E-02	8E-02	2E-01	9E-02	1E-01
LPC(22:4)	8E-02	8E-02	9E-02	4E-02	4E-02	8E-02	1E-01	2E-01	1E-01	2E-01	2E-02	5E-02	1E-01	1E-01	8E-02	6E-02	1E-01	1E-01	2E-01	1E-01	2E-01	2E-02
LPC(22:2)	2E-02	2E-02	5E-02	1E-02	2E-02	2E-02	2E-02	4E-02	3E-02	4E-02	8E-03	3E-02	2E-02	3E-02	2E-02	1E-02	4E-02	2E-02	4E-02	3E-02	5E-02	6E-03
LPC(22:1)	1E-01	5E-02	4E-02	3E-02	2E-02	8E-02	5E-02	5E-02	8E-02	6E-02	3E-02	1E-01	6E-02	5E-02	4E-02	4E-02	1E-01	5E-02	5E-02	9E-02	6E-02	4E-02
LPC(22:0)	9E-02	7E-02	7E-02	4E-02	5E-02	7E-02	1E-01	8E-02	1E-01	9E-02	5E-02	1E-01	1E-01	9E-02	7E-02	5E-02	1E-01	9E-02	8E-02	1E-01	9E-02	5E-02
LPC(24:1)	6E-02	2E-02	2E-02	1E-02	1E-02	5E-02	3E-02	3E-02	3E-02	4E-02	2E-02	5E-02	3E-02	2E-02	2E-02	4E-02	6E-02	3E-02	3E-02	5E-02	4E-02	3E-02
LPC(24:0)	1E-01	7E-02	7E-02	4E-02	6E-02	9E-02	1E-01	1E-01	9E-02	1E-01	4E-02	8E-02	9E-02	8E-02	7E-02	7E-02	1E-01	1E-01	1E-01	1E-01	1E-01	5E-02
LPC(26:0)	1E-01	8E-02	8E-02	8E-02	6E-02	7E-02	9E-02	9E-02	6E-02	9E-02	8E-02	1E-01	9E-02	6E-02	8E-02	8E-02	8E-02	7E-02	6E-02	1E-01	9E-02	7E-02
LPC(26:1)	2E-02	8E-03	1E-02	6E-03	9E-03	2E-02	2E-02	1E-02	2E-02	3E-02	7E-03	2E-02	2E-02	1E-02	1E-02	2E-02	3E-02	2E-02	2E-02	2E-02	2E-02	1E-02
PC(28:0)	1E-01	5E-01	1E-01	9E-02	3E-01	3E-01	2E-01	1E+00	2E-01	8E-01	1E-01	1E-01	7E-01	1E-01	2E-01	3E-01	5E-01	4E-01	2E+00	5E-01	1E+00	1E-01
PC(30:0)	5E+00	1E+01	5E+00	5E+00	8E+00	8E+00	1E+01	2E+01	9E+00	2E+01	4E+00	5E+00	1E+01	5E+00	7E+00	9E+00	1E+01	1E+01	2E+01	1E+01	2E+01	7E+00
PC(32:0)	1E+02	2E+02	1E+02	7E+01	1E+02	2E+02	2E+02	2E+02	2E+02	3E+02	6E+01	1E+02	2E+02	1E+02	1E+02	1E+02	2E+02	2E+02	2E+02	2E+02	3E+02	7E+01
PC(34:0)	6E+01	6E+01	5E+01	3E+01	4E+01	7E+01	6E+01	7E+01	7E+01	9E+01	3E+01	5E+01	7E+01	6E+01	6E+01	5E+01	1E+02	6E+01	7E+01	8E+01	1E+02	3E+01
PC(36:0)	3E+01	5E+01	2E+01	1E+01	4E+01	4E+01	3E+01	5E+01	4E+01	4E+01	3E+01	4E+01	4E+01	2E+01	2E+01	2E+01	3E+01	2E+01	3E+01	3E+01	5E+01	2E+01
PC(32:1)	2E+01	3E+01	1E+01	7E+00	2E+01	3E+01	2E+01	4E+01	3E+01	7E+01	1E+01	2E+01	4E+01	2E+01	2E+01	2E+01	4E+01	3E+01	4E+01	4E+01	8E+01	1E+01
PC(34:1)	3E+02	4E+02	3E+02	2E+02	3E+02	4E+02	4E+02	4E+02	4E+02	5E+02	2E+02	3E+02	4E+02	3E+02	3E+02	3E+02	4E+02	4E+02	4E+02	5E+02	5E+02	3E+02
PC(36:1)	2E+02	3E+02	2E+02	1E+02	2E+02	3E+02	2E+02	3E+02	3E+02	4E+02	9E+01	2E+02	3E+02	2E+02	2E+02	2E+02	3E+02	3E+02	3E+02	4E+02	4E+02	1E+02
PC(38:1)	1E+01	1E+01	7E+00	4E+00	8E+00	1E+01	1E+01	1E+01	1E+01	1E+01	3E+00	1E+01	1E+01	1E+01	1E+01	9E+00	2E+01	2E+01	2E+01	2E+01	2E+01	4E+00
PC(40:1)	4E-01	4E-01	3E-01	2E-01	3E-01	5E-01	4E-01	5E-01	5E-01	6E-01	2E-01	5E-01	5E-01	4E-01	3E-01	3E-01	7E-01	6E-01	6E-01	7E-01	6E-01	2E-01
PC(32:2)	2E+00	3E+00	1E+00	9E-01	2E+00	2E+00	2E+00	8E+00	4E+00	8E+00	7E-01	2E+00	4E+00	2E+00	2E+00	3E+00	3E+00	3E+00	9E+00	6E+00	1E+01	9E-01
PC(34:2)	2E+02	2E+02	2E+02	1E+02	2E+02	2E+02	2E+02	3E+02	2E+02	4E+02	9E+01	2E+02	3E+02	2E+02	2E+02	2E+02	3E+02	3E+02	3E+02	3E+02	4E+02	1E+02
PC(36:2)	2E+02	1E+02	1E+02	6E+01	9E+01	2E+02	2E+02	2E+02	2E+02	2E+02	5E+01	1E+02	2E+02	1E+02	1E+02	1E+02	2E+02	2E+02	2E+02	2E+02	3E+02	7E+01
PC(38:2)a	9E+00	8E+00	8E+00	4E+00	7E+00	1E+01	1E+01	2E+01	1E+01	2E+01	3E+00	9E+00	1E+01	1E+01	9E+00	9E+00	2E+01	1E+01	2E+01	2E+01	2E+01	3E+00
PC(38:2)b	9E+00	9E+00	6E+00	4E+00	8E+00	1E+01	9E+00	1E+01	1E+01	2E+01	3E+00	8E+00	1E+01	8E+00	7E+00	9E+00	1E+01	1E+01	1E+01	2E+01	2E+01	4E+00
PC(34:3)	6E+00	5E+00	3E+00	2E+00	3E+00	4E+00	7E+00	7E+00	8E+00	9E+00	1E+00	5E+00	6E+00	4E+00	4E+00	4E+00	7E+00	9E+00	8E+00	1E+01	1E+01	2E+00
PC(36:3)	4E+01	5E+01	4E+01	2E+01	3E+01	6E+01	6E+01	7E+01	7E+01	1E+02	1E+01	4E+01	6E+01	5E+01	4E+01	4E+01	8E+01	6E+01	7E+01	9E+01	1E+02	2E+01
PC(38:3)	3E+01	3E+01	2E+01	1E+01	1E+01	3E+01	3E+01	4E+01	3E+01	5E+01	1E+01	2E+01	4E+01	2E+01	2E+01	2E+01	5E+01	3E+01	4E+01	4E+01	6E+01	1E+01
PC(40:3)	9E-01	1E+00	6E-01	4E-01	7E-01	1E+00	1E+00	2E+00	1E+00	2E+00	3E-01	9E-01	1E+00	9E-01	8E-01	8E-01	2E+00	2E+00	2E+00	2E+00	3E+00	4E-01
PC(36:4)a	1E+01	9E+00	9E+00	5E+00	7E+00	1E+01	2E+01	2E+01	2E+01	3E+01	2E+00	1E+01	1E+01	1E+01	1E+01	8E+00	2E+01	2E+01	2E+01	3E+01	3E+01	2E+00
PC(36:4)b	2E+02	3E+02	2E+02	1E+02	2E+02	2E+02	2E+02	3E+02	2E+02	4E+02	7E+01	2E+02	3E+02	2E+02	2E+02	2E+02	3E+02	3E+02	3E+02	3E+02	4E+02	8E+01
PC(38:4)a	1E+01	1E+01	1E+01	6E+00	9E+00	2E+01	2E+01	2E+01	2E+01	3E+01	4E+00	1E+01	2E+01	1E+01	1E+01	1E+01	2E+01	2E+01	2E+01	3E+01	4E+01	5E+00
PC(38:4)b	1E+01	1E+01	2E+01	1E+01	1E+01	1E+01	2E+01	3E+01	2E+01	3E+01	4E+00	9E+00	2E+01	2E+01	2E+01	1E+01	2E+01	2E+01	3E+01	2E+01	4E+01	5E+00
PC(38:4)c	1E+02	2E+02	1E+02	9E+01	1E+02	2E+02	2E+02	3E+02	2E+02	3E+02	5E+01	1E+02	2E+02	1E+02	1E+02	1E+02	2E+02	2E+02	3E+02	2E+02	3E+02	6E+01
PC(40:4)a	2E+00	4E+00	3E+00	2E+00	3E+00	2E+00	3E+00	7E+00	4E+00	7E+00	1E+00	2E+00	5E+00	4E+00	4E+00	3E+00	3E+00	4E+00	7E+00	5E+00	8E+00	1E+00
PC(40:4)b	8E+00	1E+01	8E+00	5E+00	7E+00	9E+00	1E+01	2E+01	1E+01	1E+01	3E+00	7E+00	1E+01	9E+00	8E+00	7E+00	1E+01	1E+01	2E+01	1E+01	2E+01	3E+00
PC(42:4)	3E-01	3E-01	2E-01	1E-01	2E-01	3E-01	4E-01	5E-01	3E-01	3E-01	1E-01	3E-01	4E-01	3E-01	2E-01	2E-01	5E-01	5E-01	6E-01	4E-01	6E-01	1E-01
PC(36:5)	3E+01	1E+01	4E+00	2E+00	3E+00	4E+01	9E+00	1E+01	2E+01	1E+01	7E+00	2E+01	2E+01	6E+00	5E+00	4E+00	5E+01	1E+01	2E+01	2E+01	2E+01	8E+00
PC(38:5)a	1E+01	8E+00	8E+00	5E+00	6E+00	1E+01	1E+01	2E+01	1E+01	2E+01	3E+00	1E+01	9E+00	1E+01	7E+00	6E+00	2E+01	2E+01	1E+01	2E+01	3E+01	7E+00
PC(38:5)b	4E+01	5E+01	4E+01	2E+01	3E+01	5E+01	5E+01	6E+01	6E+01	7E+01	2E+01	3E+01	5E+01	4E+01	4E+01	3E+01	6E+01	5E+01	6E+01	7E+01	8E+01	2E+01
PC(38:5)c	2E+01	2E+01	8E+00	9E+00	8E+00	3E+01	2E+01	3E+01	2E+01	2E+01	7E+00	2E+01	2E+01	1E+01	1E+01	1E+01	4E+01	2E+01	3E+01	2E+01	2E+01	7E+00
PC(40:5)a	3E+00	2E+00	2E+00	2E+00	2E+00	3E+00	3E+00	4E+00	3E+00	4E+00	1E+00	2E+00	3E+00	3E+00	3E+00	2E+00	4E+00	3E+00	5E+00	4E+00	5E+00	1E+00
PC(40:5)b	1E+01	1E+01	1E+01	7E+00	9E+00	1E+01	1E+01	2E+01	1E+01	2E+01	4E+00	1E+01	1E+01	1E+01	1E+01	9E+00	1E+01	2E+01	2E+01	2E+01	2E+01	5E+00
PC(42:5)	1E+00	7E-01	6E-01	4E-01	5E-01	9E-01	9E-01	1E+00	8E-01	1E+00	2E-01	8E-01	8E-01	6E-01	7E-01	5E-01	1E+00	1E+00	1E+00	1E+00	1E+00	3E-01
PC(38:6)a	1E+01	1E+01	9E+00	5E+00	8E+00	1E+01	2E+01	3E+01	2E+01	3E+01	2E+00	8E+00	2E+01	1E+01	1E+01	9E+00	2E+01	2E+01	3E+01	3E+01	4E+01	3E+00
PC(38:6)b	4E+01	3E+01	2E+01	1E+01	1E+01	4E+01	2E+01	3E+01	3E+01	4E+01	2E+01	3E+01	4E+01	2E+01	1E+01	1E+01	6E+01	2E+01	3E+01	4E+01	4E+01	2E+01
PC(40:6)	1E+01	8E+00	6E+00	3E+00	4E+00	1E+01	5E+00	1E+01	9E+00	7E+00	4E+00	8E+00	1E+01	6E+00	5E+00	4E+00	1E+01	6E+00	1E+01	1E+01	9E+00	4E+00
PC(42:6)	6E-01	5E-01	3E-01	2E-01	2E-01	5E-01	3E-01	5E-01	5E-01	4E-01	3E-01	4E-01	4E-01	4E-01	4E-01	3E-01	7E-01	4E-01	5E-01	7E-01	5E-01	3E-01
PC(40:7)	2E+01	1E+01	7E+00	4E+00	7E+00	3E+01	1E+01	2E+01	2E+01	2E+01	9E+00	2E+01	2E+01	1E+01	7E+00	9E+00	4E+01	1E+01	2E+01	3E+01	2E+01	1E+01
PC(e32:0)	1E+01	1E+01	5E+00	3E+00	1E+01	2E+01	1E+01	9E+00	9E+00	2E+01	4E+00	1E+01	2E+01	6E+00	6E+00	1E+01	2E+01	1E+01	9E+00	1E+01	2E+01	5E+00
PC(e34:0)	1E+01	2E+01	6E+00	3E+00	1E+01	2E+01	1E+01	1E+01	1E+01	2E+01	2E+00	1E+01	2E+01	9E+00	8E+00	1E+01	2E+01	1E+01	1E+01	2E+01	2E+01	3E+00
PC(e34:1)	2E+01	2E+01	9E+00	5E+00	1E+01	3E+01	2E+01	1E+01	2E+01	3E+01	5E+00	2E+01	3E+01	1E+01	9E+00	2E+01	4E+01	2E+01	2E+01	3E+01	4E+01	6E+00
PC(e34:2)	4E+00	4E+00	3E+00	2E+00	3E+00	4E+00	4E+00	5E+00	3E+00	5E+00	2E+00	4E+00	4E+00	3E+00	3E+00	3E+00	5E+00	4E+00	5E+00	4E+00	6E+00	3E+00
PC(e34:2)b	4E+00	5E+00	2E+00	1E+00	3E+00	4E+00	4E+00	5E+00	5E+00	6E+00	1E+00	4E+00	7E+00	3E+00	3E+00	3E+00	6E+00	5E+00	6E+00	8E+00	8E+00	2E+00
PC(e34:3)	2E+00	3E+00	2E+00	1E+00	2E+00	3E+00	3E+00	5E+00	2E+00	5E+00	7E-01	2E+00	4E+00	3E+00	2E+00	2E+00	4E+00	4E+00	5E+00	4E+00	7E+00	1E+00
PC(e36:0)	3E+00	5E+00	2E+00	1E+00	4E+00	4E+00	3E+00	6E+00	3E+00	8E+00	1E+00	3E+00	8E+00	2E+00	2E+00	4E+00	7E+00	4E+00	8E+00	5E+00	1E+01	1E+00
PC(e36:1)	4E+00	4E+00	1E+00	1E+00	3E+00	5E+00	4E+00	4E+00	4E+00	6E+00	1E+00	4E+00	7E+00	2E+00	2E+00	4E+00	9E+00	4E+00	5E+00	6E+00	9E+00	1E+00
PC(e36:2)	2E+00	3E+00	1E+00	9E-01	2E+00	3E+00	2E+00	2E+00	4E+00	4E+00	1E+00	2E+00	4E+00	2E+00	2E+00	2E+00	5E+00	3E+00	2E+00	5E+00	6E+00	2E+00
PC(e36:2)b	3E-01	4E-01	2E-01	1E-01	2E-01	4E-01	3E-01	5E-01	4E-01	4E-01	7E-02	3E-01	6E-01	3E-01	2E-01	2E-01	5E-01	4E-01	5E-01	5E-01	6E-01	1E-01
PC(e36:3)	1E+00	1E+00	9E-01	5E-01	9E-01	2E+00	1E+00	1E+00	1E+00	2E+00	8E-01	1E+00	2E+00	8E-01	8E-01	1E+00	2E+00	1E+00	9E-01	2E+00	2E+00	1E+00
PC(e36:4)	4E+01	7E+01	3E+01	2E+01	4E+01	6E+01	6E+01	6E+01	5E+01	7E+01	2E+01	4E+01	8E+01	4E+01	3E+01	4E+01	8E+01	7E+01	7E+01	6E+01	1E+02	2E+01
PC(e36:5)	4E+00	2E+00	8E-01	4E-01	5E-01	4E+00	1E+00	1E+00	2E+00	1E+00	1E+00	4E+00	2E+00	1E+00	1E+00	7E-01	6E+00	1E+00	1E+00	2E+00	2E+00	2E+00
PC(e36:5)b	1E+01	2E+01	1E+01	7E+00	1E+01	2E+01	2E+01	3E+01	2E+01	3E+01	4E+00	1E+01	3E+01	2E+01	1E+01	1E+01	2E+01	2E+01	3E+01	3E+01	3E+01	6E+00
PC(e38:0)	7E-01	9E-01	5E-01	3E-01	8E-01	9E-01	8E-01	1E+00	7E-01	2E+00	2E-01	6E-01	1E+00	7E-01	5E-01	8E-01	1E+00	9E-01	1E+00	1E+00	3E+00	3E-01
PC(e38:1)	7E-01	9E-01	4E-01	2E-01	7E-01	1E+00	7E-01	1E+00	9E-01	1E+00	2E-01	7E-01	1E+00	4E-01	5E-01	8E-01	1E+00	9E-01	1E+00	1E+00	2E+00	3E-01
PC(e38:3)	2E+00	1E+00	6E-01	4E-01	9E-01	2E+00	1E+00	2E+00	1E+00	2E+00	6E-01	1E+00	2E+00	9E-01	7E-01	1E+00	3E+00	2E+00	2E+00	2E+00	3E+00	7E-01
PC(e38:4)	3E+01	4E+01	2E+01	1E+01	2E+01	4E+01	3E+01	4E+01	3E+01	5E+01	1E+01	3E+01	6E+01	2E+01	3E+01	3E+01	6E+01	4E+01	6E+01	4E+01	6E+01	1E+01
PC(e38:5)	2E+01	4E+01	2E+01	1E+01	2E+01	3E+01	3E+01	3E+01	4E+01	4E+01	1E+01	2E+01	4E+01	2E+01	2E+01	2E+01	4E+01	3E+01	3E+01	4E+01	5E+01	1E+01
PC(e38:5)b	1E+00	3E+00	1E+00	7E-01	1E+00	2E+00	2E+00	3E+00	2E+00	2E+00	3E-01	1E+00	3E+00	1E+00	1E+00	1E+00	2E+00	2E+00	3E+00	3E+00	3E+00	5E-01
PC(e40:0)	1E-01	9E-02	7E-02	3E-02	8E-02	1E-01	1E-01	1E-01	1E-01	3E-01	4E-02	1E-01	1E-01	8E-02	6E-02	1E-01	2E-01	1E-01	1E-01	2E-01	3E-01	5E-02
PC(e40:4)	3E+00	5E+00	2E+00	2E+00	4E+00	4E+00	4E+00	8E+00	3E+00	7E+00	1E+00	3E+00	7E+00	3E+00	3E+00	5E+00	5E+00	5E+00	1E+01	4E+00	9E+00	1E+00
PC(e40:4)b	4E-01	8E-01	4E-01	2E-01	5E-01	6E-01	5E-01	1E+00	6E-01	1E+00	1E-01	4E-01	1E+00	5E-01	5E-01	7E-01	8E-01	7E-01	1E+00	8E-01	2E+00	1E-01
PC(e40:5)	2E+00	2E+00	2E+00	1E+00	2E+00	3E+00	2E+00	3E+00	2E+00	4E+00	8E-01	2E+00	3E+00	2E+00	2E+00	2E+00	4E+00	3E+00	3E+00	3E+00	5E+00	9E-01
PC(e40:6)	7E-01	7E-01	7E-01	4E-01	5E-01	7E-01	8E-01	8E-01	9E-01	1E+00	3E-01	7E-01	9E-01	8E-01	7E-01	6E-01	9E-01	9E-01	8E-01	1E+00	1E+00	4E-01
PC(e40:6)b	2E+00	2E+00	8E-01	5E-01	9E-01	2E+00	1E+00	2E+00	2E+00	2E+00	6E-01	2E+00	3E+00	1E+00	9E-01	1E+00	3E+00	1E+00	2E+00	2E+00	2E+00	8E-01
PC(e40:7)	2E+00	2E+00	1E+00	5E-01	9E-01	2E+00	1E+00	1E+00	2E+00	2E+00	7E-01	2E+00	3E+00	1E+00	9E-01	1E+00	3E+00	1E+00	2E+00	3E+00	3E+00	9E-01
PC(e42:4)	1E+00	1E+00	8E-01	4E-01	1E+00	1E+00	1E+00	2E+00	1E+00	3E+00	3E-01	1E+00	2E+00	1E+00	9E-01	1E+00	2E+00	2E+00	3E+00	2E+00	4E+00	4E-01
PC(e42:5)	1E+00	1E+00	9E-01	5E-01	1E+00	1E+00	1E+00	2E+00	1E+00	2E+00	4E-01	9E-01	2E+00	1E+00	9E-01	1E+00	2E+00	1E+00	2E+00	2E+00	3E+00	4E-01
PC(e42:6)	3E-01	3E-01	2E-01	2E-01	3E-01	3E-01	3E-01	7E-01	3E-01	7E-01	1E-01	3E-01	4E-01	3E-01	3E-01	3E-01	3E-01	4E-01	5E-01	5E-01	8E-01	2E-01
PC(e42:6)b	3E-01	4E-01	2E-01	1E-01	2E-01	4E-01	2E-01	5E-01	3E-01	5E-01	9E-02	3E-01	5E-01	3E-01	2E-01	3E-01	6E-01	3E-01	6E-01	5E-01	7E-01	1E-01
PC(e44:4)	2E-01	2E-01	1E-01	7E-02	2E-01	2E-01	3E-01	4E-01	2E-01	5E-01	6E-02	2E-01	3E-01	2E-01	1E-01	2E-01	3E-01	3E-01	4E-01	3E-01	7E-01	7E-02
PC(e44:5)	1E+00	1E+00	8E-01	4E-01	1E+00	1E+00	1E+00	2E+00	1E+00	3E+00	3E-01	1E+00	1E+00	1E+00	9E-01	1E+00	2E+00	2E+00	2E+00	2E+00	4E+00	4E-01
PC(e44:6)	3E-01	3E-01	3E-01	2E-01	4E-01	3E-01	4E-01	6E-01	4E-01	9E-01	2E-01	3E-01	3E-01	3E-01	3E-01	4E-01	4E-01	5E-01	5E-01	5E-01	1E+00	2E-01
PC(e44:6)b	1E-01	1E-01	8E-02	5E-02	9E-02	2E-01	1E-01	2E-01	2E-01	2E-01	3E-02	1E-01	2E-01	1E-01	9E-02	1E-01	2E-01	1E-01	2E-01	2E-01	4E-01	5E-02
PI(38:4)	2E+02	2E+02	2E+02	8E+01	2E+02	1E+02	3E+02	2E+02	1E+02	3E+02	6E+01	8E+01	3E+02	8E+01	8E+01	1E+02	1E+02	2E+02	1E+02	3E+02	4E+02	9E+01
PI(36:4)	1E+01	2E+01	6E+00	5E+00	1E+01	1E+01	1E+01	2E+01	1E+01	3E+01	5E+00	9E+00	2E+01	7E+00	8E+00	1E+01	2E+01	1E+01	2E+01	2E+01	3E+01	5E+00
PI(40:4)	4E-01	8E-01	5E-01	4E-01	5E-01	8E-01	8E-01	4E-01	9E-01	7E-01	3E-01	6E-01	6E-01	5E-01	5E-01	7E-01	9E-01	5E-01	8E-01	8E-01	6E-01	3E-01
PI(40:5)	1E+00	2E+00	3E+00	2E+00	2E+00	1E+00	3E+00	1E+00	2E+00	3E+00	4E-01	7E-01	4E+00	3E+00	1E+00	3E+00	1E+00	1E+00	1E+00	3E+00	3E+00	6E-01
PI(38:5)	2E+01	2E+01	1E+01	1E+01	2E+01	2E+01	2E+01	3E+01	3E+01	4E+01	7E+00	1E+01	3E+01	2E+01	1E+01	2E+01	4E+01	3E+01	3E+01	4E+01	6E+01	7E+00

Table 61. *Results of estimation of absolute lipid concentrations for LPC, PC, ePC and PI in thrombin with the platelet inhibitor and inhibitor treated samples. Results are shown as average amount (nmol) per 1 million platelets.*

	Thrombin &Platelet Inhibitor										Platelet inhibitor									
Donor:	*1*	*2*	*3*	*4*	*5*	*6*	*7*	*8*	*9*	*10*	*11*	*1*	*2*	*3*	*4*	*5*	*6*	*7*	*8*	*9*	*10*	*11*
LPC(14:0)	1E-01	3E-01	1E-01	9E-02	1E-01	2E-01	2E-01	3E-01	2E-01	3E-01	6E-02	1E-01	2E-01	8E-02	6E-02	9E-02	1E-01	8E-02	2E-01	1E-01	2E-01	6E-02
LPC(14:0)b	1E-02	3E-02	1E-02	9E-03	2E-02	2E-02	2E-02	1E-02	1E-02	2E-02	4E-03	8E-03	2E-02	1E-02	8E-03	1E-02	9E-03	1E-02	2E-02	1E-02	2E-02	8E-03
LPC(16:1)	1E-01	1E-01	1E-01	5E-02	9E-02	1E-01	2E-01	1E-01	1E-01	2E-01	3E-02	8E-02	1E-01	6E-02	5E-02	6E-02	8E-02	7E-02	7E-02	8E-02	9E-02	4E-02
LPC(16:0)	3E+01	4E+01	3E+01	2E+01	2E+01	5E+01	3E+01	4E+01	4E+01	5E+01	1E+01	3E+01	3E+01	2E+01	1E+01	2E+01	3E+01	2E+01	3E+01	3E+01	4E+01	1E+01
LPC(16:0)b	3E+00	4E+00	2E+00	1E+00	2E+00	4E+00	3E+00	3E+00	3E+00	4E+00	7E-01	2E+00	2E+00	2E+00	1E+00	2E+00	3E+00	2E+00	2E+00	2E+00	3E+00	9E-01
LPC(18:2)	1E+00	8E-01	1E+00	4E-01	1E+00	1E+00	4E+00	7E-01	4E-01	8E-01	1E-01	5E-01	3E-01	4E-01	3E-01	4E-01	4E-01	6E-01	4E-01	3E-01	5E-01	1E-01
LPC(18:2)b	7E-01	5E-01	4E-01	2E-01	3E-01	5E-01	1E+00	2E-01	1E-01	4E-01	8E-02	4E-01	3E-01	3E-01	1E-01	2E-01	2E-01	2E-01	1E-01	1E-01	2E-01	1E-01
LPC(18:1)	3E+00	3E+00	2E+00	1E+00	2E+00	3E+00	4E+00	3E+00	3E+00	5E+00	6E-01	2E+00	2E+00	2E+00	1E+00	1E+00	2E+00	2E+00	2E+00	2E+00	2E+00	6E-01
LPC(18:1)b	8E-01	9E-01	6E-01	3E-01	5E-01	9E-01	8E-01	6E-01	6E-01	1E+00	2E-01	7E-01	6E-01	4E-01	3E-01	4E-01	6E-01	4E-01	4E-01	4E-01	8E-01	4E-01
LPC(18:0)	4E+01	4E+01	3E+01	2E+01	2E+01	4E+01	3E+01	5E+01	5E+01	5E+01	1E+01	4E+01	3E+01	2E+01	2E+01	2E+01	4E+01	3E+01	3E+01	3E+01	4E+01	1E+01
LPC(18:0)b	1E+00	2E+00	2E+00	9E-01	8E-01	2E+00	1E+00	2E+00	2E+00	2E+00	5E-01	1E+00	1E+00	1E+00	8E-01	7E-01	1E+00	1E+00	1E+00	1E+00	2E+00	5E-01
LPC(20:4)	3E-01	3E-01	3E-01	2E-01	2E-01	4E-01	5E-01	4E-01	2E-01	5E-01	6E-02	2E-01	3E-01	3E-01	2E-01	2E-01	2E-01	2E-01	2E-01	2E-01	3E-01	8E-02
LPC(20:4)b	5E-01	5E-01	2E-01	2E-01	2E-01	3E-01	3E-01	4E-01	1E-01	5E-01	1E-01	4E-01	4E-01	3E-01	2E-01	2E-01	3E-01	2E-01	2E-01	2E-01	3E-01	5E-01
LPC(20:2)	2E-01	1E-01	2E-01	1E-01	2E-01	2E-01	2E-01	4E-01	2E-01	4E-01	4E-02	2E-01	1E-01	2E-01	1E-01	1E-01	2E-01	2E-01	2E-01	2E-01	3E-01	4E-02
LPC(20:1)	8E-01	7E-01	7E-01	5E-01	5E-01	8E-01	8E-01	1E+00	1E+00	1E+00	2E-01	7E-01	6E-01	6E-01	4E-01	5E-01	7E-01	7E-01	5E-01	8E-01	1E+00	2E-01
LPC(20:1)b	2E-02	1E-02	9E-03	1E-02	1E-02	3E-02	2E-02	2E-02	4E-02	3E-02	4E-03	1E-02	1E-02	1E-02	1E-02	2E-02	1E-02	2E-02	1E-02	2E-02	2E-02	5E-03
LPC(20:0)	1E+00	1E+00	2E+00	1E+00	9E-01	1E+00	1E+00	3E+00	2E+00	2E+00	5E-01	2E+00	1E+00	1E+00	1E+00	9E-01	1E+00	2E+00	1E+00	1E+00	2E+00	6E-01
LPC(20:0)b	4E-02	4E-02	4E-02	2E-02	3E-02	3E-02	4E-02	7E-02	7E-02	6E-02	1E-02	6E-02	3E-02	4E-02	3E-02	2E-02	4E-02	4E-02	4E-02	5E-02	5E-02	2E-02
LPC(22:6)	2E-01	1E-01	6E-02	3E-02	4E-02	2E-01	8E-02	9E-02	9E-02	7E-02	4E-02	2E-01	9E-02	6E-02	3E-02	4E-02	1E-01	4E-02	7E-02	8E-02	6E-02	7E-02
LPC(22:4)	6E-02	8E-02	7E-02	7E-02	6E-02	7E-02	8E-02	2E-01	7E-02	2E-01	1E-02	5E-02	6E-02	8E-02	6E-02	5E-02	6E-02	9E-02	1E-01	8E-02	2E-01	1E-02
LPC(22:2)	2E-02	2E-02	3E-02	2E-02	1E-02	2E-02	2E-02	5E-02	3E-02	4E-02	5E-03	2E-02	2E-02	2E-02	1E-02	2E-02	2E-02	2E-02	2E-02	2E-02	3E-02	1E-02
LPC(22:1)	1E-01	5E-02	5E-02	4E-02	3E-02	8E-02	7E-02	7E-02	8E-02	6E-02	3E-02	1E-01	5E-02	4E-02	3E-02	4E-02	7E-02	5E-02	4E-02	7E-02	6E-02	2E-02
LPC(22:0)	1E-01	8E-02	9E-02	6E-02	6E-02	8E-02	1E-01	1E-01	1E-01	1E-01	5E-02	1E-01	7E-02	7E-02	5E-02	7E-02	8E-02	9E-02	7E-02	8E-02	1E-01	4E-02
LPC(24:1)	5E-02	2E-02	3E-02	2E-02	3E-02	5E-02	5E-02	4E-02	5E-02	4E-02	2E-02	6E-02	2E-02	2E-02	2E-02	3E-02	4E-02	3E-02	3E-02	3E-02	3E-02	2E-02
LPC(24:0)	1E-01	8E-02	1E-01	7E-02	7E-02	1E-01	1E-01	1E-01	1E-01	2E-01	5E-02	1E-01	8E-02	7E-02	6E-02	7E-02	9E-02	9E-02	8E-02	1E-01	2E-01	4E-02
LPC(26:0)	8E-02	8E-02	8E-02	7E-02	1E-01	1E-01	9E-02	1E-01	8E-02	1E-01	8E-02	1E-01	9E-02	9E-02	9E-02	7E-02	7E-02	6E-02	9E-02	8E-02	1E-01	8E-02
LPC(26:1)	3E-02	2E-02	2E-02	1E-02	1E-02	3E-02	2E-02	2E-02	2E-02	4E-02	7E-03	3E-02	1E-02	1E-02	1E-02	1E-02	2E-02	1E-02	1E-02	2E-02	3E-02	1E-02
PC(28:0)	1E-01	5E-01	2E-01	2E-01	4E-01	3E-01	3E-01	2E+00	4E-01	1E+00	1E-01	1E-01	4E-01	1E-01	1E-01	3E-01	2E-01	3E-01	1E+00	3E-01	7E-01	1E-01
PC(30:0)	5E+00	1E+01	7E+00	6E+00	9E+00	8E+00	9E+00	2E+01	1E+01	2E+01	4E+00	6E+00	8E+00	8E+00	6E+00	7E+00	7E+00	9E+00	1E+01	8E+00	1E+01	5E+00
PC(32:0)	2E+02	2E+02	2E+02	1E+02	1E+02	2E+02	2E+02	2E+02	2E+02	3E+02	6E+01	1E+02	1E+02	1E+02	1E+02	1E+02	2E+02	2E+02	1E+02	2E+02	3E+02	7E+01
PC(34:0)	5E+01	6E+01	7E+01	5E+01	5E+01	6E+01	6E+01	8E+01	8E+01	1E+02	3E+01	5E+01	5E+01	5E+01	5E+01	4E+01	6E+01	5E+01	5E+01	6E+01	8E+01	3E+01
PC(36:0)	3E+01	4E+01	2E+01	2E+01	2E+01	5E+01	4E+01	6E+01	3E+01	4E+01	2E+01	2E+01	2E+01	2E+01	3E+01	2E+01	3E+01	3E+01	3E+01	3E+01	4E+01	2E+01
PC(32:1)	2E+01	3E+01	2E+01	1E+01	2E+01	3E+01	2E+01	5E+01	4E+01	9E+01	1E+01	2E+01	2E+01	1E+01	1E+01	2E+01	2E+01	2E+01	3E+01	2E+01	6E+01	1E+01
PC(34:1)	4E+02	4E+02	3E+02	3E+02	3E+02	4E+02	4E+02	4E+02	4E+02	5E+02	2E+02	3E+02	3E+02	3E+02	3E+02	2E+02	3E+02	3E+02	3E+02	4E+02	4E+02	3E+02
PC(36:1)	3E+02	3E+02	3E+02	2E+02	2E+02	3E+02	3E+02	3E+02	3E+02	4E+02	1E+02	2E+02	2E+02	2E+02	2E+02	2E+02	2E+02	2E+02	2E+02	3E+02	3E+02	1E+02
PC(38:1)	1E+01	1E+01	1E+01	6E+00	9E+00	2E+01	2E+01	2E+01	2E+01	4E+01	4E+00	1E+01	9E+00	8E+00	6E+00	8E+00	1E+01	1E+01	1E+01	1E+01	1E+01	5E+00
PC(40:1)	5E-01	4E-01	5E-01	3E-01	4E-01	4E-01	5E-01	6E-01	7E-01	7E-01	2E-01	4E-01	3E-01	3E-01	2E-01	3E-01	4E-01	4E-01	3E-01	4E-01	5E-01	2E-01
PC(32:2)	2E+00	3E+00	3E+00	2E+00	3E+00	2E+00	3E+00	1E+01	5E+00	1E+01	9E-01	2E+00	2E+00	2E+00	1E+00	2E+00	2E+00	2E+00	5E+00	3E+00	8E+00	1E+00
PC(34:2)	2E+02	2E+02	2E+02	2E+02	2E+02	2E+02	3E+02	3E+02	3E+02	4E+02	1E+02	2E+02	2E+02	2E+02	2E+02	2E+02	2E+02	2E+02	2E+02	2E+02	3E+02	1E+02
PC(36:2)	2E+02	2E+02	2E+02	1E+02	1E+02	2E+02	2E+02	3E+02	2E+02	3E+02	6E+01	1E+02	1E+02	1E+02	9E+01	9E+01	2E+02	1E+02	2E+02	2E+02	2E+02	7E+01
PC(38:2)a	1E+01	9E+00	1E+01	7E+00	8E+00	1E+01	1E+01	2E+01	2E+01	3E+01	3E+00	9E+00	6E+00	8E+00	6E+00	7E+00	9E+00	1E+01	1E+01	1E+01	2E+01	3E+00
PC(38:2)b	1E+01	8E+00	1E+01	6E+00	1E+01	1E+01	1E+01	1E+01	2E+01	2E+01	3E+00	8E+00	7E+00	6E+00	5E+00	7E+00	9E+00	9E+00	7E+00	1E+01	2E+01	4E+00
PC(34:3)	6E+00	5E+00	5E+00	3E+00	4E+00	4E+00	8E+00	1E+01	9E+00	1E+01	2E+00	6E+00	3E+00	3E+00	3E+00	3E+00	4E+00	6E+00	5E+00	7E+00	8E+00	2E+00
PC(40:5)b	1E+01	1E+01	1E+01	1E+01	8E+00	3E+01	2E+01	3E+01	2E+01	2E+01	5E+00	1E+01	9E+00	1E+01	1E+01	8E+00	1E+01	1E+01	1E+01	1E+01	2E+01	5E+00
PC(42:5)	1E+00	7E-01	9E-01	7E-01	6E-01	1E+00	1E+00	1E+00	1E+00	2E+00	3E-01	1E+00	5E-01	6E-01	6E-01	4E-01	8E-01	7E-01	7E-01	8E-01	9E-01	4E-01
PC(38:6)a	1E+01	1E+01	2E+01	9E+00	1E+01	1E+01	2E+01	4E+01	3E+01	5E+01	3E+00	9E+00	9E+00	1E+01	9E+00	9E+00	1E+01	2E+01	2E+01	2E+01	3E+01	3E+00
PC(38:6)b	4E+01	4E+01	3E+01	1E+01	2E+01	5E+01	3E+01	4E+01	4E+01	4E+01	2E+01	3E+01	2E+01	2E+01	1E+01	1E+01	4E+01	2E+01	2E+01	3E+01	3E+01	2E+01
PC(40:6)	1E+01	9E+00	7E+00	4E+00	4E+00	1E+01	6E+00	1E+01	1E+01	9E+00	4E+00	9E+00	7E+00	5E+00	4E+00	3E+00	9E+00	4E+00	7E+00	8E+00	7E+00	4E+00
PC(42:6)	5E-01	4E-01	5E-01	3E-01	2E-01	4E-01	4E-01	6E-01	7E-01	6E-01	3E-01	4E-01	3E-01	3E-01	3E-01	3E-01	5E-01	4E-01	5E-01	4E-01	3E-01	3E-01
PC(40:7)	3E+01	1E+01	1E+01	6E+00	9E+00	3E+01	1E+01	2E+01	3E+01	2E+01	9E+00	2E+01	1E+01	8E+00	6E+00	8E+00	2E+01	9E+00	1E+01	2E+01	2E+01	1E+01
PC(32:0)	1E+01	1E+01	8E+00	5E+00	1E+01	2E+01	1E+01	1E+01	1E+01	2E+01	4E+00	1E+01	9E+00	6E+00	5E+00	9E+00	1E+01	1E+01	6E+00	9E+00	1E+01	5E+00
PC(34:0)	1E+01	2E+01	1E+01	6E+00	1E+01	2E+01	1E+01	2E+01	2E+01	3E+01	3E+00	1E+01	1E+01	7E+00	6E+00	9E+00	1E+01	1E+01	8E+00	1E+01	1E+01	3E+00
PC(34:1)	2E+01	2E+01	1E+01	9E+00	2E+01	3E+01	2E+01	2E+01	3E+01	4E+01	5E+00	2E+01	2E+01	1E+01	7E+00	1E+01	2E+01	1E+01	1E+01	2E+01	3E+01	6E+00
PC(34:2)	4E+00	4E+00	4E+00	3E+00	3E+00	5E+00	5E+00	6E+00	4E+00	7E+00	3E+00	4E+00	3E+00	3E+00	2E+00	3E+00	4E+00	3E+00	4E+00	3E+00	5E+00	3E+00
PC(34:2)b	4E+00	6E+00	4E+00	3E+00	4E+00	5E+00	6E+00	7E+00	7E+00	8E+00	1E+00	4E+00	4E+00	3E+00	2E+00	2E+00	4E+00	4E+00	4E+00	5E+00	6E+00	2E+00
PC(34:3)	3E+00	5E+00	4E+00	2E+00	3E+00	3E+00	5E+00	6E+00	3E+00	7E+00	1E+00	2E+00	2E+00	2E+00	2E+00	2E+00	3E+00	3E+00	3E+00	3E+00	5E+00	1E+00
PC(36:0)	4E+00	5E+00	3E+00	2E+00	5E+00	4E+00	4E+00	1E+01	5E+00	1E+01	1E+00	3E+00	4E+00	2E+00	2E+00	4E+00	4E+00	3E+00	4E+00	3E+00	8E+00	1E+00
PC(36:1)	4E+00	5E+00	3E+00	2E+00	4E+00	5E+00	4E+00	7E+00	5E+00	9E+00	1E+00	4E+00	3E+00	2E+00	1E+00	3E+00	5E+00	3E+00	3E+00	4E+00	6E+00	1E+00
PC(36:2)	3E+00	3E+00	2E+00	1E+00	2E+00	3E+00	3E+00	4E+00	4E+00	6E+00	1E+00	2E+00	2E+00	1E+00	1E+00	2E+00	3E+00	2E+00	2E+00	3E+00	4E+00	1E+00
PC(e36:2)b	4E-01	5E-01	4E-01	2E-01	3E-01	4E-01	4E-01	6E-01	6E-01	8E-01	1E-01	3E-01	3E-01	2E-01	2E-01	2E-01	3E-01	2E-01	3E-01	4E-01	5E-01	8E-02
PC(e36:3)	1E+00	1E+00	9E-01	6E-01	1E+00	2E+00	1E+00	1E+00	1E+00	2E+00	1E+00	1E+00	9E-01	8E-01	6E-01	8E-01	1E+00	1E+00	7E-01	1E+00	1E+00	1E+00
PC(e36:4)	5E+01	7E+01	5E+01	3E+01	5E+01	6E+01	6E+01	9E+01	6E+01	1E+02	2E+01	4E+01	5E+01	3E+01	3E+01	3E+01	5E+01	5E+01	5E+01	4E+01	8E+01	2E+01
PC(e36:5)	4E+00	2E+00	1E+00	6E-01	7E-01	4E+00	1E+00	2E+00	2E+00	2E+00	2E+00	3E+00	1E+00	7E-01	6E-01	6E-01	4E+00	1E+00	8E-01	1E+00	2E+00	2E+00
PC(e36:5)b	1E+01	3E+01	2E+01	1E+01	1E+01	2E+01	2E+01	3E+01	3E+01	3E+01	5E+00	1E+01	2E+01	1E+01	1E+01	1E+01	1E+01	2E+01	2E+01	2E+01	3E+01	5E+00
PC(e38:0)	8E-01	9E-01	9E-01	4E-01	8E-01	9E-01	8E-01	2E+00	1E+00	3E+00	3E-01	6E-01	7E-01	5E-01	4E-01	7E-01	8E-01	7E-01	6E-01	6E-01	2E+00	3E-01
PC(e38:1)	9E-01	9E-01	7E-01	4E-01	7E-01	9E-01	7E-01	2E+00	2E+00	2E+00	3E-01	8E-01	6E-01	4E-01	8E-01	7E-01	8E-01	5E-01	7E-01	8E-01	1E+00	3E-01
PC(e38:3)	2E+00	1E+00	1E+00	7E-01	1E+00	2E+00	2E+00	2E+00	1E+00	3E+00	6E-01	1E+00	1E+00	7E-01	6E-01	8E-01	2E+00	1E+00	9E-01	1E+00	2E+00	7E-01
PC(e38:4)	4E+01	4E+01	3E+01	2E+01	3E+01	4E+01	4E+01	6E+01	4E+01	6E+01	1E+01	3E+01	3E+01	2E+01	2E+01	2E+01	3E+01	3E+01	3E+01	3E+01	4E+01	1E+01
PC(e38:5)	2E+01	3E+01	3E+01	2E+01	3E+01	3E+01	3E+01	4E+01	4E+01	5E+01	1E+01	2E+01	3E+01	2E+01	2E+01	2E+01	3E+01	3E+01	3E+01	3E+01	4E+01	1E+01
PC(e38:5)b	2E+00	2E+00	2E+00	1E+00	2E+00	2E+00	2E+00	4E+00	2E+00	3E+00	4E-01	1E+00	2E+00	1E+00	9E-01	1E+00	1E+00	1E+00	2E+00	1E+00	2E+00	4E-01
PC(e40:0)	1E-01	9E-02	1E-01	5E-02	1E-01	1E-01	1E-01	1E-01	1E-01	4E-01	4E-02	9E-02	6E-02	7E-02	4E-02	7E-02	1E-01	1E-01	7E-02	9E-02	2E-01	5E-02
PC(e40:4)	3E+00	6E+00	3E+00	2E+00	5E+00	4E+00	4E+00	1E+01	4E+00	1E+01	1E+00	3E+00	4E+00	2E+00	2E+00	4E+00	3E+00	4E+00	6E+00	3E+00	7E+00	1E+00
PC(e40:4)b	5E-01	8E-01	6E-01	4E-01	7E-01	5E-01	6E-01	2E+00	9E-01	2E+00	1E-01	4E-01	6E-01	4E-01	4E-01	6E-01	4E-01	5E-01	8E-01	5E-01	1E+00	1E-01
PC(e40:5)	2E+00	3E+00	2E+00	2E+00	2E+00	2E+00	2E+00	4E+00	3E+00	5E+00	8E-01	2E+00	2E+00	2E+00	1E+00	2E+00	2E+00	2E+00	2E+00	2E+00	4E+00	9E-01
PC(e40:6)	8E-01	7E-01	9E-01	6E-01	6E-01	9E-01	9E-01	8E-01	1E+00	1E+00	4E-01	7E-01	6E-01	6E-01	6E-01	5E-01	7E-01	7E-01	6E-01	1E+00	1E+00	3E-01
PC(e40:6)b	2E+00	2E+00	1E+00	8E-01	1E+00	2E+00	1E+00	2E+00	2E+00	2E+00	7E-01	2E+00	1E+00	9E-01	7E-01	8E-01	2E+00	9E-01	1E+00	1E+00	1E+00	7E-01
PC(e40:7)	2E+00	2E+00	1E+00	8E-01	1E+00	2E+00	1E+00	2E+00	3E+00	3E+00	9E-01	2E+00	1E+00	9E-01	7E-01	9E-01	2E+00	9E-01	9E-01	2E+00	2E+00	9E-01
PC(e42:4)	1E+00	1E+00	1E+00	7E-01	1E+00	1E+00	2E+00	4E+00	1E+00	4E+00	4E-01	1E+00	1E+00	8E-01	7E-01	1E+00	1E+00	2E+00	1E+00	1E+00	3E+00	4E-01
PC(e42:5)	1E+00	1E+00	1E+00	8E-01	1E+00	1E+00	1E+00	3E+00	2E+00	3E+00	4E-01	1E+00	1E+00	9E-01	7E-01	1E+00	1E+00	1E+00	1E+00	1E+00	2E+00	4E-01
PC(e42:6)	3E-01	2E-01	3E-01	2E-01	4E-01	3E-01	4E-01	7E-01	3E-01	9E-01	1E-01	2E-01	2E-01	2E-01	2E-01	2E-01	2E-01	3E-01	5E-01	3E-01	6E-01	2E-01
PC(e42:6)b	4E-01	4E-01	3E-01	2E-01	3E-01	4E-01	3E-01	7E-01	4E-01	8E-01	1E-01	3E-01	3E-01	2E-01	1E-01	2E-01	3E-01	2E-01	3E-01	3E-01	4E-01	1E-01
PC(e44:4)	2E-01	2E-01	2E-01	1E-01	2E-01	2E-01	3E-01	5E-01	3E-01	7E-01	6E-02	2E-01	1E-01	2E-01	1E-01	2E-01	2E-01	2E-01	2E-01	2E-01	5E-01	7E-02
PC(e44:5)	1E+00	1E+00	2E+00	7E-01	1E+00	1E+00	2E+00	3E+00	2E+00	4E+00	3E-01	1E+00	8E-01	9E-01	6E-01	1E+00	1E+00	1E+00	1E+00	1E+00	2E+00	4E-01
PC(e44:6)	4E-01	2E-01	4E-01	2E-01	3E-01	4E-01	5E-01	6E-01	5E-01	1E+00	1E-01	3E-01	2E-01	3E-01	2E-01	3E-01	3E-01	4E-01	4E-01	3E-01	8E-01	2E-01
PC(e44:6)b	1E-01	2E-01	2E-01	8E-02	1E-01	1E-01	2E-01	3E-01	2E-01	4E-01	5E-02	1E-01	9E-02	1E-01	8E-02	8E-02	1E-01	1E-01	1E-01	1E-01	3E-01	4E-02
PI(38:4)	2E+02	2E+02	2E+02	1E+02	2E+02	2E+02	1E+02	2E+02	2E+02	3E+02	5E+01	1E+02	9E+01	1E+02	1E+02	9E+01	1E+02	2E+02	9E+01	9E+01	2E+02	1E+02
PI(36:4)	1E+01	1E+01	1E+01	1E+01	2E+01	2E+01	1E+01	3E+01	2E+01	5E+01	5E+00	1E+01	1E+01	7E+00	7E+00	1E+01	1E+01	1E+01	1E+01	1E+01	2E+01	6E+00
PI(40:4)	5E-01	4E-01	5E-01	4E-01	5E-01	4E-01	6E-01	1E+00	5E-01	8E-01	3E-01	8E-01	7E-01	5E-01	4E-01	7E-01	6E-01	5E-01	7E-01	8E-01	7E-01	3E-01
PI(40:5)	1E+00	2E+00	4E+00	1E+00	1E+00	1E+00	1E+00	3E+00	2E+00	3E+00	9E-01	7E-01	3E+00	2E+00	3E+00	1E+00	4E+00	2E+00	1E+00	3E+00	5E+00	8E-01
PI(38:5)	2E+01	2E+01	3E+01	2E+01	2E+01	3E+01	2E+01	4E+01	4E+01	6E+01	7E+00	2E+01	2E+01	2E+01	1E+01	2E+01	3E+01	3E+01	2E+01	3E+01	4E+01	8E+00

Table 62. *Results of estimation of absolute lipid concentrations for LPE, PE, ePE, PS, SM, CE and cholesterol in resting and thrombin-activated platelet samples. Results are shown as average amount (nmol) per 1 million platelets.*

	Resting											Thrombin										
Donor:	*1*	*2*	*3*	*4*	*5*	*6*	*7*	*8*	*9*	*10*	*11*	*1*	*2*	*3*	*4*	*5*	*6*	*7*	*8*	*9*	*10*	*11*
LPE(16:0)	2E+00	2E+00	1E+00	9E-01	1E+00	2E+00	2E+00	3E+00	2E+00	4E+00	7E-01	2E+00	3E+00	2E+00	8E-01	1E+00	2E+00	2E+00	3E+00	2E+00	4E+00	8E-01
LPE(16:0)b	6E-02	6E-02	1E-01	3E-02	5E-02	7E-02	7E-02	7E-02	8E-02	5E-02	5E-02	4E-02	8E-02	4E-02	3E-02	4E-02	1E-01	5E-02	8E-02	6E-02	9E-02	6E-02
LPE(18:0)	6E+00	1E+01	8E+00	5E+00	5E+00	8E+00	9E+00	1E+01	1E+01	2E+01	3E+00	6E+00	1E+01	8E+00	5E+00	4E+00	9E+00	8E+00	1E+01	1E+01	2E+01	3E+00
LPE(18:0)b	9E-02	1E-01	7E-02	5E-02	9E-02	1E-01	1E-01	2E-01	1E-01	2E-01	5E-02	1E-01	2E-01	9E-02	6E-02	8E-02	2E-01	9E-02	1E-01	1E-01	2E-01	5E-02
LPE(18:1)	1E+00	1E+00	1E+00	5E-01	5E-01	1E+00	1E+00	1E+00	2E+00	2E+00	4E-01	8E-01	2E+00	1E+00	6E-01	6E-01	1E+00	1E+00	1E+00	1E+00	2E+00	3E-01
LPE(18:1)b	4E-01	5E-01	3E+00	7E-01	7E-01	5E-01	6E-01	2E-01	7E-01	4E-01	3E+00	3E-01	3E-01	3E-01	3E-01	3E-01	5E-01	3E-01	2E-01	3E-01	3E-01	4E-01
LPE(18:2)	2E-01	1E-01	3E-01	9E-02	7E-02	1E-01	2E-01	1E-01	1E-01	2E-01	1E-01	8E-02	2E-01	1E-01	1E-01	2E-01	3E-01	3E-01	2E-01	1E-01	3E-01	5E-02
LPE(18:2)b	2E-01	3E-01	2E+00	5E-01	4E-01	3E-01	5E-01	2E-01	3E-01	3E-01	2E+00	1E-01	1E-01	2E-01	2E-01	2E-01	3E-01	1E-01	1E-01	2E-01	2E-01	3E-01
LPE(20:1)	2E-01	3E-01	2E-01	1E-01	2E-01	2E-01	2E-01	3E-01	3E-01	4E-01	6E-02	1E-01	3E-01	2E-01	1E-01	1E-01	2E-01	2E-01	3E-01	4E-01	6E-01	9E-02
LPE(20:2)	4E-02	6E-02	9E-02	5E-02	3E-02	8E-02	7E-02	7E-02	7E-02	1E-01	2E-02	4E-02	7E-02	6E-02	6E-02	2E-02	5E-02	6E-02	9E-02	1E-01	1E-01	3E-02
LPE(20:3)	2E-01	2E-01	1E+00	2E-01	2E-01	2E-01	2E-01	8E-02	2E-01	1E-01	2E+00	8E-02	1E-01	9E-02	9E-02	4E-02	2E-01	8E-02	6E-02	1E-01	7E-02	2E-01
LPE(20:4)	9E+00	2E+01	1E+02	3E+01	2E+01	1E+01	2E+01	7E+00	1E+01	1E+01	1E+02	5E+00	5E+00	8E+00	7E+00	4E+00	1E+01	5E+00	5E+00	7E+00	5E+00	1E+01
LPE(20:5)	6E-01	3E-01	2E+00	4E-01	3E-01	8E-01	3E-01	8E-02	5E-01	1E-01	7E+00	3E-01	9E-02	2E-01	1E-01	8E-02	8E-01	1E-01	1E-01	3E-01	6E-02	1E+00
LPE(20:0)	2E-01	2E-01	3E-01	1E-01	2E-01	2E-01	2E-01	3E-01	3E-01	5E-01	9E-02	2E-01	3E-01	3E-01	1E-01	2E-01	3E-01	3E-01	4E-01	4E-01	5E-01	1E-01
LPE(22:4)	8E-01	2E+00	2E+01	4E+00	3E+00	1E+00	2E+00	1E+00	2E+00	2E+00	6E+00	6E-01	9E-01	1E+00	1E+00	8E-01	1E+00	7E-01	8E-01	9E-01	8E-01	9E-01
LPE(22:5)	9E-01	2E+00	2E+01	4E+00	2E+00	1E+00	2E+00	7E-01	1E+00	1E+00	8E+00	5E-01	5E-01	1E+00	1E+00	4E-01	1E+00	5E-01	5E-01	7E-01	6E-01	1E+00
LPE(22:6)	1E+00	2E+00	1E+01	2E+00	1E+00	1E+00	1E+00	6E-01	2E+00	8E-01	1E+01	6E-01	5E-01	9E-01	7E-01	3E-01	1E+00	3E-01	4E-01	8E-01	4E-01	2E+00
PE(34:0)	9E-01	8E-01	6E-01	6E-01	1E+00	1E+00	6E-01	2E+00	9E-01	2E+00	5E-01	6E-01	1E+00	7E-01	5E-01	5E-01	1E+00	8E-01	1E+00	1E+00	1E+00	6E-01
PE(36:0)	2E-01	2E-01	2E-01	2E-01	2E-01	2E-01	2E-01	4E-01	3E-01	3E-01	1E-01	2E-01	3E-01	3E-01	2E-01	2E-01	3E-01	2E-01	3E-01	3E-01	4E-01	1E-01
PE(34:1)	2E+01	3E+01	2E+01	2E+01	2E+01	3E+01	2E+01	3E+01	4E+01	4E+01	2E+01	2E+01	3E+01	2E+01	2E+01	2E+01	4E+01	2E+01	2E+01	5E+01	3E+01	2E+01
PE(36:1)	3E+01	3E+01	2E+01	2E+01	2E+01	4E+01	2E+01	3E+01	5E+01	4E+01	1E+01	2E+01	4E+01	2E+01	2E+01	2E+01	5E+01	2E+01	2E+01	6E+01	4E+01	1E+01
PE(38:1)	1E+00	1E+00	1E+00	1E+00	1E+00	2E+00	1E+00	2E+00	3E+00	1E+00	5E-01	1E+00	2E+00	1E+00	2E+00	2E+00	2E+00	1E+00	1E+00	3E+00	2E+00	7E-01
PE(40:1)	2E-01	2E-01	1E-01	1E-01	2E-01	3E-01	2E-01	3E-01	4E-01	2E-01	1E-01	2E-01	3E-01	2E-01	2E-01	2E-01	4E-01	2E-01	2E-01	4E-01	3E-01	1E-01
PE(34:2)	1E+01	9E+00	5E+00	7E+00	9E+00	2E+01	1E+01	2E+01	2E+01	2E+01	6E+00	9E+00	1E+01	7E+00	1E+01	1E+01	2E+01	9E+00	2E+01	2E+01	3E+01	6E+00
PE(36:2)	4E+01	3E+01	2E+01	3E+01	3E+01	5E+01	4E+01	7E+01	6E+01	8E+01	2E+01	3E+01	5E+01	4E+01	3E+01	3E+01	6E+01	3E+01	5E+01	7E+01	8E+01	2E+01
PE(38:2)	5E+00	5E+00	4E+00	4E+00	5E+00	7E+00	5E+00	9E+00	9E+00	8E+00	3E+00	4E+00	7E+00	4E+00	5E+00	5E+00	1E+01	5E+00	6E+00	1E+01	1E+01	3E+00
PE(36:3)	1E+01	9E+00	7E+00	9E+00	1E+01	2E+01	1E+01	2E+01	2E+01	3E+01	6E+00	1E+01	1E+01	1E+01	1E+01	1E+01	2E+01	1E+01	2E+01	3E+01	3E+01	7E+00
PE(38:3)	4E+00	4E+00	2E+00	2E+00	4E+00	4E+00	4E+00	6E+00	4E+00	5E+00	1E+00	4E+00	5E+00	2E+00	3E+00	3E+00	5E+00	3E+00	3E+00	6E+00	6E+00	2E+00
PE(40:3)	7E-01	8E-01	3E-01	7E-01	5E-01	6E-01	6E-01	2E+00	1E+00	1E+00	3E-01	3E-01	7E-01	5E-01	5E-01	5E-01	8E-01	6E-01	8E-01	1E+00	1E+00	3E-01
PE(34:4)	2E-01	1E-01	1E-01	2E-01	1E-01	2E-01	1E-01	4E-01	2E-01	2E-01	1E-01	9E-02	2E-01	1E-01	1E-01	8E-02	2E-01	1E-01	3E-01	2E-01	4E-01	1E-01
PE(36:4)a	4E+01	6E+01	3E+01	5E+01	4E+01	7E+01	5E+01	1E+02	8E+01	1E+02	2E+01	5E+01	8E+01	4E+01	5E+01	4E+01	8E+01	5E+01	1E+02	7E+01	1E+02	3E+01
PE(36:4)b	1E+00	8E-01	9E-01	2E+00	1E+00	1E+00	1E+00	3E+00	2E+00	2E+00	1E+00	1E+00	1E+00	1E+00	1E+00	1E+00	1E+00	1E+00	1E+00	2E+00	2E+00	1E+00
PE(38:4)	4E+02	5E+02	3E+02	4E+02	4E+02	5E+02	5E+02	1E+03	6E+02	8E+02	2E+02	3E+02	8E+02	4E+02	4E+02	3E+02	6E+02	5E+02	7E+02	6E+02	8E+02	2E+02
PE(40:4)a	7E+00	8E+00	5E+00	6E+00	7E+00	1E+01	9E+00	2E+01	1E+01	2E+01	4E+00	6E+00	1E+01	7E+00	7E+00	6E+00	1E+01	1E+01	2E+01	2E+01	2E+01	4E+00
PE(40:4)b	1E+01	2E+01	1E+01	2E+01	1E+01	1E+01	1E+01	4E+01	2E+01	3E+01	5E+00	9E+00	2E+01	1E+01	2E+01	1E+01	1E+01	1E+01	2E+01	2E+01	3E+01	5E+00
PE(42:4)	7E-01	8E-01	6E-01	8E-01	5E-01	1E+00	9E-01	2E+00	1E+00	1E+00	3E-01	5E-01	1E+00	8E-01	8E-01	8E-01	9E-01	8E-01	1E+00	1E+00	1E+00	7E-01
PE(38:5)	4E+01	6E+01	3E+01	5E+01	4E+01	7E+01	6E+01	1E+02	9E+01	1E+02	2E+01	4E+01	8E+01	4E+01	5E+01	4E+01	9E+01	6E+01	8E+01	9E+01	1E+02	2E+01
PE(40:5)	2E+01	2E+01	2E+01	3E+01	2E+01	3E+01	2E+01	4E+01	4E+01	4E+01	1E+01	2E+01	3E+01	2E+01	3E+01	2E+01	4E+01	2E+01	3E+01	4E+01	4E+01	1E+01
PE(42:5)	7E-01	7E-01	7E-01	5E-01	6E-01	1E+00	9E-01	1E+00	1E+00	1E+00	4E-01	7E-01	1E+00	7E-01	9E-01	6E-01	1E+00	9E-01	1E+00	2E+00	1E+00	3E-01
PE(38:6)	1E+01	1E+01	9E+00	8E+00	7E+00	1E+01	6E+00	2E+01	2E+01	2E+01	7E+00	9E+00	2E+01	7E+00	9E+00	6E+00	1E+01	7E+00	1E+01	2E+01	2E+01	7E+00
PE(40:6)a	3E+00	4E+00	3E+00	4E+00	3E+00	5E+00	5E+00	8E+00	6E+00	8E+00	2E+00	3E+00	5E+00	4E+00	4E+00	3E+00	6E+00	4E+00	7E+00	7E+00	8E+00	2E+00
PE(40:6)b	8E+01	4E+01	2E+01	3E+01	2E+01	4E+01	2E+01	4E+01	5E+01	9E+01	2E+01	5E+01	8E+01	2E+01	3E+01	3E+01	1E+02	2E+01	2E+01	5E+01	3E+01	2E+01
PE(40:7)	1E+01	8E+00	5E+00	7E+00	7E+00	9E+00	8E+00	1E+01	1E+01	1E+01	4E+00	7E+00	1E+01	6E+00	6E+00	5E+00	1E+01	8E+00	8E+00	1E+01	1E+01	5E+00
PE(40:8)	1E+00	2E+00	1E+00	1E+00	1E+00	2E+00	1E+00	4E+00	3E+00	3E+00	5E-01	1E+00	2E+00	1E+00	1E+00	9E-01	2E+00	2E+00	3E+00	3E+00	3E+00	5E-01
PE(42:9)	5E-01	6E-01	4E-01	7E-01	4E-01	9E-01	3E-01	1E+00	9E-01	8E-01	2E-01	7E-01	5E-01	4E-01	5E-01	4E-01	9E-01	3E-01	9E-01	9E-01	8E-01	9E-01
PE(42:10)	1E+00	1E+00	7E-01	6E-01	5E-01	2E+00	8E-01	2E+00	2E+00	2E+00	5E-01	8E-01	2E+00	8E-01	8E-01	5E-01	2E+00	8E-01	2E+00	2E+00	2E+00	6E-01
PE(e34:2)	1E+01	1E+01	5E+00	9E+00	1E+01	2E+01	1E+01	1E+01	2E+01	2E+01	5E+00	1E+01	2E+01	9E+00	8E+00	1E+01	2E+01	1E+01	1E+01	2E+01	2E+01	9E+00
PE(e36:2)	9E+00	8E+00	3E+00	5E+00	5E+00	9E+00	5E+00	8E+00	1E+01	7E+00	3E+00	8E+00	1E+01	5E+00	5E+00	7E+00	1E+01	6E+00	5E+00	1E+01	9E+00	4E+00
PE(e38:2)	2E+00	2E+00	8E-01	9E-01	2E+00	2E+00	1E+00	2E+00	2E+00	2E+00	6E-01	2E+00	3E+00	1E+00	1E+00	2E+00	3E+00	1E+00	2E+00	2E+00	3E+00	9E-01
PE(e40:2)	3E-01	4E-01	2E-01	1E-01	4E-01	4E-01	3E-01	5E-01	5E-01	6E-01	9E-02	3E-01	6E-01	2E-01	2E-01	4E-01	8E-01	3E-01	4E-01	6E-01	6E-01	2E-01
PE(e34:3)	4E+00	5E+00	3E+00	4E+00	4E+00	4E+00	4E+00	7E+00	6E+00	6E+00	3E+00	3E+00	6E+00	4E+00	4E+00	4E+00	4E+00	5E+00	4E+00	6E+00	6E+00	4E+00
PE(e36:3)	8E+00	7E+00	4E+00	5E+00	6E+00	9E+00	6E+00	1E+01	1E+01	1E+01	3E+00	7E+00	1E+01	5E+00	7E+00	6E+00	1E+01	6E+00	8E+00	1E+01	1E+01	6E+00
PE(e38:3)	1E+00	2E+00	6E-01	7E-01	1E+00	2E+00	1E+00	3E+00	2E+00	2E+00	5E-01	1E+00	2E+00	1E+00	1E+00	2E+00	2E+00	1E+00	2E+00	2E+00	3E+00	9E-01
PE(e36:4)	5E+00	4E+00	1E+00	3E+00	3E+00	7E+00	4E+00	5E+00	8E+00	6E+00	3E+00	4E+00	6E+00	3E+00	3E+00	3E+00	8E+00	3E+00	4E+00	6E+00	5E+00	3E+00
PE(e38:4)	6E+00	6E+00	2E+00	3E+00	4E+00	7E+00	4E+00	7E+00	9E+00	6E+00	2E+00	5E+00	8E+00	3E+00	4E+00	5E+00	1E+01	4E+00	5E+00	1E+01	7E+00	3E+00
PE(e40:4)	2E+00	3E+00	7E-01	1E+00	2E+00	3E+00	1E+00	4E+00	3E+00	3E+00	6E-01	2E+00	4E+00	1E+00	1E+00	2E+00	3E+00	2E+00	3E+00	3E+00	3E+00	8E-01
PE(e36:5)	3E+02	3E+02	1E+02	2E+02	2E+02	3E+02	2E+02	4E+02	4E+02	4E+02	1E+02	2E+02	4E+02	2E+02	2E+02	2E+02	3E+02	2E+02	3E+02	4E+02	4E+02	2E+02
PE(e38:5)a	3E+01	7E+01	2E+01	3E+01	5E+01	5E+01	4E+01	1E+02	7E+01	9E+01	1E+01	3E+01	8E+01	4E+01	4E+01	5E+01	6E+01	5E+01	8E+01	8E+01	1E+02	2E+01
PE(e38:5)b	4E+02	5E+02	2E+02	3E+02	3E+02	4E+02	3E+02	7E+02	5E+02	5E+02	1E+02	4E+02	6E+02	3E+02	3E+02	3E+02	5E+02	3E+02	4E+02	5E+02	5E+02	2E+02
PE(e40:5)a	4E+01	8E+01	3E+01	4E+01	6E+01	5E+01	4E+01	2E+02	9E+01	1E+02	9E+00	4E+01	1E+02	5E+01	6E+01	6E+01	7E+01	6E+01	1E+02	9E+01	1E+02	1E+01
PE(e40:5)b	3E+01	4E+01	2E+01	2E+01	3E+01	3E+01	2E+01	6E+01	4E+01	6E+01	1E+01	2E+01	5E+01	2E+01	3E+01	3E+01	4E+01	3E+01	5E+01	4E+01	5E+01	2E+01
PE(e42:5)a	2E+00	5E+00	2E+00	2E+00	5E+00	2E+00	3E+00	1E+01	5E+00	9E+00	7E-01	2E+00	6E+00	3E+00	3E+00	4E+00	3E+00	2E+00	9E+00	5E+00	1E+01	8E-01
PE(e42:5)b	4E+00	4E+00	2E+00	2E+00	4E+00	5E+00	4E+00	8E+00	5E+00	8E+00	2E+00	3E+00	5E+00	3E+00	3E+00	4E+00	6E+00	4E+00	6E+00	5E+00	9E+00	2E+00
PE(e44:5)a	6E-02	1E-01	9E-02	9E-02	1E-01	1E-01	9E-02	3E-01	2E-01	3E-01	6E-02	1E-01	1E-01	7E-02	9E-02	9E-02	2E-01	1E-01	2E-01	2E-01	4E-01	9E-02
PE(e44:5)b	4E-01	3E-01	2E-01	2E-01	3E-01	4E-01	4E-01	5E-01	4E-01	9E-01	2E-01	4E-01	4E-01	2E-01	3E-01	3E-01	7E-01	4E-01	4E-01	5E-01	9E-01	2E-01
PE(e36:6)	2E+01	5E+00	2E+00	3E+00	3E+00	2E+01	4E+00	5E+00	1E+01	4E+00	8E+00	2E+01	9E+00	4E+00	4E+00	5E+00	2E+01	4E+00	4E+00	1E+01	5E+00	1E+01
PE(e38:6)	9E+01	1E+02	5E+01	8E+01	8E+01	1E+02	8E+01	1E+02	2E+02	1E+02	4E+01	8E+01	1E+02	8E+01	8E+01	8E+01	1E+02	8E+01	9E+01	2E+02	1E+02	6E+01
PE(e40:6)a	1E+01	1E+01	4E+00	5E+00	6E+00	9E+00	5E+00	1E+01	2E+01	1E+01	2E+00	7E+00	2E+01	7E+00	6E+00	7E+00	1E+01	5E+00	1E+01	2E+01	2E+01	3E+00
PE(e40:6)b	5E+01	5E+01	3E+01	5E+01	3E+01	4E+01	3E+01	6E+01	6E+01	6E+01	1E+01	3E+01	6E+01	4E+01	5E+01	3E+01	5E+01	3E+01	4E+01	7E+01	6E+01	2E+01
PE(e40:6)c	6E+00	5E+00	3E+00	3E+00	4E+00	8E+00	4E+00	9E+00	6E+00	9E+00	2E+00	5E+00	7E+00	4E+00	5E+00	4E+00	8E+00	4E+00	6E+00	6E+00	1E+01	2E+00
PE(e42:6)	6E+00	6E+00	4E+00	6E+00	5E+00	6E+00	5E+00	1E+01	8E+00	1E+01	3E+00	5E+00	8E+00	6E+00	5E+00	6E+00	7E+00	5E+00	7E+00	1E+01	1E+01	3E+00
PE(e38:7)a	5E+00	3E+00	1E+00	3E+00	2E+00	8E+00	2E+00	3E+00	5E+00	3E+00	3E+00	6E+00	4E+00	2E+00	3E+00	2E+00	8E+00	2E+00	2E+00	8E+00	3E+00	5E+00
PE(e38:7)b	4E+01	3E+01	1E+01	2E+01	2E+01	5E+01	2E+01	4E+01	5E+01	4E+01	1E+01	4E+01	5E+01	2E+01	2E+01	2E+01	6E+01	2E+01	3E+01	7E+01	5E+01	2E+01
PE(e40:7)	8E+01	7E+01	2E+01	3E+01	2E+01	9E+01	2E+01	8E+01	8E+01	5E+01	2E+01	9E+01	1E+02	5E+01	7E+01	4E+01	9E+01	3E+01	4E+01	7E+01	5E+01	3E+01
PE(e42:7)	4E+00	4E+00	2E+00	2E+00	2E+00	5E+00	2E+00	8E+00	5E+00	5E+00	1E+00	4E+00	6E+00	3E+00	2E+00	3E+00	6E+00	2E+00	5E+00	6E+00	7E+00	2E+00
PE(e44:7)	2E-01	3E-01	1E-01	1E-01	2E-01	4E-01	2E-01	5E-01	4E-01	6E-01	1E-01	3E-01	3E-01	2E-01	3E-01	3E-01	5E-01	2E-01	4E-01	4E-01	4E-01	2E-01
PE(e40:8)	9E+00	9E+00	4E+00	4E+00	5E+00	1E+01	4E+00	9E+00	2E+01	1E+01	3E+00	9E+00	1E+01	6E+00	6E+00	5E+00	2E+01	4E+00	7E+00	2E+01	1E+01	5E+00
PS(34:1)	1E+00	8E-01	9E-01	8E-01	9E-01	2E+00	1E+00	8E-01	2E+00	1E+00	9E-01	2E+00	2E+00	2E+00	1E+00	2E+00	3E+00	1E+00	1E+00	1E+00	1E+00	6E-01
PS(36:1)	1E+02	1E+02	9E+01	6E+01	9E+01	2E+02	1E+02	1E+02	2E+02	2E+02	6E+01	1E+02	1E+02	1E+02	1E+02	1E+02	2E+02	1E+02	1E+02	1E+02	1E+02	6E+01
PS(38:1)	5E+00	7E+00	5E+00	3E+00	5E+00	9E+00	6E+00	9E+00	9E+00	7E+00	3E+00	6E+00	1E+01	5E+00	5E+00	4E+00	1E+01	9E+00	9E+00	1E+01	9E+00	4E+00
PS(40:1)	4E+00	3E+00	2E+00	1E+00	2E+00	3E+00	3E+00	5E+00	3E+00	3E+00	1E+00	3E+00	3E+00	2E+00	2E+00	2E+00	5E+00	5E+00	3E+00	4E+00	3E+00	2E+00
PS(42:1)	5E-01	4E-01	2E-01	2E-01	3E-01	3E-01	3E-01	6E-01	5E-01	4E-01	2E-01	4E-01	4E-01	4E-01	3E-01	3E-01	7E-01	6E-01	4E-01	4E-01	5E-01	3E-01
PS(34:2)	3E-01	2E-01	2E-01	1E-01	2E-01	4E-01	3E-01	3E-01	2E-01	3E-01	7E-02	3E-01	3E-01	2E-01	2E-01	3E-01	5E-01	3E-01	4E-01	3E-01	4E-01	1E-01
PS(36:2)	8E+00	8E+00	5E+00	4E+00	7E+00	1E+01	8E+00	1E+01	1E+01	9E+00	4E+00	8E+00	1E+01	6E+00	5E+00	7E+00	2E+01	9E+00	9E+00	1E+01	9E+00	6E+00
PS(38:2)a	2E+00	2E+00	1E+00	8E-01	2E+00	2E+00	2E+00	2E+00	3E+00	3E+00	7E-01	2E+00	2E+00	2E+00	1E+00	2E+00	3E+00	3E+00	2E+00	3E+00	3E+00	8E-01
PS(38:2)b	2E+00	2E+00	1E+00	7E-01	1E+00	2E+00	2E+00	2E+00	1E+00	3E+00	4E-01	1E+00	2E+00	8E-01	6E-01	1E+00	2E+00	2E+00	1E+00	2E+00	2E+00	1E+00
PS(40:2)	2E+00	2E+00	1E+00	6E-01	1E+00	4E+00	2E+00	2E+00	3E+00	1E+00	9E-01	3E+00	2E+00	1E+00	1E+00	1E+00	5E+00	2E+00	2E+00	3E+00	2E+00	1E+00
PS(36:3)	9E-01	8E-01	5E-01	4E-01	7E-01	1E+00	1E+00	1E+00	1E+00	1E+00	3E-01	8E-01	1E+00	5E-01	6E-01	8E-01	1E+00	1E+00	1E+00	1E+00	1E+00	4E-01
PS(38:3)	2E+01	1E+01	1E+01	6E+00	1E+01	2E+01	1E+01	2E+01	2E+01	2E+01	7E+00	2E+01	1E+01	9E+00	8E+00	1E+01	2E+01	2E+01	1E+01	3E+01	3E+01	1E+01
PS(36:4)	8E-01	1E+00	4E-01	5E-01	6E-01	8E-01	1E+00	8E-01	7E-01	2E+00	2E-01	8E-01	1E+00	5E-01	8E-01	7E-01	1E+00	1E+00	1E+00	8E-01	2E+00	3E-01
PS(38:4)	1E+02	2E+02	1E+02	9E+01	9E+01	3E+02	2E+02	2E+02	3E+02	2E+02	1E+02	2E+02	2E+02	2E+02	2E+02	1E+02	4E+02	2E+02	4E+02	2E+02	2E+02	8E+01
PS(40:4)a	3E+00	5E+00	5E+00	4E+00	3E+00	6E+00	5E+00	7E+00	8E+00	8E+00	2E+00	4E+00	5E+00	6E+00	5E+00	6E+00	8E+00	4E+00	1E+01	6E+00	8E+00	2E+00
PS(40:4)b	2E+00	3E+00	1E+00	1E+00	1E+00	2E+00	3E+00	5E+00	3E+00	3E+00	8E-01	2E+00	3E+00	2E+00	2E+00	2E+00	3E+00	3E+00	3E+00	3E+00	3E+00	1E+00
PS(38:5)	8E+00	1E+01	1E+01	9E+00	1E+01	1E+01	2E+01	3E+01	2E+01	1E+01	4E+00	9E+00	2E+01	1E+01	1E+01	1E+01	2E+01	2E+01	3E+01	3E+01	2E+01	4E+00
PS(40:5)	2E+00	2E+00	1E+00	1E+00	1E+00	1E+00	2E+00	3E+00	1E+00	4E+00	5E-01	1E+00	2E+00	1E+00	1E+00	1E+00	2E+00	2E+00	2E+00	2E+00	4E+00	8E-01
PS(40:6)a	8E-01	9E-01	7E-01	6E-01	7E-01	1E+00	1E+00	2E+00	1E+00	2E+00	4E-01	9E-01	9E-01	6E-01	7E-01	7E-01	1E+00	1E+00	1E+00	2E+00	2E+00	4E-01
PS(40:6)b	2E+01	6E+00	4E+00	2E+00	3E+00	1E+01	3E+00	1E+01	9E+00	6E+00	6E+00	1E+01	7E+00	5E+00	5E+00	3E+00	1E+01	7E+00	9E+00	1E+01	1E+01	6E+00
PS(40:7)	8E-01	9E-01	6E-01	4E-01	5E-01	1E+00	8E-01	1E+00	1E+00	8E-01	4E-01	9E-01	1E+00	6E-01	6E-01	6E-01	2E+00	8E-01	2E+00	2E+00	8E-01	5E-01
CE(18:1)	5E+01	4E+01	3E+01	2E+01	1E+01	3E+01	4E+01	1E+01	3E+01	4E+01	9E+00	2E+01	5E+01	4E+01	2E+01	2E+01	6E+01	3E+01	2E+01	2E+01	4E+01	8E+00
CE(16:1)	7E+00	8E+00	8E+00	4E+00	3E+00	7E+00	7E+00	2E+00	3E+00	8E+00	3E+00	5E+00	8E+00	1E+01	6E+00	4E+00	1E+01	5E+00	3E+00	5E+00	8E+00	2E+00
CE(18:3)	3E+01	3E+01	3E+01	1E+01	6E+00	2E+01	2E+01	7E+00	3E+01	2E+01	7E+00	2E+01	3E+01	3E+01	2E+01	1E+01	3E+01	2E+01	2E+01	2E+01	3E+01	5E+00
CE(20:3)	2E+01	2E+01	2E+01	5E+00	4E+00	2E+01	1E+01	6E+00	9E+00	1E+01	3E+00	7E+00	2E+01	2E+01	8E+00	7E+00	3E+01	1E+01	9E+00	9E+00	9E+00	3E+00
CE(20:4)	2E+02	2E+02	2E+02	6E+01	3E+01	2E+02	1E+02	5E+01	1E+02	9E+01	3E+01	8E+01	2E+02	3E+02	1E+02	7E+01	4E+02	1E+02	1E+02	8E+01	1E+02	1E+01
CE(20:5)	9E+01	4E+01	3E+01	7E+00	4E+00	9E+01	1E+01	6E+00	3E+01	1E+01	1E+01	3E+01	3E+01	4E+01	2E+01	8E+00	2E+02	1E+01	2E+01	2E+01	2E+01	6E+00
CE(22:6)	9E+01	5E+01	4E+01	1E+01	7E+00	8E+01	2E+01	9E+00	3E+01	1E+01	1E+01	3E+01	4E+01	4E+01	2E+01	2E+01	2E+02	2E+01	3E+01	4E+01	1E+01	1E+01
CE(18:2)	5E+02	3E+02	5E+02	2E+02	1E+02	4E+02	3E+02	1E+02	3E+02	2E+02	7E+01	2E+02	3E+02	4E+02	2E+02	2E+02	6E+02	3E+02	3E+02	3E+02	3E+02	5E+01
cholesterol	1E+03	2E+03	6E+02	6E+02	3E+03	4E+03	1E+03	2E+03	1E+03	1E+04	4E+02	2E+03	2E+03	7E+02	1E+03	1E+03	4E+03	1E+03	4E+03	1E+03	9E+03	9E+02
SM(d30:1)	5E+00	9E+00	5E+00	3E+00	7E+00	9E+00	7E+00	2E+01	2E+01	1E+01	3E+00	9E+00	8E+00	6E+00	1E+01	6E+00	1E+01	9E+00	3E+01	3E+01	1E+01	3E+00
SM(d31:1)	4E+00	7E+00	3E+00	2E+00	5E+00	8E+00	7E+00	1E+01	1E+01	9E+00	2E+00	7E+00	6E+00	5E+00	7E+00	4E+00	1E+01	7E+00	2E+01	2E+01	1E+01	2E+00
SM(d32:0)	6E+00	1E+01	4E+00	3E+00	7E+00	1E+01	9E+00	1E+01	1E+01	1E+01	4E+00	1E+01	1E+01	7E+00	1E+01	6E+00	2E+01	1E+01	2E+01	2E+01	2E+01	4E+00
SM(d32:1)	2E+02	3E+02	2E+02	1E+02	2E+02	4E+02	3E+02	4E+02	5E+02	5E+02	8E+01	4E+02	3E+02	3E+02	4E+02	2E+02	5E+02	3E+02	9E+02	6E+02	5E+02	1E+02
SM(d33:0)	1E+01	3E+01	5E+00	3E+00	1E+01	1E+01	1E+01	2E+01	1E+01	1E+01	3E+00	2E+01	1E+01	1E+01	1E+01	7E+00	3E+01	1E+01	3E+01	2E+01	1E+01	4E+00
SM(d33:1)	1E+02	2E+02	8E+01	5E+01	1E+02	2E+02	1E+02	2E+02	2E+02	2E+02	5E+01	2E+02	1E+02	1E+02	2E+02	1E+02	2E+02	2E+02	4E+02	3E+02	2E+02	5E+01
SM(d34:0)	3E+01	6E+01	3E+01	2E+01	4E+01	9E+01	7E+01	4E+01	6E+01	9E+01	3E+01	1E+02	6E+01	5E+01	6E+01	4E+01	1E+02	6E+01	1E+02	8E+01	7E+01	3E+01
SM(d34:1)	1E+03	2E+03	7E+02	4E+02	1E+03	1E+03	1E+03	1E+03	1E+03	3E+03	5E+02	1E+03	1E+03	9E+02	1E+03	6E+02	2E+03	2E+03	2E+03	2E+03	3E+03	6E+02
SM(d34:2)	1E+02	2E+02	1E+02	7E+01	2E+02	2E+02	2E+02	3E+02	2E+02	5E+02	6E+01	2E+02	2E+02	2E+02	2E+02	1E+02	3E+02	2E+02	6E+02	4E+02	6E+02	7E+01
SM(d35:0)	1E+00	2E+00	1E+00	7E-01	2E+00	2E+00	2E+00	1E+00	1E+00	2E+00	6E-01	2E+00	2E+00	1E+00	1E+00	1E+00	2E+00	2E+00	3E+00	3E+00	2E+00	1E+00
SM(d35:1)	8E+00	1E+01	9E+00	6E+00	1E+01	1E+01	1E+01	1E+01	1E+01	1E+01	6E+00	2E+01	2E+01	1E+01	2E+01	9E+00	2E+01	1E+01	3E+01	2E+01	2E+01	7E+00
SM(d35:2)	3E+00	4E+00	2E+00	1E+00	3E+00	4E+00	3E+00	5E+00	5E+00	5E+00	1E+00	4E+00	4E+00	3E+00	5E+00	3E+00	5E+00	4E+00	1E+01	8E+00	6E+00	1E+00
SM(d36:0)	5E+00	1E+01	4E+00	2E+00	5E+00	1E+01	8E+00	7E+00	6E+00	1E+01	3E+00	9E+00	9E+00	4E+00	7E+00	4E+00	1E+01	8E+00	1E+01	1E+01	1E+01	3E+00
SM(d36:1)	5E+01	8E+01	4E+01	3E+01	6E+01	6E+01	5E+01	1E+02	5E+01	1E+02	2E+01	7E+01	6E+01	5E+01	7E+01	4E+01	9E+01	6E+01	1E+02	1E+02	1E+02	3E+01
SM(d36:2)	7E+00	1E+01	8E+00	5E+00	1E+01	1E+01	9E+00	1E+01	9E+00	2E+01	5E+00	1E+01	1E+01	1E+01	2E+01	6E+00	2E+01	9E+00	2E+01	2E+01	2E+01	6E+00
SM(d36:3)	1E+00	4E+00	2E+00	1E+00	2E+00	3E+00	2E+00	4E+00	4E+00	3E+00	7E-01	3E+00	3E+00	3E+00	3E+00	2E+00	4E+00	3E+00	7E+00	5E+00	4E+00	6E-01
SM(d37:0)	4E+00	5E+00	2E+00	1E+00	7E+00	4E+00	3E+00	3E+00	4E+00	5E+00	2E+00	4E+00	4E+00	3E+00	4E+00	3E+00	7E+00	4E+00	5E+00	5E+00	6E+00	2E+00
SM(d37:1)	2E+00	6E+00	2E+00	2E+00	4E+00	5E+00	3E+00	5E+00	4E+00	5E+00	1E+00	3E+00	4E+00	3E+00	4E+00	2E+00	5E+00	4E+00	8E+00	6E+00	5E+00	1E+00
SM(d38:0)	1E+01	3E+01	7E+00	5E+00	1E+01	2E+01	2E+01	2E+01	2E+01	4E+01	6E+00	2E+01	3E+01	1E+01	1E+01	1E+01	3E+01	3E+01	4E+01	3E+01	4E+01	7E+00
SM(d38:1)	6E+01	1E+02	6E+01	4E+01	9E+01	1E+02	9E+01	1E+02	1E+02	2E+02	5E+01	1E+02	1E+02	9E+01	1E+02	7E+01	1E+02	1E+02	2E+02	2E+02	2E+02	5E+01
SM(d38:2)	5E+00	8E+00	5E+00	4E+00	7E+00	8E+00	7E+00	1E+01	9E+00	1E+01	4E+00	9E+00	8E+00	7E+00	1E+01	7E+00	9E+00	7E+00	2E+01	1E+01	1E+01	3E+00
SM(d39:0)	1E+00	3E+00	8E-01	6E-01	2E+00	2E+00	2E+00	2E+00	2E+00	3E+00	7E-01	3E+00	2E+00	9E-01	2E+00	1E+00	3E+00	2E+00	3E+00	3E+00	3E+00	9E-01
SM(d39:1)	2E+01	5E+01	2E+01	1E+01	3E+01	4E+01	4E+01	4E+01	3E+01	5E+01	1E+01	4E+01	4E+01	3E+01	5E+01	3E+01	5E+01	4E+01	7E+01	5E+01	4E+01	1E+01
SM(d40:0)	4E+01	1E+02	2E+01	2E+01	4E+01	7E+01	7E+01	6E+01	6E+01	1E+02	2E+01	7E+01	9E+01	4E+01	5E+01	3E+01	1E+02	7E+01	1E+02	9E+01	1E+02	3E+01
SM(d40:1)	4E+02	8E+02	3E+02	2E+02	5E+02	7E+02	6E+02	7E+02	7E+02	1E+03	3E+02	8E+02	6E+02	6E+02	8E+02	4E+02	1E+03	7E+02	1E+03	9E+02	1E+03	3E+02
SM(d40:2)	3E+01	6E+01	4E+01	3E+01	5E+01	5E+01	5E+01	7E+01	6E+01	1E+02	2E+01	5E+01	5E+01	5E+01	7E+01	3E+01	6E+01	6E+01	1E+02	9E+01	1E+02	3E+01
SM(d41:0)	4E+00	9E+00	2E+00	2E+00	4E+00	7E+00	6E+00	6E+00	7E+00	1E+01	3E+00	5E+00	9E+00	4E+00	5E+00	2E+00	1E+01	6E+00	9E+00	1E+01	1E+01	3E+00
SM(d41:1)	8E+01	2E+02	6E+01	4E+01	9E+01	1E+02	1E+02	9E+01	8E+01	1E+02	3E+01	1E+02	1E+02	1E+02	1E+02	7E+01	2E+02	1E+02	2E+02	1E+02	1E+02	3E+01
SM(d42:0)	2E+01	5E+01	1E+01	9E+00	2E+01	4E+01	3E+01	3E+01	3E+01	8E+01	1E+01	4E+01	4E+01	2E+01	3E+01	2E+01	7E+01	3E+01	5E+01	5E+01	9E+01	1E+01
SM(d42:1)	4E+02	6E+02	3E+02	2E+02	4E+02	6E+02	6E+02	5E+02	6E+02	1E+03	2E+02	7E+02	6E+02	5E+02	6E+02	3E+02	1E+03	7E+02	1E+03	8E+02	1E+03	3E+02
SM(d42:2)	4E+02	6E+02	3E+02	2E+02	4E+02	8E+02	5E+02	4E+02	6E+02	9E+02	3E+02	8E+02	5E+02	5E+02	6E+02	3E+02	1E+03	5E+02	8E+02	8E+02	1E+03	3E+02
SM(d42:3)	4E+01	5E+01	4E+01	2E+01	5E+01	7E+01	5E+01	6E+01	6E+01	1E+02	3E+01	7E+01	4E+01	6E+01	6E+01	4E+01	9E+01	6E+01	1E+02	9E+01	1E+02	4E+01
SM(d43:1)	6E+00	1E+01	5E+00	3E+00	7E+00	1E+01	1E+01	1E+01	1E+01	2E+01	3E+00	1E+01	1E+01	9E+00	1E+01	5E+00	1E+01	1E+01	2E+01	2E+01	2E+01	3E+00
SM(d43:2)	9E+00	1E+01	6E+00	4E+00	1E+01	1E+01	1E+01	1E+01	1E+01	2E+01	3E+00	1E+01	1E+01	9E+00	1E+01	7E+00	2E+01	2E+01	2E+01	2E+01	2E+01	4E+00
SM(d44:1)	5E+00	9E+00	4E+00	2E+00	6E+00	8E+00	8E+00	9E+00	8E+00	2E+01	2E+00	9E+00	9E+00	6E+00	7E+00	4E+00	1E+01	1E+01	2E+01	1E+01	2E+01	3E+00
SM(d44:2)	7E+00	9E+00	5E+00	3E+00	7E+00	2E+01	8E+00	7E+00	2E+01	2E+01	5E+00	1E+01	8E+00	7E+00	9E+00	5E+00	2E+01	8E+00	1E+01	2E+01	2E+01	6E+00

Table 63. *Results of estimation of absolute lipid concentrations for LPE, PE, ePE, PS, SM, CE and cholesterol in thrombin with the platelet inhibitor and inhibitor treated samples. Results are shown as average amount (nmol) per 1 million platelets.*

	Thrombin &Platelet Inhibitor											Platelet inhibitor										
Donor:	*1*	*2*	*3*	*4*	*5*	*6*	*7*	*8*	*9*	*10*	*11*	*1*	*2*	*3*	*4*	*5*	*6*	*7*	*8*	*9*	*10*	*11*
LPE(16:0)	1E+00	2E+00	2E+00	9E-01	1E+00	1E+00	2E+00	4E+00	2E+00	4E+00	6E-01	2E+00	2E+00	1E+00	1E+00	2E+00	2E+00	2E+00	2E+00	2E+00	4E+00	1E+00
LPE(16:0)b	5E-02	7E-02	8E-02	4E-02	7E-02	7E-02	6E-02	1E-01	5E-02	1E-01	4E-02	5E-02	4E-02	3E-02	3E-02	5E-02	4E-02	2E-02	6E-02	3E-02	9E-02	2E-02
LPE(18:0)	7E+00	8E+00	8E+00	5E+00	5E+00	6E+00	7E+00	2E+01	7E+00	2E+01	3E+00	1E+01	1E+01	9E+00	6E+00	6E+00	7E+00	8E+00	1E+01	9E+00	2E+01	3E+00
LPE(18:0)b	1E-01	1E-01	1E-01	7E-02	9E-02	2E-01	1E-01	3E-01	1E-01	2E-01	4E-02	1E-01	1E-01	8E-02	8E-02	8E-02	2E-01	1E-01	1E-01	1E-01	1E-01	4E-02
LPE(18:1)	9E-01	9E-01	9E-01	5E-01	7E-01	8E-01	1E+00	2E+00	1E+00	2E+00	2E-01	1E+00	1E+00	1E+00	6E-01	8E-01	1E+00	1E+00	1E+00	1E+00	2E+00	4E-01
LPE(18:1)b	2E-01	2E-01	3E-01	1E-01	2E-01	3E-01	4E-01	2E-01	2E-01	2E-01	2E-01	2E-01	2E-01	3E-01	3E-01	2E-01	4E-01	3E-01	1E-01	2E-01	2E-01	8E-01
LPE(18:2)	2E-01	1E-01	1E-01	5E-02	2E-01	2E-01	4E-01	2E-01	8E-02	2E-01	4E-02	1E-01	6E-02	1E-01	6E-02	1E-01	9E-02	1E-01	9E-02	1E-01	2E-01	6E-02
LPE(18:2)b	2E-01	1E-01	2E-01	8E-02	1E-01	1E-01	2E-01	1E-01	8E-02	7E-02	1E-01	9E-02	1E-01	1E-01	1E-01	1E-01	2E-01	2E-01	7E-02	8E-02	1E-01	5E-01
LPE(20:1)	1E-01	2E-01	1E-01	7E-02	2E-01	1E-01	2E-01	5E-01	2E-01	4E-01	6E-02	2E-01	2E-01	2E-01	1E-01	2E-01	2E-01	2E-01	2E-01	2E-01	3E-01	1E-01
LPE(20:2)	7E-02	5E-02	6E-02	3E-02	4E-02	7E-02	5E-02	1E-01	6E-02	1E-01	3E-02	6E-02	4E-02	5E-02	3E-02	3E-02	6E-02	7E-02	5E-02	8E-02	9E-02	1E-01
LPE(20:3)	1E-01	7E-02	6E-02	4E-02	4E-02	1E-01	9E-02	3E-02	5E-02	7E-02	5E-02	6E-02	5E-02	6E-02	7E-02	6E-02	1E-01	8E-02	4E-02	3E-02	6E-02	4E-01
LPE(20:4)	8E+00	5E+00	4E+00	3E+00	3E+00	4E+00	6E+00	3E+00	2E+00	2E+00	4E+00	3E+00	5E+00	5E+00	6E+00	4E+00	8E+00	6E+00	4E+00	3E+00	3E+00	2E+01
LPE(20:5)	5E-01	9E-02	5E-02	7E-02	4E-02	3E-01	1E-01	5E-02	9E-02	3E-02	3E-01	2E-01	1E-01	9E-02	1E-01	5E-02	4E-01	1E-01	7E-02	1E-01	4E-02	2E+00
LPE(20:0)	2E-01	2E-01	2E-01	1E-01	1E-01	2E-01	2E-01	7E-01	2E-01	3E-01	6E-02	2E-01	2E-01	3E-01	1E-01	2E-01	2E-01	2E-01	3E-01	2E-01	3E-01	8E-02
LPE(22:4)	7E-01	1E+00	1E+00	5E-01	6E-01	4E-01	8E-01	7E-01	4E-01	4E-01	6E-01	4E-01	7E-01	1E+00	1E+00	8E-01	1E+00	1E+00	7E-01	5E-01	6E-01	2E+00
LPE(22:5)	8E-01	6E-01	7E-01	3E-01	3E-01	5E-01	5E-01	4E-01	2E-01	2E-01	4E-01	3E-01	5E-01	8E-01	1E+00	5E-01	8E-01	7E-01	4E-01	4E-01	4E-01	2E+00
LPE(22:6)	1E+00	6E-01	4E-01	2E-01	2E-01	7E-01	3E-01	3E-01	2E-01	2E-01	6E-01	4E-01	5E-01	6E-01	6E-01	3E-01	9E-01	4E-01	4E-01	4E-01	3E-01	3E+00
PE(34:0)	8E-01	1E+00	9E-01	9E-01	6E-01	1E+00	7E-01	2E+00	9E-01	3E+00	6E-01	6E-01	5E-01	9E-01	4E-01	6E-01	1E+00	8E-01	1E+00	5E-01	2E+00	7E-01
PE(36:0)	2E-01	2E-01	3E-01	2E-01	2E-01	3E-01	2E-01	4E-01	2E-01	6E-01	9E-02	2E-01	2E-01	2E-01	2E-01	2E-01	2E-01	2E-01	2E-01	2E-01	2E-01	1E-01
PE(34:1)	2E+01	3E+01	3E+01	2E+01	2E+01	3E+01	2E+01	3E+01	3E+01	6E+01	2E+01	2E+01	3E+01	2E+01	1E+01	2E+01	3E+01	2E+01	2E+01	3E+01	4E+01	2E+01
PE(36:1)	3E+01	3E+01	3E+01	2E+01	3E+01	3E+01	3E+01	3E+01	4E+01	7E+01	1E+01	2E+01	2E+01	2E+01	1E+01	2E+01	4E+01	3E+01	2E+01	4E+01	4E+01	1E+01
PE(38:1)	1E+00	1E+00	2E+00	1E+00	1E+00	2E+00	1E+00	2E+00	2E+00	3E+00	7E-01	1E+00	1E+00	1E+00	8E-01	2E+00	2E+00	1E+00	8E-01	2E+00	2E+00	6E-01
PE(40:1)	2E-01	2E-01	3E-01	2E-01	2E-01	2E-01	2E-01	3E-01	3E-01	7E-01	2E-01	2E-01	2E-01	2E-01	1E-01	2E-01	3E-01	2E-01	2E-01	2E-01	2E-01	1E-01
PE(34:2)	1E+01	9E+00	1E+01	1E+01	1E+01	1E+01	1E+01	3E+01	1E+01	5E+01	7E+00	1E+01	7E+00	8E+00	5E+00	9E+00	2E+01	1E+01	1E+01	1E+01	3E+01	5E+00
PE(36:2)	4E+01	3E+01	5E+01	4E+01	4E+01	4E+01	4E+01	7E+01	5E+01	1E+02	2E+01	3E+01	3E+01	3E+01	2E+01	4E+01	5E+01	4E+01	4E+01	4E+01	7E+01	2E+01
PE(38:2)	5E+00	5E+00	7E+00	5E+00	5E+00	6E+00	7E+00	8E+00	9E+00	2E+01	3E+00	4E+00	4E+00	5E+00	3E+00	6E+00	7E+00	6E+00	4E+00	7E+00	9E+00	3E+00
PE(36:3)	1E+01	1E+01	2E+01	1E+01	1E+01	1E+01	1E+01	2E+01	2E+01	4E+01	7E+00	1E+01	8E+00	9E+00	6E+00	1E+01	2E+01	2E+01	1E+01	2E+01	2E+01	6E+00
PE(38:3)	4E+00	4E+00	4E+00	4E+00	4E+00	4E+00	4E+00	4E+00	4E+00	1E+01	2E+00	3E+00	4E+00	3E+00	2E+00	5E+00	4E+00	5E+00	5E+00	3E+00	6E+00	1E+00
PE(40:3)	6E-01	8E-01	6E-01	7E-01	9E-01	8E-01	8E-01	1E+00	7E-01	1E+00	4E-01	6E-01	6E-01	5E-01	6E-01	8E-01	7E-01	8E-01	7E-01	7E-01	7E-01	4E-01
PE(34:4)	1E-01	2E-01	2E-01	2E-01	1E-01	9E-02	1E-01	5E-01	2E-01	5E-01	7E-02	8E-02	1E-01	1E-01	9E-02	1E-01	1E-01	2E-01	3E-01	1E-01	2E-01	8E-02
PE(36:4)a	5E+01	6E+01	6E+01	5E+01	4E+01	5E+01	6E+01	2E+02	7E+01	2E+02	3E+01	5E+01	5E+01	4E+01	3E+01	5E+01	7E+01	7E+01	8E+01	6E+01	1E+02	3E+01
PE(36:4)b	1E+00	9E-01	2E+00	2E+00	1E+00	1E+00	1E+00	2E+00	2E+00	4E+00	7E-01	9E-01	1E+00	1E+00	9E-01	1E+00	1E+00	2E+00	1E+00	2E+00	3E+00	8E-01
PE(38:4)	4E+02	5E+02	5E+02	5E+02	4E+02	4E+02	5E+02	9E+02	5E+02	1E+03	3E+02	4E+02	4E+02	4E+02	3E+02	3E+02	5E+02	6E+02	6E+02	5E+02	8E+02	2E+02
PE(40:4)a	7E+00	8E+00	1E+01	9E+00	7E+00	8E+00	1E+01	3E+01	1E+01	3E+01	5E+00	7E+00	8E+00	7E+00	5E+00	8E+00	1E+01	1E+01	1E+01	9E+00	1E+01	3E+00
PE(40:4)b	1E+01	2E+01	2E+01	2E+01	1E+01	1E+01	2E+01	4E+01	2E+01	5E+01	5E+00	9E+00	1E+01	2E+01	1E+01	2E+01	1E+01	2E+01	2E+01	1E+01	3E+01	5E+00
PE(42:4)	6E-01	1E+00	1E+00	1E+00	7E-01	6E-01	1E+00	2E+00	9E-01	2E+00	4E-01	6E-01	8E-01	9E-01	6E-01	8E-01	8E-01	1E+00	9E-01	8E-01	1E+00	3E-01
PE(38:5)	4E+01	6E+01	6E+01	5E+01	5E+01	6E+01	7E+01	1E+02	7E+01	2E+02	3E+01	4E+01	6E+01	5E+01	3E+01	6E+01	8E+01	8E+01	6E+01	6E+01	1E+02	2E+01
PE(40:5)	2E+01	2E+01	4E+01	3E+01	2E+01	3E+01	3E+01	4E+01	3E+01	7E+01	1E+01	2E+01	2E+01	3E+01	2E+01	2E+01	4E+01	3E+01	3E+01	3E+01	4E+01	1E+01
PE(42:5)	8E-01	8E-01	1E+00	1E+00	7E-01	8E-01	1E+00	2E+00	1E+00	2E+00	4E-01	9E-01	5E-01	9E-01	7E-01	6E-01	1E+00	1E+00	9E-01	1E+00	1E+00	3E-01
PE(38:6)	1E+01	1E+01	1E+01	9E+00	8E+00	1E+01	9E+00	1E+01	2E+01	4E+01	8E+00	1E+01	9E+00	9E+00	5E+00	6E+00	1E+01	9E+00	9E+00	1E+01	2E+01	7E+00
PE(40:6)a	4E+00	4E+00	5E+00	5E+00	3E+00	4E+00	4E+00	8E+00	6E+00	1E+01	2E+00	3E+00	3E+00	4E+00	3E+00	3E+00	4E+00	5E+00	5E+00	5E+00	8E+00	2E+00
PE(40:6)b	4E+01	4E+01	4E+01	3E+01	3E+01	2E+01	5E+01	5E+01	5E+01	1E+02	3E+01	3E+01	3E+01	3E+01	2E+01	4E+01	7E+01	3E+01	2E+01	3E+01	1E+02	2E+01
PE(40:7)	1E+01	8E+00	1E+01	8E+00	6E+00	1E+01	9E+00	1E+01	1E+01	2E+01	5E+00	6E+00	8E+00	7E+00	5E+00	6E+00	1E+01	1E+01	7E+00	1E+01	1E+01	5E+00
PE(40:8)	1E+00	1E+00	2E+00	1E+00	1E+00	1E+00	2E+00	4E+00	2E+00	6E+00	7E-01	1E+00	1E+00	1E+00	9E-01	1E+00	1E+00	2E+00	2E+00	2E+00	3E+00	5E-01
PE(42:9)	5E-01	4E-01	6E-01	1E+00	6E-01	5E-01	5E-01	7E-01	9E-01	2E+00	5E-01	3E-01	6E-01	7E-01	5E-01	4E-01	8E-01	4E-01	5E-01	7E-01	8E-01	8E-01
PE(42:10)	1E+00	1E+00	1E+00	8E-01	6E-01	1E+00	9E-01	2E+00	1E+00	2E+00	6E-01	1E+00	1E+00	9E-01	5E-01	7E-01	1E+00	1E+00	9E-01	1E+00	2E+00	5E-01
PE(e34:2)	1E+01	2E+01	1E+01	1E+01	1E+01	2E+01	1E+01	1E+01	2E+01	3E+01	7E+00	1E+01	1E+01	9E+00	6E+00	1E+01	2E+01	1E+01	7E+00	2E+01	2E+01	7E+00
PE(e36:2)	8E+00	1E+01	7E+00	7E+00	6E+00	1E+01	7E+00	7E+00	8E+00	1E+01	5E+00	7E+00	7E+00	5E+00	3E+00	8E+00	1E+01	8E+00	4E+00	8E+00	7E+00	3E+00
PE(e38:2)	2E+00	2E+00	2E+00	1E+00	2E+00	2E+00	2E+00	2E+00	2E+00	5E+00	1E+00	2E+00	2E+00	1E+00	8E-01	2E+00	3E+00	2E+00	1E+00	2E+00	2E+00	7E-01
PE(e40:2)	4E-01	4E-01	3E-01	3E-01	5E-01	4E-01	4E-01	5E-01	5E-01	1E+00	2E-01	3E-01	3E-01	2E-01	1E-01	4E-01	4E-01	4E-01	3E-01	4E-01	5E-01	1E-01
PE(e34:3)	4E+00	6E+00	5E+00	5E+00	4E+00	4E+00	7E+00	5E+00	5E+00	1E+01	4E+00	3E+00	4E+00	5E+00	3E+00	3E+00	5E+00	6E+00	4E+00	5E+00	6E+00	3E+00
PE(e36:3)	8E+00	9E+00	9E+00	7E+00	7E+00	8E+00	8E+00	1E+01	9E+00	2E+01	4E+00	8E+00	9E+00	6E+00	6E+00	7E+00	1E+01	8E+00	7E+00	1E+01	1E+01	4E+00
PE(e38:3)	1E+00	2E+00	2E+00	9E-01	2E+00	2E+00	2E+00	3E+00	2E+00	5E+00	9E-01	1E+00	1E+00	9E-01	8E-01	2E+00	1E+00	2E+00	1E+00	1E+00	3E+00	8E-01
PE(e36:4)	4E+00	5E+00	3E+00	4E+00	4E+00	4E+00	4E+00	4E+00	5E+00	9E+00	4E+00	5E+00	5E+00	3E+00	2E+00	4E+00	5E+00	4E+00	3E+00	5E+00	6E+00	3E+00
PE(e38:4)	6E+00	6E+00	4E+00	4E+00	5E+00	7E+00	6E+00	7E+00	7E+00	1E+01	3E+00	6E+00	5E+00	3E+00	2E+00	5E+00	7E+00	6E+00	4E+00	6E+00	6E+00	3E+00
PE(e40:4)	2E+00	3E+00	2E+00	2E+00	2E+00	2E+00	2E+00	4E+00	2E+00	5E+00	8E-01	2E+00	2E+00	1E+00	9E-01	3E+00	2E+00	2E+00	2E+00	2E+00	3E+00	6E-01
PE(e36:5)	3E+02	3E+02	3E+02	3E+02	2E+02	3E+02	3E+02	4E+02	3E+02	6E+02	2E+02	2E+02	3E+02	2E+02	2E+02	2E+02	3E+02	3E+02	2E+02	3E+02	3E+02	1E+02
PE(e38:5)a	3E+01	7E+01	6E+01	5E+01	5E+01	4E+01	5E+01	1E+02	6E+01	2E+02	2E+01	3E+01	6E+01	4E+01	3E+01	6E+01	5E+01	6E+01	6E+01	5E+01	9E+01	1E+01
PE(e38:5)b	4E+02	5E+02	4E+02	4E+02	3E+02	4E+02	4E+02	6E+02	4E+02	8E+02	2E+02	4E+02	4E+02	3E+02	2E+02	3E+02	4E+02	4E+02	3E+02	4E+02	5E+02	2E+02
PE(e40:5)a	4E+01	1E+02	9E+01	7E+01	7E+01	5E+01	6E+01	2E+02	7E+01	2E+02	2E+01	3E+01	7E+01	5E+01	4E+01	7E+01	5E+01	7E+01	8E+01	7E+01	1E+02	1E+01
PE(e40:5)b	3E+01	4E+01	3E+01	3E+01	4E+01	3E+01	3E+01	6E+01	3E+01	1E+02	2E+01	3E+01	4E+01	3E+01	2E+01	4E+01	3E+01	4E+01	3E+01	3E+01	5E+01	1E+01
PE(e42:5)a	2E+00	6E+00	4E+00	4E+00	4E+00	2E+00	3E+00	1E+01	3E+00	2E+01	1E+00	2E+00	4E+00	3E+00	2E+00	4E+00	3E+00	3E+00	7E+00	3E+00	9E+00	8E-01
PE(e42:5)b	3E+00	3E+00	4E+00	4E+00	4E+00	4E+00	4E+00	8E+00	4E+00	2E+01	2E+00	3E+00	3E+00	4E+00	2E+00	4E+00	4E+00	5E+00	4E+00	3E+00	7E+00	2E+00
PE(e44:5)a	1E-01	8E-02	2E-01	1E-01	1E-01	2E-01	2E-01	3E-01	2E-01	6E-01	9E-02	1E-01	9E-02	7E-02	6E-02	1E-01	8E-02	1E-01	2E-01	1E-01	4E-01	5E-02
PE(e44:5)b	4E-01	3E-01	4E-01	3E-01	3E-01	3E-01	6E-01	8E-01	4E-01	2E+00	2E-01	3E-01	2E-01	3E-01	2E-01	3E-01	4E-01	5E-01	3E-01	3E-01	7E-01	2E-01
PE(e36:6)	2E+01	7E+00	5E+00	4E+00	3E+00	2E+01	6E+00	4E+00	1E+01	9E+00	1E+01	2E+01	6E+00	4E+00	2E+00	4E+00	2E+01	5E+00	3E+00	8E+00	4E+00	1E+01
PE(e38:6)	1E+02	1E+02	1E+02	1E+02	9E+01	1E+02	1E+02	1E+02	1E+02	2E+02	6E+01	8E+01	1E+02	9E+01	6E+01	9E+01	1E+02	1E+02	7E+01	1E+02	1E+02	6E+01
PE(e40:6)a	1E+01	1E+01	1E+01	8E+00	7E+00	1E+01	6E+00	1E+01	1E+01	2E+01	3E+00	2E+01	1E+01	1E+01	4E+00	7E+00	9E+00	7E+00	7E+00	1E+01	1E+01	3E+00
PE(e40:6)b	4E+01	5E+01	7E+01	6E+01	4E+01	4E+01	4E+01	5E+01	5E+01	1E+02	2E+01	3E+01	4E+01	4E+01	4E+01	4E+01	5E+01	5E+01	4E+01	5E+01	6E+01	2E+01
PE(e40:6)c	6E+00	6E+00	7E+00	6E+00	4E+00	7E+00	4E+00	1E+01	4E+00	2E+01	3E+00	5E+00	5E+00	4E+00	3E+00	5E+00	5E+00	5E+00	5E+00	3E+00	1E+01	2E+00
PE(e42:6)	6E+00	6E+00	8E+00	7E+00	7E+00	7E+00	6E+00	9E+00	7E+00	2E+01	4E+00	5E+00	6E+00	5E+00	5E+00	7E+00	6E+00	6E+00	7E+00	6E+00	1E+01	3E+00
PE(e38:7)a	6E+00	4E+00	3E+00	2E+00	2E+00	6E+00	3E+00	3E+00	5E+00	6E+00	5E+00	5E+00	4E+00	3E+00	1E+00	3E+00	6E+00	4E+00	2E+00	4E+00	4E+00	4E+00
PE(e38:7)b	4E+01	5E+01	4E+01	3E+01	2E+01	4E+01	2E+01	4E+01	5E+01	7E+01	3E+01	4E+01	3E+01	3E+01	1E+01	2E+01	5E+01	2E+01	2E+01	4E+01	4E+01	2E+01
PE(e40:7)	6E+01	6E+01	7E+01	4E+01	2E+01	7E+01	3E+01	7E+01	8E+01	9E+01	4E+01	5E+01	7E+01	6E+01	2E+01	3E+01	7E+01	6E+01	3E+01	7E+01	5E+01	3E+01
PE(e42:7)	4E+00	5E+00	4E+00	3E+00	3E+00	5E+00	3E+00	8E+00	4E+00	1E+01	2E+00	3E+00	4E+00	3E+00	2E+00	3E+00	4E+00	3E+00	3E+00	4E+00	5E+00	2E+00
PE(e44:7)	3E-01	4E-01	3E-01	2E-01	2E-01	3E-01	3E-01	5E-01	3E-01	8E-01	2E-01	2E-01	2E-01	2E-01	1E-01	2E-01	3E-01	2E-01	2E-01	2E-01	4E-01	2E-01
PE(e40:8)	1E+01	9E+00	8E+00	6E+00	5E+00	1E+01	7E+00	1E+01	1E+01	2E+01	5E+00	8E+00	9E+00	6E+00	3E+00	6E+00	1E+01	6E+00	5E+00	1E+01	9E+00	4E+00
PS(34:1)	1E+00	1E+00	1E+00	1E+00	1E+00	1E+00	1E+00	3E+00	1E+00	2E+00	8E-01	2E+00	2E+00	9E-01	1E+00	2E+00	3E+00	1E+00	1E+00	2E+00	3E+00	5E-01
PS(36:1)	1E+02	1E+02	1E+02	6E+01	9E+01	1E+02	1E+02	2E+02	2E+02	2E+02	6E+01	1E+02	1E+02	7E+01	9E+01	1E+02	1E+02	1E+02	1E+02	1E+02	1E+02	7E+01
PS(38:1)	7E+00	8E+00	5E+00	4E+00	6E+00	7E+00	8E+00	1E+01	1E+01	1E+01	3E+00	6E+00	6E+00	4E+00	4E+00	5E+00	5E+00	6E+00	5E+00	6E+00	6E+00	3E+00
PS(40:1)	4E+00	3E+00	2E+00	3E+00	3E+00	5E+00	5E+00	4E+00	5E+00	5E+00	1E+00	2E+00	2E+00	2E+00	2E+00	2E+00	2E+00	3E+00	2E+00	2E+00	2E+00	1E+00
PS(42:1)	5E-01	4E-01	3E-01	4E-01	4E-01	8E-01	7E-01	7E-01	8E-01	6E-01	2E-01	4E-01	3E-01	2E-01	2E-01	2E-01	3E-01	4E-01	2E-01	4E-01	3E-01	2E-01
PS(34:2)	4E-01	3E-01	2E-01	2E-01	2E-01	4E-01	3E-01	4E-01	3E-01	5E-01	1E-01	3E-01	2E-01	1E-01	2E-01	3E-01	3E-01	3E-01	2E-01	2E-01	4E-01	9E-02
PS(36:2)	1E+01	8E+00	6E+00	6E+00	7E+00	1E+01	9E+00	1E+01	2E+01	1E+01	4E+00	8E+00	6E+00	5E+00	5E+00	1E+01	9E+00	9E+00	8E+00	9E+00	6E+00	5E+00
PS(38:2)a	2E+00	2E+00	2E+00	1E+00	2E+00	2E+00	2E+00	2E+00	4E+00	3E+00	8E-01	1E+00	2E+00	1E+00	1E+00	2E+00	2E+00	3E+00	1E+00	2E+00	2E+00	8E-01
PS(38:2)b	2E+00	2E+00	1E+00	1E+00	2E+00	2E+00	2E+00	2E+00	3E+00	3E+00	6E-01	9E-01	1E+00	9E-01	9E-01	1E+00	2E+00	2E+00	8E-01	1E+00	2E+00	8E-01
PS(40:2)	3E+00	2E+00	1E+00	1E+00	1E+00	2E+00	2E+00	2E+00	3E+00	3E+00	8E-01	3E+00	1E+00	9E-01	8E-01	2E+00	2E+00	2E+00	1E+00	2E+00	1E+00	8E-01
PS(36:3)	9E-01	8E-01	7E-01	6E-01	9E-01	1E+00	1E+00	2E+00	2E+00	1E+00	4E-01	7E-01	6E-01	4E-01	5E-01	9E-01	9E-01	9E-01	9E-01	9E-01	8E-01	4E-01
PS(38:3)	3E+01	1E+01	1E+01	1E+01	1E+01	3E+01	2E+01	2E+01	3E+01	4E+01	1E+01	2E+01	1E+01	9E+00	8E+00	9E+00	2E+01	2E+01	1E+01	1E+01	2E+01	1E+01
PS(36:4)	1E+00	1E+00	7E-01	9E-01	9E-01	1E+00	1E+00	2E+00	8E-01	2E+00	3E-01	8E-01	8E-01	4E-01	7E-01	9E-01	1E+00	1E+00	7E-01	4E-01	1E+00	3E-01
PS(38:4)	2E+02	2E+02	1E+02	1E+02	1E+02	2E+02	1E+02	4E+02	2E+02	3E+02	9E+01	2E+02	2E+02	1E+02	1E+02	2E+02	1E+02	2E+02	2E+02	3E+02	2E+02	7E+01
PS(40:4)a	4E+00	7E+00	7E+00	4E+00	3E+00	4E+00	4E+00	2E+01	6E+00	1E+01	2E+00	5E+00	6E+00	5E+00	5E+00	6E+00	5E+00	5E+00	9E+00	7E+00	1E+01	2E+00
PS(40:4)b	2E+00	3E+00	2E+00	2E+00	2E+00	3E+00	4E+00	5E+00	3E+00	4E+00	1E+00	2E+00	2E+00	2E+00	2E+00	2E+00	2E+00	2E+00	3E+00	2E+00	3E+00	8E-01
PS(38:5)	1E+01	2E+01	1E+01	1E+01	1E+01	1E+01	2E+01	3E+01	3E+01	2E+01	4E+00	9E+00	1E+01	9E+00	1E+01	1E+01	1E+01	2E+01	2E+01	2E+01	1E+01	4E+00
PS(40:5)	2E+00	2E+00	2E+00	2E+00	1E+00	2E+00	2E+00	3E+00	2E+00	5E+00	8E-01	1E+00	1E+00	1E+00	1E+00	1E+00	1E+00	2E+00	2E+00	9E-01	3E+00	7E-01
PS(40:6)a	1E+00	1E+00	1E+00	7E-01	8E-01	1E+00	1E+00	2E+00	2E+00	2E+00	4E-01	9E-01	7E-01	6E-01	7E-01	7E-01	1E+00	1E+00	1E+00	9E-01	1E+00	4E-01
PS(40:6)b	2E+01	6E+00	5E+00	4E+00	4E+00	2E+01	5E+00	1E+01	2E+01	1E+01	6E+00	9E+00	5E+00	3E+00	3E+00	4E+00	8E+00	3E+00	5E+00	8E+00	5E+00	5E+00
PS(40:7)	1E+00	1E+00	7E-01	5E-01	6E-01	1E+00	7E-01	2E+00	2E+00	1E+00	4E-01	1E+00	7E-01	5E-01	6E-01	6E-01	1E+00	8E-01	1E+00	1E+00	6E-01	5E-01
CE(18:1)	5E+01	1E+02	6E+01	4E+01	4E+01	6E+01	9E+01	2E+01	3E+01	4E+01	1E+01	3E+01	4E+01	3E+01	2E+01	3E+01	2E+01	2E+01	6E+00	1E+01	2E+01	7E+00
CE(16:1)	9E+00	2E+01	1E+01	6E+00	7E+00	7E+00	1E+01	6E+00	3E+00	7E+00	3E+00	9E+00	8E+00	8E+00	6E+00	5E+00	4E+00	7E+00	2E+00	3E+00	7E+00	2E+00
CE(18:3)	4E+01	1E+02	5E+01	2E+01	2E+01	2E+01	8E+01	2E+01	2E+01	2E+01	7E+00	3E+01	2E+01	2E+01	1E+01	2E+01	8E+00	2E+01	6E+00	2E+01	2E+01	4E+00
CE(20:3)	2E+01	6E+01	2E+01	2E+01	1E+01	3E+01	6E+01	7E+00	1E+01	1E+01	4E+00	1E+01	1E+01	1E+01	7E+00	9E+00	7E+00	1E+01	3E+00	7E+00	6E+00	2E+00
CE(20:4)	2E+02	7E+02	2E+02	1E+02	1E+02	3E+02	4E+02	1E+02	7E+01	9E+01	2E+01	2E+02	2E+02	1E+02	7E+01	9E+01	8E+01	1E+02	3E+01	6E+01	8E+01	2E+01
CE(20:5)	1E+02	1E+02	4E+01	2E+01	9E+00	1E+02	6E+01	1E+01	2E+01	1E+01	1E+01	8E+01	3E+01	2E+01	1E+01	1E+01	3E+01	2E+01	6E+00	2E+01	1E+01	7E+00
CE(22:6)	1E+02	1E+02	5E+01	2E+01	2E+01	1E+02	1E+02	2E+01	3E+01	2E+01	1E+01	9E+01	3E+01	3E+01	1E+01	2E+01	4E+01	3E+01	6E+00	2E+01	1E+01	8E+00
CE(18:2)	5E+02	8E+02	5E+02	4E+02	2E+02	5E+02	1E+03	3E+02	2E+02	2E+02	7E+01	4E+02	2E+02	3E+02	2E+02	3E+02	2E+02	3E+02	9E+01	2E+02	2E+02	5E+01
cholesterol	2E+03	9E+02	1E+03	8E+02	8E+02	1E+03	2E+03	3E+03	2E+03	2E+03	3E+02	1E+03	2E+03	5E+02	1E+03	2E+03	2E+03	1E+03	9E+02	2E+03	2E+03	6E+02
SM(d30:1)	9E+00	7E+00	7E+00	6E+00	7E+00	6E+00	6E+00	4E+01	2E+01	1E+01	2E+00	1E+01	5E+00	5E+00	4E+00	9E+00	6E+00	9E+00	2E+01	2E+01	6E+00	3E+00
SM(d31:1)	6E+00	5E+00	5E+00	4E+00	6E+00	4E+00	5E+00	2E+01	1E+01	1E+01	1E+00	9E+00	4E+00	3E+00	3E+00	6E+00	4E+00	8E+00	1E+01	1E+01	5E+00	2E+00
SM(d32:0)	1E+01	9E+00	7E+00	5E+00	8E+00	9E+00	6E+00	2E+01	2E+01	1E+01	3E+00	2E+01	7E+00	5E+00	4E+00	1E+01	9E+00	1E+01	2E+01	1E+01	7E+00	4E+00
SM(d32:1)	3E+02	2E+02	3E+02	2E+02	2E+02	2E+02	2E+02	1E+03	5E+02	5E+02	6E+01	4E+02	2E+02	2E+02	1E+02	3E+02	2E+02	4E+02	6E+02	5E+02	3E+02	8E+01
SM(d33:0)	1E+01	9E+00	1E+01	7E+00	8E+00	1E+01	8E+00	4E+01	1E+01	1E+01	2E+00	2E+01	9E+00	7E+00	4E+00	1E+01	1E+01	1E+01	2E+01	1E+01	7E+00	4E+00
SM(d33:1)	1E+02	1E+02	1E+02	1E+02	1E+02	1E+02	1E+02	3E+02	2E+02	2E+02	3E+01	2E+02	1E+02	9E+01	7E+01	1E+02	1E+02	2E+02	2E+02	2E+02	1E+02	4E+01
SM(d34:0)	6E+01	5E+01	4E+01	2E+01	4E+01	5E+01	4E+01	9E+01	6E+01	6E+01	3E+01	1E+02	5E+01	3E+01	2E+01	6E+01	6E+01	8E+01	8E+01	7E+01	5E+01	3E+01
SM(d34:1)	2E+03	1E+03	1E+03	9E+02	1E+03	1E+03	9E+02	2E+03	2E+03	2E+03	4E+02	2E+03	7E+02	5E+02	5E+02	1E+03	7E+02	2E+03	1E+03	1E+03	9E+02	6E+02
SM(d34:2)	2E+02	2E+02	2E+02	2E+02	2E+02	2E+02	2E+02	6E+02	4E+02	5E+02	4E+01	3E+02	1E+02	1E+02	1E+02	2E+02	1E+02	2E+02	3E+02	2E+02	3E+02	6E+01
SM(d35:0)	2E+00	2E+00	2E+00	1E+00	1E+00	2E+00	2E+00	2E+00	2E+00	2E+00	5E-01	2E+00	2E+00	8E-01	7E-01	1E+00	1E+00	3E+00	2E+00	1E+00	1E+00	7E-01
SM(d35:1)	2E+01	1E+01	1E+01	1E+01	1E+01	1E+01	8E+00	2E+01	2E+01	1E+01	5E+00	2E+01	1E+01	1E+01	7E+00	1E+01	1E+01	2E+01	2E+01	1E+01	7E+00	6E+00
SM(d35:2)	4E+00	3E+00	4E+00	2E+00	3E+00	3E+00	2E+00	9E+00	6E+00	5E+00	1E+00	5E+00	3E+00	3E+00	2E+00	4E+00	2E+00	4E+00	6E+00	4E+00	4E+00	1E+00
SM(d36:0)	7E+00	9E+00	4E+00	4E+00	6E+00	8E+00	5E+00	1E+01	9E+00	1E+01	2E+00	1E+01	7E+00	3E+00	3E+00	7E+00	6E+00	8E+00	1E+01	6E+00	7E+00	3E+00
SM(d36:1)	8E+01	5E+01	5E+01	5E+01	6E+01	7E+01	4E+01	1E+02	1E+02	1E+02	2E+01	8E+01	4E+01	4E+01	3E+01	6E+01	4E+01	7E+01	9E+01	5E+01	5E+01	3E+01
SM(d36:2)	1E+01	1E+01	1E+01	9E+00	1E+01	8E+00	7E+00	2E+01	1E+01	2E+01	4E+00	1E+01	7E+00	7E+00	6E+00	9E+00	8E+00	1E+01	1E+01	1E+01	1E+01	5E+00
SM(d36:3)	2E+00	2E+00	2E+00	2E+00	2E+00	2E+00	2E+00	7E+00	5E+00	3E+00	5E-01	3E+00	2E+00	2E+00	1E+00	2E+00	2E+00	3E+00	5E+00	3E+00	2E+00	6E-01
SM(d37:0)	3E+00	3E+00	2E+00	2E+00	3E+00	7E+00	3E+00	5E+00	5E+00	5E+00	1E+00	7E+00	2E+00	2E+00	1E+00	4E+00	5E+00	4E+00	3E+00	5E+00	2E+00	2E+00
SM(d37:1)	4E+00	3E+00	2E+00	3E+00	4E+00	3E+00	3E+00	7E+00	6E+00	6E+00	1E+00	4E+00	2E+00	2E+00	2E+00	3E+00	3E+00	4E+00	6E+00	5E+00	3E+00	2E+00
SM(d38:0)	2E+01	2E+01	9E+00	9E+00	1E+01	2E+01	2E+01	4E+01	3E+01	4E+01	5E+00	2E+01	2E+01	7E+00	6E+00	1E+01	2E+01	2E+01	2E+01	2E+01	2E+01	6E+00
SM(d38:1)	1E+02	8E+01	8E+01	6E+01	9E+01	7E+01	6E+01	2E+02	2E+02	2E+02	3E+01	1E+02	7E+01	6E+01	4E+01	1E+02	7E+01	9E+01	2E+02	1E+02	9E+01	4E+01
SM(d38:2)	9E+00	8E+00	8E+00	6E+00	7E+00	6E+00	6E+00	2E+01	1E+01	1E+01	3E+00	1E+01	6E+00	5E+00	6E+00	9E+00	5E+00	7E+00	2E+01	9E+00	6E+00	3E+00
SM(d39:0)	2E+00	2E+00	1E+00	1E+00	2E+00	2E+00	1E+00	3E+00	3E+00	3E+00	5E-01	3E+00	1E+00	8E-01	5E-01	1E+00	2E+00	2E+00	2E+00	2E+00	2E+00	8E-01
SM(d39:1)	4E+01	4E+01	3E+01	3E+01	3E+01	3E+01	3E+01	7E+01	5E+01	4E+01	8E+00	4E+01	3E+01	2E+01	2E+01	4E+01	3E+01	4E+01	5E+01	3E+01	2E+01	9E+00
SM(d40:0)	6E+01	7E+01	4E+01	3E+01	4E+01	6E+01	5E+01	1E+02	8E+01	1E+02	1E+01	8E+01	6E+01	3E+01	2E+01	5E+01	5E+01	7E+01	7E+01	6E+01	7E+01	2E+01
SM(d40:1)	6E+02	6E+02	4E+02	4E+02	5E+02	5E+02	4E+02	1E+03	8E+02	1E+03	2E+02	9E+02	5E+02	4E+02	3E+02	6E+02	4E+02	8E+02	1E+03	7E+02	7E+02	3E+02
SM(d40:2)	5E+01	5E+01	4E+01	4E+01	5E+01	4E+01	4E+01	1E+02	8E+01	9E+01	2E+01	6E+01	4E+01	4E+01	3E+01	5E+01	3E+01	7E+01	9E+01	6E+01	5E+01	2E+01
SM(d41:0)	5E+00	8E+00	3E+00	3E+00	4E+00	6E+00	4E+00	1E+01	9E+00	1E+01	2E+00	7E+00	5E+00	2E+00	2E+00	4E+00	5E+00	6E+00	7E+00	7E+00	5E+00	2E+00
SM(d41:1)	1E+02	1E+02	1E+02	9E+01	1E+02	1E+02	9E+01	2E+02	1E+02	1E+02	2E+01	2E+02	9E+01	7E+01	6E+01	1E+02	1E+02	1E+02	1E+02	9E+01	7E+01	2E+01
SM(d42:0)	3E+01	4E+01	2E+01	2E+01	2E+01	3E+01	2E+01	5E+01	4E+01	7E+01	9E+00	5E+01	3E+01	2E+01	1E+01	3E+01	3E+01	4E+01	3E+01	3E+01	4E+01	1E+01
SM(d42:1)	6E+02	5E+02	5E+02	4E+02	4E+02	4E+02	4E+02	1E+03	8E+02	1E+03	2E+02	8E+02	4E+02	4E+02	3E+02	5E+02	4E+02	7E+02	8E+02	6E+02	6E+02	2E+02
SM(d42:2)	7E+02	4E+02	4E+02	3E+02	5E+02	5E+02	3E+02	8E+02	8E+02	1E+03	2E+02	9E+02	4E+02	3E+02	2E+02	6E+02	6E+02	6E+02	6E+02	6E+02	5E+02	3E+02
SM(d42:3)	7E+01	5E+01	5E+01	4E+01	5E+01	5E+01	4E+01	1E+02	8E+01	1E+02	3E+01	8E+01	3E+01	4E+01	3E+01	5E+01	4E+01	5E+01	8E+01	7E+01	7E+01	3E+01
SM(d43:1)	1E+01	1E+01	9E+00	8E+00	7E+00	9E+00	9E+00	2E+01	1E+01	2E+01	2E+00	1E+01	7E+00	7E+00	5E+00	8E+00	7E+00	1E+01	2E+01	1E+01	9E+00	3E+00
SM(d43:2)	1E+01	1E+01	1E+01	9E+00	1E+01	1E+01	1E+01	2E+01	2E+01	2E+01	2E+00	2E+01	8E+00	7E+00	5E+00	1E+01	1E+01	1E+01	1E+01	1E+01	8E+00	3E+00
SM(d44:1)	9E+00	7E+00	7E+00	5E+00	6E+00	6E+00	7E+00	2E+01	1E+01	2E+01	2E+00	1E+01	5E+00	4E+00	4E+00	6E+00	6E+00	1E+01	1E+01	7E+00	1E+01	2E+00
SM(d44:2)	1E+01	7E+00	7E+00	5E+00	7E+00	1E+01	5E+00	1E+01	2E+01	1E+01	4E+00	1E+01	5E+00	5E+00	3E+00	8E+00	9E+00	9E+00	1E+01	1E+01	8E+00	5E+00

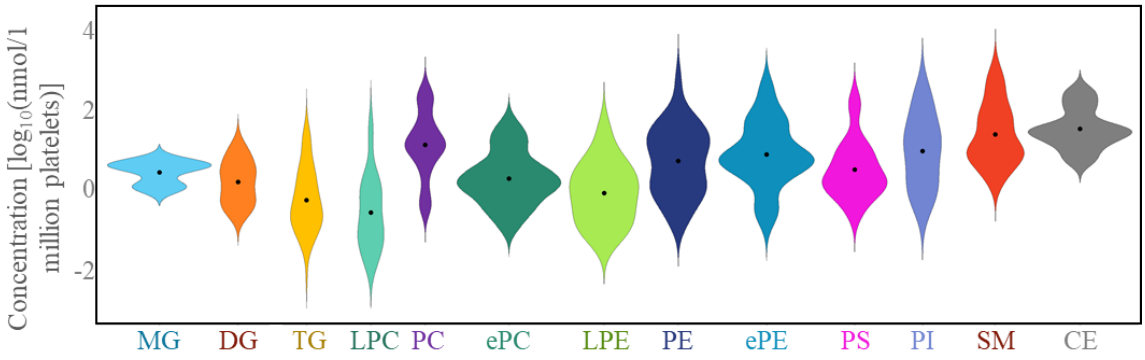

Figure 98. *Violin plots showing distribution of lipid species concentration (in logarithmic scale) within different lipid classes. Average values of 11 resting platelet samples. Black dots show mean concentration.*

4.5.7. Final results of 44 platelet samples with 4 different treatments – results of statistical analysis

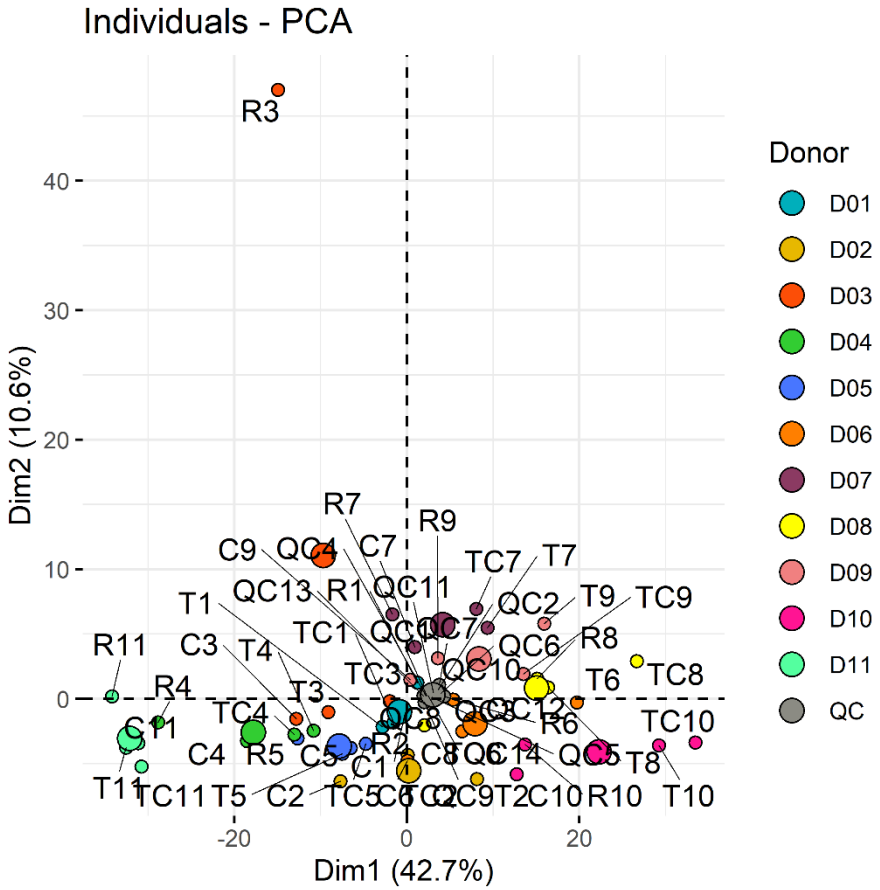

Figure 99. *Score plot from PCA of lipid signal intensities from the 44 samples. The R3 sample (resting platelets from the 3rd donor) is an outlier and was removed from the further analysis.*

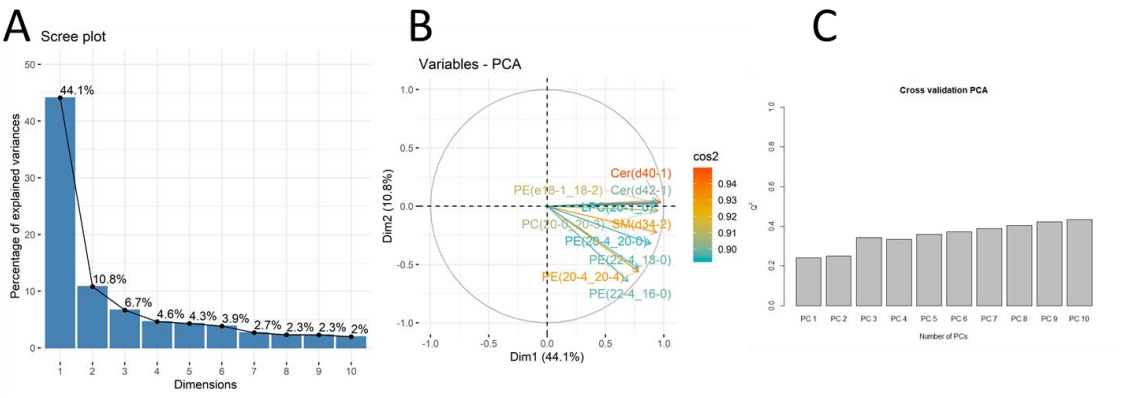

Figure 100. A: *Scree plot and* ***B****: graph of 10 top variables and their contribution to principal components (the arrows are coloured by the quality of representation) and* ***C****: cumulative Q2. The data is related to PCA (Figure 79A of the main document).*

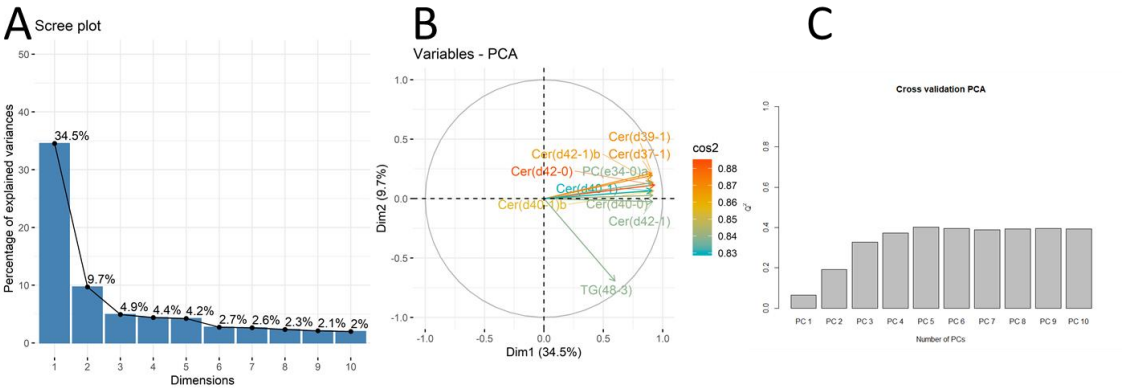

Figure 101. A: *Scree plot and* ***B****: graph of 10 top variables and their contribution to principal components (the arrows are coloured by the quality of representation) and* ***C****: cumulative Q2. The data is related to PCA (Figure 79B of the main document).*

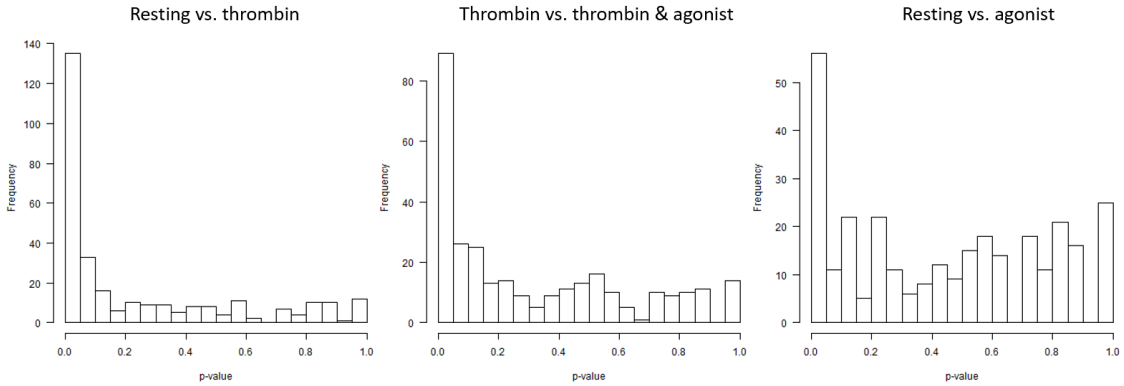

Figure 102. *Histograms showing distribution of p-values for the 3 comparisons.*

Table 64. *Percentage of lipid species in each lipid class, which showed q-value lower than 0.05 for the 3 comparisons and the corresponding mean value of FC for all the lipids in a class.*

	Resting vs. Thrombin		Thrombin vs. Thrombin & Platelet inhibitor		Resting vs. Platelet inhibitor	
	% q-values < 0.05	mean FC	% q-values < 0.05	mean FC	% q-values < 0.05	mean FC
FA	19.0	1.06	0.0	0.86	14.3	0.80
MG	0.0	0.98	0.0	1.01	0.0	0.92
DG	0.0	1.03	23.8	0.67	33.3	0.64
TG	3.4	1.06	22.4	1.32	1.7	0.99
LPC	53.6	1.20	0.0	0.91	10.7	0.86
PC	18.4	1.07	0.0	1.00	0.0	1.01
ePC	63.6	1.15	0.0	1.00	0.0	1.01
LPE	47.1	0.75	5.9	0.79	47.1	0.64
PE	35.0	1.12	0.0	0.97	0.0	0.99
ePE	65.7	1.17	0.0	0.98	0.0	1.03
LPI	100.0	3.27	80.0	0.40	0.0	1.03
PI	0.0	1.01	0.0	1.06	0.0	1.04
LPS	0.0	1.25	0.0	0.60	100.0	0.47
PS	12.0	1.07	0.0	1.02	0.0	0.99
ACar	12.5	1.09	50.0	2.86	56.3	2.31
CE	11.1	1.08	33.3	1.40	0.0	0.84
Cer	89.3	1.23	0.0	1.00	0.0	1.02
HexCer	20.0	1.27	0.0	1.03	0.0	1.01
SM	44.4	1.13	0.0	0.98	0.0	0.98
Oxylipins	80.0	17.34	40.0	0.49	0.0	0.78

Table 65. *Significant findings as shown in the volcano plots (Figure 80 in the main document).*

Lipid species	Resting vs. Thrombin		Thrombin vs. Thrombin & Platelet inhibitor		Resting vs. Platelet inhibitor	
	q-value	FC	q-value	FC	q-value	FC
FA(18:0)	0.021	1.51	0.290	0.98	0.988	1.10
FA(20:4)	0.044	0.37	0.374	0.58	0.453	0.58
FA(20:5)	0.025	0.38	0.761	1.12	0.075	0.43
FA(22:6)	0.037	0.31	0.527	0.81	0.046	0.37
TXB2	0.016	32.56	0.044	0.07	0.506	0.74
HHT	0.016	48.28	0.044	0.12	0.828	0.94
HETE	0.016	2.06	0.673	0.91	0.874	0.78
HODE	0.016	2.10	0.074	0.55	0.707	0.71
DG(10:0_16:0)	0.543	1.24	0.443	0.67	0.047	0.49
DG(12:0_18:1)	0.438	1.02	0.502	0.68	0.046	0.49
DG(14:0_18:1)	0.407	0.91	0.443	0.49	0.046	0.50
DG(16:0_18:1)	0.124	1.29	0.044	0.50	0.046	0.46
DG(16:0_18:2)	0.543	1.21	0.044	0.53	0.047	0.49
DG(18:0_18:1)	0.407	1.06	0.044	0.44	0.046	0.48
DG(18:0_18:2)	0.438	1.26	0.044	0.47	0.062	0.53
DG(18:1_18:2)	0.376	0.82	0.044	0.62	0.091	0.56
LPC(18:1)b	0.510	1.04	0.108	0.79	0.046	0.60
LPC(18:2)b	0.308	0.90	0.673	0.73	0.046	0.44
LPC(20:4)b	0.044	0.57	0.160	0.86	0.046	0.39
LPC(24:1)	0.021	1.57	0.708	1.02	0.453	1.07
LPE(18:1)b	0.016	0.61	0.044	0.67	0.046	0.39
LPE(18:2)b	0.016	0.47	0.290	0.75	0.046	0.32
LPE(20:3)	0.016	0.44	0.131	0.65	0.046	0.37
LPE(20:4)	0.016	0.51	0.090	0.66	0.046	0.44
LPE(20:5)	0.016	0.35	0.561	0.94	0.046	0.31
LPE(22:4)	0.016	0.36	0.131	0.59	0.046	0.38
LPE(22:5)	0.016	0.37	0.227	0.77	0.046	0.32
LPE(22:6)	0.016	0.45	0.052	0.41	0.046	0.34
LPI(16:0)	0.016	3.68	0.044	0.49	0.803	1.42
LPI(18:0)	0.016	3.94	0.044	0.30	0.075	0.63
LPI(18:1)	0.016	2.48	0.044	0.49	0.957	1.01
LPI(20:0)	0.016	4.77	0.044	0.16	0.672	1.52
LPS(18:0)	0.278	1.25	0.059	0.60	0.046	0.47
ACar(14:0)	0.231	1.34	0.052	1.55	0.046	1.79
ACar(16:0)	0.633	0.96	0.044	4.29	0.046	4.43
ACar(16:1)	0.407	0.78	0.044	3.40	0.047	2.04
ACar(18:0)	0.089	1.40	0.044	2.58	0.046	2.32
ACar(18:1)	0.181	0.72	0.044	5.49	0.046	3.40
ACar(18:2)	0.438	0.99	0.044	6.93	0.046	3.34
ACar(20:2)	0.139	1.34	0.044	3.35	0.046	3.67
ACar(20:3)	0.407	0.96	0.044	5.11	0.047	3.90
CE(18:1)	0.639	0.88	0.044	1.54	0.707	0.77
CE(18:3)	0.633	0.95	0.044	1.53	0.628	0.82
Cer(d35:1)	0.016	1.52	0.738	1.03	0.988	0.97
HexCer(d18:0/24:0)	0.021	1.50	0.502	0.95	0.828	0.95
TG(42:2)	0.207	0.91	0.044	1.51	0.780	0.97
TG(48:2)	0.407	0.97	0.044	1.69	0.828	0.84
TG(48:3)	0.476	1.07	0.044	1.61	0.957	1.10
TG(52:2)	0.207	0.93	0.044	1.55	0.536	0.80
TG(54:2)	0.231	0.87	0.044	1.56	0.957	0.91
TG(54:5)	0.639	0.99	0.044	1.58	0.933	1.08
sphingosine (18:1)	0.016	1.74	0.673	1.04	0.091	1.31
sphinganine (18:0)	0.016	1.66	0.329	0.85	0.755	1.15

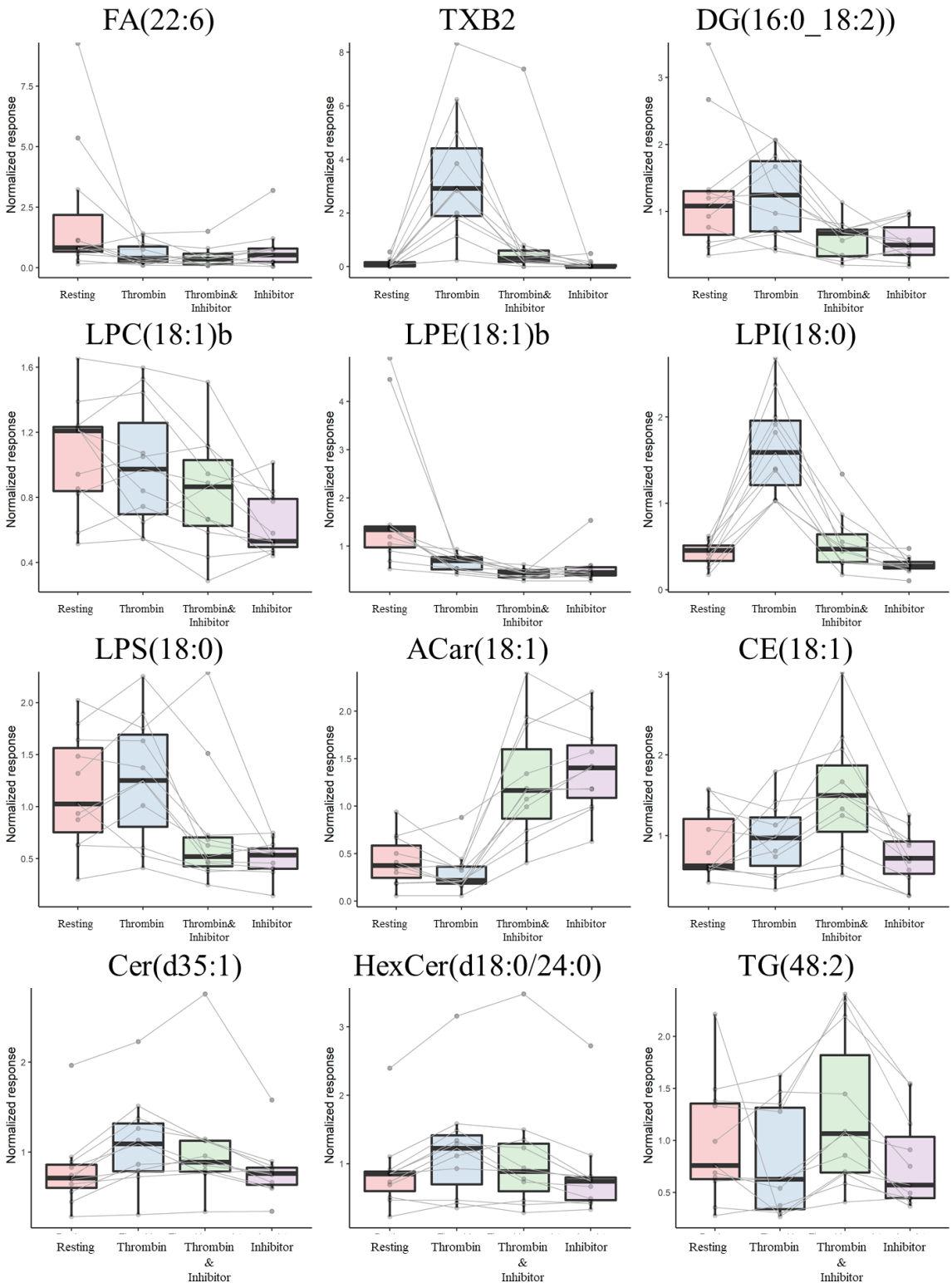

Figure 103. *Exemplary boxplots of significantly altered lipids. One example per lipid class. The first box (red) represents resting platelets, the second (blue) thrombin treated, the third (green) thrombin and platelet inhibitor treated and the last one (purple) the platelet inhibitor treated samples. Lines connect samples from the same donor.*

FINAL REMARKS

The research carried out in the course of my PhD thesis contributed to the field of lipid research and platelet lipidomics. New analytical methods based on the state of the art LC-MS/MS technologies have been developed. Especially the challenging problem of detection and quantification of low abundant oxylipins has been addressed in my work and two new methods have been established. The first one was achiral, highly sensitive μUHPLC analysis for simultaneous quantification of a larger set of oxylipins, while the second one was an enantioselective method for analysing chiral hydroxy fatty acids.

Another analytical issue communicated in my work was the hypothesis generating untargeted analysis of lipids. New ideas for post-acquisition data processing suitable for study of hundreds to thousands of lipid species have been stated and developed. It resulted in improvements in peak picking, lipid identification and in more selective compound quantification.

All the methods established during my PhD research and described in this thesis were carefully and systematically optimized, so that they could well serve their analytical purpose. The methods were validated to show their good performance especially in terms of sufficient sensitivity and proper selectivity. Issues of analyte calibration in biological matrices as well as peak normalization without isotopically labelled analogues were addressed and successfully resolved. Moreover, this thesis describes other important analytical aspects, like sample treatment, storage and extraction procedures.

The described methods were used for analysis of platelet cellular lipidome and platelet releasates and important discoveries were made. For the first time the release of PUFAs and their presence in platelet releasate was described. Furthermore, enantioselective characterisation of oxylipins released from platelets was reported. What is more, the platelet cellular lipidome was described by untargeted analysis of the general lipid classes and by targeted, sensitive analysis of oxylipins. Finally the influence to platelet lipidome by treatment with thrombin and/or platelet inhibitor – the selective CXCR7 receptor agonist has been reported.

REFERENCES

[1] R. Cammack *et al.*, *Oxford Dictionary of Biochemistry and Molecular Biology*. Oxford University Press, 2008.

[2] W. W. Christie and X. Han, *Lipid analysis*. 2010.

[3] E. Fahy, D. Cotter, M. Sud, and S. Subramaniam, "Lipid classification, structures and tools," *Biochim Biophys Acta,* vol. 1811, no. 11, pp. 637-47, Nov 2011, doi: 10.1016/j.bbalip.2011.06.009.

[4] E. Fahy *et al.*, "A comprehensive classification system for lipids," *J Lipid Res,* vol. 46, no. 5, pp. 839-61, May 2005, doi: 10.1194/jlr.E400004-JLR200.

[5] E. Fahy *et al.*, "Update of the LIPID MAPS comprehensive classification system for lipids," *J Lipid Res,* vol. 50 Suppl, pp. S9-14, Apr 2009, doi: 10.1194/jlr.R800095-JLR200.

[6] J. P. Koelmel, C. Z. Ulmer, C. M. Jones, R. A. Yost, and J. A. Bowden, "Common cases of improper lipid annotation using high-resolution tandem mass spectrometry data and corresponding limitations in biological interpretation," *Biochim Biophys Acta Mol Cell Biol Lipids,* vol. 1862, no. 8, pp. 766-770, Aug 2017, doi: 10.1016/j.bbalip.2017.02.016.

[7] G. Liebisch *et al.*, "Shorthand notation for lipid structures derived from mass spectrometry," *J Lipid Res,* vol. 54, no. 6, pp. 1523-30, Jun 2013, doi: 10.1194/jlr.M033506.

[8] J. Yeung, M. Hawley, and M. Holinstat, "The expansive role of oxylipins on platelet biology," *J Mol Med (Berl),* vol. 95, no. 6, pp. 575-588, Jun 2017, doi: 10.1007/s00109-017-1542-4.

[9] M. A. Nayeem, "Role of oxylipins in cardiovascular diseases," *Acta Pharmacol Sin,* vol. 39, no. 7, pp. 1142-1154, Jul 2018, doi: 10.1038/aps.2018.24.

[10] B. E. Tourdot, I. Ahmed, and M. Holinstat, "The emerging role of oxylipins in thrombosis and diabetes," *Front Pharmacol,* vol. 4, p. 176, Jan 7 2014, doi: 10.3389/fphar.2013.00176.

[11] G. Astarita, A. C. Kendall, E. A. Dennis, and A. Nicolaou, "Targeted lipidomic strategies for oxygenated metabolites of polyunsaturated fatty acids," *Biochim Biophys Acta,* vol. 1851, no. 4, pp. 456-68, Apr 2015, doi: 10.1016/j.bbalip.2014.11.012.

[12] I. Willenberg, A. I. Ostermann, and N. H. Schebb, "Targeted metabolomics of the arachidonic acid cascade: current state and challenges of LC-MS analysis of oxylipins," *Anal Bioanal Chem,* vol. 407, no. 10, pp. 2675-83, Apr 2015, doi: 10.1007/s00216-014-8369-4.

[13] J. D. Imig and B. D. Hammock, "Soluble epoxide hydrolase as a therapeutic target for cardiovascular diseases," *Nat Rev Drug Discov,* vol. 8, no. 10, pp. 794-805, Oct 2009, doi: 10.1038/nrd2875.

[14] B. Z. Paul, J. Jin, and S. P. Kunapuli, "Molecular mechanism of thromboxane A(2)-induced platelet aggregation. Essential role for p2t(ac) and alpha(2a) receptors," *J Biol Chem,* vol. 274, no. 41, pp. 29108-14, Oct 8 1999, doi: 10.1074/jbc.274.41.29108.

[15] E. Niki, Y. Yoshida, Y. Saito, and N. Noguchi, "Lipid peroxidation: mechanisms, inhibition, and biological effects," *Biochem Biophys Res Commun,* vol. 338, no. 1, pp. 668-76, Dec 9 2005, doi: 10.1016/j.bbrc.2005.08.072.

[16] J. Griffiths, "A brief history of mass spectrometry," *Anal Chem,* vol. 80, no. 15, pp. 5678-83, Aug 1 2008, doi: 10.1021/ac8013065.

[17] Á. Somogyi, *Medical Applications of Mass Spectrometry*. Elsevier Science, 2007.

[18] X. Han, *Lipidomics: Comprehensive Mass Spectrometry of Lipids* (Wiley Series on Mass Spectrometry). Hoboken, New Jersey: John Wiley & Sons, Inc, 2016.
[19] J. Kool and W. M. A. Niessen, *Analyzing Biomolecular Interactions by Mass Spectrometry*. Wiley-VCH Verlag GmbH & Co. KGaA, 2015.
[20] E. Hoffmann and V. Stroobant, *Mass Spectrometry Principles and Applications*. John Wiley & Sons Ltd, 2007.
[21] G. Siuzdak, "An introduction to mass spectrometry ionization: An excerpt from The Expanding Role of Mass Spectrometry in Biotechnology, 2nd ed.; MCC Press: San Diego, 2005," *Journal of the Association for Laboratory Automation,* vol. 9, no. 2, pp. 50-63, 2004, doi: 10.1016/j.jala.2004.01.004.
[22] B. K. Matuszewski, M. L. Constanzer, and C. M. Chavez-Eng, "Matrix effect in quantitative LC/MS/MS analyses of biological fluids: a method for determination of finasteride in human plasma at picogram per milliliter concentrations," *Anal Chem,* vol. 70, no. 5, pp. 882-9, Mar 1 1998, doi: 10.1021/ac971078+.
[23] G. Hart-Smith and S. J. Blanksby, *Mass Spectrometry in Polymer Chemistry: 1. Mass Analysis*. Wiley-VCH Verlag GmbH & Co. KGaA., 2012.
[24] P. L. Urban, Y.-C. Chen, and Y.-S. Wang, *Time-Resolved Mass Spectrometry: From Concept to Applications*. John Wiley & Sons, Ltd., 2016.
[25] D. L. Shinholt, S. N. Anthony, A. W. Alexander, B. E. Draper, and M. F. Jarrold, "A frequency and amplitude scanned quadrupole mass filter for the analysis of high m/z ions," *Rev Sci Instrum,* vol. 85, no. 11, p. 113109, Nov 2014, doi: 10.1063/1.4900627.
[26] P. E. Miller and M. B. Denton, "The quadrupole mass filter: Basic operating concepts," *Journal of Chemical Education,* vol. 63, no. 7, 1986, doi: 10.1021/ed063p617.
[27] A. R. Johnson and E. E. Carlson, "Collision-Induced Dissociation Mass Spectrometry: A Powerful Tool for Natural Product Structure Elucidation," *Anal Chem,* vol. 87, no. 21, pp. 10668-78, Nov 3 2015, doi: 10.1021/acs.analchem.5b01543.
[28] http://www.massspecpro.com/technology/mass-analyzers/linear-ion-trap-lit (accessed 26.08.2020.
[29] D. J. Douglas, A. J. Frank, and D. Mao, "Linear ion traps in mass spectrometry," *Mass Spectrom Rev,* vol. 24, no. 1, pp. 1-29, Jan-Feb 2005, doi: 10.1002/mas.20004.
[30] I. V. Chernushevich, A. V. Loboda, and B. A. Thomson, "An introduction to quadrupole-time-of-flight mass spectrometry," *J Mass Spectrom,* vol. 36, no. 8, pp. 849-65, Aug 2001, doi: 10.1002/jms.207.
[31] D. W. Koppenaal *et al.*, "MS detectors," *Anal Chem,* vol. 77, no. 21, pp. 418A-427A, Nov 1 2005, doi: 10.1021/ac053495p.
[32] G. L. Andrews, B. L. Simons, J. B. Young, A. M. Hawkridge, and D. C. Muddiman, "Performance characteristics of a new hybrid quadrupole time-of-flight tandem mass spectrometer (TripleTOF 5600)," *Anal Chem,* vol. 83, no. 13, pp. 5442-6, Jul 1 2011, doi: 10.1021/ac200812d.
[33] M. Holcapek, G. Liebisch, and K. Ekroos, "Lipidomic Analysis," *Anal Chem,* vol. 90, no. 7, pp. 4249-4257, Apr 3 2018, doi: 10.1021/acs.analchem.7b05395.
[34] T. Hyotylainen and M. Oresic, "Optimizing the lipidomics workflow for clinical studies--practical considerations," *Anal Bioanal Chem,* vol. 407, no. 17, pp. 4973-93, Jul 2015, doi: 10.1007/s00216-015-8633-2.

[35] M. Wang, C. Wang, R. H. Han, and X. Han, "Novel advances in shotgun lipidomics for biology and medicine," *Prog Lipid Res,* vol. 61, pp. 83-108, Jan 2016, doi: 10.1016/j.plipres.2015.12.002.
[36] M. Lisa, E. Cifkova, M. Khalikova, M. Ovcacikova, and M. Holcapek, "Lipidomic analysis of biological samples: Comparison of liquid chromatography, supercritical fluid chromatography and direct infusion mass spectrometry methods," *J Chromatogr A,* vol. 1525, pp. 96-108, Nov 24 2017, doi: 10.1016/j.chroma.2017.10.022.
[37] A. T. James and A. J. Martin, "Gas-liquid chromatography: the separation and identification of the methyl esters of saturated and unsaturated acids from formic acid to n-octadecanoic acid," *Biochem J,* vol. 63, no. 1, pp. 144-52, May 1956, doi: 10.1042/bj0630144.
[38] L. D. Roberts, G. McCombie, C. M. Titman, and J. L. Griffin, "A matter of fat: an introduction to lipidomic profiling methods," *J Chromatogr B Analyt Technol Biomed Life Sci,* vol. 871, no. 2, pp. 174-81, Aug 15 2008, doi: 10.1016/j.jchromb.2008.04.002.
[39] O. Quehenberger, A. M. Armando, and E. A. Dennis, "High sensitivity quantitative lipidomics analysis of fatty acids in biological samples by gas chromatography-mass spectrometry," *Biochim Biophys Acta,* vol. 1811, no. 11, pp. 648-56, Nov 2011, doi: 10.1016/j.bbalip.2011.07.006.
[40] T. Cajka and O. Fiehn, "Comprehensive analysis of lipids in biological systems by liquid chromatography-mass spectrometry," *Trends Analyt Chem,* vol. 61, pp. 192-206, Oct 1 2014, doi: 10.1016/j.trac.2014.04.017.
[41] P. Wood, *Lipidomics* (Neuromethods). 2017.
[42] G. Paglia, M. Kliman, E. Claude, S. Geromanos, and G. Astarita, "Applications of ion-mobility mass spectrometry for lipid analysis," *Anal Bioanal Chem,* vol. 407, no. 17, pp. 4995-5007, Jul 2015, doi: 10.1007/s00216-015-8664-8.
[43] B. C. Bohrer, S. I. Merenbloom, S. L. Koeniger, A. E. Hilderbrand, and D. E. Clemmer, "Biomolecule analysis by ion mobility spectrometry," *Annu Rev Anal Chem (Palo Alto Calif),* vol. 1, pp. 293-327, 2008, doi: 10.1146/annurev.anchem.1.031207.113001.
[44] M. Lange, Z. Ni, A. Criscuolo, and M. Fedorova, "Liquid Chromatography Techniques in Lipidomics Research," *Chromatographia,* vol. 82, no. 1, pp. 77-100, 2018, doi: 10.1007/s10337-018-3656-4.
[45] J. G. Dorsey and W. T. Cooper, "Retention mechanisms of bonded-phase liquid chromatography," *Anal Chem,* vol. 66, no. 17, pp. 857A-867A, Sep 1 1994, doi: 10.1021/ac00089a002.
[46] T. P. Silverstein, "The Real Reason Why Oil and Water Don't Mix," *Journal of Chemical Education,* vol. 75, no. 1, 1998, doi: 10.1021/ed075p116.
[47] A. Vailaya, "Fundamentals of Reversed Phase Chromatography: Thermodynamic and Exothermodynamic Treatment," *Journal of Liquid Chromatography & Related Technologies,* vol. 28, no. 7-8, pp. 965-1054, 2007, doi: 10.1081/jlc-200052969.
[48] M. Ovcacikova, M. Lisa, E. Cifkova, and M. Holcapek, "Retention behavior of lipids in reversed-phase ultrahigh-performance liquid chromatography-electrospray ionization mass spectrometry," *J Chromatogr A,* vol. 1450, pp. 76-85, Jun 10 2016, doi: 10.1016/j.chroma.2016.04.082.
[49] M. Witting, T. V. Maier, S. Garvis, and P. Schmitt-Kopplin, "Optimizing a ultrahigh pressure liquid chromatography-time of flight-mass spectrometry approach using a novel sub-2mum core-shell particle for in depth lipidomic

profiling of Caenorhabditis elegans," *J Chromatogr A,* vol. 1359, pp. 91-9, Sep 12 2014, doi: 10.1016/j.chroma.2014.07.021.
[50] M. Narvaez-Rivas and Q. Zhang, "Comprehensive untargeted lipidomic analysis using core-shell C30 particle column and high field orbitrap mass spectrometer," *J Chromatogr A,* vol. 1440, pp. 123-134, Apr 1 2016, doi: 10.1016/j.chroma.2016.02.054.
[51] J. Layne, "Characterization and comparison of the chromatographic performance of conventional, polar-embedded, and polar-endcapped reversed-phase liquid chromatography stationary phases," *Journal of Chromatography A,* vol. 957, no. 2, pp. 149-164, 2002, doi: 10.1016/s0021-9673(02)00193-0.
[52] T. Cajka and O. Fiehn, "Increasing lipidomic coverage by selecting optimal mobile-phase modifiers in LC–MS of blood plasma," *Metabolomics,* vol. 12, no. 2, 2016, doi: 10.1007/s11306-015-0929-x.
[53] K. Jurowski, K. Kochan, J. Walczak, M. Barańska, W. Piekoszewski, and B. Buszewski, "Comprehensive review of trends and analytical strategies applied for biological samples preparation and storage in modern medical lipidomics: State of the art," *TrAC Trends in Analytical Chemistry,* vol. 86, pp. 276-289, 2017, doi: 10.1016/j.trac.2016.10.014.
[54] M. Cebo, X. Fu, M. Gawaz, M. Chatterjee, and M. Lammerhofer, "Micro-UHPLC-MS/MS method for analysis of oxylipins in plasma and platelets," *J Pharm Biomed Anal,* vol. 189, p. 113426, Jun 20 2020, doi: 10.1016/j.jpba.2020.113426.
[55] B. Drotleff and M. Lammerhofer, "Guidelines for Selection of Internal Standard-Based Normalization Strategies in Untargeted Lipidomic Profiling by LC-HR-MS/MS," *Anal Chem,* vol. 91, no. 15, pp. 9836-9843, Aug 6 2019, doi: 10.1021/acs.analchem.9b01505.
[56] M. Wang, C. Wang, and X. Han, "Selection of internal standards for accurate quantification of complex lipid species in biological extracts by electrospray ionization mass spectrometry-What, how and why?," *Mass Spectrom Rev,* vol. 36, no. 6, pp. 693-714, Nov 2017, doi: 10.1002/mas.21492.
[57] S. Abreu, A. Solgadi, and P. Chaminade, "Optimization of normal phase chromatographic conditions for lipid analysis and comparison of associated detection techniques," *J Chromatogr A,* vol. 1514, pp. 54-71, Sep 8 2017, doi: 10.1016/j.chroma.2017.07.063.
[58] P. Jiang and C. A. Lucy, "Coupling normal phase liquid chromatography with electrospray ionization mass spectrometry: strategies and applications," *Analytical Methods,* vol. 8, no. 35, pp. 6478-6488, 2016, doi: 10.1039/c6ay01419d.
[59] W. Naidong, "Bioanalytical liquid chromatography tandem mass spectrometry methods on underivatized silica columns with aqueous/organic mobile phases," *J Chromatogr B Analyt Technol Biomed Life Sci,* vol. 796, no. 2, pp. 209-24, Nov 5 2003, doi: 10.1016/j.jchromb.2003.08.026.
[60] B. Buszewski and S. Noga, "Hydrophilic interaction liquid chromatography (HILIC)--a powerful separation technique," *Anal Bioanal Chem,* vol. 402, no. 1, pp. 231-47, Jan 2012, doi: 10.1007/s00216-011-5308-5.
[61] H. P. Nguyen and K. A. Schug, "The advantages of ESI-MS detection in conjunction with HILIC mode separations: Fundamentals and applications," *J Sep Sci,* vol. 31, no. 9, pp. 1465-80, May 2008, doi: 10.1002/jssc.200700630.
[62] A. U. S. J. Kumari, S. R. Acharya, and J. Bergquist, "A novel, fast and sensitive supercritical fluid chromatography-tandem mass spectrometry (SFC-MS/MS)

method for analysis of arachidonic acid metabolites," *Analyst,* vol. 143, no. 15, pp. 3661-3669, Jul 23 2018, doi: 10.1039/c8an00788h.
[63] M. Lisa and M. Holcapek, "UHPSFC/ESI-MS Analysis of Lipids," *Methods Mol Biol,* vol. 1730, pp. 73-82, 2018, doi: 10.1007/978-1-4939-7592-1_5.
[64] L. Laboureur, M. Ollero, and D. Touboul, "Lipidomics by Supercritical Fluid Chromatography," *Int J Mol Sci,* vol. 16, no. 6, pp. 13868-84, Jun 17 2015, doi: 10.3390/ijms160613868.
[65] J. Teixeira, M. E. Tiritan, M. M. M. Pinto, and C. Fernandes, "Chiral Stationary Phases for Liquid Chromatography: Recent Developments," *Molecules,* vol. 24, no. 5, Feb 28 2019, doi: 10.3390/molecules24050865.
[66] F. Ianni, G. Saluti, R. Galarini, S. Fiorito, R. Sardella, and B. Natalini, "Enantioselective high-performance liquid chromatography analysis of oxygenated polyunsaturated fatty acids," *Free Radical Biology and Medicine,* vol. 144, no. January, pp. 35-54, 2019 2019, doi: 10.1016/j.freeradbiomed.2019.04.038.
[67] P. Montuschi, P. J. Barnes, and L. J. Roberts, "Isoprostanes: Markers and mediators of oxidative stress," *FASEB Journal,* vol. 18, no. 15, pp. 1791-1800, 2004 2004, doi: 10.1096/fj.04-2330rev.
[68] A. Czajkowska-Myslek, U. Siekierko, and M. Gajewska, "Application of Silver Ion High-Performance Liquid Chromatography for Quantitative Analysis of Selected n-3 and n-6 PUFA in Oil Supplements," *Lipids,* vol. 51, no. 4, pp. 413-21, Apr 2016, doi: 10.1007/s11745-016-4133-1.
[69] M. Lisa, H. Velinska, and M. Holcapek, "Regioisomeric characterization of triacylglycerols using silver-ion HPLC/MS and randomization synthesis of standards," *Anal Chem,* vol. 81, no. 10, pp. 3903-10, May 15 2009, doi: 10.1021/ac900150j.
[70] B. Nikolova-Damyanova, "Retention of lipids in silver ion high-performance liquid chromatography: facts and assumptions," *J Chromatogr A,* vol. 1216, no. 10, pp. 1815-24, Mar 6 2009, doi: 10.1016/j.chroma.2008.10.097.
[71] R. H. Perry, R. G. Cooks, and R. J. Noll, "Orbitrap mass spectrometry: instrumentation, ion motion and applications," *Mass Spectrom Rev,* vol. 27, no. 6, pp. 661-99, Nov-Dec 2008, doi: 10.1002/mas.20186.
[72] I. V. Chernushevich, "Duty cycle improvement for a quadrupole-time-of-flight mass spectrometer and its use for precursor ion scans," (in English), *Eur J Mass Spectrom,* vol. 6, no. 6, pp. 471-479, 2000, doi: DOI 10.1255/ejms.377.
[73] J. H. Gross, *Mass Spectrometry*. 2017.
[74] S. Zhou, Q. Song, Y. Tang, and W. Naidong, "Critical Review of Development, Validation, and Transfer for High Throughput Bioanalytical LC-MS/MS Methods," *Current Pharmaceutical Analysis,* vol. 1, no. 1, pp. 3-14, 2005, doi: 10.2174/1573412052953346.
[75] B. Drotleff, M. Hallschmid, and M. Lammerhofer, "Quantification of steroid hormones in plasma using a surrogate calibrant approach and UHPLC-ESI-QTOF-MS/MS with SWATH-acquisition combined with untargeted profiling," *Anal Chim Acta,* vol. 1022, pp. 70-80, Aug 31 2018, doi: 10.1016/j.aca.2018.03.040.
[76] Y. Fillatre, D. Rondeau, A. Jadas-Hecart, and P. Y. Communal, "Advantages of the scheduled selected reaction monitoring algorithm in liquid chromatography/electrospray ionization tandem mass spectrometry multi-residue analysis of 242 pesticides: a comparative approach with classical selected reaction

monitoring mode," *Rapid Commun Mass Spectrom,* vol. 24, no. 16, pp. 2453-61, Aug 30 2010, doi: 10.1002/rcm.4649.
[77] B. Peng *et al.*, "Identification of key lipids critical for platelet activation by comprehensive analysis of the platelet lipidome," *Blood,* vol. 132, no. 5, pp. e1-e12, Aug 2 2018, doi: 10.1182/blood-2017-12-822890.
[78] B. Drotleff, J. Illison, J. Schlotterbeck, R. Lukowski, and M. Lammerhofer, "Comprehensive lipidomics of mouse plasma using class-specific surrogate calibrants and SWATH acquisition for large-scale lipid quantification in untargeted analysis," *Anal Chim Acta,* vol. 1086, pp. 90-102, Dec 4 2019, doi: 10.1016/j.aca.2019.08.030.
[79] J. Rubert, M. Zachariasova, and J. Hajslova, "Advances in high-resolution mass spectrometry based on metabolomics studies for food--a review," *Food Addit Contam Part A Chem Anal Control Expo Risk Assess,* vol. 32, no. 10, pp. 1685-708, 2015, doi: 10.1080/19440049.2015.1084539.
[80] X. Zhu, Y. Chen, and R. Subramanian, "Comparison of information-dependent acquisition, SWATH, and MS(All) techniques in metabolite identification study employing ultrahigh-performance liquid chromatography-quadrupole time-of-flight mass spectrometry," *Anal Chem,* vol. 86, no. 2, pp. 1202-9, Jan 21 2014, doi: 10.1021/ac403385y.
[81] F. Koopmans, J. T. C. Ho, A. B. Smit, and K. W. Li, "Comparative Analyses of Data Independent Acquisition Mass Spectrometric Approaches: DIA, WiSIM-DIA, and Untargeted DIA," *Proteomics,* vol. 18, no. 1, Jan 2018, doi: 10.1002/pmic.201700304.
[82] R. S. Plumb *et al.*, "UPLC/MS(E); a new approach for generating molecular fragment information for biomarker structure elucidation," *Rapid Commun Mass Spectrom,* vol. 20, no. 13, pp. 1989-94, 2006, doi: 10.1002/rcm.2550.
[83] G. Hopfgartner, D. Tonoli, and E. Varesio, "High-resolution mass spectrometry for integrated qualitative and quantitative analysis of pharmaceuticals in biological matrices," *Anal Bioanal Chem,* vol. 402, no. 8, pp. 2587-96, Mar 2012, doi: 10.1007/s00216-011-5641-8.
[84] B. Simons, D. Kauhanen, T. Sylvanne, K. Tarasov, E. Duchoslav, and K. Ekroos, "Shotgun Lipidomics by Sequential Precursor Ion Fragmentation on a Hybrid Quadrupole Time-of-Flight Mass Spectrometer," *Metabolites,* vol. 2, no. 1, pp. 195-213, Feb 20 2012, doi: 10.3390/metabo2010195.
[85] M. Cebo, J. Schlotterbeck, M. Gawaz, M. Chatterjee, and M. Lämmerhofer, "Simultaneous targeted and untargeted UHPLC-ESI-MS/MS method with data-independent acquisition for quantification and profiling of (oxidized) fatty acids released upon platelet activation by thrombin," *Analytica Chimica Acta,* vol. 1094, pp. 57-69, 2020/01 2020, doi: 10.1016/j.aca.2019.10.005.
[86] J. Schlotterbeck, M. Chatterjee, M. Gawaz, and M. Lammerhofer, "Comprehensive MS/MS profiling by UHPLC-ESI-QTOF-MS/MS using SWATH data-independent acquisition for the study of platelet lipidomes in coronary artery disease," *Anal Chim Acta,* vol. 1046, pp. 1-15, Jan 10 2019, doi: 10.1016/j.aca.2018.08.060.
[87] G. Xu, J. Stupak, L. Yang, L. Hu, B. Guo, and J. Li, "Deconvolution in mass spectrometry based proteomics," *Rapid Commun Mass Spectrom,* vol. 32, no. 10, pp. 763-774, May 30 2018, doi: 10.1002/rcm.8103.
[88] J. Zhou, C. Liu, D. Si, B. Jia, L. Zhong, and Y. Yin, "Workflow development for targeted lipidomic quantification using parallel reaction monitoring on a

quadrupole-time of flight mass spectrometry," *Anal Chim Acta,* vol. 972, pp. 62-72, Jun 15 2017, doi: 10.1016/j.aca.2017.04.008.
[89] J. Neumüller, A. Ellinger, and T. Wagner, "Transmission Electron Microscopy of Platelets FROM Apheresis and Buffy-Coat-Derived Platelet Concentrates," in *The Transmission Electron Microscope - Theory and Applications,* 2015, ch. Chapter 11.
[90] J. L. Fitch-Tewfik and R. Flaumenhaft, "Platelet granule exocytosis: a comparison with chromaffin cells," *Front Endocrinol (Lausanne),* vol. 4, p. 77, 2013, doi: 10.3389/fendo.2013.00077.
[91] K. Broos, D. S. F. Meyer, H. B. Feys, K. Vanhoorelbeke, and H. Deckmyn, "Blood platelet biochemistry," *Thrombosis Research,* vol. 129, no. 3, pp. 245-249, 2012 2012, doi: 10.1016/j.thromres.2011.11.002.
[92] S. G. Thomas, "The Structure of Resting and Activated Platelets," in *Platelets*, 2019, pp. 47-77.
[93] A. T. Nurden, "Platelets, inflammation and tissue regeneration," *Thromb Haemost,* vol. 105 Suppl 1, pp. S13-33, May 2011, doi: 10.1160/THS10-11-0720.
[94] R. E. Rumbaut and P. Thiagarajan, *Platelet-Vessel Wall Interactions in Hemostasis and Thrombosis*. Morgan & Claypool Life Sciences, 2010.
[95] A. A. Ponomareva, T. A. Nevzorova, E. R. Mordakhanova, I. A. Andrianova, and R. I. Litvinov, "Structural characterization of platelets and platelet microvesicles," *Cell and Tissue Biology,* vol. 10, no. 3, pp. 217-226, 2016, doi: 10.1134/s1990519x1603010x.
[96] M. V. Selvadurai and J. R. Hamilton, "Structure and function of the open canalicular system - the platelet's specialized internal membrane network," *Platelets,* vol. 29, no. 4, pp. 319-325, Jun 2018, doi: 10.1080/09537104.2018.1431388.
[97] K. Jurk and B. E. Kehrel, "Platelets: physiology and biochemistry," *Semin Thromb Hemost,* vol. 31, no. 4, pp. 381-92, 2005, doi: 10.1055/s-2005-916671.
[98] T. Hla, S. Galvani, S. Rafii, and R. Nachman, "S1P and the birth of platelets," *J Exp Med,* vol. 209, no. 12, pp. 2137-40, Nov 19 2012, doi: 10.1084/jem.20122284.
[99] R. H. Aster, "Pooling of platelets in the spleen: role in the pathogenesis of "hypersplenic" thrombocytopenia," *J Clin Invest,* vol. 45, no. 5, pp. 645-57, May 1966, doi: 10.1172/JCI105380.
[100] C. A. Finch, L. A. Harker, and J. D. Cook, "Kinetics of the formed elements of human blood," *Blood,* vol. 50, no. 4, pp. 699-707, 1977, doi: 10.1182/blood.V50.4.699.699.
[101] M. Lebois and E. C. Josefsson, "Regulation of platelet lifespan by apoptosis," *Platelets,* vol. 27, no. 6, pp. 497-504, Sep 2016, doi: 10.3109/09537104.2016.1161739.
[102] R. J. Davey and J. P. AuBuchon, "Post-Transfusion Red Blood Cell and Platelet Survival and Kinetics: Basic Principles and Practical Aspects," in *Blood Banking and Transfusion Medicine,* 2007, pp. 455-466.
[103] C. Weber, "Platelets and chemokines in atherosclerosis: partners in crime," *Circ Res,* vol. 96, no. 6, pp. 612-6, Apr 1 2005, doi: 10.1161/01.RES.0000160077.17427.57.
[104] M. Chatterjee, D. Rath, and M. Gawaz, "Role of chemokine receptors CXCR4 and CXCR7 for platelet function," *Biochem Soc Trans,* vol. 43, no. 4, pp. 720-6, Aug 2015, doi: 10.1042/BST20150113.

[105] C. Wang, W. Chen, and J. Shen, "CXCR7 Targeting and Its Major Disease Relevance," *Front Pharmacol*, vol. 9, p. 641, 2018, doi: 10.3389/fphar.2018.00641.
[106] V. B. O'Donnell, R. C. Murphy, and S. P. Watson, "Platelet lipidomics: modern day perspective on lipid discovery and characterization in platelets," *Circ Res*, vol. 114, no. 7, pp. 1185-203, Mar 28 2014, doi: 10.1161/CIRCRESAHA.114.301597.
[107] M. Masoodi, M. Eiden, A. Koulman, D. Spaner, and D. A. Volmer, "Comprehensive lipidomics analysis of bioactive lipids in complex regulatory networks," *Anal Chem*, vol. 82, no. 19, pp. 8176-85, Oct 1 2010, doi: 10.1021/ac1015563.
[108] A. M. Wolfer, M. Gaudin, S. D. Taylor-Robinson, E. Holmes, and J. K. Nicholson, "Development and Validation of a High-Throughput Ultrahigh-Performance Liquid Chromatography-Mass Spectrometry Approach for Screening of Oxylipins and Their Precursors," *Anal Chem*, vol. 87, no. 23, pp. 11721-31, Dec 1 2015, doi: 10.1021/acs.analchem.5b02794.
[109] M. T. Duvernay, A. Matafonov, C. W. Lindsley, and H. E. Hamm, "Platelet Lipidomic Profiling: Novel Insight into Cytosolic Phospholipase A2alpha Activity and Its Role in Human Platelet Activation," *Biochemistry*, vol. 54, no. 36, pp. 5578-88, Sep 15 2015, doi: 10.1021/acs.biochem.5b00549.
[110] A. Derksen and P. Cohen, "Patterns of fatty acid release from endogenous substrates by human platelet homogenates and membranes," *J Biol Chem*, vol. 250, no. 24, pp. 9342-7, Dec 25 1975. [Online]. Available: https://www.ncbi.nlm.nih.gov/pubmed/394.
[111] T. K. Bills, J. B. Smith, and M. J. Silver, "Selective release of archidonic acid from the phospholipids of human platelets in response to thrombin," *J Clin Invest*, vol. 60, no. 1, pp. 1-6, Jul 1977, doi: 10.1172/JCI108745.
[112] S. Rittenhouse-Simmons and D. Deykin, "The mobilization of arachidonic acid in platelets exposed to thrombin or ionophore A23187. Effects of adenosine triphosphate deprivation," *J Clin Invest*, vol. 60, no. 2, pp. 495-8, Aug 1977, doi: 10.1172/JCI108801.
[113] J. F. Meal, "Polyunsaturated Fatty acids," *Science*, vol. 188, no. 4194, pp. 1225-6, Jun 20 1975, doi: 10.1126/science.188.4194.1225.
[114] T. Okuno, Y. Iizuka, H. Okazaki, T. Yokomizo, R. Taguchi, and T. Shimizu, "12(S)-Hydroxyheptadeca-5Z, 8E, 10E-trienoic acid is a natural ligand for leukotriene B4 receptor 2," *J Exp Med*, vol. 205, no. 4, pp. 759-66, Apr 14 2008, doi: 10.1084/jem.20072329.
[115] A. P. Agins, M. J. Thomas, C. G. Edmonds, and J. A. McCloskey, "Identification of 12-keto-5,8,10-heptadecatrienoic acid as an arachidonic acid metabolite produced by human HL-60 leukemia cells," *Biochemical Pharmacology*, vol. 36, no. 11, pp. 1799-1805, 1987, doi: 10.1016/0006-2952(87)90241-3.
[116] J. M. Roodhart *et al.*, "Mesenchymal stem cells induce resistance to chemotherapy through the release of platinum-induced fatty acids," *Cancer Cell*, vol. 20, no. 3, pp. 370-83, Sep 13 2011, doi: 10.1016/j.ccr.2011.08.010.
[117] D. A. Slatter *et al.*, "Mapping the Human Platelet Lipidome Reveals Cytosolic Phospholipase A2 as a Regulator of Mitochondrial Bioenergetics during Activation," *Cell Metab*, vol. 23, no. 5, pp. 930-44, May 10 2016, doi: 10.1016/j.cmet.2016.04.001.

[118] M. Chatterjee *et al.*, "Regulation of oxidized platelet lipidome: implications for coronary artery disease," *Eur Heart J*, vol. 38, no. 25, pp. 1993-2005, Jul 1 2017, doi: 10.1093/eurheartj/ehx146.
[119] S. Valkonen *et al.*, "Lipid mediators in platelet concentrate and extracellular vesicles: Molecular mechanisms from membrane glycerophospholipids to bioactive molecules," *Biochim Biophys Acta Mol Cell Biol Lipids*, vol. 1864, no. 8, pp. 1168-1182, Aug 2019, doi: 10.1016/j.bbalip.2019.03.011.
[120] U. Hofmann, S. Seefried, C. O. Meese, T. Mettang, E. Hübel, and U. Kuhlmann, "Measurement of 12(S)-hydroxy-5Z,8E,10E-heptadecatrienoic acid and its metabolite 12-oxo-5Z,8E,10E-heptadecatrienoic acid in human plasma by gas chromatography/negative ion chemical ionization mass spectrometry," *Analytical Biochemistry*, vol. 189, no. 2, pp. 244-248, 1990, doi: 10.1016/0003-2697(90)90115-p.
[121] T. Sanaki *et al.*, "A hybrid strategy using global analysis of oxidized fatty acids and bioconversion by Bacillus circulans," *Rapid Commun Mass Spectrom*, vol. 30, no. 6, pp. 751-62, Mar 30 2016, doi: 10.1002/rcm.7504.
[122] Y. Huang *et al.*, "Serum metabolomics study and eicosanoid analysis of childhood atopic dermatitis based on liquid chromatography-mass spectrometry," *J Proteome Res*, vol. 13, no. 12, pp. 5715-23, Dec 5 2014, doi: 10.1021/pr5007069.
[123] M. Chocholouskova, R. Jirasko, D. Vrana, J. Gatek, B. Melichar, and M. Holcapek, "Reversed phase UHPLC/ESI-MS determination of oxylipins in human plasma: a case study of female breast cancer," *Anal Bioanal Chem*, vol. 411, no. 6, pp. 1239-1251, Feb 2019, doi: 10.1007/s00216-018-1556-y.
[124] L. Kortz, J. Dorow, and U. Ceglarek, "Liquid chromatography-tandem mass spectrometry for the analysis of eicosanoids and related lipids in human biological matrices: a review," *J Chromatogr B Analyt Technol Biomed Life Sci*, vol. 964, pp. 1-11, Aug 1 2014, doi: 10.1016/j.jchromb.2014.01.046.
[125] X. Han and R. W. Gross, "Shotgun lipidomics: electrospray ionization mass spectrometric analysis and quantitation of cellular lipidomes directly from crude extracts of biological samples," *Mass Spectrom Rev*, vol. 24, no. 3, pp. 367-412, May-Jun 2005, doi: 10.1002/mas.20023.
[126] B. Peng *et al.*, "A Comprehensive High-Resolution Targeted Workflow for the Deep Profiling of Sphingolipids," *Anal Chem*, vol. 89, no. 22, pp. 12480-12487, Nov 21 2017, doi: 10.1021/acs.analchem.7b03576.
[127] A. Triebl, M. Trotzmuller, J. Hartler, T. Stojakovic, and H. C. Kofeler, "Lipidomics by ultrahigh performance liquid chromatography-high resolution mass spectrometry and its application to complex biological samples," *J Chromatogr B Analyt Technol Biomed Life Sci*, vol. 1053, pp. 72-80, May 15 2017, doi: 10.1016/j.jchromb.2017.03.027.
[128] E. Rampler *et al.*, "A Novel Lipidomics Workflow for Improved Human Plasma Identification and Quantification Using RPLC-MSn Methods and Isotope Dilution Strategies," *Anal Chem*, vol. 90, no. 11, pp. 6494-6501, Jun 5 2018, doi: 10.1021/acs.analchem.7b05382.
[129] G. La Barbera *et al.*, "Delving into the Polar Lipidome by Optimized Chromatographic Separation, High-Resolution Mass Spectrometry, and Comprehensive Identification with Lipostar: Microalgae as Case Study," *Anal Chem*, vol. 90, no. 20, pp. 12230-12238, Oct 16 2018, doi: 10.1021/acs.analchem.8b03482.

[130] R. Bonner and G. Hopfgartner, "SWATH data independent acquisition mass spectrometry for metabolomics," *TrAC Trends in Analytical Chemistry,* vol. 120, 2019, doi: 10.1016/j.trac.2018.10.014.
[131] H. Tsugawa *et al.*, "MS-DIAL: data-independent MS/MS deconvolution for comprehensive metabolome analysis," *Nat Methods,* vol. 12, no. 6, pp. 523-6, Jun 2015, doi: 10.1038/nmeth.3393.
[132] J. Schlotterbeck, A. Kolb, and M. Lammerhofer, "Free fatty acid profiling in marine algae extract by LC-MS/MS and isolation as well as quantification of the omega-3 fatty acid hexadeca-4,7,10,13-tetraenoic acid," *J Sep Sci,* vol. 41, no. 23, pp. 4286-4295, Dec 2018, doi: 10.1002/jssc.201800780.
[133] J. Schlotterbeck, M. Cebo, A. Kolb, and M. Lammerhofer, "Quantitative analysis of chemoresistance-inducing fatty acid in food supplements using UHPLC-ESI-MS/MS," *Anal Bioanal Chem,* vol. 411, no. 2, pp. 479-491, Jan 2019, doi: 10.1007/s00216-018-1468-x.
[134] D. B. Dess and J. C. Martin, "A useful 12-I-5 triacetoxyperiodinane (the Dess-Martin periodinane) for the selective oxidation of primary or secondary alcohols and a variety of related 12-I-5 species," *Journal of the American Chemical Society,* vol. 113, no. 19, pp. 7277-7287, 1991, doi: 10.1021/ja00019a027.
[135] O. Borst *et al.*, "The inflammatory chemokine CXC motif ligand 16 triggers platelet activation and adhesion via CXC motif receptor 6-dependent phosphatidylinositide 3-kinase/Akt signaling," *Circ Res,* vol. 111, no. 10, pp. 1297-307, Oct 26 2012, doi: 10.1161/CIRCRESAHA.112.276444.
[136] V. Matyash, G. Liebisch, T. V. Kurzchalia, A. Shevchenko, and D. Schwudke, "Lipid extraction by methyl-tert-butyl ether for high-throughput lipidomics," *J Lipid Res,* vol. 49, no. 5, pp. 1137-46, May 2008, doi: 10.1194/jlr.D700041-JLR200.
[137] B. K. Matuszewski, M. L. Constanzer, and C. M. Chavez-Eng, "Strategies for the assessment of matrix effect in quantitative bioanalytical methods based on HPLC-MS/MS," *Anal Chem,* vol. 75, no. 13, pp. 3019-30, Jul 1 2003, doi: 10.1021/ac020361s.
[138] http://www.ich.org/fileadmin/Public_Web_Site/ICH_Products/Guidelines/Quality/Q2_R1/Step4/Q2_R1__Guideline.pdf (accessed 01.09.2019.
[139] C. Calderon, C. Sanwald, J. Schlotterbeck, B. Drotleff, and M. Lammerhofer, "Comparison of simple monophasic versus classical biphasic extraction protocols for comprehensive UHPLC-MS/MS lipidomic analysis of Hela cells," *Anal Chim Acta,* vol. 1048, pp. 66-74, Feb 7 2019, doi: 10.1016/j.aca.2018.10.035.
[140] J. G. Bollinger *et al.*, "Improved sensitivity mass spectrometric detection of eicosanoids by charge reversal derivatization," *Anal Chem,* vol. 82, no. 16, pp. 6790-6, Aug 15 2010, doi: 10.1021/ac100720p.
[141] T. Kind, K. H. Liu, D. Y. Lee, B. DeFelice, J. K. Meissen, and O. Fiehn, "LipidBlast in silico tandem mass spectrometry database for lipid identification," *Nat Methods,* vol. 10, no. 8, pp. 755-8, Aug 2013, doi: 10.1038/nmeth.2551.
[142] A. P. Bye, A. J. Unsworth, and J. M. Gibbins, "Platelet signaling: a complex interplay between inhibitory and activatory networks," *J Thromb Haemost,* vol. 14, no. 5, pp. 918-30, May 2016, doi: 10.1111/jth.13302.
[143] F. Sekiya *et al.*, "12S-Hydroxyeicosatetraenoic acid plays a central role in the regulation of platelet activation," *Biochemical and Biophysical Research Communications,* vol. 179, no. 1, pp. 345-351, 1991, doi: 10.1016/0006-291x(91)91376-n.

[144] D. A. Slatter *et al.*, "Enzymatically oxidized phospholipids restore thrombin generation in coagulation factor deficiencies," *JCI Insight,* vol. 3, no. 6, Mar 22 2018, doi: 10.1172/jci.insight.98459.
[145] S. N. Lauder *et al.*, "Networks of enzymatically oxidized membrane lipids support calcium-dependent coagulation factor binding to maintain hemostasis," *Sci Signal,* vol. 10, no. 507, Nov 28 2017, doi: 10.1126/scisignal.aan2787.
[146] H. M. and U. V., "12(S)-Hydroxy-5,8,10 (Z,E,E)-heptadecatrienoic acid (HHT) is preferentially metabolized to its 12-keto derivative by human erythrocytes in vitro.," *Eicosanoids.,* vol. 1, no. 1, pp. 19-25, 1988.
[147] K. Strassburg *et al.*, "Quantitative profiling of oxylipins through comprehensive LC-MS/MS analysis: application in cardiac surgery," *Anal Bioanal Chem,* vol. 404, no. 5, pp. 1413-26, Sep 2012, doi: 10.1007/s00216-012-6226-x.
[148] C. Gladine, A. I. Ostermann, J. W. Newman, and N. H. Schebb, "MS-based targeted metabolomics of eicosanoids and other oxylipins: Analytical and inter-individual variabilities," *Free Radic Biol Med,* vol. 144, pp. 72-89, Nov 20 2019, doi: 10.1016/j.freeradbiomed.2019.05.012.
[149] H. S. Jonasdottir, H. Brouwers, R. E. M. Toes, A. Ioan-Facsinay, and M. Giera, "Effects of anticoagulants and storage conditions on clinical oxylipid levels in human plasma," *Biochim Biophys Acta Mol Cell Biol Lipids,* vol. 1863, no. 12, pp. 1511-1522, Dec 2018, doi: 10.1016/j.bbalip.2018.10.003.
[150] N. M. Hartung, M. Mainka, N. Kampschulte, A. I. Ostermann, and N. H. Schebb, "A strategy for validating concentrations of oxylipin standards for external calibration," *Prostaglandins Other Lipid Mediat,* vol. 141, pp. 22-24, Apr 2019, doi: 10.1016/j.prostaglandins.2019.02.006.
[151] D. Tsikas and A. A. Zoerner, "Analysis of eicosanoids by LC-MS/MS and GC-MS/MS: a historical retrospect and a discussion," *J Chromatogr B Analyt Technol Biomed Life Sci,* vol. 964, pp. 79-88, Aug 1 2014, doi: 10.1016/j.jchromb.2014.03.017.
[152] P. Le Faouder *et al.*, "LC-MS/MS method for rapid and concomitant quantification of pro-inflammatory and pro-resolving polyunsaturated fatty acid metabolites," *J Chromatogr B Analyt Technol Biomed Life Sci,* vol. 932, pp. 123-33, Aug 1 2013, doi: 10.1016/j.jchromb.2013.06.014.
[153] J. T. English, P. C. Norris, R. R. Hodges, D. A. Dartt, and C. N. Serhan, "Identification and Profiling of Specialized Pro-Resolving Mediators in Human Tears by Lipid Mediator Metabolomics," *Prostaglandins Leukot Essent Fatty Acids,* vol. 117, pp. 17-27, Feb 2017, doi: 10.1016/j.plefa.2017.01.004.
[154] A. I. Ostermann *et al.*, "Intra-individual variance of the human plasma oxylipin pattern: low inter-day variability in fasting blood samples versus high variability during the day," *Analytical Methods,* vol. 10, no. 40, pp. 4935-4944, 2018, doi: 10.1039/c8ay01753k.
[155] K. M. Rund *et al.*, "Development of an LC-ESI(-)-MS/MS method for the simultaneous quantification of 35 isoprostanes and isofurans derived from the major n3- and n6-PUFAs," *Anal Chim Acta,* vol. 1037, pp. 63-74, Dec 11 2018, doi: 10.1016/j.aca.2017.11.002.
[156] R. A. Colas, M. Shinohara, J. Dalli, N. Chiang, and C. N. Serhan, "Identification and signature profiles for pro-resolving and inflammatory lipid mediators in human tissue," *Am J Physiol Cell Physiol,* vol. 307, no. 1, pp. C39-54, Jul 1 2014, doi: 10.1152/ajpcell.00024.2014.

[157] L. Kutzner *et al.*, "Development of an Optimized LC-MS Method for the Detection of Specialized Pro-Resolving Mediators in Biological Samples," *Front Pharmacol,* vol. 10, p. 169, 2019, doi: 10.3389/fphar.2019.00169.
[158] M. Cebo, J. Schlotterbeck, M. Gawaz, M. Chatterjee, and M. Lammerhofer, "Simultaneous targeted and untargeted UHPLC-ESI-MS/MS method with data-independent acquisition for quantification and profiling of (oxidized) fatty acids released upon platelet activation by thrombin," *Anal Chim Acta,* vol. 1094, pp. 57-69, Jan 15 2020, doi: 10.1016/j.aca.2019.10.005.
[159] R. Berkecz, M. Lisa, and M. Holcapek, "Analysis of oxylipins in human plasma: Comparison of ultrahigh-performance liquid chromatography and ultrahigh-performance supercritical fluid chromatography coupled to mass spectrometry," *J Chromatogr A,* vol. 1511, pp. 107-121, Aug 18 2017, doi: 10.1016/j.chroma.2017.06.070.
[160] C. Hinz *et al.*, "A Comprehensive UHPLC Ion Mobility Quadrupole Time-of-Flight Method for Profiling and Quantification of Eicosanoids, Other Oxylipins, and Fatty Acids," *Anal Chem,* vol. 91, no. 13, pp. 8025-8035, Jul 2 2019, doi: 10.1021/acs.analchem.8b04615.
[161] M. Cebo, X. Fu, M. Gawaz, M. Chatterjee, and M. Lammerhofer, "Enantioselective ultra-high performance liquid chromatography-tandem mass spectrometry method based on sub-2microm particle polysaccharide column for chiral separation of oxylipins and its application for the analysis of autoxidized fatty acids and platelet releasates," *J Chromatogr A,* vol. 1624, p. 461206, Aug 2 2020, doi: 10.1016/j.chroma.2020.461206.
[162] F. Ianni, G. Saluti, R. Galarini, S. Fiorito, R. Sardella, and B. Natalini, "Enantioselective high-performance liquid chromatography analysis of oxygenated polyunsaturated fatty acids," *Free Radic Biol Med,* vol. 144, pp. 35-54, Nov 20 2019, doi: 10.1016/j.freeradbiomed.2019.04.038.
[163] A. I. Ostermann, I. Willenberg, and N. H. Schebb, "Comparison of sample preparation methods for the quantitative analysis of eicosanoids and other oxylipins in plasma by means of LC-MS/MS," *Anal Bioanal Chem,* vol. 407, no. 5, pp. 1403-14, Feb 2015, doi: 10.1007/s00216-014-8377-4.
[164] https://www.fda.gov/ (accessed 01.07.2020.
[165] A.-L. Hauswaldt *et al.*, "Uncertainty of standard addition experiments: a novel approach to include the uncertainty associated with the standard in the model equation," *Accreditation and Quality Assurance,* vol. 17, no. 2, pp. 129-138, 2011, doi: 10.1007/s00769-011-0827-5.
[166] G. Y. Chen and Q. Zhang, "Comprehensive analysis of oxylipins in human plasma using reversed-phase liquid chromatography-triple quadrupole mass spectrometry with heatmap-assisted selection of transitions," *Anal Bioanal Chem,* vol. 411, no. 2, pp. 367-385, Jan 2019, doi: 10.1007/s00216-018-1446-3.
[167] C. N. Serhan, P. A. Ward, D. W. Gilroy, and S. S. Ayoub, *Fundamentals of Inflammation*. 2010.
[168] K. Broos, S. F. De Meyer, H. B. Feys, K. Vanhoorelbeke, and H. Deckmyn, "Blood platelet biochemistry," *Thromb Res,* vol. 129, no. 3, pp. 245-9, Mar 2012, doi: 10.1016/j.thromres.2011.11.002.
[169] J. D. Morrow, T. M. Harris, and L. Jackson Roberts, "Noncyclooxygenase oxidative formation of a series of novel prostaglandins: Analytical ramifications for measurement of eicosanoids," *Analytical Biochemistry,* vol. 184, no. 1, pp. 1-10, 1990, doi: 10.1016/0003-2697(90)90002-q.

[170] P. Montuschi, P. J. Barnes, and L. J. Roberts, 2nd, "Isoprostanes: markers and mediators of oxidative stress," *FASEB J,* vol. 18, no. 15, pp. 1791-800, Dec 2004, doi: 10.1096/fj.04-2330rev.
[171] M. Lammerhofer, "Chiral recognition by enantioselective liquid chromatography: mechanisms and modern chiral stationary phases," *J Chromatogr A,* vol. 1217, no. 6, pp. 814-56, Feb 5 2010, doi: 10.1016/j.chroma.2009.10.022.
[172] F. Ianni *et al.*, "Direct enantioseparation of underivatized aliphatic 3-hydroxyalkanoic acids with a quinine-based zwitterionic chiral stationary phase," *J Chromatogr A,* vol. 1363, pp. 101-8, Oct 10 2014, doi: 10.1016/j.chroma.2014.03.060.
[173] C. Calderon, C. Santi, and M. Lammerhofer, "Chiral separation of disease biomarkers with 2-hydroxycarboxylic acid structure," *J Sep Sci,* vol. 41, no. 6, pp. 1224-1231, Mar 2018, doi: 10.1002/jssc.201701243.
[174] C. Calderon and M. Lammerhofer, "Chiral separation of short chain aliphatic hydroxycarboxylic acids on cinchonan carbamate-based weak chiral anion exchangers and zwitterionic chiral ion exchangers," *J Chromatogr A,* vol. 1487, pp. 194-200, Mar 3 2017, doi: 10.1016/j.chroma.2017.01.060.
[175] D. Norton, B. Crow, M. Bishop, K. Kovalcik, J. George, and J. A. Bralley, "High performance liquid chromatography-tandem mass spectrometry (HPLC/MS/MS) assay for chiral separation of lactic acid enantiomers in urine using a teicoplanin based stationary phase," *J Chromatogr B Analyt Technol Biomed Life Sci,* vol. 850, no. 1-2, pp. 190-8, May 1 2007, doi: 10.1016/j.jchromb.2006.11.020.
[176] T. Ikai and Y. Okamoto, "Structure control of polysaccharide derivatives for efficient separation of enantiomers by chromatography," *Chem Rev,* vol. 109, no. 11, pp. 6077-101, Nov 2009, doi: 10.1021/cr8005558.
[177] B. Chankvetadze, "Recent developments on polysaccharide-based chiral stationary phases for liquid-phase separation of enantiomers," *J Chromatogr A,* vol. 1269, pp. 26-51, Dec 21 2012, doi: 10.1016/j.chroma.2012.10.033.
[178] U. Garscha, T. Nilsson, and E. H. Oliw, "Enantiomeric separation and analysis of unsaturated hydroperoxy fatty acids by chiral column chromatography-mass spectrometry," *J Chromatogr B Analyt Technol Biomed Life Sci,* vol. 872, no. 1-2, pp. 90-8, Sep 1 2008, doi: 10.1016/j.jchromb.2008.07.013.
[179] M. Blum, I. Dogan, M. Karber, M. Rothe, and W. H. Schunck, "Chiral lipidomics of monoepoxy and monohydroxy metabolites derived from long-chain polyunsaturated fatty acids," *J Lipid Res,* vol. 60, no. 1, pp. 135-148, Jan 2019, doi: 10.1194/jlr.M089755.
[180] M. Bayer, A. Mosandl, and D. Thaci, "Improved enantioselective analysis of polyunsaturated hydroxy fatty acids in psoriatic skin scales using high-performance liquid chromatography," *J Chromatogr B Analyt Technol Biomed Life Sci,* vol. 819, no. 2, pp. 323-8, May 25 2005, doi: 10.1016/j.jchromb.2005.02.008.
[181] C. Schneider, Z. Yu, W. E. Boeglin, Y. Zheng, and A. R. Brash, "Enantiomeric separation of hydroxy and hydroperoxy eicosanoids by chiral column chromatography," *Methods Enzymol,* vol. 433, pp. 145-57, 2007, doi: 10.1016/S0076-6879(07)33008-5.
[182] S. H. Lee, M. V. Williams, and I. A. Blair, "Targeted chiral lipidomics analysis," *Prostaglandins Other Lipid Mediat,* vol. 77, no. 1-4, pp. 141-57, Sep 2005, doi: 10.1016/j.prostaglandins.2004.01.009.
[183] C. Mesaros, S. H. Lee, and I. A. Blair, "Targeted quantitative analysis of eicosanoid lipids in biological samples using liquid chromatography-tandem mass

spectrometry," *J Chromatogr B Analyt Technol Biomed Life Sci,* vol. 877, no. 26, pp. 2736-45, Sep 15 2009, doi: 10.1016/j.jchromb.2009.03.011.
[184] R. Sardella, F. Ianni, A. Lisanti, M. Marinozzi, S. Scorzoni, and B. Natalini, "The effect of mobile phase composition in the enantioseparation of pharmaceutically relevant compounds with polysaccharide-based stationary phases," *Biomed Chromatogr,* vol. 28, no. 1, pp. 159-67, Jan 2014, doi: 10.1002/bmc.3015.
[185] T. Zhang and P. Franco, "Analytical and Preparative Potential of Immobilized Polysaccharide-Derived Chiral Stationary Phases," in *Chiral Separation Techniques*, 2006, pp. 99-134.
[186] A. R. Brash, W. E. Boeglin, J. H. Capdevila, S. Yeola, and I. A. Blair, "7-HETE, 10-HETE, and 13-HETE are major products of NADPH-dependent arachidonic acid metabolism in rat liver microsomes: analysis of their stereochemistry, and the stereochemistry of their acid-catalyzed rearrangement," *Arch Biochem Biophys,* vol. 321, no. 2, pp. 485-92, Aug 20 1995, doi: 10.1006/abbi.1995.1421.
[187] K. V. Penmetsa *et al.*, "Development of Reversed-Phase Chiral Hplc Methods Using Mass Spectrometry Compatible Mobile Phases," *Journal of Liquid Chromatography & Related Technologies,* vol. 23, no. 6, pp. 831-839, 2007, doi: 10.1081/jlc-100101492.
[188] W. Schafer *et al.*, "Improved chiral SFC screening for analytical method development," *Chirality,* vol. 25, no. 11, pp. 799-804, Nov 2013, doi: 10.1002/chir.22218.
[189] F. T. Mattrey *et al.*, "Current challenges and future prospects in chromatographic method development for pharmaceutical research," *TrAC Trends in Analytical Chemistry,* vol. 95, pp. 36-46, 2017, doi: 10.1016/j.trac.2017.07.021.
[190] J. Homann *et al.*, "Chiral chromatography-tandem mass spectrometry applied to the determination of pro-resolving lipid mediators," *J Chromatogr A,* vol. 1360, pp. 150-63, Sep 19 2014, doi: 10.1016/j.chroma.2014.07.068.
[191] M. Chatterjee, "Platelet lipidome: Dismantling the "Trojan horse" in the bloodstream," *J Thromb Haemost,* vol. 18, no. 3, pp. 543-557, Mar 2020, doi: 10.1111/jth.14721.
[192] J. Yeung and M. Holinstat, "Who is the real 12-HETrE?," *Prostaglandins Other Lipid Mediat,* vol. 132, pp. 25-30, Sep 2017, doi: 10.1016/j.prostaglandins.2017.02.005.
[193] J. Yeung *et al.*, "12(S)-HETrE, a 12-Lipoxygenase Oxylipin of Dihomo-gamma-Linolenic Acid, Inhibits Thrombosis via Galphas Signaling in Platelets," *Arterioscler Thromb Vasc Biol,* vol. 36, no. 10, pp. 2068-77, Oct 2016, doi: 10.1161/ATVBAHA.116.308050.
[194] M. Laniado-Schwartzman and M. W. Dunn, "Cytochrome P450-derived eicosanoids mediators of ocular surface inflammation. are," *Adv Exp Med Biol,* vol. 525, pp. 47-54, 2003, doi: 10.1007/978-1-4419-9194-2_10.
[195] M. Rosolowsky and W. B. Campbell, "Synthesis of hydroxyeicosatetraenoic (HETEs) and epoxyeicosatrienoic acids (EETs) by cultured bovine coronary artery endothelial cells," *Biochimica et Biophysica Acta (BBA) - Lipids and Lipid Metabolism,* vol. 1299, no. 2, pp. 267-277, 1996, doi: 10.1016/0005-2760(95)00216-2.
[196] C. Schneider and A. R. Brash, "Lipoxygenase-catalyzed formation of R-configuration hydroperoxides," *Prostaglandins & Other Lipid Mediators,* vol. 68-69, pp. 291-301, 2002, doi: 10.1016/s0090-6980(02)00041-2.
[197] J. Capdevila, P. Yadagiri, S. Manna, and J. R. Falck, "Absolute configuration of the hydroxyeicosatetraenoic acids (HETEs) formed during catalytic oxygenation

of arachidonic acid by microsomal cytochrome P-450," *Biochemical and Biophysical Research Communications,* vol. 141, no. 3, pp. 1007-1011, 1986, doi: 10.1016/s0006-291x(86)80144-9.
[198] H. Kawajiri *et al.*, "Arachidonic and linoleic acid metabolism in mouse intestinal tissue: evidence for novel lipoxygenase activity," *Arch Biochem Biophys,* vol. 398, no. 1, pp. 51-60, Feb 1 2002, doi: 10.1006/abbi.2001.2685.
[199] F. Bürger, P. Krieg, F. Marks, and G. Fürstenberger, "Positional- and stereo-selectivity of fatty acid oxygenation catalysed by mouse (12S)-lipoxygenase isoenzymes," *Biochemical Journal,* vol. 348, no. 2, pp. 329-335, 2000, doi: 10.1042/bj3480329.
[200] P. E. J. van der Meijden and J. W. M. Heemskerk, "Platelet biology and functions: new concepts and clinical perspectives," *Nat Rev Cardiol,* vol. 16, no. 3, pp. 166-179, Mar 2019, doi: 10.1038/s41569-018-0110-0.
[201] G. A. FitzGerald, "Human Platelet Lipidomics: Variance, Visualization, Flux, and Fuel," *Cell Metab,* vol. 23, no. 5, pp. 757-9, May 10 2016, doi: 10.1016/j.cmet.2016.04.025.
[202] V. B. O'Donnell and R. C. Murphy, "Directing eicosanoid esterification into phospholipids," *J Lipid Res,* vol. 58, no. 5, pp. 837-839, May 2017, doi: 10.1194/jlr.C075986.
[203] S. Zhong *et al.*, "An update on lipid oxidation and inflammation in cardiovascular diseases," *Free Radic Biol Med,* vol. 144, pp. 266-278, Nov 20 2019, doi: 10.1016/j.freeradbiomed.2019.03.036.
[204] A. Anesi and G. Guella, "A fast liquid chromatography-mass Spectrometry methodology for membrane lipid profiling through hydrophilic interaction liquid chromatography," *J Chromatogr A,* vol. 1384, pp. 44-52, Mar 6 2015, doi: 10.1016/j.chroma.2015.01.035.
[205] D. Q. Tang, L. Zou, X. X. Yin, and C. N. Ong, "HILIC-MS for metabolomics: An attractive and complementary approach to RPLC-MS," *Mass Spectrom Rev,* vol. 35, no. 5, pp. 574-600, Sep 2016, doi: 10.1002/mas.21445.
[206] T. Bamba, J. W. Lee, A. Matsubara, and E. Fukusaki, "Metabolic profiling of lipids by supercritical fluid chromatography/mass spectrometry," *J Chromatogr A,* vol. 1250, pp. 212-9, Aug 10 2012, doi: 10.1016/j.chroma.2012.05.068.
[207] T. Uchikata, A. Matsubara, E. Fukusaki, and T. Bamba, "High-throughput phospholipid profiling system based on supercritical fluid extraction-supercritical fluid chromatography/mass spectrometry for dried plasma spot analysis," *J Chromatogr A,* vol. 1250, pp. 69-75, Aug 10 2012, doi: 10.1016/j.chroma.2012.06.031.
[208] C. Calderon, L. Rubarth, M. Cebo, I. Merfort, and M. Lammerhofer, "Lipid Atlas of Keratinocytes and Betulin Effects on its Lipidome Profiled by Comprehensive UHPLC-MS/MS with Data Independent Acquisition Using Targeted Data Processing," *Proteomics,* vol. 20, no. 11, p. e1900113, Jun 2020, doi: 10.1002/pmic.201900113.
[209] M. Groessl, S. Graf, and R. Knochenmuss, "High resolution ion mobility-mass spectrometry for separation and identification of isomeric lipids," *Analyst,* vol. 140, no. 20, pp. 6904-11, Oct 21 2015, doi: 10.1039/c5an00838g.
[210] G. Paglia *et al.*, "Ion mobility-derived collision cross section as an additional measure for lipid fingerprinting and identification," *Anal Chem,* vol. 87, no. 2, pp. 1137-44, Jan 20 2015, doi: 10.1021/ac503715v.

[211] R. Wang, Y. Yin, and Z. J. Zhu, "Advancing untargeted metabolomics using data-independent acquisition mass spectrometry technology," *Anal Bioanal Chem*, vol. 411, no. 19, pp. 4349-4357, Jul 2019, doi: 10.1007/s00216-019-01709-1.
[212] H. Tsugawa, K. Ikeda, W. Tanaka, Y. Senoo, M. Arita, and M. Arita, "Comprehensive identification of sphingolipid species by in silico retention time and tandem mass spectral library," *J Cheminform*, vol. 9, p. 19, 2017, doi: 10.1186/s13321-017-0205-3.
[213] M. Raetz, E. Duchoslav, R. Bonner, and G. Hopfgartner, "Hybrid SWATH/MS and HR-SRM/MS acquisition for phospholipidomics using QUAL/QUANT data processing," *Anal Bioanal Chem*, vol. 411, no. 22, pp. 5681-5690, Sep 2019, doi: 10.1007/s00216-019-01946-4.
[214] M. Wijtmans *et al.*, "Synthesis, modeling and functional activity of substituted styrene-amides as small-molecule CXCR7 agonists," *Eur J Med Chem*, vol. 51, pp. 184-92, May 2012, doi: 10.1016/j.ejmech.2012.02.041.
[215] F. Rigano, M. Oteri, M. Russo, P. Dugo, and L. Mondello, "Proposal of a Linear Retention Index System for Improving Identification Reliability of Triacylglycerol Profiles in Lipid Samples by Liquid Chromatography Methods," *Anal Chem*, vol. 90, no. 5, pp. 3313-3320, Mar 6 2018, doi: 10.1021/acs.analchem.7b04837.
[216] Y. Benjamini and Y. Hochberg, "Controlling the False Discovery Rate: A Practical and Powerful Approach to Multiple Testing," *Journal of the Royal Statistical Society: Series B (Methodological)*, vol. 57, no. 1, pp. 289-300, 1995, doi: 10.1111/j.2517-6161.1995.tb02031.x.

LIST OF FIGURES

LIST OF TABLES

ACKNOWLEDGEMENTS

"Coming together is a beginning. Keeping together is progress. Working together is success." - *Henry Ford*

I could never accomplish all this work without help of other people; and to all the people, who directly or indirectly contributed to this thesis I am sincerely thankful.

I am very grateful to **Prof. Michael Lämmerhofer** for accepting me in his group, for guiding me through all the years of the laboratory research and through the process of writing this thesis. I honestly admire his ingenuity, unconventional thinking and optimism, which have always inspired me to work better and harder. I am also thankful to **Prof. Pierre Koch** for being my second supervisor and for evaluating this thesis.

I would like to especially thank to **Dr. Stefan Neubauer** for his professional advice, critical thinking and novel ideas as well as personal care of me and Nusi. He motivated me as nobody else to accomplish this thesis.

I would like to also thank to all my dear colleagues: to **Dr. Jörg Schlotterbeck** for his warm welcome in the beginning of my work and for answering all of my million questions about lipidomics; to **Dr. Jeannie Horak** for her broad knowledge and the great willingness to share it; to **Dr. Bernhard Drotleff** for solving even the weirdest problems with our MS instruments; to **Dr. Carlos Calderón Castro** for countless discussions on lipidomics related (or not) topics; to **Dr. Siyao Liu** for her kindness and for bringing always nice atmosphere, to **Stefanie Bäurer** for great trips during conferences; to **Ryan Karongo** for being the best officemate; to **Ece Aydin** for organizing our monthly science meetings; to **Peng Li** and **Xiaoqing Fu** - working together was always a pleasure; to **Christian Geibel** for caring about everybody in our group; to **Dr. Adrian Sievers-Engler** and **Marc Wolter** for their great sense of humour; to **Simon Jaag** for his willingness to help with the LC issues; to **Dr. Ulrich Woiwode** for inspiring me to work hard; to **Corinna Sanwald** for taking care of our working group; to **Kristina Dittrich** for her ideas in complex data processing; to **Feiyang Li** for his expertise in laboratory work and to **Mike Kaupert** for taking care of our instruments. I am also grateful to our secretaries, **Eveline Wachendorfer** and **Ingrid Straub** for keeping our group running.

Many thanks to **Dr. Madhumita Chatterjee** for our successful collaboration on platelet lipidomics, for her scientific advice and for encouraging discussions.

Special thanks to my dear friends **Dr. Zuzanna Misiewicz** and **Agnieszka Pukało** for always being there for me (next to a phone).

Finally, I am very grateful to my family **Czesława Cebo**, **Sławomir Cebo**, **Tomasz Cebo** and **Danuta Jabłońska** for their love, care and understandings. They have always supported me and motivated to fulfil my dreams.

This work was funded by the Deutsche Forschungsgemeinschaft (DFG, German Research Foundation) – Project number 374031971 – TRR 240.